Pacific Northwest
NATIONAL LABORATORY

PNNL-28838 Rev 2
EWG-RPT-021 Rev. 2

# Enhanced Hanford Low-Activity Waste Glass Property Data Development: Phase 2

February 2021

RL Russell
BP McCarthy
SK Cooley
EA Cordova
SE Sannoh
V Gervasio
MJ Schweiger
JB Lang
CH Skidmore
CE Lonergan
BA Stanfill
JM Meline
JD Vienna

U.S. DEPARTMENT OF ENERGY

Prepared for the U.S. Department of Energy
under Contract DE-AC05-76RL01830

**DISCLAIMER**



PACIFIC NORTHWEST NATIONAL LABORATORY
*operated by*
BATTELLE
*for the*
UNITED STATES DEPARTMENT OF ENERGY
*under Contract DE-AC05-76RL01830*

**Printed in the United States of America**

**Available to DOE and DOE contractors from the**
**Office of Scientific and Technical Information,**
**P.O. Box 62, Oak Ridge, TN 37831-0062;**
**ph: (865) 576-8401**
**fax: (865) 576-5728**
**email: reports@adonis.osti.gov**

**Available to the public from the National Technical Information Service**
**5301 Shawnee Rd., Alexandria, VA 22312**
**ph: (800) 553-NTIS (6847)**
**email: orders@ntis.gov <https://www.ntis.gov/about>**
**Online ordering: http://www.ntis.gov**

PNNL-28838 Rev 2
EWG-RPT-021 Rev. 2

# Enhanced Hanford Low-Activity Waste Glass Property Data Development: Phase 2

February 2021

RL Russell
BP McCarthy
SK Cooley
EA Cordova
SE Sannoh
V Gervasio
MJ Schweiger
JB Lang
CH Skidmore
CE Lonergan
BA Stanfill
JM Meline
JD Vienna

Prepared for
the U.S. Department of Energy
under Contract DE-AC05-76RL01830

Pacific Northwest National Laboratory
Richland, Washington 99354

# Executive Summary

This report summarizes and analyzes the data collected on a second test matrix of 42 low-activity waste (LAW) glass compositions intended to expand the LAW glass composition region over which glass property-composition models are valid. The 42 LAW glass compositions were selected using a statistical layered experimental design approach to explore a new glass composition region that overlaps and expands beyond the previously explored LAW glass composition region. The layered design of 42 LAW glasses consisted of 21 outer-layer glasses, 15 inner-layer glasses, a center glass (three replicates), and two glasses previously tested at another laboratory. The outer-layer glass compositions include extrema based on current projections of the LAW feeds and melter operating temperatures. One of the outer-layer compositions was eliminated due to the inability to form a glass. Therefore, only 41 glasses were analyzed. The analyses performed on these glasses include chemical composition (for target compositional verification), density, viscosity, electrical conductivity, crystal fraction, canister centerline cooling with crystal identification, the Product Consistency Test, sulfur solubility, and the Vapor Hydration Test. This report discusses the results obtained from this testing.

# Acknowledgments

The authors gratefully acknowledge the financial support provided by the U.S. Department of Energy Office of River Protection Waste Treatment and Immobilization Plant Project managed by Tom Fletcher, with technical oversight by Albert Kruger.

The authors thank Kevin Fox and Thomas Edwards of Savannah River National Laboratory for their help in the analysis and testing of the glasses. We also thank Tongan Jin (PNNL) for his technical review, Heather Culley (PNNL) for her editorial review, and Hans Brandal and Veronica Perez (PNNL) for programmatic support during the conduct of this work.

# Acronyms and Abbreviations

| | |
|---|---|
| ARM | Approved Reference Material |
| BNI | Bechtel National, Inc. |
| CCC | canister centerline cooling (heat treatment) |
| CUA | The Catholic University of America |
| DIW | deionized water |
| DOE | U.S. Department of Energy |
| EA | Environmental Assessment |
| EC | electrical conductivity |
| EGCR | experimental glass composition region |
| EWG | Enhanced Waste Glass |
| η | Viscosity |
| HDI | "How Do I…?" |
| IA | image analysis |
| IC | ion chromatography |
| ICP-AES | inductively coupled plasma – atomic emissions spectroscopy |
| IL | inner layer |
| KH | potassium hydroxide digestion |
| LAW | low-activity waste |
| LM | lithium metaborate/tetraborate fusion |
| LRM | low-activity waste reference material |
| NIST | National Institute of Standards and Technology |
| NQAP | Nuclear Quality Assurance Program |
| OL | outer layer |
| OM | optical microscopy |
| ORP | Office of River Protection |
| PCT | Product Consistency Test |
| PF | sodium peroxide fusion |
| PNNL | Pacific Northwest National Laboratory |
| PSAL | Process Science Analytical Laboratory |
| PVDF | polyvinylidene difluoride |
| QA | quality assurance |
| QGCR | qualified glass composition region |
| R&D | research and development |
| SRNL | Savannah River National Laboratory |
| S/V | surface area-to-solution volume |
| VHT | Vapor Hydration Test |
| vol% | volume percent |
| VFT | Vogel-Fulcher-Tammann |

| | |
|---|---|
| wt% | weight percent |
| WTP | Hanford Tank Waste Treatment and Immobilization Plant |
| XRD | x-ray diffraction |
| XRF | x-ray fluorescence |

# Contents

# Figures

## Tables

# 1.0 Introduction

The U.S. Department of Energy's (DOE) Office of River Protection (ORP) requested Pacific Northwest National Laboratory (PNNL) to support the River Protection Project vitrification in an effort to support operations upon completion of startup activities (DOE 2012). This work was performed under the PNNL project titled "ORP Glass Support Work." One task of this project—Enhanced Hanford Waste Glass Models—is the subject of this report. A previous task focused on generating property-composition data and models for the Hanford site low-activity waste (LAW) glasses with lower waste loadings, which are relevant to the commissioning of the LAW vitrification facility. The current task has the long-term objective of expanding the Hanford site LAW glass database and property-composition models for the balance of the Hanford site tank waste treatment and immobilization mission. During the balance of the mission, LAW glasses with higher waste loadings will be produced.

This report presents the glass compositions and glass property data developed in Phase 2 of the enhanced Hanford LAW glass property data development effort. When this effort is complete, enhanced LAW glass property models will be developed. Section 1.1 summarizes the status of the LAW glass composition regions and waste loading constraints prior to the data development effort documented in this report. Section 1.2 summarizes the LAW Phase 2 glass composition region and test matrix. Section 1.3 documents the quality assurance program used in performing the work discussed in this report.

## 1.1 Status of LAW Experimental Glass Composition Regions and Waste Loading Constraints

The Hanford Waste Treatment and Immobilization Plant (WTP) project has previously developed glass property-composition models to formulate LAW glass compositions and qualify LAW glasses for disposal (Piepel et al. 2007). These models are based on data from crucible-scale tests with simulants, crucible-scale tests with actual waste, and scaled-melter tests with simulants collected under the Bechtel National, Inc. (BNI) contract to design, construct, and commission the WTP (DOE 2000). The scope of the BNI contract is limited to operating the plant over a limited commissioning period with LAW glasses with limited waste loadings (i.e., the proportion of waste in the glass). Hence, the data and resulting glass property-composition models only cover a fraction of the LAW glass composition region needed for the entire Hanford site mission. In addition, the data and models developed by BNI are targeted at glasses that modestly exceed contract minimum waste loadings rather than maximum achievable waste loadings.

In this document, the term *experimental glass composition region* (EGCR) is used to refer to a composition region of glasses that has been (or will be) experimentally explored through fabricating glasses and testing their properties. Ideally, an EGCR should include all glass compositions that will satisfy processing and product-quality related constraints, as well as glass compositions that fail one or more constraints. Experimental data collected on glass compositions covering the EGCR then provide for developing property-composition models that can 1) discriminate between glass compositions that satisfy and fail the requirements, and 2) adequately predict glass properties of compositions that satisfy all requirements. The term *qualified glass composition region* (QGCR) refers to the subset of the EGCR where all processing and product-quality constraints are satisfied with sufficient confidence after accounting for applicable uncertainties.

EGCRs are specified using processing and product-quality constraints of two main kinds. Single-component constraints (SCCs) involve lower and/or upper limits on individual LAW glass components. Multiple-component constraints (MCCs) involve lower and/or upper limits on combinations of LAW glass components. For some MCCs, the combinations of components are existing property-composition models for LAW glasses. In other cases, the combinations are stand-in expressions for properties that

have not yet been modeled or are not easily measured or predicted. Examples of stand-in constraints are discussed in the following paragraph. The set of all SCCs and MCCs specifying the EGCR are referred to as *model validity constraints* because these constraints specify the region of qualified data available for developing models to predict the LAW glass properties of interest.

Stand-in constraints are used in lieu of constraints on the properties to be controlled. For example, we previously limited the weight percent (wt%) $SO_3$ targeted in glass because the salt accumulation in the melter was not predictable. We also limited the equilibrium fraction of crystals at 950°C to one volume percent (vol%) because crystal blockages of the melter pour-spout are not currently predictable. To determine the ultimate waste loading of glass, these constraints based on limited data availability need to be replaced with constraints based on true operating and product performance property limits. To this end, we seek to develop (1) glass property data across broader glass composition regions to increase waste loadings and (2) methods to measure (directly or indirectly) and model the properties that fundamentally limit the melter operations or the performance of the glass.

The LAW is dominated by sodium salts (DOE 2000). The ratio of sulfur (as $SO_3$) to sodium (as $Na_2O$) in the waste is a key determinant of waste loading and glass formulation. At high-alkali concentrations, the waste loading is limited primarily by the chemical durability (measured by the VHT and PCT responses) of the resulting LAW glass. At high $SO_3$ concentrations, the waste loading is limited primarily by salt accumulation in the melter.

The LAW glasses currently formulated for WTP (Kim and Vienna 2012) have relatively conservative alkali and $SO_3$ loading limits, as shown by the red constraint in Figure 1.1. The waste loading is currently determined by the ratio of normalized alkali ($Na_2O+0.66K_2O$) to $SO_3$ in the waste. Where the ($Na_2O+0.66K_2O$):$SO_3$ ratio for a waste intersects the red line determines the loading of that waste in glass using the current WTP LAW glass constraints. Additional constraints are used to limit the concentrations of halides in the glass, which are functions of chromium, phosphorus, and potassium (Kim and Vienna 2012).

More recently, new high waste loading formulations have been developed by The Catholic University of America (CUA) and PNNL in support of ORP (Matlack et al. 2005a, 2005b, 2006a, 2006b, 2007, 2009; Vienna et al. 2003a, 2004a, 2004b; and Kim et al. 2003). The resulting data are summarized in Muller et al. (2012, 2015), Vienna et al. (2013, 2016), and Russell et al. (2017), with some newer data not yet reported. The basic conclusions of these studies are that loadings for specific wastes in glass can be increased significantly over what would be allowed by current WTP constraints. Examples of the gains made in recent studies include the following:

- Glass $SO_3$ loadings of >1.5 wt% were successfully processed, which is double the 0.77 wt% allowed by the current WTP LAW EGCR.
- LAW normalized alkali loadings of 26 wt% have been achieved compared to the 21 wt% maximum in the current WTP LAW EGCR.

These advances (upper blue line) are compared with the WTP baseline waste loading constraints (lower red line) in Figure 1.1. In this figure, the $SO_3$ limits ($SO_3$ = 0.77 or 1.5 wt%) are used to reduce the risk of salt accumulation in the melter. If salt does accumulate in the melter, the useful life of components that are adjacent to or pass through the melt line may be significantly reduced. The horizontal lines represent alkali limits in glass ($Na_2O+0.66K_2O$ = 21.5 or 24 wt%) above which there is high risk of exceeding the current WTP contract specifications for the Product Consistency Test (PCT) and the Vapor Hydration Test (VHT) responses for glass durability (DOE 2000). The sloped lines between these two end constraints represent the limits of the formulations tested to date in trading off how high $SO_3$ or alkali can be when the other is at its upper limit. Therefore, glasses can be formulated for high $SO_3$ loading or for

high-alkali loading, but compromises must be made to achieve high concentrations of both. The sloped lines therefore represent the current state of formulations tested to achieve this balance. Future testing and modeling efforts are underway to describe each of the fundamental properties (e.g., salt formation, PCT and VHT responses, viscosity, electrical conductivity) as functions of target glass compositions. Although these models exist for projecting the amount of glass to be expected during Hanford's mission (Vienna et al. 2016), they need to be updated for WTP processing within the expanded glass composition region to ensure that optimized glasses simultaneously satisfy all the processing and product-quality constraints.

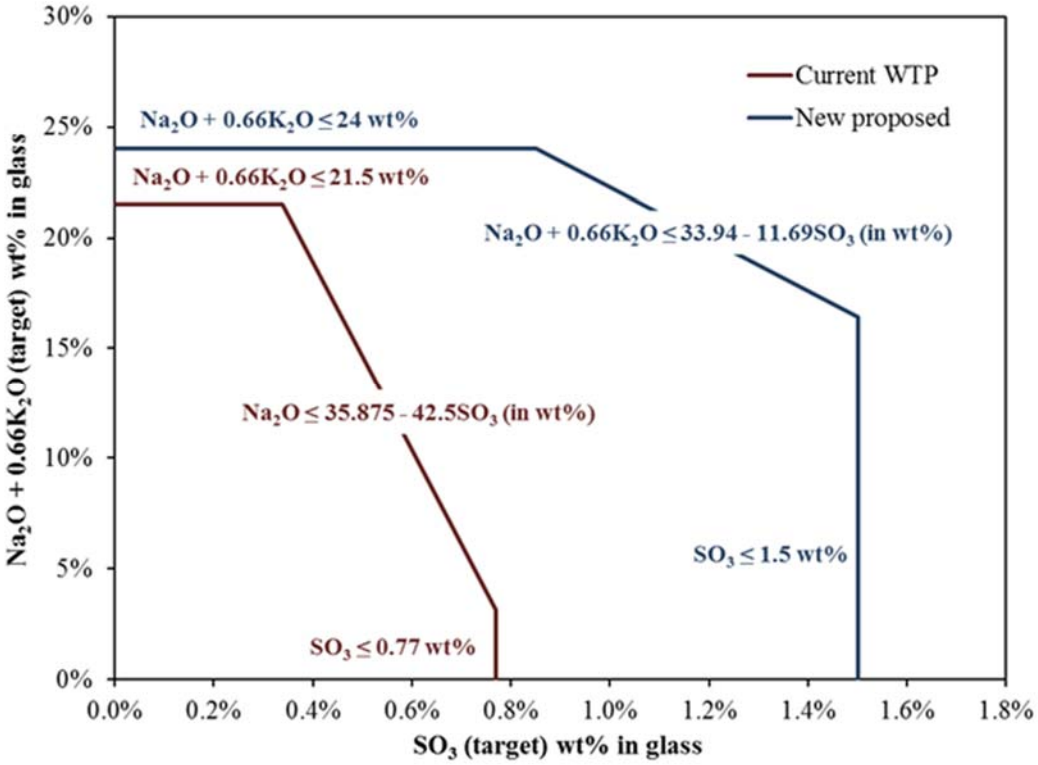


Figure 1.1. Plot of Glass Waste Loading Constraints for the Current WTP and Advanced ORP LAW Glasses as Projected Based on $Na_2O+0.66K_2O$ Versus $SO_3$ Concentrations in Glass (Vienna et al. 2016)

The LAW glass compositions that have available property data have two somewhat distinct composition sub-regions (the current WTP and the advanced ORP glasses). The question is raised whether we need to develop 1) a single, combined EGCR, or 2) an advanced LAW EGCR without ties to the subregion with lower waste loadings. This question is being addressed by current property-composition modeling work at PNNL. For this Phase 2 study, PNNL explored only the advanced LAW EGCR corresponding to the sub-region with higher waste loadings. The current CUA testing program is attempting to bridge the gap between the two sub-regions (Muller et al. 2013a, 2013b, 2015, 2017).

## 1.2 Phase 2 Enhanced LAW Experimental Glass Composition Region and Test Matrix

The objective of this task was to generate data for different LAW glass compositions to ultimately support the development, validation, and implementation of glass property models that can achieve high waste loading for the full region of Hanford LAW compositions. To extend the models beyond our current knowledge space, a new enhanced LAW EGCR was developed. Table 1.1 lists the 15 LAW glass

components selected for variation in the experimental work, including an Others component mix. Certain components were chosen for variation in the experimental work for specific reasons. The components $SnO_2$ and $ZrO_2$ were included because they can decrease the VHT response. The components $V_2O_5$ and $Li_2O$ were included because they can increase the $SO_3$ tolerance in the melter. Finally, the components ZnO and $Cr_2O_3$ were included because they can decrease refractory corrosion.

Table 1.1. Lower and Upper Bounds of Single-Component Constraints[(a)] for the Outer and Inner Layers of the 15-Component Enhanced Low-Activity Waste Experimental Glass Composition Region

| | Outer Layer | | Inner Layer | | |
|---|---|---|---|---|---|
| **Component** | **Lower Bound** | **Upper Bound** | **Lower Bound** | **Upper Bound** | **Center Point** |
| $Al_2O_3$ | 0.06 | 0.125 | 0.075 | 0.1075 | 0.10 |
| $B_2O_3$ | 0.06 | 0.1375 | 0.08 | 0.12 | 0.095 |
| CaO | 0.02 | 0.11 | 0.02 | 0.08 | 0.05 |
| $Cr_2O_3$ | 0.003 | 0.006 | 0.00375 | 0.00525 | 0.0045 |
| $Fe_2O_3$ | 0.00 | 0.015 | 0.002 | 0.01 | 0.006 |
| $K_2O$ | 0.00 | 0.0575 | 0.005 | 0.02 | 0.01 |
| $Li_2O$ | 0.00 | 0.00 | 0.00 | 0.00 | 0.00 |
| MgO | 0.00 | 0.0135 | 0.003 | 0.01 | 0.0065 |
| $Na_2O$ | 0.21 | 0.26 | 0.22 | 0.245 | 0.23 |
| $SiO_2$ | 0.349 | 0.47 | 0.37 | 0.43 | 0.388 |
| $SO_3$ | 0.001 | 0.02 | 0.002 | 0.008 | 0.005 |
| $SnO_2$ | 0.00 | 0.035 | 0.005 | 0.025 | 0.015 |
| $V_2O_5$ | 0.00 | 0.04 | 0.005 | 0.02 | 0.01 |
| ZnO | 0.02 | 0.036 | 0.024 | 0.032 | 0.028 |
| $ZrO_2$ | 0.0295 | 0.065 | 0.03 | 0.055 | 0.04 |
| Others[(b)] | 0.0036 | 0.0269 | 0.01 | 0.02 | 0.012 |

(a) The lower and upper bounds of the SCCs are in terms of mass fractions of the components, such that the mass fractions of all 15 components must sum to 1.0000.
(b) The Others component was composed of the following mixture of three minor components (expressed as mass fractions): Cl = 0.173, F = 0.263, and $P_2O_5$ = 0.564.

The enhanced LAW EGCR was specified by the SCCs listed in Table 1.1 and the MCCs listed in Table 1.2. Table 1.1 and Table 1.2 list SCCs and MCCs separately for the outer and inner layers of the enhanced LAW EGCR. The outer-layer SCCs and MCCs were chosen to overlap and expand beyond the previously explored EGCR and to include more extreme LAW glass compositions based on current projections of the LAW feed.

Table 1.2. Lower and Upper Bounds of Multiple-Component Constraints for the Outer and Inner Layers of a 15-Component Enhanced Low-Activity Waste Experimental Glass Composition Region

| | Outer Layer | | Inner Layer | |
|---|---|---|---|---|
| **Expression (units)[a]** | **Lower Bound** | **Upper Bound** | **Lower Bound** | **Upper Bound** |
| Nalk (mf)[b] | 0.15 | 0.265 | 0.195 | 0.2515 |
| $ZrO_2$+$SnO_2$ (mf) | 0.03 | 0.11 | 0.04 | 0.08 |
| $\eta_{1150}$ (poise)[c] | 10 | 100 | 30 | 70 |
| $SO_3$ Solubility (wt%) | – | Solubility Limit[d] | – | Solubility Limit[d] |

(a) mf = mass fraction, wt% = weight percent.
(b) Nalk = $Na_2O$ + 0.66($K_2O$) + 2($Li_2O$)
(c) $\eta_{1150}$ = viscosity at 1150ºC, expressed as a linear mixture model, as discussed by Piepel et al. (2015, 2016).
(d) The $SO_3$ solubility limit is expressed as a partial quadratic mixture model, as discussed by Piepel et al. (2015, 2016).

The 42 Phase 2 enhanced LAW glass compositions that were tested comprise a statistical layered design (Piepel et al. 1993; Cooley et al. 2003; Piepel et al. 2005) consisting of 21 outer-layer glasses, 15 inner-layer glasses, a center glass (three replicates), and two glasses previously tested at another laboratory. The 42 LAW glass compositions are listed in Table 1.3.

Four of the glasses in this study required some modifications to their compositions for them to melt and form glasses. These glasses had sulfate salts segregate from the melt, and therefore had to have the sulfate decreased in their final glass compositions. These four glasses also were opaque, which required their compositions to be modified. One other glass, LP2-OL-06, was eliminated because of continual chemical dissolution issues that caused it not to form a glass even after a couple of modifications. This is understandable because LP2-OL-06 was an outer-layer extreme vertex of the EGCR. The test matrix included outer-layer extreme vertices of to investigate LAW glasses with significantly higher waste loadings. This topic is discussed in more detail in Section 2.2. The modified glass compositions are listed in Table 1.4, with the extension “MOD” added to the glass identification. One glass, LP2-OL-03, required two modifications to obtain a glass and therefore is noted as “MOD2”. Note that glass property data were generated only for the “MOD” glasses, not their original “as-designed” counterparts.

This report summarizes the experimental methods used at PNNL to fabricate, heat treat, and test the remaining and modified 41 glasses in the LAW Phase 2 test matrix. These 41 glasses included the following:

- 20 outer-layer glass compositions (after one glass composition eliminated)
- 15 inner-layer glass compositions
- a repeated outer-layer glass composition (LP2-OL-10)
- a centroid glass, EWG-LAW-Centroid (three replicates; named LP2-IL-16, LP2-OL-2, and LP2-OL-21)
- a CUA-tested glass designated as LAW-ORP- LD1 (named LP2-OL-7)
- a CUA-tested glass designated as ORLEC33 (named LP2-IL-17).

Measured values of glass-quality and processing properties for the 41 Phase 2 LAW glasses are described in this report and data are provided in appendices.

Table 1.3. Targeted Compositions (mass fractions) for the Phase 2 Enhanced LAW Glasses

| | Glass ID | | | | | | | | | | | | |
|---|---|---|---|---|---|---|---|---|---|---|---|---|---|
| **Component** | **LP2-IL-01** | **LP2-IL-02** | **LP2-IL-03** | **LP2-IL-04** | **LP2-IL-05** | **LP2-IL-06** | **LP2-IL-07** | **LP2-IL-08** | **LP2-IL-09** | **LP2-IL-10** | **LP2-IL-11** | **LP2-IL-12** | **LP2-IL-13** |
| $Al_2O_3$ | 0.07500 | 0.07500 | 0.08725 | 0.07500 | 0.07500 | 0.10680 | 0.07500 | 0.07500 | 0.07500 | 0.10000 | 0.09000 | 0.07500 | 0.07500 |
| $B_2O_3$ | 0.08000 | 0.08129 | 0.08732 | 0.08000 | 0.12000 | 0.12000 | 0.12000 | 0.08000 | 0.12000 | 0.09500 | 0.08000 | 0.08000 | 0.11255 |
| CaO | 0.07617 | 0.02000 | 0.02000 | 0.07494 | 0.07025 | 0.02000 | 0.05147 | 0.08000 | 0.02000 | 0.05000 | 0.03080 | 0.03117 | 0.02320 |
| Cl | 0.00174 | 0.00174 | 0.00347 | 0.00347 | 0.00347 | 0.00347 | 0.00347 | 0.00347 | 0.00173 | 0.00208 | 0.00347 | 0.00347 | 0.00174 |
| $Cr_2O_3$ | 0.00525 | 0.00375 | 0.00525 | 0.00525 | 0.00375 | 0.00525 | 0.00375 | 0.00525 | 0.00525 | 0.00450 | 0.00375 | 0.00375 | 0.00525 |
| F | 0.00263 | 0.00263 | 0.00526 | 0.00527 | 0.00526 | 0.00526 | 0.00527 | 0.00526 | 0.00263 | 0.00316 | 0.00526 | 0.00527 | 0.00263 |
| $Fe_2O_3$ | 0.00200 | 0.00577 | 0.00200 | 0.01000 | 0.00200 | 0.00200 | 0.00200 | 0.01000 | 0.01000 | 0.00600 | 0.01000 | 0.00200 | 0.01000 |
| $K_2O$ | 0.02000 | 0.02000 | 0.00758 | 0.02000 | 0.00500 | 0.02000 | 0.02000 | 0.00500 | 0.00500 | 0.01000 | 0.02000 | 0.00500 | 0.02000 |
| MgO | 0.00300 | 0.01000 | 0.00300 | 0.01000 | 0.00300 | 0.01000 | 0.01000 | 0.01000 | 0.01000 | 0.00650 | 0.00300 | 0.01000 | 0.00300 |
| $Na_2O$ | 0.23680 | 0.23680 | 0.24500 | 0.23680 | 0.22000 | 0.22000 | 0.22327 | 0.22000 | 0.24373 | 0.23000 | 0.22000 | 0.23787 | 0.22000 |
| $P_2O_5$ | 0.00563 | 0.00563 | 0.01127 | 0.01127 | 0.01127 | 0.01127 | 0.01127 | 0.01127 | 0.00563 | 0.00676 | 0.01127 | 0.01127 | 0.00563 |
| $SiO_2$ | 0.37978 | 0.41808 | 0.40360 | 0.38200 | 0.37000 | 0.37000 | 0.39450 | 0.38975 | 0.37000 | 0.38800 | 0.38845 | 0.42920 | 0.43000 |
| $SO_3$ | 0.00800 | 0.00800 | 0.00200 | 0.00200 | 0.00200 | 0.00800 | 0.00800 | 0.00800 | 0.00200 | 0.00500 | 0.00200 | 0.00200 | 0.00200 |
| $SnO_2$ | 0.00500 | 0.02500 | 0.02500 | 0.02500 | 0.02500 | 0.00820 | 0.00500 | 0.00500 | 0.02203 | 0.01500 | 0.02500 | 0.00500 | 0.00500 |
| $V_2O_5$ | 0.02000 | 0.00500 | 0.00500 | 0.00500 | 0.00500 | 0.01075 | 0.00500 | 0.00500 | 0.02000 | 0.01000 | 0.02000 | 0.02000 | 0.00500 |
| ZnO | 0.02400 | 0.02631 | 0.03200 | 0.02400 | 0.02400 | 0.02400 | 0.03200 | 0.03200 | 0.03200 | 0.02800 | 0.03200 | 0.02400 | 0.02400 |
| $ZrO_2$ | 0.05500 | 0.05500 | 0.05500 | 0.03000 | 0.05500 | 0.05500 | 0.03000 | 0.05500 | 0.05500 | 0.04000 | 0.05500 | 0.05500 | 0.05500 |
| **Total** | 1.00000 | 1.00000 | 1.00000 | 1.00000 | 1.00000 | 1.00000 | 1.00000 | 1.00000 | 1.00000 | 1.00000 | 1.00000 | 1.00000 | 1.00000 |

Table 1.3. Targeted Compositions (mass fractions) for the Phase 2 Enhanced LAW Glasses (cont.)

| | Glass ID | | | | | | | | | | | |
|---|---|---|---|---|---|---|---|---|---|---|---|---|
| **Component** | **LP2-IL-14** | **LP2-IL-15** | **LP2-IL-16 (Centroid)** | **LP2-IL-17 (CUA ORLEC33)** | **LP2-OL-01** | **LP2-OL-02 (Centroid)** | **LP2-OL-03** | **LP2-OL-04** | **LP2-OL-05** | **LP2-OL-06 (eliminated)** | **LP2-OL-07 (CUA LD1)** | **LP2-OL-08** |
| $Al_2O_3$ | 0.08795 | 0.07500 | 0.10000 | 0.09227 | 0.06000 | 0.10000 | 0.10550 | 0.10500 | 0.12500 | 0.12500 | 0.10150 | 0.06000 |
| $B_2O_3$ | 0.12000 | 0.10752 | 0.09500 | 0.11000 | 0.06000 | 0.09500 | 0.06000 | 0.06000 | 0.06000 | 0.06000 | 0.12040 | 0.06000 |
| CaO | 0.03830 | 0.02000 | 0.05000 | 0.02500 | 0.0909 | 0.05000 | 0.10714 | 0.07840 | 0.11000 | 0.09130 | 0.08010 | 0.10664 |
| Cl | 0.00347 | 0.00347 | 0.00208 | 0.00073 | 0.00062 | 0.00208 | 0.00062 | 0.00062 | 0.00467 | 0.00467 | 0.00330 | 0.00062 |
| $Cr_2O_3$ | 0.00375 | 0.00525 | 0.00450 | 0.00080 | 0.00600 | 0.00450 | 0.00600 | 0.00600 | 0.00300 | 0.00600 | 0.00500 | 0.00600 |
| $Cs_2O$ | 0.00000 | 0.00000 | 0.00000 | 0.00000 | 0.00000 | 0.00000 | 0.00000 | 0.00000 | 0.00000 | 0.00000 | 0.00130 | 0.00000 |
| F | 0.00526 | 0.00527 | 0.00316 | 0.00110 | 0.00095 | 0.00316 | 0.00095 | 0.00095 | 0.00708 | 0.00708 | 0.00170 | 0.00095 |
| $Fe_2O_3$ | 0.01000 | 0.01000 | 0.00600 | 0.00200 | 0.00000 | 0.00600 | 0.00000 | 0.01500 | 0.01500 | 0.00000 | 0.01000 | 0.01500 |
| $K_2O$ | 0.00500 | 0.00500 | 0.01000 | 0.00500 | 0.00000 | 0.01000 | 0.00000 | 0.05750 | 0.00000 | 0.05750 | 0.00160 | 0.00000 |
| MgO | 0.00300 | 0.00300 | 0.00650 | 0.01000 | 0.01350 | 0.00650 | 0.01350 | 0.01350 | 0.00000 | 0.00000 | 0.01000 | 0.00000 |
| $Na_2O$ | 0.24500 | 0.22000 | 0.23000 | 0.23000 | 0.21000 | 0.23000 | 0.26000 | 0.21000 | 0.21000 | 0.21000 | 0.20980 | 0.26000 |
| NiO | 0.00000 | 0.00000 | 0.00000 | 0.00000 | 0.00000 | 0.00000 | 0.00000 | 0.00000 | 0.00000 | 0.00000 | 0.00040 | 0.00000 |
| $P_2O_5$ | 0.01127 | 0.01127 | 0.00676 | 0.00237 | 0.00203 | 0.00676 | 0.00203 | 0.00203 | 0.01515 | 0.01515 | 0.00290 | 0.00203 |
| $SiO_2$ | 0.37000 | 0.42722 | 0.38800 | 0.40943 | 0.47000 | 0.38800 | 0.34900 | 0.34900 | 0.39080 | 0.34900 | 0.37140 | 0.34900 |
| $SO_3$ | 0.00800 | 0.00800 | 0.00500 | 0.01000 | 0.00100 | 0.00500 | 0.01076 | 0.00100 | 0.00980 | 0.00880 | 0.01060 | 0.01476 |
| $SnO_2$ | 0.00500 | 0.02500 | 0.01500 | 0.00000 | 0.00000 | 0.01500 | 0.03500 | 0.00000 | 0.00000 | 0.00000 | 0.00000 | 0.00000 |
| $V_2O_5$ | 0.00500 | 0.02000 | 0.01000 | 0.02100 | 0.00000 | 0.01000 | 0.00000 | 0.00000 | 0.00000 | 0.00000 | 0.01000 | 0.04000 |
| ZnO | 0.02400 | 0.02400 | 0.02800 | 0.03000 | 0.02000 | 0.02800 | 0.02000 | 0.03600 | 0.02000 | 0.03600 | 0.03000 | 0.02000 |
| $ZrO_2$ | 0.05500 | 0.03000 | 0.04000 | 0.05030 | 0.06500 | 0.04000 | 0.02950 | 0.06500 | 0.02950 | 0.02950 | 0.03000 | 0.06500 |
| **Total**[(a)] | 1.00000 | 1.00000 | 1.00000 | 1.00000 | 1.00000 | 1.00000 | 1.00000 | 1.00000 | 1.00000 | 1.00000 | 1.00000 | 1.00000 |

Table 1.3. Targeted Compositions (mass fractions) for the Phase 2 Enhanced LAW Glasses (cont.)

| | Glass ID | | | | | | | | | | | |
|---|---|---|---|---|---|---|---|---|---|---|---|---|
| **Component** | **LP2-OL-09** | **LP2-OL-10 (Rep. of LP2-OL-5)** | **LP2-OL-11** | **LP2-OL-12** | **LP2-OL-13** | **LP2-OL-14** | **LP2-OL-15** | **LP2-OL-16** | **LP2-OL-17** | **LP2-OL-18** | **LP2-OL-19** | **LP2-OL-20** |
| $Al_2O_3$ | 0.12500 | 0.12500 | 0.06000 | 0.06000 | 0.06000 | 0.06000 | 0.06000 | 0.06000 | 0.06000 | 0.06000 | 0.06000 | 0.06000 |
| $B_2O_3$ | 0.13750 | 0.06000 | 0.13750 | 0.13750 | 0.06000 | 0.13750 | 0.13750 | 0.07474 | 0.06000 | 0.06000 | 0.06000 | 0.06000 |
| CaO | 0.02000 | 0.11000 | 0.07990 | 0.07991 | 0.11000 | 0.07171 | 0.11000 | 0.03050 | 0.04550 | 0.08723 | 0.03345 | 0.08050 |
| Cl | 0.00062 | 0.00467 | 0.00062 | 0.00467 | 0.00467 | 0.00062 | 0.00062 | 0.00062 | 0.00467 | 0.00467 | 0.00062 | 0.00062 |
| $Cr_2O_3$ | 0.00600 | 0.00300 | 0.00300 | 0.00600 | 0.00300 | 0.00600 | 0.00600 | 0.00600 | 0.00300 | 0.00600 | 0.00300 | 0.00300 |
| $Cs_2O$ | 0.00000 | 0.00000 | 0.00000 | 0.00000 | 0.00000 | 0.00000 | 0.00000 | 0.00000 | 0.00000 | 0.00000 | 0.00000 | 0.00000 |
| F | 0.00095 | 0.00708 | 0.00095 | 0.00708 | 0.00708 | 0.00095 | 0.00095 | 0.00095 | 0.00708 | 0.00708 | 0.00095 | 0.00095 |
| $Fe_2O_3$ | 0.00000 | 0.01500 | 0.00000 | 0.01500 | 0.00000 | 0.00000 | 0.01500 | 0.01500 | 0.01500 | 0.00000 | 0.01500 | 0.00000 |
| $K_2O$ | 0.00000 | 0.00000 | 0.05750 | 0.00000 | 0.05750 | 0.05750 | 0.00000 | 0.00000 | 0.05750 | 0.00000 | 0.05750 | 0.00000 |
| MgO | 0.00000 | 0.00000 | 0.01350 | 0.01350 | 0.00000 | 0.00000 | 0.00000 | 0.01350 | 0.01350 | 0.01350 | 0.00000 | 0.00000 |
| $Na_2O$ | 0.21000 | 0.21000 | 0.21000 | 0.25941 | 0.22205 | 0.21000 | 0.21000 | 0.21000 | 0.22205 | 0.21000 | 0.21000 | 0.26000 |
| NiO | 0.00000 | 0.00000 | 0.00000 | 0.00000 | 0.00000 | 0.00000 | 0.00000 | 0.00000 | 0.00000 | 0.00000 | 0.00000 | 0.00000 |
| $P_2O_5$ | 0.00203 | 0.01515 | 0.00203 | 0.01515 | 0.01515 | 0.00203 | 0.00203 | 0.00203 | 0.01515 | 0.01515 | 0.00203 | 0.00203 |
| $SiO_2$ | 0.39190 | 0.39080 | 0.34900 | 0.35128 | 0.35405 | 0.34900 | 0.35640 | 0.47000 | 0.37105 | 0.34900 | 0.46499 | 0.46640 |
| $SO_3$ | 0.00100 | 0.00980 | 0.00100 | 0.00100 | 0.00100 | 0.01519 | 0.00100 | 0.01116 | 0.00100 | 0.01137 | 0.00796 | 0.00100 |
| $SnO_2$ | 0.01550 | 0.00000 | 0.00000 | 0.00000 | 0.00000 | 0.00000 | 0.03500 | 0.00000 | 0.03500 | 0.03500 | 0.03500 | 0.00000 |
| $V_2O_5$ | 0.04000 | 0.00000 | 0.00000 | 0.00000 | 0.04000 | 0.04000 | 0.00000 | 0.04000 | 0.04000 | 0.04000 | 0.00000 | 0.00000 |
| ZnO | 0.02000 | 0.02000 | 0.02000 | 0.02000 | 0.03600 | 0.02000 | 0.03600 | 0.03600 | 0.02000 | 0.03600 | 0.02000 | 0.03600 |
| $ZrO_2$ | 0.02950 | 0.02950 | 0.06500 | 0.02950 | 0.02950 | 0.02950 | 0.02950 | 0.02950 | 0.02950 | 0.06500 | 0.02950 | 0.02950 |
| **Total** | 1.00000 | 1.00000 | 1.00000 | 1.00000 | 1.00000 | 1.00000 | 1.00000 | 1.00000 | 1.00000 | 1.00000 | 1.00000 | 1.00000 |

Table 1.3. Targeted Compositions (mass fractions) for the Phase 2 Enhanced LAW Glasses (cont.)

| | Glass ID | | | | |
|---|---|---|---|---|---|
| **Component** | **LP2-OL-21 (Centroid)** | **LP2-OL-22** | **LP2-OL-23** | **LP2-OL-24** | **LP2-OL-25** |
| $Al_2O_3$ | 0.10000 | 0.07000 | 0.06000 | 0.12500 | 0.06000 |
| $B_2O_3$ | 0.09500 | 0.06000 | 0.13725 | 0.06000 | 0.13750 |
| CaO | 0.05000 | 0.11000 | 0.11000 | 0.07245 | 0.02578 |
| Cl | 0.00208 | 0.00062 | 0.00062 | 0.00062 | 0.00062 |
| $Cr_2O_3$ | 0.00450 | 0.00300 | 0.00300 | 0.00300 | 0.00300 |
| $Cs_2O$ | 0.00000 | 0.00000 | 0.00000 | 0.00000 | 0.00000 |
| F | 0.00316 | 0.00095 | 0.00095 | 0.00095 | 0.00095 |
| $Fe_2O_3$ | 0.00600 | 0.01500 | 0.00000 | 0.01500 | 0.01500 |
| $K_2O$ | 0.01000 | 0.00000 | 0.00000 | 0.00000 | 0.00000 |
| MgO | 0.00650 | 0.00000 | 0.01350 | 0.01350 | 0.00000 |
| $Na_2O$ | 0.23000 | 0.21000 | 0.21000 | 0.25195 | 0.26000 |
| NiO | 0.00000 | 0.00000 | 0.00000 | 0.00000 | 0.00000 |
| $P_2O_5$ | 0.00676 | 0.00203 | 0.00203 | 0.00203 | 0.00203 |
| $SiO_2$ | 0.38800 | 0.36740 | 0.34900 | 0.34900 | 0.34900 |
| $SO_3$ | 0.00500 | 0.00100 | 0.01315 | 0.00100 | 0.01012 |
| $SnO_2$ | 0.01500 | 0.03500 | 0.03500 | 0.00000 | 0.03500 |
| $V_2O_5$ | 0.01000 | 0.04000 | 0.00000 | 0.04000 | 0.00000 |
| ZnO | 0.02800 | 0.02000 | 0.03600 | 0.03600 | 0.03600 |
| $ZrO_2$ | 0.04000 | 0.06500 | 0.02950 | 0.02950 | 0.06500 |
| **Total** | 1.00000 | 1.00000 | 1.00000 | 1.00000 | 1.00000 |

Table 1.4. Targeted Compositions (mass fractions) for the Modified Outer-Layer Phase 2 Enhanced LAW Glasses

| | Glass ID | | | |
|---|---|---|---|---|
| **Component** | **LP2-OL-03-MOD2** | **LP2-OL-08-MOD** | **LP2-OL-10-MOD** | **LP2-OL-16-MOD** |
| $Al_2O_3$ | 0.10738 | 0.06121 | 0.12523 | 0.06008 |
| $B_2O_3$ | 0.06107 | 0.06121 | 0.06011 | 0.07483 |
| CaO | 0.10905 | 0.10879 | 0.11020 | 0.03054 |
| Cl | 0.00063 | 0.00063 | 0.00468 | 0.00062 |
| $Cr_2O_3$ | 0.00611 | 0.00612 | 0.00301 | 0.00601 |
| F | 0.00097 | 0.00097 | 0.00709 | 0.00095 |
| $Fe_2O_3$ | 0.00000 | 0.01530 | 0.01503 | 0.01502 |
| $K_2O$ | 0.00000 | 0.00000 | 0.00000 | 0.00000 |
| MgO | 0.01374 | 0.00000 | 0.00000 | 0.01352 |
| $Na_2O$ | 0.26464 | 0.26524 | 0.21038 | 0.21026 |
| $P_2O_5$ | 0.00207 | 0.00207 | 0.01518 | 0.00203 |
| $SiO_2$ | 0.35523 | 0.35604 | 0.39151 | 0.47059 |
| $SO_3$ | 0.00754 | 0.00816 | 0.00800 | 0.00992 |
| $SnO_2$ | 0.02779 | 0.00000 | 0.00000 | 0.00000 |
| $V_2O_5$ | 0.00000 | 0.04081 | 0.00000 | 0.04005 |
| ZnO | 0.02036 | 0.02040 | 0.02004 | 0.03605 |
| $ZrO_2$ | 0.02342 | 0.05305 | 0.02955 | 0.02954 |
| **Total** | 1.00000 | 1.00000 | 1.00000 | 1.00000 |

## 1.3 Quality Assurance

### 1.3.1 PNNL QA Program

The PNNL Quality Assurance (QA) Program is based upon the requirements as defined in the DOE Order 414.1D, *Quality Assurance*, and 10 CFR 830, *Energy/Nuclear Safety Management*, Subpart A, *Quality Assurance Requirements* (a.k.a., the Quality Rule). PNNL has chosen to implement the following consensus standards in a graded approach:

- ASME NQA-1-2000, *Quality Assurance Requirements for Nuclear Facility Applications*, Part I, "Requirements for Quality Assurance Programs for Nuclear Facilities"
- ASME NQA-1-2000, Part II, Subpart 2.7, "Quality Assurance Requirements for Computer Software for Nuclear Facility Applications", including problem reporting and corrective action
- ASME NQA-1-2000, Part IV, Subpart 4.2, "Guidance on Graded Application of Quality Assurance (QA) for Nuclear-Related Research and Development."

The PNNL *Quality Assurance Program Description/Quality Management M&O Program Description* describes the Laboratory-level QA program that applies to all work performed by PNNL. Laboratory-level procedures for implementing the QA requirements described in the standards identified above are deployed through PNNL's web-based "How Do I…?" (HDI) system, a standards-based system for managing and deploying requirements and procedures to PNNL staff. The HDI procedures (called Workflows and Work Controls) provide detailed guidance for performing tasks, such as protecting classified information and procuring items and services, as well as general guidelines for performing research-related tasks, such as preparing and reviewing calculations and calibrating and controlling measuring and test equipment.

### 1.3.2 ORP Glass Support Work QA Program

The ORP Glass Support Work project is performed under the PNNL nuclear quality assurance program (NQAP); this program establishes an ASME NQA-1-2012, 10 CFR 830, Subpart A DOE Order (O) 414.1D compliant QA program for use by research and development (R&D) projects and programs that are compatible with the editions of ASME NQA-1 2000 through 2012.

The work of this report was performed to the QA level of applied research:

> *Applied research work activities (or deliverables) apply to nuclear and non-nuclear R&D (work activities or deliverables) that are processes initiated-with-the-intent of solving a specific problem or meeting a practical need. For applied research activities, grading is minimal and largely contingent upon the complexity of the research and the ability to duplicate the research if data were lost. The elements of QA grading, including the level of documentation, were applied to the program-, project-, and task-levels.*

# 2.0 Test Methods

This section describes how the data were obtained for the 41 enhanced LAW glasses described in Section 1.0. The descriptions include the methods for 1) glass fabrication, 2) needed composition modification 3) chemical composition analysis, 4) density determination, 5) viscosity measurement, 6) electrical conductivity (EC) measurement, 7) crystal fraction (CF) determination, 8) secondary phase identification from canister centerline cooling (CCC), 9) PCT response, 10) VHT response, and 11) sulfate solubility measurement.

## 2.1 Glass Fabrication

Glass fabrication was performed according to the PNNL procedure, *Glass Batching and Melting* (WFDL-GBM-1, Rev 2).[1] Single metal oxides, single metal carbonates, and sodium salts were weighed out in the appropriate masses to form the target glass composition for each glass and then placed in a plastic bag. After thoroughly mixing in the plastic bag for at least 30 s until uniform color developed, the powders were transferred into an agate milling chamber and milled for 2 min in the Angstrom vibratory mill. The powders were then transferred to a clean Pt-10%Rh crucible for melting using a two-step melt process. The first melt was of the raw materials after mixing in the agate milling chamber. Initial melting was performed at a temperature of 1150 °C for 1 h to 1.8 h for the compositions to melt and form macroscopically homogenous glasses. A second melt of the glass was accomplished after the first melt was quenched and the glass was ground to a fine powder in a tungsten carbide vibratory mill. Some glasses required a third melt or more to be performed. Generally, the second melt and subsequent melts were at the same temperature, or 25 °C to 100 °C higher, than the initial melt, and 1 h to 2.3 h in duration. See Table 2.1 for specific melt times and temperatures used for each glass.

Four of the matrix glasses required a melt temperature of 1200 °C, with one glass requiring a melt temperature of 1250 °C. In addition, 18 of the glasses required more than two iterations of grinding and melting to fully dissolve all the starting materials and adequately melt the glasses. Using a higher melting temperature is deemed to be an acceptable method of fabricating challenging glass compositions. The laboratory crucible-scale fabrication of glasses is not intended to mimic the actual melter process or feed processing. Rather, it is intended to fabricate a glass sample with a controlled composition for property testing. Composition is the primary variable in determining glass properties. The other primary impact of temperature history of glass melts is the impact on phase assemblage. Both liquid and crystalline phase separation may occur in some glasses. The impacts of thermal history on phase assemblage is measured for test glasses by systematic isothermal heat treatments at a range of temperatures and the CCC heat treatments bounding the anticipated behavior in the plant.

The morphology and color of each quenched glass is shown in Appendix A.

(1) Russell, RL. 2016. *Glass Batching and Melting.* WFDL-GBM-1, Rev. 2.

Table 2.1. Melting Temperatures and Times Used in Fabricating the Phase 2 Enhanced LAW Waste Glasses

| | First Melt | | | Second and More Melts | | |
|---|---|---|---|---|---|---|
| Glass ID | Date | Temp. (°C) | Time (h) | Date | Temp. (°C) | Time (h) |
| LP2-IL-01 | 1/12/17 | 1150 | 1 | 1/13/17, 1/20/17 | 1150, 1175 | 1.5, 1 |
| LP2-IL-02 | 1/11/17 | 1150 | 1 | 1/12/17, 1/13/17, 1/16/17, 1/17/17 | 1150, 1150, 1150, 1150 | 1.5, 0.5, 0.5, 0.33 |
| LP2-IL-03 | 1/20/17 | 1150 | 1 | 1/24/17 | 1150 | 1.5 |
| LP2-IL-04 | 1/23/17 | 1150 | 1 | 1/23/17 | 1150 | 2.3 |
| LP2-IL-05 | 1/26/17 | 1150 | 1 | 1/27/17 | 1150 | 1.5 |
| LP2-IL-06 | 2/20/17 | 1175 | 1 | 2/22/17, 2/27/17, 3/3/17 | 1175, 1175, 1175 | 2, 1, 1 |
| LP2-IL-07 | 1/26/17 | 1150 | 1 | 1/27/17 | 1150 | 1 |
| LP2-IL-08 | 2/27/17 | 1150 | 1 | 2/28/17, 3/3/17, 3/3/17 | 1175, 1175, 1200 | 1.5, 1, 1 |
| LP2-IL-09 | 1/30/17 | 1150 | 1 | 1/31/17, 2/2/17 | 1150, 1175 | 1.75, 1 |
| LP2-IL-10 | 2/3/17 | 1150 | 1 | 2/6/17, 2/10/17 | 1150, 1175 | 1, 1.5 |
| LP2-IL-11 | 2/10/17 | 1150 | 1 | 2/13/17, 2/14/17 | 1150, 1175 | 1.5, 1 |
| LP2-IL-12 | 2/16/17 | 1150 | 1 | 2/16/17, 2/17/17 | 1150, 1175 | 1.5, 1 |
| LP2-IL-13 | 2/16/17 | 1150 | 1 | 2/17/17 | 1150 | 1.5 |
| LP2-IL-14 | 2/20/17 | 1150 | 1 | 2/21/17, 2/22/17 | 1150, 1150 | 1.5, 0.75 |
| LP2-IL-15 | 2/21/17 | 1150 | 1 | 2/23/17, 2/23/17 | 1150, 1150 | 1.5, 1 |
| LP2-IL-16 | 3/3/17 | 1150 | 1 | 3/3/17, 3/4/17 | 1175, 1175 | 1.5, 0.75 |
| LP2-IL-17 | 2/24/17 | 1150 | 1 | 2/24/17 | 1150 | 1.5 |
| LP2-OL-01-3 | 10/31/17 | 1150 | 1.5 | 11/1/17 | 1150 | NR |
| LP2-OL-02-1 | 11/8/17 | 1150 | 1.5 | 11/8/17 | 1150 | 1.33 |
| LP2-OL-03-MOD2 | 3/5/18 | 1150 | 1.7 | 3/6/18, 3/1/18 | 1150, 1200 | 1.5, 1.3 |
| LP2-OL-04-1 | 11/2/17 | 1150 | 1.6 | 11/6/17 | 1150 | 1.5 |
| LP2-OL-05 | 10/23/17 | 1150 | 1.5 | 10/24/17, 10/26/17 | 1150, 1150 | 1.5, 1.5 |
| LP2-OL-07-1 | 11/14/17 | 1150 | 1.5 | 11/14/17 | 1150 | NR |
| LP2-OL-08-MOD | 2/26/18 | 1150 | 1.6 | 2/27/18 | 1150 | 1.4 |
| LP2-OL-09-1 | 11/20/17 | 1150 | 1.5 | 11/20/17 | 1150 | 1.5 |
| LP2-OL-10-MOD | 2/22/18 | 1150 | 1.5 | 2/26/18, 2/27/18 | 1150, 1150 | 1.5, 1.6 |
| LP2-OL-11 | 11/21/17 | 1150 | 1.4 | 11/21/17 | 1150 | 1.6 |
| LP2-OL-12 | 11/22/17 | 1150 | 1.5 | 11/27/17 | 1150 | 1.5 |
| LP2-OL-13 | 11/27/17 | 1150 | 1.5 | 11/28/17 | 1150 | 1.7 |
| LP2-OL-14 | 11/28/17 | 1150 | 1.5 | 11/29/17 | 1150 | 1.5 |
| LP2-OL-15 | 11/29/17 | 1150 | 1.5 | 11/30/17 | 1150 | 1.5 |
| LP2-OL-16-MOD | 2/20/18 | 1150 | 1.5 | 2/20/18, 2/21/18 | 1150, 1200 | 1.5, 2 |
| LP2-OL-17 | 12/4/17 | 1150 | 1.8 | 12/5/17 | 1150 | 1.5 |
| LP2-OL-18 | 12/5/17 | 1150 | 1.5 | 12/5/17, 12/28/17 | 1150, 1250 | 1.3, 1.6 |
| LP2-OL-19 | 12/8/17 | 1150 | 1.5 | 12/11/17 | 1150 | 1.5 |
| LP2-OL-20 | 12/11/17 | 1150 | 1.5 | 12/12/17 | 1150 | 1.5 |
| LP2-OL-21 | 12/12/17 | 1150 | 1.5 | 12/14/17 | 1150 | 1.4 |
| LP2-OL-22 | 12/14/17 | 1150 | 1.6 | 12/17/17, 12/21/17 | 1150, 1150 | 1.4, 1.5 |
| LP2-OL-23 | 12/18/17 | 1150 | 1.4 | 12/18/17 | 1150 | 1.5 |
| LP2-OL-24 | 12/17/17 | 1150 | 1.6 | 12/19/17, 12/28/17 | 1150, 1200 | 1.5, 1.7 |
| LP2-OL-25 | 12/20/17 | 1150 | 1.5 | 12/20/17 | 1150 | 1.4 |

NR = not recorded

## 2.2 Matrix Glasses Needing Composition Modification

Five outer-layer matrix glasses needed some modification to their compositions to form homogeneous glasses. Modifications to these glasses are discussed in detail in the following sections.

### 2.2.1 LP2-OL-03

The original composition of the LP2-OL-03 glass had salt segregation on the glass surface and around the crucible edges (see Figure 2.1) following the third melt at 1150 °C for 95 min. Iterations of composition modifications made to this glass are shown in Table 2.2 with the changes in boldface.

The first modification of the LP2-OL-03 glass decreased the $SO_3$ by ~15 % (from 0.01076 to 0.01058 mf) and renormalized the composition. This modified composition was melted five times. The first three times it was melted at 1150 °C for 90 min each. The next two times it was melted at 1200 °C for 120 min and 30 min, respectively. The first three melts all showed undissolved particles and sulfur on the crucible walls, as shown in Figure 2.2 and Figure 2.3. By the fourth melt, the undissolved particles were gone, but sulfur was still being deposited on the crucible walls. After the last melt, there also appeared to be phase separation, as the glass touching the pour plate was transparent, but the top part of the glass was cloudy (see Figure 2.4).

Table 2.2. Composition Modifications Made to Glass LP2-OL-03

| | Glass Oxide Fraction | | |
|---|---|---|---|
| **Component** | **Original** | **1st Mod** | **2nd Mod and Final** |
| $SiO_2$ | 0.34900 | 0.34906 | 0.35523 |
| $Al_2O_3$ | 0.10550 | 0.10552 | 0.10738 |
| $B_2O_3$ | 0.06000 | 0.06001 | 0.06107 |
| $Na_2O$ | 0.26000 | 0.26005 | 0.26464 |
| $Fe_2O_3$ | 0.00000 | 0.00000 | 0.00000 |
| CaO | 0.10714 | 0.10716 | 0.10905 |
| $SnO_2$ | 0.03500 | 0.03501 | **0.02779** |
| ZnO | 0.02000 | 0.02000 | 0.02036 |
| $ZrO_2$ | 0.02950 | 0.02951 | **0.02342** |
| $V_2O_5$ | 0.00000 | 0.00000 | 0.00000 |
| Cl | 0.00062 | 0.00062 | 0.00063 |
| $Cr_2O_3$ | 0.00600 | 0.00600 | 0.00611 |
| $K_2O$ | 0.00000 | 0.00000 | 0.00000 |
| MgO | 0.01350 | 0.01350 | 0.01374 |
| $P_2O_5$ | 0.00203 | 0.00203 | 0.00207 |
| F | 0.00095 | 0.00095 | 0.00097 |
| $SO_3$ | 0.01076 | **0.01058** | **0.00754** |
| Sum | 1.00000 | 1.00000 | 1.00000 |
| Melt Temp (°C) | 1150/1150/1150 | 1150/1150/1150/**1200/1200** | 1150/1150 |
| Melt Time (min) | 90/95/95 | 90/90/90/**120/30** | 102/90 |

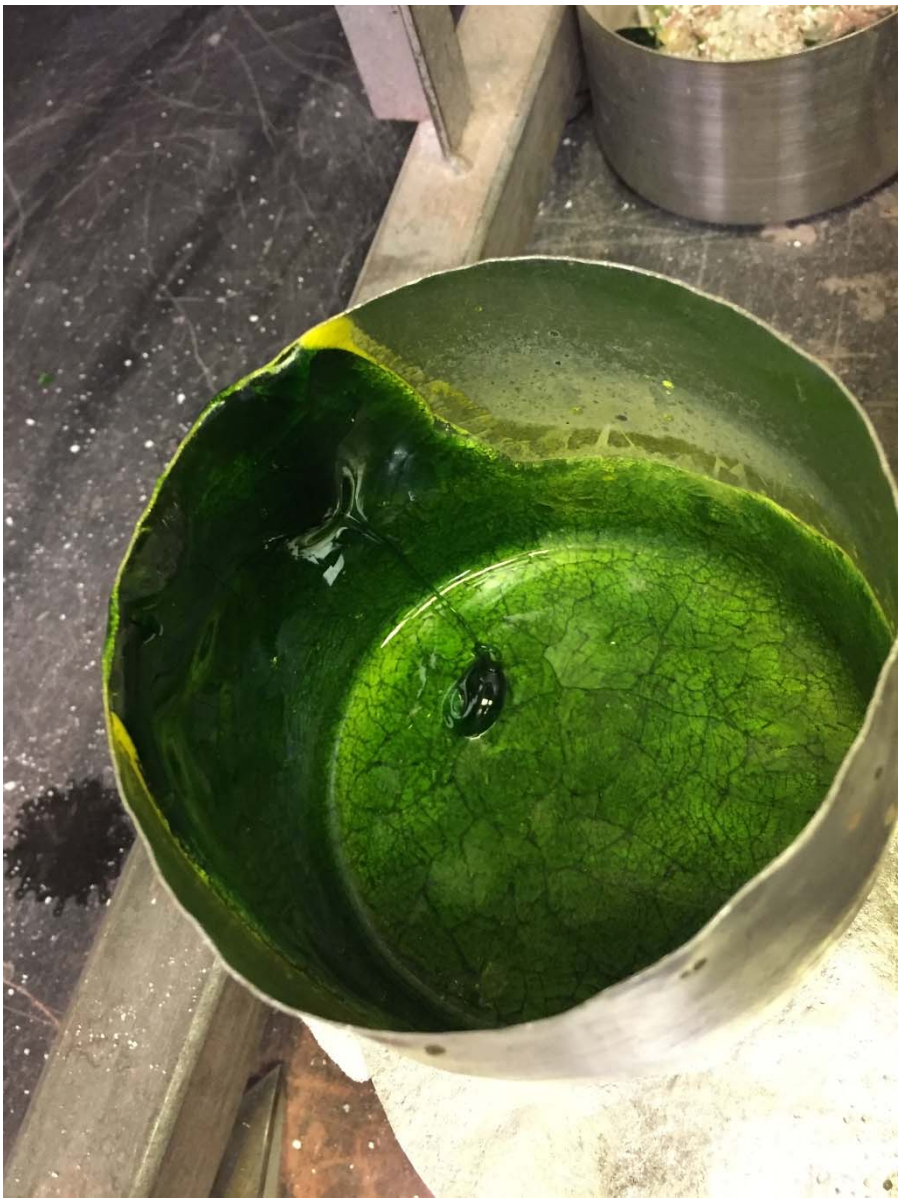

Figure 2.1. Glass LP2-OL-03 Original Composition

Figure 2.2. Glass LP2-OL-03 First Modified Composition after First Melt

Figure 2.3. Glass LP2-OL-03 First Modified Composition after Third Melt

Figure 2.4. Glass LP2-OL-03 First Modified Composition after Final Melt

Due to the appearance of a phase separation, the glass composition was modified again. The second modification of the LP2-OL-03 glass composition decreased the $SO_3$ by 30 % (from 0.01508 to 0.00754 mf) as well as decreasing the $SnO_2$ and $ZrO_2$ together by ~22 % (from 0.03501 to 0.02779 mf for $SnO_2$ and from 0.02951 to 0.02342 mf for $ZrO_2$) based on the first modification. The entire composition was then renormalized to a sum of 1.00000 and is shown in Table 2.2. After the first melt of this modified composition at 1150 °C for 102 min, a few big undissolved particles were observed, but there was no sulfur on the edges. After a second melt at the same temperature for 90 min, the glass was transparent with no sulfur or undissolved particles present. Therefore, it was decided that this would be the final composition, which would be characterized.

### 2.2.2 LP2-OL-06

The original composition of the LP2-OL-06 glass had salt segregation and undissolved particles following the third melt at 1150 °C for 95 min (see Figure 2.5). Iterations of composition modifications made to this glass are shown in Table 2.3 with the changes in boldface.

For the first modification, the $SO_3$ was reduced by 11 % (from 0.00880 to 0.00787 mf) and the composition was renormalized, as shown in Table 2.3. After three melts at 1150 °C for 90 min each, the glass was still opaque, with evidence of sulfur and undissolved particles (see Figure 2.6). Due to the evidence of sulfur and undissolved particles, another modification was performed.

For the second modification, the $SO_3$ was reduced by 20 % (from 0.00787 to 0.00612 mf) from the first modified value and the $P_2O_5$ was reduced by 50 % from the original value (from 0.01515 to 0.00765 mf). Then, the composition was renormalized and is shown in Table 2.3. After two melts at 1150 °C for 90 min each, there was still a large amount of undissolved particles and sulfur on the surface of the glass (see Figure 2.7).

Table 2.3. Composition Modifications Made to Glass LP2-OL-06

| | Glass Oxide Fraction | | | |
|---|---|---|---|---|
| **Component** | **Original** | **1st Mod** | **2nd Mod** | **3rd Mod** |
| $SiO_2$ | 0.34900 | 0.34933 | 0.35264 | 0.35551 |
| $Al_2O_3$ | 0.12500 | 0.12512 | 0.12630 | 0.12733 |
| $B_2O_3$ | 0.06000 | 0.06006 | 0.06063 | 0.06112 |
| $Na_2O$ | 0.21000 | 0.21020 | 0.21219 | 0.21392 |
| $Fe_2O_3$ | 0.00000 | 0.00000 | 0.00000 | 0.00000 |
| CaO | 0.09130 | 0.09138 | 0.09225 | 0.09300 |
| $SnO_2$ | 0.00000 | 0.00000 | 0.00000 | 0.00000 |
| ZnO | 0.03600 | 0.03603 | 0.03638 | 0.03667 |
| $ZrO_2$ | 0.02950 | 0.02953 | 0.02981 | **0.02344** |
| $V_2O_5$ | 0.00000 | 0.00000 | 0.00000 | 0.00000 |
| Cl | 0.00467 | 0.00467 | 0.00472 | 0.00476 |
| $Cr_2O_3$ | 0.00600 | 0.00601 | 0.00606 | 0.00611 |
| $K_2O$ | 0.05750 | 0.05755 | 0.05810 | 0.05857 |
| MgO | 0.00000 | 0.00000 | 0.00000 | 0.00000 |
| $P_2O_5$ | 0.01515 | 0.01516 | **0.00765** | **0.00772** |
| F | 0.00708 | 0.00709 | 0.00715 | 0.00721 |
| $SO_3$ | 0.00880 | **0.00787** | **0.00612** | **0.00463** |
| Sum | 1.00000 | 1.00000 | 1.00000 | 0.99999 |
| Melt Temp (°C) | 1150/1150/1150 | 1150/1150/1150 | 1150/1150 | 1150/1150/1150 |
| Melt Time (min) | 90/90/95 | 91/91/100 | 90/110 | 90/90/90 |

Figure 2.5. Glass LP2-OL-06 Original Composition

Figure 2.6. Glass LP2-OL-06 First Modification

Figure 2.7. Glass LP2-OL-06 Second Modification

For the third modification, the $SO_3$ was reduced another 25 % from the second modification (from 0.00612 to 0.00463 mf), the $ZrO_2$ was reduced 21 % (from 0.02981 to 0.02344 mf), and the $P_2O_5$ was kept at the level of the second modification. The composition was then renormalized, as shown in Table 2.3. Although the number of undissolved particles appeared to decrease after three melts at 1150 °C for 90 min each, there still appeared to be streaks of sulfur present with a slightly opaque glass (see Figure 2.8). Therefore, it was decided to eliminate this glass from further testing.

Figure 2.8. Glass LP2-OL-06 Third Modification

### 2.2.3 LP2-OL-08

When melted at 1150 °C for 90 min, the original composition of LP2-OL-08 formed clear glass on the bottom, but crystals formed upon cooling in the rest of the glass (causing it to be very opaque, Figure 2.9). An XRD analysis found the crystals to be sodium sulfate (Figure 2.10). Iterations of composition modifications made to this glass are shown in Table 2.4 with the changes in boldface.

For the first modification, shown in Table 2.4, the $SO_3$ was decreased by 45 % (from 0.01476 to 0.00816 mf) and the $ZrO_2$ was decreased by 20 % (from 0.06500 to 0.05305 mf). Then, the composition with modified values was renormalized. The batch was melted at 1150 °C for ~90 min twice, and then the temperature was increased to 1200 °C for ~80 min due to the presence of undissolved particles. Raising the temperature of the melt resulted in a smooth and shiny glass (Figure 2.11), so the modified and renormalized composition was determined to be final.

Table 2.4. Composition Modifications Made to Glass LP2-OL-08

| | Glass Oxide Mass Fractions | |
|---|---|---|
| **Component** | **Original** | **1st Mod and Final** |
| $SiO_2$ | 0.34900 | 0.35604 |
| $Al_2O_3$ | 0.06000 | 0.06121 |
| $B_2O_3$ | 0.06000 | 0.06121 |
| $Na_2O$ | 0.26000 | 0.26524 |
| $Fe_2O_3$ | 0.01500 | 0.01530 |
| CaO | 0.10664 | 0.10879 |
| $SnO_2$ | 0.00000 | 0.00000 |
| $V_2O_5$ | 0.04000 | 0.04081 |
| ZnO | 0.02000 | 0.02040 |
| $ZrO_2$ | 0.06500 | **0.05305** |
| Cl | 0.00062 | 0.00063 |
| $Cr_2O_3$ | 0.00600 | 0.00612 |
| $K_2O$ | 0.00000 | 0.00000 |
| MgO | 0.00000 | 0.00000 |
| $P_2O_5$ | 0.00203 | 0.00207 |
| F | 0.00095 | 0.00097 |
| $SO_3$ | 0.01476 | **0.00816** |
| Sum | 1.00000 | 1.00000 |
| Melt Temp (°C) | 1150/1150 | 1150/1150/**1200** |
| Melt Time (min) | 90/90 | 91/82/79 |

Figure 2.9. Glass LP2-OL-08 Original Composition

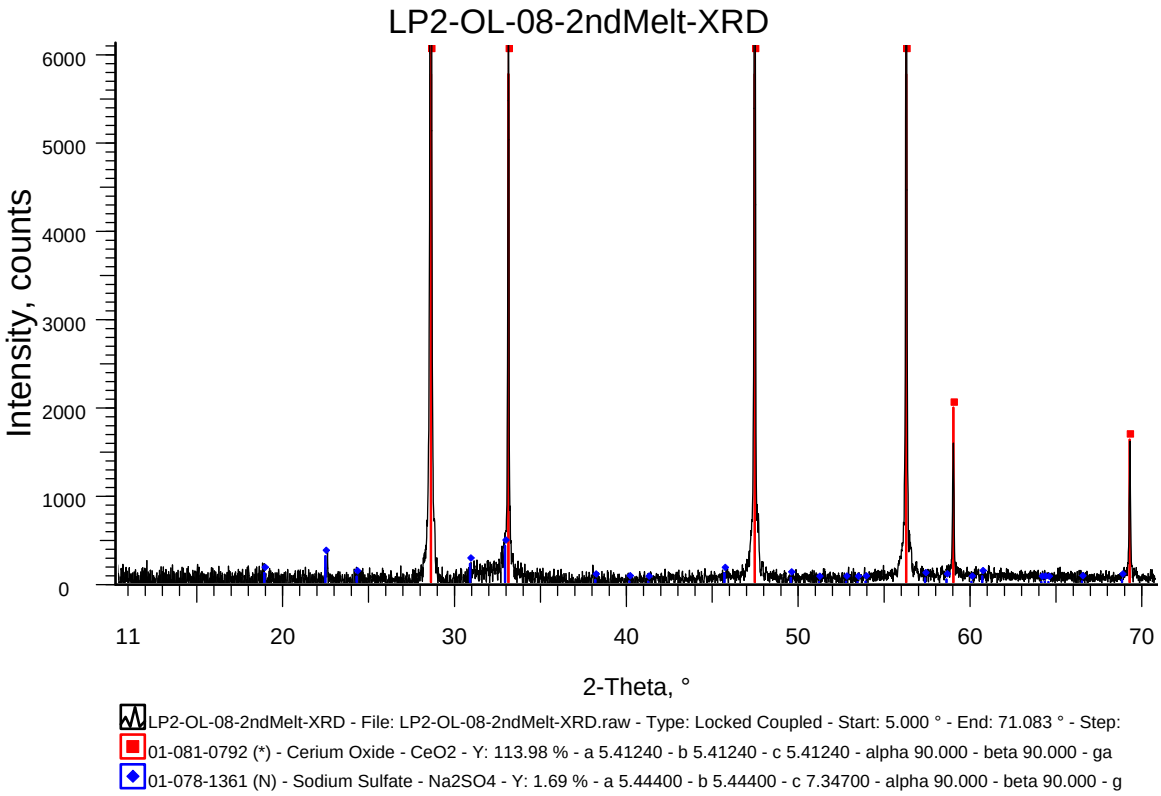


Figure 2.10. XRD Pattern of Original LP2-OL-08 Composition

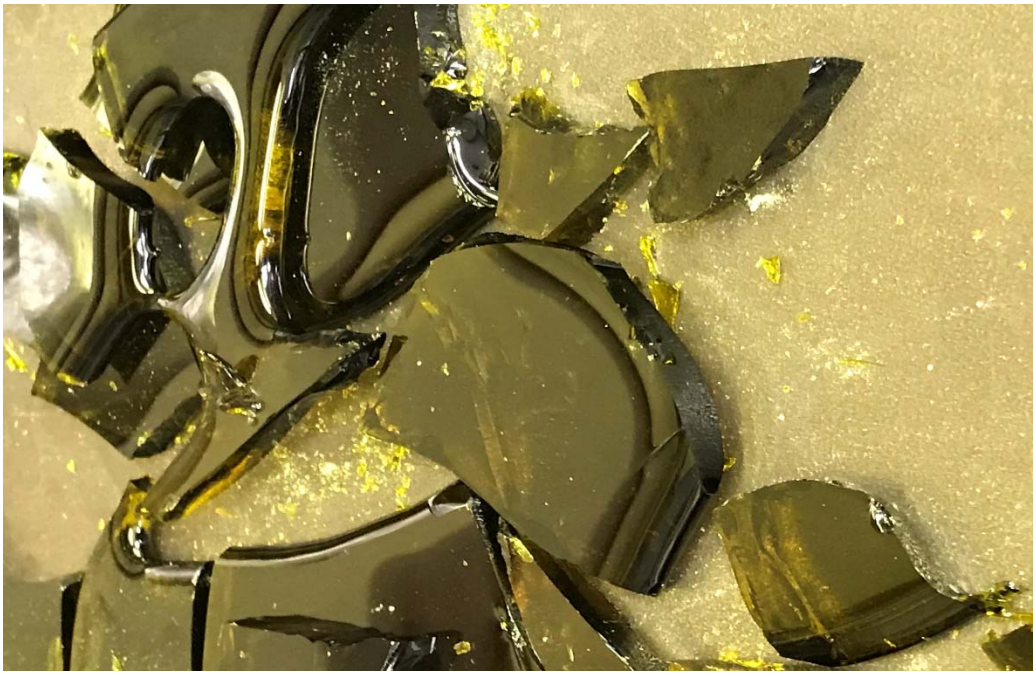

Figure 2.11. Glass LP2-OL-08 after First Modification

### 2.2.4 LP2-OL-10

When melted three times at 1150 °C for 90 min, the original composition of LP2-OL-10 formed an opaque glass with a slight amount of sulfate salt, as shown in Figure 2.12. Iterations of composition modifications made to this glass are shown in Table 2.5 with the changes in boldface.

For the first modification, the $SO_3$ was reduced by 20 % (from 0.00980 to 0.00800 mf) and the modified composition was renormalized. The batch was melted at 1150 °C three times. This composition resulted in a smooth and shiny glass (Figure 2.13), and therefore was determined to be the final composition.

Table 2.5. Composition Modifications Made to Glass LP2-OL-10

| | Glass Oxide Mass Fractions | |
|---|---|---|
| **Component** | **Original** | **1st Mod and Final** |
| $SiO_2$ | 0.39080 | 0.39151 |
| $Al_2O_3$ | 0.12500 | 0.12523 |
| $B_2O_3$ | 0.06000 | 0.06011 |
| $Na_2O$ | 0.21000 | 0.21038 |
| $Fe_2O_3$ | 0.01500 | 0.01503 |
| CaO | 0.11000 | 0.11020 |
| $SnO_2$ | 0.00000 | 0.00000 |
| $V_2O_5$ | 0.00000 | 0.00000 |
| ZnO | 0.02000 | 0.02004 |
| $ZrO_2$ | 0.02950 | 0.02955 |
| Cl | 0.00467 | 0.00468 |
| $Cr_2O_3$ | 0.00300 | 0.00301 |
| $K_2O$ | 0.00000 | 0.00000 |
| MgO | 0.00000 | 0.00000 |
| $P_2O_5$ | 0.01515 | 0.01518 |
| F | 0.00708 | 0.00709 |
| $SO_3$ | 0.00980 | **0.00800** |
| Sum | 1.00000 | 1.00001 |
| Melt Temp (°C) | 1150/1150/1150 | 1150/1150/1150 |
| Melt Time (min) | 90/90/95 | 90/150/34 |

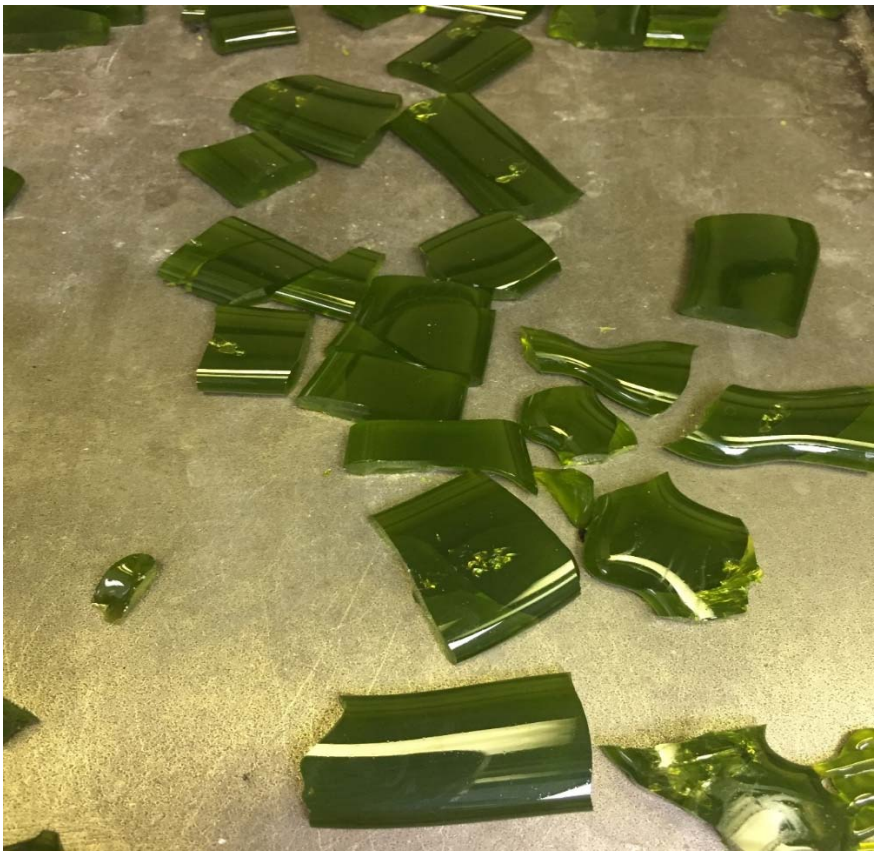

Figure 2.12. Glass LP2-OL-10 Original Composition

Figure 2.13. Glass LP2-OL-10 after First Modification

### 2.2.5 LP2-OL-16

When melted twice at 1150 °C for 90 min, the original composition of the LP2-OL-16 formed an opaque glass with a small amount of sulfate salt present, as shown in Figure 2.14. Iterations of composition modifications made to this glass are shown in Table 2.6 with the changes in bold face.

For the first modification, the $SO_3$ was reduced by 11 % (from 0.01116 to 0.00992 mf) and the modified composition was renormalized. The batch was melted at 1150 °C twice for 90 min each, and then the temperature was increased to 1200 °C for 120 min due to the presence of undissolved particles. Raising the temperature of the melt resulted in a smooth and shiny glass (Figure 2.15), and therefore was determined to be the final composition.

Table 2.6. Composition Modifications Made to Glass LP2-OL-16

| | Glass Oxide Mass Fractions | |
|---|---|---|
| **Component** | **Original** | **1st Mod and Final** |
| $SiO_2$ | 0.47000 | 0.47059 |
| $Al_2O_3$ | 0.06000 | 0.06008 |
| $B_2O_3$ | 0.07474 | 0.07483 |
| $Na_2O$ | 0.21000 | 0.21026 |
| $Fe_2O_3$ | 0.01500 | 0.01502 |
| CaO | 0.03050 | 0.03054 |
| $SnO_2$ | 0.00000 | 0.00000 |
| $V_2O_5$ | 0.04000 | 0.04005 |
| ZnO | 0.03600 | 0.03605 |
| $ZrO_2$ | 0.02950 | 0.02954 |
| Cl | 0.00062 | 0.00062 |
| $Cr_2O_3$ | 0.00600 | 0.00601 |
| $K_2O$ | 0.00000 | 0.00000 |
| MgO | 0.01350 | 0.01352 |
| $P_2O_5$ | 0.00203 | 0.00203 |
| F | 0.00095 | 0.00095 |
| $SO_3$ | 0.01116 | **0.00992** |
| Sum | 1.00000 | 1.00001 |
| Melt Temp (°C) | 1150/1150 | 1150/1150/**1200** |
| Melt Time (min) | 85/100 | 90/87/**120** |

Figure 2.14. Glass LP2-OL-16 Original Composition

Figure 2.15. Glass LP2-OL-16 after First Modification

## 2.3 Chemical Analysis of Glass Composition

To confirm that the "as-fabricated" glasses corresponded to the specified target compositions, a representative sample of each glass was chemically analyzed at the Savannah River National Laboratory (SRNL) Process Science Analytical Laboratory (PSAL). Three preparation techniques, including sodium peroxide fusion (PF), lithium metaborate/tetraborate fusion (LM), and potassium hydroxide digestion (KH), were used to prepare duplicate glass samples for analysis.

Each of the six preparations (two duplicate glass samples for each for the three preparation techniques) was analyzed twice by inductively coupled plasma-atomic emission spectroscopy (ICP-AES). All elements of interest and appropriate for a given preparation method were determined for each analysis. The duplicate samples were analyzed twice resulting in four measurements of each element. These measurements were then averaged, and the average value was reported. Glass composition standards were also intermittently prepared and analyzed to assess the performance of the ICP-AES instrument over the course of these analyses. Specifically, several samples of the low-activity reference material (LRM) (Ebert and Wolfe 1999) were included as part of the SRNL-PSAL analytical plan. The anions (Cl and F) were analyzed by ion chromatography (IC) also. The preparation and measurement methods used for each of the reported glass elements are listed in Table 2.7.

A detailed data analysis of the chemical composition measurements is published elsewhere (Fox et al. 2017, 2018). A short summary of these data analyses is included in Section 3.1.

Table 2.7. Preparation and Measurement Methods Used in Reporting the Measured Concentrations of Each of the Elements of the Study Glasses

| Element | Preparation Method | Measurement Method |
|---|---|---|
| Al | PF | ICP-AES |
| B | PF | ICP-AES |
| Ca | LM | ICP-AES |
| Cl | KH | IC |
| Cr | LM | ICP-AES |
| F | KH | IC |
| Fe | PF | ICP-AES |
| K | LM | ICP-AES |
| Li | PF | ICP-AES |
| Mg | LM | ICP-AES |
| Na | LM | ICP-AES |
| P | LM | ICP-AES |
| Si | PF | ICP-AES |
| Sn | PF | ICP-AES |
| S | LM | ICP-AES |
| V | LM | ICP-AES |
| Zn | LM | ICP-AES |
| Zr | LM | ICP-AES |

PF = peroxide fusion
LM = lithium metaborate/tetraborate fusion
KH = potassium hydroxide digestion
ICP-AES = inductively coupled plasma-atomic emission spectrometry
IC = ion chromatography

## 2.4 Glass Density

The room temperature density of each glass was measured according to PNNL procedure, *Density Using a Gas Pycnometer* (EWG-OP-0045),[2] using a MicroMeritics AccuPyc II 1340 gas pycnometer (MicroMeritics, Norcross, GA) with approximately 0.5 g of glass. The glass was loaded into a vial and placed within the instrument. The instrument then determined the density by the difference in amount of helium gas needed to fill the vial with and without the glass present. After five runs for each glass, the average glass density for that glass was calculated. The pycnometer was calibrated before and after measurements for that day using a National Institute of Standards and Technology (NIST) traceable standard tungsten carbide ball. These results are discussed in Section 3.2.

## 2.5 Viscosity

The viscosities (η) of the quenched glasses were measured as a function of temperature, with a fully automated Anton Parr FRS 1600 Furnace Rheometer System, according to the PNNL procedure, *High-Temperature Viscosity Measurement Using Anton Paar FRS1600* (EWG-OP-0046, Rev. 0.0).[3] Approximately 200 g of each glass was first crushed in a tungsten carbide mill for 0.05 min and about 25 to 30 mL, or ~70 g, of glass was placed into a Pt-alloy cylindrical cup. It was then heated to ~1150 °C and maintained until thermal equilibrium was reached. A Pt-alloy spindle was then lowered into the cup of molten glass. An initial torque reading (at a constant spindle speed) was taken at ~1150 °C. Subsequent measurements were taken at both higher and lower temperatures, ranging from 950 °C to 1250 °C, using a hysteresis approach. The hysteresis approach allows for the potential impacts of crystallization (at lower temperatures) to be assessed (via reproducibility). Duplicate measurements were taken at approximately the melting temperature ($T_M$) and volatilization (at higher temperatures) was minimized by measuring viscosity at temperatures above $T_M$ as the final viscosity measurement(s). The temperature sequence used was 1150 °C, 1050 °C, 950 °C, 1150 °C, 1250 °C, and then 1150 °C a third time. The soak time was 30 min at each temperature. Prior to quenched glass viscosity measurements, the test instrumentation was calibrated using a standard glass (Defense Waste Processing Facility (DWPF) Startup Frit) as discussed in the literature (Crum et al. 2012). These results are discussed in Section 3.3.

## 2.6 Electrical Conductivity

The electrical conductivities (ECs) of the quenched glasses were measured with an Anton Parr FRS 1600 Furnace Rheometer System as the high-temperature furnace and a Solartron Analytical 1455 Cell Test System (Solartron Analytical, Oak Ridge, TN) impedance analyzer according to PNNL procedure, *High-Temperature Electrical Conductivity Measurement* (EWG-OP-0047, Rev. 0.0).[4] Platinum plates (1.3 in. long by 0.28 in. wide) were placed parallel to each other with a separation of 0.367 in. A 30-mL glass sample was used for EC measurement in a Pt-alloy crucible. Before measuring ECs of the test matrix glasses, calibration was conducted at room temperature with reference solutions of KCl (0.1 M and 1 M) by measuring the resistance values over a range of frequencies (between 0.1 Hz and 1 MHz). Four readings were taken at each frequency over a period of two to five minutes. The calibration was then checked with DWPF standard glass at the higher temperatures (Crum et al. 2012). The averaged values of the four readings were then used to calculate the cell constant. For glass measurement, the sample was first heated to melting temperature and the probe was slowly lowered into the molten glass to a depth of 12.7-mm. After the temperature was stabilized, a scan from 1 MHz to 0.1 Hz in 3 min was conducted and

(2) Russell RL. 2017. *Density Using a Gas Pycnometer*. EWG-OP-0045, Rev. 0.0.
(3) McCarthy, BM. 2017. *High-Temperature Viscosity Measurement Using Anton Paar FRS1600*. EWG-OP-0046, Rev. 0.0.
(4) McCarthy, BM. 2017. *High-Temperature Electrical Conductivity Measurement*. EWG-OP-0047, Rev. 0.0.

resistance at 1 kHz was used to calculate the EC. Two scans were made for each temperature after the glass was held for 10 min at each temperature before measurement for temperature stabilization. The EC was measured at four different temperatures in a range around the melting temperature of the glass. These results are discussed in Section 3.4.

## 2.7 Equilibrium Crystal Fraction

Equilibrium crystal fraction at a fixed temperature was measured in Pt-alloy crucibles and boats with tight fitting lids (to minimize volatility) according to the ASTM International standard procedure, *Standard Test Method for Determining Liquidus Temperature of Immobilized Waste Glasses and Simulated Waste Glasses* (ASTM C1720). The heat treatment times and temperatures were 24 ± 2 h at 950 °C to ensure equilibrium was achieved without excessive volatility. The samples were then quenched and analyzed by x-ray diffraction (XRD).

The crystal fraction formed during heat treatment was analyzed by XRD according to Section 12.4.4 of the ASTM International standard procedure, *Standard Test Method for Determining Liquidus Temperature of Immobilized Waste Glasses and Simulated Waste Glasses* (ASTM C1720). Powdered glass samples were prepared using 5 wt% $CeO_2$ as an internal standard phase with between 1.5 g and 2.5 g of glass powder. Glass and $CeO_2$ were milled together for 2 min in a 10 $cm^3$ tungsten carbide disc mill. The powdered samples were loaded into XRD sample holders and scanned at a 0.04° 2θ step size, 4 sec dwell time, from 10° to 70° 2θ scan range. XRD spectra were analyzed with TOPAS® 4.2 Software (Bruker AXS Inc., Madison, Wisconsin) for phase identification and Rietveld refinement to semi-quantify the amounts of crystal phases in some samples with high crystalline content. These results are discussed in Section 3.5.

## 2.8 Canister Centerline Cooling (CCC) and Crystal Identification

A portion (~30 g) of each test glass was subjected to the simulated CCC temperature profile shown in Table 2.8 and Figure 2.16. This profile is the temperature schedule of CCC heat-treatment for Hanford LAW glasses planned for use at WTP[5] and modified by PNNL. Pieces of quenched glass, <1cm in diameter, were placed in a Pt-alloy crucible and covered with a Pt-alloy lid. The glass samples were brought to a target temperature of the glass melt temperature and held for 30 min. Then they were quickly cooled to 1114 °C. The cooling profile was then started from 1114 °C to room temperature based on nine cooling segments (see Table 2.3). The starting temperature for the seven segments of cooling are melting temperature, 1114 °C, 1000 °C, 900 °C, 825 °C, 775 °C, 725 °C, 600 °C, and room temperature.

Several of the glasses formed a crystalline layer around the edge of the Pt-alloy crucible during the CCC heat-treatment. Therefore, a quartz crucible was tried in order to eliminate the crystals. However, when a quartz crucible was used, it was found that the glass still formed a layer of crystals around the crucible walls. Therefore, this phenomenon did not appear to be due to the Pt.

(5) Memorandum, Canister Centerline Cooling Data, Revision 1, CCN: 074851, RPP-WTP, October 29, 2003.

Table 2.8. Temperature Schedule During Canister Centerline Cooling (CCC) Treatment of Hanford LAW Glasses

| Segment | Time (min) | Start Temp. (°C) | Rate (°C/min) |
|---|---|---|---|
| 1 | -30 | Melt temp. | 0 |
| 2 | 0 | 1114 | -7.125 |
| 3 | 0-16 | 1000 | -1.754 |
| 4 | 16-73 | 900 | -0.615 |
| 5 | 73-195 | 825 | -0.312 |
| 6 | 195-355 | 775 | -0.175 |
| 7 | 355-640 | 725 | -0.130 |
| 8 | 640-1600 | 600 | -0.095 |
| 9 | 1600-3710 | Room temp. | NA |

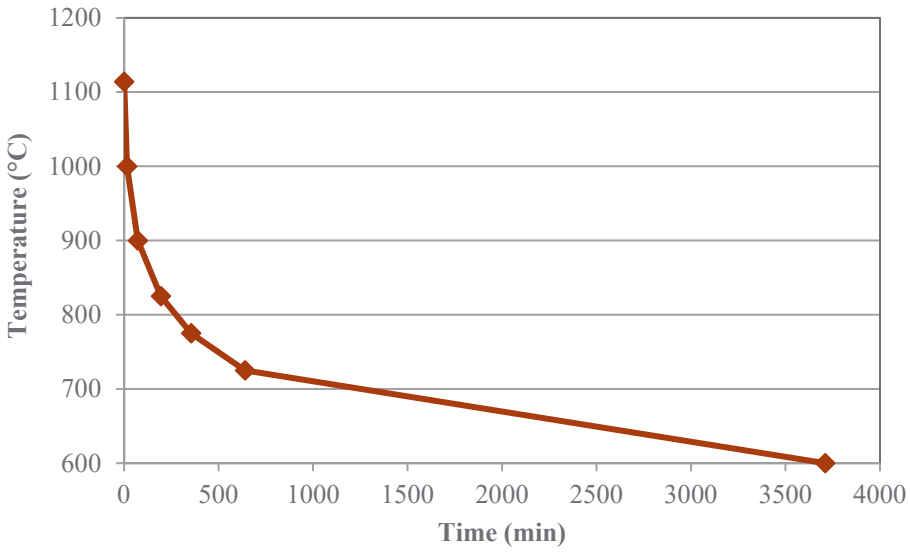


Figure 2.16. Plot of Temperature Schedule During CCC Heat-Treatment of Hanford LAW Glasses

The amount and type of crystalline phases that formed during CCC heat-treatment were analyzed by XRD according to Section 12.4.4 of the ASTM International standard procedure, *Standard Test Method for Determining Liquidus Temperature of Immobilized Waste Glasses and Simulated Waste Glasses* (ASTM C1720). Powdered glass samples were prepared using 5 wt% $CeO_2$ as an internal standard phase with between 1.5 g and 2.5 g of powdered glass. Glass and $CeO_2$ were milled together for 2 min in a 10 $cm^3$ tungsten carbide disc mill. The powdered glass samples were loaded into XRD sample holders and scanned at a 0.04° 2θ step size, 4 sec dwell time, from 10° to 70° 2θ scan range. XRD spectra were analyzed with TOPAS® 4.2 Software (Bruker AXS Inc., Madison, Wisconsin) for phase identification and Rietveld refinement to semi-quantify the amounts of crystal phases in some samples with high crystalline content. These results are discussed in Section 3.6.

## 2.9 Product Consistency Test (PCT)

PCT responses were measured in triplicate at SRNL for quenched and CCC samples of each glass using Method A of the ASTM International standard procedure, *Standard Test Methods for Determining Chemical Durability of Nuclear, Hazardous, and Mixed Waste Glasses and Multiphase Glass Ceramics: The Product Consistency Test (PCT)* (ASTM C1285). Also included in the PCT experimental test matrix and tested in triplicate were the Approved Reference Material (ARM) glass (Mellinger and Daniel 1984) and blanks. Glass samples were ground, sieved to -100 +200 mesh, washed, and prepared according to the ASTM C1285 procedure. The prepared glass was added to deionized water in a 1 g to 10 mL ratio, resulting in a surface area-to-solution volume (S/V) ratio of approximately 2000 $m^{-1}$. The vessels used were desensitized Type 304L stainless steel. The vessels were closed, sealed, and placed into an oven at 90 ± 2 °C for 7 days ± 3 h.

After the seven days at 90 °C, the vessels were removed from the oven and allowed to cool to room temperature. The final mass of the vessel and the solution pH were recorded on a data sheet. Each test solution was then filtered through a 0.45-µm-size filter and acidified with concentrated, high-purity $HNO_3$ to 1 vol% to assure that the cations present remained in solution. The resulting solutions were analyzed by SRNL for Si, Na, B, and Li. Samples of a multi-element, standard solution were also analyzed as a check on the accuracy of the ICP-AES. Normalized releases (g/L) were calculated based on both target and measured compositions using the average of the logarithms of the leachate concentrations. Results from the PCT work are published elsewhere (Fox et al. 2017, 2018), and a short summary of these results is included in Section 3.7.

## 2.10 Vapor Hydration Test (VHT)

In the VHT, monolithic glass samples were exposed to water vapor at 200 °C in sealed stainless-steel vessels according to the ASTM International standard procedure, *Standard Test Method for Measuring Waste Glass or Glass Ceramic Durability by Vapor Hydration Test* (ASTM C1663). Roughly 1-mm by 10-mm by 10-mm samples were cut from annealed or CCC-treated LAW glass bars using a diamond-impregnated saw. All sides of the cut sample were polished to 600-grit surface finishes with silicon carbide paper.

Polished samples were hung from stainless-steel supports on Pt wire within a stainless-steel container (see Figure 2.17). Deionized water (DIW) was added to the bottom of the vessel so that enough water was present to react with the specimen without enough water to reflux during testing (~0.20 g). The samples were heated and held at 200 °C in a convection oven for either 7, 11, or 24 days. All samples were initially tested for 24 days. Samples found to fully react in 24 days were then tested for shorter times to enable estimating a numerical alteration rate (as opposed to > values).

After removal from the oven, vessels were weighed and then quenched in cold water. The specimens were removed from the vessels and cross-sectioned with or without epoxy (depending on the stability of each sample) for analysis by optical microscopy-image analysis (OM-IA) to determine the amount of glass altered during the test.

The remaining glass thickness of the VHT specimen was determined by performing at least 10 measurements distributed (roughly equally) across the crack-free cross section of the sample. Then, the average and standard deviation of the 10 thickness measurements of the remaining glass were calculated. The amount of glass altered per unit surface area of specimen was determined from the average thickness of unaltered glass according to Equation (2.1):

$$m = \frac{1}{2}\rho(d_i - d_r) = \frac{m_i}{2w_i l_i}\left(1 - \frac{d_r}{d_i}\right) \quad (2.1)$$

where $w_i$, $d_i$, $l_i$ = initial width, thickness, and length of the specimen, respectively (m)
$d_r$ = average thickness of remaining glass layer (m)
$m_i$ = initial specimen mass (g)
$m$ = mass of glass converted to alteration products per unit surface area (g/m$^2$)
$\rho$ = glass density (g/m$^2$).

The average rate of corrosion was calculated as $r_a = m/t$, where $t$ is the corrosion time. Vienna et al. (2001) showed that, if the average rate of corrosion at 200°C is

$$r_a = m / t < 50 \text{ g/(m}^2\cdot\text{d)} \quad (2.2)$$

then the final rate of corrosion, $r_\infty < 50$ g/(m$^2$·d), meets the current ORP requirement for LAW glass performance. Although the contract limit for VHT response is stated in rates (50 g/m$^2$/d), the test directly measures alteration depth (D) in µm at different times. In previous studies (Piepel et al. 2007 and Muller et al. 2014), the directly measured parameter of D in µm after 24 days was modeled. This value can be converted to a rate by: D (µm) *10$^{-6}$ (m/µm) *density (g/cm$^3$) *10$^6$ (cm$^3$/m$^3$)/t(d). Assuming a density of 2.65 g/cm$^3$, the limit of 50 g/m$^2$/d is equivalent to a D of 453 µm for a 24-d test duration.

These results are discussed in Section 0.

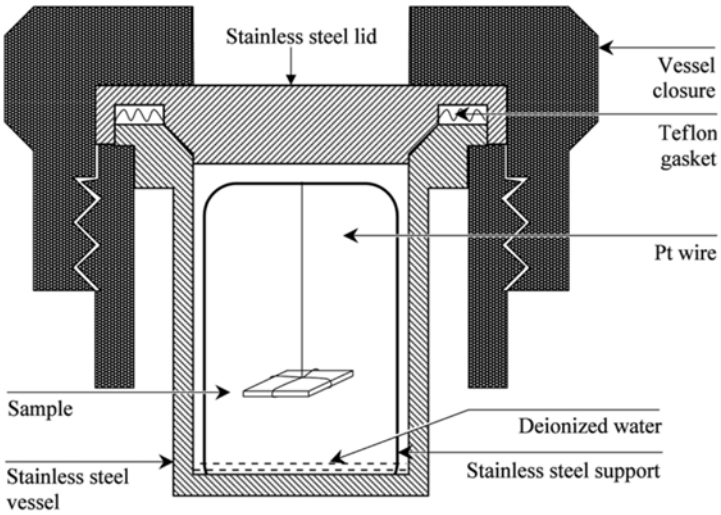


Figure 2.17. Apparatus for Conducting VHTs

## 2.11 Sulfur Solubility

Sulfur solubility was measured on the quenched glass samples. The procedure was developed by PNNL using *Test Instruction for Sulfate Solubility for LAW Phase 1 Matrix Glasses* (EWG-TI-026).[6]

There are three primary phases of testing with each glass:

1. Saturation with sodium sulfate
2. DIW wash
3. Analysis

Saturation with sodium sulfate was performed by taking 50 or 100 g of each LAW matrix glass for melting with sodium sulfate. The baseline glass was ground and sieved through a #120 sieve (125 µm). Then, 7.64 g of $Na_2SO_4$ per 100 g of glass was added to the sieved powdered glass to maintain 4 mol% $SO_3$ in the glass/salt system, and the combination was mixed for homogeneity. The mixture of baseline glass and $Na_2SO_4$ was melted at 1150 °C for 1 h in a Pt-alloy crucible with a tight-fitting lid. After melting, the mixture was poured onto a steel plate and quenched. The mixture was again mixed by crushing and sieving through a #120 sieve (125 µm) and placed back into the Pt-alloy crucible to melt at 1150 °C for 1 h the second time. After the second melting, the mixture was quenched by pouring on a steel plate, mixed by crushing and sieving, and melted under the same conditions for the third time. The glass, after three times re-melting and re-mixing, was crushed and sieved through the #120 sieve (125 µm) sieve.

Each of the melted samples that were ground and sieved three times were then washed with DIW to remove excess salt prior to further analysis. This was done by adding 4 g of glass/salt mixture to a beaker and then adding 50 g of DIW to the beaker. The beaker was placed in an ultrasonic bath for 3 min to wash the glass powder. After washing, the water and glass from the beaker were vacuum filtered through a 0.2 µm polyvinylidene difluoride (PVDF) membrane disc filter installed on a 47-mm magnetic filter funnel. An additional 50 g DIW was used to rinse all of the glass powder from the beaker and the glass powder sample in the filter funnel. A total of 100 g DIW was used for washing one sample. The washed and filtered glass was then dried at 90 °C.

The washed and filtered glasses and the wash solutions recovered from filtering were then analyzed by ICP-AES and IC at SRNL. A total of 18 elements were analyzed. The following 16 elements were analyzed by ICP-AES: Al, B, Ca, Cr, Fe, K, Li, Mg, Na, P, Si, S, Sn, V, Zn, and Zr. The elements Cl and F were analyzed by IC. A detailed data analysis of the sulfur solubility measurements is published elsewhere (Fox et al. 2017, 2018). These results are discussed in Section 3.9.

(6) Jin, T. 2016. *Test Instruction for Sulfate Solubility for LAW Phase 1 Matrix Glasses*. EWG-TI-026.

# 3.0 Results and Discussion

This section describes the test results for the chemical composition, density, viscosity, EC, crystal fraction, secondary phase identification, PCT, VHT, and sulfate solubility for the LAW glasses studied.

As a part of the discussion of the property data for the Phase 2 enhanced LAW glasses, a previously developed property-composition model for each property is used to predict the property values. Often these models are the most recent ones developed prior to collecting the Phase 2 enhanced LAW glass data. In this report, attention is limited to plotting the model-predicted versus measured property values and assessing how well the previous model predicts the measured values for Phase 2 enhanced LAW glasses.

## 3.1 Chemical Analysis of Glass Composition

The targeted and average measured component concentrations (wt%) in the quenched glasses are presented in Appendix B along with the percent differences. The composition analyses of the glass samples were performed as described in Section 2.3. The purpose of these comparisons was to identify whether (i) any Phase 2 enhanced LAW glass(es) was(were) mis-batched, (ii) there was non-negligible volatility in any component(s) during glass melting, or (iii) whether there were any component(s) that was(were) not completely incorporated into the glass melts. The analyzed compositions are not intended for use in modeling glass properties, except for the measured semi-volatile component $SO_3$. Compositions for property modeling will be the measured $SO_3$ concentrations and target compositions renormalized to sum to one minus the measured $SO_3$. This approach was selected due to the relatively high uncertainty in analyzed component concentrations (5 to 20 relative percent) compared to the relatively low uncertainty in chemical additive concentrations (typically 98 to 99% pure) and weighing methods.

The results presented in this section are summarized from the reports by Fox et al. (2017, 2018). The analytical sequences of the measurements were reviewed, the average chemical composition for each glass was determined, and comparisons were made between the measurements and the targeted compositions of the glasses. JMP™ Pro Version 11.2.1 (SAS Institute, Inc.) was used to support these data analyses. Ideally, Fox et al. (2017, 2018) would have used statistical methods for objective comparisons rather than relying on subjective assessment of tables and graphs of data and data summary values. That way differences that were statistically significant could have been detected. However, the data analyses they performed were minimally sufficient for the project needs.

Plots of the wt% glass component concentrations measured for each sample by oxide and analytical block were provided in Fox et al. (2017, 2018). The plots were in analytical sequence within each calibration block, with different symbols and colors being used to represent each of the study and standard glasses. These plots include all the measurement data. Plotting the data in this format provides an opportunity to identify gross trends in performance of the analytical instruments within and among calibration blocks. A review of these plots did not identify any gross patterns or trends in the analytical process over the course of these measurements. Only minor, block-to-block calibration shifts were seen. For example, minor calibration effects were visible between the two sub-blocks within each analytical block for the $Na_2O$ measurements. Minor calibration effects were also visible between the two sub-blocks of Block 1 for the $SnO_2$ measurements. In all cases, the instrument check standards were within specification. These small calibration effects are typical of ICP-AES analyses and are “averaged out” by taking the mean of the measurements for each element.

Plots showing the individual measurements across the duplicates of each preparation method and the two instrument calibrations for each glass were also prepared in Fox et al. (2017, 2018). Plotting the data in this format provides an opportunity to review the values for each individual glass as a function of the duplicate preparations and duplicate measurements. A review of the plots reveals the repeatability of the four individual values for each oxide for each glass. Some degree of scatter among the $Al_2O_3$, $B_2O_3$, $Na_2O$, $SiO_2$, $SnO_2$, and $ZrO_2$ measurements was noted for the study glasses. There were no indications of an error in preparation or measurement that had to be addressed in treatment of the data. Therefore, the entire set of measurement data were used in determining representative, measured compositions for the study glasses.

A comparison of the LRM results to their acceptability limits was performed by SRNL. The review was in the form of plots of the measurements arranged by preparation method and element, framed by upper and lower acceptability limits for the concentration of the element in question. The results show that all the measurements for the elements present in the LRM standard glass were within the acceptability limits utilized by SRNL in conducting instrument and procedure assessments during the execution of these analyses.

The four measurements (duplicates of two glass preparations) for each oxide in each glass were averaged to determine a representative chemical composition for each glass. A sum of oxide wt% values was also computed for each glass based upon the averaged, measured values. The following observations were noted based on these results:

- The measured concentrations of Cl and F were on average ~20% low (compared to targeted values) for most of the study glasses. This is most likely due to volatility during melting.
- The measured concentrations of $P_2O_5$ were below the targeted values for those glasses that targeted higher concentrations of this component (>1 wt %). $ZrO_2$ concentrations were below the targeted values for several of the study glasses. As described in Fox et al. (2018), this appears to be related to the dissolution method used in analysis.
- The measured concentration of $Cr_2O_3$ and $Fe_2O_3$ were on average ~20% above the targeted values for the outer-layer glasses, most likely due to how close the concentrations were to the detection limit.
- There were some deviations in the measured $SiO_2$ concentrations of the outer-layer glasses, both above and below the targeted values of the outer-layer glasses.
- All the sums of measured oxides for the study glasses fell within the interval of 97.8 to 101.7 wt % for the inner-layer glasses and 94.7 to 101.9 wt% for the outer-layer glasses, indicating excellent recovery of the glass components.

Based on the observations above, along with the overall analysis results shown in Appendix B, it was determined that analyzed glass compositions are subject to biased analyses and volatility. Hence, analyzed glass compositions are useful only for assessing if (i) glasses were correctly batched according to their targeted compositions, and (ii) if any components were subject to non-negligible volatility during melting. It was concluded by SRNL that the glasses had been batched correctly and there were no components subject to non-negligible volatility. However, as anticipated, the targeted concentrations of $SO_3$ were not always incorporated into the Phase 2 enhanced LAW glasses.

Hence, it was decided that the targeted values of components (except for $SO_3$ for which measured values were used) were best used in the subsequent calculations. Specifically, the Phase 2 enhanced LAW glass compositions were obtained by normalizing the targeted compositions with the measured $SO_3$ value used instead of the targeted value. Also, target values of B and Na were used to calculate normalized PCT releases of those components.

## 3.2 Density

This section presents and discusses the results of the glass density measurements for the Phase 2 enhanced LAW glasses obtained using the methods discussed in Section 2.4. The prediction of glass density uses a distinctly different process than the other properties. Specifically, specific or molar volumes of the constituent oxides are additive for ideal mixtures. Ionic radii from constituent cations and anions are then used to estimate the partial-specific volumes of glass oxides and halogens. Two constants used to account for non-ideality were fitted to experimental data on waste glasses in the same manner as described in Vienna et al. (2002).

The results of the glass density measurements are shown in Table 3.1. The mode of these 41 density values is 2.64 g/cm$^3$, with a minimum of 2.59 g/cm$^3$ and a maximum of 2.75 g/cm$^3$. The density of LAW glasses varies little—60% of the glasses have density values between 2.64 g/cm$^3$ and 2.70 g/cm$^3$.

Figure 3.1 compares these measured density results to predicted density results obtained from the density model

$$\rho = \frac{\sum_{i=1}^{N} M_i x_i}{\mathrm{V}} \tag{3.1}$$

where $M_i$ is the molecular mass of the $i$-th component, $x_i$ is the mole fraction of the $i$-th component, and $V$ is molar volume (Vienna et al. 2003b). In an ideal mixture, the molar volume of the mixture is given by the sum of partial molar volumes of the mixture constituents. Clearly, glass is not an ideal mixture. However, a model based on volume is more likely to be linear than one based on density. This model tends to overpredict the density for all but two glasses, indicating that the density model is not very accurate in this composition region. This is most likely due to the glass not being an ideal mixture and the molar volume being assumed to be constant irrespective of bonding environment.

However, all density values are well below the contractual limit of 3.7 g/cm$^3$. Thus, the available density data for LAW glasses indicate that it is not necessary to develop a property-composition model to comply with the contractual requirement for density of LAW glasses.

Table 3.1. Measured Densities of Phase 2 Enhanced LAW Glasses

| Glass ID | Measured Density (g/cm$^3$) | Glass ID | Measured Density (g/cm$^3$) |
|---|---|---|---|
| LP2-IL-01 | 2.6864 | LP2-OL-05 | 2.6771 |
| LP2-IL-02 | 2.6881 | LP2-OL-07-1 | 2.6154 |
| LP2-IL-03 | 2.6808 | LP2-OL-08-MOD | 2.6867 |
| LP2-IL-04 | 2.6986 | LP2-OL-09-1 | 2.5882 |
| LP2-IL-05 | 2.7014 | LP2-OL-10-MOD | 2.6326 |
| LP2-IL-06 | 2.6306 | LP2-OL-11 | 2.6503 |
| LP2-IL-07 | 2.6329 | LP2-OL-12 | 2.6280 |
| LP2-IL-08 | 2.7031 | LP2-OL-13 | 2.6591 |
| LP2-IL-09 | 2.6861 | LP2-OL-14 | 2.5884 |
| LP2-IL-10 | 2.6625 | LP2-OL-15 | 2.7081 |
| LP2-IL-11 | 2.7011 | LP2-OL-16-MOD | 2.5838 |
| LP2-IL-12 | 2.6508 | LP2-OL-17 | 2.6448 |
| LP2-IL-13 | 2.6443 | LP2-OL-18 | 2.7360 |
| LP2-IL-14 | 2.6506 | LP2-OL-19 | 2.6082 |
| LP2-IL-15 | 2.6422 | LP2-OL-20 | 2.6351 |
| LP2-IL-16 | 2.6665 | LP2-OL-21 | 2.6409 |
| LP2-IL-17 | 2.6250 | LP2-OL-22 | 2.7456 |
| LP2-OL-01-3 | 2.6435 | LP2-OL-23 | 2.7296 |
| LP2-OL-02-1 | 2.6121 | LP2-OL-24 | 2.6658 |
| LP2-OL-03-MOD2 | 2.6597 | LP2-OL-25 | 2.7053 |
| LP2-OL-04-1 | 2.6779 | | |

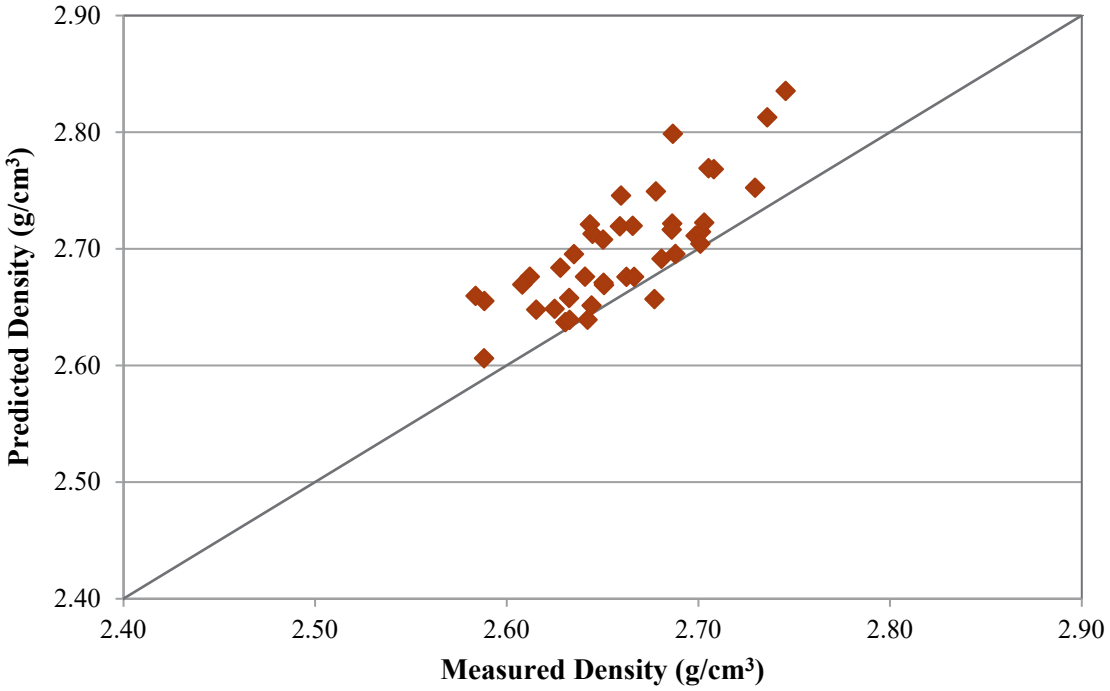


Figure 3.1. Predicted versus Measured Density for Phase 2 Enhanced LAW Glasses. The predicted values were obtained using the model in Equation (3.1).

## 3.3 Viscosity ($\eta$)

This section presents and discusses the viscosity results for the Phase 2 enhanced LAW glasses obtained using the methods discussed in Section 2.5. The results of the viscosity measurements are listed in Appendix C and summarized in Table 3.2.

Two model forms are widely used to fit viscosity-temperature data for each waste glass. The first model form is the Arrhenius equation

$$\ln(\eta) = A + \frac{B}{T_K} , \tag{3.2}$$

where $A$ and $B$ are independent of temperature ($T_K$), which is in K (T(°C) + 273.15), and potentially composition dependent. The values for the A and B coefficients are shown in Table 3.3 for each glass. The second model is the Vogel-Fulcher-Tammann (VFT) model

$$\ln(\eta) = E + \frac{F}{T_k - T_0} , \tag{3.3}$$

where E, F, and $T_0$ are temperature independent and potentially composition dependent coefficients and $T_K$ is the temperature in K. This model can be used to estimate the effect of temperature on viscosity over a wide range of temperatures for silicate-based glasses. Therefore, this model was also applied to the data for each glass; the E, F, and $T_0$ coefficients for each glass are also shown in Table 3.3. Furthermore, Table 3.3 summarizes the viscosity results at 1150 °C ($\eta_{1150}$) calculated using the VFT equation (Equation (3.3)) for the Phase 2 enhanced LAW glasses.

Figure 3.2 displays a plot of the ln (predicted viscosity) values against the ln (measured viscosity) values based on the latest LAW model from Piepel et al. (2016) given by

$$\begin{aligned}\ln(\eta_{1150}) = {} & 15.0259(g_{Al_2O_3}) - 5.8836(g_{B_2O_3}) - 5.3224(g_{CaO}) - 0.0395(g_{Fe_2O_3}) \\ & - 0.9015(g_{K_2O}) - 31.5781(g_{Li_2O}) - 3.2548(g_{MgO}) - 7.3212(g_{Na_2O}) \\ & + 11.3813(g_{SiO_2}) + 3.7336(g_{SO_3}) + 5.1123(g_{SnO_2}) - 4.8736(g_{V_2O_5}) \\ & - 2.0498(g_{ZnO}) + 11.5939(g_{ZrO_2}) + 0.4703(g_{Others1})\end{aligned} \quad (3.4)$$

Although this model produced very good predictions as seen in Figure 3.2, it slightly overpredicts the measured ln($\eta_{1150}$) values for the Phase 2 enhanced LAW glasses. Therefore, it would be useful to re-fit the model to account for the Phase 2 data as well as the entire LAW glass composition region.

Table 3.2. Measured Viscosity (P) Values Versus Target Temperature (in the sequence of measurement) for the Phase 2 Enhanced LAW Glasses Tested

| **Target *T*, °C** | **1150** | **1050** | **950** | **1150** | **1250** | **1150** |
|---|---|---|---|---|---|---|
| **Glass ID** | | | **Viscosity (P)** | | | |
| LP2-IL-01 | 25.078 | 70.056 | 258.950 | 25.300 | 10.900 | 25.189 |
| LP2-IL-02 | 62.771 | 197.680 | 840.620 | 62.883 | 24.668 | 62.517 |
| LP2-IL-03 | 56.953 | 174.980 | 721.650 | 57.084 | 22.522 | 55.956 |
| LP2-IL-04 | 24.808 | 68.137 | 249.000 | 25.100 | 11.100 | 25.263 |
| LP2-IL-05 | 24.355 | 70.386 | 278.41 | 24.600 | 10.600 | 24.704 |
| LP2-IL-06 | 46.437 | 132.000 | 494.400 | 47.110 | 20.212 | 47.424 |
| LP2-IL-07 | 25.601 | 65.778 | 217.620 | 25.974 | 12.200 | 26.192 |
| LP2-IL-08 | 35.711 | 107.000 | 434.12 | 36.093 | 14.997 | 36.204 |
| LP2-IL-09 | 24.098 | 66.425 | 243.000 | 24.222 | 10.795 | 24.300 |
| LP2-IL-10 | 46.916 | 134.580 | 508.790 | 47.276 | 20.114 | 47.246 |
| LP2-IL-11 | 58.537 | 182.920 | 764.970 | 59.055 | 23.859 | 60.265 |
| LP2-IL-12 | 62.078 | 182.830 | 697.660 | 62.585 | 25.958 | 62.543 |
| LP2-IL-13 | 56.397 | 160.500 | 608.710 | 55.994 | 23.912 | 56.011 |
| LP2-IL-14 | 27.252 | 72.645 | 249.220 | 27.555 | 12.555 | 27.906 |
| LP2-IL-15 | 55.414 | 160.090 | 613.200 | 55.377 | 23.700 | 55.780 |
| LP2-IL-16 | 43.301 | 123.130 | 461.020 | 43.809 | 18.619 | 43.665 |
| LP2-IL-17 | 51.172 | 139.000 | 500.000 | 50.442 | 22.340 | 51.314 |
| LP2-OL-01-3 | 85.343 | 287.000 | 1390.000 | 85.906 | 32.400 | 86.130 |
| LP2-OL-02-1 | 54.029 | 137.750 | 532.560 | 52.799 | 22.929 | 53.837 |
| LP2-OL-03 MOD2 | 25.618 | 73.108 | 275.070 | 25.866 | 11.100 | 26.043 |
| LP2-OL-04-1 | 38.693 | 119.000 | 490.670 | 38.804 | 15.787 | 39.790 |
| LP2-OL-05 | 67.671 | 212.000 | 1658.687 | 68.443 | 27.717 | 69.974 |
| LP2-OL-07-1 | 29.977 | 77.385 | 268.350 | 29.646 | 13.761 | 30.927 |
| LP2-OL-08 MOD | 12.800 | 33.548 | 125.190 | 12.900 | 5.902 | 12.806 |
| LP2-OL-09-1 | 63.768 | 170.300 | 630.374 | 63.776 | 28.548 | 64.592 |

| Target *T*, °C | 1150 | 1050 | 950 | 1150 | 1250 | 1150 |
|---|---|---|---|---|---|---|
| **Glass ID** | **Viscosity (P)** | | | | | |
| LP2-OL-10 MOD | 63.721 | 197.000 | 1450.000 | 65.037 | 26.566 | 67.690 |
| LP2-OL-11 | 11.300 | 27.304 | 83.927 | 11.400 | 5.592 | 11.609 |
| LP2-OL-12 | 7.970 | 17.577 | 48.700 | 8.029 | 4.240 | 8.119 |
| LP2-OL-13 | 13.167 | 31.861 | 90.966 | 13.266 | 6.420 | 13.467 |
| LP2-OL-14 | 9.563 | 21.329 | 59.802 | 9.643 | 5.042 | 9.800 |
| LP2-OL-15 | 12.726 | 33.842 | 122.000 | 12.856 | 6.003 | 12.900 |
| LP2-OL-16 MOD | 72.672 | 199.230 | 742.860 | 73.708 | 31.831 | 73.868 |
| LP2-OL-17 | 24.736 | 66.816 | 229.210 | 25.350 | 11.283 | 25.582 |
| LP2-OL-18 | 26.037 | 94.031 | 408.640 | 25.782 | 10.600 | 26.407 |
| LP2-OL-19 | 94.658 | 286.220 | 1140.300 | 96.150 | 38.812 | 97.627 |
| LP2-OL-20 | 46.287 | 122.000 | 419.930 | 45.714 | 20.366 | 45.952 |
| LP2-OL-21 | 41.915 | 116.000 | 423.520 | 42.674 | 18.500 | 43.189 |
| LP2-OL-22 | 32.000 | 106.000 | 515.778 | 32.362 | 12.700 | 32.200 |
| LP2-OL-23 | 12.000 | 31.800 | 116.000 | 12.196 | 5.635 | 12.200 |
| LP2-OL-24 | 37.241 | 103.720 | 372.040 | 37.409 | 16.000 | 37.457 |
| LP2-OL-25 | 14.843 | 39.062 | 138.000 | 15.000 | 6.879 | 15.050 |

Table 3.3. Fitted Coefficients of Arrhenius and VFT Models for Viscosity (Poise) as Functions of Temperature, and Predicted Viscosity at 1150 °C Using the VFT Model for the Phase 2 Enhanced LAW Glasses

| | Arrhenius Coefficients | | VFT Coefficients | | | |
|---|---|---|---|---|---|---|
| **Glass ID** | **A (ln P)** | **B (ln P· K)** | **E (ln P)** | **F (ln P· K)** | **$T_0$ (K)** | **$\eta_{1150}$ (P)** |
| LP2-IL-01 | -10.634 | 19748 | -5.560 | 8378 | 469.4 | 25.14 |
| LP2-IL-02 | -11.311 | 22015 | -5.854 | 9698 | 452.7 | 62.78 |
| LP2-IL-03 | -11.137 | 21620 | -5.962 | 9856 | 437.4 | 56.59 |
| LP2-IL-04 | -10.391 | 19398 | -4.997 | 7520 | 507.8 | 25.00 |
| LP2-IL-05 | -11.119 | 20413 | -4.906 | 7032 | 555.7 | 24.53 |
| LP2-IL-06 | -10.140 | 19935 | -4.851 | 8152 | 485.7 | 46.75 |
| LP2-IL-07 | -9.360 | 17978 | -4.396 | 7011 | 506.2 | 25.79 |
| LP2-IL-08 | -11.159 | 21012 | -5.236 | 8010 | 514.8 | 35.98 |
| LP2-IL-09 | -10.458 | 19449 | -4.856 | 7212 | 526.3 | 24.18 |
| LP2-IL-10 | -10.292 | 20156 | -5.122 | 8566 | 468.7 | 47.13 |
| LP2-IL-11 | -11.105 | 21644 | -5.391 | 8912 | 482.4 | 59.28 |
| LP2-IL-12 | -10.276 | 20531 | -5.542 | 9691 | 421.5 | 62.44 |
| LP2-IL-13 | -10.144 | 20195 | -4.939 | 8538 | 470.9 | 56.10 |
| LP2-IL-14 | -9.766 | 18643 | -4.891 | 7760 | 477.6 | 27.56 |
| LP2-IL-15 | -10.236 | 20314 | -4.795 | 8229 | 489.3 | 55.55 |
| LP2-IL-16 | -10.267 | 20007 | -5.256 | 8717 | 457.7 | 43.53 |
| LP2-IL-17 | -9.664 | 19370 | -4.803 | 8422 | 458.6 | 50.87 |
| LP2-OL-01-3 | -12.005 | 23456 | -5.036 | 8347 | 543.0 | 85.42 |
| LP2-OL-02-1 | -9.669 | 19430 | -1.404 | 3596 | 755.1 | 53.41 |

| | Arrhenius Coefficients | | VFT Coefficients | | | |
|---|---|---|---|---|---|---|
| Glass ID | A (ln P) | B (ln P· K) | E (ln P) | F (ln P· K) | $T_0$ (K) | $\eta_{1150}$ (P) |
| LP2-OL-03 MOD2 | -10.801 | 20025 | -5.562 | 8330 | 478.0 | 25.82 |
| LP2-OL-04-1 | -11.376 | 21434 | -5.833 | 9029 | 472.5 | 39.05 |
| LP2-OL-05 | -13.579 | 25414 | -0.963 | 2694 | 901.1 | 66.51 |
| LP2-OL-07-1 | -9.566 | 18481 | -4.482 | 7258 | 502.4 | 30.01 |
| LP2-OL-08 MOD | -10.807 | 19043 | -4.377 | 5585 | 616.4 | 12.75 |
| LP2-OL-09-1 | -9.362 | 19266 | -3.636 | 6859 | 542.6 | 63.66 |
| LP2-OL-10 MOD | -13.213 | 24816 | -1.070 | 2791 | 888.4 | 63.33 |
| LP2-OL-11 | -9.409 | 16878 | -4.717 | 6533 | 508.8 | 11.35 |
| LP2-OL-12 | -8.594 | 15216 | -4.239 | 5680 | 524.0 | 7.99 |
| LP2-OL-13 | -9.008 | 16514 | -7.316 | 12135 | 197.1 | 13.22 |
| LP2-OL-14 | -8.545 | 15408 | -3.956 | 5472 | 543.2 | 9.60 |
| LP2-OL-15 | -10.658 | 18837 | -4.395 | 5667 | 607.1 | 12.80 |
| LP2-OL-16 MOD | -9.458 | 19593 | -4.186 | 7896 | 491.5 | 72.96 |
| LP2-OL-17 | -9.942 | 18762 | -5.476 | 8599 | 435.0 | 25.17 |
| LP2-OL-18 | -12.919 | 23100 | -6.192 | 8449 | 531.8 | 26.74 |
| LP2-OL-19 | -10.210 | 21048 | -5.053 | 9368 | 448.4 | 95.40 |
| LP2-OL-20 | -9.396 | 18837 | -4.381 | 7737 | 480.7 | 46.00 |
| LP2-OL-21 | -9.929 | 19488 | -4.313 | 7248 | 523.7 | 42.32 |
| LP2-OL-22 | -12.777 | 23171 | -4.972 | 6829 | 614.5 | 32.18 |
| LP2-OL-23 | -10.752 | 18887 | -4.469 | 5682 | 607.0 | 12.10 |
| LP2-OL-24 | -10.136 | 19596 | -5.530 | 9111 | 427.4 | 37.33 |
| LP2-OL-25 | -10.418 | 18704 | -4.836 | 6621 | 544.9 | 14.92 |

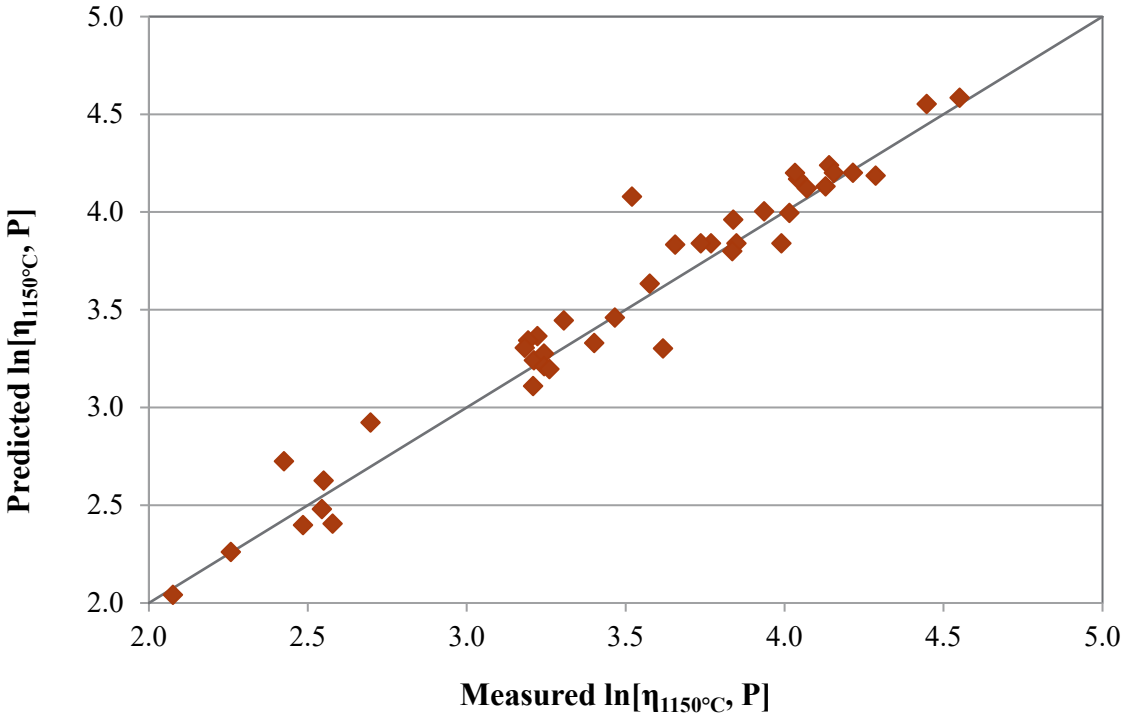


Figure 3.2. Predicted Versus Measured Viscosity at 1150ºC Values for Phase 2 Enhanced LAW Glasses. The predicted values were obtained using the model in Equation (3.4).

## 3.4 Electrical Conductivity (EC)

This section presents and discusses the EC results for the Phase 2 enhanced LAW glasses obtained using the methods discussed in Section 2.6. Table 3.4 lists the EC versus temperature data for each of the glasses and Appendix D shows the plots for the EC versus temperature data obtained from the EC experiments.

The Arrhenius equation is widely used to fit EC-temperature data for waste glass. It is

$$\ln(\varepsilon) = A + \frac{B}{T_K} \ , \tag{3.5}$$

where $A$ and $B$ are independent of temperature ($T_K$), which is in K (T(°C) + 273.15), and potentially composition dependent. The values for the A and B coefficients are shown in Table 3.3 for each glass.

The second model is the Vogel-Fulcher-Tammann (VFT) model

$$\ln(\varepsilon) = E + \frac{F}{T_k - T_0} \ , \tag{3.6}$$

where E, F, and $T_0$ are temperature independent and potentially composition dependent coefficients and $T_K$ is the temperature in K. This model can be used to estimate the effect of temperature on EC over a wide range of temperatures for silicate-based glasses. Therefore, this model was also applied to the data for each glass; the E, F, and $T_0$ coefficients for each glass are also shown in Table 3.3. Furthermore, Table 3.3 summarizes the EC results at 1150 °C ($\varepsilon_{1150}$) calculated using the VFT equation (Equation (3.3)) for the Phase 2 enhanced LAW glasses.

Figure 3.3 shows the ln(EC) plot for predicted versus measured EC, where the predicted values were produced by the modified Arrhenius equation parameters expanded as linear mixture models plus three alkali and alkaline earth cross-product terms (Piepel et al. 2007), given by

$$\ln(\varepsilon) = \sum_{i=1}^{q} a_i x_i + a_{CaOLi2O} x_{CaO} x_{Li2O} + a_{CaONa2O} x_{CaO} x_{Na2O} + a_{Li2ONa2O} x_{Li2O} x_{Na2O} + \sum_{i=1}^{q} b_i \frac{x_i}{\frac{T}{1000}} \quad (3.7)$$

where $x_i$ is the mass fraction of the $i^{th}$ oxide component and $T$ is the measured temperature in K. The model coefficients are shown in The measured value at 1 kHz is plotted in Figure 3.3 because this is the frequency used in the model and is closest to the real impedance. This model overpredicted the EC in all but one instance. This could be because of the different glass composition region that the Phase 2 enhanced LAW glass study explored compared to the composition region with lower waste loadings explored for the models in Piepel et al. (2007). Therefore, a new model exploring a wider composition region with higher waste loadings would be useful to account for the Phase 2 data.

Table 3.. The measured value at 1 kHz is plotted in Figure 3.3 because this is the frequency used in the model and is closest to the real impedance. This model overpredicted the EC in all but one instance. This could be because of the different glass composition region that the Phase 2 enhanced LAW glass study explored compared to the composition region with lower waste loadings explored for the models in Piepel et al. (2007). Therefore, a new model exploring a wider composition region with higher waste loadings would be useful to account for the Phase 2 data.

Table 3.The measured value at 1 kHz is plotted in Figure 3.3 because this is the frequency used in the model and is closest to the real impedance. This model overpredicted the EC in all but one instance. This could be because of the different glass composition region that the Phase 2 enhanced LAW glass study explored compared to the composition region with lower waste loadings explored for the models in Piepel et al. (2007). Therefore, a new model exploring a wider composition region with higher waste loadings would be useful to account for the Phase 2 data.

Table 3.4. Measured Electrical Conductivity (S/cm) Values versus Temperatures for the Phase 2 Enhanced LAW Glasses

| **Target *T*, °C** | **950** | **950** | **1250** | **1250** | **1150** | **1150** | **1050** | **1050** |
|---|---|---|---|---|---|---|---|---|
| **Glass ID** | **Electrical Conductivity (S/cm)** | | | | | | | |
| LP2-IL-01 | 0.2869 | 0.2891 | 0.7199 | 0.7188 | 0.5695 | 0.5702 | 0.4219 | 0.4238 |
| LP2-IL-02 | 0.2914 | 0.2939 | 0.7311 | 0.7298 | 0.5799 | 0.5808 | 0.4277 | 0.4297 |
| LP2-IL-03 | 0.3071 | 0.3092 | 0.7379 | -- | 0.5905 | 0.5928 | 0.4421 | 0.4450 |
| LP2-IL-04 | 0.2906 | 0.2926 | 0.7374 | 0.7345 | 0.5839 | 0.5852 | 0.4293 | 0.4312 |
| LP2-IL-05 | 0.2347 | 0.2365 | 0.6502 | 0.6477 | 0.5030 | 0.5055 | 0.3593 | 0.3609 |

| Target *T*, °C | 950 | 950 | 1250 | 1250 | 1150 | 1150 | 1050 | 1050 |
|---|---|---|---|---|---|---|---|---|
| Glass ID | Electrical Conductivity (S/cm) | | | | | | | |
| LP2-IL-06 | 0.2737 | 0.2754 | 0.6752 | 0.6716 | 0.5387 | 0.5394 | 0.4006 | 0.4020 |
| LP2-IL-07 | 0.2681 | 0.2700 | 0.6753 | -- | 0.5348 | 0.5359 | 0.3952 | 0.3969 |
| LP2-IL-08 | 0.2310 | 0.2327 | 0.6359 | 0.6335 | 0.4916 | 0.4926 | 0.3525 | 0.3540 |
| LP2-IL-09 | 0.3209 | 0.3233 | 0.7802 | 0.7809 | 0.6290 | 0.6309 | 0.4669 | 0.4703 |
| LP2-IL-10 | 0.2598 | 0.2615 | 0.6630 | -- | 0.5245 | 0.5249 | 0.3843 | 0.3858 |
| LP2-IL-11 | 0.2628 | 0.2646 | 0.6731 | 0.6715 | 0.5336 | 0.5351 | 0.3920 | 0.3935 |
| LP2-IL-12 | 0.3138 | 0.3156 | 0.7280 | 0.7257 | 0.5867 | 0.5876 | 0.4461 | 0.4476 |
| LP2-IL-13 | 0.2323 | 0.2343 | 0.5973 | 0.5959 | 0.4695 | 0.4702 | 0.3451 | 0.3464 |
| LP2-IL-14 | 0.3340 | 0.3360 | 0.7716 | 0.7708 | 0.6261 | 0.6267 | 0.4755 | 0.4771 |
| LP2-IL-15 | 0.3128 | 0.3154 | 0.7613 | 0.7599 | 0.6116 | 0.6125 | 0.4569 | 0.4583 |
| LP2-IL-16 | 0.2792 | 0.2812 | 0.7128 | -- | 0.5626 | 0.5644 | 0.4134 | 0.4153 |
| LP2-IL-17 | 0.2644 | 0.2674 | 0.6345 | 0.6335 | 0.5145 | 0.5158 | 0.3874 | 0.3895 |
| LP2-OL-01-3 | 0.1483 | 0.1496 | 0.4400 | 0.4401 | 0.3344 | 0.3352 | 0.2348 | 0.2357 |
| LP2-OL-02-1 | 0.2345 | 0.2359 | 0.5798 | 0.5783 | 0.4624 | 0.4641 | 0.3437 | 0.3450 |
| LP2-OL-03 MOD2 | 0.3138 | 0.3162 | 0.7508 | -- | 0.6088 | 0.6102 | 0.4559 | 0.4577 |
| LP2-OL-04-1 | 0.1923 | 0.1940 | 0.5431 | -- | 0.4244 | 0.4253 | 0.3020 | 0.3034 |
| LP2-OL-05 | 0.1627 | 0.1640 | 0.4629 | 0.4613 | 0.3581 | 0.3590 | 0.2542 | 0.2555 |
| LP2-OL-07-1 | 0.1750 | 0.1764 | 0.4869 | -- | 0.3782 | 0.3784 | 0.2705 | 0.2717 |
| LP2-OL-08 MOD | 0.3685 | 0.3708 | 0.8067 | -- | 0.6599 | 0.6609 | 0.5118 | 0.5128 |
| LP2-OL-09-1 | 0.1936 | 0.1949 | 0.4963 | 0.4952 | 0.3948 | 0.3956 | 0.2889 | 0.2901 |
| LP2-OL-10 MOD | 0.1728 | 0.1743 | 0.4747 | -- | 0.3695 | 0.3705 | 0.2660 | 0.2672 |
| LP2-OL-11 | 0.2342 | 0.2358 | 0.6158 | -- | 0.4862 | 0.4877 | 0.3557 | 0.3570 |
| LP2-OL-12 | 0.3216 | 0.3233 | 0.7487 | -- | 0.6044 | 0.6068 | 0.4587 | 0.4609 |
| LP2-OL-13 | 0.2913 | 0.2943 | 0.6977 | 0.6952 | 0.5689 | 0.5702 | 0.4286 | 0.4301 |
| LP2-OL-14 | 0.2546 | 0.2564 | 0.6431 | 0.6406 | 0.5132 | -- | 0.3798 | 0.3818 |
| LP2-OL-15 | 0.1636 | 0.1652 | 0.5312 | 0.5290 | 0.3976 | 0.3988 | 0.2704 | 0.2720 |
| LP2-OL-16 MOD | 0.2194 | 0.2210 | 0.5245 | -- | 0.4211 | 0.4205 | 0.3169 | 0.3184 |
| LP2-OL-17 | 0.2946 | 0.2965 | 0.7024 | -- | 0.5652 | -- | 0.4263 | 0.4274 |
| LP2-OL-18 | 0.1986 | 0.1999 | 0.5639 | -- | 0.4340 | 0.4360 | 0.3072 | 0.3084 |
| LP2-OL-19 | 0.2175 | 0.2189 | 0.5718 | 0.5716 | 0.4511 | 0.4525 | 0.3279 | 0.3291 |
| LP2-OL-20 | 0.2906 | 0.2923 | 0.6615 | 0.6595 | 0.5417 | 0.5430 | 0.4149 | 0.4161 |
| LP2-OL-21 | 0.2505 | 0.2522 | 0.6249 | -- | 0.4987 | 0.5000 | 0.3703 | 0.3718 |
| LP2-OL-22 | 0.1760 | 0.1774 | 0.5376 | -- | 0.4065 | 0.4075 | 0.2818 | 0.2833 |
| LP2-OL-23 | 0.1838 | 0.1852 | 0.5599 | 0.5578 | 0.4251 | 0.4264 | 0.2949 | 0.2963 |
| LP2-OL-24 | 0.2796 | 0.2813 | 0.6454 | 0.6438 | 0.5260 | 0.5273 | 0.4006 | 0.4024 |
| LP2-OL-25 | 0.2942 | 0.2961 | 0.6878 | 0.6864 | 0.5578 | 0.5588 | 0.4220 | 0.4230 |

-- = not measured

Table 3.5. Fitted Coefficients of the Arrhenius and VFT Models for Electrical Conductivity as a Function of Temperature, and Predicted Electrical Conductivity at 1150 °C Using the VFT Model for the Phase 2 Enhanced LAW Glasses

| | Arrhenius Coefficients | | VFT Coefficients | | | |
|---|---|---|---|---|---|---|
| Glass ID | A (ln S/cm) | B (ln S/cm· K) | E (ln S/cm) | F (ln S/cm· K) | $T_0$ (K) | $\varepsilon_{1150}$ (S/cm) |
| LP2-IL-01 | 8.0308 | -5694.1 | 6.3033 | -1953.5 | 559.43 | 0.569 |
| LP2-IL-02 | 8.0499 | -5698.5 | 6.3331 | -1974.4 | 555.53 | 0.578 |

| | Arrhenius Coefficients | | VFT Coefficients | | | |
|---|---|---|---|---|---|---|
| Glass ID | A (ln S/cm) | B (ln S/cm· K) | E (ln S/cm) | F (ln S/cm· K) | $T_0$ (K) | $\varepsilon_{1150}$ (S/cm) |
| LP2-IL-03 | 7.9364 | -5500.4 | 6.2899 | -1947.5 | 542.79 | 0.590 |
| LP2-IL-04 | 8.1048 | -5768.3 | 6.2875 | -1872.7 | 580.81 | 0.582 |
| LP2-IL-05 | 8.3388 | -6314.2 | 6.3795 | -2096.8 | 572.11 | 0.502 |
| LP2-IL-06 | 7.8972 | -5587.4 | 6.0819 | -1729.2 | 598.84 | 0.537 |
| LP2-IL-07 | 8.0433 | -5795.2 | 6.2402 | -1943.1 | 564.08 | 0.534 |
| LP2-IL-08 | 8.2859 | -6269.9 | 6.3937 | -2167.1 | 556.50 | 0.491 |
| LP2-IL-09 | 8.0048 | -5523.3 | 6.1477 | -1615.5 | 619.59 | 0.626 |
| LP2-IL-10 | 8.0872 | -5888.4 | 6.2856 | -2022.5 | 554.72 | 0.523 |
| LP2-IL-11 | 8.0575 | -5830.7 | 6.0918 | -1697.5 | 621.25 | 0.532 |
| LP2-IL-12 | 7.7200 | -5207.4 | 6.1592 | -1817.2 | 552.70 | 0.586 |
| LP2-IL-13 | 7.9411 | -5841.8 | 6.1815 | -2024.6 | 555.44 | 0.469 |
| LP2-IL-14 | 7.7712 | -5191.9 | 6.1097 | -1645.5 | 589.93 | 0.625 |
| LP2-IL-15 | 7.9688 | -5509.5 | 6.1161 | -1611.1 | 619.65 | 0.610 |
| LP2-IL-16 | 8.1560 | -5883.6 | 6.3426 | -2000.0 | 558.77 | 0.562 |
| LP2-IL-17 | 7.7243 | -5409.7 | 5.7059 | -1300.4 | 687.03 | 0.514 |
| LP2-OL-01-3 | 8.2301 | -6739.5 | 6.1158 | -2202.1 | 578.34 | 0.334 |
| LP2-OL-02-1 | 7.7624 | -5611.7 | 5.9324 | -1726.4 | 601.07 | 0.462 |
| LP2-OL-03 MOD2 | 7.9641 | -5503.2 | 6.0269 | -1509.2 | 637.67 | 0.607 |
| LP2-OL-04-1 | 8.3389 | -6553.4 | 5.8871 | -1597.5 | 677.39 | 0.423 |
| LP2-OL-05 | 8.1106 | -6477.6 | 5.8755 | -1811.0 | 635.72 | 0.357 |
| LP2-OL-07-1 | 8.1412 | -6431.9 | 5.9762 | -1907.4 | 609.94 | 0.377 |
| LP2-OL-08 MOD | 7.6300 | -4904.2 | 6.1653 | -1741.8 | 541.53 | 0.660 |
| LP2-OL-09-1 | 7.7621 | -5842.8 | 5.7559 | -1650.5 | 632.05 | 0.393 |
| LP2-OL-10 MOD | 8.0608 | -6348.5 | 5.9008 | -1848.7 | 616.49 | 0.369 |
| LP2-OL-11 | 8.1500 | -6085.1 | 5.9539 | -1593.0 | 653.63 | 0.486 |
| LP2-OL-12 | 7.8230 | -5305.1 | 6.1475 | -1740.1 | 572.50 | 0.605 |
| LP2-OL-13 | 7.8152 | -5400.4 | 5.6900 | -1154.4 | 724.25 | 0.567 |
| LP2-OL-14 | 7.9294 | -5710.6 | 5.8882 | -1486.9 | 661.63 | 0.512 |
| LP2-OL-15 | 8.7855 | -7292.3 | 6.2776 | -2050.6 | 633.67 | 0.397 |
| LP2-OL-16 MOD | 7.5684 | -5459.4 | 5.8380 | -1781.2 | 574.53 | 0.421 |
| LP2-OL-17 | 7.8404 | -5431.4 | 6.0646 | -1680.9 | 595.57 | 0.565 |
| LP2-OL-18 | 8.3738 | -6565.6 | 6.3525 | -2235.4 | 558.14 | 0.433 |
| LP2-OL-19 | 8.0097 | -6003.6 | 5.9948 | -1761.2 | 618.50 | 0.450 |
| LP2-OL-20 | 7.5560 | -5094.4 | 5.0720 | -1288.4 | 670.25 | 0.541 |
| LP2-OL-21 | 7.9400 | -5749.0 | 5.9601 | -1639.6 | 623.92 | 0.498 |
| LP2-OL-22 | 8.6223 | -7013.2 | 6.3747 | -2249.9 | 580.91 | 0.406 |
| LP2-OL-23 | 8.5824 | -6905.8 | 6.2600 | -2019.0 | 619.74 | 0.424 |
| LP2-OL-24 | 7.5888 | -5182.2 | 5.7449 | -1369.1 | 655.44 | 0.525 |
| LP2-OL-25 | 7.7052 | -5264.5 | 5.9505 | -1562.6 | 614.24 | 0.556 |

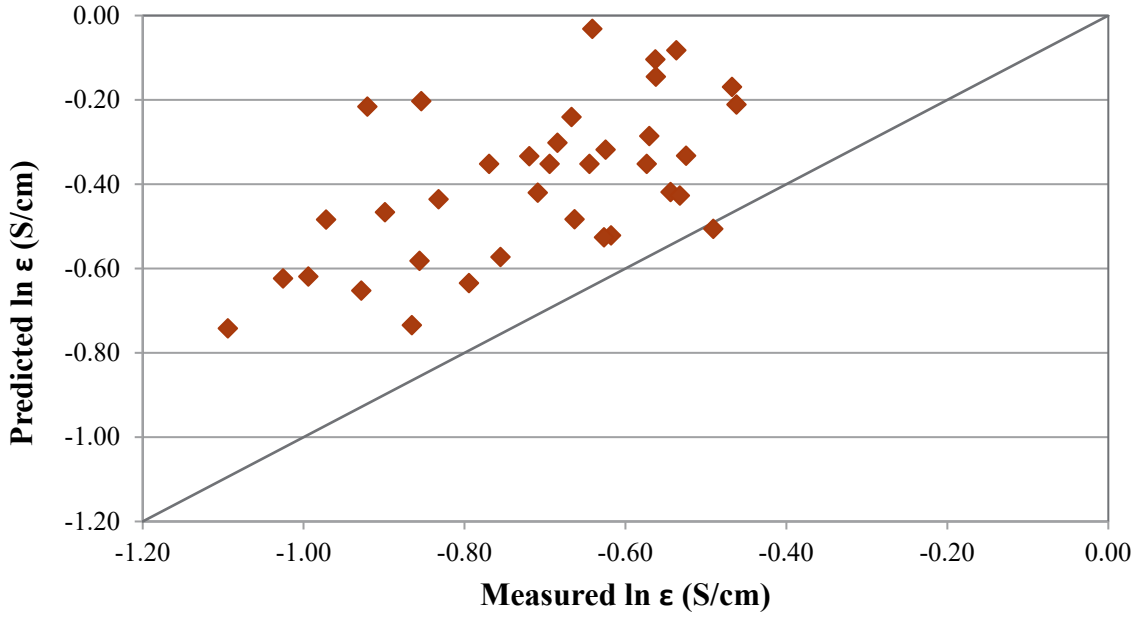


Figure 3.3. Predicted versus Measured Electrical Conductivity at 1150 ºC Values for Phase 2 Enhanced LAW Glasses. The predicted values were obtained using the model in Equation (3.7) with coefficients in Table 3.6.

The measured value at 1 kHz is plotted in Figure 3.3 because this is the frequency used in the model and is closest to the real impedance. This model overpredicted the EC in all but one instance. This could be because of the different glass composition region that the Phase 2 enhanced LAW glass study explored compared to the composition region with lower waste loadings explored for the models in Piepel et al. (2007). Therefore, a new model exploring a wider composition region with higher waste loadings would be useful to account for the Phase 2 data.

Table 3.6. List of Electrical Conductivity Model Components and Coefficients (Piepel et al. 2007)

| Component | Coefficient | Component | Coefficient |
|---|---|---|---|
| $Al_2O_3$ | 2.3854 | $Al_2O_3$/(T/1000) | -9.0593 |
| $B_2O_3$ | 7.9750 | $B_2O_3$/(T/1000) | -11.0983 |
| CaO | 5.2093 | CaO/(T/1000) | -30.6535 |
| $Fe_2O_3$ | 4.3935 | $Fe_2O_3$/(T/1000) | -9.2407 |
| $K_2O$ | 7.6774 | $K_2O$/(T/1000) | -11.5299 |
| MgO | 15.1675 | MgO/(T/1000) | -25.0634 |
| $Na_2O$ | -2.0291 | $Na_2O$/(T/1000) | 12.3822 |
| $SiO_2$ | 3.6811 | $SiO_2$/(T/1000) | -10.1563 |
| $ZrO_2$ | 7.8740 | $ZrO_2$/(T/1000) | -16.5390 |
| Others (1) | 11.2070 | Others(1)/(T/1000) | -17.7117 |
| $Na_2O$ x CaO | 79.0190 | | |

(1) Others includes $SO_3$, Cl, $P_2O_5$, F, $Cr_2O_3$, $SnO_2$, $V_2O_5$, and ZnO

## 3.5 Crystal Fraction of Heat-Treated Glasses

This section presents and discusses the crystal fraction results for the Phase 2 enhanced LAW glasses obtained using the methods discussed in Section 2.7. For each glass composition, specimens were prepared, and heat treated at 950 °C. Heat-treated specimens were spiked with 5 mass% $CeO_2$, milled to powderize them and adequately mix the glass, and analyzed using XRD. The $CeO_2$ spiked into the specimen was used as a standard for semi-quantitative analysis to determine the mass fraction of crystal phase(s) in a specimen. See Appendix E for photos of crystal fraction heat-treated glasses and Appendix F for XRD spectra obtained from them.

All but 14 glasses had insufficient crystals to perform XRD analysis when treated at 950 °C for 24 h. Nine glasses contained Nasicon ($Na_{1+x}Zr_2Si_xP_{3-x}O_{12}$, $0 < x < 3$) and six glasses contained lazurite, $(Na,Ca)_8[(S,Cl,SO_4,OH)_2|(Al_6Si_6O_{24})]$, and/or combeite ($Na_2Ca_2Si_3O_9$). The wt% total crystallinity ranged from 0 to 17.5 wt%. These results are summarized in Table 3..

Table 3.7. Weight Percent Crystallinity and Identification of Crystals by XRD in 24 h Heat-Treated Phase 2 Enhanced LAW Glasses

| Glass ID | Heat-Treated Temp. (°C) | Wt% Crystallinity | Crystal Phase Identification |
|---|---|---|---|
| LP2-IL-01 | 950 | 0.67<br>0.29 | Nasicon<br>Baddeleyite |
| LP2-IL-02 | 950 | 1.20<br>0.29 | Nasicon<br>Baddeleyite |
| LP2-IL-03 | 950 | 1.96<br>0.59 | Nasicon<br>Baddeleyite |
| LP2-IL-04 | 950 | 0 | Amorphous |
| LP2-IL-05 | 950 | 0 | Amorphous |
| LP2-IL-06 | 950 | 0 | Amorphous |
| LP2-IL-07 | 950 | 0 | Amorphous |
| LP2-IL-08 | 950 | 0 | Amorphous |
| LP2-IL-09 | 950 | 0 | Amorphous |
| LP2-IL-10 | 950 | 0 | Amorphous |
| LP2-IL-11 | 950 | 1.96 | Nasicon |
| LP2-IL-12 | 950 | 0 | Amorphous |
| LP2-IL-13 | 950 | 0 | Amorphous |
| LP2-IL-14 | 950 | 0 | Amorphous |
| LP2-IL-15 | 950 | 0 | Amorphous |
| LP2-IL-16 | 950 | 0 | Amorphous |
| LP2-IL-17 | 950 | 0 | Amorphous |
| LP2-OL-01-3 | 950 | ~0 | Not enough crystals |
| LP2-OL-02-1 | 950 | 0 | Amorphous |
| LP2-OL-03 MOD2 | 950 | 2.02<br>5.29<br>4.25<br>0.11 | Nasicon<br>Combeite high<br>Lazurite 4A<br>Tin Fluoride |

| Glass ID | Heat-Treated Temp. (°C) | Wt% Crystallinity | Crystal Phase Identification |
|---|---|---|---|
| LP2-OL-04-1 | 950 | 5.31 | Nasicon |
| LP2-OL-05 | 950 | 2.07 | Lazurite 1C |
| LP2-OL-07-1 | 950 | ~0 | Not enough crystals |
| LP2-OL-08 MOD | 950 | 6.56<br>10.90 | Nasicon<br>Combeite high |
| LP2-OL-09-1 | 950 | 0 | Amorphous with bubbles |
| LP2-OL-10 MOD | 950 | 10.57 | Lazurite 1C |
| LP2-OL-11 | 950 | 0 | Amorphous |
| LP2-OL-12 | 950 | 0 | Amorphous |
| LP2-OL-13 | 950 | 1.72<br>0.261 | Nasicon<br>Quartz low |
| LP2-OL-14 | 950 | 0 | Amorphous |
| LP2-OL-15 | 950 | 0 | Amorphous |
| LP2-OL-16 MOD | 950 | 0 | Amorphous |
| LP2-OL-17 | 950 | ~0 | Not enough crystals |
| LP2-OL-18 | 950 | 0.336<br>0.287<br>0.313 | Cassiterite<br>Calcium Sodium Tin<br>Halite |
| LP2-OL-19 | 950 | ~0 | Not enough crystals |
| LP2-OL-20 | 950 | 0.544<br>0.224<br>0.131<br>0.292<br>1.18 | Mullite (Al, Si, O)<br>Lazurite<br>Zircon<br>Zirconium Aluminum<br>Silicon |
| LP2-OL-21 | 950 | 0 | Amorphous |
| LP2-OL-22 | 950 | 2.48 | Nasicon |
| LP2-OL-23 | 950 | 0 | Amorphous |
| LP2-OL-24 | 950 | 1.22<br>0.033<br>2.22 | Hauyne<br>Lazurite 1C<br>Aluminum Phosphate |
| LP2-OL-25 | 950 | ~0 | Not enough crystals |

## 3.6 Crystal Identification in Canister Centerline Cooling (CCC) Glasses

This section presents and discusses the crystal fraction results from CCC heat treatments of Phase 2 enhanced LAW glasses obtained using the methods discussed in Section 2.8. XRD scans of CCC glass samples identified various crystal types. The crystal types and wt% crystallinity results are summarized in Table 3.. A total of 28 samples were not analyzed by XRD because there were either no crystals or very few crystals (not enough for XRD to detect) observed by optical microscope. Four glasses had crystal content of less than 5 mass%, while eight glasses had crystal content greater than 10 mass% crystals. Only one glass (LP2-IL-06) had a crystal content between 5 and 10 mass%. The major crystalline phases appearing in the glasses containing crystals were nepheline, sodalite, and combeite, which are all feldspathoids. See Appendix G for photos of CCC-treated glasses and Appendix H for XRD spectra obtained from them.

During cooling, several of the glasses seemed to form a layer of crystals around the Pt crucible walls (see Figure 3.4). When a quartz crucible was used, the glass still formed a layer of crystals around the crucible walls (Figure 3.5). Therefore, this phenomenon did not appear to be due to the Pt.

Table 3.8. Weight Percent Crystallinity and Identification of Crystals by XRD in CCC-Treated Phase 2 Enhanced LAW Glasses

| Glass ID | Starting CCC Temp (°C) | Wt% Crystallinity | Crystal Phase Identification |
|---|---|---|---|
| LP2-IL-01 | 1150 | 1.22<br>2.48 | Lazurite 4A<br>Combeite low |
| LP2-IL-02 | 1150 | 0 | Amorphous |
| LP2-IL-03 | 1150 | 0 | Amorphous |
| LP2-IL-04 | 1150 | 0 | Amorphous |
| LP2-IL-05 | 1150 | 0 | Amorphous |
| LP2-IL-06 | 1150 | 8.83<br>1.07 | Lazurite 4A<br>Sodalite |
| LP2-IL-07 | 1150 | 0 | Amorphous |
| LP2-IL-08 | 1150 | 0 | Amorphous |
| LP2-IL-09 | 1150 | 0 | Amorphous |
| LP2-IL-10 | 1150 | 0 | Amorphous |
| LP2-IL-11 | 1150 | 0 | Amorphous |
| LP2-IL-12 | 1150 | 0 | Amorphous |
| LP2-IL-13 | 1150 | 0 | Amorphous |
| LP2-IL-14 | 1150 | 0 | Amorphous |
| LP2-IL-15 | 1150 | 0 | Amorphous |
| LP2-IL-16 | 1150 | 0 | Amorphous |
| LP2-IL-17 | 1150 | 0.576 | Lazurite 4A |
| LP2-OL-01-3 | 1150 | 0 | Amorphous |
| LP2-OL-02-1 | 1150 | 0 | Amorphous |
| LP2-OL-03 MOD2 | 1150 | 40.78<br>6.72<br>18.87<br>0.943 | Combeite high<br>Nepheline, sodian<br>SodiumAluminumSilicate<br>CalciumZinc |
| LP2-OL-04-1 | 1150 | 37.52<br>18.16<br>5.17<br>0.72<br>1.25<br>2.98<br>0.46<br>3.11 | Combeite high<br>Nepheline (Si-rich)<br>Sodium Peroxide<br>Zirconium Oxide<br>65-9834_AlMg<br>Zeolite<br>Zirconium Oxide<br>Periclase |
| LP2-OL-05 | 1150 | 11.91<br>8.51<br>3.00 | Haueyne [(b)]<br>Nosean [(a)]<br>Combeite high |
| LP2-OL-07-1 | 1150 | 4.06 | Haueyne [(b)] |
| LP2-OL-08 MOD | 1150 | 6.68<br>49.56<br>6.36<br>7.12 | Nasicon<br>Combeite high<br>Sodium Aluminum Silicate<br>nepheline<br>Sodium Iron Aluminum Oxide |

| Glass ID | Starting CCC Temp (°C) | Wt% Crystallinity | Crystal Phase Identification |
|---|---|---|---|
| LP2-OL-09 | 1150 | 0 | Amorphous |
| LP2-OL-10 MOD | 1150 | 11.45<br>2.04<br>10.25<br>4.55 | Nepheline, sodian<br>Lazurite 4A<br>Combeite high<br>Nosean [(a)] |
| LP2-OL-11 | 1150 | 0 | Amorphous |
| LP2-OL-12 | 1150 | 0 | Amorphous |
| LP2-OL-13 | 1150 | 42.36<br>2.84 | Combeite high<br>Nepheline (Si-rich) |
| LP2-OL-14 | 1150 | 0 | Amorphous |
| LP2-OL-15 | 1150 | 0 | Amorphous |
| LP2-OL-16 MOD | 1150 | 0 | Amorphous |
| LP2-OL-17 | 1150 | 0 | Amorphous |
| LP2-OL-18 | 1150 | 3.76 | Lazurite 4A |
| LP2-OL-19 | 1150 | 0 | Amorphous |
| LP2-OL-20 | 1150 | 16.46 | Combeite high |
| LP2-OL-21 | 1150 | 0 | Amorphous |
| LP2-OL-22 | 1150 | 0 | Amorphous |
| LP2-OL-23 | 1150 | 0 | Amorphous |
| LP2-OL-24 | 1150 | 66.22<br>0.41 | SodiumAluminumSiliconOxide<br>SodiumMagnesiumSulfate |
| LP2-OL-25 | 1150 | 0 | Amorphous |

(a) Nosean is very similar to nepheline except it also contains sulfate.
(b) Hauyne is also similar to nepheline but contains Ca and sulfate.

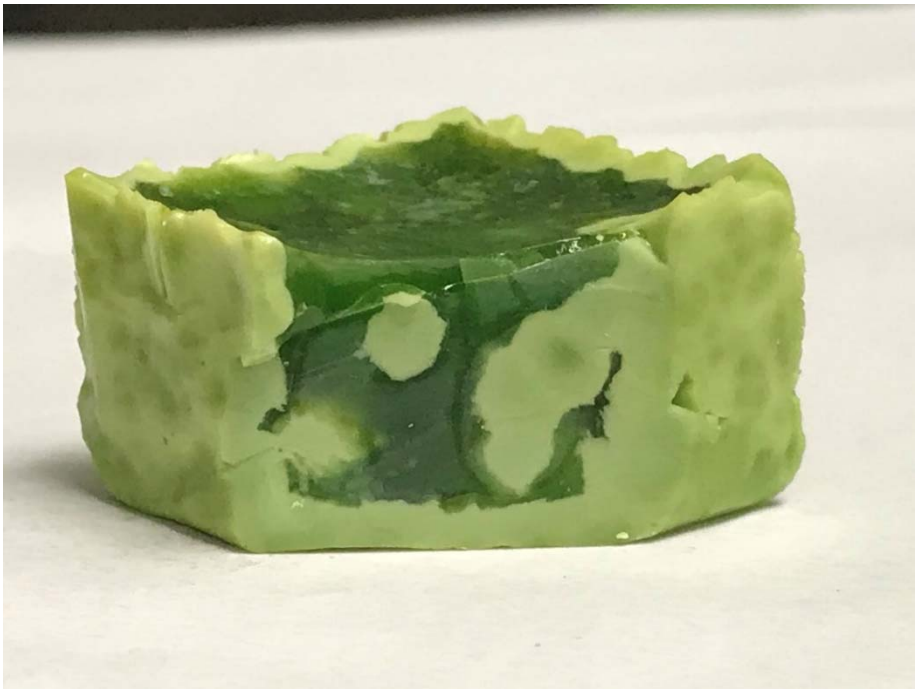

Figure 3.4. Glass LP2-OL-05 Cooled in a Pt Crucible with Crystals along Edge

Figure 3.5. Glass LP2-OL-05 Cooled in a Quartz Crucible with Crystals along Edge

## 3.7 Product Consistency Test (PCT)

This section presents and discusses the PCT results for the Phase 2 enhanced LAW glasses obtained using the methods discussed in Section 2.9. The PCT results are published elsewhere (Fox et al. 2017, 2018), but are summarized here in Table 3.. The PCT results were normalized to the target values of the glasses. A review of the PCT data shows that none of the inner-layer glasses had normalized releases for boron (NR [B]) and sodium (NR [Na]) that were higher than the WTP contract limit of 4 g/L for either quenched or CCC-treated glasses. However, several of the outer-layer glasses did exceed this limit (which was intended in generating the outer-layer test matrix).

A review of the PCT data resulted in the following observations:

- The CCC heat treatment had little impact on the PCT results as compared to the quenched versions of the study glasses for the inner-layer glasses. For the outer-layer glasses, the CCC heat treatment increased PCT normalized releases for most glasses that formed crystals.
- Glass LP2-OL-18 showed a decrease in PCT normalized releases after CCC heat treatment.
- The quenched and CCC glass LP2-OL-12 had the highest $NR_B$ and $NR_{Na}$ values based on normalization to the targeted composition.

Table 3.9. PCT Normalized Releases (g/L) Using Targeted Glass Compositions from Fox et al. (2017 and 2018)

| Glass ID | Type | B (g/L) | Na (g/L) | Si (g/L) |
|---|---|---|---|---|
| LP2-IL-01 | Quenched | 1.375 | 1.854 | 0.483 |
| | CCC | 2.090 | 2.725 | 0.565 |
| LP2-IL-02 | Quenched | 1.139 | 1.319 | 0.391 |
| | CCC | 1.124 | 1.366 | 0.415 |
| LP2-IL-03 | Quenched | 0.768 | 1.111 | 0.353 |
| | CCC | 0.746 | 1.091 | 0.369 |
| LP2-IL-04 | Quenched | 1.359 | 1.908 | 0.535 |
| | CCC | 1.485 | 2.135 | 0.597 |
| LP2-IL-05 | Quenched | 1.003 | 1.138 | 0.294 |
| | CCC | 1.165 | 1.358 | 0.340 |
| LP2-IL-06 | Quenched | 2.522 | 1.868 | 0.266 |
| | CCC | 2.248 | 1.729 | 0.274 |
| LP2-IL-07 | Quenched | 2.948 | 2.561 | 0.639 |
| | CCC | 2.639 | 2.535 | 0.629 |
| LP2-IL-08 | Quenched | 1.317 | 1.571 | 0.418 |
| | CCC | 1.188 | 1.474 | 0.419 |
| LP2-IL-09 | Quenched | 3.468 | 2.693 | 0.447 |
| | CCC | 3.291 | 2.550 | 0.475 |
| LP2-IL-10 | Quenched | 0.881 | 1.146 | 0.316 |
| | CCC | 0.945 | 1.201 | 0.358 |
| LP2-IL-11 | Quenched | 0.581 | 0.960 | 0.286 |
| | CCC | 0.616 | 0.944 | 0.312 |
| LP2-IL-12 | Quenched | 1.384 | 1.497 | 0.467 |
| | CCC | 1.082 | 1.362 | 0.443 |
| LP2-IL-13 | Quenched | 2.022 | 1.632 | 0.332 |
| | CCC | 1.512 | 1.358 | 0.325 |
| LP2-IL-14 | Quenched | 2.911 | 2.356 | 0.379 |
| | CCC | 2.713 | 2.231 | 0.409 |
| LP2-IL-15 | Quenched | 1.780 | 1.361 | 0.350 |
| | CCC | 0.922 | 0.901 | 0.321 |
| LP2-IL-16 | Quenched | 0.971 | 1.197 | 0.328 |
| | CCC | 0.906 | 1.143 | 0.337 |
| LP2-IL-17 | Quenched | 1.777 | 1.412 | 0.309 |
| | CCC | 1.613 | 1.339 | 0.340 |
| LP2-OL-01-3 | Quenched | 0.665 | 1.140 | 0.337 |
| | CCC | 0.625 | 0.955 | 0.292 |
| LP2-OL-02-1 | Quenched | 0.937 | 1.045 | 0.334 |
| | CCC | 0.959 | 0.983 | 0.314 |

| Glass ID | Type | B (g/L) | Na (g/L) | Si (g/L) |
|---|---|---|---|---|
| LP2-OL-03MOD2 | Quenched | 0.741 | 2.552 | 0.398 |
| | CCC | 1.642 | 14.511 | 1.693 |
| LP2-OL-04-1 | Quenched | 1.531 | 2.115 | 0.444 |
| | CCC | 9.449 | 20.573 | 2.304 |
| LP2-OL-05 | Quenched | 0.319 | 0.725 | 0.184 |
| | CCC | 0.862 | 0.990 | 0.190 |
| LP2-OL-07-1 | Quenched | 0.874 | 1.001 | 0.271 |
| | CCC | 0.813 | 0.845 | 0.224 |
| LP2-OL-08MOD | Quenched | 2.535 | 4.522 | 0.872 |
| | CCC | 18.526 | 22.386 | 1.979 |
| LP2-OL-09-1 | Quenched | 3.117 | 1.843 | 0.250 |
| | CCC | 2.309 | 1.453 | 0.246 |
| LP2-OL-10MOD | Quenched | 0.339 | 0.809 | 0.187 |
| | CCC | 9.581 | 5.007 | 0.408 |
| LP2-OL-11 | Quenched | 7.737 | 7.210 | 1.214 |
| | CCC | 7.129 | 6.675 | 1.235 |
| LP2-OL-12 | Quenched | 34.223 | 26.813 | 4.068 |
| | CCC | 35.740 | 28.587 | 4.489 |
| LP2-OL-13 | Quenched | 1.031 | 3.885 | 0.640 |
| | CCC | 11.643 | 14.231 | 1.560 |
| LP2-OL-14 | Quenched | 14.466 | 12.760 | 2.076 |
| | CCC | 9.921 | 9.293 | 1.788 |
| LP2-OL-15 | Quenched | 0.552 | 0.875 | 0.243 |
| | CCC | 0.477 | 0.840 | 0.221 |
| LP2-OL-16MOD | Quenched | 2.608 | 2.612 | 0.904 |
| | CCC | 2.179 | 2.153 | 0.753 |
| LP2-OL-17 | Quenched | 11.233 | 9.488 | 2.306 |
| | CCC | 12.632 | 10.825 | 2.582 |
| LP2-OL-18 | Quenched | 2.366 | 2.371 | 0.581 |
| | CCC | 0.350 | 0.968 | 0.259 |
| LP2-OL-19 | Quenched | 0.777 | 1.825 | 0.533 |
| | CCC | 0.739 | 1.743 | 0.483 |
| LP2-OL-20 | Quenched | 0.540 | 2.182 | 0.331 |
| | CCC | 1.848 | 4.560 | 0.886 |
| LP2-OL-21 | Quenched | 0.901 | 1.041 | 0.354 |
| | CCC | 0.985 | 1.003 | 0.328 |
| LP2-OL-22 | Quenched | 0.395 | 1.078 | 0.222 |
| | CCC | 0.459 | 1.051 | 0.215 |
| LP2-OL-23 | Quenched | 0.961 | 1.194 | 0.323 |

| Glass ID | Type | B (g/L) | Na (g/L) | Si (g/L) |
|---|---|---|---|---|
| | CCC | 0.753 | 1.077 | 0.266 |
| LP2-OL-24 | Quenched | 0.914 | 1.746 | 0.448 |
| | CCC | 3.242 | 4.030 | 0.718 |
| LP2-OL-25 | Quenched | 5.148 | 3.864 | 0.624 |
| | CCC | 5.697 | 4.138 | 0642 |

Figure 3.6 compares the PCT normalized releases of B with the normalized releases of Na for the quenched glass samples. Figure 3.6 shows that B values tend to be lower than Na values below approximately the natural log of 0.7 g/m$^2$. Above approximately the natural log of 1 g/m$^2$, the B values tend to be at or slightly above the Na values. Figure 3.7 compares the PCT normalized releases of B with the normalized releases of Na for the CCC glass samples. Figure 3.7 shows that the PCT normalized releases of B are typically lower than those of Na for CCC glass samples.

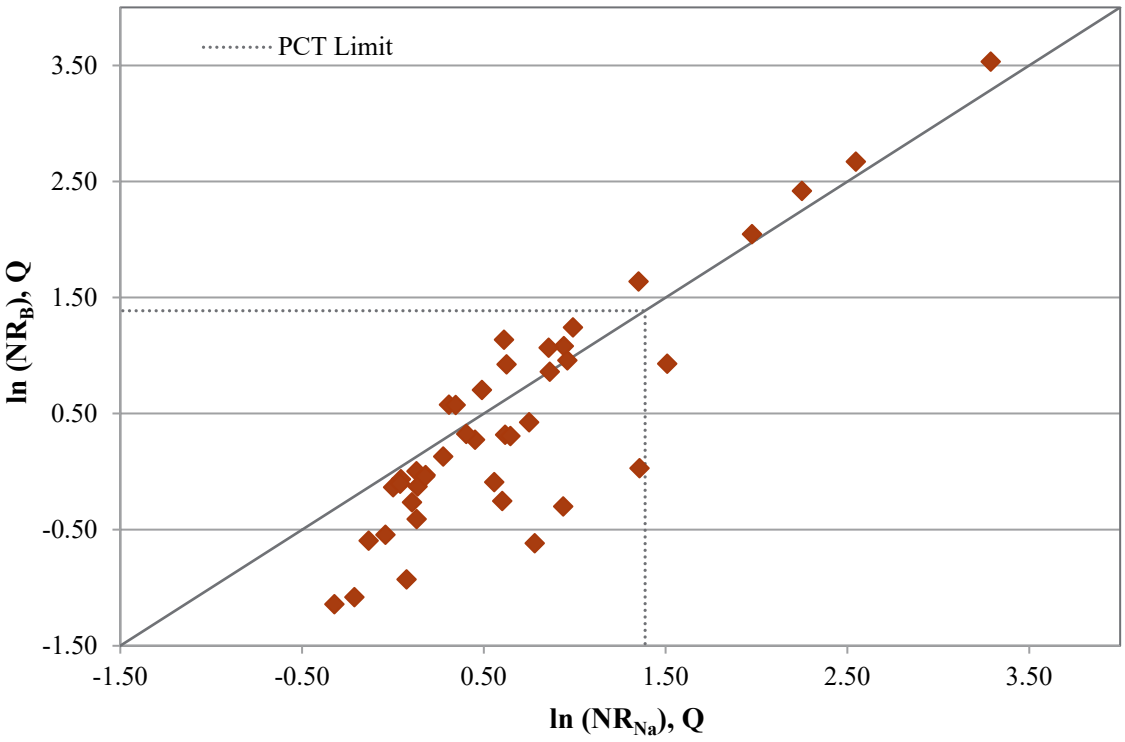


Figure 3.6. Comparison of Natural Logarithms of PCT Normalized Releases of B and Na (both g/L) for Quenched Samples of Phase 2 Enhanced LAW Glasses

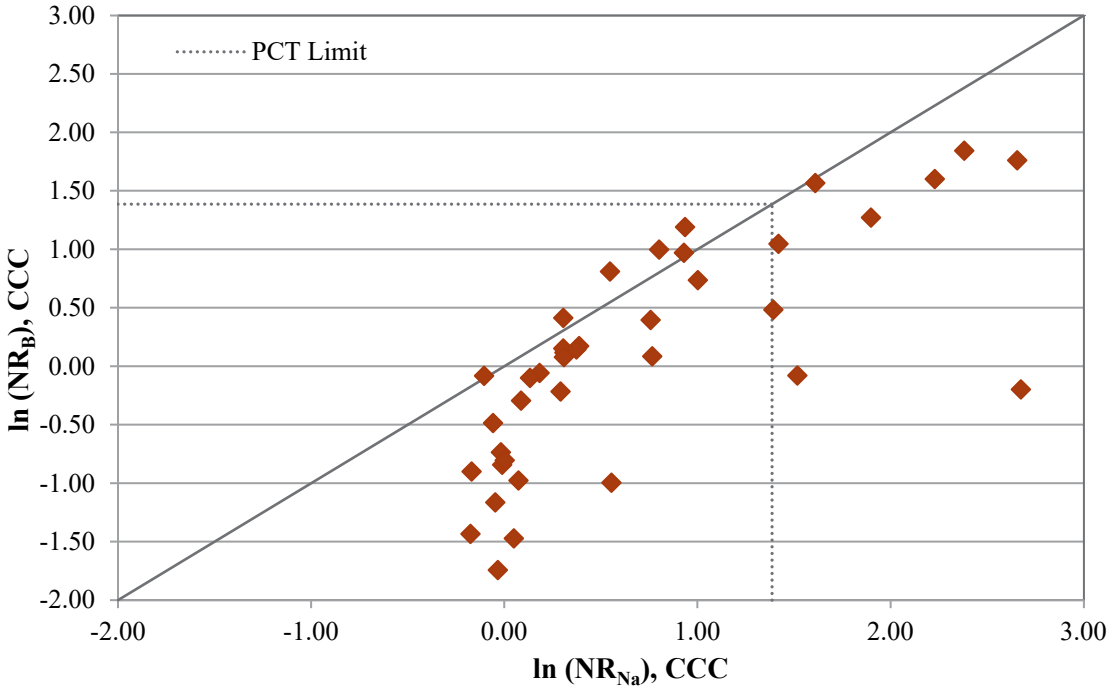


Figure 3.7. Comparison of Natural Logarithms of PCT Normalized Releases of B and Na (g/L) for CCC Samples of Phase 2 Enhanced LAW Glasses

Figure 3.8 shows the measured Na and B normalized releases compared to the predictions using previous models for Na and B normalized releases of LAW glasses from Piepel et al. (2007). These models were partial quadratic mixture (PQM) models of the form

$$\ln(NR) = \sum_{i=1}^{q} b_i x_i + \text{selected}\left\{ \sum_{i=1}^{q} b_{ii} x_i^2 + \sum_{j=1}^{q-1} \sum_{k=j+1}^{q} b_{jk} x_j x_k \right\} \quad (3.8)$$

where

| | |
|---|---|
| $NR$ | normalized release of B or Na (g/L) |
| $q$ | number of components in the waste glass |
| $x_i$ | mass fraction of the $i$th component |
| $b_i$ | coefficient of the $i$th component |
| $b_{ii}$ | coefficient for the $i$th component squared |
| $b_{jk}$ | coefficient for the crossproduct of the $j$th and $k$th components |

However, the models from that report were for a different LAW glass composition region that did not include enhanced waste glasses. The coefficients for the B model are listed in Table 3. and for the Na model are listed in Table 3.5. It appears that the B releases are generally overpredicted, and the Na releases are generally underpredicted using these models. These prediction differences in PCT releases for the Phase 2 LAW glasses are likely a result of the Piepel et al. (2007) models being developed from data over a composition region that did not include enhanced waste glasses. Also, it was noted in Piepel et al. (2007) that the recommend partial quadratic mixture models were not as accurate with higher waste

loadings and higher Na and B releases. Since the current effort is to increase waste loading, new PCT models are needed to ensure that the LAW glasses meet the release limit of 2 g/m$^2$ (4 g/L).

Table 3.10. Coefficients for PCT Boron (g/L) Model (Piepel 2007)

| Component | Coefficient | Component | Coefficient |
|---|---|---|---|
| $Al_2O_3$ | -31.3612 | $P_2O_5$ | -19.254 |
| $B_2O_3$ | 11.8101 | $SiO_2$ | -1.6161 |
| CaO | -13.8404 | $ZrO_2$ | -6.6289 |
| $Fe_2O_3$ | -16.5948 | Others (1) | -5.169 |
| $K_2O$ | 7.9687 | $B_2O_3$ x MgO | 488.8612 |
| MgO | -21.2343 | $Na_2O$ x $SiO_2$ | -74.3462 |
| $Na_2O$ | 46.1599 | CaO x $Fe_2O_3$ | 212.0947 |

(1) The data Piepel et al. (2007) used to fit this model contained many minor components in Others. However, in the Phase 2 LAW glasses for which the model was used to predict, Others included only $SO_3$, Cl, F, $Cr_2O_3$ and ZnO.

Table 3.5. Coefficients for PCT Sodium (g/L) Model (Piepel 2007)

| Component | Coefficient | Component | Coefficient |
|---|---|---|---|
| $Al_2O_3$ | -20.7142 | $P_2O_5$ | -14.5324 |
| $B_2O_3$ | -6.5489 | $SiO_2$ | -4.8834 |
| CaO | 0.0151 | $ZrO_2$ | -0.62 |
| $Fe_2O_3$ | -8.4617 | Others (1) | 3.345 |
| $K_2O$ | -0.8724 | $B_2O_3$ x MgO | 437.4267 |
| MgO | -13.8667 | $Na_2O$ x $B_2O_3$ | 87.6716 |
| $Na_2O$ | 9.9942 | CaO x $Fe_2O_3$ | 182.6191 |
| | | $K_2O$ x $K_2O$ | 315.6867 |

(1) The data Piepel et al. (2007) used to fit this model contained many minor components in Others. However, in the Phase 2 LAW glasses for which the model was used to predict, Others included only $SO_3$, Cl, F, $Cr_2O_3$ and ZnO.

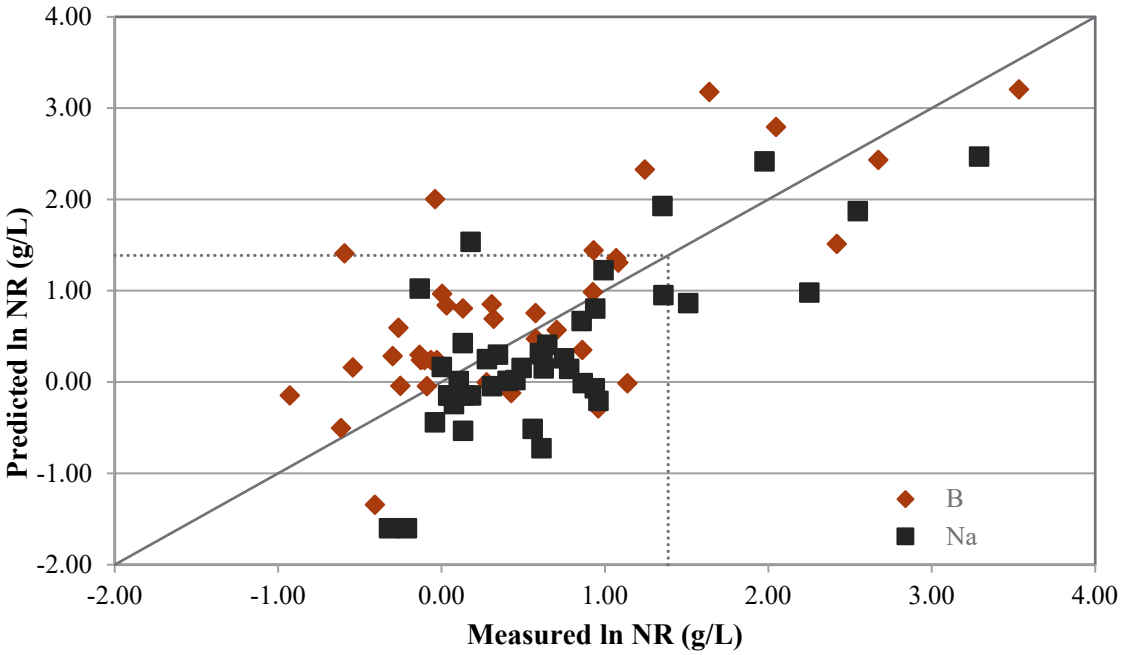


Figure 3.8. Predicted Versus Measured Natural Logarithms of Normalized Releases (g/L) of Boron and Sodium for Phase 2 Enhanced LAW Glasses. The predicted values were obtained using the model form in Equation (3.8) with coefficients listed in Tables 3.10 and 3.11.

Figure 3.9 compares the normalized releases (g/L) of the quenched and CCC glasses. When significant crystals containing Al and Si (>10 wt%) are present in the glass, CCC-treated samples can have notably higher releases than quenched samples. This may be because the crystals remove the glass formers (Si and Al) from the bulk glass structure and composition, making it less durable.

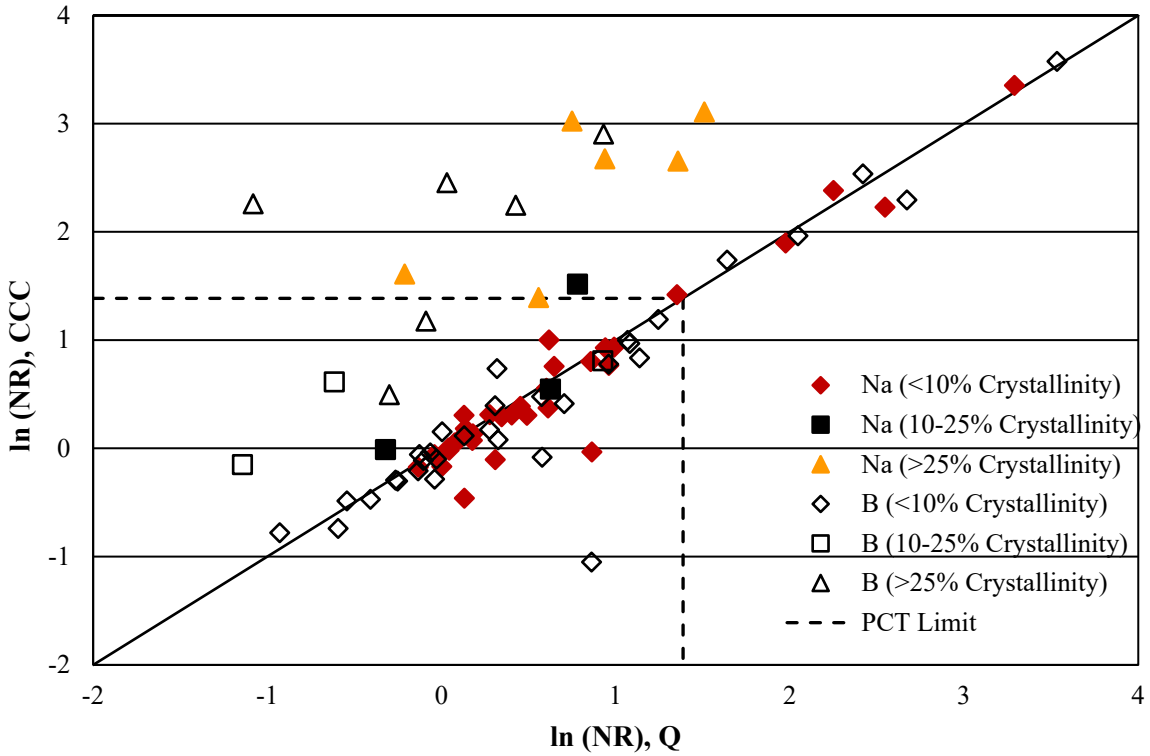


Figure 3.9. Comparison of Natural Logarithm of PCT Normalized Release (g/L) of B and Na for Quenched and CCC-Treated Samples of Phase 2 Enhanced LAW Glasses that Contain Aluminosilicates

## 3.8 Vapor Hydration Test (VHT)

This section presents and discusses the VHT results obtained using the methods discussed in Section 2.10.

Table 3. shows the alteration depth (µm) and corrosion rate (g/m$^2$/d) of each glass based on the VHT. For VHT, alteration depth equal to or less than 50 µm, the measured values were rounded to nearest 0.05 µm; and for VHT alteration depth larger than 50 µm, the measured values were rounded to nearest 0.5 µm. See Appendix I for photos of the glass samples after the VHT. A total of 14 of the 41 quenched glasses failed the VHT, with a corrosion rate of >50 g/m$^2$/d (

Table 3.). A total of 11 of the 41 CCC glasses failed the VHT, with a corrosion rate of >50 g/m$^2$/d (Table 3.). The glasses tested performed either extremely well or extremely poor, with only three quenched glasses and one CCC glass near the corrosion rate limit. Ideally there would have been a better distribution of VHT corrosion rates for the Phase 2 LAW glasses. Still, glasses with corrosion rates above and below the limit are necessary for developing property-composition models that can predict glasses that meet or fail the limit.

Table 3.6. VHT Results from the Quenched Phase 2 Enhanced LAW Glasses

| Glass ID | Density ($g/cm^3$) | Temp. (°C) | Days | Alteration Depth (µm) | Rate ($g/m^2/d$) | Comparison to Limit of 50 $g/m^2/d$ |
|---|---|---|---|---|---|---|
| LP2-IL-01-Q | 2.6864 | 200 | 7 | 131.5 | 49.8 | 100% |
| LP2-IL-02-Q | 2.6881 | 200 | 7 | 86.0 | 32.6 | 65% |
| | | | 24 | 7.10 | 0.80 | 2% |
| LP2-IL-03-Q | 2.6808 | 200 | 7 | 447.5 | 169.4 | 339% |
| LP2-IL-04-Q | 2.6986 | 200 | 7 | 21.15 | 8.0 | 16% |
| | | | 24 | 9.00 | 1.0 | 2% |
| LP2-IL-05-Q | 2.7014 | 200 | 7 | 1.00 | 0.4 | 1% |
| | | | 24 | 46.70 | 5.2 | 10% |
| LP2-IL-06-Q | 2.6306 | 200 | 7 | 351.0 | 132.9 | 266% |
| LP2-IL-07-Q | 2.6329 | 200 | 7 | 299.0 | 113.2 | 226% |
| LP2-IL-08-Q | 2.7031 | 200 | 7 | 0.60 | 0.2 | 1% |
| | | | 24 | 111.0 | 12.3 | 25% |
| LP2-IL-09-Q | 2.6861 | 200 | 7 | 93.5 | 35.4 | 71% |
| | | | 24 | 286.5 | 31.6 | 63% |
| LP2-IL-10-Q | 2.6625 | 200 | 7 | 281.5 | 106.6 | 213% |
| LP2-IL-11-Q | 2.7011 | 200 | 7 | 14.80 | 5.6 | 11% |
| | | | 24 | 246.0 | 27.2 | 54% |
| LP2-IL-12-Q | 2.6508 | 200 | 7 | 95.5 | 36.2 | 72% |
| | | | 24 | 416.0 | 45.9 | 92% |
| LP2-IL-13-Q | 2.6443 | 200 | 7 | 7.60 | 2.9 | 6% |
| | | | 24 | 19.35 | 2.1 | 4.% |
| LP2-IL-14-Q | 2.6506 | 200 | 7 | 96.5 | 36.5 | 73% |
| | | | 24 | 355.5 | 39.3 | 79% |
| LP2-IL-15-Q | 2.6422 | 200 | 7 | 3.20 | 1.2 | 2% |
| | | | 24 | 57.0 | 6.3 | 13% |
| LP2-IL-16-Q | 2.6665 | 200 | 7 | 88.0 | 33.3 | 67% |
| | | | 24 | 431.0 | 47.6 | 95% |
| LP2-IL-17-Q | 2.6250 | 200 | 7 | 165.5 | 62.7 | 125% |
| LP2-OL-01-3-Q | 2.6435 | 200 | 11 | 66.5 | 16.0 | 32% |
| | | | 24 | 4.85 | 0.5 | 1% |

| Glass ID | Density (g/cm$^3$) | Temp. (°C) | Days | Alteration Depth (µm) | Rate (g/m$^2$/d) | Comparison to Limit of 50 g/m$^2$/d |
|---|---|---|---|---|---|---|
| LP2-OL-02-1-Q | 2.6121 | 200 | 11 | 104.5 | 25.2 | 50% |
| | | | 24 | 11.30 | 1.2 | 3% |
| LP2-OL-03-MOD2-Q | 2.6597 | 200 | 24 | 210.0 | 23.2 | 46% |
| LP2-OL-04-1-Q | 2.6779 | 200 | 11 | 0.00 | 0.0 | 0% |
| | | | 24 | 24.20 | 2.7 | 5% |
| LP2-OL-05-Q | 2.6771 | 200 | 11 | 117.0 | 28.2 | 56% |
| | | | 24 | 47.25 | 5.2 | 10% |
| LP2-OL-07-1-Q | 2.6154 | 200 | 11 | 68.0 | 16.4 | 33% |
| | | | 24 | 143.0 | 15.8 | 32% |
| LP2-OL-08-MOD-Q | 2.6867 | 200 | 7 | 289.0 | 109.4 | 219% |
| | | | 24 | >680 | >75.1 | >150% |
| LP2-OL-09-1-Q | 2.5882 | 200 | 11 | 125.5 | 30.2 | 61% |
| | | | 24 | 92.5 | 10.2 | 20% |
| LP2-OL-10-MOD-Q | 2.6326 | 200 | 24 | 78.5 | 8.7 | 17% |
| LP2-OL-11-Q | 2.6503 | 200 | 11 | 483.0 | 116.4 | 233% |
| | | | 24 | 501.5 | 55.4 | 111% |
| LP2-OL-12-Q | 2.6280 | 200 | 11 | 666.5 | 160.6 | 321% |
| | | | 24 | >775 | >85.6 | >171% |
| LP2-OL-13-Q | 2.6591 | 200 | 11 | >675 | >162.6 | >325% |
| | | | 24 | 460.0 | 50.8 | 102% |
| LP2-OL-14-Q | 2.5884 | 200 | 7 | >480 | >181.7 | >363% |
| | | | 24 | >555 | >61.3 | >123% |
| LP2-OL-15-Q | 2.7081 | 200 | 24 | 11.30 | 1.2 | 3% |
| LP2-OL-16-MOD-Q | 2.5838 | 200 | 24 | 34.65 | 3.8 | 8% |
| LP2-OL-17-Q | 2.6448 | 200 | 7 | >730 | >276.4 | >553% |
| | | | 24 | >700 | >77.3 | >155% |
| LP2-OL-18-Q | 2.7360 | 200 | 24 | 86.0 | 9.5 | 19% |
| LP2-OL-19-Q | 2.6082 | 200 | 7 | 320.0 | 121.1 | 242% |
| | | | 24 | >770 | >85 | >170% |
| LP2-OL-20-Q | 2.6351 | 200 | 7 | 689.7 | 261 | 522% |
| | | | 24 | >705 | >77.8 | >156% |
| LP2-OL-21-Q | 2.6409 | 200 | 24 | 222.5 | 24.6 | 49% |
| LP2-OL-22-Q | 2.7456 | 200 | 24 | 12.55 | 1.4 | 3% |
| LP2-OL-23-Q | 2.7296 | 200 | 24 | 19.40 | 2.1 | 4% |
| LP2-OL-24-Q | 2.6658 | 200 | 24 | 126.0 | 13.9 | 28% |

| Glass ID | Density (g/cm$^3$) | Temp. (°C) | Days | Alteration Depth (µm) | Rate (g/m$^2$/d) | Comparison to Limit of 50 g/m$^2$/d |
|---|---|---|---|---|---|---|
| LP2-OL-25-Q | 2.7053 | 200 | 24 | 251.0 | 27.7 | 55% |

Table 3.7. VHT Results from the CCC Phase 2 Enhanced LAW Glasses

| Glass ID | Days | Alteration Depth (µm) | Rate (g/m$^2$/d) | Comparison to Limit of 50 g/m$^2$/d |
|---|---|---|---|---|
| LP2-IL-01-CCC | 7 | 111.0 | 42.0 | 84% |
| | 24 | 410.5 | 45.3 | 91% |
| LP2-IL-02-CCC | 7 | 55.0 | 20.8 | 42% |
| | 24 | 377.5 | 41.7 | 83% |
| LP2-IL-03-CCC | 7 | 2.85 | 1.1 | 2% |
| | 24 | 183.0 | 20.2 | 40% |
| LP2-IL-04-CCC | 7 | 478.0 | 181.0 | 362% |
| LP2-IL-05-CCC | 7 | 10.85 | 4.1 | 8% |
| | 24 | 116.5 | 12.9 | 26% |
| LP2-IL-06-CCC | 7 | 279.5 | 105.8 | 212% |
| LP2-IL-07-CCC | 7 | 204.0 | 77.2 | 154% |
| LP2-IL-08-CCC | 7 | 34.55 | 13.1 | 26% |
| | 24 | 240.0 | 26.5 | 53% |
| LP2-IL-09-CCC | 7 | 24.00 | 9.1 | 18% |
| | 24 | 142.5 | 15.7 | 31% |
| LP2-IL-10-CCC | 7 | 21.6 | 8.2 | 16% |
| | 24 | 331.0 | 36.5 | 73% |
| LP2-IL-11-CCC | 7 | 27.55 | 10.4 | 21% |
| | 24 | 160.0 | 17.7 | 35% |
| LP2-IL-12-CCC | 7 | 3.90 | 1.5 | 3% |
| | 24 | 37.30 | 4.1 | 8% |
| LP2-IL-13-CCC | 24 | 44.20 | 4.9 | 10% |
| LP2-IL-14-CCC | 7 | 172.5 | 65.3 | 131% |
| LP2-IL-15-CCC | 7 | 37.40 | 14.2 | 28% |
| | 24 | 115.5 | 12.8 | 26% |
| LP2-IL-16-CCC | 24 | 87.5 | 9.7 | 19% |
| LP2-IL-17-CCC | 7 | 10.30 | 3.9 | 8% |
| | 24 | 283.5 | 31.3 | 63% |
| LP2-OL-01-3-CCC | 11 | 90.5 | 21.8 | 44% |

| Glass ID | Days | Alteration Depth (µm) | Rate ($g/m^2/d$) | Comparison to Limit of 50 $g/m^2/d$ |
|---|---|---|---|---|
| LP2-OL-02-1-CCC | 24 | 35.30 | 3.9 | 8% |
| | 24 | 219.5 | 24.2 | 48% |
| LP2-OL-03-MOD2-CCC | 7 | 5.75 | 2.2 | 4% |
| | 24 | 265.0 | 29.3 | 59% |
| LP2-OL-04-1-CCC | 11 | 294.0 | 70.8 | 142% |
| LP2-OL-05-CCC | 7 | 5.75 | 2.2 | 4% |
| | 24 | 41.10 | 4.5 | 9% |
| LP2-OL-07-1-CCC | 24 | 18.15 | 2.0 | 4% |
| LP2-OL-08-MOD-CCC | 7 | 18.25 | 6.9 | 14% |
| | 24 | 372.5 | 41.1 | 82% |
| LP2-OL-09-1-CCC | 24 | 46.45 | 5.1 | 10% |
| LP2-OL-10-MOD-CCC | 7 | 66.0 | 25.0 | 50% |
| | 24 | 33.90 | 3.7 | 7% |
| LP2-OL-11-CCC | 24 | 26.45 | 2.9 | 6% |
| LP2-OL-12-CCC | 7 | 114.0 | 43.2 | 86% |
| | 24 | >570.0 | >62.9 | >126% |
| LP2-OL-13-CCC | 7 | ≥755.0 | 285.8 | 572% |
| | 24 | 612.5 | 67.6 | 135% |
| LP2-OL-14-CCC | 7 | >625.0 | >236.6 | >473% |
| | 24 | 521.5 | 57.6 | 115% |
| LP2-OL-15-CCC | 24 | 19.35 | 2.1 | 4% |
| LP2-OL-16-MOD-CCC | 24 | 8.10 | 0.9 | 2% |
| LP2-OL-17-CCC | 7 | >770.0 | >291.5 | >583% |
| | 24 | >725.0 | >80.1 | >160% |
| LP2-OL-18- CCC | 7 | 56.50 | 21.4 | 43% |
| | 24 | 53.0 | 5.9 | 12% |
| LP2-OL-19-CCC | 24 | 0.00 | 0.0 | 0% |
| LP2-OL-20-CCC | 7 | ≥715.0 | 270.7 | 541% |
| | 24 | >895.0 | >98.8 | >198% |
| LP2-OL-21-CCC | 24 | 197.5 | 21.8 | 44% |
| LP2-OL-22-CCC | 24 | 28.30 | 3.1 | 6% |
| LP2-OL-23-CCC | 24 | 126.5 | 14.0 | 28% |
| LP2-OL-24-CCC | 7 | 339.0 | 128.3 | 257% |
| | 24 | >735.0 | >81.2 | >162% |
| LP2-OL-25-CCC | 24 | 240.5 | 26.6 | 53% |

Figure 3.10 shows how much the total normalized alkali [Nalk = $Na_2O$ + 0.66($K_2O$) + 2($Li_2O$)] decreases the durability of the LAW glasses by plotting the VHT results against the total normalized alkali values. Basically, all the glasses up to 23 wt% alkali passed the VHT. Above 23 wt% alkali, the glasses began failing; at about 26 wt%, all but one of the current glasses failed the VHT.

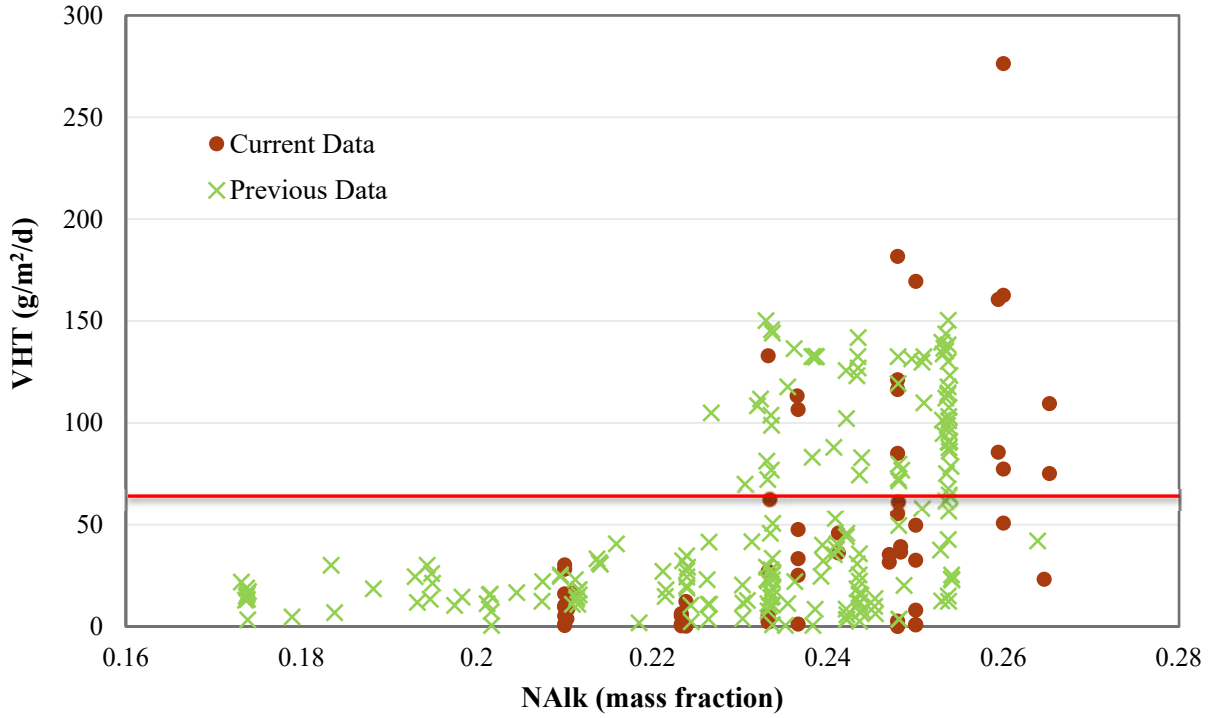


Figure 3.10. VHT Response Compared to the Total Normalized Alkali [Nalk = $Na_2O$ + 0.66($K_2O$) + 2($Li_2O$)] Content of the Glass

Figure 3.11 shows the quenched glass alteration depth versus the CCC glass alteration depth results depending on amount of crystallinity in the glass. There does not appear to be any correlation between amount of crystallinity in the glass and the depth of glass alteration. The corrosion rate per day was also looked at and did not appear to have a direct correlation.

The VHT data were also compared to predictions from a VHT model (Piepel et al. 2007), which is a 15-term reduced partial cubic mixture model based on alteration depth (Figure 3.12), with the coefficients shown in Table 3.8. The VHT data were also compared to predictions from another VHT model (Piepel et al. 2007), a 16-term reduced partial quadratic mixture model based on alteration depth (Figure 3.13), with the coefficients shown in Table 3.9. There was relatively large scatter in data points using the models from Piepel et al. (2007). There are likely several reasons for this. First, the VHT is known to produce large variability in VHT results, even for the same glass composition. Second, Piepel et al. (2007) noted that their models had large, and statistically significant lack-of-fits, possibly due to the large variability in VHT results. Third, the Phase 2 LAW glasses have higher waste loadings than the glasses used to develop the Piepel et al. (2007) models. Hence, models developed using glasses with higher waste loadings and other approaches should be tried to produce a model that would fit the data closer.

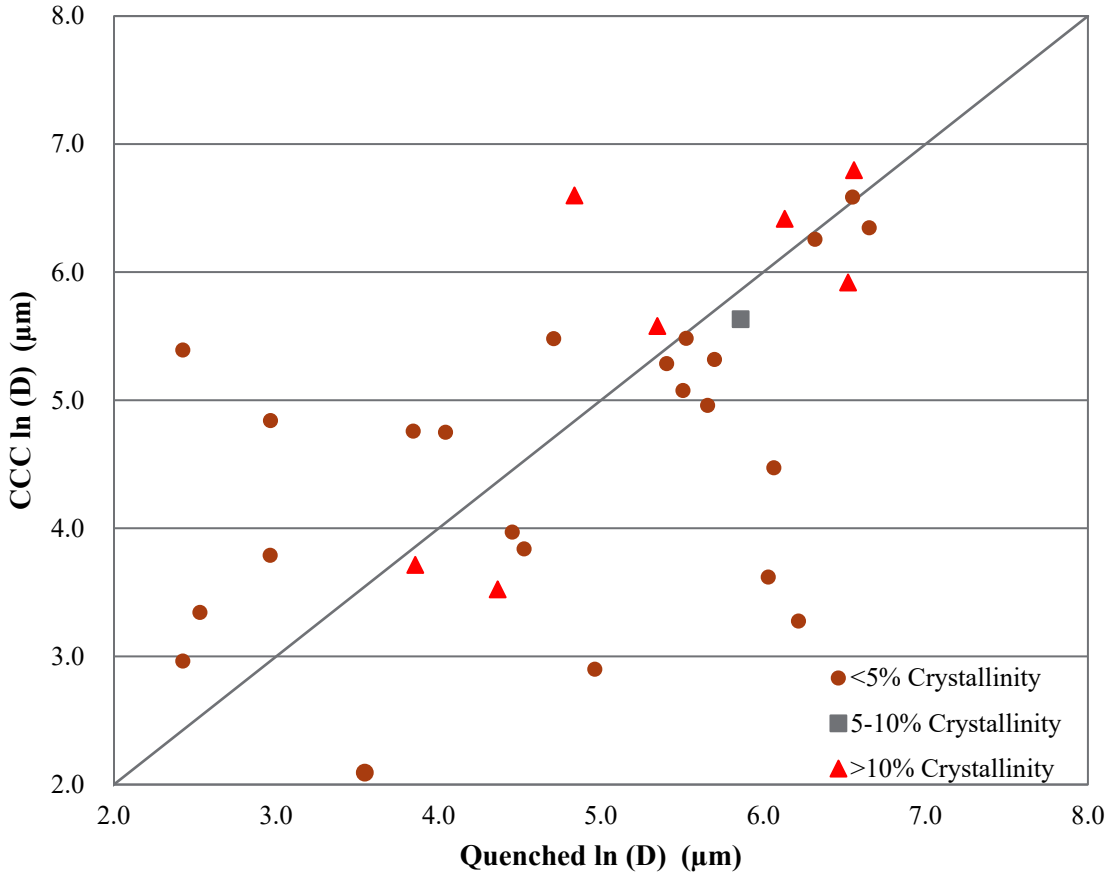


Figure 3.11 Natural Logarithm of VHT Alteration Depth Results for CCC versus Quenched Versions of Phase 2 Enhanced LAW Glasses

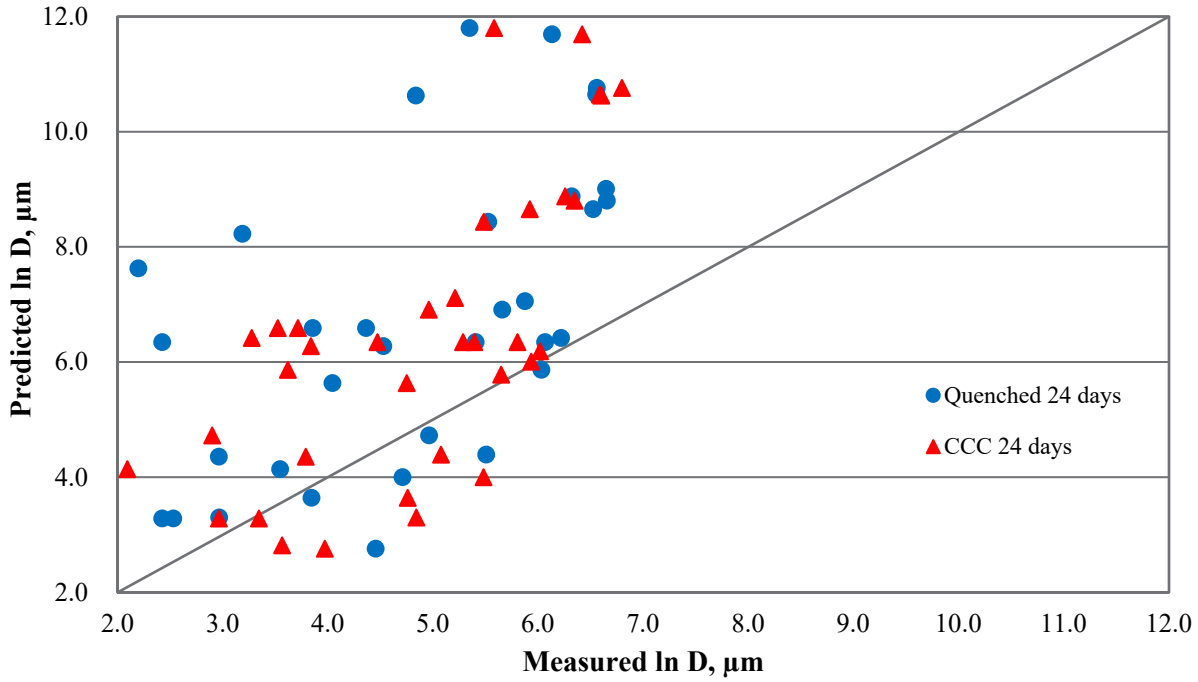


Figure 3.12. Natural Logarithm of VHT Alteration Depth Results Predicted using 15-Term Reduced Partial Cubic Mixture Model Versus Measured Values for Phase 2 Enhanced LAW Glasses

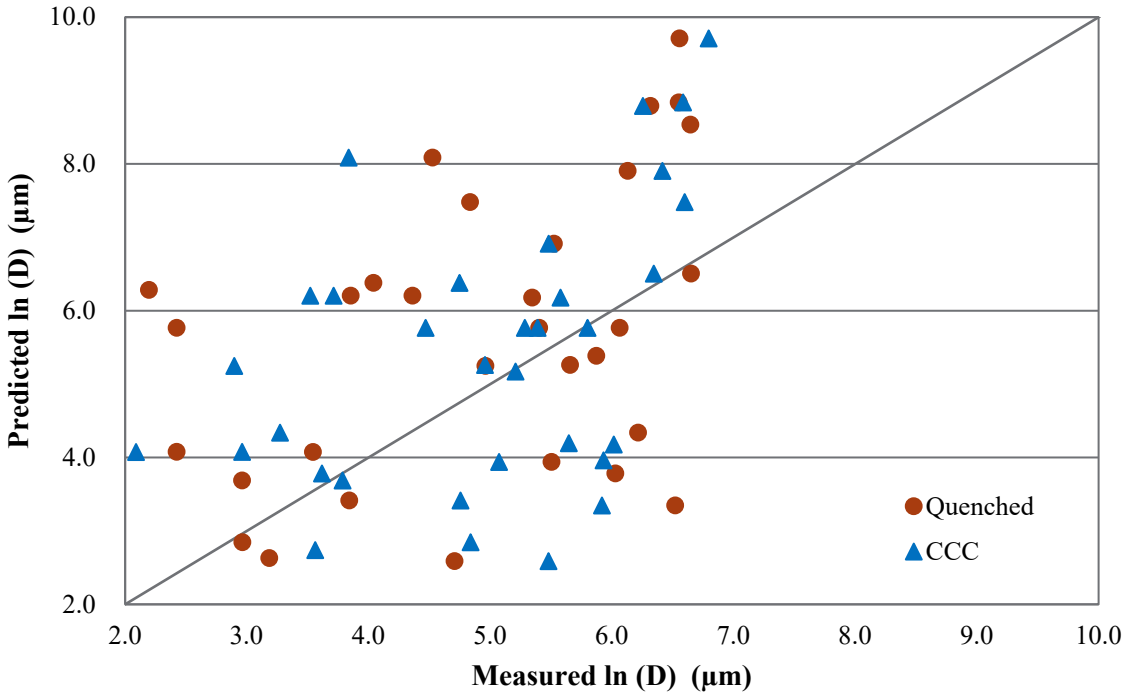


Figure 3.13. Natural Logarithm of VHT Alteration Depth Results Predicted using 16-Term Reduced Partial Quadratic Mixture Model Versus Measured VHT Values for Phase 2 Enhanced LAW Glasses

Table 3.8. Coefficients for 15-Term Reduced Partial Cubic Mixture Model Based on Alteration Depth for VHT Data (Piepel 2007)

| Component | Coefficient | Component | Coefficient |
|---|---|---|---|
| $Al_2O_3$ | 19.5685 | $SiO_2$ | -0.5137 |
| $B_2O_3$ | 18.5336 | $ZrO_2$ | -62.8457 |
| CaO | 38.2412 | Others (1) | -0.4293 |
| $Fe_2O_3$ | -8.4126 | $K_2O$ x $K_2O$ x $Na_2O$ | 10138.2817 |
| $K_2O$ | -39.3124 | $(Na_2O)^3$ | 872.6563 |
| MgO | -8.3068 | $Na_2O$ x CaO x $B_2O_3$ | -1943.0687 |
| $Na_2O$ | -20.6518 | | |

(1) The data Piepel et al. (2007) used to fit this model contained many minor components in Others. However, in the Phase 2 LAW glasses for which the model was used to predict, Others included only $SO_3$, Cl, F, $Cr_2O_3$ and ZnO.

Table 3.9. Coefficients for 16-Term Reduced Partial Quadratic Mixture Model on Natural Logarithm of VHT Alteration Depth (Piepel 2007)

| Component | Coefficient | Component | Coefficient |
|---|---|---|---|
| $Al_2O_3$ | 66.1577 | $SiO_2$ | -29.0882 |
| $B_2O_3$ | 5.2229 | $ZrO_2$ | 77.6908 |
| CaO | -233.0861 | Others (1) | 1.7371 |
| $Fe_2O_3$ | -5.2172 | $Al_2O_3$ x $ZrO_2$ | -1479.4599 |
| $K_2O$ | -33.5013 | $Na_2O$ x MgO | -920.4672 |
| MgO | 111.5235 | CaO x $SiO_2$ | 556.6025 |
| $Na_2O$ | 75.4548 | $K_2O$ x $K_2O$ | 1605.6605 |
| | | $Na_2O$ x $ZrO_2$ | -336.1985 |

(1) The data Piepel et al. (2007) used to fit this model contained many minor components in Others. However, in the Phase 2 LAW glasses for which the model was used to predict, Others included only $SO_3$, Cl, F, $Cr_2O_3$ and ZnO.

## 3.9 Sulfur Solubility Results

This section presents and discusses the sulfur solubility results of test glasses obtained using the methods discussed in Section 2.11. For each glass, the as melted sample (called baseline in this subsection) and the "sulfur-saturated" (SSM) sample were analyzed by ICP-AES and IC. The chemical analysis results of the baseline glasses have been presented and discussed in Section 3.1. More detailed chemical analysis results have been reported by Fox et al. (2017, 2018).

Note that 41 glass samples were prepared based on the glasses listed in Table 1.3. The measured $Na_2O$ concentrations were slightly below the targeted values for both baseline (0.011 mf) and SSM samples. There were no indications of errors in glass preparation or measurement that had to be addressed in using the data. Therefore, the entire set of measurement data was used in determining representative, measured compositions for the SSM versions of the glasses.

Table 3. and Figure 3.14 summarize the analyzed $SO_3$ concentrations in the baseline and the sulfur-saturated glasses. The $SO_3$ concentrations in the baseline glasses were mostly below 0.015 mass fraction (including several glasses with low $SO_3$ at 0.001 mass fraction). After sulfur-saturation, there was a significant increase of $SO_3$ in the Phase 2 LAW glasses, which is considered the experimentally determined $SO_3$ solubility of the glass. In most glasses, the $SO_3$ solubilities (i.e., the saturated $SO_3$ concentrations) were between 1.1 wt% and 1.5 wt%. Three glasses had a $SO_3$ solubility slightly above 2.0 wt%, with the highest $SO_3$ solubility being 2.6 wt% in glass LP2-OL-14.

Appendix J shows the analyzed glass compositions after normalization of the baseline and sulfur-saturated glass samples. Comparisons of the compositions showed that after the sulfur-saturation, other major glass components only have negligible changes except when the $SO_3$ reaches a sulfur-saturation mass fraction greater than about 0.015. For the minor components, $K_2O$ decreases, which may be due to ion-exchange, and the losses of the Cl, F, and $P_2O_5$ may be due to volatilization during multiple times of melting and/or extraction into the salt.

The compositions of the sulfur-saturated glasses based on chemical analyses and normalization have been used to evaluate a preliminary $SO_3$ solubility model (Vienna et al. 2014). The empirical model produces the predicted $SO_3$ solubility using a PQM model of the form

$$w_{SO_3}^{Pred} = \sum_{i=1}^{q} s_i n_i + \text{selected}\left\{ \sum_{i=1}^{q} s_{ii} n_i^2 + \sum_{j=1}^{q-1} \sum_{k=j+1}^{q} s_{jk} n_j n_k \right\} \quad (3.8)$$

where

| | |
|---|---|
| $w_{SO_3}^{Pred}$ | the predicted $SO_3$ solubility (in wt%) |
| $q$ | the number of components in the waste glass except for $SO_3$ |
| $n_i$ | normalized (after removing $SO_3$) mass fraction of the $i$th component |
| $s_i$ | coefficient of the $i$th component |
| $s_{ii}$ | coefficient for the $i$th component squared |
| $s_{jk}$ | coefficient for the crossproduct of the $j$th and $k$th components |

The model coefficients are listed in Table 3.11. In this preliminary model, only $Li_2O$ has a squared term ($s_{ii}$) and there are no crossproduct terms ($s_{jk}$).

The model predicted and measured $SO_3$ solubility values are compared in Figure 3.15. The data points are below the equal line, indicating the $SO_3$ solubility values for the Phase 2 LAW glasses are underpredicted by the model. The underprediction is expected because a large portion of data used to develop the preliminary model were not fully saturated with $SO_3$. The previous samples were prepared by one-time mixing and melting of the baseline glasses with $Na_2SO_4$, which could not fully saturate the glass and achieve the true $SO_3$ solubility. On the other hand, the three-times-mixing-and-melting sulfur-saturation method developed in this work (see Section 2.10) can fabricate glasses fully saturated by $SO_3$ and determine the true $SO_3$ solubility of the glass (Jin et al. 2019; Skidmore et al. 2019). Future work will help modify the preliminary model using this new experimentally determined $SO_3$ solubility data to improve the empirical model.

Table 3.10. Target and Measured Baseline Values of $SO_3$ (mass fraction) and $SO_3$ Solubility (wt%) Values for Phase 2 Enhanced LAW Glasses

| | $SO_3$, Mass Fraction | | $SO_3$ |
|---|---|---|---|
| Sample ID | Target Baseline | Measured Baseline | Solubility (wt%) |
| LP2-IL-01 | 0.00800 | 0.00806 | 1.503 |
| LP2-IL-02 | 0.00800 | 0.00792 | 1.180 |
| LP2-IL-03 | 0.00200 | 0.00211 | 1.180 |
| LP2-IL-04 | 0.00200 | 0.00229 | 1.484 |
| LP2-IL-05 | 0.00200 | 0.00212 | 1.489 |
| LP2-IL-06 | 0.00800 | 0.00782 | 1.035 |
| LP2-IL-07 | 0.00800 | 0.00782 | 1.632 |
| LP2-IL-08 | 0.00800 | 0.00763 | 1.373 |
| LP2-IL-09 | 0.00200 | 0.00212 | 1.444 |
| LP2-IL-10 | 0.00500 | 0.00469 | 1.337 |
| LP2-IL-11 | 0.00200 | 0.00199 | 1.189 |
| LP2-IL-12 | 0.00200 | 0.00206 | 1.468 |
| LP2-IL-13 | 0.00200 | 0.00199 | 1.236 |
| LP2-IL-14 | 0.00800 | 0.00767 | 1.496 |
| LP2-IL-15 | 0.00800 | 0.00741 | 1.252 |
| LP2-IL-16 | 0.00500 | 0.00486 | 1.338 |
| LP2-IL-17 | 0.01000 | 0.00954 | 1.321 |
| LP2-OL-01-3 | 0.00100 | 0.00154 | 1.489 |
| LP2-OL-02-1 | 0.00500 | 0.00479 | 1.098 |
| LP2-OL-03-MOD2 | 0.00754 | 0.00725 | 1.445 |
| LP2-OL-04-1 | 0.00100 | 0.00154 | 1.092 |
| LP2-OL-05 | 0.00980 | 0.00929 | 1.427 |
| LP2-OL-07-1 | 0.01060 | 0.01011 | 1.634 |
| LP2-OL-08-MOD | 0.00816 | 0.00633 | 1.816 |
| LP2-OL-09-1 | 0.00100 | 0.00108 | 1.096 |
| LP2-OL-10-MOD | 0.00800 | 0.00718 | 1.082 |
| LP2-OL-11 | 0.00100 | 0.00147 | 1.470 |
| LP2-OL-12 | 0.00100 | 0.00137 | 2.319 |
| LP2-OL-13 | 0.00100 | 0.00102 | 1.500 |
| LP2-OL-14 | 0.01519 | 0.01503 | 2.603 |
| LP2-OL-15 | 0.00100 | 0.00119 | 2.022 |
| LP2-OL-16-MOD | 0.00992 | 0.00896 | 1.190 |
| LP2-OL-17 | 0.00100 | 0.00138 | 1.786 |
| LP2-OL-18 | 0.01140 | 0.01003 | 1.195 |
| LP2-OL-19 | 0.00796 | 0.00620 | 0.956 |
| LP2-OL-20 | 0.00100 | 0.00120 | 1.870 |
| LP2-OL-21 | 0.00500 | 0.00502 | 1.127 |
| LP2-OL-22 | 0.00100 | 0.00104 | 1.139 |
| LP2-OL-23 | 0.01315 | 0.01160 | 1.707 |

| Sample ID | $SO_3$, Mass Fraction | | $SO_3$ |
|---|---|---|---|
| | Target Baseline | Measured Baseline | Solubility (wt%) |
| LP2-OL-24 | 0.00100 | 0.00128 | 1.385 |
| LP2-OL-25 | 0.01012 | 0.00790 | 1.248 |

Table 3.11. List of $SO_3$ Solubility Model Components and Coefficients (Vienna et al. 2016)

| Model Term | $s_i$ Coefficient |
|---|---|
| $Al_2O_3$ | -2.091901 |
| $B_2O_3$ | 3.0440748 |
| CaO | 4.4422886 |
| Cl | -22.65353 |
| $Cr_2O_3$ | -13.14139 |
| $K_2O$ | 0.615785 |
| $Li_2O$ | 2.473926 |
| $Na_2O$ | 2.8972089 |
| $P_2O_5$ | 4.606083 |
| $SiO_2$ | 0.2407285 |
| $SnO_2$ | -1.775325 |
| $V_2O_5$ | 7.5345478 |
| $ZrO_2$ | -1.871916 |
| Others * | -0.280272 |
| $(Li_2O)^2$ | 260.203 |

* Others is the sum of all components not specifically listed as model terms (i.e., those not anticipated to have a significant effect).

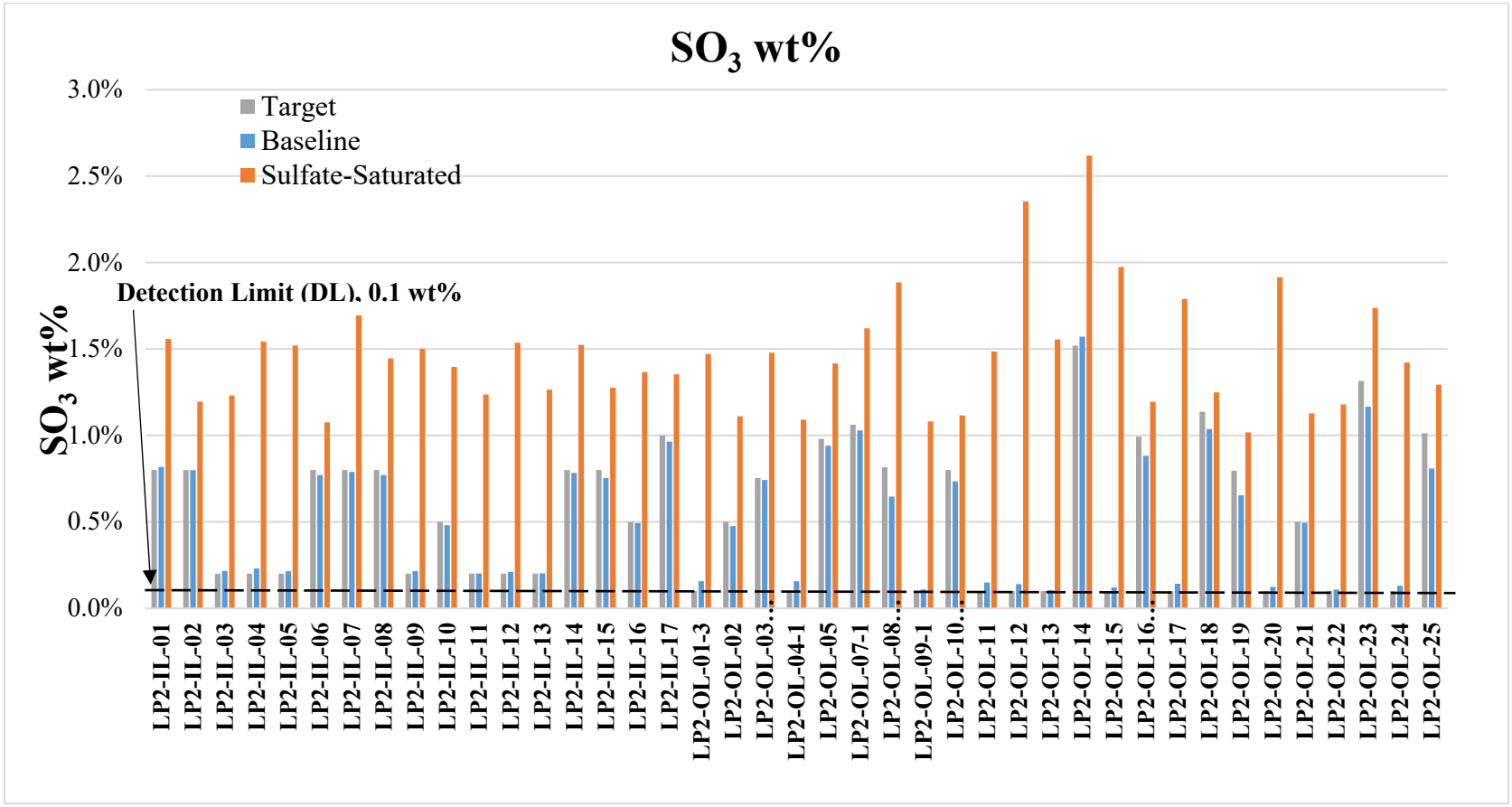


Figure 3.14. Analyzed Sulfur Concentration (wt%) in the Baseline and the Sulfur-Saturated Glasses

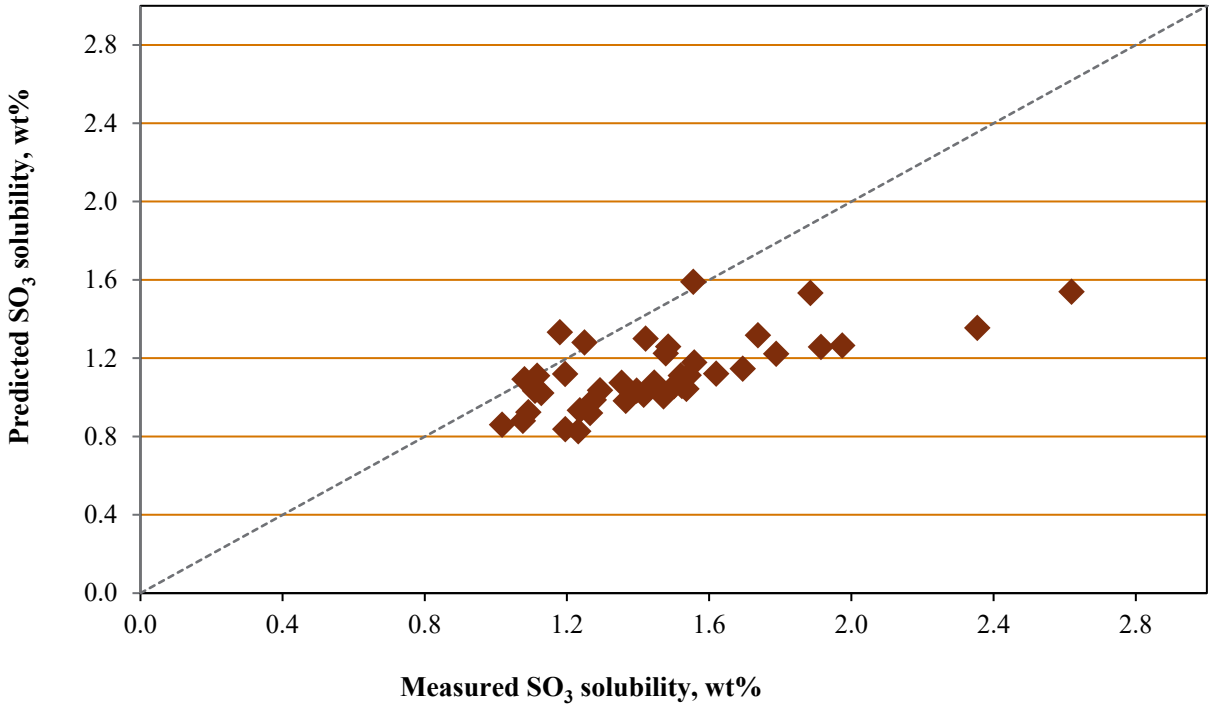


Figure 3.15. Predicted versus Measured $SO_3$ Solubility (wt%) for Phase 2 Enhanced LAW Glasses. The predicted values were obtained using the model in Equation (3.6) with coefficients as listed in Table 3.16.

# 4.0 Summary

The objective of the task in this report was to generate data on enhanced LAW glass compositions to ultimately support the development, validation, and implementation of glass property models that can achieve high waste loading for the full region of Hanford LAW compositions. To extend the models beyond our current knowledge space, a new enhanced LAW EGCR was developed. Fifteen LAW glass components were selected for variation in the experimental work, including an Others component mix. Certain components were chosen for variation in the experimental work for specific reasons. The components $SnO_2$ and $ZrO_2$ were included because they can decrease the VHT response. The components $V_2O_5$ and $Li_2O$ were included because they can increase the $SO_3$ tolerance in the melter. Finally, the components ZnO and $Cr_2O_3$ were included because they can decrease refractory corrosion.

A statistical layered experimental design approach (Piepel et al. 1993; Cooley et al. 2003; Piepel et al. 2005) was used to generate a test matrix of 42 Phase 2 enhanced LAW glass compositions. The test matrix consisted of 21 outer-layer glasses, 15 inner-layer glasses, a center glass (three replicates), and two glasses previously tested at another laboratory. Five of the outer-layer matrix glasses needed some modification to their composition and/or melt temperature to form homogeneous glasses. However, one of the outer-layer matrix glasses (LP2-OL-06) was not able to be modified to produce a homogenous glass and was dropped from testing.

The purpose of the chemical composition analysis was to identify whether (i) any Phase 2 enhanced LAW glass(es) was(were) mis-batched, (ii) there was non-negligible volatility in any component(s) during glass melting, or (iii) whether there were any component(s) that was(were) not completely incorporated into the glass melts. All the measured sums of oxides for the study glasses fell within the interval of 97.8 to 101.7 wt% for the inner-layer glasses and 94.7 to 101.9 wt% for the outer-layer glasses, indicating excellent recovery of the glass components.

XRD scans of CCC glass samples identified several crystal types. The major crystalline phases appearing (in the glasses containing crystals) were nepheline, sodalite, and combeite, which are all feldspathoids. A total of 28 samples were not analyzed by XRD because there were either no crystals or very few crystals (not enough for XRD to detect) observed by optical microscope. Four glasses had crystal content of less than 5 mass%, while eight glasses had crystal content greater than 10 mass% crystals. Only one glass (LP2-IL-06) had a crystal content between 5 and 10 mass%.

During the CCC heat-treatment, several of the Phase 2 enhanced LAW glasses seemed to form a layer of crystals around the Pt crucible walls. When a quartz crucible was used, the glass still formed a layer of crystals around the crucible walls. Therefore, this crystal formation did not appear to be due to the Pt.

The mode of the 41 measured density values was 2.64 g/cm$^3$, with a minimum of 2.59 g/cm$^3$and a maximum of 2.75 g/cm$^3$. The density of LAW glasses varied little—60% of the glasses had density values between 2.64 g/cm$^3$ and 2.70 g/cm$^3$. The predicted glass density based on the model discussed in Section 3.2 was higher than the measured density for all but one of the Phase 2 enhanced LAW glass compositions. However, all density values were well below the contractual limit of 3.7 g/cm$^3$. Thus, the available density data for LAW glasses indicated that it is not necessary to develop a property-composition model to comply with the contractual requirement for LAW density.

Although a previous model (Piepel et al. 2016) produced very good predictions of $\eta_{1150}$ for the Phase 2 enhanced LAW glasses, the model slightly overpredicted the measured values. Therefore, it would be useful to re-fit the model to account for the Phase 2 data, as well as the entire LAW glass composition region.

A previous model expressed as a function of glass composition and melt temperature (Piepel et al. 2007), overpredicted electrical conductivity at 1150°C ($\varepsilon_{1150}$) for all but one of the Phase 2 LAW glasses. This could be because of the different glass composition region that the Phase 2 enhanced LAW glass study explored compared to the composition region explored for the models in Piepel et al. (2007). Therefore, a new model exploring a wider composition region would be useful to account for the Phase 2 data.

In measuring the crystal fraction of the glasses by holding them at 950°C for 24 ± 2 h, all but 14 glasses had insufficient crystals to perform XRD analysis. Nine glasses contained Nasicon ($Na_{1+x}Zr_2Si_xP_{3-x}O_{12}$, $0 < x < 3$) and six glasses contained lazurite, $(Na,Ca)_8[(S,Cl,SO_4,OH)_2|(Al_6Si_6O_{24})]$, and/or combeite ($Na_2Ca_2Si_3O_9$). The wt% total crystallinity ranged from 0 to 17.46 wt%.

A review of the PCT data shows that none of the inner-layer glasses had normalized release values for boron (NR [B]) and sodium (NR [Na]) that are higher than the WTP contract limit of 2 g/m$^2$ for both quenched and CCC-treated glasses. However, several of the outer-layer glasses did exceed this limit. The test matrix was developed in this way so that PCT-composition models would be able to predict whether a given glass meets the PCT limits. It appeared that the CCC heat treatment had little impact on the PCT results as compared to the quenched versions of the study glasses for the inner-layer glasses. For the outer-layer glasses, the CCC heat treatment resulted in increased normalized release values of glasses with crystals. It appears that the B release is generally overpredicted, and the Na release is generally underpredicted using the PCT models from Piepel et al. (2007). It was noted in Piepel et al. (2007) that the given partial quadratic mixture models were not as accurate with higher waste loadings and higher Na and B releases. Since the current effort is to increase waste loading, new PCT models are needed to ensure that the glasses meet the release limit of 2 g/m$^2$ (4 g/L).

A total of 14 of the 41 quenched glasses and 11 of the 41 CCC glasses failed the VHT with a corrosion rate of >50 g/m$^2$/d. The glasses tested performed either extremely well or extremely poor, with only three quenched and one CCC glasses near the corrosion rate limit. Ideally the VHT results for the Phase 2 LAW glasses would have been better distributed, but the goal of having some VHT results above the limit for modeling purposes was achieved.

The VHT data were also predicted using two VHT models (Piepel et al. 2007) based on alteration depth (see Section 3.8). The data in predicted versus measured plots are quite scattered, with the models generally overpredicting the VHT response. There are likely several reasons for this. First, the VHT is known to produce large variability in VHT results, even for the same glass composition. Second, Piepel et al. (2007) noted that their models had large, and statistically significant lack-of-fits, possibly due to the large variability in VHT results. Third, the Phase 2 LAW glasses have higher waste loadings than the glasses used to develop the Piepel et al. (2007) models. Hence, models developed using glasses with higher waste loadings and other approaches should be tried to produce a model that would fit the data closer.

The $SO_3$ concentrations (mass fractions) in the baseline glasses were mostly below 0.015 (including several glasses with low $SO_3$ at 0.001). After sulfur-saturation, there was a significant increase of $SO_3$ mass fraction, which is considered the experimentally determined $SO_3$ solubility of the glass. In most glasses, the $SO_3$ solubility (i.e., the saturated $SO_3$ concentrations) was between 1.2 wt% and 1.5 wt%. Two glasses had a $SO_3$ solubility slightly above 2.0 wt%, with the highest $SO_3$ being 2.62 wt% in glass LP2-OL-14.

# 5.0 References

ASTM. "Standard Test Methods for Determining Chemical Durability of Nuclear, Hazardous, and Mixed Waste Glasses and Multiphase Glass Ceramics: The Product Consistency Test (PCT)," ASTM C1285, ASTM International, West Conshohocken, PA.

ASTM. "Standard Test Method for Measuring Waste Glass or Glass Ceramic Durability by Vapor Hydration Test," ASTM C1663, ASTM International, West Conshohocken, PA.

ASTM. "Standard Test Method for Determining Liquidus Temperature of Immobilized Waste Glasses and Simulated Waste Glasses," ASTM C1720, ASTM International, West Conshohocken, PA.

Cooley SK, GF Piepel, H Gan, WK Kot, and IL Pegg. 2003. “A Two-Stage Layered Mixture Experiment Design for a Nuclear Waste Glass Application—Part 2”, *2003 Proceedings of the American Statistical Association*, pp. 1044-1051. American Statistical Association, Alexandria, VA.

Crum, JV, TB Edwards, RL Russell, PJ Workman, M.J. Schweiger, R.F. Schumacher, D.E. Smith, D.K. Peeler, and J.D. Vienna. 2012. "DWPF Startup Frit Viscosity Measurement Round Robin Results," Journal of the American Ceramic Society, 95(7):2196-2205.

DOE. 2000. *Design, Construction, and Commissioning of the Hanford Tank Waste Treatment and Immobilization Plant*. Contract DE-AC27-01RV14136, as amended, U.S. Department of Energy, Office of River Protection, Richland, WA.

DOE. 2012. Memorandum, "Enhanced WTP Glass Composition Envelope Development," to C. Swan, Inter-Entity Work Order M0ORV00020, October 18, 2012, U.S. Department of Energy, Office of River Protection, Richland, WA.

Ebert, WL and SF Wolfe. 1999. *Round-robin Testing of a Refernce Glass for Low-Activity Waste Forms*. ANL-99/22, Argonne National Laboratory, Argonne, IL.

Fox, KM, TB Edwards, ME Caldwell, and WT Riley. 2017. *Sulfur Solubility Testing and Characterization of LAW Phase 2, Inner Layer Matrix Glasses*. SRNL-STI-2017-00709, Rev. 0, Westinghouse Savannah River Company, Aiken, SC.

Fox, KM, TB Edwards, and WT Riley. 2018. *Sulfur Solubility Testing and Characterization of LAW Phase 2, Outer Layer Matrix Glasses*. SRNL-STI-2018-00150, Rev. 0, Westinghouse Savannah River Company, Aiken, SC.

Kim DS, JD Vienna, PR Hrma, MJ Schweiger, J Matyas, JV Crum, DE Smith, GJ Sevigny, WC Buchmiller, JS Tixier, JD Yeager, and KB Belew. 2003. *Development and Testing of Icv Glasses for Hanford LAW*. PNNL-14351, Pacific Northwest National Laboratory, Richland, WA.

Kim DS and JD Vienna. 2012. *Preliminary ILAW Formulation Algorithm Description*. 24590-LAW-RPT-RT-04-0003, Rev. 1, River Protection Project, Hanford Tank Waste Treatment and Immobilization Plant, Richland, WA.

Matlack KS, M Chaudhuri, H Gan, IS Muller, WK Kot, W Gong, and IL Pegg. 2005a. *Glass Formulation Testing to Increase Sulfate Incorporation*. VSL-04R4960-1, Vitreous State Laboratory, The Catholic University of America, Washington, DC.

Matlack KS, W Gong, and IL Pegg. 2005b. *Glass Formulation Testing to Increase Sulfate Volatilization from Melter*. VSL-04R4970-1, Vitreous State Laboratory, The Catholic University of America, Washington, DC.

Matlack KS, W Gong, IS Muller, I Joseph, and IL Pegg. 2006a. *LAW Envelope C Glass Formulation Testing to Increase Waste Loading*. VSL-05R5900-1, Vitreous State Laboratory, The Catholic University of America, Washington, DC.

Matlack KS, W Gong, IS Muller, I Joseph, and IL Pegg. 2006b. *LAW Envelope A and B Glass Formulations Testing to Increase Waste Loading*. VSL-06R6900-1, Vitreous State Laboratory, The Catholic University of America, Washington, DC.

Matlack KS, I Joseph, W Gong, IS Muller, and IL Pegg. 2007. *Enhanced LAW Glass Formulation Testing*. VSL-07R1130-1, Vitreous State Laboratory, The Catholic University of America, Washington, DC.

Matlack KS, I Joseph, W Gong, IS Muller, and IL Pegg. 2009. *Glass Formulation Development and Dm10 Melter Testing with ORP LAW Glasses*. VSL-09R1510-2, Vitreous State Laboratory, The Catholic University of America, Washington, DC.

Mellinger GB and JL Daniel. 1984. *Approved Reference and Testing Materials for Use in Nuclear Waste Management Research and Development Programs*. PNL-4955-2, Pacific Northwest Laboratory, Richland, WA.

Muller IS, WK Kot, HK Pasieka, K Gilbo, FC Perez-Cardenas, I Joseph, and IL Pegg. 2012. *Compilation and Management of Orp Glass Formulation Database*. VSL-12R2470-1, Vitreous State Laboratory, The Catholic University of America, Washington, DC.

Muller IS, M Chaudhuri, IL Pegg, and I Joseph. 2013a. *Test Plan: Improved High-Alkali Low-Activity Waste Formulations*. VSL-13T3290-1, Vitreous State Laboratory, The Catholic University of America, Washington, DC.

Muller IS, IL Pegg, and I Joseph. 2013b. *Test Plan: Enhanced LAW Glass Property-Composition Models, Phase 2*. VSL-13T3050-1, Vitreous State Laboratory, The Catholic University of America, Washington, DC.

Muller, IS, K Gilbo, I Joseph, and IL Pegg. 2014. *Enhanced LAW Glass Property-Composition Models—Phase 1*. VSL-13R2940-1, Vitreous State Laboratory, The Catholic University of America, Washington, DC.

Muller IS, M Chaudhuri, H Gan, AC Buechele, X Xie, IL Pegg, and I Joseph. 2015. *Improved High-Alkali Low-Activity Waste Formulations*. VSL-15R3290-1, Rev. 0, Vitreous State Laboratory, The Catholic University of America, Washington, DC.

Muller, IS, KS Matlack, IL Pegg, and I Joseph. 2017. *Enhanced LAW Glass Correlation-Phase 3*. VSL-17R4230-1, Vitreous State Laboratory, The Catholic University of America, Washington, DC.

Petkus LL. 2003. "Low Activity Container Centerline Cooling Data," to C.A. Musick, CCN: 074181, October 16, 2003, River Protection Project, Hanford Tank Waste Treatment and Immobilization Plant, Richland, WA.

Piepel GF, CM Anderson, and PE Redgate. 1993. “Response Surface Designs for Irregularly-Shaped Regions” (Parts 1, 2, and 3). *1993 Proceedings of the Section on Physical and Engineering Sciences*, 205-227, American Statistical Association, Alexandria, VA.

Piepel GF, JM Szychowski, and JL Loeppky. 2002. “Augmenting Scheffé Linear Mixture Models with Squared and/or Crossproduct Terms”. *Journal of Quality Technology* 34, 297-314.

Piepel GF, SK Cooley, and B Jones. 2005. “Construction of a 21-Component Layered Mixture Experiment Design Using a New Mixture Coordinate-Exchange Algorithm”. *Quality Engineering* 17, 579-594.

Piepel GF, SK Cooley, IS Muller, H Gan, I Joseph, and IL Pegg. 2007. *ILAW PCT, VHT, Viscosity, and Electrical Conductivity Model Development*. VSL-07R1230-1, Rev. 0, Vitreous State Laboratory, The Catholic University of America, Washington, D.C.

Piepel GF, SK Cooley, JD Vienna, and JV Crum. 2015. “Designing a Mixture Experiment when the Components are Subject to a Nonlinear Multiplecomponent Constraint,” *Quality Engineering*, DOI: 10.1080/08982112.2015.1086003.

Piepel GF, SK Cooley, JD Vienna, and JV Crum. 2016. *Experimental Design for Hanford Low-Activity Waste Glasses with High Waste Loading*. PNNL-24391, Rev. 1, Pacific Northwest National Laboratory, Richland, WA.

Russell, RL, T Jin, BP McCarthy, LP Darnell, DE Rinehart, CC Bonham, V Gervasio, JM Mayer, CL Arendt, JB Lang, MJ Schweiger, and JD Vienna. 2017. *Enhanced Hanford Low-Activity Waste Glass Property Data Development: Phase 1*. PNNL-26630, Rev. 0, Pacific Northwest National Laboratory, Richland, WA.

Vienna JD. 2002. *The Effects of Temperature and Composition on the Solubility of Chromium in Multi-component Alkali-borosilicate Glass Melts*. Ph.D. Dissertation, Washington State University, Pullman, Washington.

Vienna, JD, P Hrma, A Jiricka, DE Smith, TH Lorier, IA Reamer, and RL Schultz. 2001. *Hanford Immobilized LAW Product Acceptance Testing: Tanks Focus Area Results*. PNNL-13744, Pacific Northwest National Laboratory, Richland, WA.

Vienna, JD, DS Kim, and DK Peeler. 2003a. “Glass Formulation for INEEL Sodium Bearing Waste.” *Ceramic Transactions* 143:169-176.

Vienna JD, DS Kim, and P Hrma. 2003b. "Interim Models Developed to Predict Key Hanford Waste Glass Properties Using Composition," *Ceramic Transactions*, 143, 151-157, American Ceramic Society, Westerville, OH.

Vienna JD, DS Kim, MJ Schweiger, P Hrma, J Matyas, JV Crum, and DE Smith. 2004a. "Preliminary Glass Development and Testing for in-Container Vitrification of Hanford Low-Activity Waste," *Ceramic Transactions*, 97(10), 261-268, American Ceramic Society, Westerville, OH.

Vienna, JD, P Hrma, WC Buchmiller, and JS Ricklefs. 2004b. *Preliminary Investigation of Sulfur Loading in Hanford LAW Glass*. PNNL-14649, Pacific Northwest National Laboratory, Richland, WA.

Vienna JD, DC Skorski, D Kim, J Matyas, 2013. Glass Property Models and Constraints for Estimating Glass to be Produced at Hanford by Implementing Current Advanced Glass Formulation Efforts, PNNL-22631 Rev.1, ORP-58289, Pacific Northwest National Laboratory, Richland, WA.

Vienna JD, DS Kim, IS Muller, GF Piepel, and AA Kruger. 2014. "Toward Understanding the Effect of Low-Activity Waste Glass Composition on Sulfur Solubility." *Journal of the American Ceramic Society* 97(10):3135-3142.

Vienna, JD, GF Piepel, DS Kim, JV Crum, CE Lonergan, BA Stanfill, BJ Riley, SK Cooley, and T Jin. 2016. *2016 Update of Hanford Glass Property Models and Constraints for Use in Estimating the Glass Mass to be Produced at Hanford by Implementing Current Enhanced Glass Formulation Efforts*. PNNL-25835, Pacific Northwest National Laboratory, Richland, WA.

# Appendix A – Morphology/Color of Each Quenched Glass

The photos in this appendix show quenched samples of each Phase 2 enhanced LAW glass after melting in a Pt/Rh crucible twice at the specified melt temperature.

Figure A.1. Photo of Glass LP2-IL-01 Morphology of Second Melt at 1150 °C for 1.5 h

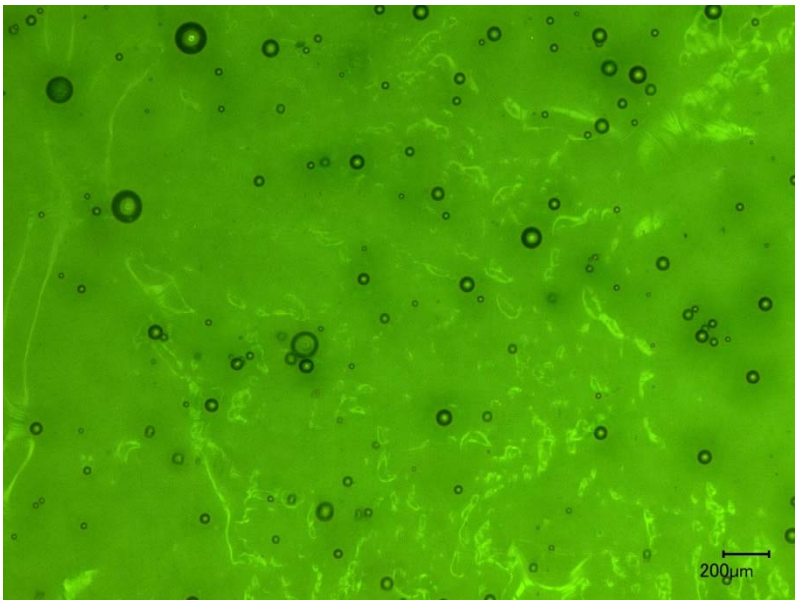


Figure A.2. Photo of Glass LP2-IL-02 Morphology of Fourth Melt at 1150 °C for 0.5 h

Figure A.3. Photo of Glass LP2-IL-03 Morphology of Second Melt at 1150 °C for 1.5 h

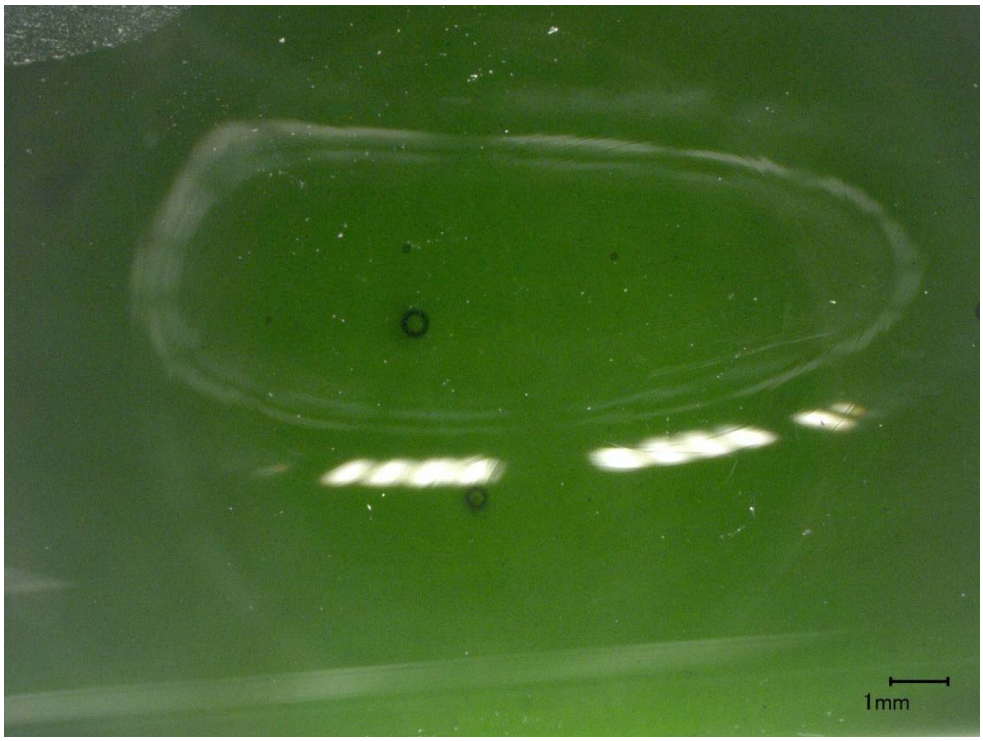


Figure A.4. Photo of Glass LP2-IL-04 Morphology of Second Melt at 1150 °C for 2.3 h

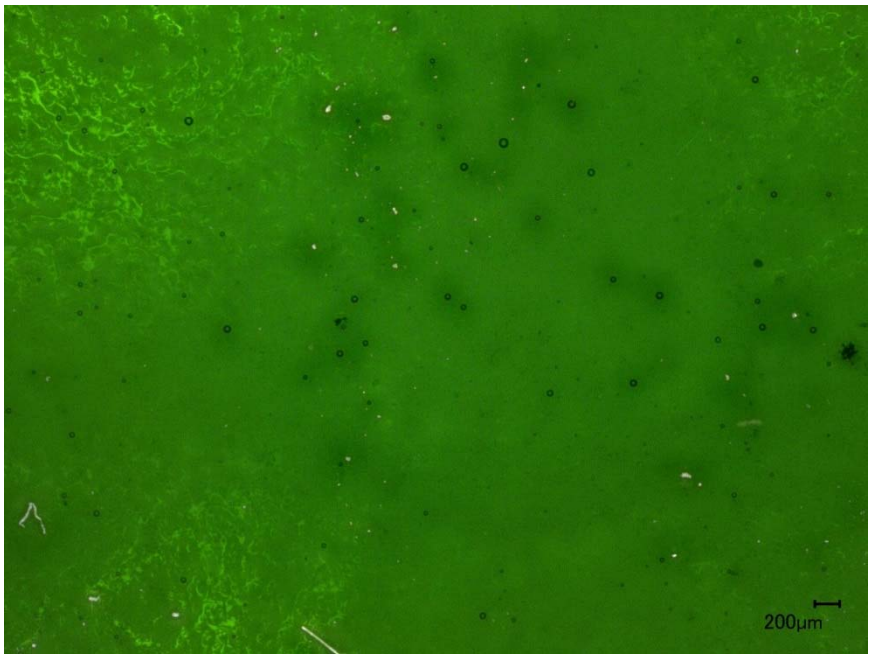


Figure A.5. Photo of Glass LP2-IL-05 Morphology of Second Melt at 1150 °C for 1.5 h

Figure A.6. Photo of Glass LP2-IL-06 Morphology of Fourth Melt at 1175 °C for 1 h

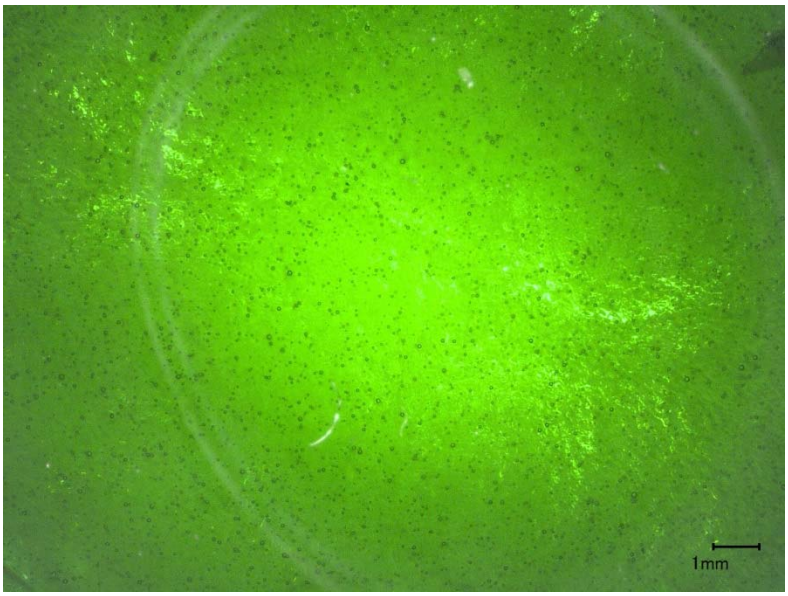


Figure A.7. Photo of Glass LP2-IL-07 Morphology of Second Melt at 1150 °C for 1 h

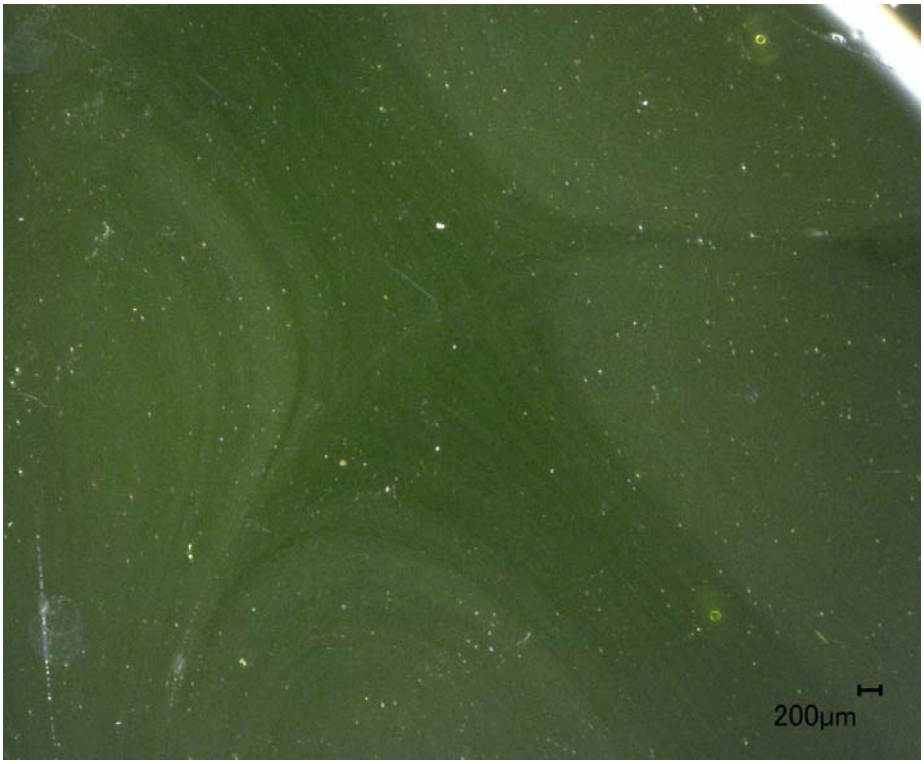


Figure A.8. Photo of Glass LP2-IL-08 Morphology of Third Melt at 1175 °C for 1.1 h

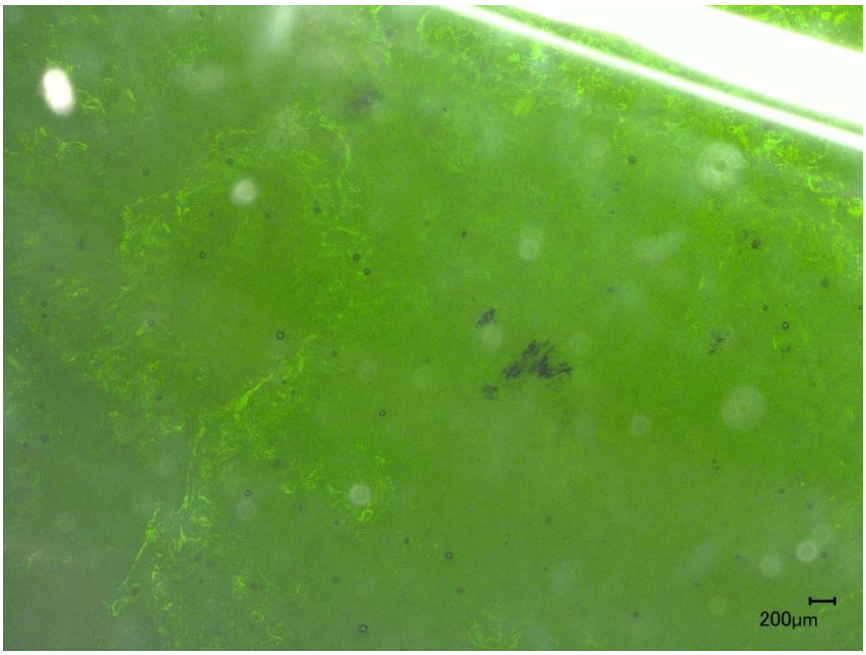


Figure A.9. Photo of Glass LP2-IL-09 Morphology of Third Melt at 1175 °C for 1 h

Figure A.10. Photo of Glass LP2-IL-10 Morphology of Third Melt at 1175 °C for 1.5 h

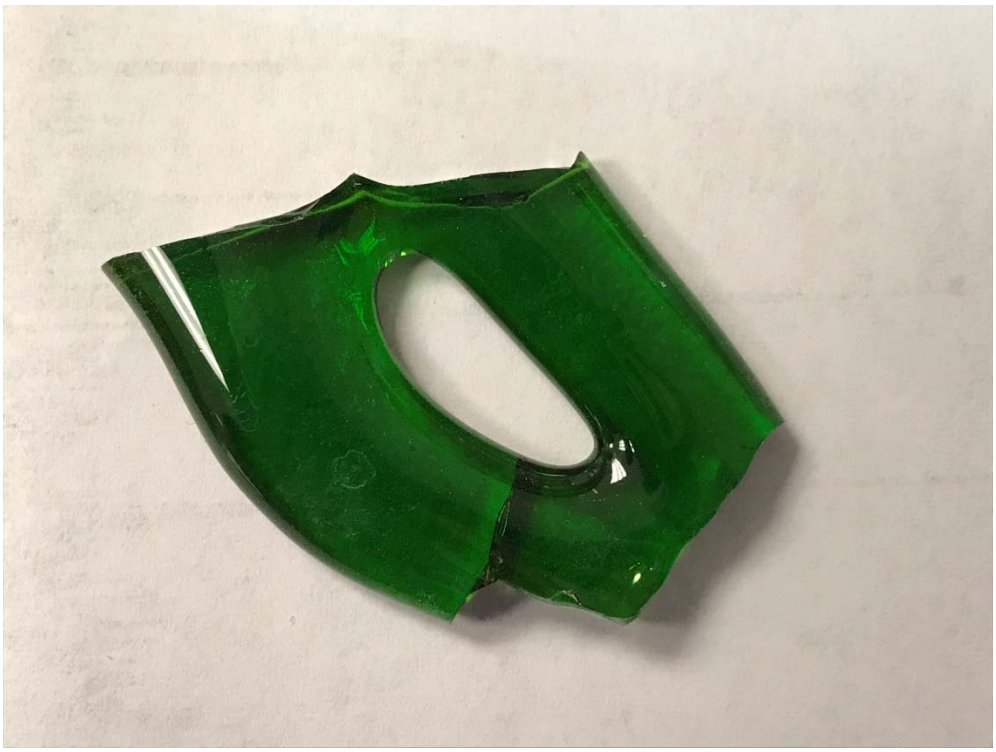

Figure A.11. Photo of Glass LP2-IL-11 Morphology of Third Melt at 1175 °C for 1 h

Figure A.12. Photo of Glass LP2-IL-12 Morphology of Third Melt at 1175 °C for 1 h

Figure A.13. Photo of Glass LP2-IL-13 Morphology of Second Melt at 1150 °C for 1.5 h

Figure A.14. Photo of Glass LP2-IL-14 Morphology of Second Melt at 1150 °C for 1.5 h

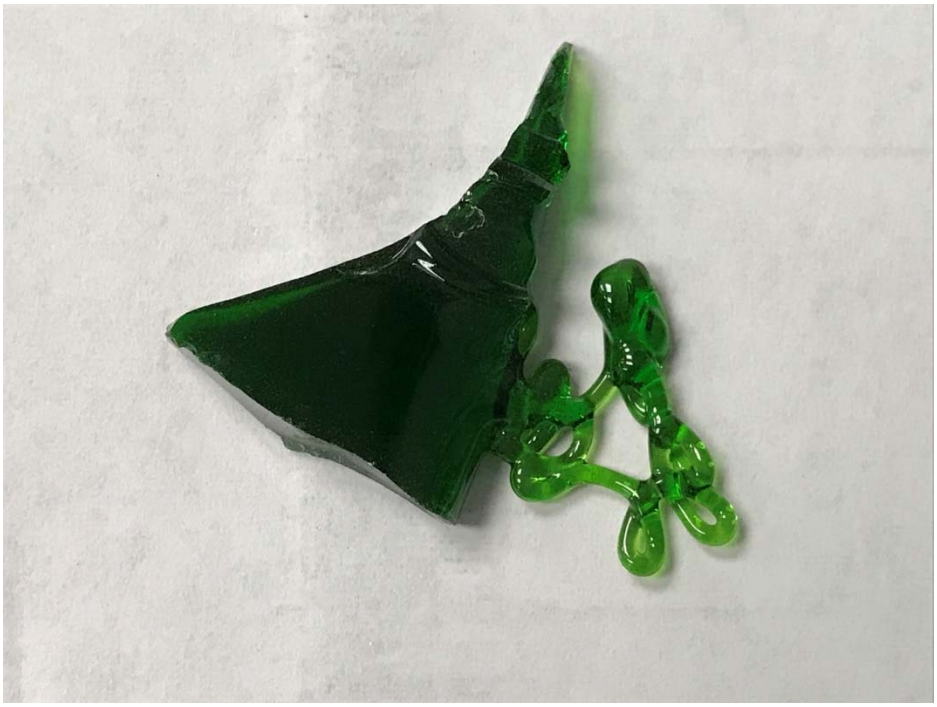

Figure A.15. Photo of Glass LP2-IL-15 Morphology of Third Melt at 1150 °C for 1 h

Figure A.16. Photo of Glass LP2-IL-16 Morphology of Second Melt at 1175 °C for 0.75 h

Figure A.17. Photo of Glass LP2-IL-17 Morphology of Second Melt at 1150 °C for 1.5 h

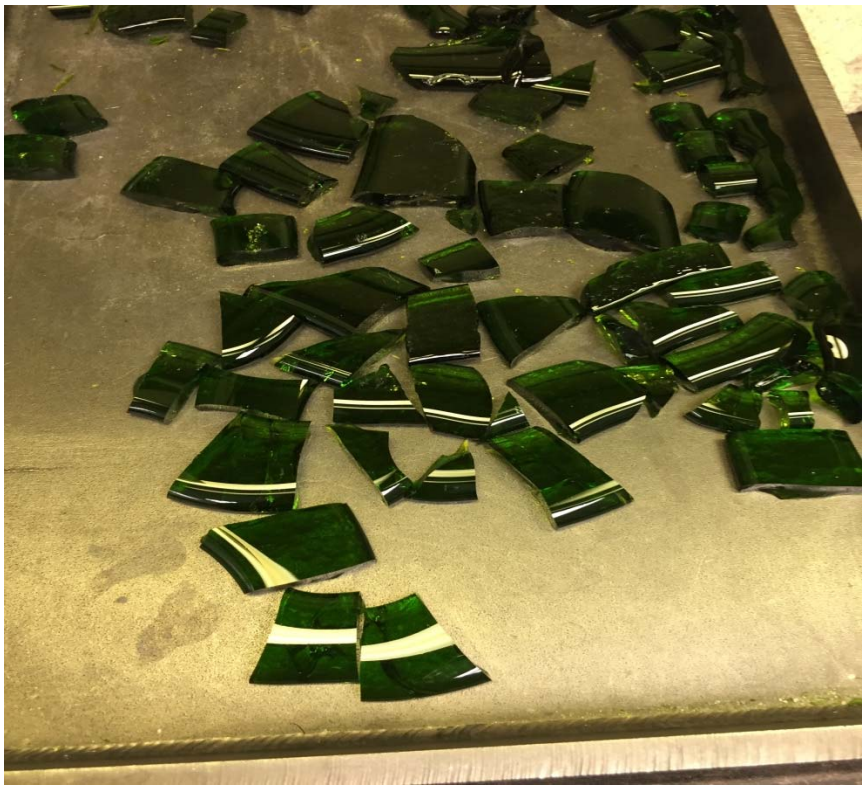

Figure A.18. Photo of Glass LP2-OL-01-3 Morphology of Second Melt at 1150 °C for 1.5 h

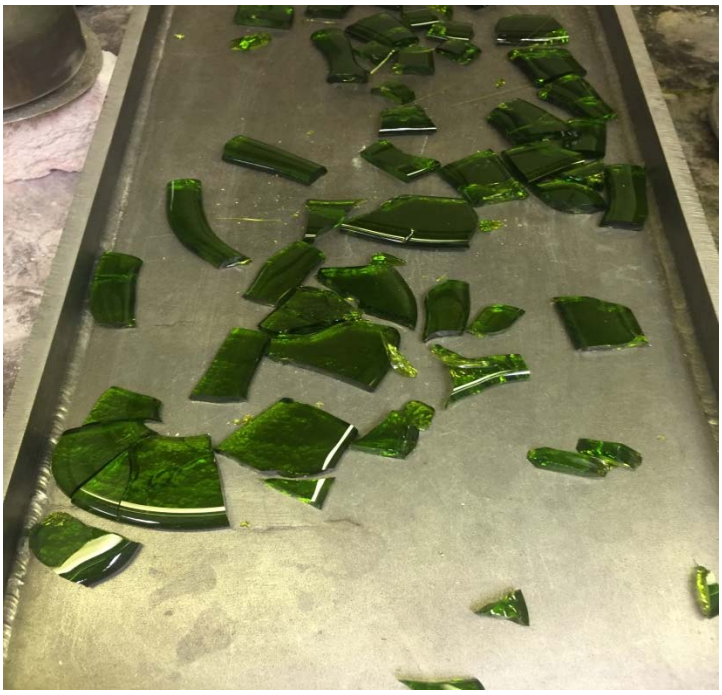

Figure A.19. Photo of Glass LP2-OL-02-1 Morphology of Second Melt at 1150 °C for 1.3 h

Figure A.20. Photo of Glass LP2-OL-03MOD2 Morphology of Second Melt at 1150 °C for 1.5 h

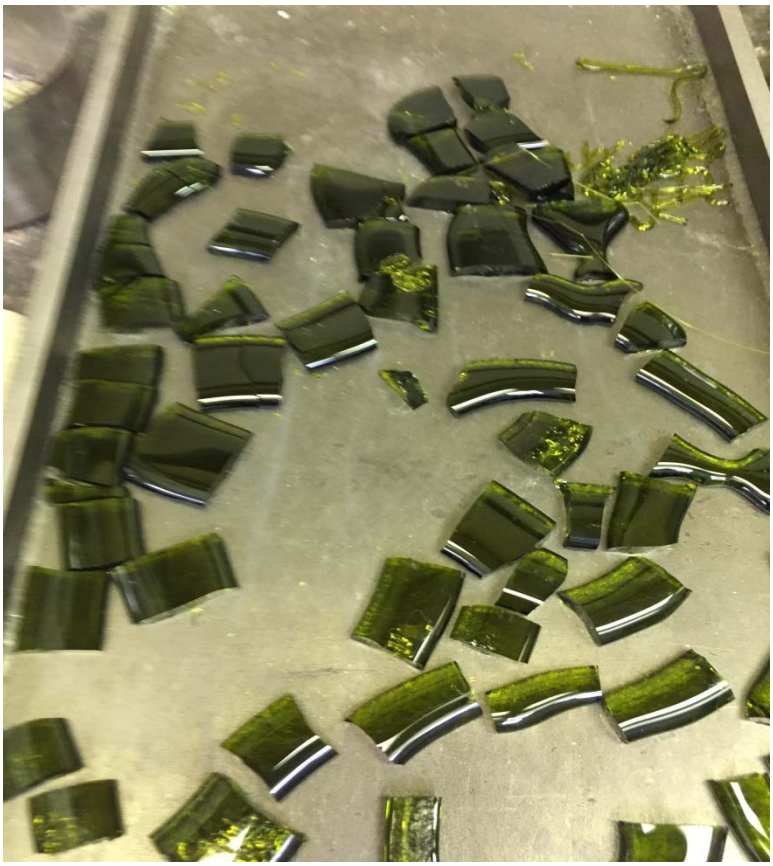

Figure A.21. Photo of Glass LP2-OL-04-1 Morphology of Second Melt at 1150 °C for 1.5 h

Figure A.22. Photo of Glass LP2-OL-05 Morphology of Third Melt at 1150 °C for 1.5 h

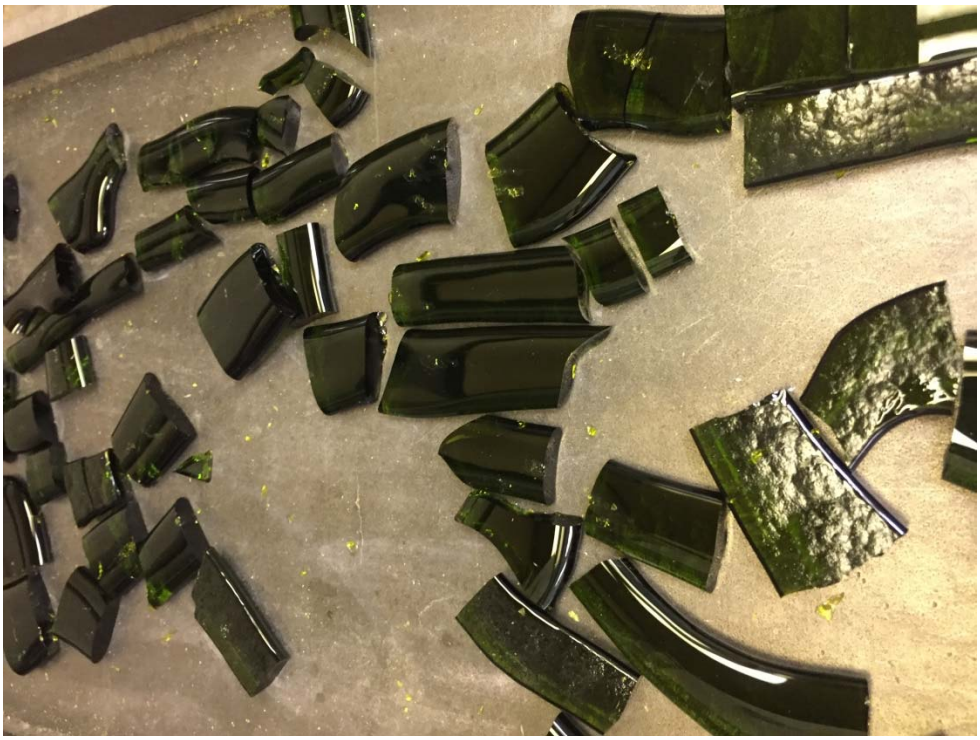

Figure A.23. Photo of Glass LP2-OL-07-1 Morphology of Second Melt at 1150 °C for 1.5 h

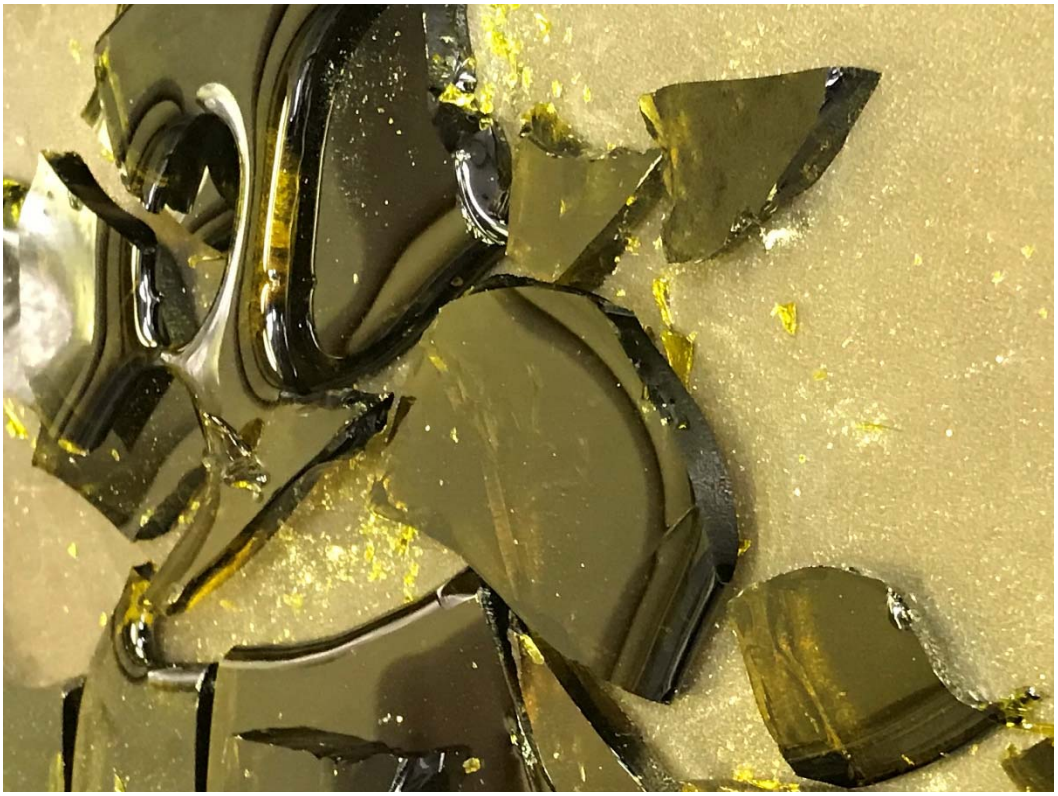

Figure A.24. Photo of Glass LP2-OL-08MOD Morphology of Second Melt at 1200 °C for 1.3 h

Figure A.25. Photo of Glass LP2-OL-09-1 Morphology of Second Melt at 1150 °C for 1.5 h

Figure A.26. Photo of Glass LP2-OL-10 MOD Morphology of Second Melt at 1150 °C for 1.5 h

Figure A.27. Photo of Glass LP2-OL-11 Morphology of Second Melt at 1150 °C for 1.6 h

Figure A.28. Photo of Glass LP2-OL-12 Morphology of Second Melt at 1150 °C for 1.5 h

Figure A.29. Photo of Glass LP2-OL-13 of Morphology Third Melt at 1150 °C for 1.7 h

Figure A.30. Photo of Glass LP2-OL-14 Morphology of Second Melt at 1150 °C for 1.5 h

Figure A.31. Photo of Glass LP2-OL-15 Morphology of Third Melt at 1150 °C for 1 h

Figure A.32. Photo of Glass LP2-OL-16 MOD of Third Melt at 1200 °C for 2 h

Figure A.33. Photo of Glass LP2-OL-17 Morphology of Second Melt at 1150 °C for 1.5 h

Figure A.34. Photo of Glass LP2-OL-18 Morphology of Second Melt at 1250 °C for 1.6 h

Figure A.35. Photo of Glass LP2-OL-19 Morphology of Second Melt at 1150 °C for 1.5 h

Figure A.36. Photo of Glass LP2-OL-20 Morphology of First Melt at 1150 °C for 1.5 h

Figure A.37. Photo of Glass LP2-OL-21 Morphology of Second Melt at 1150 °C for 1.4 h

Figure A.38. Photo of Glass LP2-OL-22 Morphology of Third Melt at 1150 °C for 1.5 h

Figure A.39. Photo of Glass LP2-OL-23 Morphology of Second Melt at 1150 °C for 1.5 h

Figure A.40. Photo of Glass LP2-OL-24 Morphology of Third Melt at 1200 °C for 1.5 h

Figure A.41. Photo of Glass LP2-OL-25 Morphology of Second Melt at 1150 °C for 1.6 h

# Appendix B – Analyzed Glass Compositions

The tables in this appendix compare the targeted glass compositions with the analyzed glass compositions and their percent differences for the Phase 2 enhanced LAW glasses. There were two main purposes for analyzing the compositions of these glasses. First, the analyzed $SO_3$ values estimate the concentrations of that component incorporated into the glass melts. Second, comparing target and analyzed values of components provides for detecting glasses that were mis-batched, or components subject to volatilization during melting.

There appeared to be overall agreement between targeted and analyzed components for all Phase 2 LAW glasses. Hence, renormalized versions of the targeted compositions, with use of the measured instead of targeted $SO_3$ values, will be used in future work to develop property-composition models.

Table B.1. Comparison of Targeted and Analyzed LAW Phase 2 Enhanced Glass Compositions

| Glass ID | LP2-IL-01 | | | LP2-IL-02 | | | LP2-IL-03 | | | LP2-IL-04 | | |
|---|---|---|---|---|---|---|---|---|---|---|---|---|
| Component | Targeted (wt%) | Analyzed (wt%) | % Diff | Targeted (wt%) | Analyzed (wt%) | % Diff | Targeted (wt%) | Analyzed (wt%) | % Diff | Targeted (wt%) | Analyzed (wt%) | % Diff |
| $Al_2O_3$ | 7.500 | 6.906 | -7.92 | 7.500 | 7.275 | -3.00 | 8.730 | 8.073 | -7.53 | 7.500 | 7.213 | -3.83 |
| $B_2O_3$ | 8.000 | 7.631 | -4.61 | 8.130 | 8.138 | 0.10 | 8.730 | 8.549 | -2.07 | 8.000 | 8.227 | 2.84 |
| CaO | 7.620 | 7.877 | 3.37 | 2.000 | 2.305 | 15.25 | 2.000 | 2.337 | 16.85 | 7.490 | 7.615 | 1.67 |
| Cl | 0.170 | 0.124 | -27.06 | 0.170 | 0.115 | -32.35 | 0.350 | 0.262 | -25.14 | 0.350 | 0.226 | -35.43 |
| $Cr_2O_3$ | 0.530 | 0.520 | -1.89 | 0.380 | 0.372 | -2.11 | 0.530 | 0.520 | -1.89 | 0.530 | 0.520 | -1.89 |
| F | 0.260 | 0.225 | -13.46 | 0.260 | 0.219 | -15.77 | 0.530 | 0.462 | -12.83 | 0.530 | 0.462 | -12.83 |
| $Fe_2O_3$ | 0.200 | 0.217 | 8.50 | 0.580 | 0.603 | 3.97 | 0.200 | 0.221 | 10.50 | 1.000 | 1.069 | 6.90 |
| $K_2O$ | 2.000 | 1.985 | -0.75 | 2.000 | 1.985 | -0.75 | 0.760 | 0.813 | 6.97 | 2.000 | 1.945 | -2.75 |
| MgO | 0.300 | 0.315 | 5.00 | 1.000 | 0.979 | -2.10 | 0.300 | 0.313 | 4.33 | 1.000 | 0.985 | -1.50 |
| $Na_2O$ | 23.680 | 22.242 | -6.07 | 23.680 | 22.410 | -5.36 | 24.500 | 22.107 | -9.77 | 23.680 | 22.411 | -5.36 |
| $P_2O_5$ | 0.560 | 0.661 | 18.04 | 0.560 | 0.517 | -7.68 | 1.130 | 0.828 | -26.73 | 1.130 | 0.835 | -26.11 |
| $SiO_2$ | 37.980 | 39.096 | 2.94 | 41.810 | 42.572 | 1.82 | 40.360 | 42.305 | 4.82 | 38.200 | 39.737 | 4.02 |
| $SO_3$ | 0.800 | 0.806 | 0.75 | 0.800 | 0.792 | -1.00 | 0.200 | 0.211 | 5.50 | 0.200 | 0.229 | 14.50 |
| $SnO_2$ | 0.500 | 0.504 | 0.80 | 2.500 | 2.517 | 0.68 | 2.500 | 2.571 | 2.84 | 2.500 | 2.634 | 5.36 |
| $V_2O_5$ | 2.000 | 2.008 | 0.40 | 0.500 | 0.491 | -1.80 | 0.500 | 0.481 | -3.80 | 0.500 | 0.488 | -2.40 |
| ZnO | 2.400 | 2.427 | 1.13 | 2.630 | 2.627 | -0.11 | 3.200 | 3.165 | -1.09 | 2.400 | 2.409 | 0.38 |
| $ZrO_2$ | 5.500 | 5.096 | -7.35 | 5.500 | 5.174 | -5.93 | 5.500 | 4.498 | -18.22 | 3.000 | 2.313 | -22.90 |
| Total | 100.000 | 98.856 | -1.14 | 100.000 | 99.305 | -0.70 | 100.020 | 97.930 | -2.09 | 100.010 | 99.534 | -0.48 |

Table B.1. Comparison of Targeted and Analyzed LAW Phase 1 Enhanced Glass Compositions (cont.)

| Glass ID | LP2-IL-05 | | | LP2-IL-06 | | | LP2-IL-07 | | | LP2-IL-08 | | |
|---|---|---|---|---|---|---|---|---|---|---|---|---|
| Component | Targeted (wt%) | Analyzed (wt%) | % Diff | Targeted (wt%) | Analyzed (wt%) | % Diff | Targeted (wt%) | Analyzed (wt%) | % Diff | Targeted (wt%) | Analyzed (wt%) | % Diff |
| $Al_2O_3$ | 7.500 | 7.048 | -6.03 | 10.680 | 10.397 | -2.65 | 7.500 | 6.986 | -6.85 | 7.500 | 7.227 | -3.64 |
| $B_2O_3$ | 12.000 | 11.423 | -4.81 | 12.000 | 12.107 | 0.89 | 12.000 | 11.938 | -0.52 | 8.000 | 8.501 | 6.26 |
| CaO | 7.030 | 7.227 | 2.80 | 2.000 | 2.295 | 14.75 | 5.150 | 5.369 | 4.25 | 8.000 | 8.108 | 1.35 |
| Cl | 0.350 | 0.244 | -30.29 | 0.350 | 0.218 | -37.71 | 0.350 | 0.270 | -22.86 | 0.350 | 0.206 | -41.14 |
| $Cr_2O_3$ | 0.380 | 0.369 | -2.89 | 0.530 | 0.524 | -1.13 | 0.380 | 0.368 | -3.16 | 0.530 | 0.508 | -4.15 |
| F | 0.530 | 0.441 | -16.79 | 0.530 | 0.424 | -20.00 | 0.530 | 0.466 | -12.08 | 0.530 | 0.443 | -16.42 |
| $Fe_2O_3$ | 0.200 | 0.225 | 12.50 | 0.200 | 0.218 | 9.00 | 0.200 | 0.123 | -38.50 | 1.000 | 0.988 | -1.20 |
| $K_2O$ | 0.500 | 0.527 | 5.40 | 2.000 | 2.003 | 0.15 | 2.000 | 1.985 | -0.75 | 0.500 | 0.537 | 7.40 |
| MgO | 0.300 | 0.305 | 1.67 | 1.000 | 0.988 | -1.20 | 1.000 | 0.963 | -3.70 | 1.000 | 0.973 | -2.70 |
| $Na_2O$ | 22.000 | 20.658 | -6.10 | 22.000 | 22.276 | 1.25 | 22.330 | 22.040 | -1.30 | 22.000 | 20.928 | -4.87 |
| $P_2O_5$ | 1.130 | 0.749 | -33.72 | 1.130 | 0.872 | -22.83 | 1.130 | 0.745 | -34.07 | 1.130 | 0.866 | -23.36 |
| $SiO_2$ | 37.000 | 38.721 | 4.65 | 37.000 | 39.203 | 5.95 | 39.450 | 40.433 | 2.49 | 38.980 | 39.898 | 2.36 |
| $SO_3$ | 0.200 | 0.212 | 6.00 | 0.800 | 0.782 | -2.25 | 0.800 | 0.782 | -2.25 | 0.800 | 0.763 | -4.63 |
| $SnO_2$ | 2.500 | 2.606 | 4.24 | 0.820 | 0.831 | 1.34 | 0.500 | 0.379 | -24.20 | 0.500 | 0.401 | -19.80 |
| $V_2O_5$ | 0.500 | 0.484 | -3.20 | 1.080 | 1.023 | -5.28 | 0.500 | 0.486 | -2.80 | 0.500 | 0.483 | -3.40 |
| ZnO | 2.400 | 2.402 | 0.08 | 2.400 | 2.353 | -1.96 | 3.200 | 3.124 | -2.38 | 3.200 | 3.109 | -2.84 |
| $ZrO_2$ | 5.500 | 5.140 | -6.55 | 5.500 | 4.978 | -9.49 | 3.000 | 2.678 | -10.73 | 5.500 | 5.022 | -8.69 |
| Total | 100.020 | 98.996 | -1.02 | 100.020 | 101.705 | 1.68 | 100.020 | 99.351 | -0.67 | 100.020 | 99.176 | -0.84 |

Table B.1. Comparison of Targeted and Analyzed LAW Phase 1 Enhanced Glass Compositions (cont.)

| Glass ID | LP2-IL-09 | | | LP2-IL-10 | | | LP2-IL-11 | | | LP2-IL-12 | | |
|---|---|---|---|---|---|---|---|---|---|---|---|---|
| Component | Targeted (wt%) | Analyzed (wt%) | % Diff | Targeted (wt%) | Analyzed (wt%) | % Diff | Targeted (wt%) | Analyzed (wt%) | % Diff | Targeted (wt%) | Analyzed (wt%) | % Diff |
| $Al_2O_3$ | 7.500 | 7.076 | -5.65 | 10.000 | 9.060 | -9.40 | 9.000 | 8.663 | -3.74 | 7.500 | 6.878 | -8.29 |
| $B_2O_3$ | 12.000 | 12.155 | 1.29 | 9.500 | 10.054 | 5.83 | 8.000 | 8.460 | 5.75 | 8.000 | 7.921 | -0.99 |
| CaO | 2.000 | 2.281 | 14.05 | 5.000 | 5.216 | 4.32 | 3.080 | 3.337 | 8.34 | 3.120 | 3.400 | 8.97 |
| Cl | 0.170 | 0.120 | -29.41 | 0.210 | 0.137 | -34.76 | 0.350 | 0.206 | -41.14 | 0.350 | 0.256 | -26.86 |
| $Cr_2O_3$ | 0.530 | 0.511 | -3.58 | 0.450 | 0.434 | -3.56 | 0.380 | 0.367 | -3.42 | 0.380 | 0.366 | -3.68 |
| F | 0.260 | 0.223 | -14.23 | 0.320 | 0.269 | -15.94 | 0.530 | 0.438 | -17.36 | 0.530 | 0.454 | -14.34 |
| $Fe_2O_3$ | 1.000 | 0.938 | -6.20 | 0.600 | 0.552 | -8.00 | 1.000 | 0.970 | -3.00 | 0.200 | 0.119 | -40.50 |
| $K_2O$ | 0.500 | 0.545 | 9.00 | 1.000 | 1.080 | 8.00 | 2.000 | 1.930 | -3.50 | 0.500 | 0.528 | 5.60 |
| MgO | 1.000 | 0.975 | -2.50 | 0.650 | 0.627 | -3.54 | 0.300 | 0.294 | -2.00 | 1.000 | 0.966 | -3.40 |
| $Na_2O$ | 24.370 | 23.489 | -3.62 | 23.000 | 21.871 | -4.91 | 22.000 | 21.332 | -3.04 | 23.790 | 22.545 | -5.23 |
| $P_2O_5$ | 0.560 | 0.625 | 11.61 | 0.680 | 0.603 | -11.32 | 1.130 | 0.770 | -31.86 | 1.130 | 0.754 | -33.27 |
| $SiO_2$ | 37.000 | 37.224 | 0.61 | 38.800 | 38.668 | -0.34 | 38.850 | 39.042 | 0.49 | 42.920 | 43.695 | 1.81 |
| $SO_3$ | 0.200 | 0.212 | 6.00 | 0.500 | 0.469 | -6.20 | 0.200 | 0.199 | -0.50 | 0.200 | 0.206 | 3.00 |
| $SnO_2$ | 2.200 | 2.123 | -3.50 | 1.500 | 1.495 | -0.33 | 2.500 | 2.549 | 1.96 | 0.500 | 0.408 | -18.40 |
| $V_2O_5$ | 2.000 | 1.999 | -0.05 | 1.000 | 0.939 | -6.10 | 2.000 | 1.986 | -0.70 | 2.000 | 1.999 | -0.05 |
| ZnO | 3.200 | 3.128 | -2.25 | 2.800 | 2.739 | -2.18 | 3.200 | 3.090 | -3.44 | 2.400 | 2.365 | -1.46 |
| $ZrO_2$ | 5.500 | 5.049 | -8.20 | 4.000 | 3.377 | -15.58 | 5.500 | 5.532 | 0.58 | 5.500 | 5.035 | -8.45 |
| Total | 99.990 | 98.887 | -1.10 | 100.010 | 97.804 | -2.21 | 100.020 | 99.382 | -0.64 | 100.020 | 98.112 | -1.91 |

Table B.1. Comparison of Targeted and Analyzed LAW Phase 1 Enhanced Glass Compositions (cont.)

| Glass ID | LP2-IL-13 | | | LP2-IL-14 | | | LP2-IL-15 | | | LP2-IL-16 | | |
|---|---|---|---|---|---|---|---|---|---|---|---|---|
| Component | Targeted (wt%) | Analyzed (wt%) | % Diff | Targeted (wt%) | Analyzed (wt%) | % Diff | Targeted (wt%) | Analyzed (wt%) | % Diff | Targeted (wt%) | Analyzed (wt%) | % Diff |
| $Al_2O_3$ | 7.500 | 7.237 | -3.51 | 8.800 | 8.106 | -7.89 | 7.500 | 7.062 | -5.84 | 10.000 | 9.452 | -5.48 |
| $B_2O_3$ | 11.260 | 10.964 | -2.63 | 12.000 | 11.302 | -5.82 | 10.750 | 10.328 | -3.93 | 9.500 | 9.136 | -3.83 |
| CaO | 2.320 | 2.575 | 10.99 | 3.830 | 4.117 | 7.49 | 2.000 | 2.176 | 8.80 | 5.000 | 5.271 | 5.42 |
| Cl | 0.170 | 0.127 | -25.29 | 0.350 | 0.243 | -30.57 | 0.350 | 0.254 | -27.43 | 0.210 | 0.139 | -33.81 |
| $Cr_2O_3$ | 0.530 | 0.509 | -3.96 | 0.380 | 0.365 | -3.95 | 0.530 | 0.519 | 2.08 | 0.450 | 0.439 | 2.44 |
| F | 0.260 | 0.202 | -22.31 | 0.530 | 0.422 | -20.38 | 0.530 | 0.416 | -21.51 | 0.320 | 0.263 | -17.81 |
| $Fe_2O_3$ | 1.000 | 0.954 | -4.60 | 1.000 | 0.914 | -8.60 | 1.000 | 0.941 | -5.90 | 0.600 | 0.558 | -7.00 |
| $K_2O$ | 2.000 | 1.927 | -3.65 | 0.500 | 0.541 | 8.20 | 0.500 | 0.542 | 8.40 | 1.000 | 1.087 | 8.70 |
| MgO | 0.300 | 0.291 | -3.00 | 0.300 | 0.297 | -1.00 | 0.300 | 0.299 | -0.33 | 0.650 | 0.641 | -1.38 |
| $Na_2O$ | 22.000 | 21.433 | -2.58 | 24.500 | 23.489 | -4.13 | 22.000 | 21.130 | -3.95 | 23.000 | 22.478 | -2.27 |
| $P_2O_5$ | 0.560 | 0.600 | 7.14 | 1.130 | 0.777 | -31.24 | 1.130 | 0.923 | -18.32 | 0.680 | 0.617 | -9.26 |
| $SiO_2$ | 43.000 | 43.374 | 0.87 | 37.000 | 38.240 | 3.35 | 42.720 | 43.535 | 1.91 | 38.800 | 39.149 | 0.90 |
| $SO_3$ | 0.200 | 0.199 | -0.50 | 0.800 | 0.767 | -4.13 | 0.800 | 0.741 | -7.38 | 0.500 | 0.486 | -2.80 |
| $SnO_2$ | 0.500 | 0.430 | -14.00 | 0.500 | 0.471 | -5.80 | 2.500 | 2.409 | -3.64 | 1.500 | 1.441 | -3.93 |
| $V_2O_5$ | 0.500 | 0.480 | -4.00 | 0.500 | 0.487 | -2.60 | 2.000 | 2.022 | 1.10 | 1.000 | 0.959 | -4.10 |
| ZnO | 2.400 | 2.365 | -1.46 | 2.400 | 2.365 | -1.46 | 2.400 | 2.390 | -0.42 | 2.800 | 2.760 | -1.43 |
| $ZrO_2$ | 5.500 | 4.735 | -13.91 | 5.500 | 5.045 | -8.27 | 3.000 | 2.749 | -8.37 | 4.000 | 3.681 | -7.98 |
| Total | 100.000 | 98.618 | -1.38 | 100.020 | 98.164 | -1.86 | 100.010 | 98.650 | -1.36 | 100.010 | 98.774 | -1.24 |

Table B.1. Comparison of Targeted and Analyzed LAW Phase 1 Enhanced Glass Compositions (cont.)

| Glass ID | LP2-IL-17 | | | LP2-OL-01-3 | | | LP2-OL-02-1 | | | LP2-OL-03 MOD2 | | |
|---|---|---|---|---|---|---|---|---|---|---|---|---|
| Component | Targeted (wt%) | Analyzed (wt%) | % Diff | Targeted (wt%) | Analyzed (wt%) | % Diff | Targeted (wt%) | Analyzed (wt%) | % Diff | Targeted (wt%) | Analyzed (wt%) | % Diff |
| $Al_2O_3$ | 9.230 | 8.678 | -5.98 | 6.000 | 5.697 | -5.05 | 10.000 | 9.122 | -8.78 | 10.738 | 9.773 | -8.99 |
| $B_2O_3$ | 11.000 | 10.408 | -5.38 | 6.000 | 6.037 | 0.62 | 9.500 | 9.225 | -2.89 | 6.107 | 5.691 | -6.81 |
| CaO | 2.500 | 2.753 | 10.12 | 9.090 | 8.500 | -6.49 | 5.000 | 5.069 | 1.38 | 10.905 | 10.802 | -0.94 |
| Cl | 0.070 | 0.062 | -11.43 | 0.062 | <0.050 | -- | 0.208 | 0.146 | -29.81 | 0.063 | 0.067 | 6.35 |
| $Cr_2O_3$ | 0.080 | 0.087 | 8.75 | 0.600 | 0.717 | 19.50 | 0.450 | 0.559 | 24.22 | 0.611 | 0.685 | 12.11 |
| F | 0.110 | 0.087 | -20.91 | 0.095 | 0.072 | -24.21 | 0.316 | 0.260 | -17.72 | 0.097 | 0.102 | 5.15 |
| $Fe_2O_3$ | 0.200 | 0.165 | -17.50 | 0.000 | 0.418 | -- | 0.600 | 1.011 | 68.50 | 0.000 | 0.471 | -- |
| $K_2O$ | 0.500 | 0.558 | 11.60 | 0.000 | <0.120 | -- | 1.000 | 0.977 | -2.30 | 0.000 | <0.120 | -- |
| MgO | 1.000 | 0.970 | -3.00 | 1.350 | 1.282 | -5.04 | 0.650 | 0.654 | 0.62 | 1.374 | 1.347 | -1.97 |
| $Na_2O$ | 23.000 | 22.714 | -1.24 | 21.000 | 19.580 | -6.76 | 23.000 | 22.748 | -1.10 | 26.464 | 26.185 | -1.05 |
| $P_2O_5$ | 0.240 | 0.176 | -26.67 | 0.203 | <0.243 | -- | 0.676 | 0.577 | -14.65 | 0.207 | 0.180 | -13.04 |
| $SiO_2$ | 40.940 | 41.609 | 1.63 | 47.000 | 47.947 | 2.01 | 38.800 | 41.117 | 5.97 | 35.523 | 34.122 | -3.94 |
| $SO_3$ | 1.000 | 0.954 | -4.60 | 0.1000 | 0.154 | 54.00 | 0.500 | 0.479 | -4.20 | 0.754 | 0.725 | -3.85 |
| $SnO_2$ | 0.000 | <0.127 | --- | 0.000 | <0.127 | -- | 1.500 | 1.717 | 14.47 | 2.779 | 2.965 | 6.69 |
| $V_2O_5$ | 2.100 | 2.089 | -0.52 | 0.000 | <0.179 | -- | 1.000 | 0.952 | -4.80 | 0.000 | <0.179 | -- |
| ZnO | 3.000 | 2.947 | -1.77 | 2.000 | 1.923 | -3.85 | 2.800 | 2.692 | -3.86 | 2.036 | 2.088 | 2.55 |
| $ZrO_2$ | 5.030 | 4.620 | -8.15 | 6.500 | 5.194 | -20.09 | 4.000 | 3.451 | -13.73 | 2.342 | 2.431 | 3.80 |
| Total | 100.000 | 99.219 | -0.78 | 100.000 | 98.683 | -1.32 | 100.000 | 101.099 | 1.099 | 100.000 | 98.276 | -1.72 |

Table B.1. Comparison of Targeted and Analyzed LAW Phase 1 Enhanced Glass Compositions (cont.)

| Glass ID | LP2-OL-04-1 | | | LP2-OL-05 | | | LP2-OL-07-1 | | |
|---|---|---|---|---|---|---|---|---|---|
| Component | Targeted (wt%) | Analyzed (wt%) | % Diff | Targeted (wt%) | Analyzed (wt%) | % Diff | Targeted (wt%) | Analyzed (wt%) | % Diff |
| $Al_2O_3$ | 10.500 | 10.147 | -3.36 | 12.500 | 11.814 | -5.49 | 10.150 | 9.523 | -6.18 |
| $B_2O_3$ | 6.000 | 6.263 | 4.38 | 6.000 | 5.989 | -0.18 | 12.040 | 12.332 | 2.43 |
| CaO | 7.840 | 7.283 | -7.10 | 11.000 | 10.798 | -1.84 | 8.010 | 8.063 | 0.66 |
| Cl | 0.062 | <0.050 | -- | 0.467 | 0.292 | -37.47 | 0.330 | 0.204 | -38.18 |
| $Cr_2O_3$ | 0.600 | 0.628 | 4.67 | 0.300 | 0.385 | 28.33 | 0.500 | 0.584 | 16.80 |
| $Cs_2O$ | 0.000 | -- | -- | 0.000 | -- | -- | 0.130 | -- | -- |
| F | 0.095 | 0.079 | -16.84 | 0.708 | 0.595 | -15.96 | 0.170 | 0.122 | -28.24 |
| $Fe_2O_3$ | 1.500 | 1.855 | 23.67 | 1.500 | 1.916 | 27.73 | 1.000 | 1.339 | 33.90 |
| $K_2O$ | 5.750 | 5.267 | -8.40 | 0.000 | <0.120 | -- | 0.160 | 0.211 | 31.88 |
| MgO | 1.350 | 1.251 | -7.33 | 0.000 | <0.166 | -- | 1.000 | 0.983 | -1.70 |
| $Na_2O$ | 21.000 | 19.748 | -5.96 | 21.000 | 19.007 | -9.49 | 20.980 | 19.344 | -7.80 |
| NiO | 0.000 | <0.127 | -- | 0.000 | <0.127 | -- | 0.040 | <0.127 | -- |
| $P_2O_5$ | 0.203 | <0.241 | -- | 1.515 | 1.461 | -3.56 | 0.290 | 0.261 | -10.00 |
| $SiO_2$ | 34.900 | 36.037 | 3.26 | 39.080 | 40.641 | 3.99 | 37.140 | 37.502 | 0.97 |
| $SO_3$ | 0.100 | 0.154 | 54.00 | 0.980 | 0.929 | -5.20 | 1.060 | 1.011 | -4.62 |
| $SnO_2$ | 0.000 | <0.127 | -- | 0.000 | <0.127 | -- | 0.000 | <0.127 | -- |
| $V_2O_5$ | 0.000 | <0.179 | -- | 0.000 | <0.179 | -- | 1.000 | 0.929 | -7.10 |
| ZnO | 3.600 | 3.457 | -3.97 | 2.000 | 1.998 | -0.10 | 3.000 | 3.053 | 1.77 |
| $ZrO_2$ | 6.500 | 5.545 | -14.69 | 2.950 | 2.161 | -26.75 | 3.000 | 2.452 | -18.27 |
| Total | 100.000 | 98.652 | -1.35 | 100.000 | 98.922 | -1.08 | 100.000 | 98.382 | -1.62 |

Table B.1. Comparison of Targeted and Analyzed LAW Phase 1 Enhanced Glass Compositions (cont.)

| Glass ID | LP2-OL-08 MOD | | | LP2-OL-09-1 | | | LP2-OL-10 MOD | | | LP2-OL-11 | | |
|---|---|---|---|---|---|---|---|---|---|---|---|---|
| Component | Targeted (wt%) | Analyzed (wt%) | % Diff | Targeted (wt%) | Analyzed (wt%) | % Diff | Targeted (wt%) | Analyzed (wt%) | % Diff | Targeted (wt%) | Analyzed (wt%) | % Diff |
| $Al_2O_3$ | 6.121 | 5.763 | -5.85 | 12.500 | 11.876 | -4.99 | 12.523 | 11.441 | -8.64 | 6.000 | 5.508 | -8.20 |
| $B_2O_3$ | 6.121 | 6.037 | -1.37 | 13.750 | 13.805 | 0.40 | 6.011 | 5.627 | -6.39 | 13.750 | 13.242 | -3.69 |
| CaO | 10.879 | 10.532 | -3.19 | 2.000 | 1.948 | -2.60 | 11.020 | 10.721 | -2.71 | 7.990 | 7.832 | -1.98 |
| Cl | 0.060 | 0.063 | -5.00 | 0.062 | <0.050 | -- | 0.468 | 0.378 | -19.23 | 0.062 | 0.051 | -17.74 |
| $Cr_2O_3$ | 0.612 | 0.694 | 13.40 | 0.600 | 0.691 | 15.17 | 0.301 | 0.404 | 34.22 | 0.300 | 0.402 | 34.00 |
| F | 0.097 | 0.077 | -20.62 | 0.095 | 0.067 | -29.47 | 0.709 | 0.648 | -8.60 | 0.095 | 0.077 | -18.95 |
| $Fe_2O_3$ | 1.530 | 1.891 | 23.60 | 0.000 | 0.570 | -- | 1.503 | 1.919 | 27.68 | 0.000 | 0.330 | -- |
| $K_2O$ | 0.000 | <0.120 | -- | 0.000 | <0.120 | -- | 0.000 | <0.120 | -- | 5.750 | 5.336 | -7.20 |
| MgO | 0.000 | <0.166 | -- | 0.000 | <0.166 | -- | 0.000 | <0.166 | -- | 1.350 | 1.332 | -1.33 |
| $Na_2O$ | 26.524 | 24.904 | -6.11 | 21.000 | 19.175 | -8.69 | 21.038 | 20.523 | -2.45 | 21.000 | 20.153 | -4.03 |
| $P_2O_5$ | 0.207 | 0.227 | 9.66 | 0.203 | <0.241 | -- | 1.518 | 1.723 | 13.5 | 0.203 | 0.234 | 15.3 |
| $SiO_2$ | 35.604 | 35.486 | -0.33 | 39.190 | 39.978 | 2.01 | 39.151 | 38.454 | -1.78 | 34.900 | 36.646 | 5.00 |
| $SO_3$ | 0.816 | 0.633 | -22.43 | 0.100 | 0.108 | 8.00 | 0.800 | 0.718 | -10.25 | 0.100 | 0.147 | 47.00 |
| $SnO_2$ | 0.000 | 0.472 | -- | 1.550 | 1.536 | -0.90 | 0.000 | 0.262 | -- | 0.000 | 0.265 | -- |
| $V_2O_5$ | 4.081 | 3.945 | -3.33 | 4.000 | 3.776 | -5.60 | 0.000 | <0.179 | -- | 0.000 | <0.179 | -- |
| ZnO | 2.040 | 2.020 | -0.98 | 2.000 | 1.945 | -2.75 | 2.004 | 2.013 | 0.45 | 2.000 | 1.957 | -2.15 |
| $ZrO_2$ | 5.305 | 5.268 | -0.70 | 2.950 | 2.060 | -30.17 | 2.955 | 3.033 | 2.64 | 6.500 | 5.187 | -20.20 |
| Total | 100.000 | 98.637 | -1.36 | 100.000 | 98.455 | -1.55 | 100.000 | 98.673 | -1.33 | 100.000 | 99.220 | -0.78 |

Table B.1. Comparison of Targeted and Analyzed LAW Phase 1 Enhanced Glass Compositions (cont.)

| Glass ID | LP2-OL-12 | | | LP2-OL-13 | | | LP2-OL-14 | | | LP2-OL-15 | | |
|---|---|---|---|---|---|---|---|---|---|---|---|---|
| Component | Targeted (wt%) | Analyzed (wt%) | % Diff | Targeted (wt%) | Analyzed (wt%) | % Diff | Targeted (wt%) | Analyzed (wt%) | % Diff | Targeted (wt%) | Analyzed (wt%) | % Diff |
| $Al_2O_3$ | 6.000 | 5.768 | -3.87 | 6.000 | 5.621 | -6.32 | 6.000 | 5.541 | -7.65 | 6.000 | 5.796 | -3.40 |
| $B_2O_3$ | 13.750 | 13.741 | -0.07 | 6.000 | 5.933 | -1.12 | 13.750 | 13.717 | -0.24 | 13.750 | 13.894 | 1.05 |
| CaO | 7.991 | 7.930 | -0.76 | 11.000 | 10.886 | -1.04 | 7.171 | 7.125 | -0.64 | 11.000 | 10.662 | -3.07 |
| Cl | 0.467 | 0.348 | -25.48 | 0.467 | 0.299 | -35.97 | 0.062 | <0.053 | -- | 0.062 | <0.054 | -- |
| $Cr_2O_3$ | 0.600 | 0.688 | 14.67 | 0.300 | 0.374 | 24.67 | 0.600 | 0.671 | 11.83 | 0.600 | 0.692 | 15.33 |
| F | 0.708 | 0.586 | -17.23 | 0.708 | 0.595 | -15.96 | 0.095 | 0.070 | -26.32 | 0.095 | 0.070 | -26.32 |
| $Fe_2O_3$ | 1.500 | 1.862 | 24.13 | 0.000 | 0.365 | -- | 0.000 | 0.286 | -- | 1.500 | 2.009 | 33.93 |
| $K_2O$ | 0.000 | <0.120 | -- | 5.750 | 5.562 | -3.27 | 5.750 | 5.580 | -2.96 | 0.000 | <0.120 | -- |
| MgO | 1.350 | 1.324 | -1.93 | 0.000 | <0.166 | -- | 0.000 | <0.166 | -- | 0.000 | <0.166 | -- |
| $Na_2O$ | 25.941 | 24.331 | -6.21 | 22.205 | 20.523 | -7.58 | 21.000 | 18.939 | -9.81 | 21.000 | 19.142 | -8.85 |
| $P_2O_5$ | 1.515 | 1.431 | -5.55 | 1.515 | 1.760 | 16.17 | 0.203 | <0.233 | -- | 0.203 | <0.232 | -- |
| $SiO_2$ | 35.128 | 36.336 | 3.44 | 35.405 | 35.208 | -0.56 | 34.900 | 33.737 | -3.33 | 35.640 | 36.459 | 2.30 |
| $SO_3$ | 0.100 | 0.137 | 37.00 | 0.100 | 0.102 | 2.00 | 1.519 | 1.503 | -1.05 | 0.100 | 0.119 | 19.00 |
| $SnO_2$ | 0.000 | <0.127 | -- | 0.000 | 0.277 | -- | 0.000 | <0.127 | -- | 3.500 | 3.463 | -1.06 |
| $V_2O_5$ | 0.000 | <0.179 | -- | 4.000 | 3.963 | -0.93 | 4.000 | 3.974 | -0.65 | 0.000 | <0.179 | -- |
| ZnO | 2.000 | 2.013 | 0.65 | 3.600 | 3.675 | 2.08 | 2.000 | 2.017 | 0.85 | 3.600 | 3.551 | -1.36 |
| $ZrO_2$ | 2.950 | 2.148 | -27.19 | 2.950 | 2.499 | -15.29 | 2.950 | 1.898 | -35.66 | 2.950 | 2.080 | -29.49 |
| Total | 100.000 | 98.437 | -1.56 | 100.000 | 98.149 | -1.85 | 100.000 | 95.977 | -4.02 | 100.000 | 99.028 | -0.97 |

Table B.1. Comparison of Targeted and Analyzed LAW Phase 1 Enhanced Glass Compositions (cont.)

| Glass ID | LP2-OL-16 MOD | | | LP2-OL-17 | | | LP2-OL-18 | | | LP2-OL-19 | | |
|---|---|---|---|---|---|---|---|---|---|---|---|---|
| Component | Targeted (wt%) | Analyzed (wt%) | % Diff | Targeted (wt%) | Analyzed (wt%) | % Diff | Targeted (wt%) | Analyzed (wt%) | % Diff | Targeted (wt%) | Analyzed (wt%) | % Diff |
| $Al_2O_3$ | 6.008 | 5.475 | -8.87 | 6.000 | 5.720 | -4.67 | 6.000 | 5.772 | -3.80 | 6.000 | 5.692 | -5.13 |
| $B_2O_3$ | 7.483 | 7.309 | -2.33 | 6.000 | 6.182 | 3.03 | 6.000 | 5.925 | -1.25 | 6.000 | 6.037 | 0.62 |
| CaO | 3.054 | 3.064 | 0.33 | 4.550 | 4.345 | -4.51 | 8.720 | 8.626 | -1.08 | 3.345 | 3.505 | 4.78 |
| Cl | 0.062 | 0.052 | -16.13 | 0.467 | 0.329 | -29.55 | 0.470 | 0.318 | -32.34 | 0.062 | 0.055 | -11.29 |
| $Cr_2O_3$ | 0.601 | 0.710 | 18.14 | 0.300 | 0.378 | 26.00 | 0.600 | 0.657 | 9.50 | 0.300 | 0.424 | 41.33 |
| F | 0.095 | 0.075 | -21.05 | 0.708 | 0.603 | -14.83 | 0.710 | 0.630 | -11.27 | 0.095 | 0.081 | -14.74 |
| $Fe_2O_3$ | 1.502 | 1.880 | 25.17 | 1.500 | 1.769 | 17.93 | 0.000 | 0.462 | -- | 1.500 | 1.969 | 31.27 |
| $K_2O$ | 0.000 | <0.120 | -- | 5.750 | 5.388 | -6.30 | 0.000 | <0.120 | -- | 5.750 | 5.641 | -1.90 |
| MgO | 1.352 | 1.301 | -3.77 | 1.350 | 1.288 | -4.59 | 1.350 | 1.281 | -5.11 | 0.000 | <0.166 | -- |
| $Na_2O$ | 21.026 | 20.490 | -2.55 | 22.205 | 20.523 | -7.58 | 21.000 | 20.287 | -3.40 | 21.000 | 19.175 | -8.69 |
| $P_2O_5$ | 0.203 | 0.204 | 0.49 | 1.515 | 1.463 | -3.43 | 1.520 | 1.277 | -15.99 | 0.203 | 0.242 | 19.21 |
| $SiO_2$ | 47.059 | 49.894 | 6.02 | 37.105 | 38.037 | 2.51 | 34.900 | 34.111 | -2.26 | 46.499 | 43.150 | -7.20 |
| $SO_3$ | 0.992 | 0.896 | -9.68 | 0.100 | 0.138 | 38.0 | 1.140 | 1.003 | -12.02 | 0.796 | 0.620 | -22.11 |
| $SnO_2$ | 0.000 | 0.440 | -- | 3.500 | 3.399 | -2.89 | 3.500 | 3.847 | 9.91 | 3.500 | 3.625 | 3.57 |
| $V_2O_5$ | 4.005 | 3.771 | -5.84 | 4.000 | 3.834 | -4.15 | 4.000 | 3.972 | -0.70 | 0.000 | <0.179 | -- |
| ZnO | 3.605 | 3.439 | -4.61 | 2.000 | 1.967 | -1.65 | 3.600 | 3.706 | 2.94 | 2.000 | 2.010 | 0.50 |
| $ZrO_2$ | 2.954 | 2.465 | -16.55 | 2.950 | 2.242 | -24.00 | 6.500 | 4.903 | -24.57 | 2.950 | 2.668 | -9.56 |
| Total | 100.000 | 101.928 | 1.93 | 100.000 | 97.949 | -2.05 | 100.000 | 97.242 | -2.76 | 100.000 | 95.582 | -4.42 |

Table B.1. Comparison of Targeted and Analyzed LAW Phase 1 Enhanced Glass Compositions (cont.)

| Glass ID | LP2-OL-20 | | | LP2-OL-21 | | | LP2-OL-22 | | | LP2-OL-23 | | |
|---|---|---|---|---|---|---|---|---|---|---|---|---|
| Component | Targeted (wt%) | Analyzed (wt%) | % Diff | Targeted (wt%) | Analyzed (wt%) | % Diff | Targeted (wt%) | Analyzed (wt%) | % Diff | Targeted (wt%) | Analyzed (wt%) | % Diff |
| $Al_2O_3$ | 6.000 | 5.560 | -7.33 | 10.000 | 9.358 | -6.42 | 7.000 | 6.514 | -6.94 | 6.000 | 5.513 | -8.12 |
| $B_2O_3$ | 6.000 | 5.796 | -3.40 | 9.500 | 9.434 | -0.70 | 6.000 | 5.884 | -1.93 | 13.725 | 13.266 | -3.34 |
| CaO | 8.050 | 8.063 | 0.16 | 5.000 | 5.128 | 2.56 | 11.000 | 10.714 | -2.60 | 11.000 | 10.438 | -5.11 |
| Cl | 0.062 | 0.064 | 3.23 | 0.208 | 0.162 | -22.12 | 0.062 | <0.050 | -- | 0.062 | 0.056 | -9.68 |
| $Cr_2O_3$ | 0.300 | 0.433 | 44.33 | 0.450 | 0.553 | 22.89 | 0.300 | 0.376 | 25.33 | 0.300 | 0.423 | 41.00 |
| F | 0.095 | 0.081 | -14.74 | 0.316 | 0.278 | -12.03 | 0.095 | 0.075 | -21.05 | 0.095 | 0.072 | -24.21 |
| $Fe_2O_3$ | 0.000 | 0.535 | -- | 0.600 | 0.953 | 58.83 | 1.500 | 1.898 | 26.53 | 0.000 | 0.599 | -- |
| $K_2O$ | 0.000 | <0.120 | -- | 1.000 | 1.056 | 5.60 | 0.000 | <0.120 | -- | 0.000 | <0.120 | -- |
| MgO | 0.000 | <0.166 | -- | 0.650 | 0.643 | -1.08 | 0.000 | <0.166 | -- | 1.350 | 1.306 | -3.26 |
| $Na_2O$ | 26.000 | 25.545 | -1.75 | 23.000 | 21.972 | -4.47 | 21.000 | 19.243 | -8.37 | 21.000 | 20.456 | -2.59 |
| $P_2O_5$ | 0.203 | 0.214 | 5.42 | 0.676 | 0.632 | -6.51 | 0.203 | 0.275 | 35.47 | 0.203 | 0.195 | -3.94 |
| $SiO_2$ | 46.640 | 44.540 | -4.50 | 38.800 | 42.096 | 8.50 | 36.740 | 36.320 | -1.14 | 34.900 | 36.411 | 4.33 |
| $SO_3$ | 0.100 | 0.120 | 20.00 | 0.500 | 0.502 | 0.40 | 0.100 | 0.104 | 4.00 | 1.315 | 1.160 | -11.79 |
| $SnO_2$ | 0.000 | 0.258 | -- | 1.500 | 1.796 | 19.73 | 3.500 | 3.571 | 2.03 | 3.500 | 3.545 | 1.29 |
| $V_2O_5$ | 0.000 | <0.179 | -- | 1.000 | 0.951 | -4.90 | 4.000 | 3.905 | -2.38 | 0.000 | <0.179 | -- |
| ZnO | 3.600 | 3.716 | 3.22 | 2.800 | 2.742 | -2.07 | 2.000 | 2.001 | 0.05 | 3.600 | 3.417 | -5.08 |
| $ZrO_2$ | 2.950 | 2.533 | 14.14 | 4.000 | 3.228 | -19.30 | 6.500 | 5.214 | -19.79 | 2.950 | 2.573 | -12.78 |
| Total | 100.000 | 98.263 | -1.74 | 100.000 | 101.825 | 1.83 | 100.000 | 96.773 | -3.23 | 100.000 | 100.072 | 0.07 |

Table B.1. Comparison of Targeted and Analyzed LAW Phase 1 Enhanced Glass Compositions (cont.)

| Glass ID | LP2-OL-24 | | | LP2-OL-25 | | |
|---|---|---|---|---|---|---|
| Component | Targeted (wt%) | Analyzed (wt%) | % Diff | Targeted (wt%) | Analyzed (wt%) | % Diff |
| $Al_2O_3$ | 12.500 | 11.403 | -8.78 | 6.000 | 5.782 | -3.63 |
| $B_2O_3$ | 6.000 | 5.804 | -3.27 | 13.750 | 13.419 | -2.41 |
| CaO | 7.245 | 7.423 | 2.5 | 2.578 | 2.624 | 1.8 |
| Cl | 0.062 | 0.061 | -1.61 | 0.062 | 0.058 | -6.45 |
| $Cr_2O_3$ | 0.300 | 0.421 | 40.33 | 0.300 | 0.402 | 34.00 |
| F | 0.095 | 0.095 | 0.00 | 0.095 | 0.076 | -20.00 |
| $Fe_2O_3$ | 1.500 | 1.916 | 27.73 | 1.500 | 1.991 | 32.73 |
| $K_2O$ | 0.000 | <0.120 | -- | 0.000 | <0.120 | -- |
| MgO | 1.350 | 1.351 | 0.07 | 0.000 | <0.166 | -- |
| $Na_2O$ | 25.195 | 25.241 | 0.18 | 26.000 | 23.860 | -8.23 |
| $P_2O_5$ | 0.203 | 0.192 | -5.42 | 0.203 | 0.279 | 37.44 |
| $SiO_2$ | 34.900 | 33.956 | -2.71 | 34.900 | 35.823 | 2.65 |
| $SO_3$ | 0.100 | 0.128 | 28.00 | 1.012 | 0.790 | -21.9 |
| $SnO_2$ | 0.000 | 0.250 | -- | 3.500 | 3.710 | 6.00 |
| $V_2O_5$ | 4.000 | 4.084 | 2.10 | 0.000 | <0.179 | -- |
| ZnO | 3.600 | 3.809 | 5.81 | 3.600 | 3.535 | -1.81 |
| $ZrO_2$ | 2.950 | 2.627 | -10.95 | 6.500 | 5.356 | -17.60 |
| Total | 100.000 | 99.225 | -0.78 | 100.000 | 98.511 | -1.49 |

# Appendix C – Viscosity Data

This appendix contains the measured viscosity data for each of the Phase 2 enhanced LAW glasses. The plots shown in this appendix were fitted to the Arrhenius equation

$$\ln(\eta) = A + \frac{B}{T_K} \quad \text{(C.1)}$$

where $A$ and $B$ are independent of temperature and possibly composition dependent, and temperature ($T_K$) is in K (T(°C) + 273.15). If the plots showed curvature, the data would be better fit to the Vogel- Fulcher-Tammann (VFT) model

$$\ln(\eta) = E + \frac{F}{T_k - T_0} \quad \text{(C.2)}$$

where $E$, $F$, and $T_0$ are temperature independent and possibly composition dependent coefficients, and $T_K$ is the temperature in K (T(°C) + 273.15). The intent of the figures and Arrhenius equation fits shown in this appendix is mainly to assess trends of the data and provide some observations about whether there may be sufficient curvature in the data to consider VFT fits in the subsequent work that will decide between fitting the viscosity-temperature data to the Arrhenius or VFT equations.

## C.1 Glass LP2-IL-01 Viscosity Data

Table C.1. Viscosity Data for Glass LP2-IL-01

| Measured Temp., °C | Viscosity, P | 1/T x10000, $K^{-1}$ | ln η, P |
|---|---|---|---|
| 1150 | 25.078 | 7.027 | 3.222 |
| 1050 | 70.056 | 7.559 | 4.249 |
| 950 | 258.950 | 8.177 | 5.557 |
| 1150 | 25.300 | 7.027 | 3.231 |
| 1250 | 10.900 | 6.566 | 2.389 |
| 1150 | 25.189 | 7.027 | 3.226 |

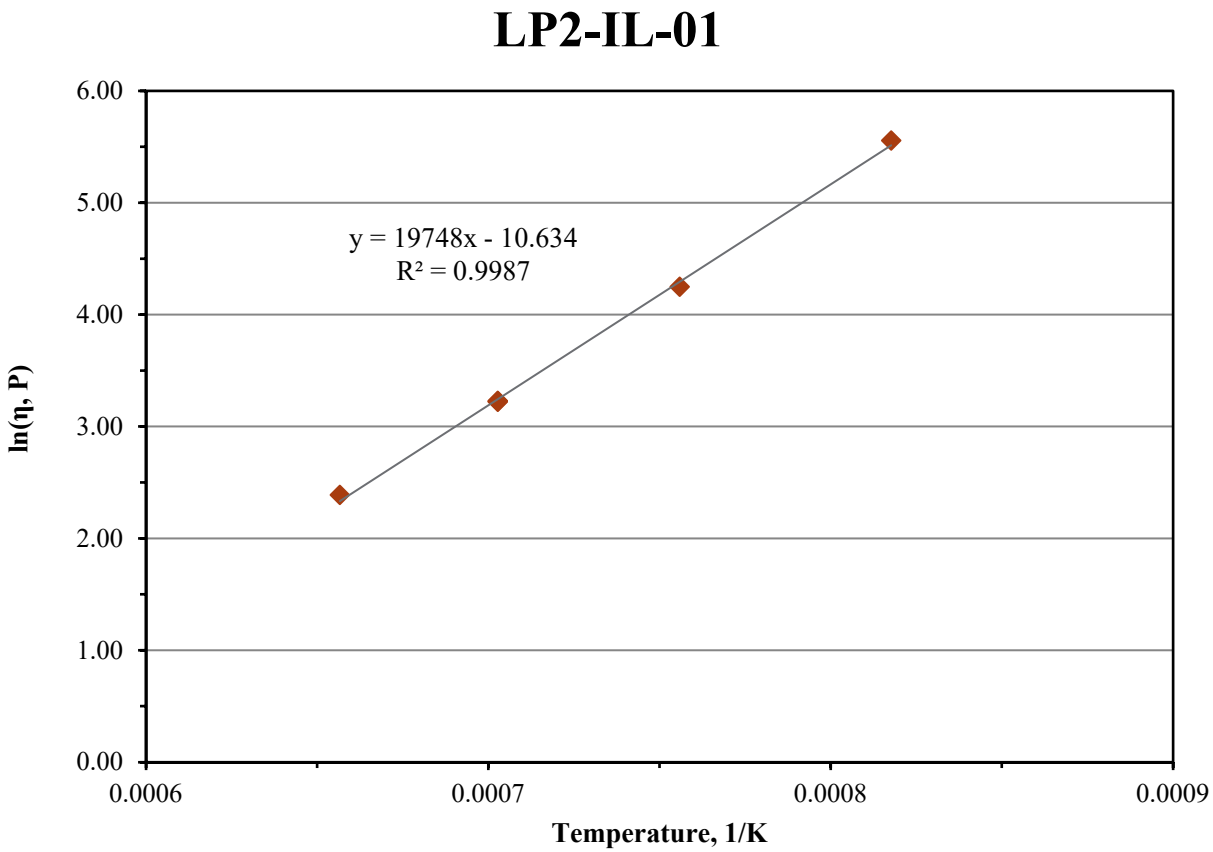


Figure C.1. Viscosity-Temperature Data and Arrhenius Equation Fit for Glass LP2-IL-01

## C.2 Glass LP2-IL-02 Viscosity Data

Table C.2. Viscosity Data for Glass LP2-IL-02

| Measured Temp., °C | Viscosity, P | 1/T x10000, $K^{-1}$ | ln η, P |
|---|---|---|---|
| 1150 | 62.771 | 7.027 | 4.139 |
| 1050 | 197.680 | 7.559 | 5.287 |
| 950 | 840.620 | 8.177 | 6.734 |
| 1150 | 62.883 | 7.027 | 4.141 |
| 1250 | 24.668 | 6.566 | 3.206 |
| 1150 | 62.517 | 7.027 | 4.135 |

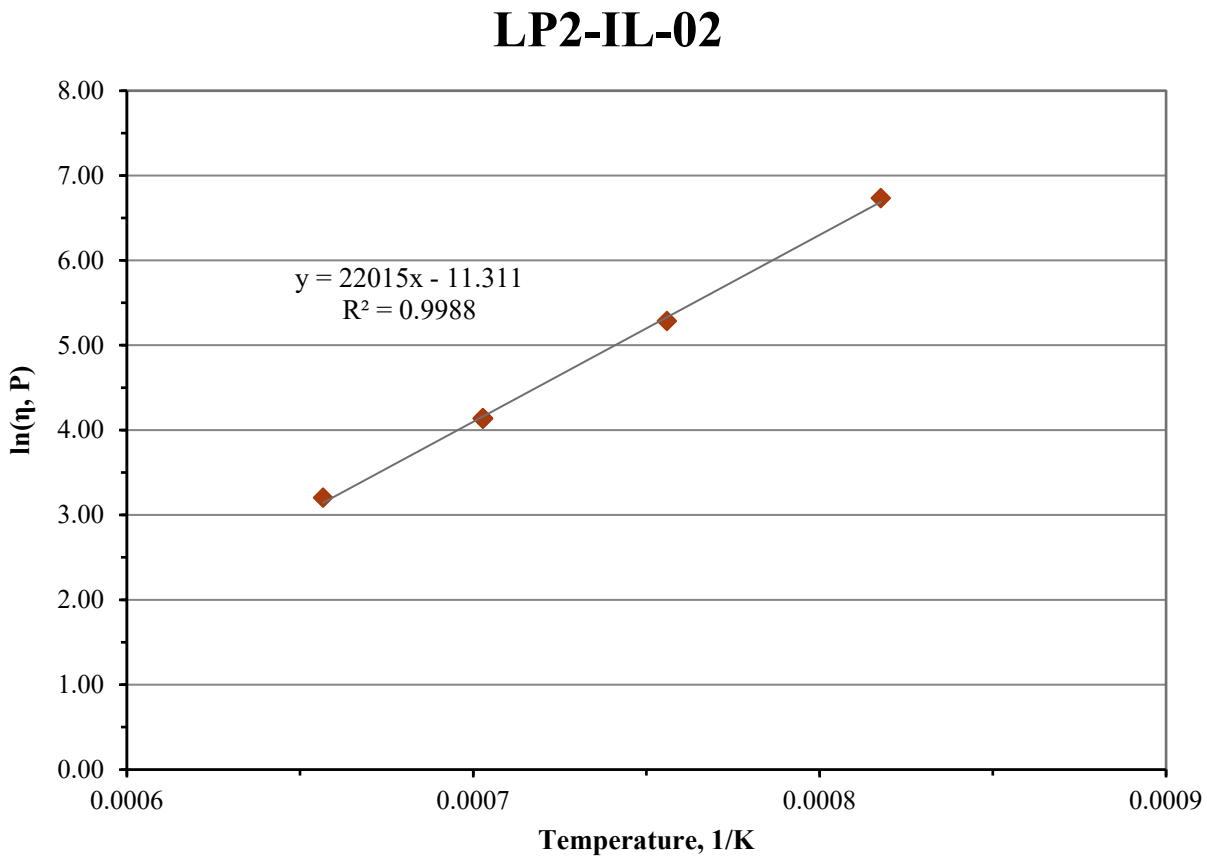


Figure C.2. Viscosity-Temperature Data and Arrhenius Equation Fit for Glass LP2-IL-02

## C.3 Glass LP2-IL-03 Viscosity Data

Table C.3. Viscosity Data for Glass LP2-IL-03

| Measured Temp., °C | Viscosity, P | 1/T x10000, $K^{-1}$ | ln η, P |
|---|---|---|---|
| 1150 | 56.953 | 7.027 | 4.042 |
| 1050 | 174.980 | 7.559 | 5.165 |
| 950 | 721.650 | 8.177 | 6.582 |
| 1150 | 57.084 | 7.027 | 4.045 |
| 1250 | 22.522 | 6.566 | 3.114 |
| 1150 | 55.956 | 7.027 | 4.025 |

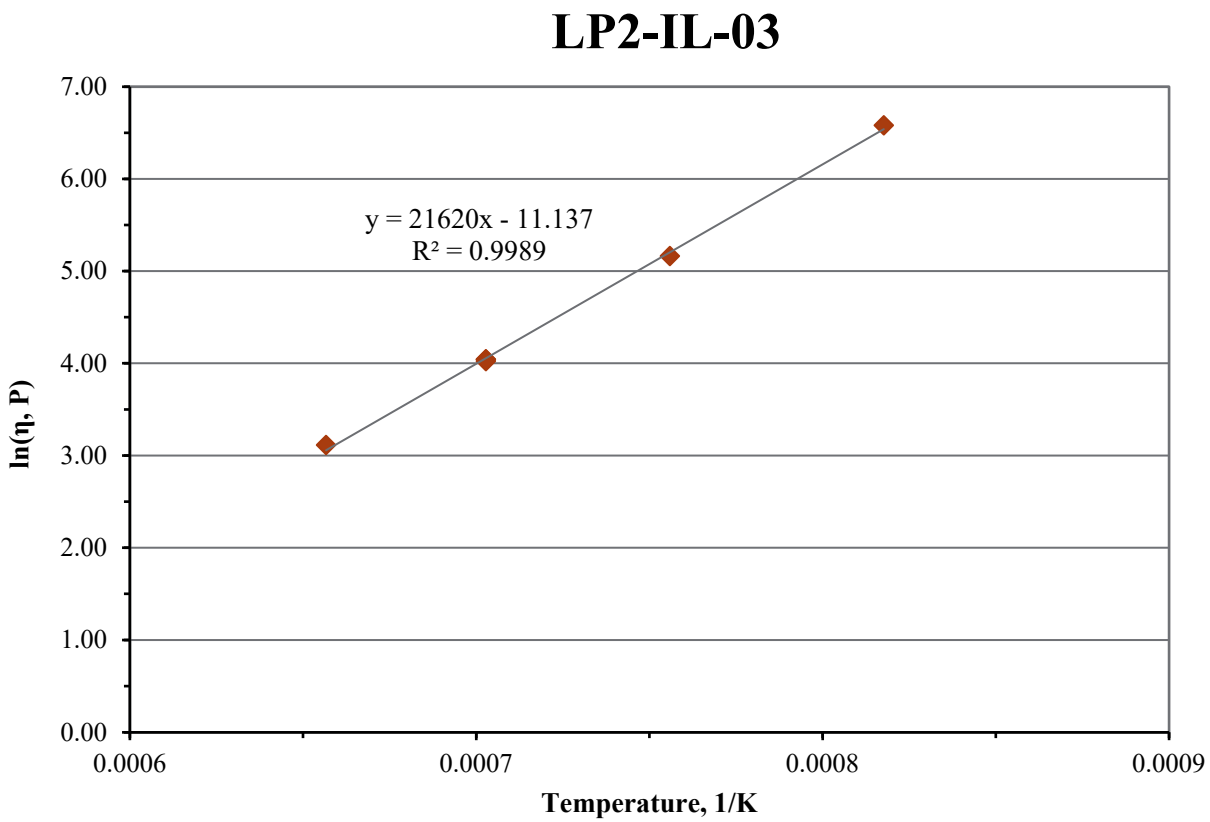


Figure C.3. Viscosity-Temperature Data and Arrhenius Equation Fit for Glass LP2-IL-03

## C.4 Glass LP2-IL-04 Viscosity Data

Table C.4. Viscosity Data for Glass LP2-IL-04

| Measured Temp., °C | Viscosity, P | 1/T x10000, K-1 | ln η, P |
|---|---|---|---|
| 1150 | 24.808 | 7.027 | 3.211 |
| 1050 | 68.137 | 7.559 | 4.222 |
| 950 | 249.000 | 8.177 | 5.517 |
| 1150 | 25.100 | 7.027 | 3.223 |
| 1250 | 11.100 | 6.566 | 2.407 |
| 1150 | 25.263 | 7.027 | 3.229 |

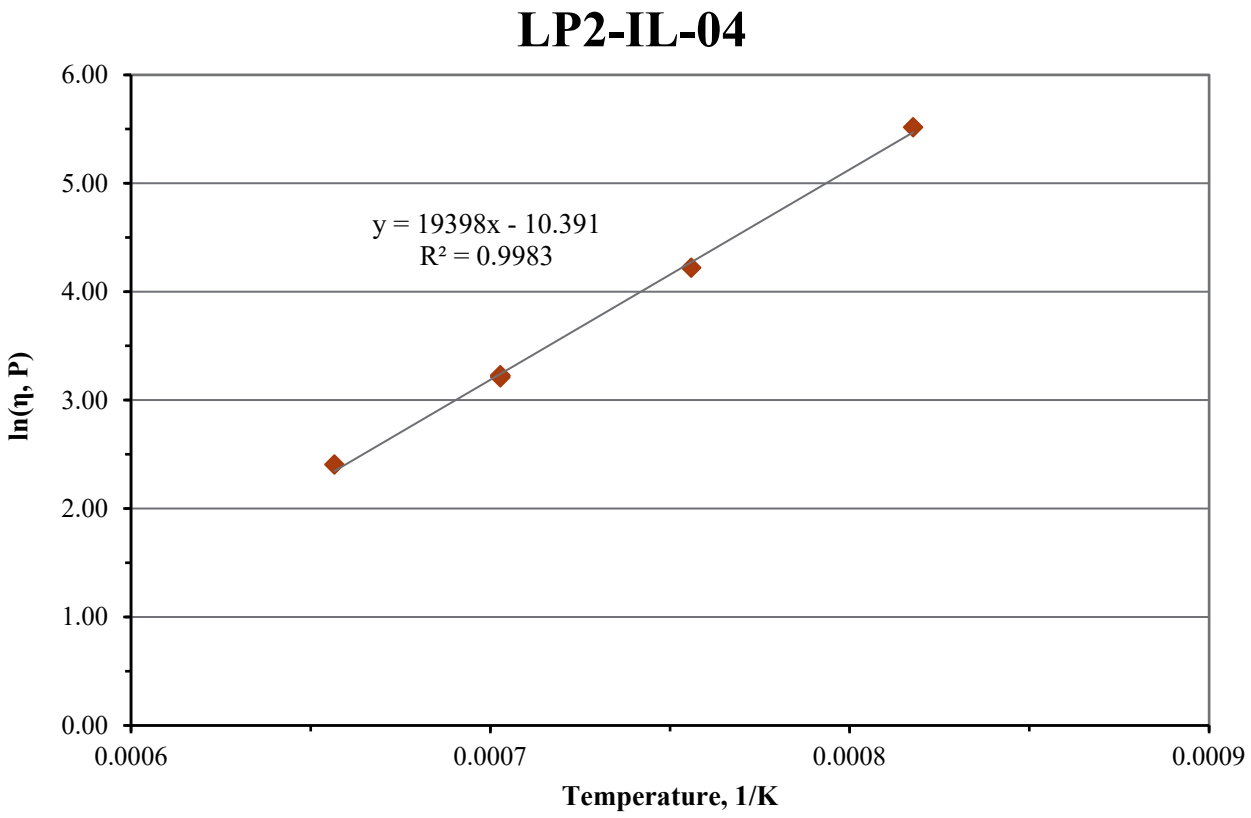


Figure C.4. Viscosity-Temperature Data and Arrhenius Equation Fit for Glass LP2-IL-04

## C.5 Glass LP2-IL-05 Viscosity Data

Table C.5. Viscosity Data for Glass LP2-IL-05

| Measured Temp., °C | Viscosity, P | 1/T x10000, $K^{-1}$ | ln η, P |
|---|---|---|---|
| 1150 | 24.355 | 7.027 | 3.193 |
| 1050 | 70.386 | 7.559 | 4.254 |
| 950 | 278.410 | 8.177 | 5.629 |
| 1150 | 24.600 | 7.027 | 3.203 |
| 1250 | 10.600 | 6.566 | 2.361 |
| 1150 | 24.704 | 7.027 | 3.207 |

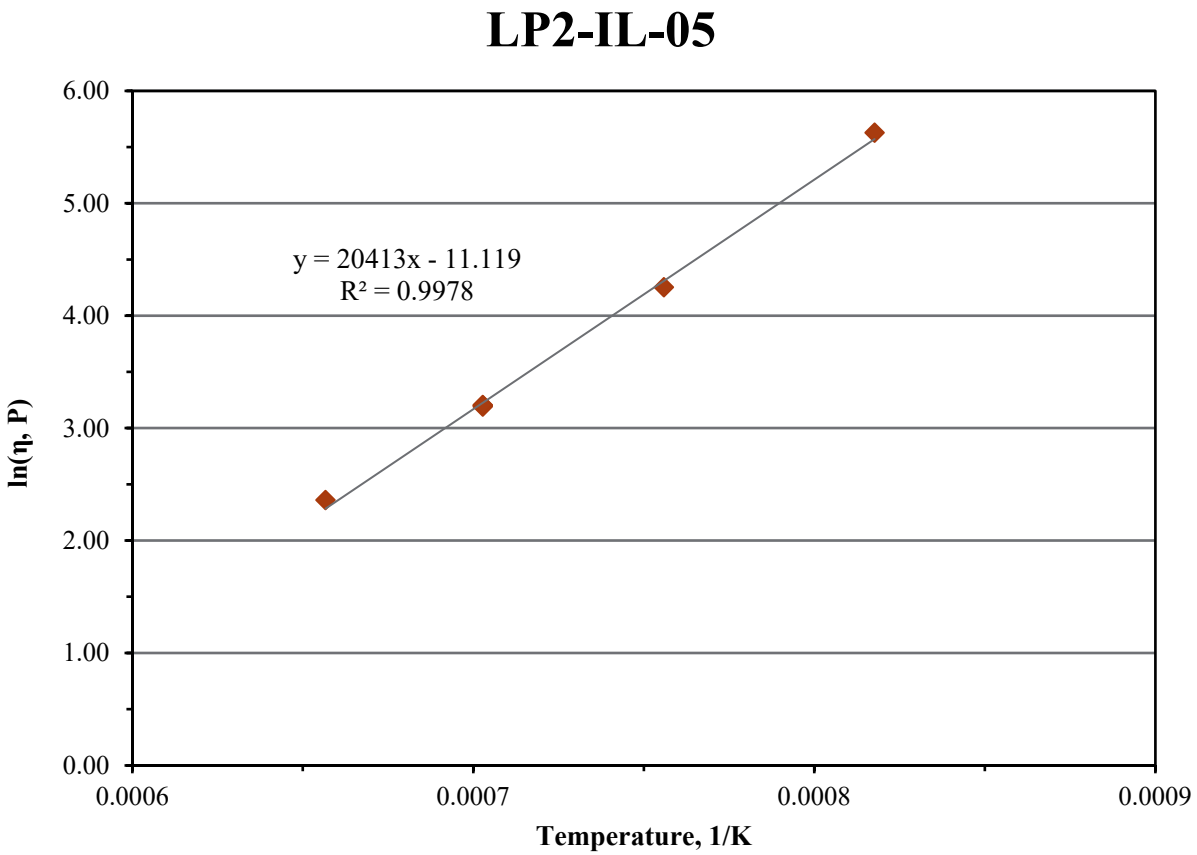


Figure C.5. Viscosity-Temperature Data and Arrhenius Equation Fit for Glass LP2-IL-05

## C.6 Glass LP2-IL-06 Viscosity Data

Table C.6. Viscosity Data for Glass LP2-IL-06

| Measured Temp., °C | Viscosity, P | 1/T x10000, $K^{-1}$ | ln η, P |
|---|---|---|---|
| 1150 | 46.437 | 7.027 | 3.838 |
| 1050 | 132.000 | 7.559 | 4.883 |
| 950 | 494.400 | 8.177 | 6.203 |
| 1150 | 47.110 | 7.027 | 3.852 |
| 1250 | 20.212 | 6.566 | 3.006 |
| 1150 | 47.424 | 7.027 | 3.859 |

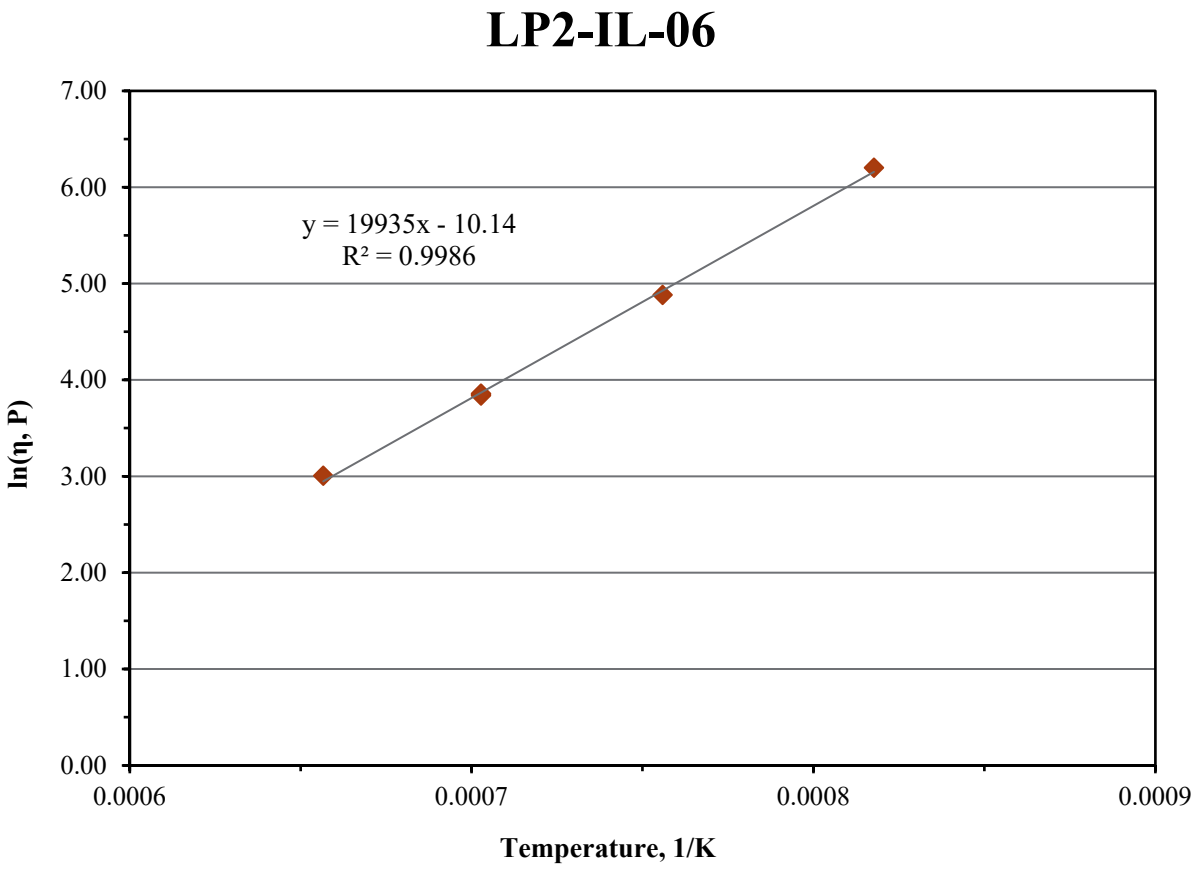


Figure C.6. Viscosity-Temperature Data and Arrhenius Equation Fit for Glass LP2-IL-06

## C.7 Glass LP2-IL-07 Viscosity Data

Table C.7. Viscosity Data for Glass LP2-IL-07

| Measured Temp., °C | Viscosity, P | 1/T x10000, $K^{-1}$ | ln η, P |
|---|---|---|---|
| 1150 | 25.601 | 7.027 | 3.243 |
| 1050 | 65.778 | 7.559 | 4.186 |
| 950 | 217.620 | 8.177 | 5.383 |
| 1150 | 25.974 | 7.027 | 3.257 |
| 1250 | 12.200 | 6.566 | 2.501 |
| 1150 | 26.192 | 7.027 | 3.265 |

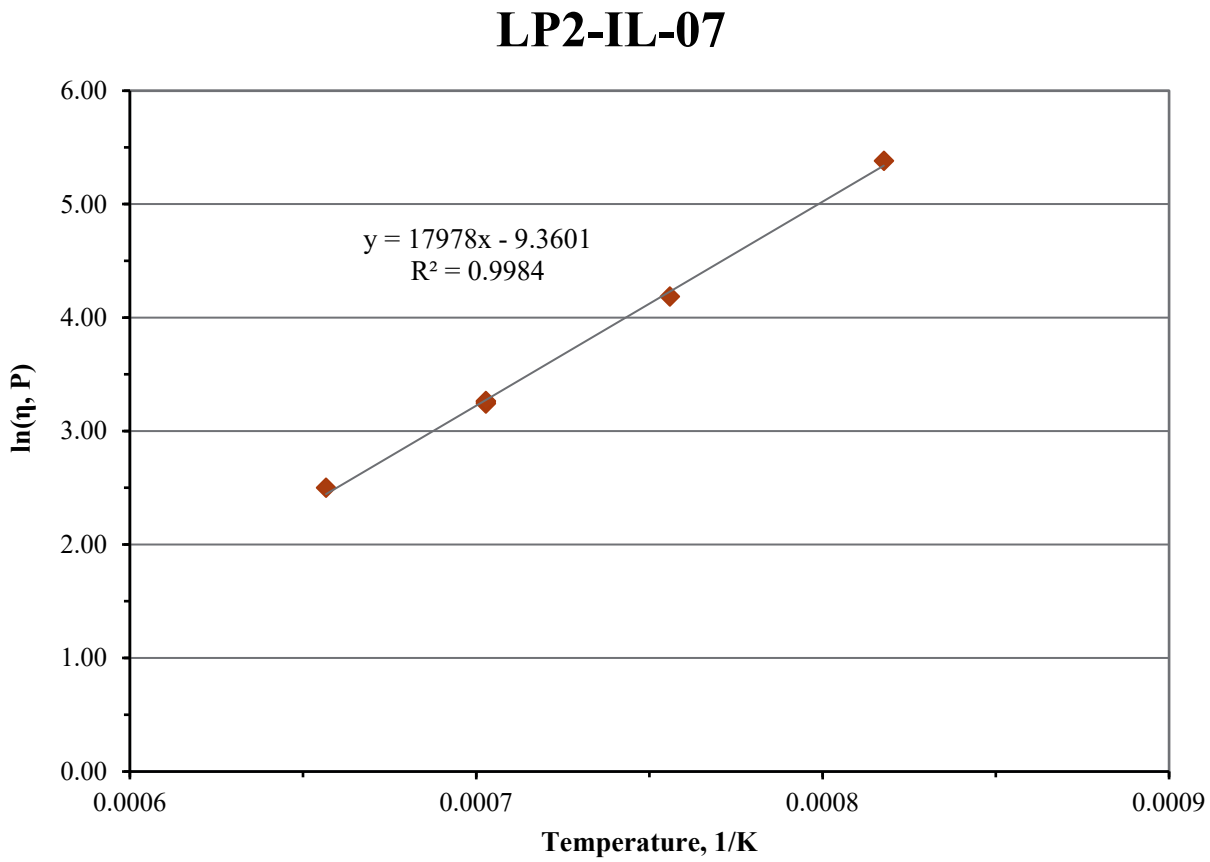


Figure C.7. Viscosity-Temperature Data and Arrhenius Equation Fit for Glass LP2-IL-07

## C.8 Glass LP2-IL-08 Viscosity Data

Table C.8. Viscosity Data for Glass LP2-IL-08

| Measured Temp., °C | Viscosity, P | 1/T x10000, $K^{-1}$ | ln η, P |
|---|---|---|---|
| 1150 | 35.711 | 7.027 | 3.575 |
| 1050 | 107.000 | 7.559 | 4.673 |
| 950 | 434.120 | 8.177 | 6.073 |
| 1150 | 36.093 | 7.027 | 3.586 |
| 1250 | 14.997 | 6.566 | 2.708 |
| 1150 | 36.204 | 7.027 | 3.589 |

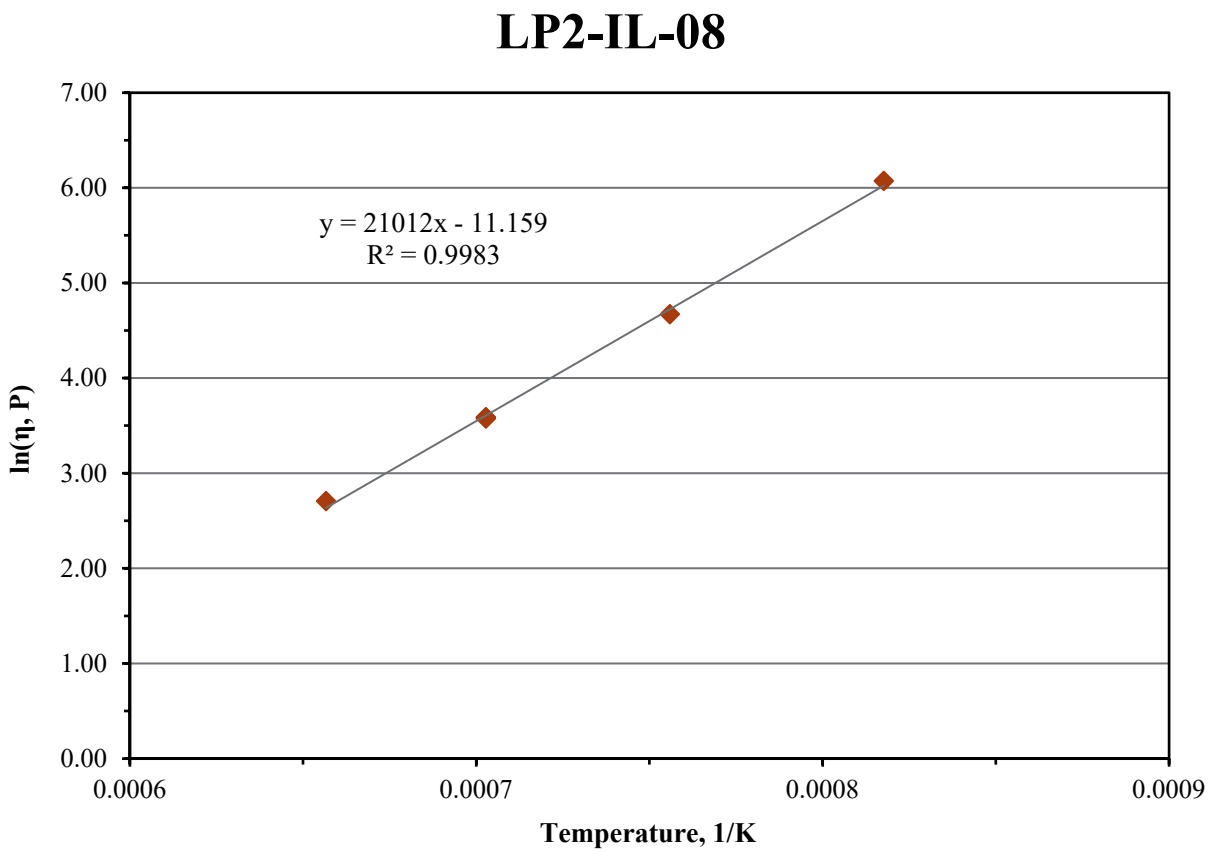


Figure C.8. Viscosity-Temperature Data and Arrhenius Equation Fit for Glass LP2-IL-08

## C.9 Glass LP2-IL-09 Viscosity Data

Table C.9. Viscosity Data for Glass LP2-IL-09

| Measured Temp., °C | Viscosity, P | 1/T x10000, $K^{-1}$ | ln η, P |
|---|---|---|---|
| 1150 | 24.098 | 7.027 | 3.182 |
| 1050 | 66.425 | 7.559 | 4.196 |
| 950 | 243.000 | 8.177 | 5.493 |
| 1150 | 24.222 | 7.027 | 3.187 |
| 1250 | 10.795 | 6.566 | 2.379 |
| 1150 | 24.300 | 7.027 | 3.190 |

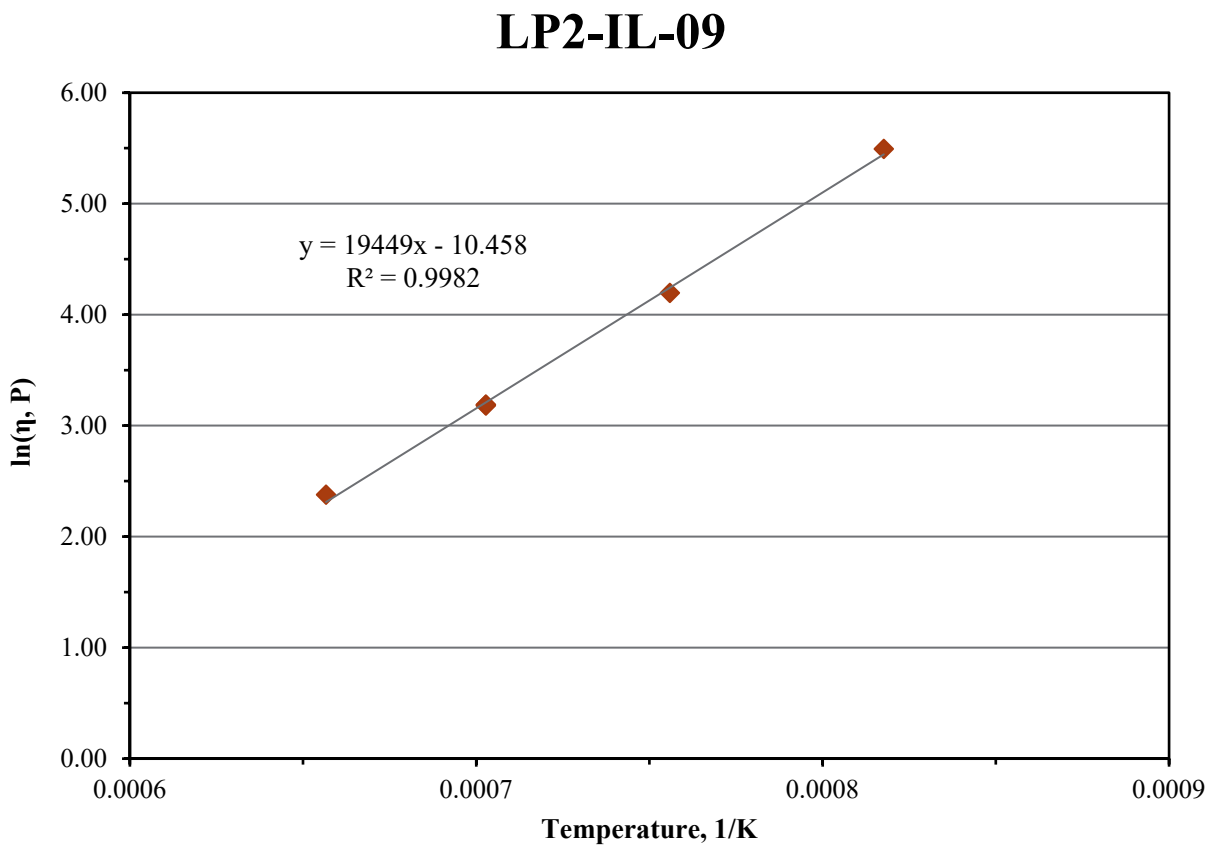


Figure C.9. Viscosity-Temperature Data and Arrhenius Equation Fit for Glass LP2-IL-09

## C.10 Glass LP2-IL-10 Viscosity Data

Table C.10. Viscosity Data for Glass LP2-IL-10

| Measured Temp., °C | Viscosity, P | 1/T x10000, $K^{-1}$ | ln η, P |
|---|---|---|---|
| 1150 | 46.916 | 7.027 | 3.848 |
| 1050 | 134.580 | 7.559 | 4.902 |
| 950 | 508.790 | 8.177 | 6.232 |
| 1150 | 47.276 | 7.027 | 3.856 |
| 1250 | 20.114 | 6.566 | 3.001 |
| 1150 | 47.246 | 7.027 | 3.855 |

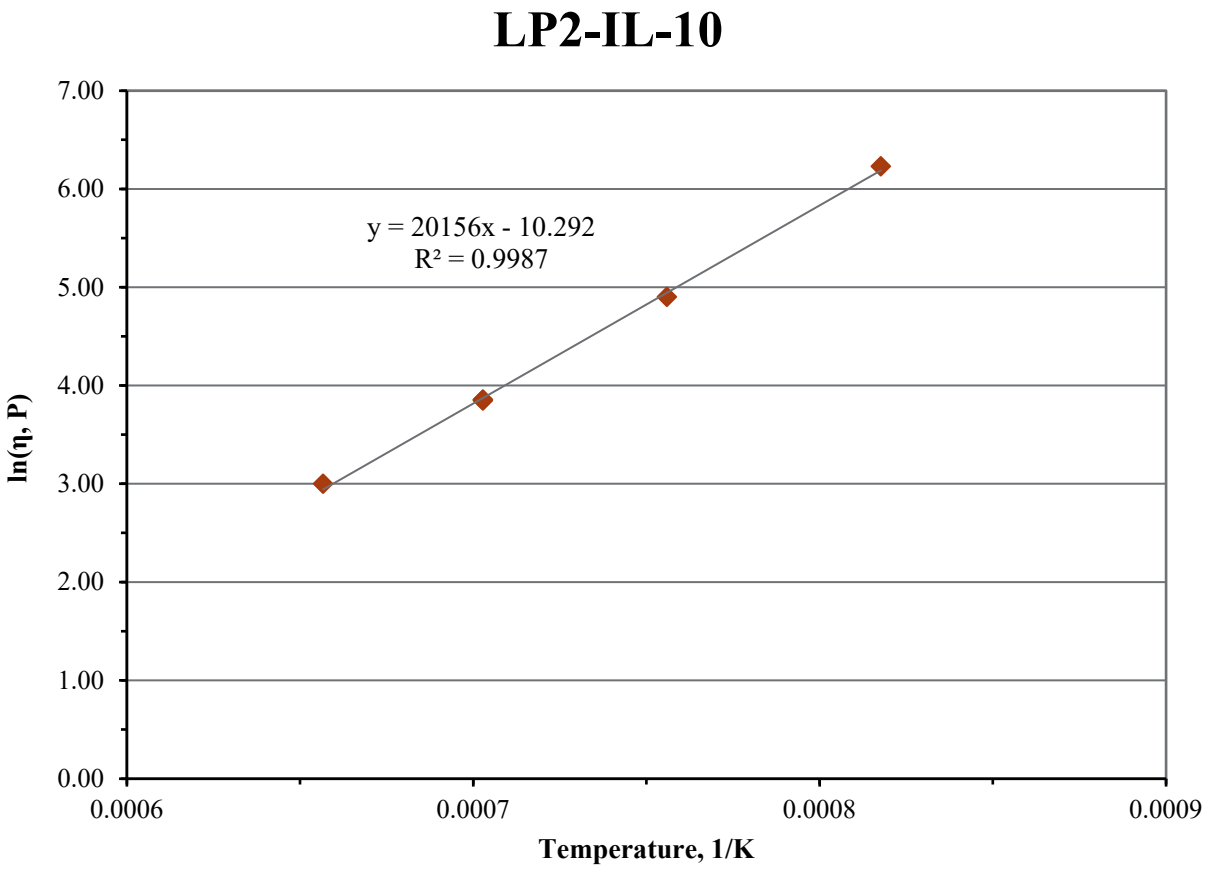


Figure C.10. Viscosity-Temperature Data and Arrhenius Equation Fit for Glass LP2-IL-10

## C.11 Glass LP2-IL-11 Viscosity Data

Table C.11. Viscosity Data for Glass LP2-IL-11

| Measured Temp., °C | Viscosity, P | 1/T x10000, $K^{-1}$ | ln η, P |
|---|---|---|---|
| 1150 | 58.537 | 7.027 | 4.070 |
| 1050 | 182.920 | 7.559 | 5.209 |
| 950 | 764.970 | 8.177 | 6.640 |
| 1150 | 59.055 | 7.027 | 4.078 |
| 1250 | 23.859 | 6.566 | 3.172 |
| 1150 | 60.265 | 7.027 | 4.099 |

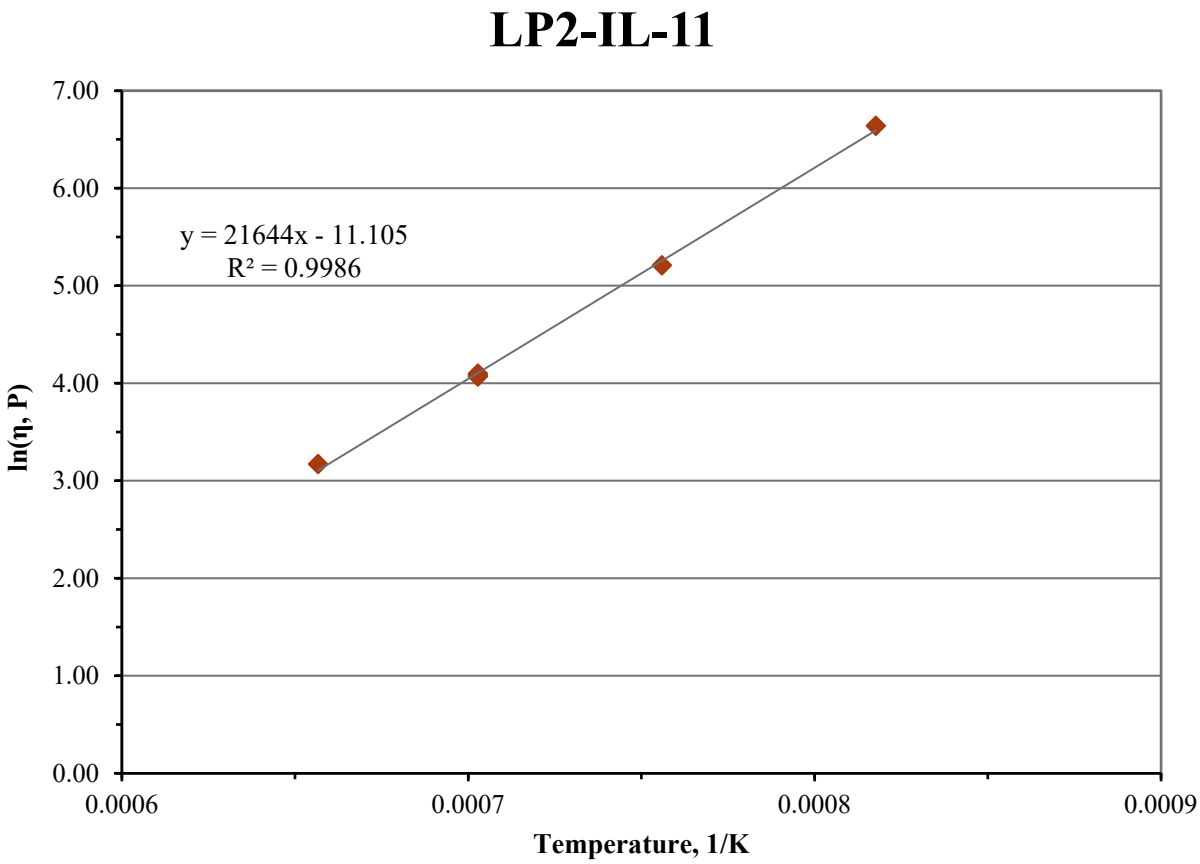


Figure C.11. Viscosity-Temperature Data and Arrhenius Equation Fit for Glass LP2-IL-11

## C.12 Glass LP2-IL-12 Viscosity Data

Table C.12. Viscosity Data for Glass LP2-IL-12

| Measured Temp., °C | Viscosity, P | 1/T x10000, $K^{-1}$ | ln η, P |
|---|---|---|---|
| 1150 | 62.078 | 7.027 | 4.128 |
| 1050 | 182.830 | 7.559 | 5.209 |
| 950 | 697.660 | 8.177 | 6.548 |
| 1150 | 62.585 | 7.027 | 4.137 |
| 1250 | 25.958 | 6.566 | 3.256 |
| 1150 | 62.543 | 7.027 | 4.136 |

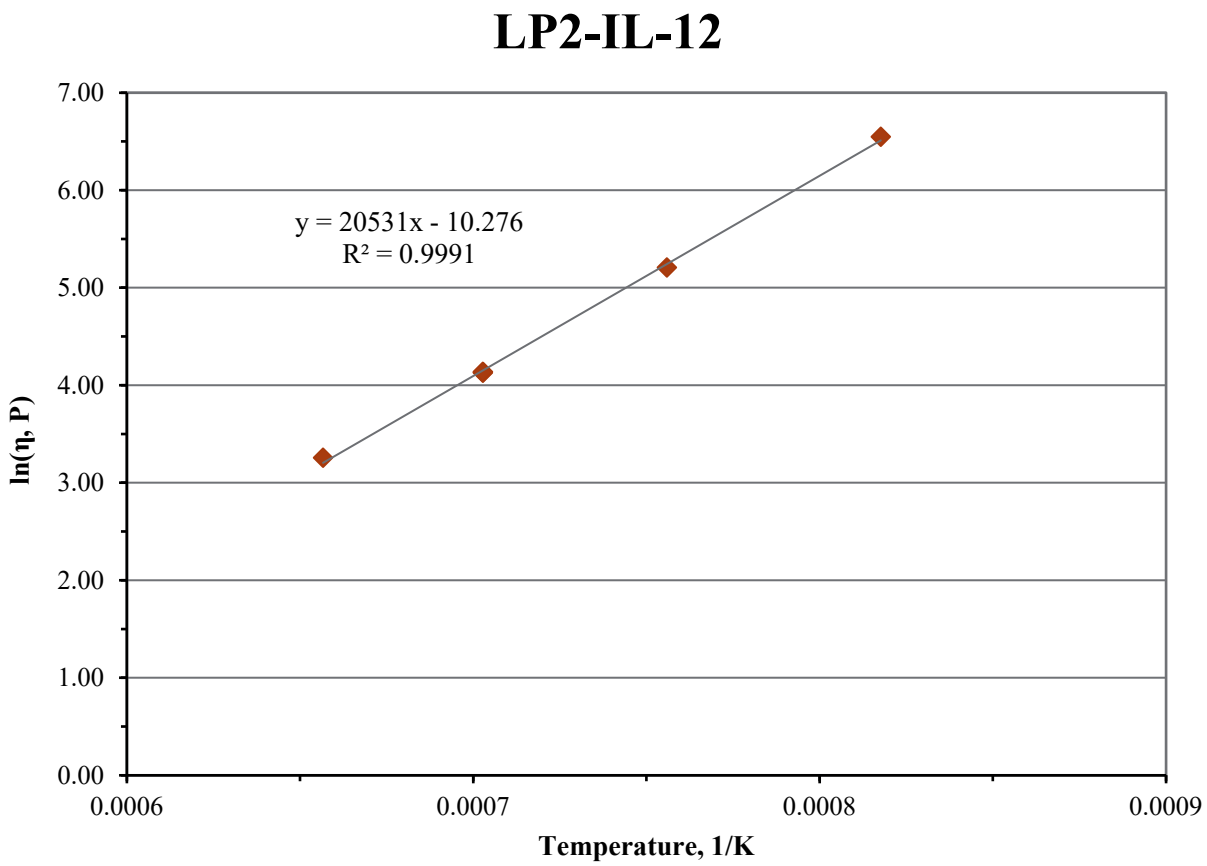


Figure C.12. Viscosity-Temperature Data and Arrhenius Equation Fit for Glass LP2-IL-12

## C.13 Glass LP2-IL-13 Viscosity Data

Table C.13. Viscosity Data for Glass LP2-IL-13

| Measured Temp., °C | Viscosity, P | 1/T x10000, $K^{-1}$ | ln η, P |
|---|---|---|---|
| 1150 | 56.397 | 7.027 | 4.032 |
| 1050 | 160.500 | 7.559 | 5.078 |
| 950 | 608.710 | 8.177 | 6.411 |
| 1150 | 55.994 | 7.027 | 4.025 |
| 1250 | 23.912 | 6.566 | 3.174 |
| 1150 | 56.011 | 7.027 | 4.026 |

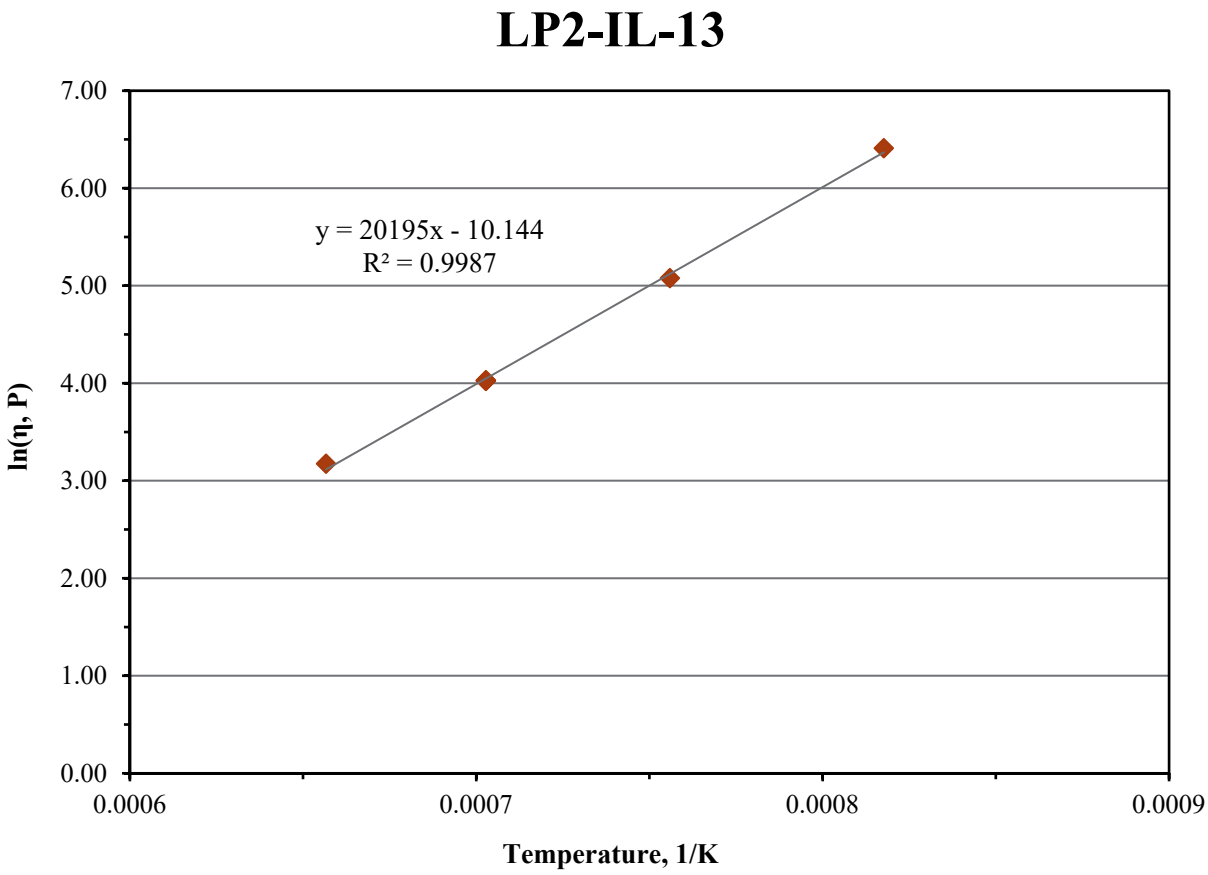


Figure C.13. Viscosity-Temperature Data and Arrhenius Equation Fit for Glass LP2-IL-13

## C.14 Glass LP2-IL-14 Viscosity Data

Table C.14. Viscosity Data for Glass LP2-IL-14

| Measured Temp., °C | Viscosity, P | 1/T x10000, $K^{-1}$ | ln η, P |
|---|---|---|---|
| 1150 | 27.252 | 7.027 | 3.305 |
| 1050 | 72.645 | 7.559 | 4.286 |
| 950 | 249.220 | 8.177 | 5.518 |
| 1150 | 27.555 | 7.027 | 3.316 |
| 1250 | 12.555 | 6.566 | 2.530 |
| 1150 | 27.906 | 7.027 | 3.329 |

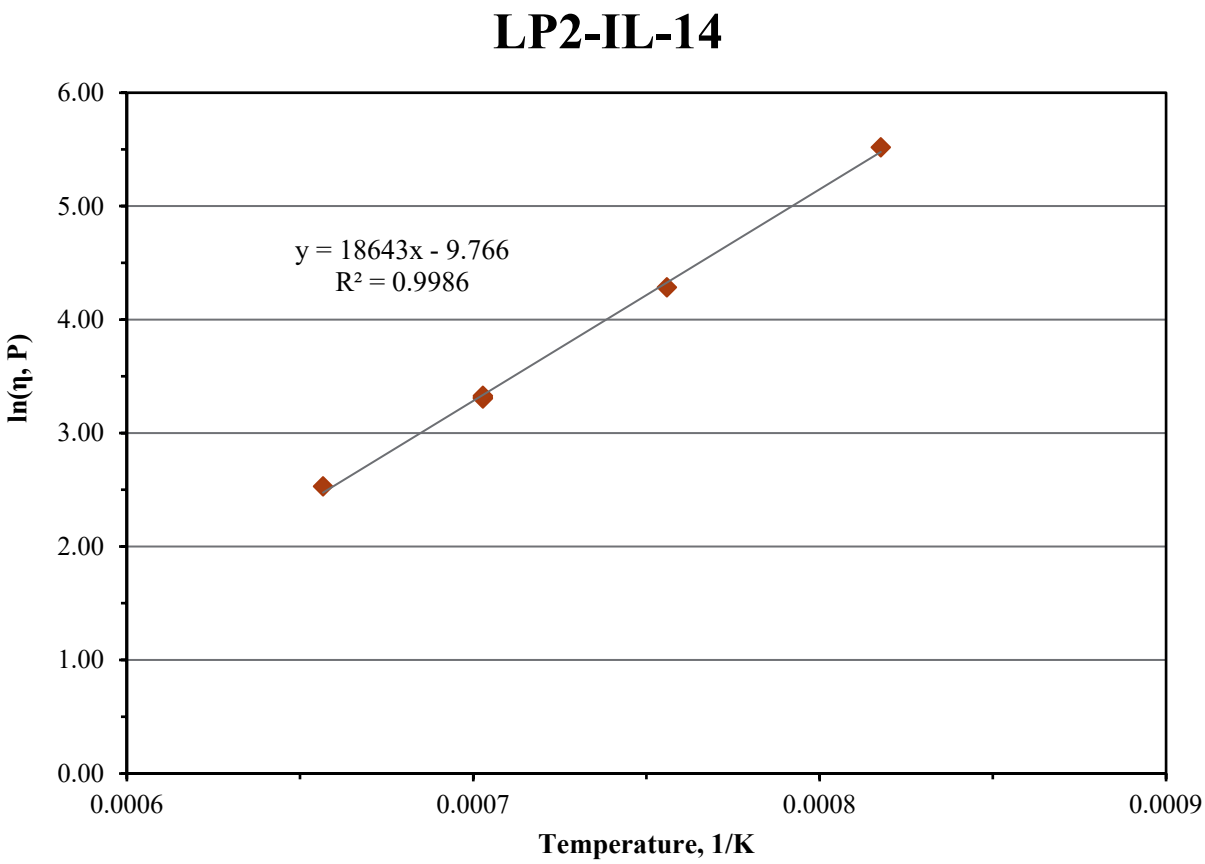


Figure C.14. Viscosity-Temperature Data and Arrhenius Equation Fit for Glass LP2-IL-14

## C.15 Glass LP2-IL-15 Viscosity Data

Table C.15. Viscosity Data for Glass LP2-IL-15

| Measured Temp., °C | Viscosity, P | 1/T x10000, $K^{-1}$ | ln η, P |
|---|---|---|---|
| 1150 | 55.414 | 7.027 | 4.015 |
| 1050 | 160.090 | 7.559 | 5.076 |
| 950 | 613.200 | 8.177 | 6.419 |
| 1150 | 55.377 | 7.027 | 4.014 |
| 1250 | 23.700 | 6.566 | 3.165 |
| 1150 | 55.780 | 7.027 | 4.021 |

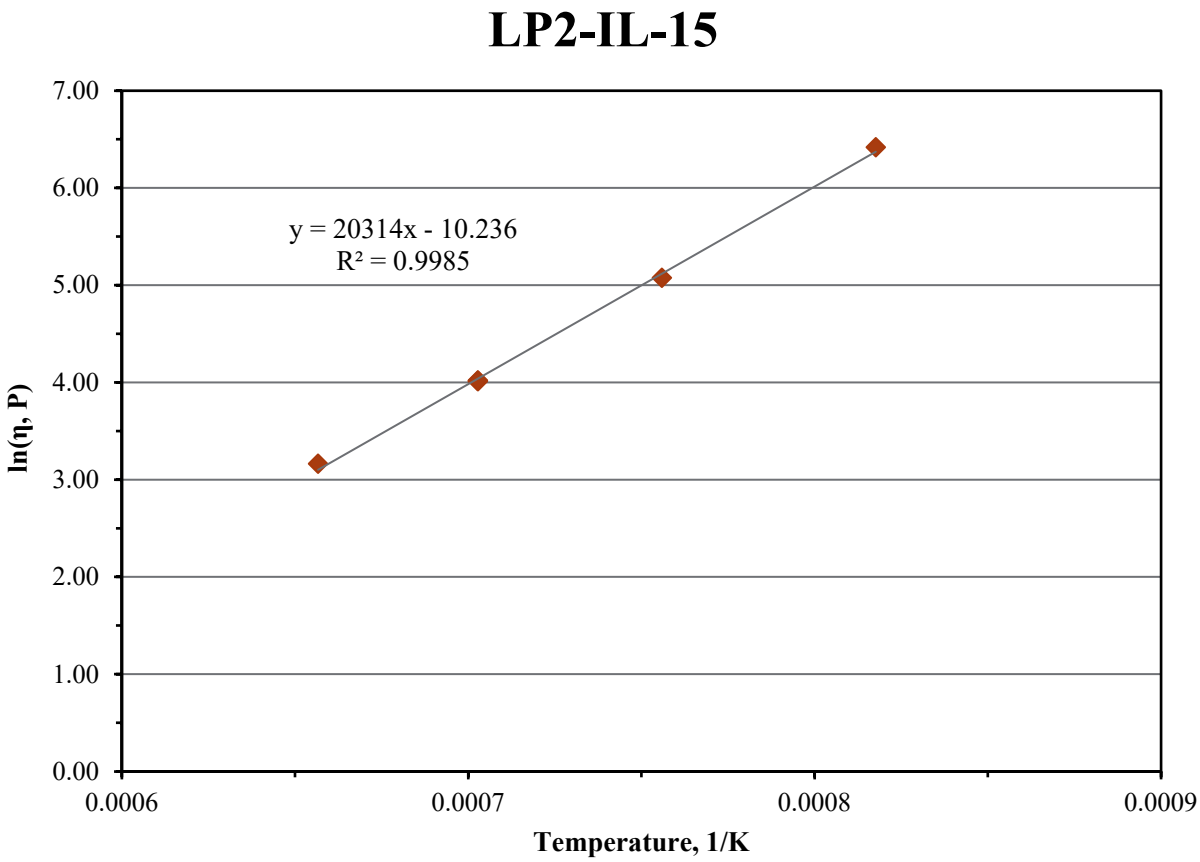


Figure C.15. Viscosity-Temperature Data and Arrhenius Equation Fit for Glass LP2-IL-15

## C.16 Glass LP2-IL-16 Viscosity Data

Table C.16. Viscosity Data for Glass LP2-IL-16

| Measured Temp., °C | Viscosity, P | 1/T x10000, $K^{-1}$ | ln η, P |
|---|---|---|---|
| 1150 | 43.301 | 7.027 | 3.768 |
| 1050 | 123.130 | 7.559 | 4.813 |
| 950 | 461.020 | 8.177 | 6.133 |
| 1150 | 43.809 | 7.027 | 3.780 |
| 1250 | 18.619 | 6.566 | 2.924 |
| 1150 | 43.665 | 7.027 | 3.777 |

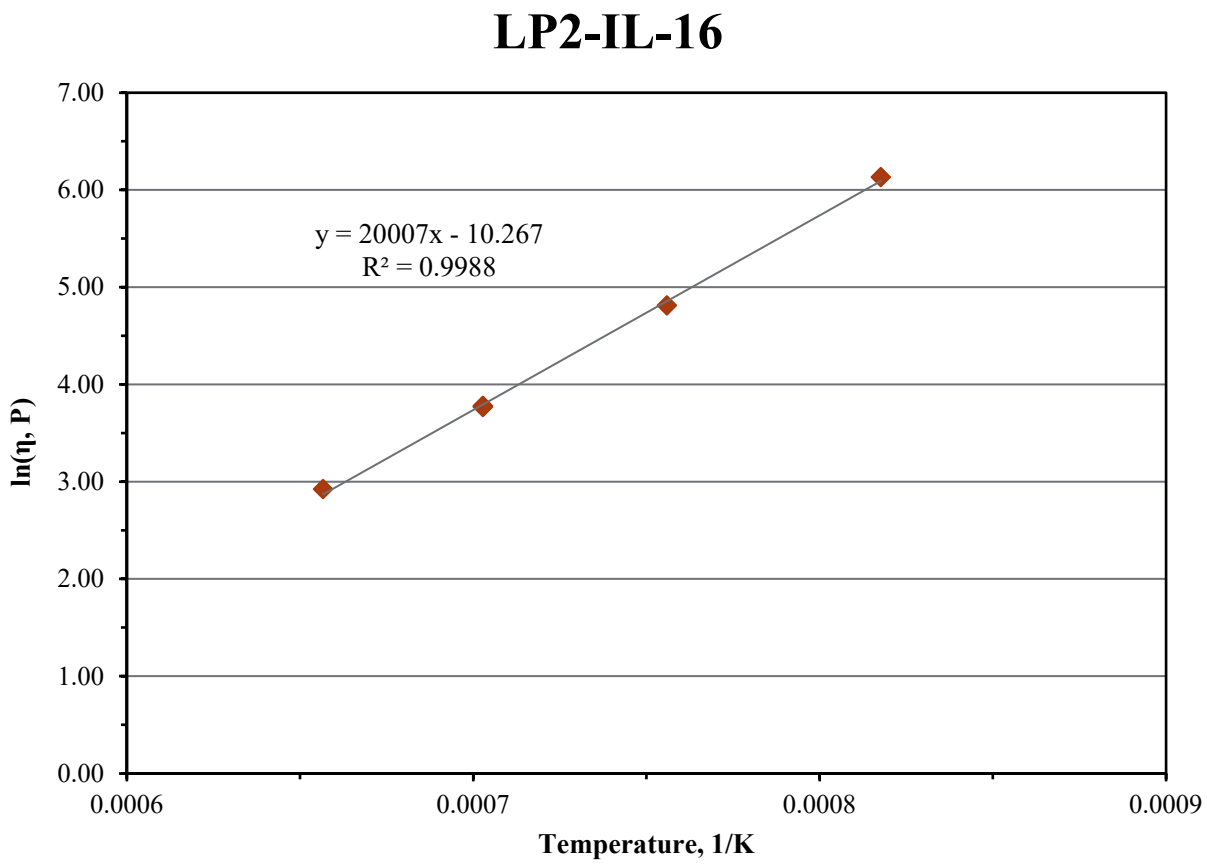


Figure C.16. Viscosity-Temperature Data and Arrhenius Equation Fit for Glass LP2-IL-16

## C.17 Glass LP2-IL-17 Viscosity Data

Table C.17. Viscosity Data for Glass LP2-IL-17

| Measured Temp., °C | Viscosity, P | 1/T x10000, $K^{-1}$ | ln η, P |
|---|---|---|---|
| 1150 | 51.172 | 7.027 | 3.935 |
| 1050 | 139.000 | 7.559 | 4.934 |
| 950 | 500.000 | 8.177 | 6.215 |
| 1150 | 50.442 | 7.027 | 3.921 |
| 1250 | 22.340 | 6.566 | 3.106 |
| 1150 | 51.314 | 7.027 | 3.938 |

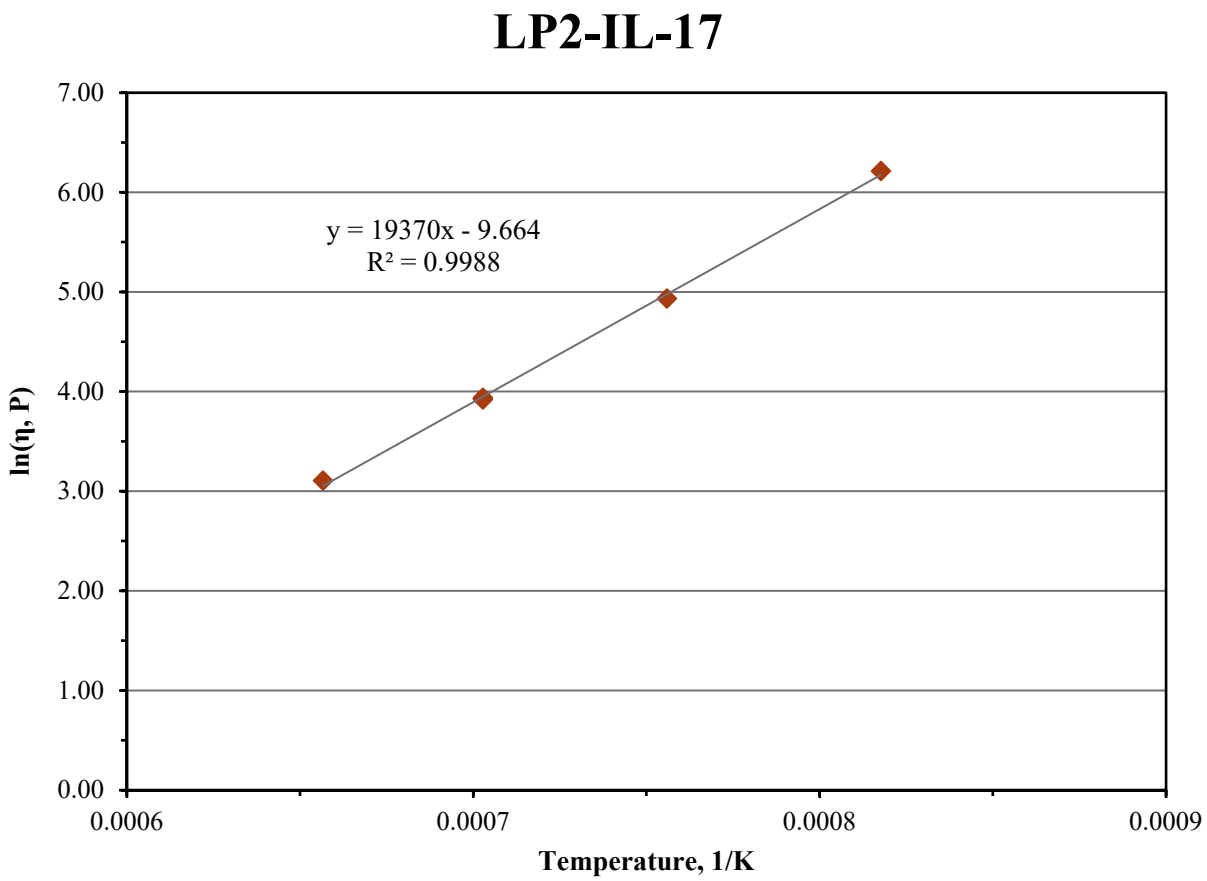


Figure C.17. Viscosity-Temperature Data and Arrhenius Equation Fit for Glass LP2-IL-17

## C.18 Glass LP2-OL-01-3 Viscosity Data

Table C.18. Viscosity Data for Glass LP2-OL-01-3

| Measured Temp., °C | Viscosity, P | 1/T x10000, $K^{-1}$ | ln η, P |
|---|---|---|---|
| 1150 | 85.343 | 7.027 | 4.447 |
| 1050 | 287.000 | 7.559 | 5.659 |
| 950 | 1390.000 | 8.177 | 7.2437 |
| 1150 | 85.906 | 7.027 | 4.453 |
| 1250 | 32.400 | 6.566 | 3.478 |
| 1150 | 86.130 | 7.027 | 4.456 |

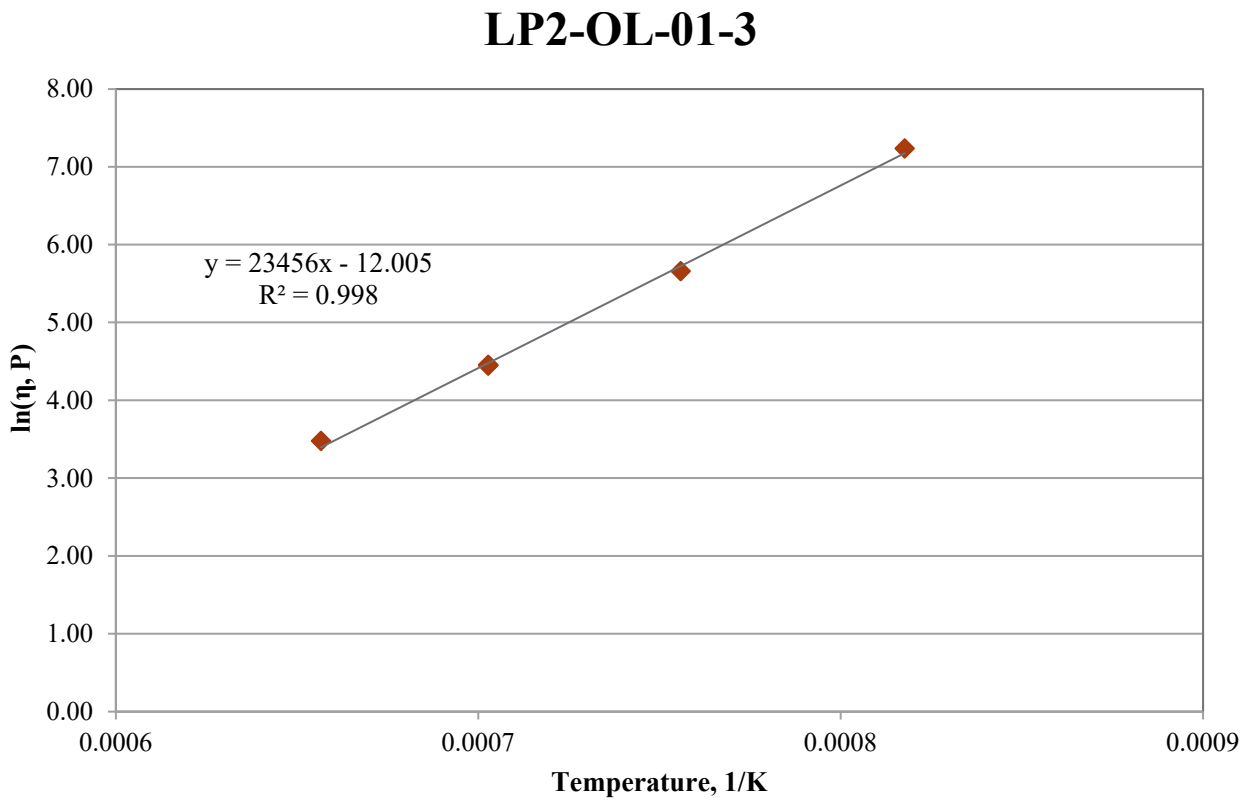


Figure C.18. Viscosity-Temperature Data and Arrhenius Equation Fit for Glass LP2-OL-01-3

## C.19 Glass LP2-OL-02-1 Viscosity Data

Table C.19. Viscosity Data for Glass LP2-OL-02-1

| Measured Temp., °C | Viscosity, P | 1/T x10000, $K^{-1}$ | ln η, P |
|---|---|---|---|
| 1150 | 54.029 | 7.027 | 3.990 |
| 1050 | 137.750 | 7.559 | 4.925 |
| 950 | 532.560 | 8.177 | 6.278 |
| 1150 | 52.799 | 7.027 | 3.966 |
| 1250 | 22.929 | 6.566 | 3.132 |
| 1150 | 53.837 | 7.027 | 3.986 |

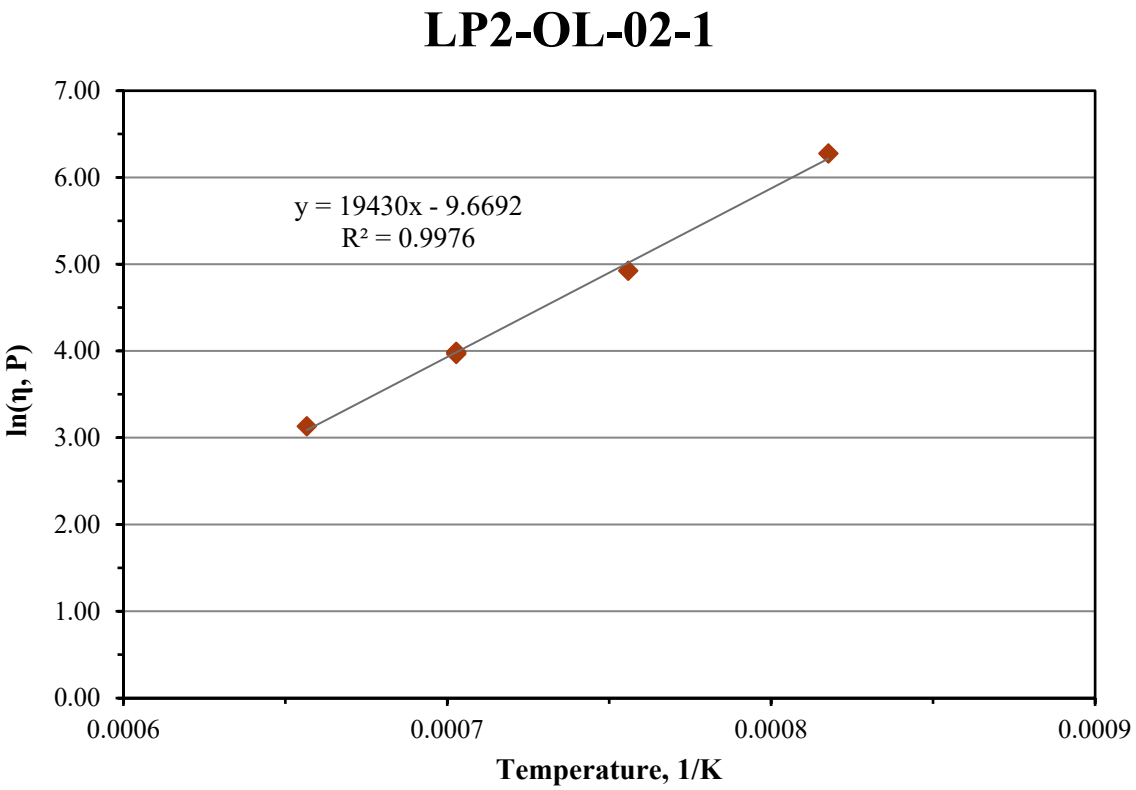


Figure C.19. Viscosity-Temperature Data and Arrhenius Equation Fit for Glass LP2-OL-02-1

## C.20 Glass LP2-OL-03 MOD2 Viscosity Data

Table C.20. Viscosity Data for Glass LP2-OL-03 MOD2

| Measured Temp., °C | Viscosity, P | 1/T x10000, $K^{-1}$ | ln η, P |
|---|---|---|---|
| 1150 | 25.618 | 7.027 | 3.243 |
| 1050 | 73.108 | 7.559 | 4.292 |
| 950 | 275.070 | 8.177 | 5.617 |
| 1150 | 25.866 | 7.027 | 3.253 |
| 1250 | 11.100 | 6.566 | 2.407 |
| 1150 | 26.043 | 7.027 | 3.260 |

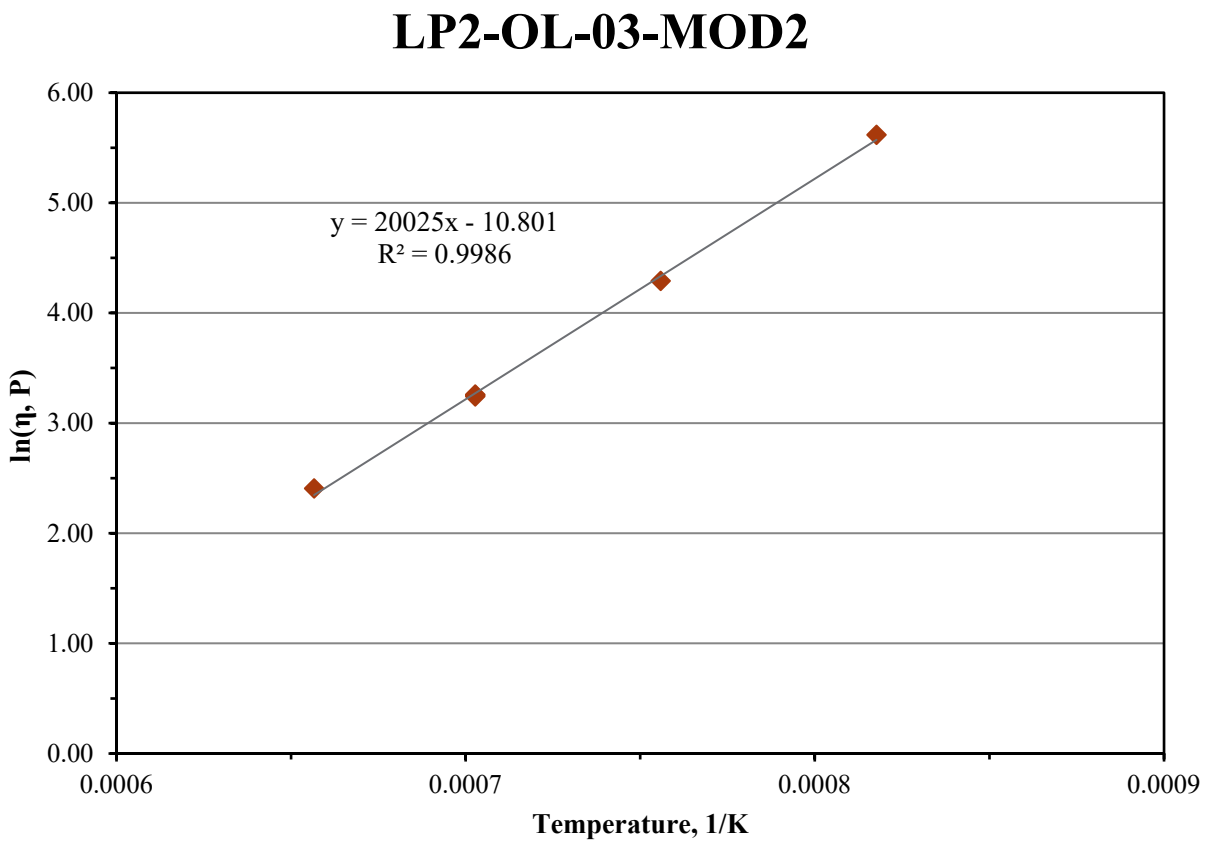


Figure C.20. Viscosity-Temperature Data and Arrhenius Equation Fit for Glass LP2-OL-03 MOD2

## C.21 Glass LP2-OL-04-1 Viscosity Data

Table C.21. Viscosity Data for Glass LP2-OL-04-1

| Measured Temp., °C | Viscosity, P | 1/T x10000, $K^{-1}$ | ln η, P |
|---|---|---|---|
| 1150 | 38.693 | 7.027 | 3.656 |
| 1050 | 119.000 | 7.559 | 4.779 |
| 950 | 490.670 | 8.177 | 6.196 |
| 1150 | 38.804 | 7.027 | 3.659 |
| 1250 | 15.787 | 6.566 | 2.759 |
| 1150 | 39.790 | 7.027 | 3.684 |

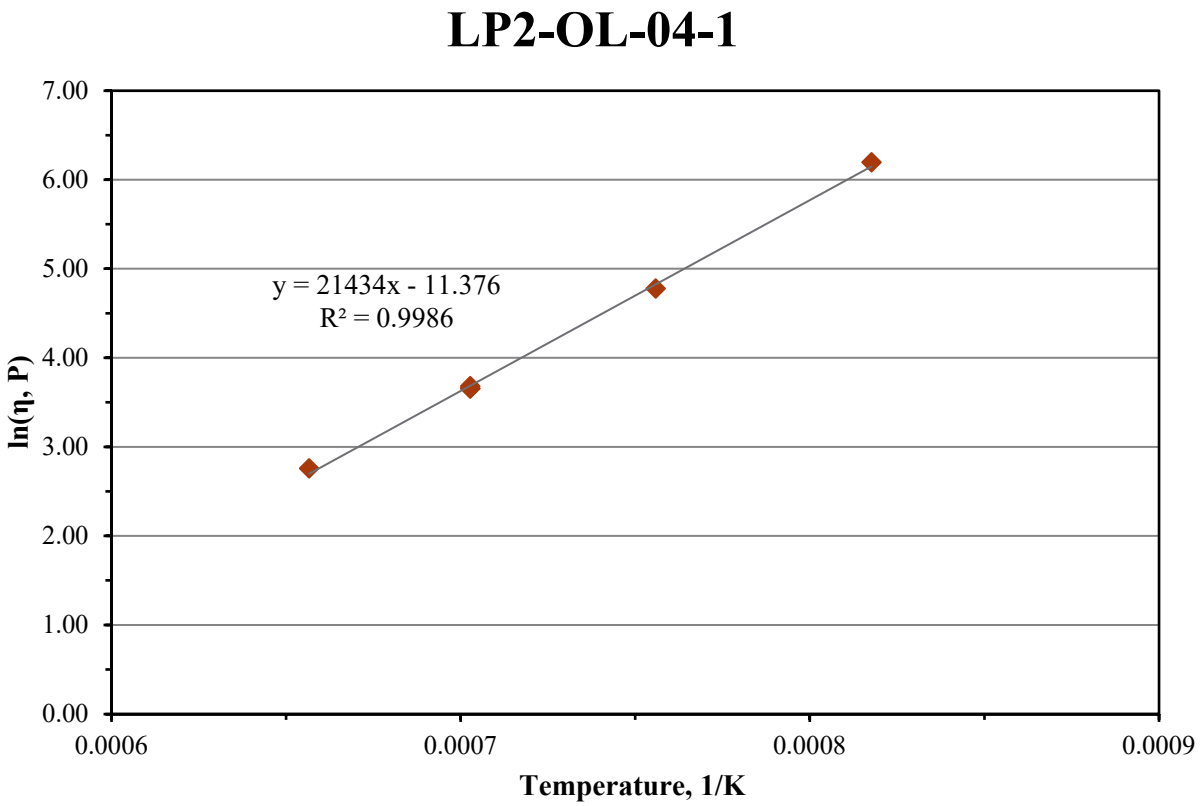


Figure C.21. Viscosity-Temperature Data and Arrhenius Equation Fit for Glass LP2-OL-04-1

## C.22 Glass LP2-OL-05 Viscosity Data

Table C.22. Viscosity Data for Glass LP2-OL-05

| Measured Temp., °C | Viscosity, P | 1/T x10000, $K^{-1}$ | ln η, P |
|---|---|---|---|
| 1150 | 67.671 | 7.027 | 4.215 |
| 1050 | 212.000 | 7.559 | 5.357 |
| 950 | 1658.687 | 8.177 | 7.414 |
| 1150 | 68.443 | 7.027 | 4.226 |
| 1250 | 27.717 | 6.566 | 3.322 |
| 1150 | 69.974 | 7.027 | 4.248 |

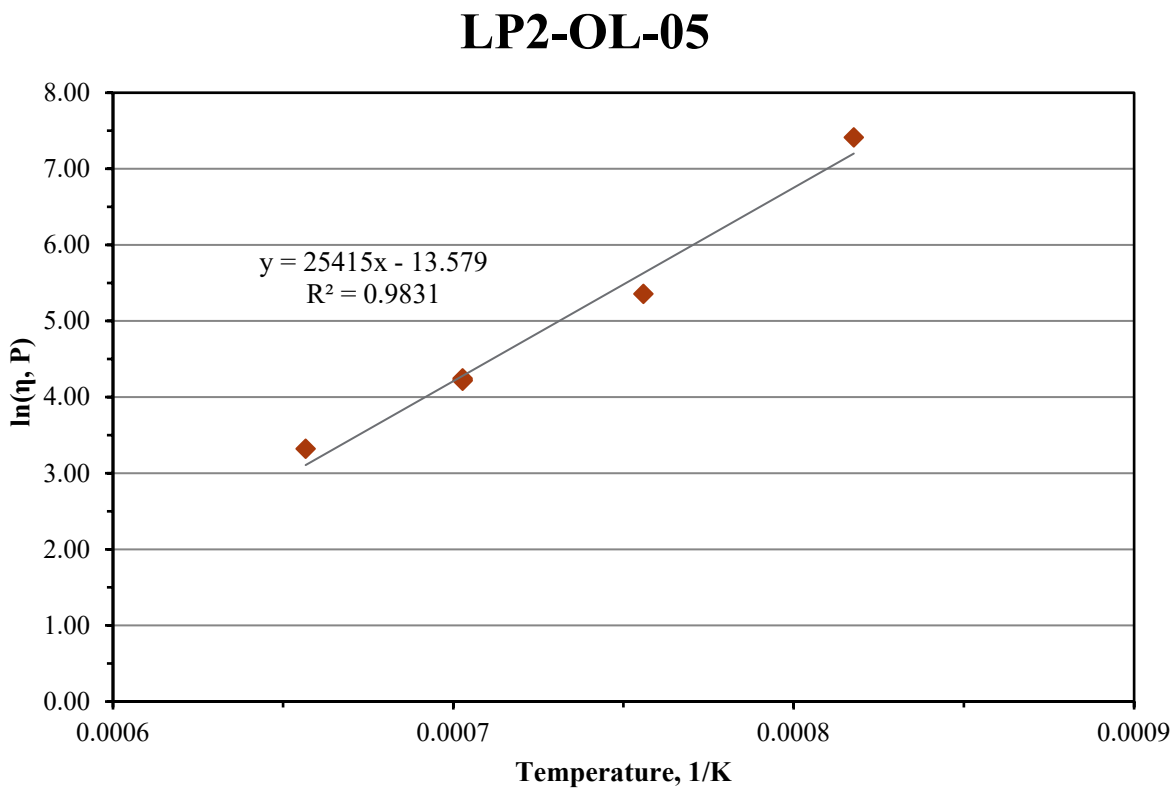


Figure C.22. Viscosity-Temperature Data and Arrhenius Equation Fit for Glass LP2-OL-05

## C.23 Glass LP2-OL-07-1 Viscosity Data

Table C.23. Viscosity Data for LP2-OL-07-1

| Measured Temp., °C | Viscosity, P | 1/T x10000, $K^{-1}$ | ln η, P |
|---|---|---|---|
| 1150 | 29.977 | 7.027 | 3.400 |
| 1050 | 77.385 | 7.559 | 4.349 |
| 950 | 268.350 | 8.177 | 5.592 |
| 1150 | 29.646 | 7.027 | 3.389 |
| 1250 | 13.761 | 6.566 | 2.622 |
| 1150 | 30.927 | 7.027 | 3.432 |

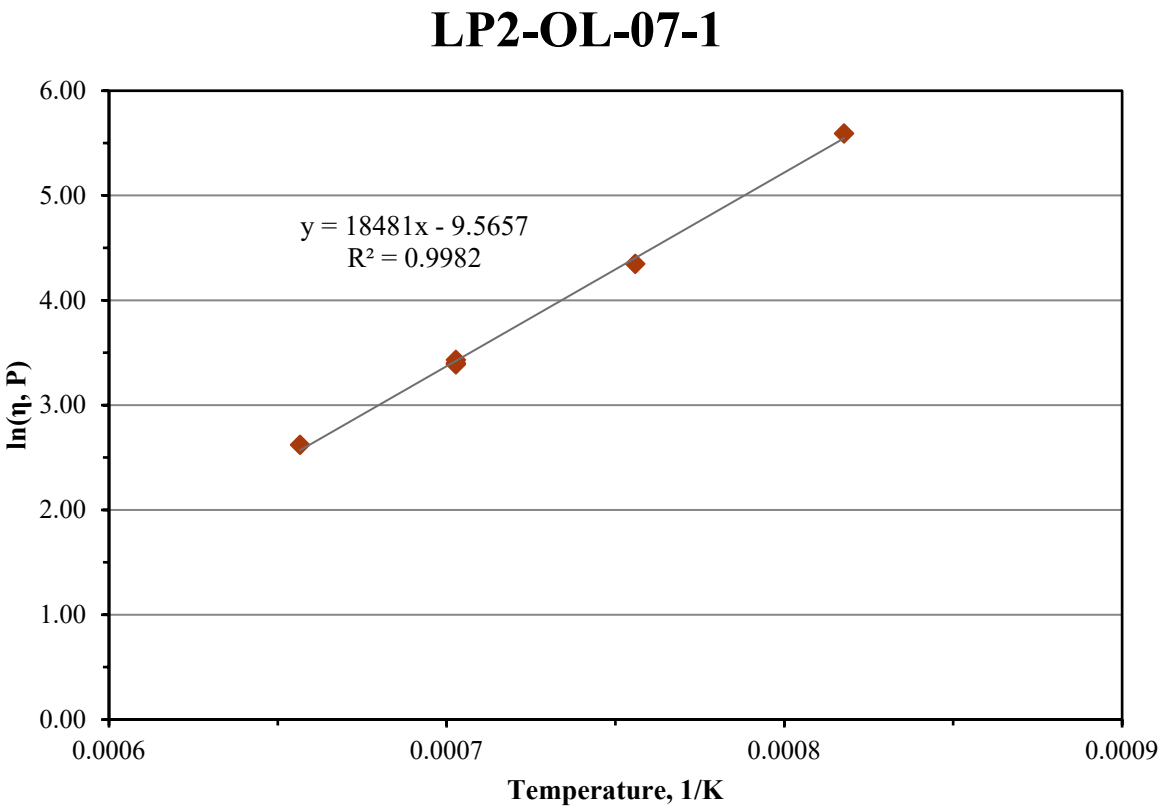


Figure C.23. Viscosity-Temperature Data and Arrhenius Equation Fit for Glass LP2-OL-07-1

## C.24 Glass LP2-OL-08 MOD Viscosity Data

Table C.24. Viscosity Data for Glass LP2-OL-08 MOD

| Measured Temp., °C | Viscosity, P | 1/T x10000, $K^{-1}$ | ln η, P |
|---|---|---|---|
| 1150 | 12.800 | 7.027 | 2.549 |
| 1050 | 33.548 | 7.559 | 3.513 |
| 950 | 125.190 | 8.177 | 4.830 |
| 1150 | 12.900 | 7.027 | 2.557 |
| 1250 | 5.902 | 6.566 | 1.775 |
| 1150 | 12.806 | 7.027 | 2.550 |

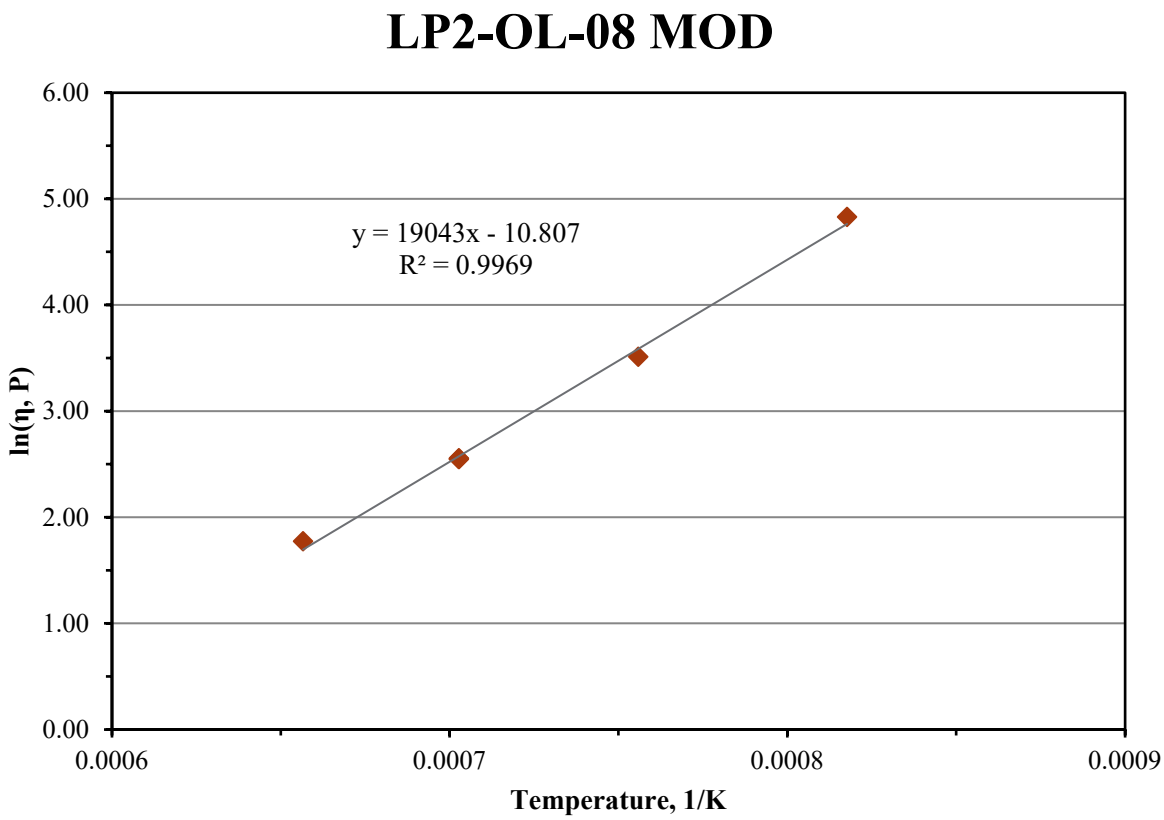


Figure C.24. Viscosity-Temperature Data and Arrhenius Equation Fit for Glass LP2-OL-08 MOD

## C.25 Glass LP2-OL-09-1 Viscosity Data

Table C.25. Viscosity Data for Glass LP2-OL-09-1

| Measured Temp., °C | Viscosity, P | 1/T x10000, $K^{-1}$ | ln η, P |
|---|---|---|---|
| 1150 | 63.768 | 7.027 | 4.155 |
| 1050 | 170.300 | 7.559 | 5.138 |
| 950 | 630.374 | 8.177 | 6.446 |
| 1150 | 63.776 | 7.027 | 4.155 |
| 1250 | 28.548 | 6.566 | 3.352 |
| 1150 | 64.592 | 7.027 | 4.168 |

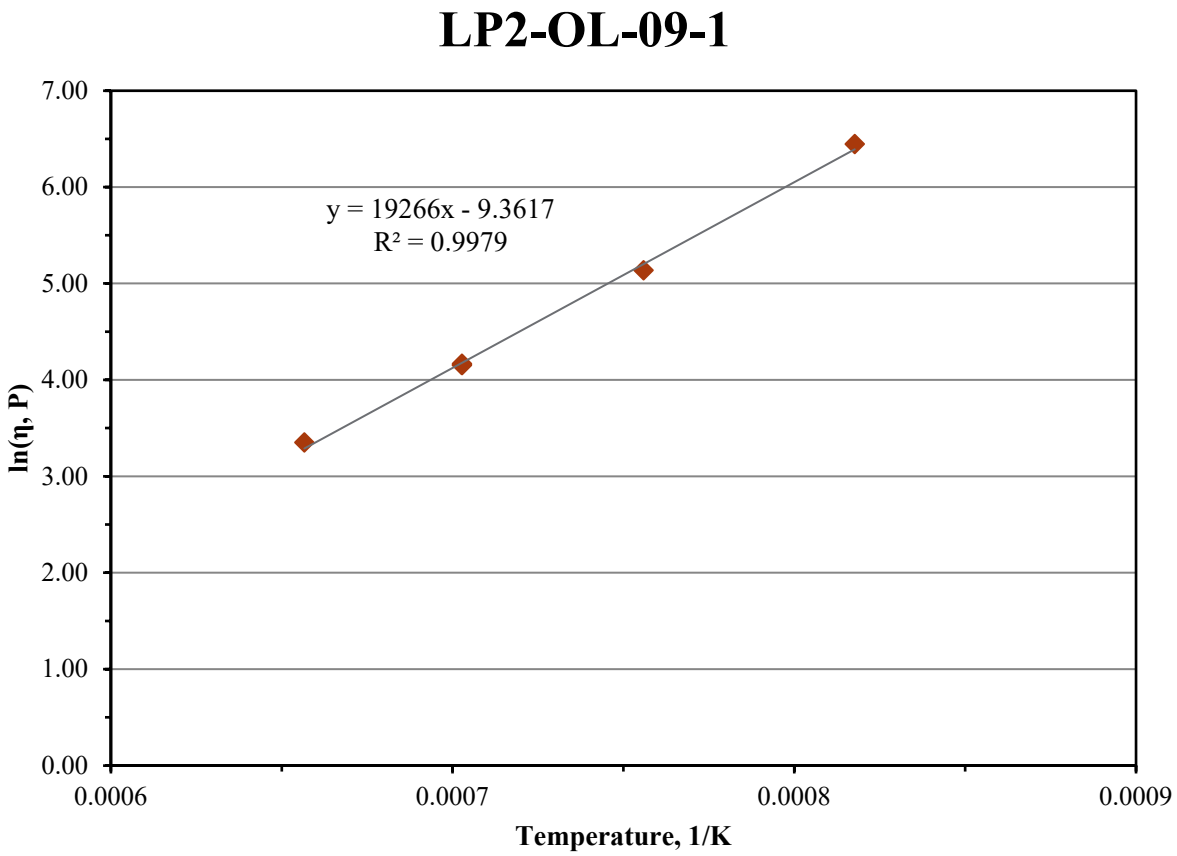


Figure C.25. Viscosity-Temperature Data and Arrhenius Equation Fit for Glass LP2-OL-09-1

## C.26 Glass LP2-OL-10 MOD Viscosity Data

Table C.26. Viscosity Data for Glass LP2-OL-10 MOD

| Measured Temp., °C | Viscosity, P | 1/T x10000, $K^{-1}$ | ln η, P |
|---|---|---|---|
| 1150 | 63.721 | 7.027 | 4.155 |
| 1050 | 197.000 | 7.559 | 5.283 |
| 950 | 1450.000 | 8.177 | 7.279 |
| 1150 | 65.037 | 7.027 | 4.175 |
| 1250 | 26.566 | 6.566 | 3.280 |
| 1150 | 67.690 | 7.027 | 4.215 |

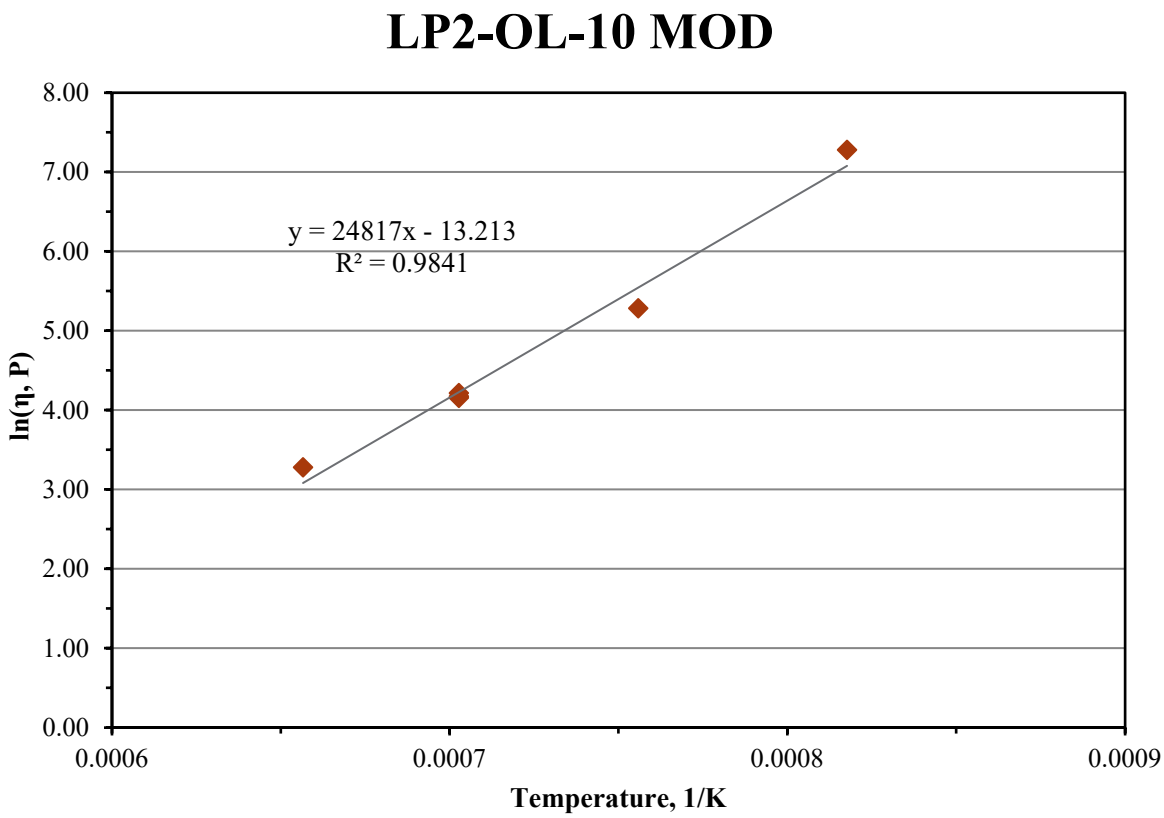


Figure C.26. Viscosity-Temperature Data and Arrhenius Equation Fit for Glass LP2-OL-10 MOD

## C.27 Glass LP2-OL-11 Viscosity Data

Table C.27. Viscosity Data for Glass LP2-OL-11

| Measured Temp., °C | Viscosity, P | 1/T x10000, $K^{-1}$ | ln η, P |
|---|---|---|---|
| 1150 | 11.300 | 7.027 | 2.425 |
| 1050 | 27.304 | 7.559 | 3.307 |
| 950 | 83.927 | 8.177 | 4.430 |
| 1150 | 11.400 | 7.027 | 2.434 |
| 1250 | 5.592 | 6.566 | 1.721 |
| 1150 | 11.609 | 7.027 | 2.452 |

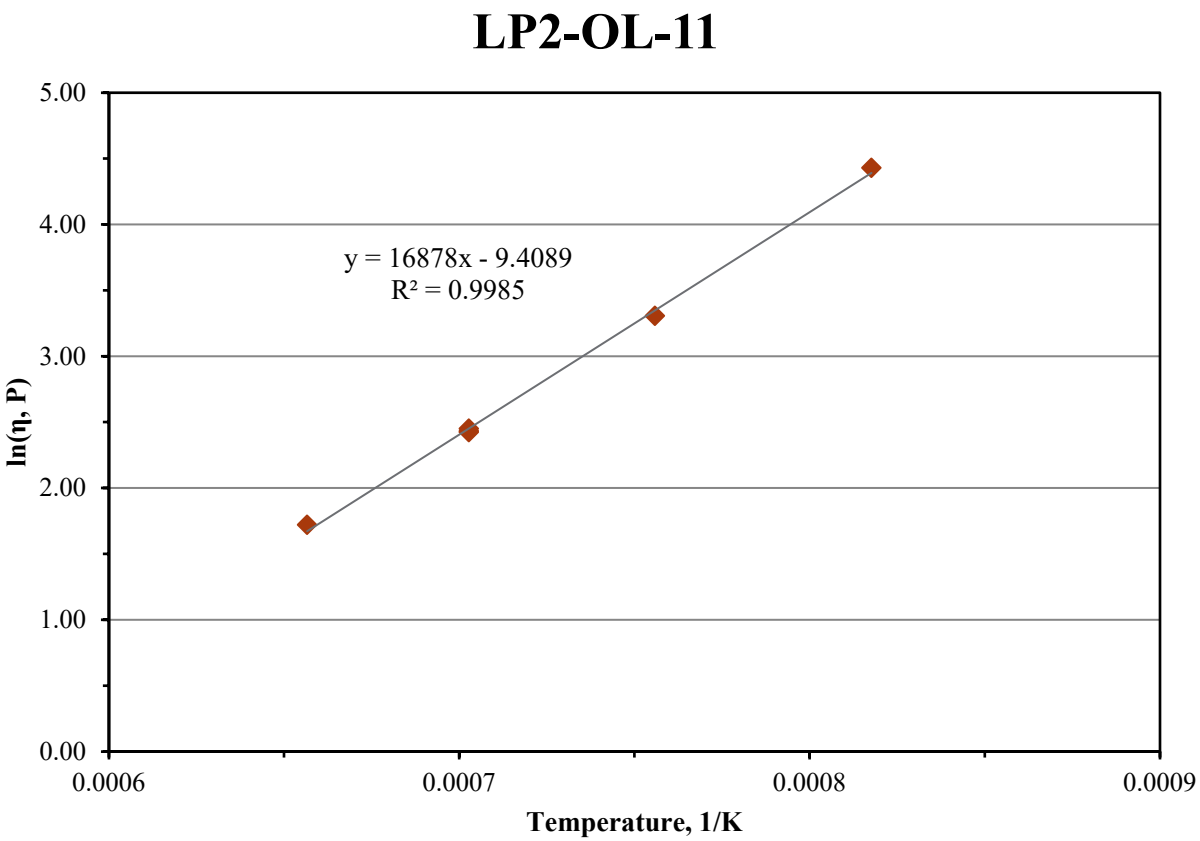


Figure C.27. Viscosity-Temperature Data and Arrhenius Equation Fit for Glass LP2-OL-11

## C.28 Glass LP2-OL-12 Viscosity Data

Table C.28. Viscosity Data for Glass LP2-OL-12

| Measured Temp., °C | Viscosity, P | 1/T x10000, $K^{-1}$ | ln η, P |
|---|---|---|---|
| 1150 | 7.970 | 7.027 | 2.076 |
| 1050 | 17.577 | 7.559 | 2.867 |
| 950 | 48.700 | 8.177 | 3.886 |
| 1150 | 8.029 | 7.027 | 2.083 |
| 1250 | 4.240 | 6.566 | 1.445 |
| 1150 | 8.119 | 7.027 | 2.094 |

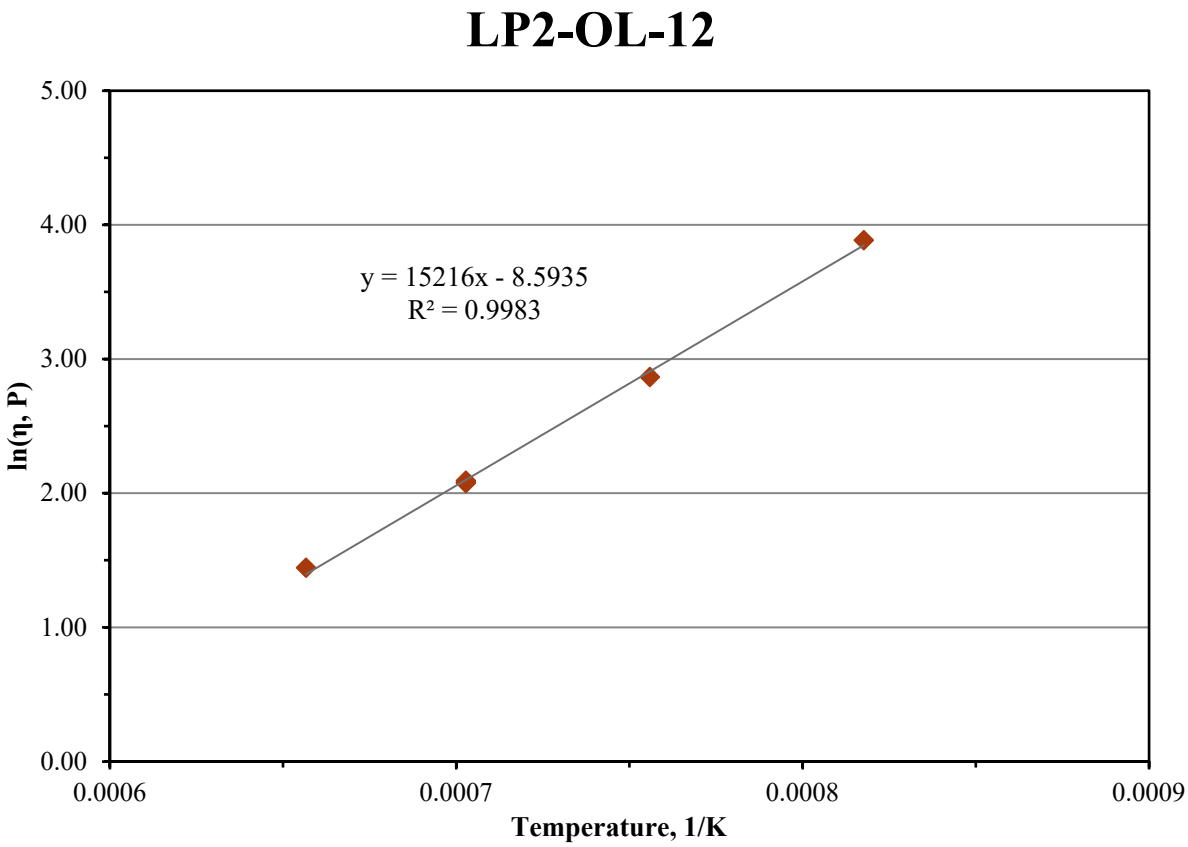


Figure C.28. Viscosity-Temperature Data and Arrhenius Equation Fit for Glass LP2-OL-12

## C.29 Glass LP2-OL-13 Viscosity Data

Table C.29. Viscosity Data for Glass LP2-OL-13

| Measured Temp., °C | Viscosity, P | 1/T x10000, $K^{-1}$ | ln η, P |
|---|---|---|---|
| 1150 | 13.167 | 7.027 | 2.578 |
| 1050 | 31.861 | 7.559 | 3.461 |
| 950 | 90.966 | 8.177 | 4.510 |
| 1150 | 13.266 | 7.027 | 2.585 |
| 1250 | 6.420 | 6.566 | 1.859 |
| 1150 | 13.467 | 7.027 | 2.600 |

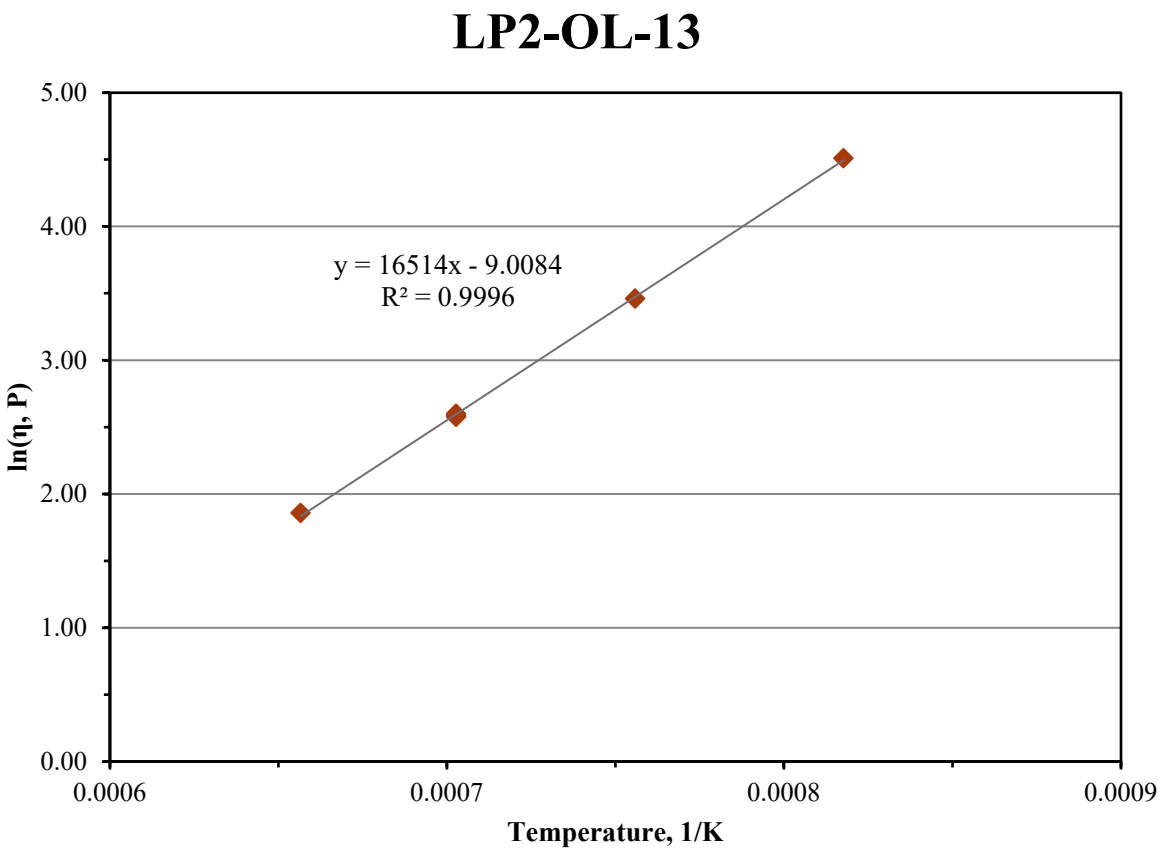


Figure C.29. Viscosity-Temperature Data and Arrhenius Equation Fit for Glass LP2-OL-13

## C.30 Glass LP2-OL-14 Viscosity Data

Table C.30. Viscosity Data for Glass LP2-OL-14

| Measured Temp., °C | Viscosity, P | 1/T x10000, $K^{-1}$ | ln η, P |
|---|---|---|---|
| 1150 | 9.563 | 7.027 | 2.258 |
| 1050 | 21.329 | 7.559 | 3.060 |
| 950 | 59.802 | 8.177 | 4.091 |
| 1150 | 9.643 | 7.027 | 2.266 |
| 1250 | 5.042 | 6.566 | 1.618 |
| 1150 | 9.800 | 7.027 | 2.282 |

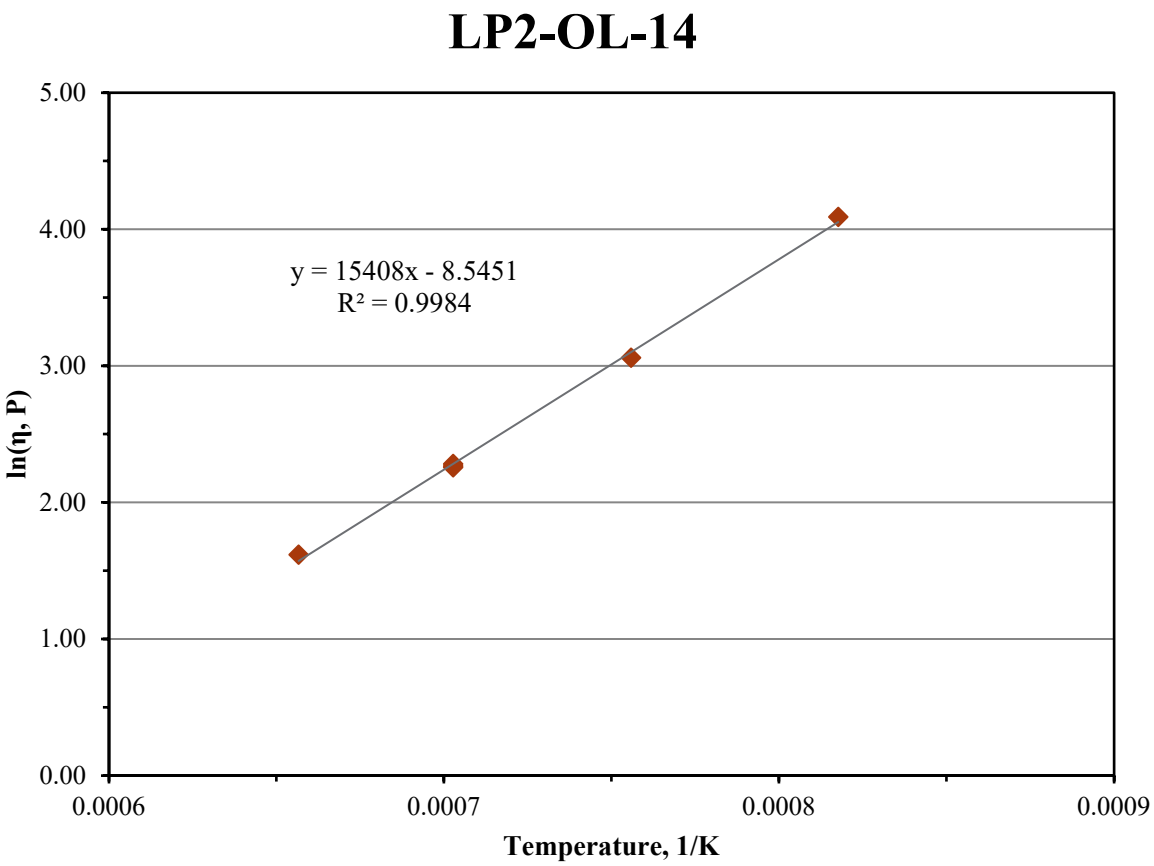


Figure C.30. Viscosity-Temperature Data and Arrhenius Equation Fit for Glass LP2-OL-14

## C.31 Glass LP2-OL-15 Viscosity Data

Table C.31. Viscosity Data for Glass LP2-OL-15

| Measured Temp., °C | Viscosity, P | 1/T x10000, $K^{-1}$ | ln η, P |
|---|---|---|---|
| 1150 | 12.726 | 7.027 | 2.544 |
| 1050 | 33.842 | 7.559 | 3.522 |
| 950 | 122.000 | 8.177 | 4.804 |
| 1150 | 12.856 | 7.027 | 2.554 |
| 1250 | 6.003 | 6.566 | 1.792 |
| 1150 | 12.900 | 7.027 | 2.557 |

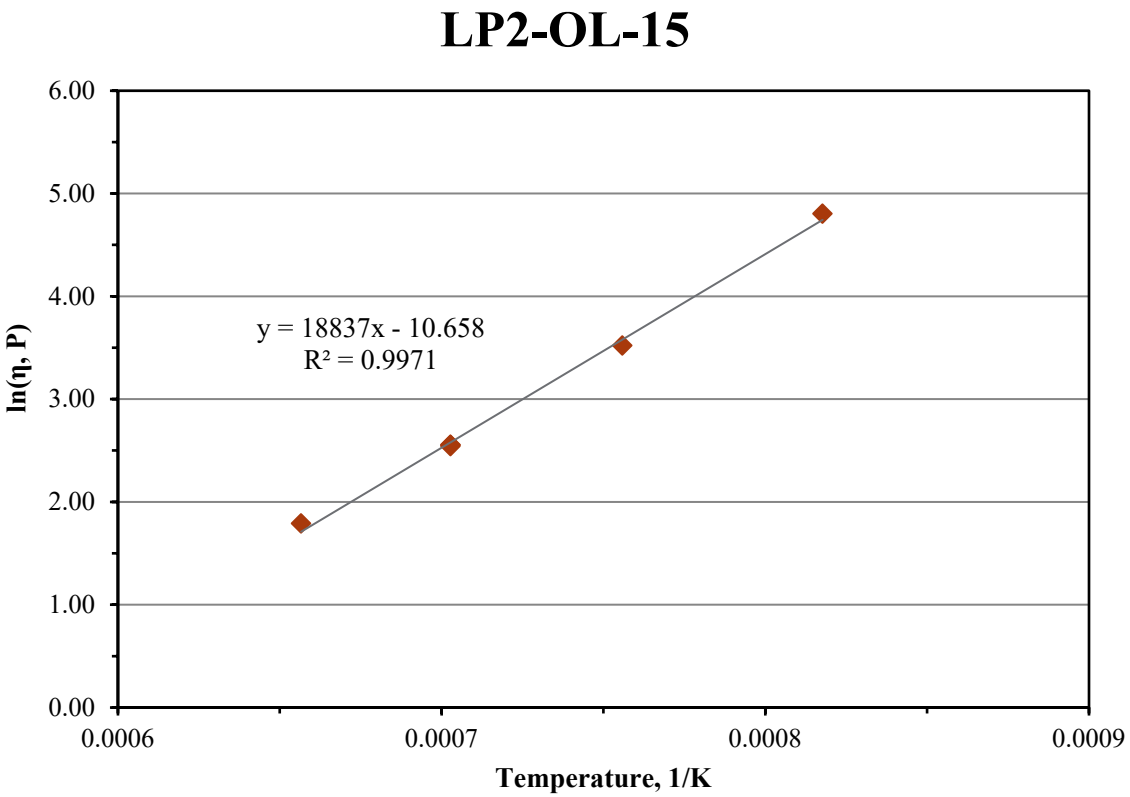


Figure C.31. Viscosity-Temperature Data and Arrhenius Equation Fit for Glass LP2-OL-15

## C.32 Glass LP2-OL-16 MOD Viscosity Data

Table C.32. Viscosity Data for Glass LP2-OL-16 MOD

| Measured Temp., °C | Viscosity, P | 1/T x10000, $K^{-1}$ | ln η, P |
|---|---|---|---|
| 1150 | 72.672 | 7.027 | 4.286 |
| 1050 | 199.230 | 7.559 | 5.294 |
| 950 | 742.860 | 8.177 | 6.611 |
| 1150 | 73.708 | 7.027 | 4.300 |
| 1250 | 31.831 | 6.566 | 3.460 |
| 1150 | 73.868 | 7.027 | 4.302 |

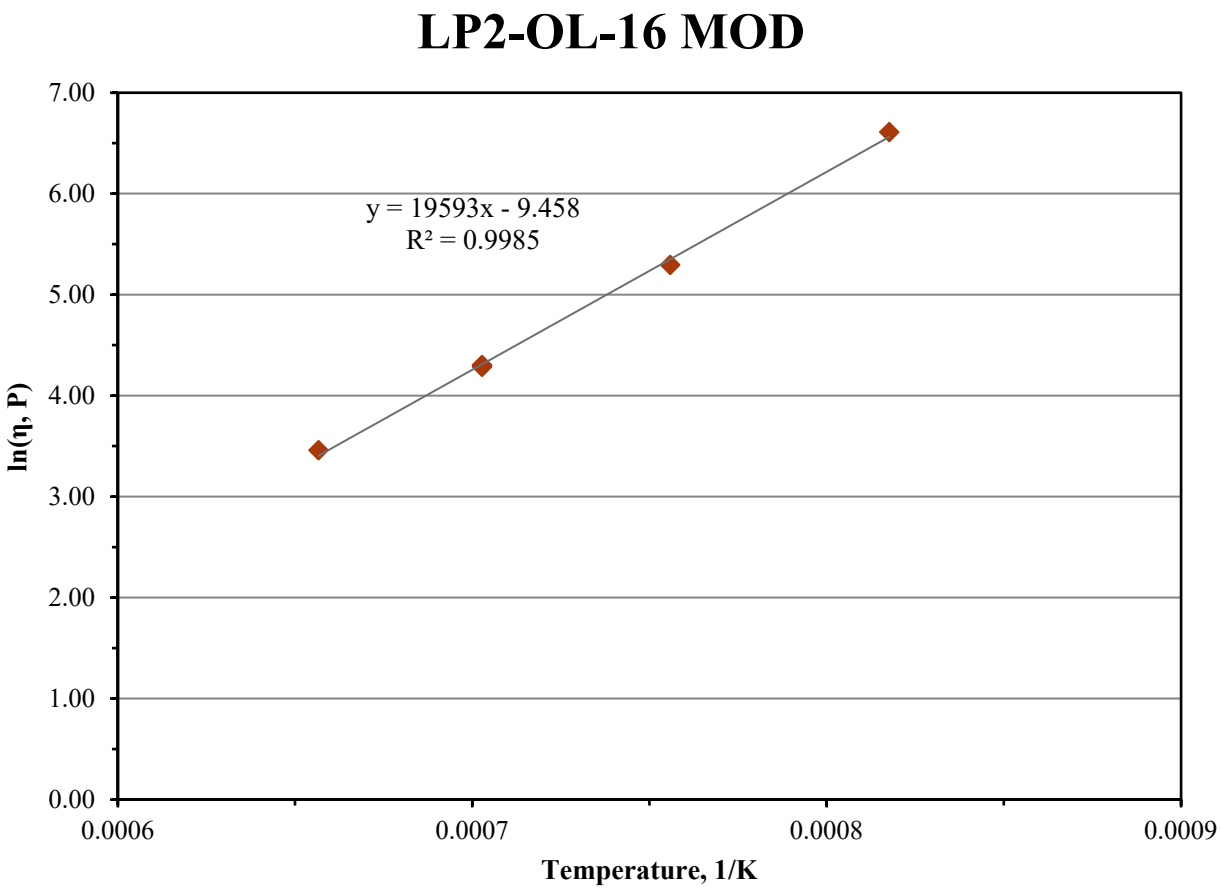


Figure C.32. Viscosity-Temperature Data and Arrhenius Equation Fit for Glass LP2-OL-16 MOD

## C.33 Glass LP2-OL-17 Viscosity Data

Table C.33. Viscosity Data for Glass LP2-OL-17

| Measured Temp., °C | Viscosity, P | 1/T x10000, $K^{-1}$ | ln η, P |
|---|---|---|---|
| 1150 | 24.736 | 7.027 | 3.208 |
| 1050 | 66.816 | 7.559 | 4.202 |
| 950 | 229.210 | 8.177 | 5.435 |
| 1150 | 25.350 | 7.027 | 3.233 |
| 1250 | 11.283 | 6.566 | 2.423 |
| 1150 | 25.582 | 7.027 | 3.242 |

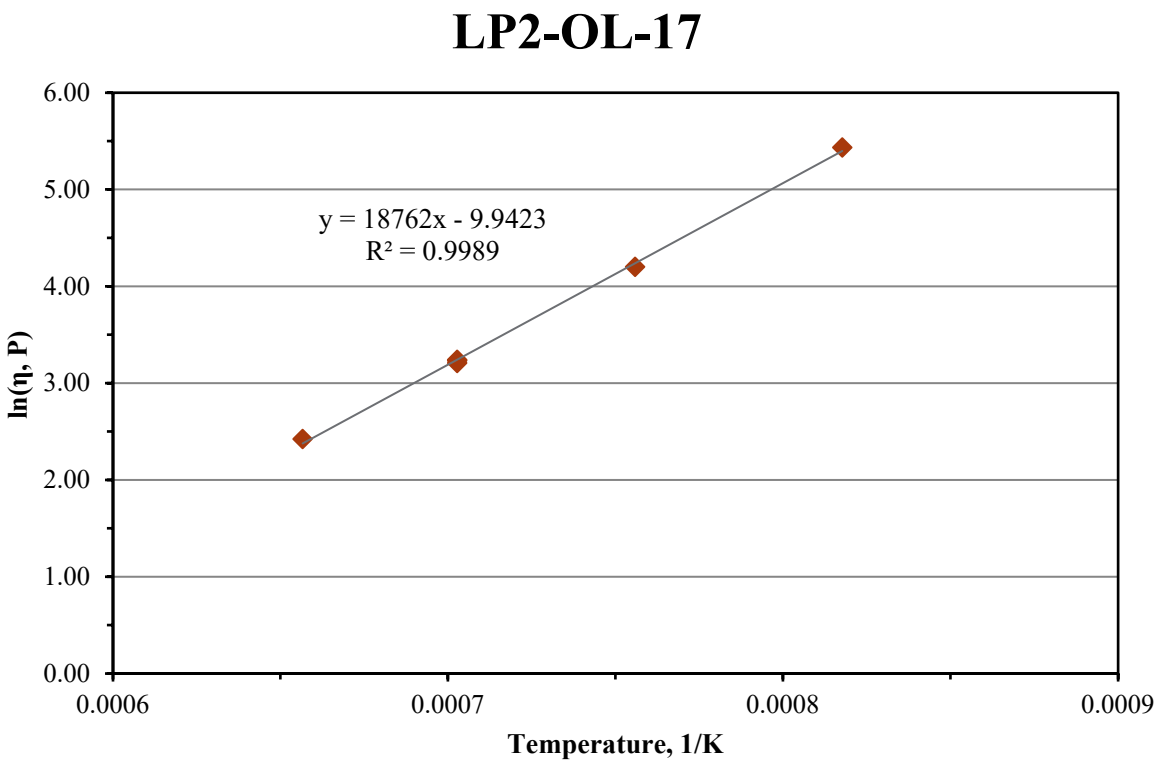


Figure C.33. Viscosity-Temperature Data and Arrhenius Equation Fit for Glass LP2-OL-17

## C.34 Glass LP2-OL-18 Viscosity Data

Table C.34. Viscosity Data for Glass LP2-OL-18

| Measured Temp., °C | Viscosity, P | 1/T x10000, $K^{-1}$ | ln η, P |
|---|---|---|---|
| 1150 | 26.037 | 7.027 | 3.260 |
| 1050 | 94.031 | 7.559 | 4.544 |
| 950 | 408.640 | 8.177 | 6.013 |
| 1150 | 25.782 | 7.027 | 3.250 |
| 1250 | 10.600 | 6.566 | 2.361 |
| 1150 | 26.407 | 7.027 | 3.274 |

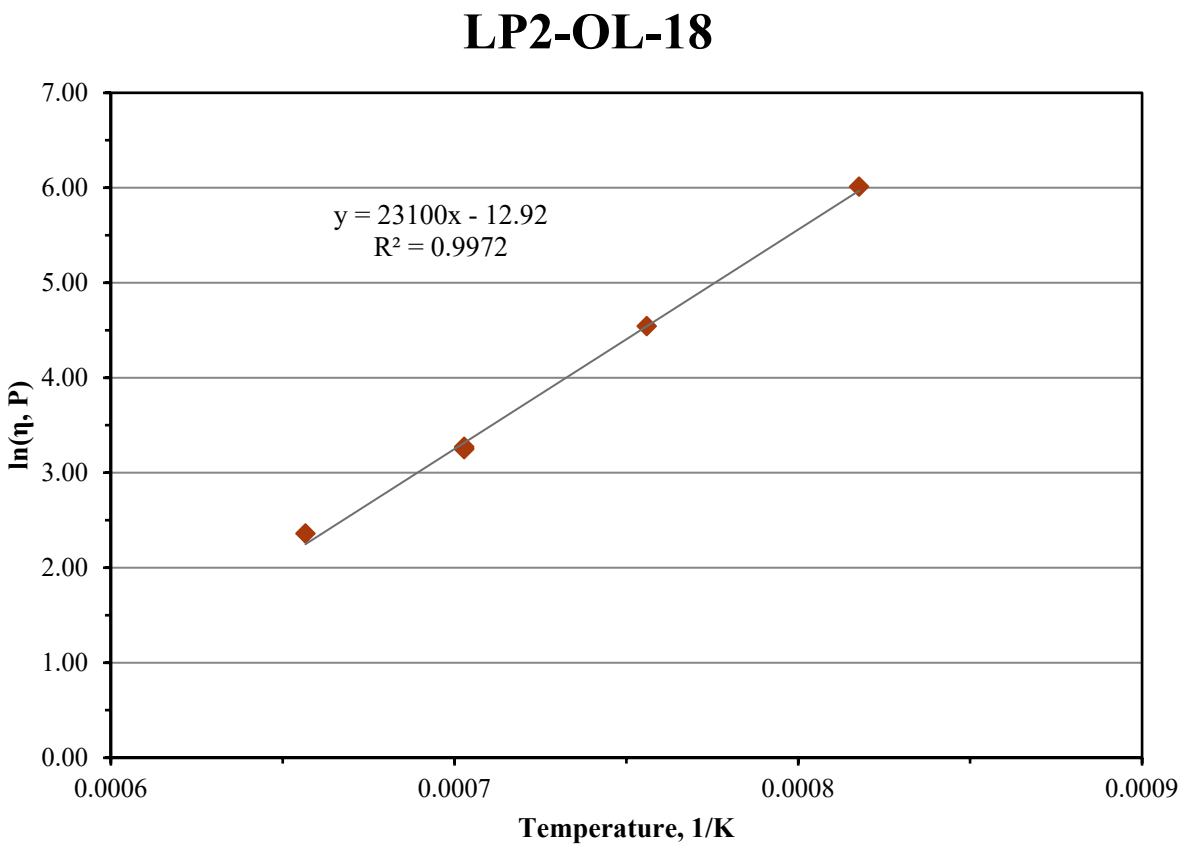


Figure C.34. Viscosity-Temperature Data and Arrhenius Equation Fit for Glass LP2-OL-18

## C.35 Glass LP2-OL-19 Viscosity Data

Table C.35. Viscosity Data for Glass LP2-OL-19

| Measured Temp., °C | Viscosity, P | 1/T x10000, $K^{-1}$ | ln η, P |
|---|---|---|---|
| 1150 | 94.658 | 7.027 | 4.550 |
| 1050 | 286.220 | 7.559 | 5.657 |
| 950 | 1140.300 | 8.177 | 7.039 |
| 1150 | 96.150 | 7.027 | 4.566 |
| 1250 | 38.812 | 6.566 | 3.659 |
| 1150 | 97.627 | 7.027 | 4.581 |

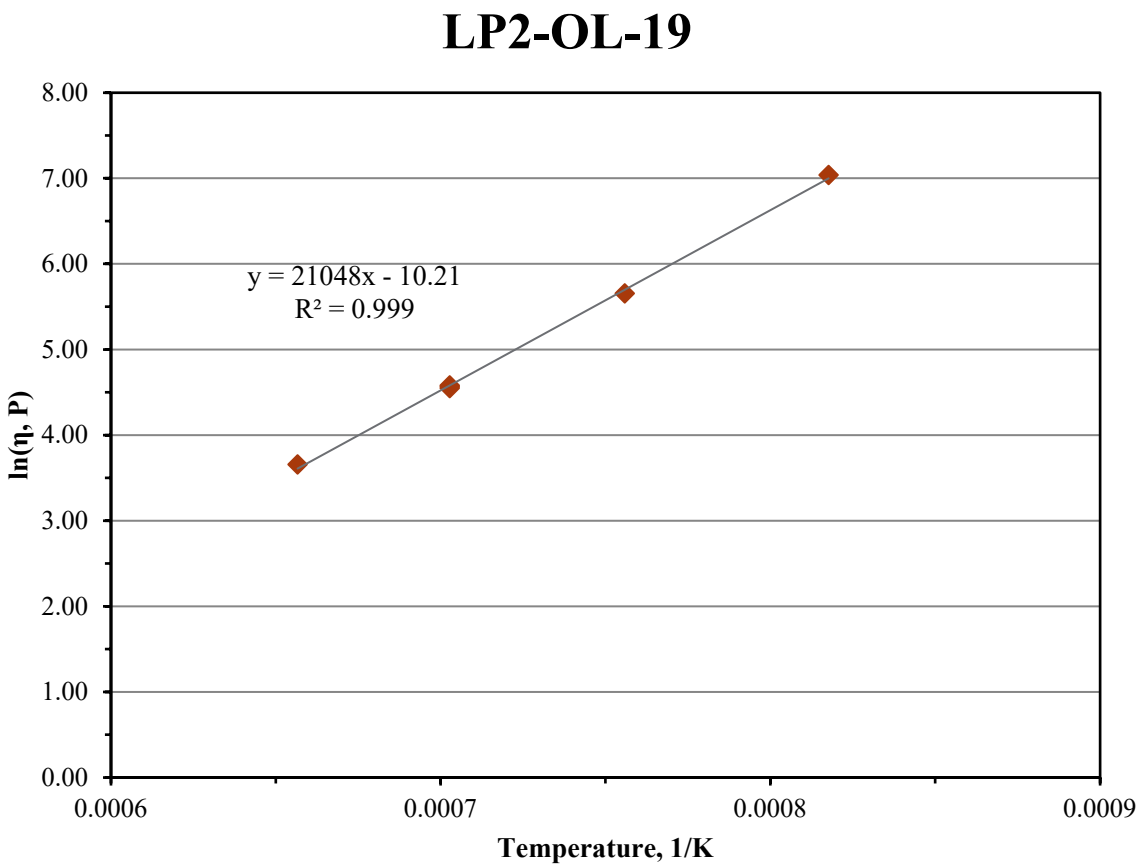


Figure C.35. Viscosity-Temperature Data and Arrhenius Equation Fit for Glass LP2-OL-19

## C.36 Glass LP2-OL-20 Viscosity Data

Table C.36. Viscosity Data for Glass LP2-OL-20

| Measured Temp., °C | Viscosity, P | 1/T x10000, $K^{-1}$ | ln η, P |
|---|---|---|---|
| 1150 | 46.287 | 7.027 | 3.835 |
| 1050 | 122.000 | 7.559 | 4.804 |
| 950 | 419.930 | 8.177 | 6.040 |
| 1150 | 45.714 | 7.027 | 3.822 |
| 1250 | 20.366 | 6.566 | 3.014 |
| 1150 | 45.952 | 7.027 | 3.828 |

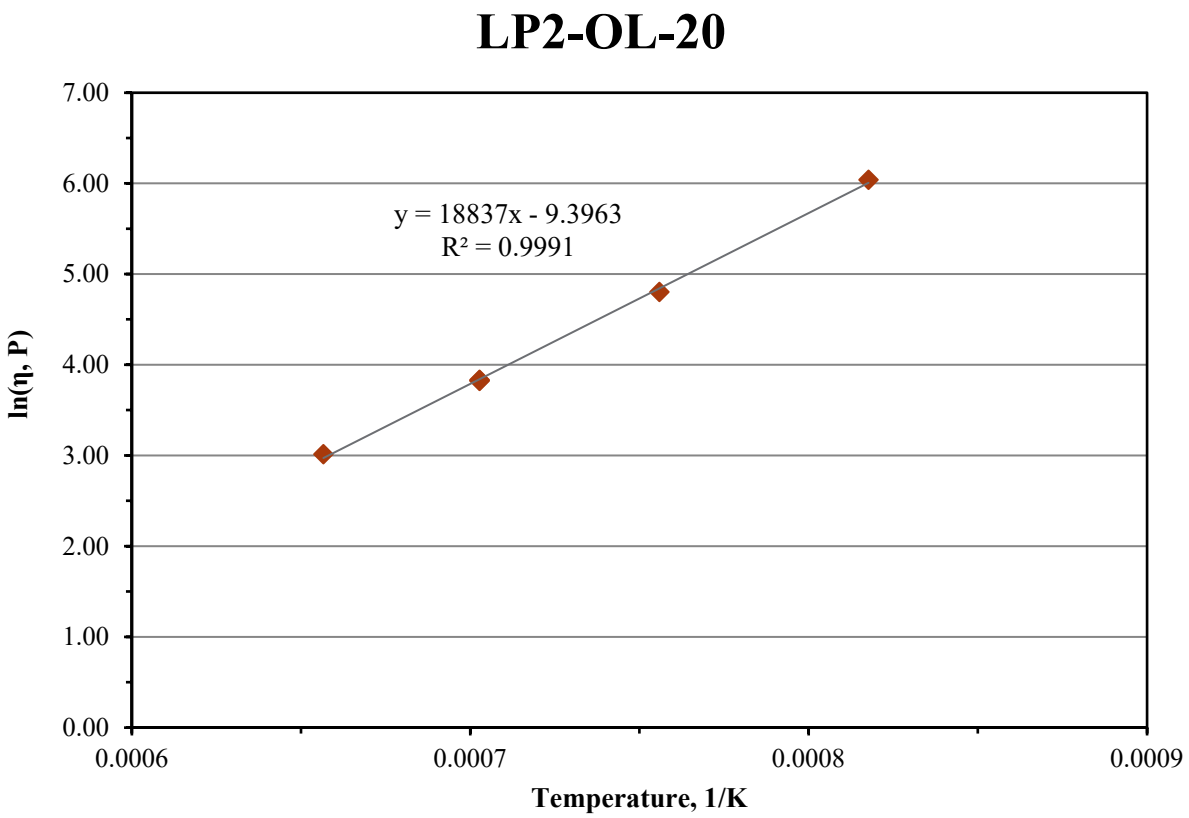


Figure C.36. Viscosity-Temperature Data and Arrhenius Equation Fit for Glass LP2-OL-20

## C.37 Glass LP2-OL-21 Viscosity Data

Table C.37. Viscosity Data for Glass LP2-OL-21

| Measured Temp., °C | Viscosity, P | 1/T x10000, $K^{-1}$ | ln η, P |
|---|---|---|---|
| 1150 | 41.915 | 7.027 | 3.736 |
| 1050 | 116.000 | 7.559 | 4.754 |
| 950 | 423.520 | 8.177 | 6.049 |
| 1150 | 42.674 | 7.027 | 3.754 |
| 1250 | 18.500 | 6.566 | 2.918 |
| 1150 | 43.189 | 7.027 | 3.766 |

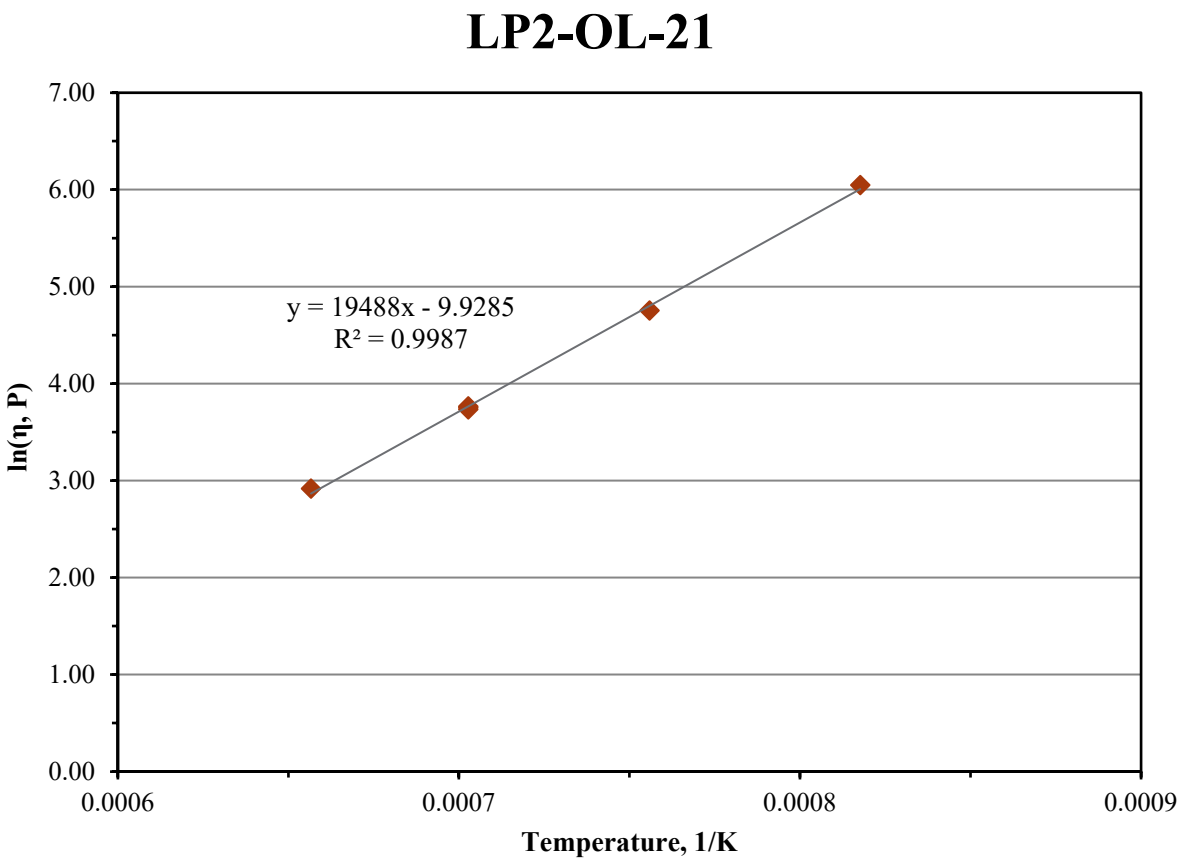


Figure C.37. Viscosity-Temperature Data and Arrhenius Equation Fit for Glass LP2-OL-21

## C.38 Glass LP2-OL-22 Viscosity Data

Table C.38. Viscosity Data for Glass LP2-OL-22

| Measured Temp., °C | Viscosity, P | 1/T x10000, $K^{-1}$ | ln η, P |
|---|---|---|---|
| 1150 | 32.000 | 7.027 | 3.466 |
| 1050 | 106.000 | 7.559 | 4.663 |
| 950 | 515.778 | 8.177 | 6.246 |
| 1150 | 32.362 | 7.027 | 3.477 |
| 1250 | 12.700 | 6.566 | 2.542 |
| 1150 | 32.200 | 7.027 | 3.472 |

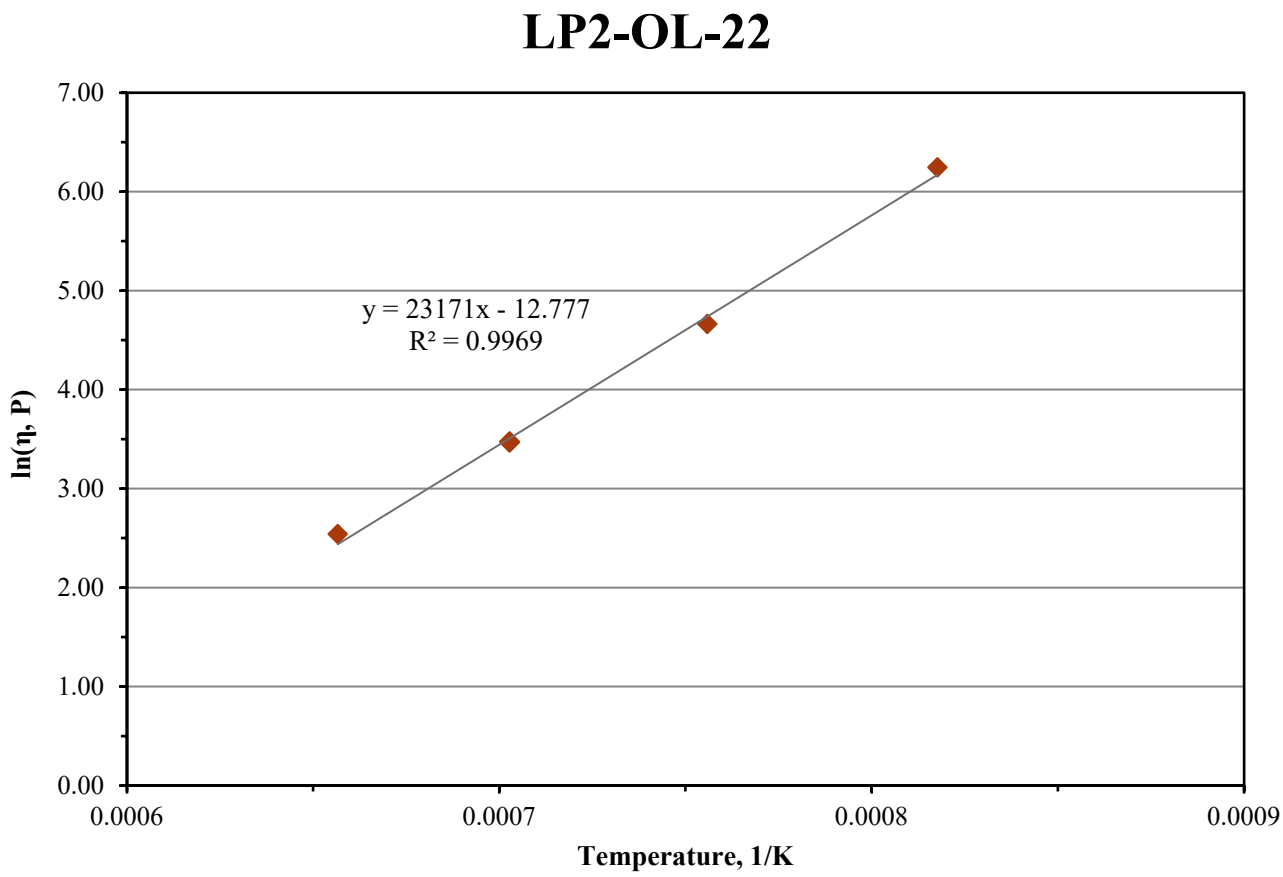


Figure C.38. Viscosity-Temperature Data and Arrhenius Equation Fit for Glass LP2-OL-22

## C.39 Glass LP2-OL-23 Viscosity Data

Table C.39. Viscosity Data for Glass LP2-OL-23

| Measured Temp., °C | Viscosity, P | 1/T x10000, $K^{-1}$ | ln η, P |
|---|---|---|---|
| 1150 | 12.000 | 7.027 | 2.485 |
| 1050 | 31.800 | 7.559 | 3.459 |
| 950 | 116.000 | 8.177 | 4.754 |
| 1150 | 12.196 | 7.027 | 2.501 |
| 1250 | 5.635 | 6.566 | 1.729 |
| 1150 | 12.200 | 7.027 | 2.501 |

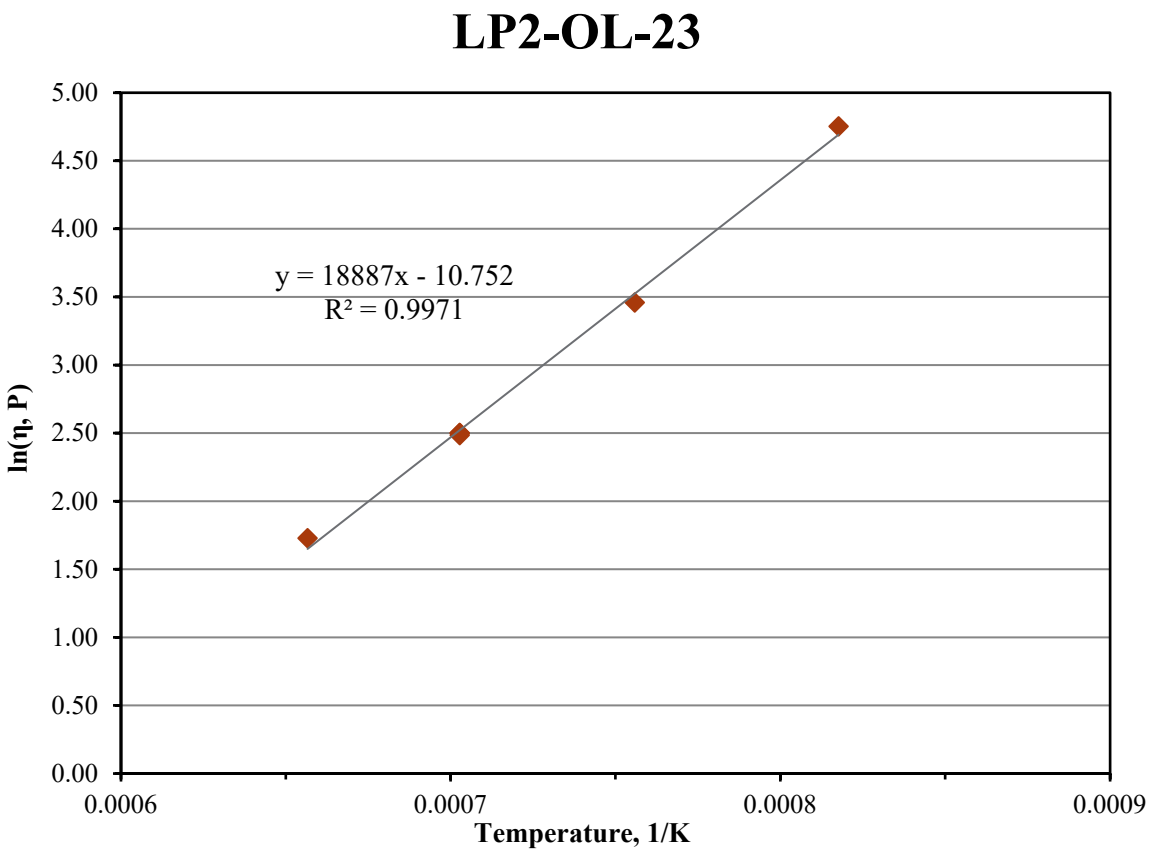


Figure C.39. Viscosity-Temperature Data and Arrhenius Equation Fit for Glass LP2-OL-23

## C.40 Glass LP2-OL-24 Viscosity Data

Table C.40. Viscosity Data for Glass LP2-OL-24

| Measured Temp., °C | Viscosity, P | 1/T x10000, $K^{-1}$ | ln η, P |
|---|---|---|---|
| 1150 | 37.241 | 7.027 | 3.617 |
| 1050 | 103.720 | 7.559 | 4.642 |
| 950 | 372.040 | 8.177 | 5.919 |
| 1150 | 37.409 | 7.027 | 3.622 |
| 1250 | 16.000 | 6.566 | 2.773 |
| 1150 | 37.457 | 7.027 | 3.623 |

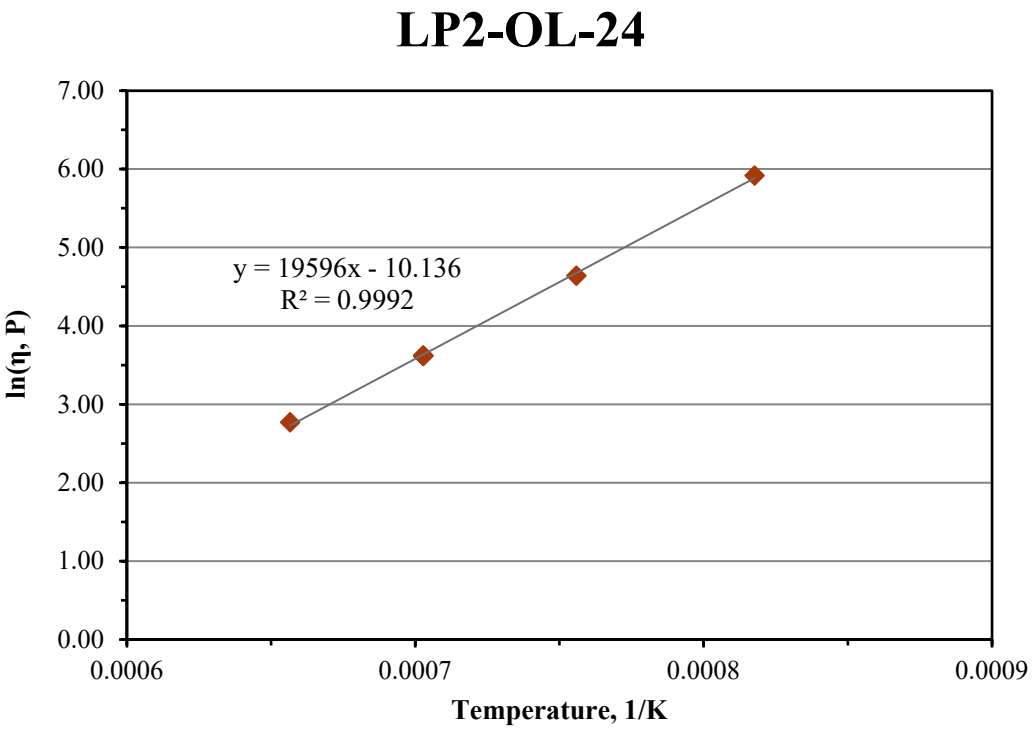


Figure C.40. Viscosity-Temperature Data and Arrhenius Equation Fit for Glass LP2-OL-24

## C.41 Glass LP2-OL-25 Viscosity Data

Table C.41. Viscosity Data for Glass LP2-OL-25

| Measured Temp., °C | Viscosity, P | 1/T x10000, $K^{-1}$ | ln η, P |
|---|---|---|---|
| 1150 | 14.843 | 7.027 | 2.698 |
| 1050 | 39.062 | 7.559 | 3.665 |
| 950 | 138.000 | 8.177 | 4.927 |
| 1150 | 15.000 | 7.027 | 2.708 |
| 1250 | 6.879 | 6.566 | 1.928 |
| 1150 | 15.050 | 7.027 | 2.711 |

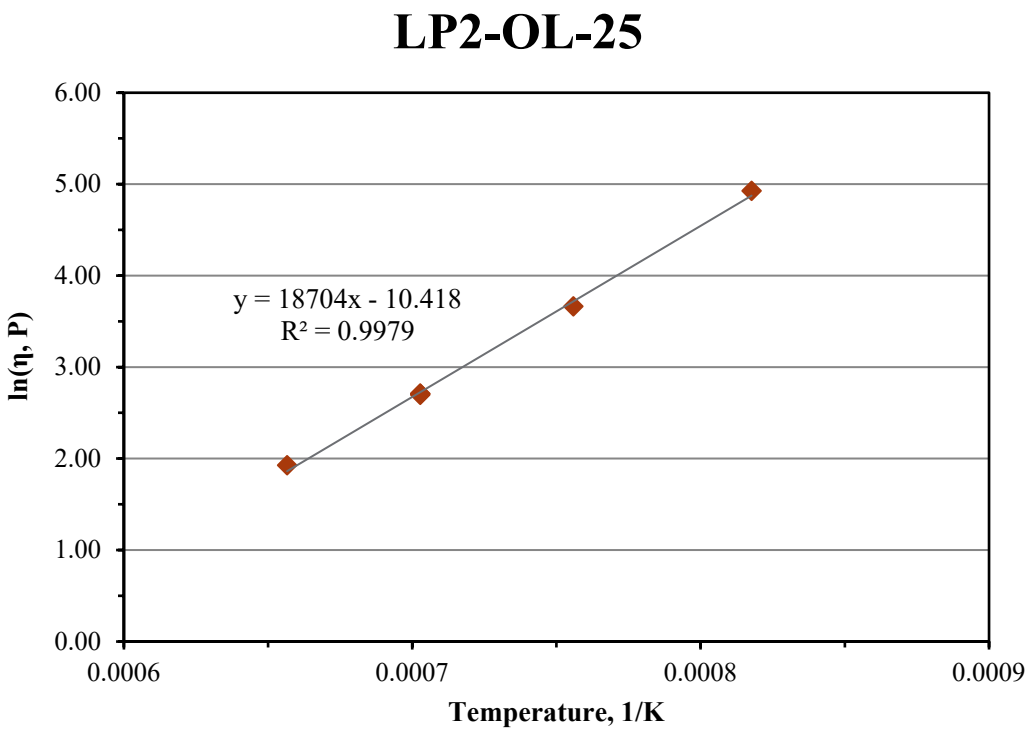


Figure C.41. Viscosity-Temperature Data and Arrhenius Equation Fit for Glass LP2-OL-25

# Appendix D – Electrical Conductivity Data

This appendix contains the measured electrical conductivity data for each of the Phase 2 enhanced LAW glasses. The plots shown in this appendix were fitted to the Arrhenius equation

$$\ln(\varepsilon) = A + \frac{B}{T_K} \quad \text{(D.1)}$$

where *A* and *B* are independent of temperature ($T_K$) is in K (T(°C) + 273.15)**.** If some of the plots showed curvature, the data would be better fit to the Vogel-Fulcher-Tamman (VFT) model

$$\ln(\varepsilon) = E + \frac{F}{T_K - T_0} \quad \text{(D.2)}$$

where E, F, and $T_0$ are temperature independent coefficients and composition dependent coefficients and $T_K$ is in °K (T(°C) + 273.15). The intent of the figures and Arrhenius equation fits shown in this appendix is mainly to assess trends of the data and provide some observations about whether there may be sufficient curvature in the data to consider VFT fits in the subsequent work that will decide between fitting the electrical conductivity-temperature data to the Arrhenius or VFT equations. All of the Phase 2 enhanced LAW glasses appear to have very good fits to the Arrhenius equation and do not show a need for fitting to the VFT model.

## D.1 Glass LP2-IL-01 Electrical Conductivity Data

Table D.1. Electrical Conductivity Data for Glass LP2-IL-01

| Temperature, °C | Conductivity, S/m | 1/T, $K^{-1}$ | ln ε (S/m) |
|---|---|---|---|
| 950 | 28.69 | 0.000818 | 3.356 |
| 950 | 28.91 | 0.000818 | 3.364 |
| 1250 | 71.99 | 0.000657 | 4.276 |
| 1250 | 71.88 | 0.000657 | 4.275 |
| 1150 | 56.95 | 0.000703 | 4.042 |
| 1150 | 57.02 | 0.000703 | 4.043 |
| 1050 | 42.19 | 0.000756 | 3.742 |
| 1050 | 42.38 | 0.000756 | 3.747 |

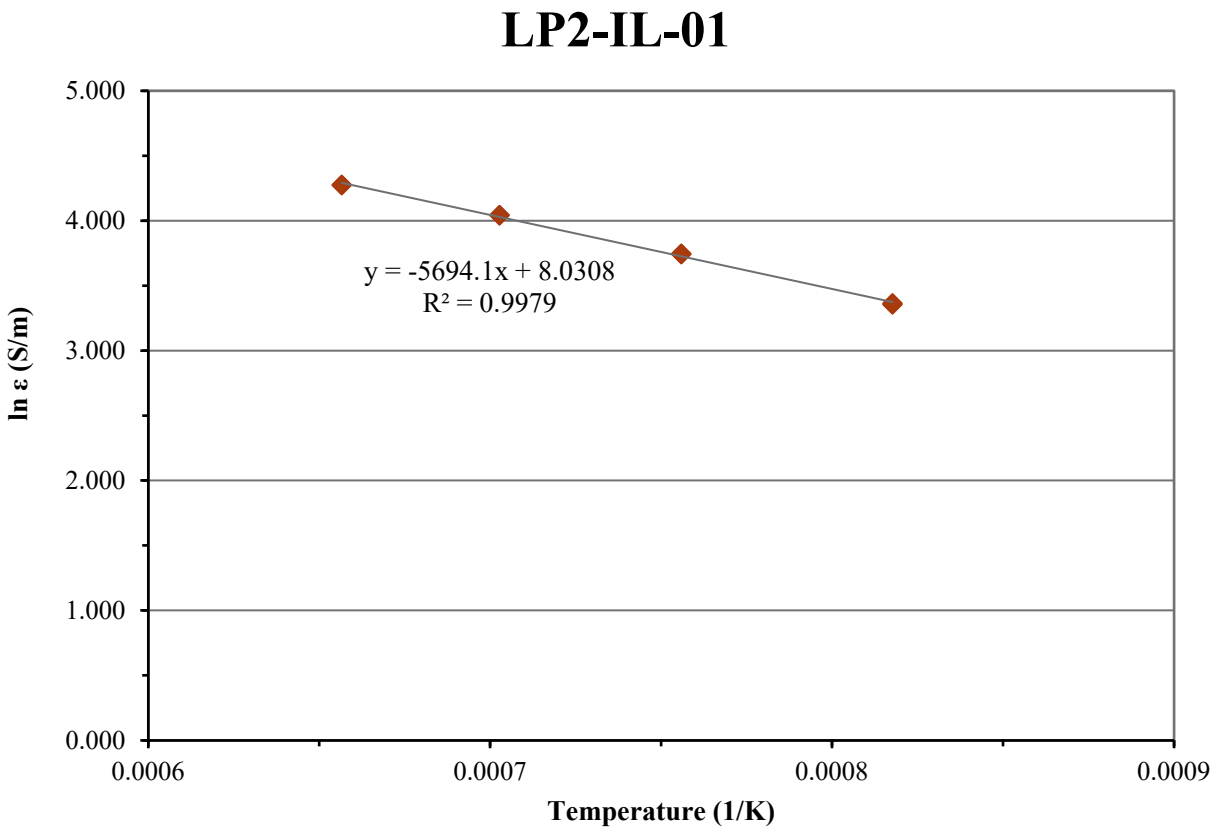


Figure D.1. Electrical Conductivity-Temperature Data and Arrhenius Equation Fit for Glass LP2-IL-01

## D.2 Glass LP2-IL-02 Electrical Conductivity Data

Table D.2. Electrical Conductivity Data for Glass LP2-IL-02

| Temperature, °C | Conductivity, S/m | 1/T, $K^{-1}$ | ln (ε, S/m) |
|---|---|---|---|
| 950 | 29.14 | 0.000818 | 3.372 |
| 950 | 29.39 | 0.000818 | 3.381 |
| 1250 | 73.11 | 0.000657 | 4.292 |
| 1250 | 72.98 | 0.000657 | 4.290 |
| 1150 | 57.99 | 0.000703 | 4.060 |
| 1150 | 58.08 | 0.000703 | 4.062 |
| 1050 | 42.77 | 0.000756 | 3.756 |
| 1050 | 42.97 | 0.000756 | 3.760 |

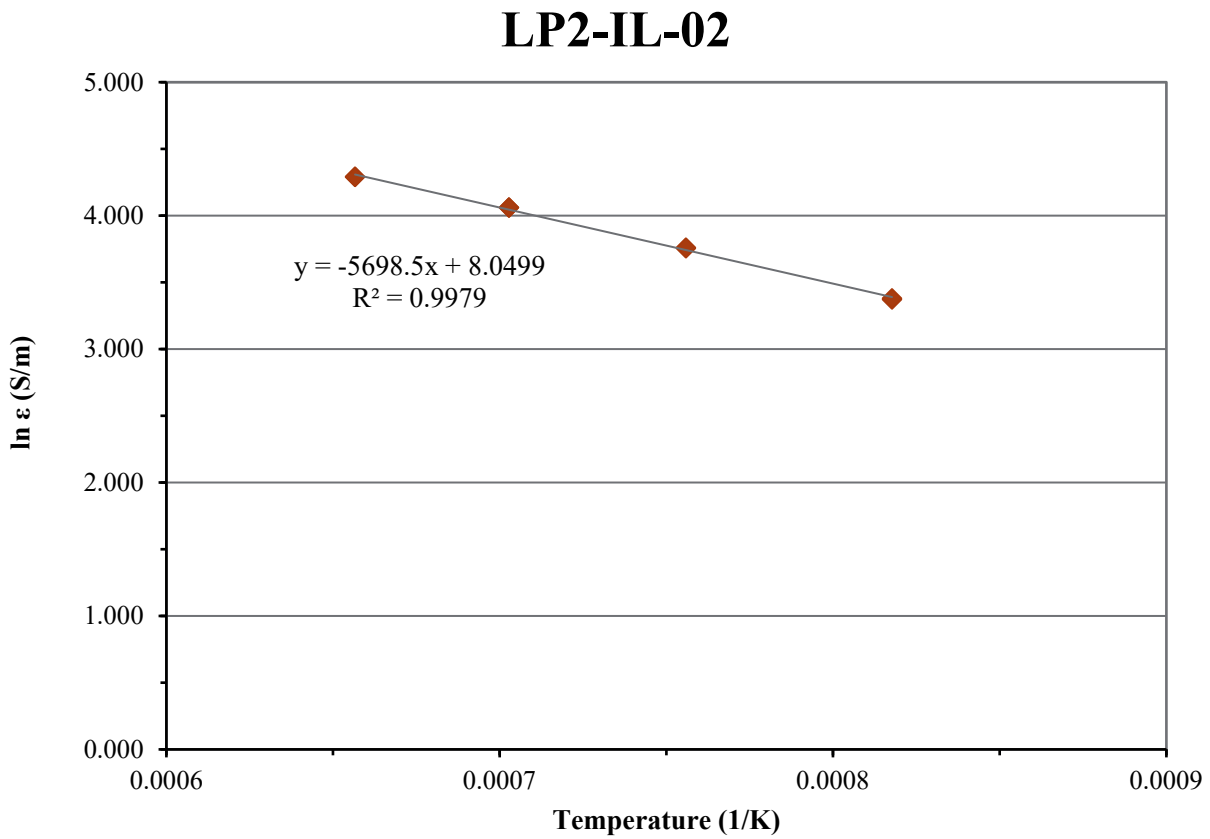


Figure D.2. Electrical Conductivity-Temperature Data and Arrhenius Equation Fit for Glass LP2-IL-02

## D.3 Glass LP2-IL-03 Electrical Conductivity Data

Table D.3. Electrical Conductivity Data for Glass LP2-IL-03

| Temperature, °C | Conductivity, S/m | 1/T, $K^{-1}$ | ln (ε, S/m) |
|---|---|---|---|
| 950 | 30.71 | 0.000818 | 3.425 |
| 950 | 30.92 | 0.000818 | 3.431 |
| 1250 | 73.79 | 0.000657 | 4.301 |
| 1150 | 59.05 | 0.000703 | 4.078 |
| 1150 | 59.28 | 0.000703 | 4.082 |
| 1050 | 44.21 | 0.000756 | 3.789 |
| 1050 | 44.50 | 0.000756 | 3.796 |

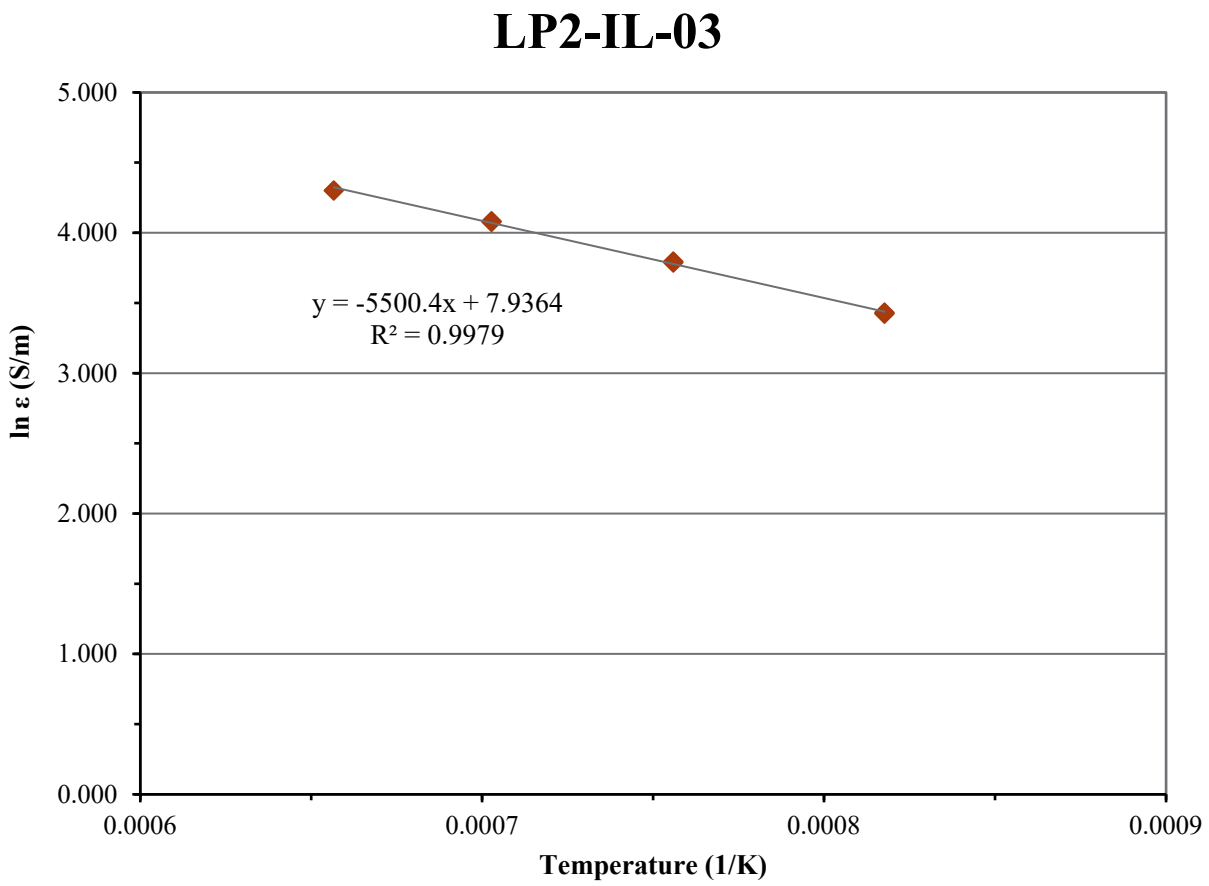


Figure D.3. Electrical Conductivity-Temperature Data and Arrhenius Equation Fit for Glass LP2-IL-03

## D.4 Glass LP2-IL-04 Electrical Conductivity Data

Table D.4. Electrical Conductivity Data for Glass LP2-IL-04

| Temperature, °C | Conductivity, S/m | 1/T, $K^{-1}$ | ln (ε, S/m) |
|---|---|---|---|
| 950 | 29.06 | 0.000818 | 3.369 |
| 950 | 29.26 | 0.000818 | 3.376 |
| 1250 | 73.74 | 0.000657 | 4.301 |
| 1250 | 73.45 | 0.000657 | 4.297 |
| 1150 | 58.39 | 0.000703 | 4.067 |
| 1150 | 58.52 | 0.000703 | 4.069 |
| 1050 | 42.93 | 0.000756 | 3.760 |
| 1050 | 43.12 | 0.000756 | 3.764 |

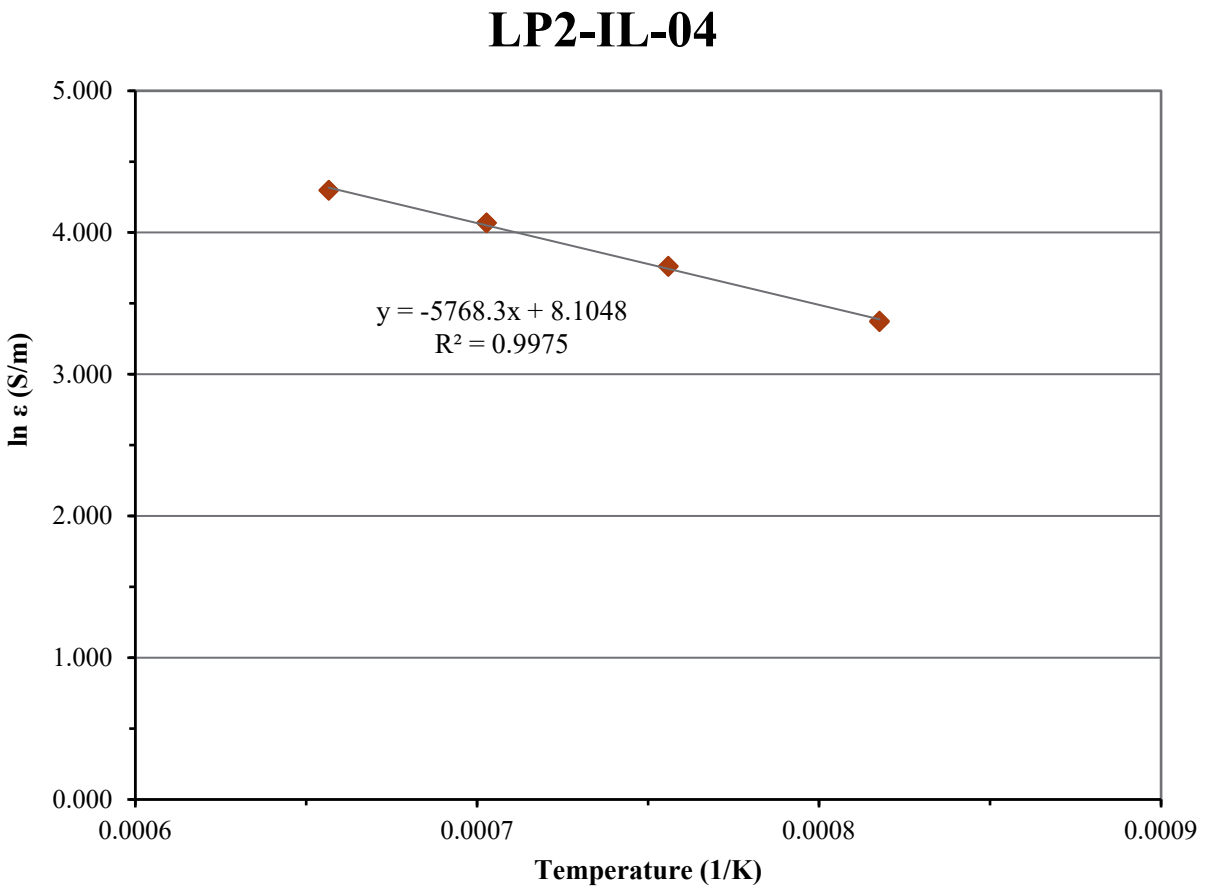


Figure D.4. Electrical Conductivity-Temperature Data and Arrhenius Equation Fit for Glass LP2-IL-04

## D.5 Glass LP2-IL-05 Electrical Conductivity Data

Table D.5. Electrical Conductivity Data for Glass LP2-IL-05

| Temperature, °C | Conductivity, S/m | 1/T, $K^{-1}$ | ln (ε, S/m) |
|---|---|---|---|
| 950 | 23.47 | 0.000818 | 3.156 |
| 950 | 23.65 | 0.000818 | 3.164 |
| 1250 | 65.02 | 0.000657 | 4.175 |
| 1250 | 64.77 | 0.000657 | 4.171 |
| 1150 | 50.30 | 0.000703 | 3.918 |
| 1150 | 50.55 | 0.000703 | 3.923 |
| 1050 | 35.93 | 0.000756 | 3.582 |
| 1050 | 36.09 | 0.000756 | 3.586 |

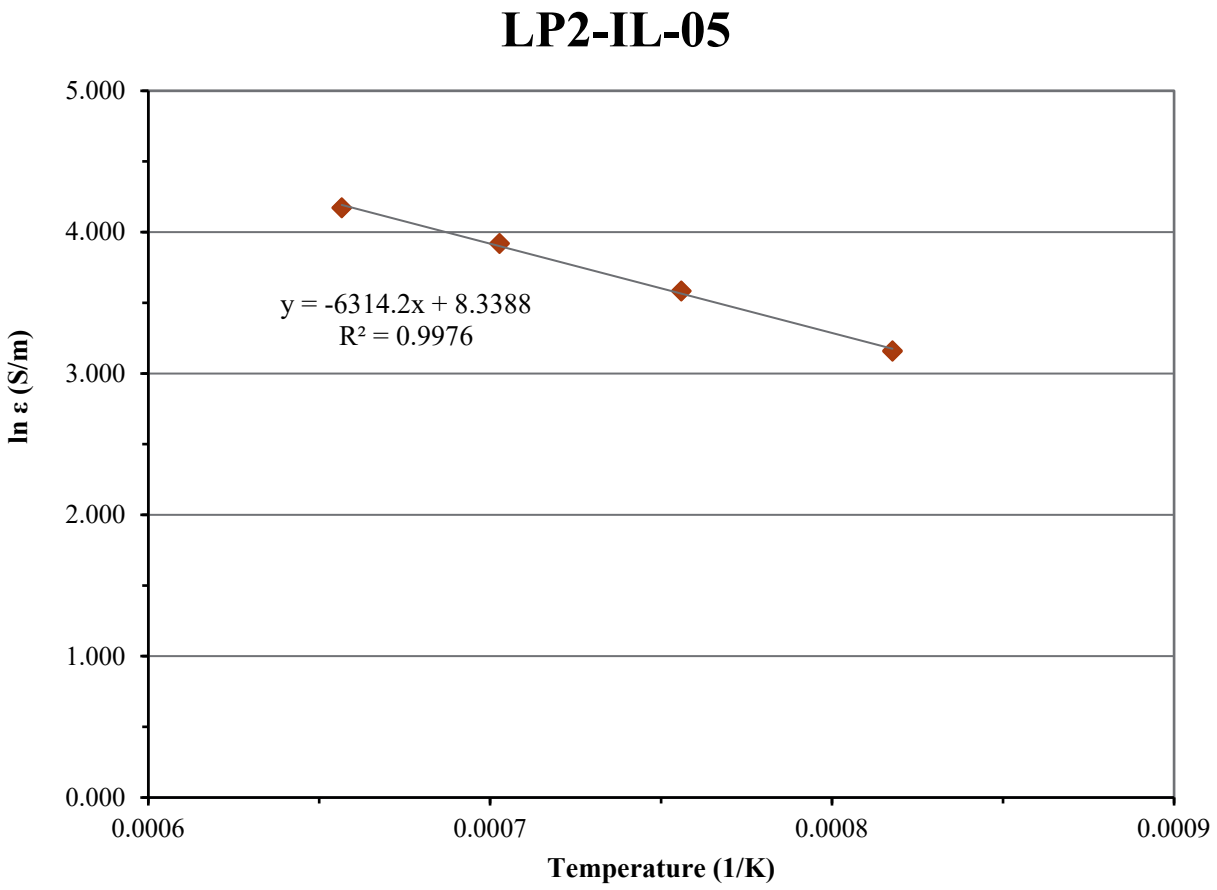


Figure D.5. Electrical Conductivity-Temperature Data and Arrhenius Equation Fit for Glass LP2-IL-05

## D.6 Glass LP2-IL-06 Electrical Conductivity Data

Table D.6. Electrical Conductivity Data for Glass LP2-IL-06

| Temperature, °C | Conductivity, S/m | 1/T, $K^{-1}$ | ln (ε, S/m) |
|---|---|---|---|
| 950 | 27.37 | 0.000818 | 3.310 |
| 950 | 27.54 | 0.000818 | 3.316 |
| 1250 | 67.52 | 0.000657 | 4.212 |
| 1250 | 67.16 | 0.000657 | 4.207 |
| 1150 | 53.87 | 0.000703 | 3.987 |
| 1150 | 53.94 | 0.000703 | 3.988 |
| 1050 | 40.06 | 0.000756 | 3.690 |
| 1050 | 40.20 | 0.000756 | 3.694 |

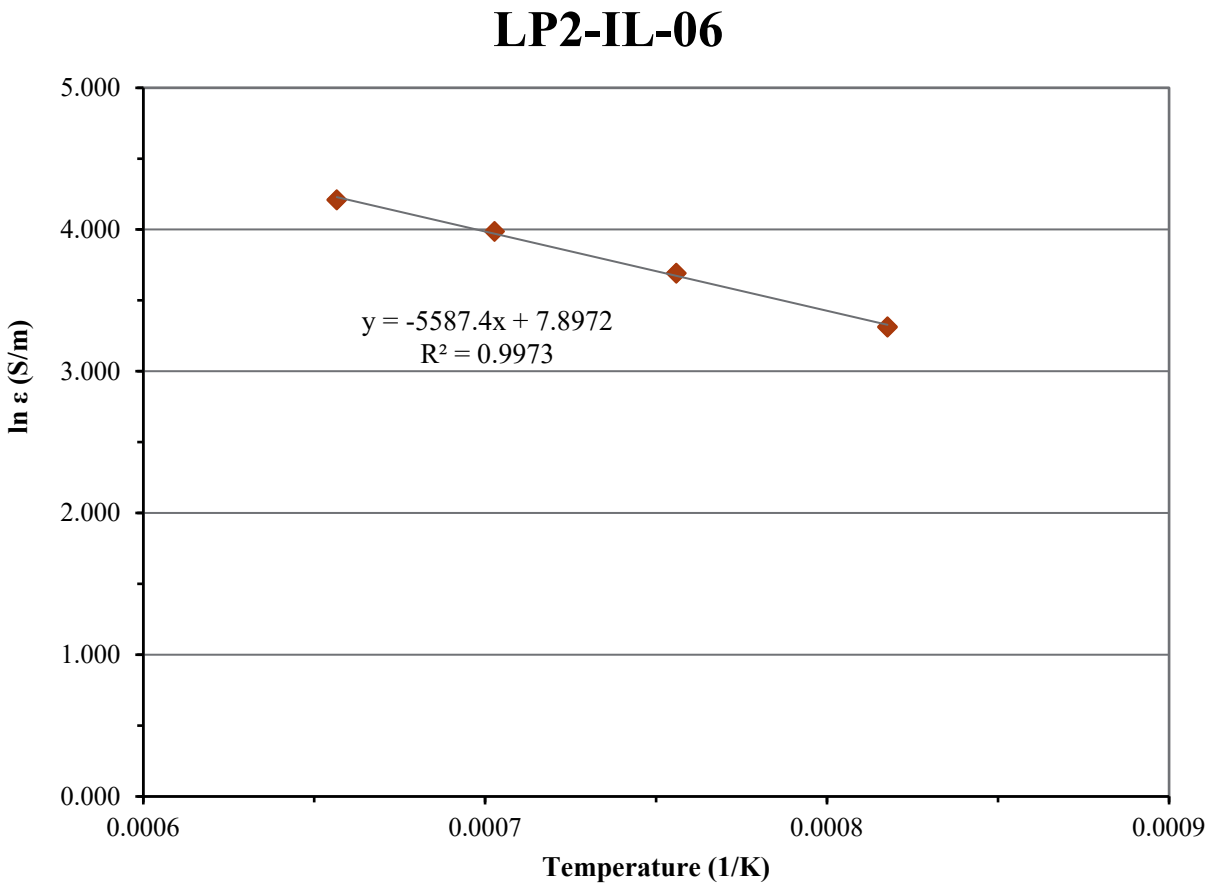


Figure D.6. Electrical Conductivity-Temperature Data and Arrhenius Equation Fit for Glass LP2-IL-06

## D.7 Glass LP2-IL-07 Electrical Conductivity Data

Table D.7. Electrical Conductivity Data for Glass LP2-IL-07

| Temperature, °C | Conductivity, S/m | 1/T, $K^{-1}$ | ln (ε, S/m) |
|---|---|---|---|
| 950 | 26.81 | 0.000818 | 3.289 |
| 950 | 27.00 | 0.000818 | 3.296 |
| 1250 | 67.53 | 0.000657 | 4.213 |
| 1150 | 53.48 | 0.000703 | 3.979 |
| 1150 | 53.59 | 0.000703 | 3.981 |
| 1050 | 39.52 | 0.000756 | 3.677 |
| 1050 | 39.69 | 0.000756 | 3.681 |

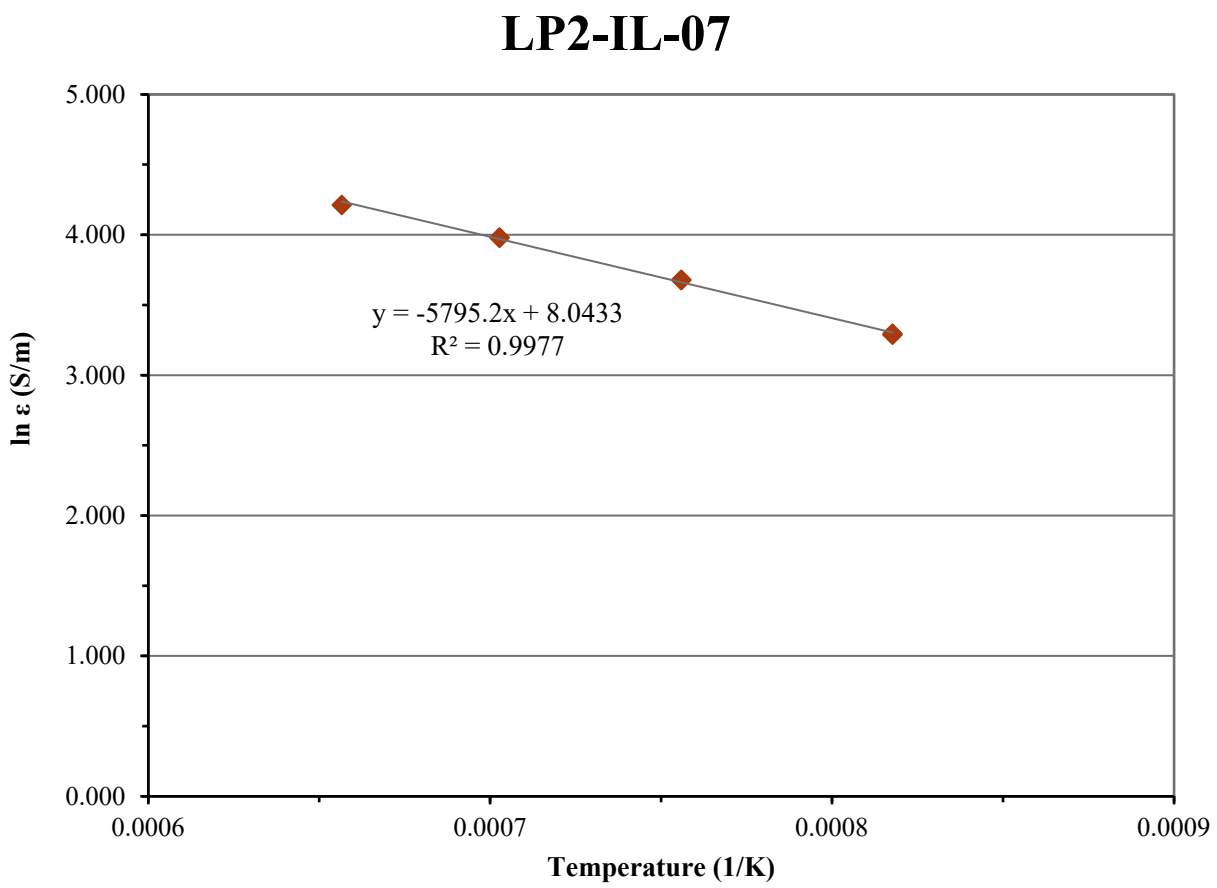


Figure D.7. Electrical Conductivity-Temperature Data and Arrhenius Equation Fit for Glass LP2-IL-07

## D.8 Glass LP2-IL-08 Electrical Conductivity Data

Table D.8. Electrical Conductivity Data for Glass LP2-IL-08

| Temperature, °C | Conductivity, S/m | 1/T, $K^{-1}$ | ln (ε, S/m) |
|---|---|---|---|
| 950 | 23.10 | 0.000818 | 3.140 |
| 950 | 23.27 | 0.000818 | 3.147 |
| 1250 | 63.59 | 0.000657 | 4.153 |
| 1250 | 63.35 | 0.000657 | 4.149 |
| 1150 | 49.16 | 0.000703 | 3.895 |
| 1150 | 49.26 | 0.000703 | 3.897 |
| 1050 | 35.25 | 0.000756 | 3.563 |
| 1050 | 35.40 | 0.000756 | 3.567 |

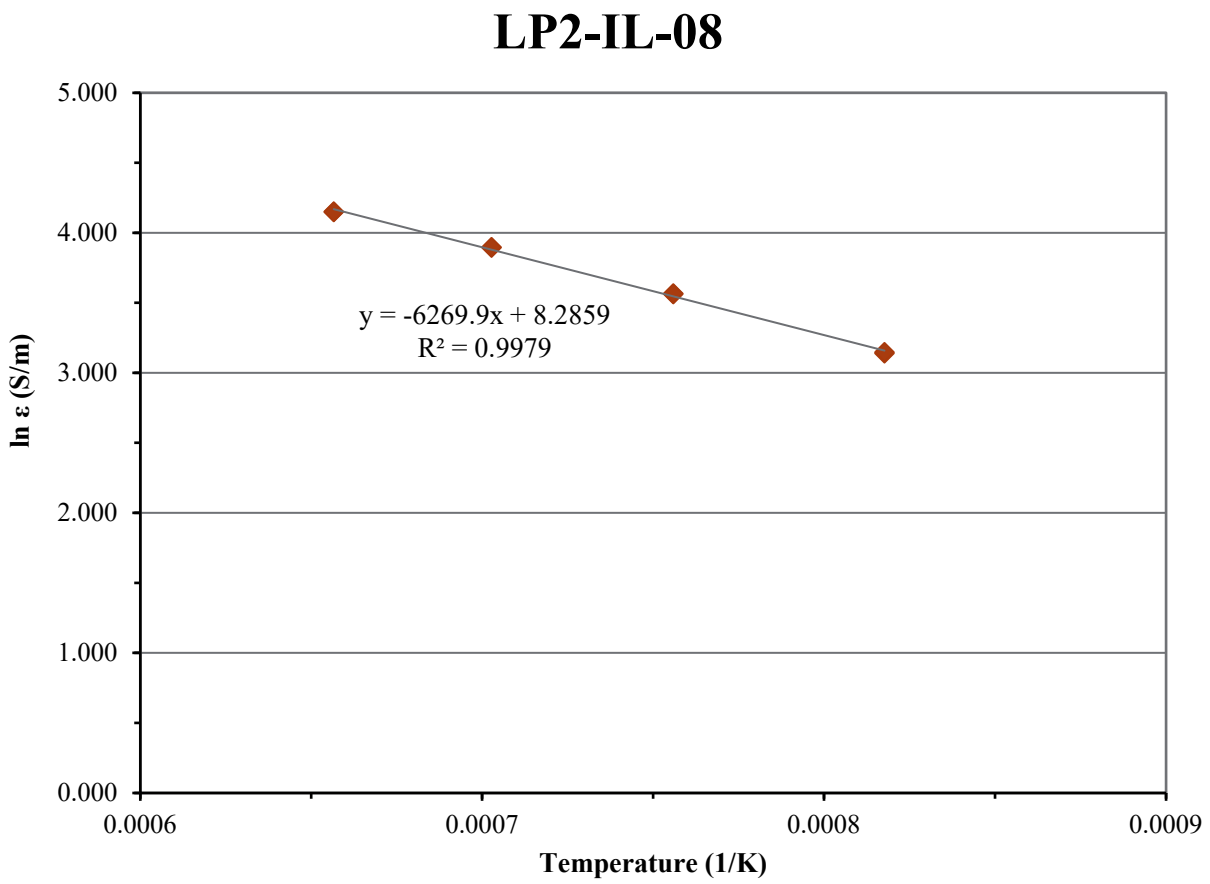


Figure D.8. Electrical Conductivity-Temperature Data and Arrhenius Equation Fit for Glass LP2-IL-08

## D.9 Glass LP2-IL-09 Electrical Conductivity Data

Table D.9. Electrical Conductivity Data for Glass LP2-IL-09

| Temperature, °C | Conductivity, S/m | 1/T, $K^{-1}$ | ln (ε, S/m) |
|---|---|---|---|
| 950 | 32.09 | 0.000818 | 3.468 |
| 950 | 32.33 | 0.000818 | 3.476 |
| 1250 | 78.02 | 0.000657 | 4.357 |
| 1250 | 78.09 | 0.000657 | 4.358 |
| 1150 | 62.90 | 0.000703 | 4.142 |
| 1150 | 63.09 | 0.000703 | 4.145 |
| 1050 | 46.69 | 0.000756 | 3.844 |
| 1050 | 47.03 | 0.000756 | 3.851 |

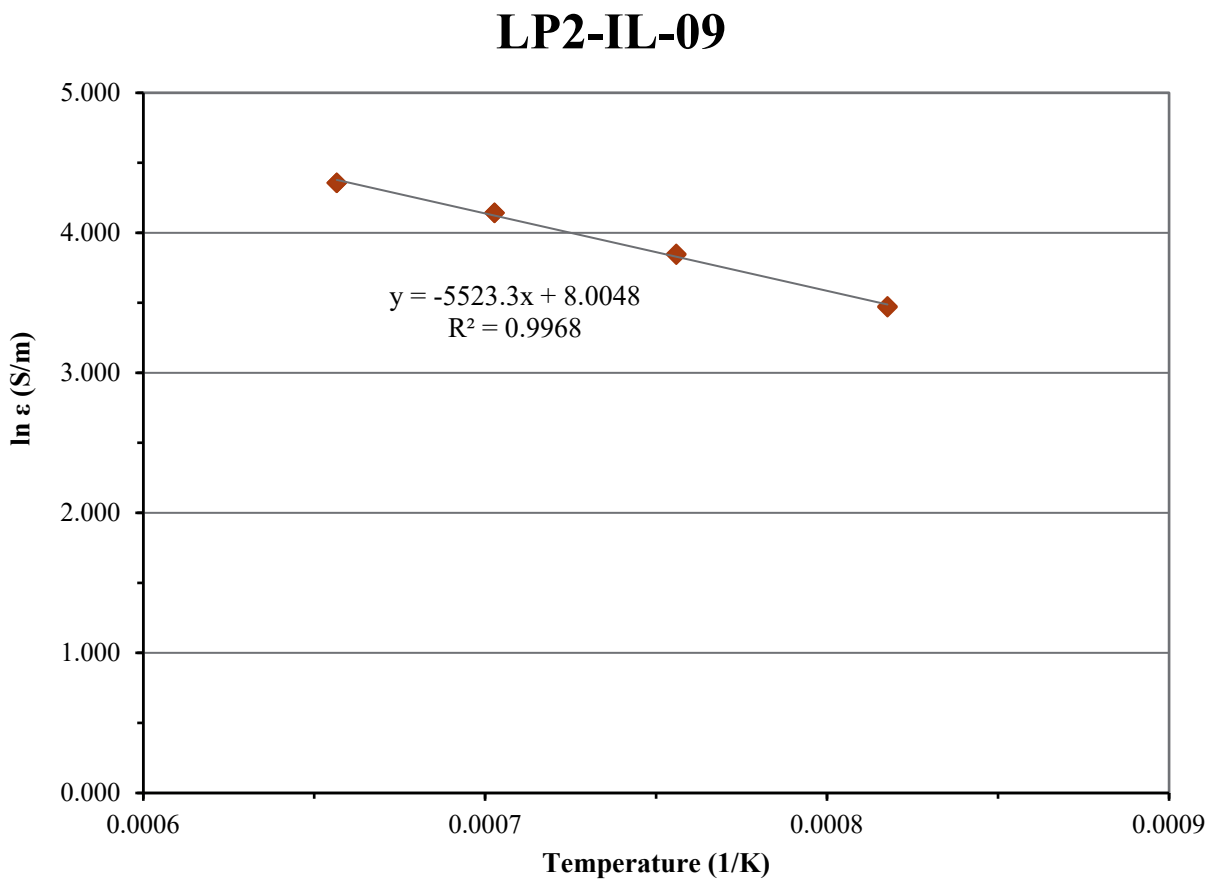


Figure D.9. Electrical Conductivity-Temperature Data and Arrhenius Equation Fit for Glass LP2-IL-09

## D.10 Glass LP2-IL-10 Electrical Conductivity Data

Table D.10. Electrical Conductivity Data for Glass LP2-IL-10

| Temperature, °C | Conductivity, S/m | 1/T, $K^{-1}$ | ln (ε, S/m) |
|---|---|---|---|
| 950 | 25.98 | 0.000818 | 3.257 |
| 950 | 26.15 | 0.000818 | 3.264 |
| 1250 | 66.30 | 0.000657 | 4.194 |
| 1150 | 52.45 | 0.000703 | 3.960 |
| 1150 | 52.49 | 0.000703 | 3.961 |
| 1050 | 38.43 | 0.000756 | 3.649 |
| 1050 | 38.58 | 0.000756 | 3.653 |

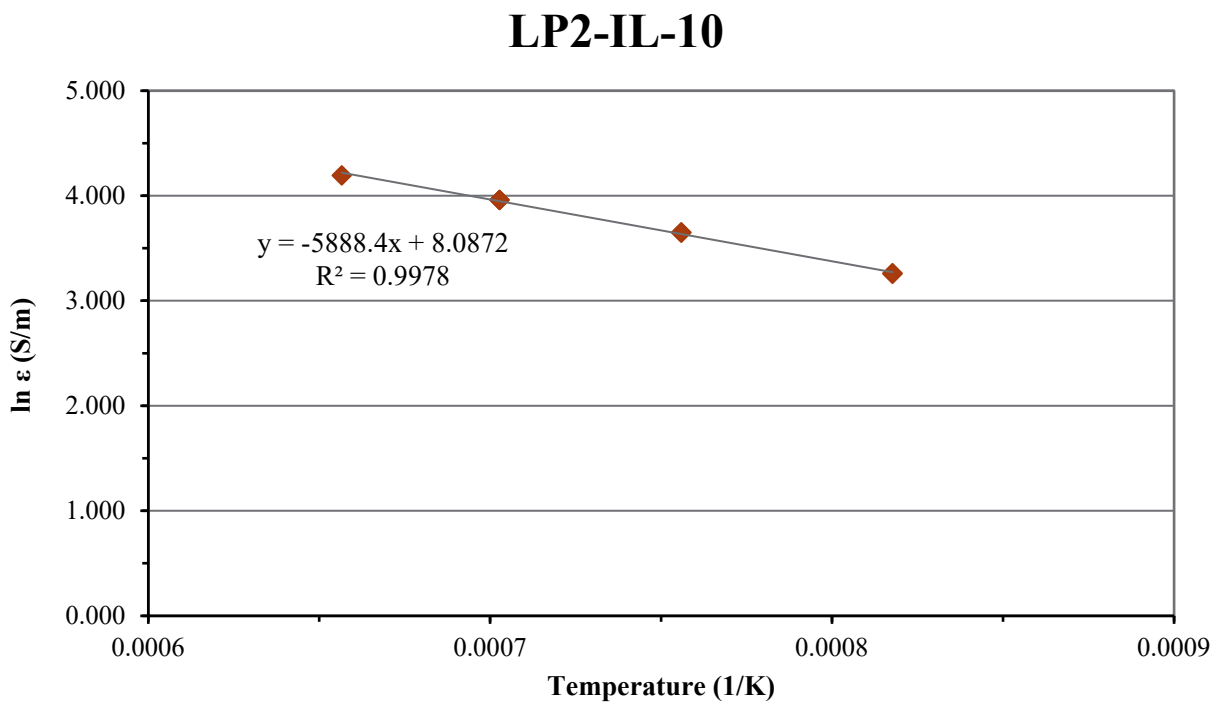


Figure D.10. Electrical Conductivity-Temperature Data and Arrhenius Equation Fit for Glass LP2-IL-10

## D.11 Glass LP2-IL-11 Electrical Conductivity Data

Table D.11. Electrical Conductivity Data for Glass LP2-IL-11

| Temperature, °C | Conductivity, S/m | 1/T, $K^{-1}$ | ln (ε, S/m) |
|---|---|---|---|
| 950 | 26.28 | 0.000818 | 3.269 |
| 950 | 26.46 | 0.000818 | 3.275 |
| 1250 | 67.31 | 0.000657 | 4.209 |
| 1250 | 67.15 | 0.000657 | 4.207 |
| 1150 | 53.36 | 0.000703 | 3.977 |
| 1150 | 53.51 | 0.000703 | 3.980 |
| 1050 | 39.20 | 0.000756 | 3.669 |
| 1050 | 39.35 | 0.000756 | 3.673 |

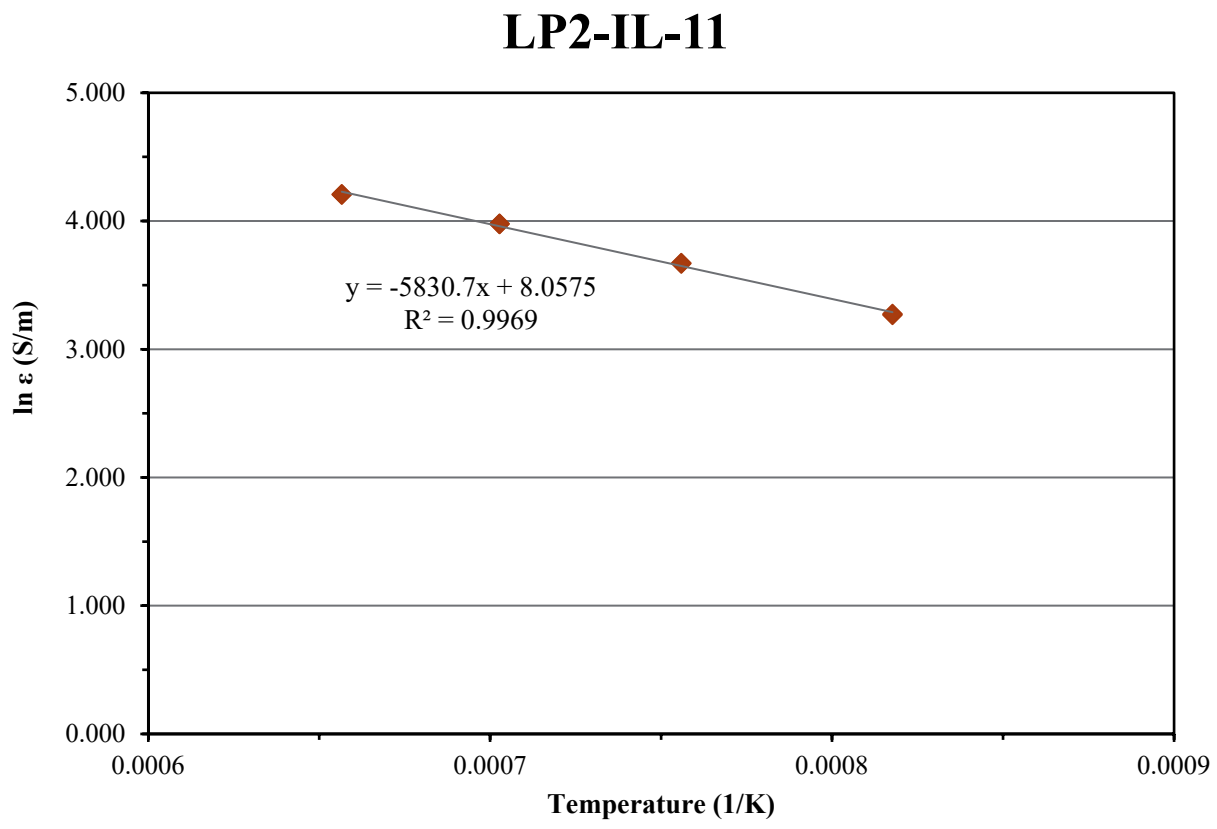


Figure D.11. Electrical Conductivity-Temperature Data and Arrhenius Equation Fit for Glass LP2-IL-11

## D.12 Glass LP2-IL-12 Electrical Conductivity Data

Table D.12. Electrical Conductivity Data for Glass LP2-IL-12

| Temperature, °C | Conductivity, S/m | 1/T, $K^{-1}$ | ln (ε, S/m) |
|---|---|---|---|
| 950 | 31.38 | 0.000818 | 3.446 |
| 950 | 31.56 | 0.000818 | 3.452 |
| 1250 | 72.80 | 0.000657 | 4.288 |
| 1250 | 72.57 | 0.000657 | 4.285 |
| 1150 | 58.67 | 0.000703 | 4.072 |
| 1150 | 58.76 | 0.000703 | 4.074 |
| 1050 | 44.61 | 0.000756 | 3.798 |
| 1050 | 44.76 | 0.000756 | 3.801 |

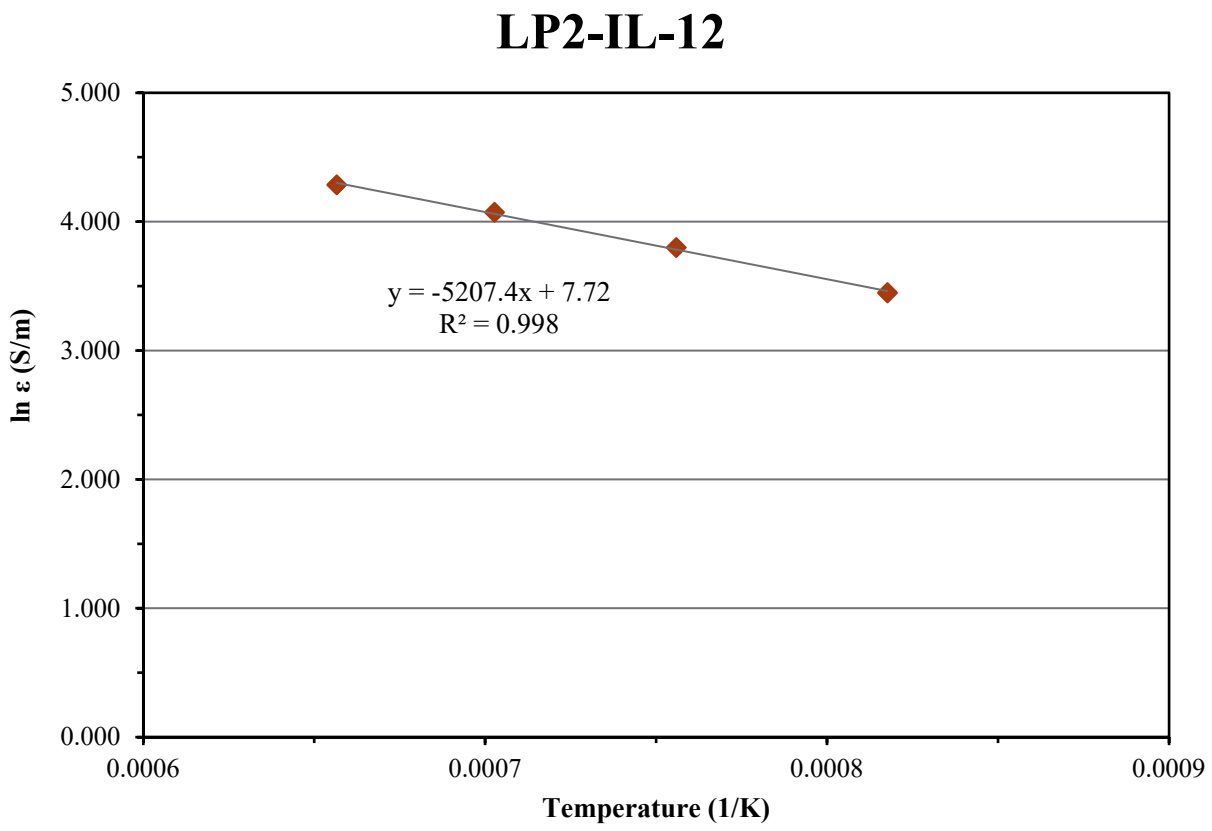


Figure D.12. Electrical Conductivity-Temperature Data and Arrhenius Equation Fit for Glass LP2-IL-12

## D.13 Glass LP2-IL-13 Electrical Conductivity Data

Table D.13. Electrical Conductivity Data for Glass LP2-IL-13

| Temperature, °C | Conductivity, S/m | 1/T, $K^{-1}$ | ln (ε, S/m) |
|---|---|---|---|
| 950 | 23.23 | 0.000818 | 3.146 |
| 950 | 23.43 | 0.000818 | 3.154 |
| 1250 | 59.73 | 0.000657 | 4.090 |
| 1250 | 59.59 | 0.000657 | 4.088 |
| 1150 | 46.95 | 0.000703 | 3.849 |
| 1150 | 47.02 | 0.000703 | 3.851 |
| 1050 | 34.51 | 0.000756 | 3.541 |
| 1050 | 34.64 | 0.000756 | 3.545 |

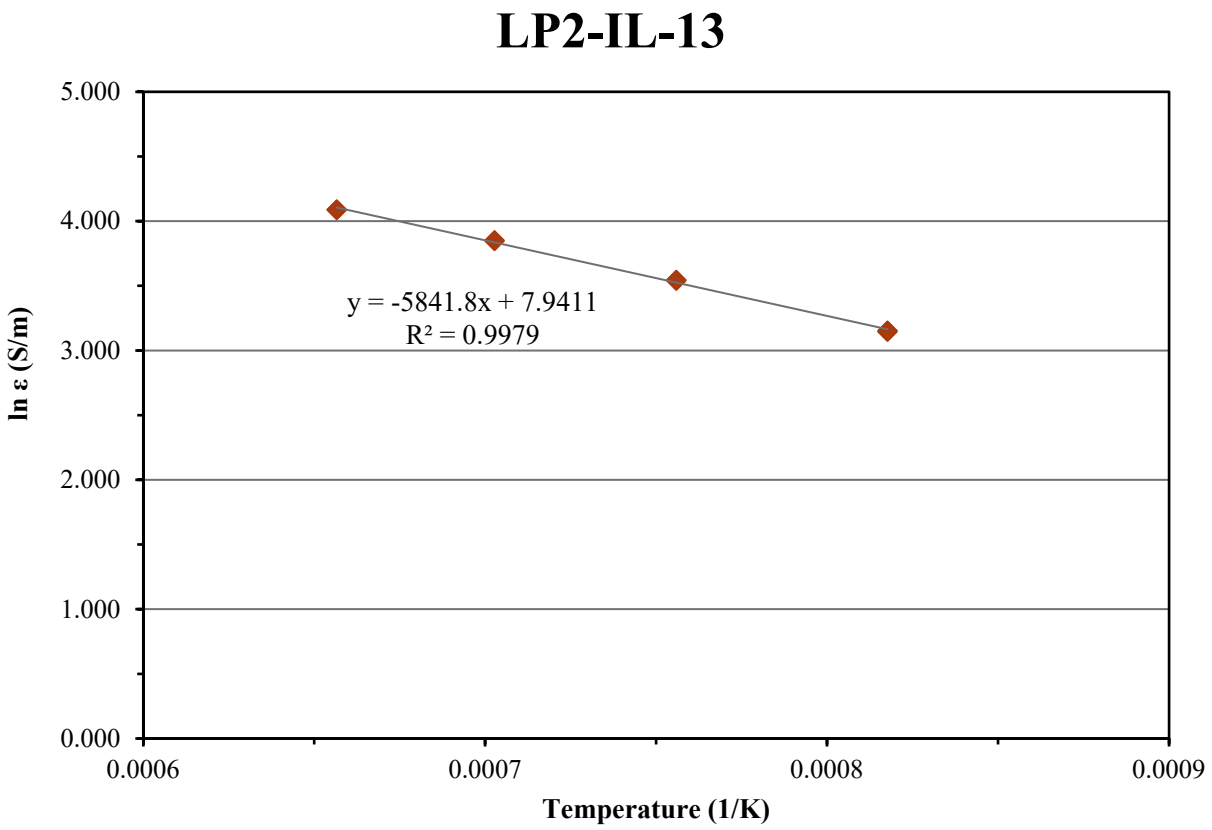


Figure D.13. Electrical Conductivity-Temperature Data and Arrhenius Equation Fit for Glass LP2-IL-13

## D.14 Glass LP2-IL-14 Electrical Conductivity Data

Table D.14. Electrical Conductivity Data for Glass LP2-IL-14

| Temperature, °C | Conductivity, S/m | 1/T, $K^{-1}$ | ln (ε, S/m) |
|---|---|---|---|
| 950 | 33.40 | 0.000818 | 3.509 |
| 950 | 33.60 | 0.000818 | 3.515 |
| 1250 | 77.16 | 0.000657 | 4.346 |
| 1250 | 77.08 | 0.000657 | 4.345 |
| 1150 | 62.61 | 0.000703 | 4.137 |
| 1150 | 62.67 | 0.000703 | 4.138 |
| 1050 | 47.55 | 0.000756 | 3.862 |
| 1050 | 47.71 | 0.000756 | 3.865 |

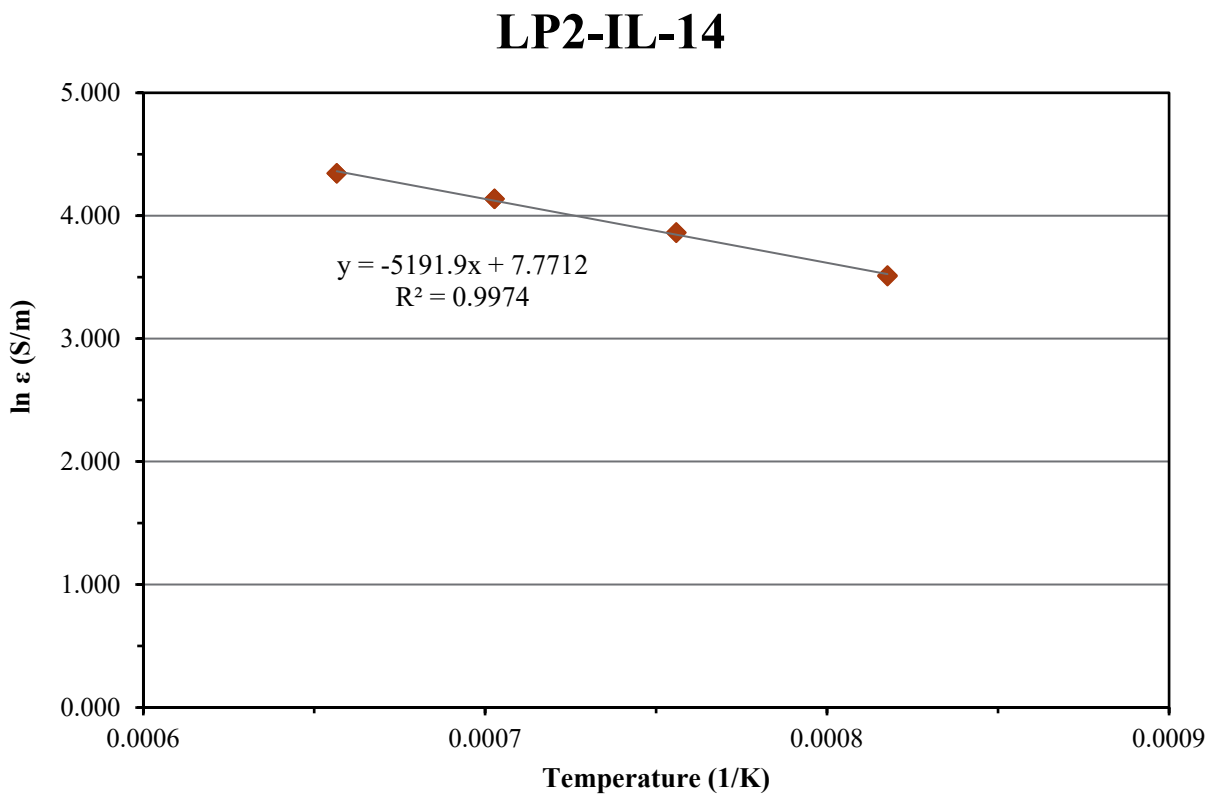


Figure D.14. Electrical Conductivity-Temperature Data and Arrhenius Equation Fit for Glass LP2-IL-14

## D.15 Glass LP2-IL-15 Electrical Conductivity Data

Table D.15. Electrical Conductivity Data for Glass LP2-IL-15

| Temperature, °C | Conductivity, S/m | 1/T, $K^{-1}$ | ln (ε, S/m) |
|---|---|---|---|
| 950 | 31.28 | 0.000818 | 3.443 |
| 950 | 31.54 | 0.000818 | 3.451 |
| 1250 | 76.13 | 0.000657 | 4.332 |
| 1250 | 75.99 | 0.000657 | 4.331 |
| 1150 | 61.16 | 0.000703 | 4.114 |
| 1150 | 61.25 | 0.000703 | 4.115 |
| 1050 | 45.69 | 0.000756 | 3.822 |
| 1050 | 45.83 | 0.000756 | 3.825 |

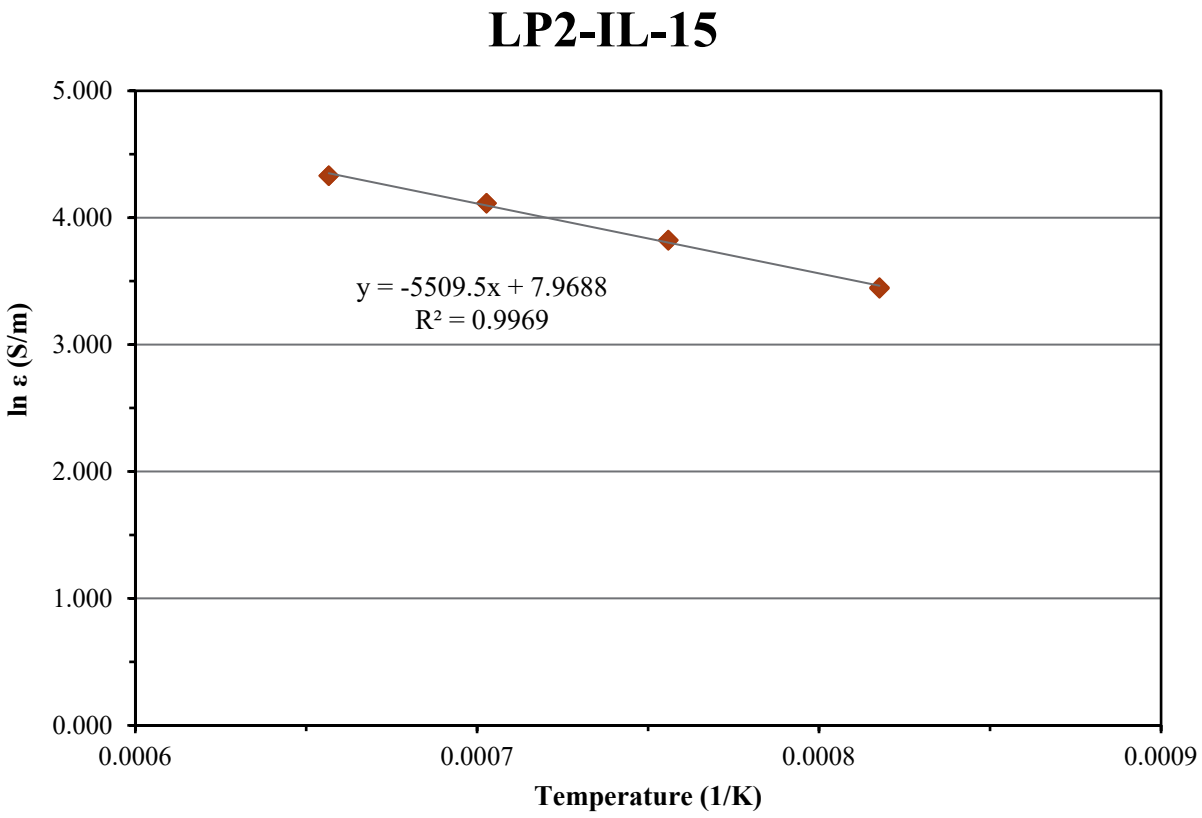


Figure D.15. Electrical Conductivity-Temperature Data and Arrhenius Equation Fit for Glass LP2-IL-15

## D.16 Glass LP2-IL-16 Electrical Conductivity Data

Table D.16. Electrical Conductivity Data for Glass LP2-IL-16

| Temperature, °C | Conductivity, S/m | 1/T, $K^{-1}$ | ln (ε, S/m) |
|---|---|---|---|
| 950 | 27.92 | 0.000818 | 3.329 |
| 950 | 28.12 | 0.000818 | 3.336 |
| 1250 | 71.28 | 0.000657 | 4.267 |
| 1150 | 56.26 | 0.000703 | 4.030 |
| 1150 | 56.44 | 0.000703 | 4.033 |
| 1050 | 41.34 | 0.000756 | 3.722 |
| 1050 | 41.53 | 0.000756 | 3.726 |

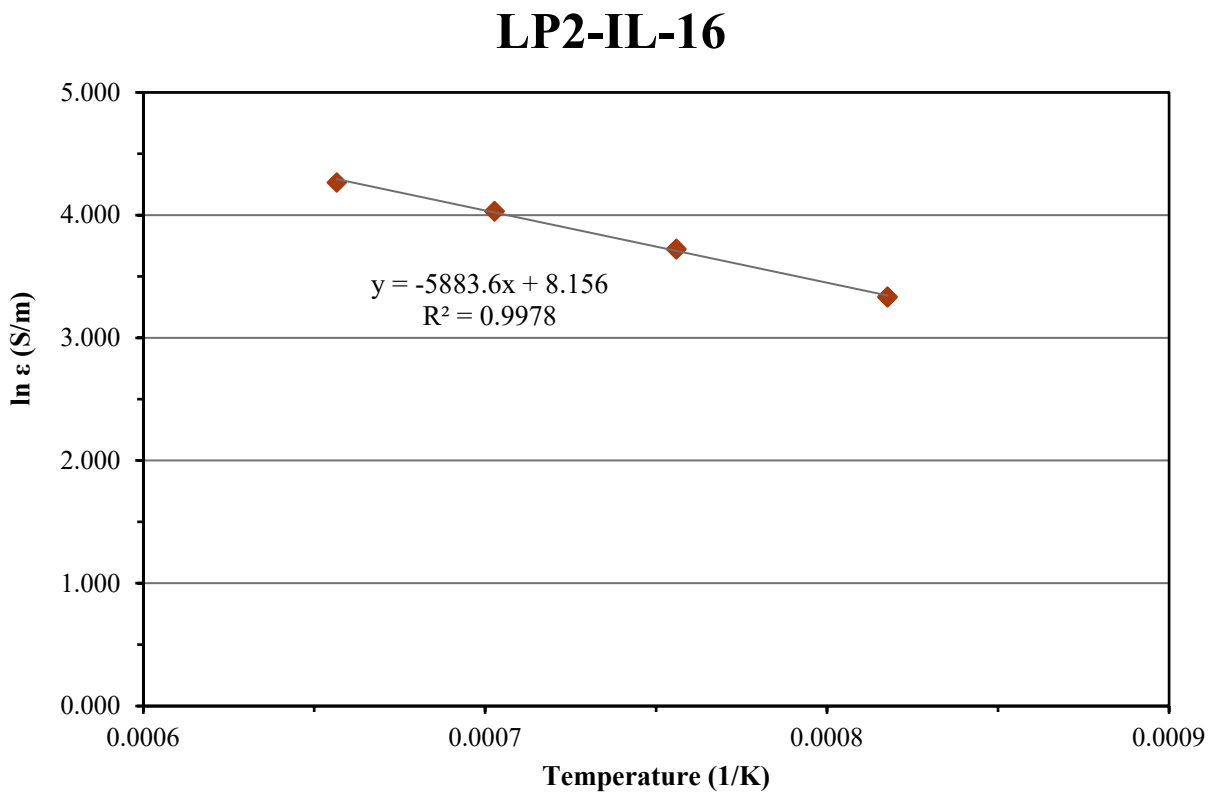


Figure D.16. Electrical Conductivity-Temperature Data and Arrhenius Equation Fit for Glass LP2-IL-16

## D.17 Glass LP2-IL-17 Electrical Conductivity Data

Table D.17. Electrical Conductivity Data for Glass LP2-IL-17

| Temperature, °C | Conductivity, S/m | 1/T, $K^{-1}$ | ln (ε, S/m) |
|---|---|---|---|
| 950 | 26.44 | 0.000818 | 3.275 |
| 950 | 26.74 | 0.000818 | 3.286 |
| 1250 | 63.45 | 0.000657 | 4.150 |
| 1250 | 63.35 | 0.000657 | 4.149 |
| 1150 | 51.45 | 0.000703 | 3.941 |
| 1150 | 51.58 | 0.000703 | 3.943 |
| 1050 | 38.74 | 0.000756 | 3.657 |
| 1050 | 38.95 | 0.000756 | 3.662 |

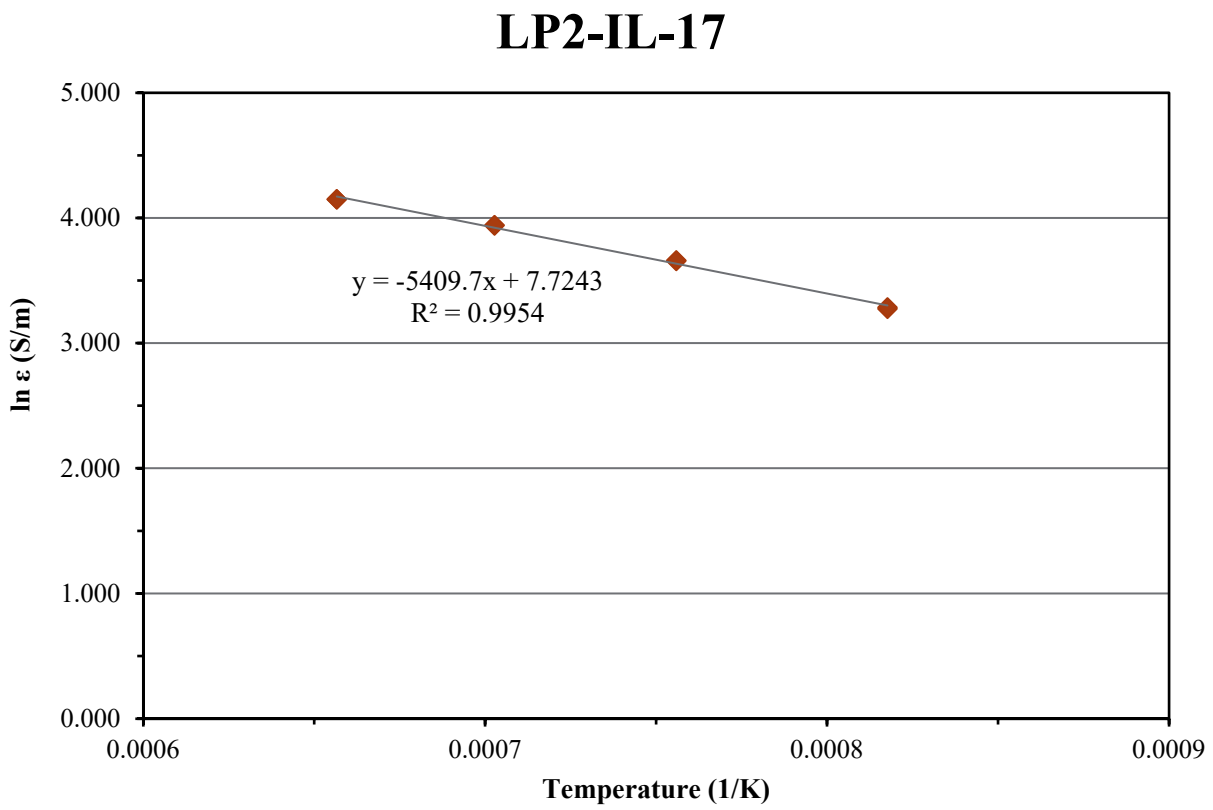


Figure D.17. Electrical Conductivity-Temperature Data and Arrhenius Equation Fit for Glass LP2-IL-17

## D.18 Glass LP2-OL-01-3 Electrical Conductivity Data

Table D.18. Electrical Conductivity Data for Glass LP2-OL-01-3

| Temperature, °C | Conductivity, S/m | 1/T, $K^{-1}$ | ln (ε, S/m) |
|---|---|---|---|
| 950 | 14.83 | 0.000818 | 2.697 |
| 950 | 14.96 | 0.000818 | 2.705 |
| 1250 | 44.00 | 0.000657 | 3.784 |
| 1250 | 44.01 | 0.000657 | 3.785 |
| 1150 | 33.44 | 0.000703 | 3.510 |
| 1150 | 33.52 | 0.000703 | 3.512 |
| 1050 | 23.48 | 0.000756 | 3.156 |
| 1050 | 23.57 | 0.000756 | 3.160 |

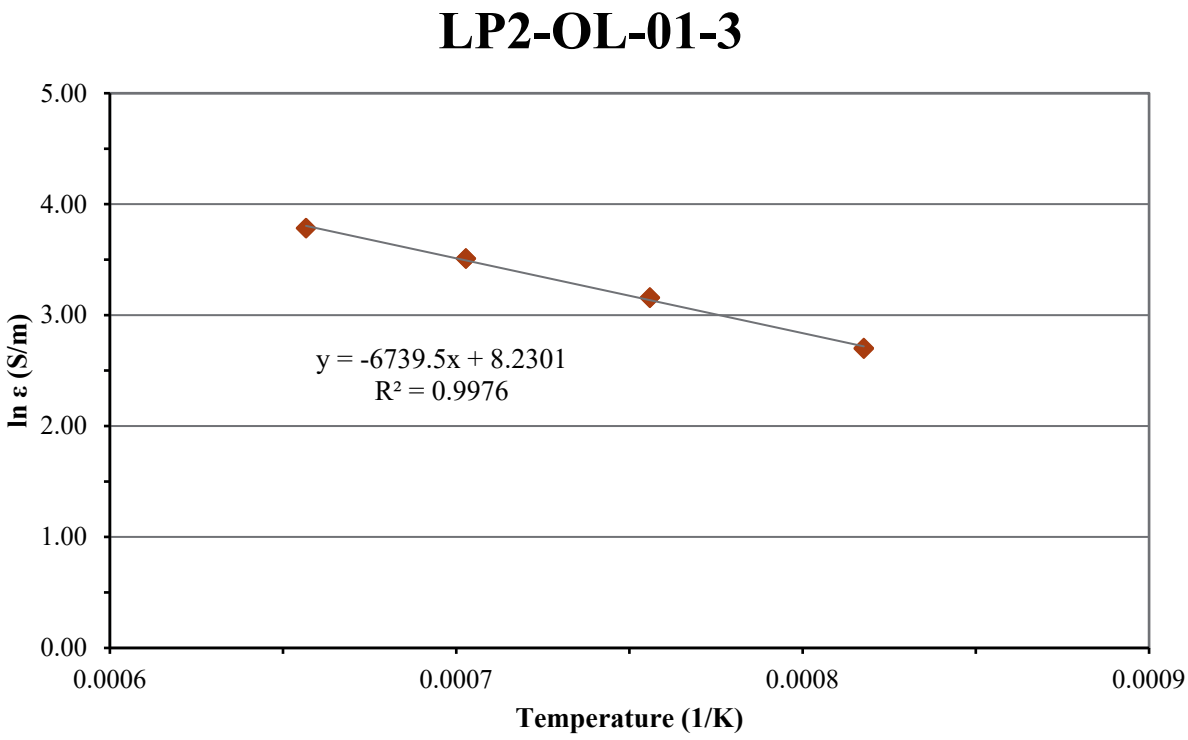


Figure D.18. Electrical Conductivity-Temperature Data and Arrhenius Equation Fit for Glass LP2-OL-01-3

## D.19 Glass LP2-OL-02-1 Electrical Conductivity Data

Table D.19. Electrical Conductivity Data for Glass LP2-OL-02-1

| Temperature, °C | Conductivity, S/m | 1/T, $K^{-1}$ | ln (ε, S/m) |
|---|---|---|---|
| 950 | 23.45 | 0.000818 | 3.155 |
| 950 | 23.59 | 0.000818 | 3.161 |
| 1250 | 57.98 | 0.000657 | 4.060 |
| 1250 | 57.83 | 0.000657 | 4.058 |
| 1150 | 46.24 | 0.000703 | 3.834 |
| 1150 | 46.41 | 0.000703 | 3.838 |
| 1050 | 34.37 | 0.000756 | 3.537 |
| 1050 | 34.50 | 0.000756 | 3.541 |

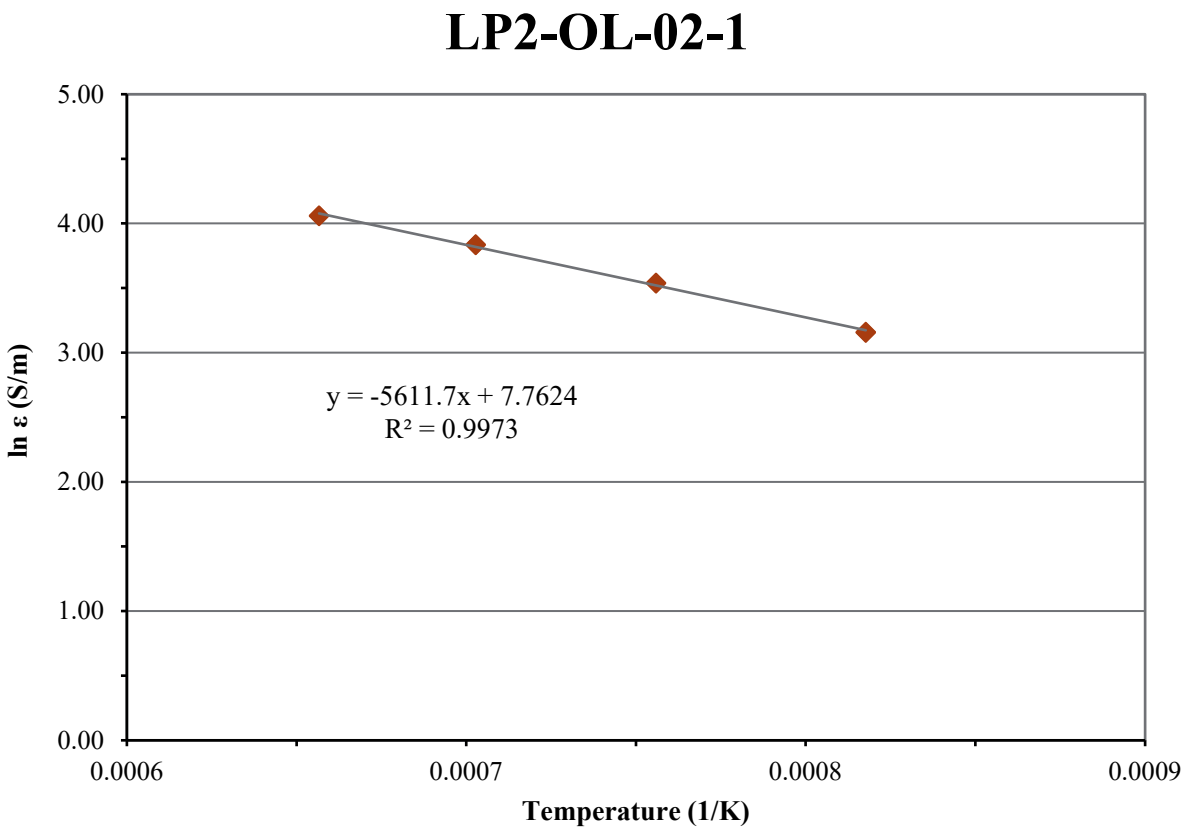


Figure D.19. Electrical Conductivity-Temperature Data and Arrhenius Equation Fit for Glass LP2-OL-02-1

## D.20 Glass LP2-OL-03 MOD2 Electrical Conductivity Data

Table D.20. Electrical Conductivity Data for Glass LP2-OL-03 MOD2

| Temperature, °C | Conductivity, S/m | 1/T, $K^{-1}$ | ln (ε, S/m) |
|---|---|---|---|
| 950 | 31.38 | 0.000818 | 3.446 |
| 950 | 31.62 | 0.000818 | 3.454 |
| 1250 | 75.08 | 0.000657 | 4.319 |
| 1150 | 60.88 | 0.000703 | 4.109 |
| 1150 | 61.02 | 0.000703 | 4.111 |
| 1050 | 45.59 | 0.000756 | 3.820 |
| 1050 | 45.77 | 0.000756 | 3.824 |

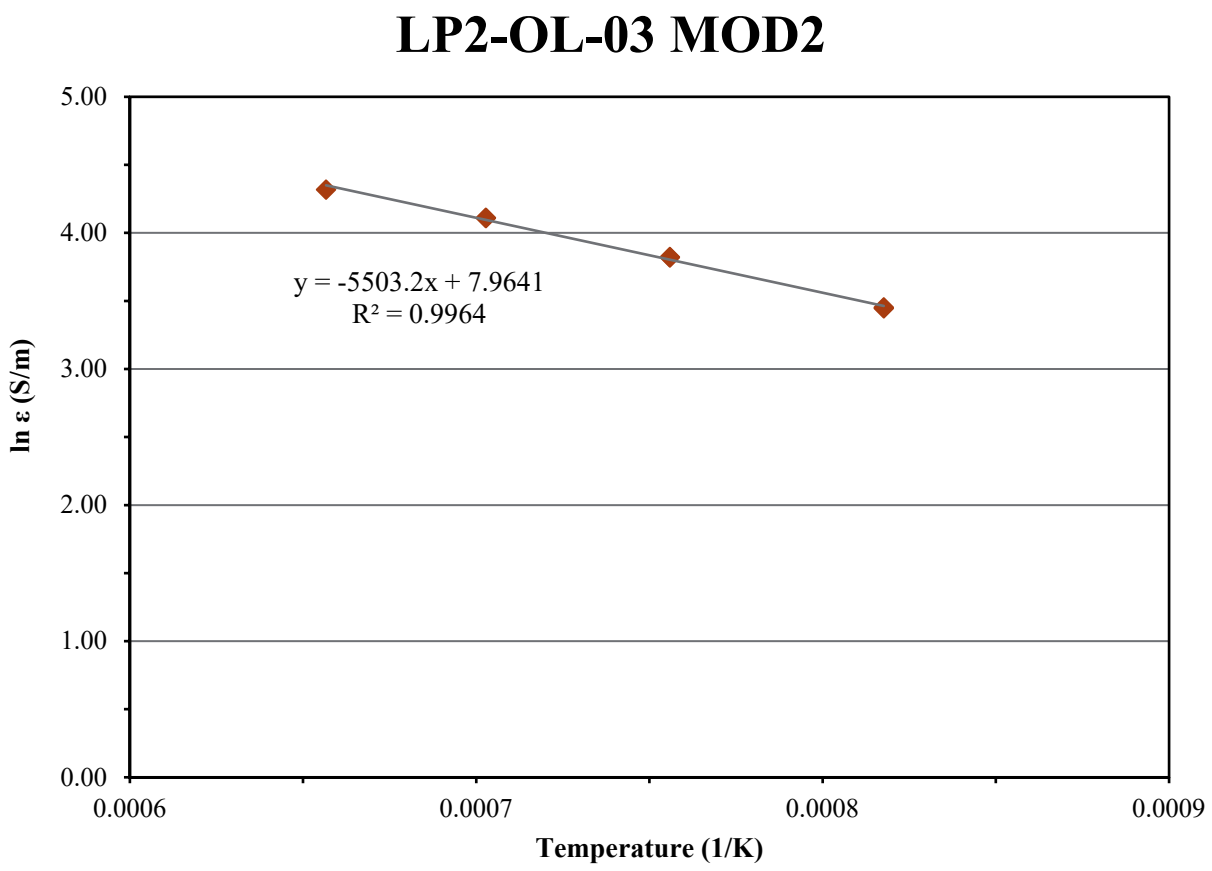


Figure D.20. Electrical Conductivity-Temperature Data and Arrhenius Equation Fit for Glass LP2-OL-03 MOD2

## D.21 Glass LP2-OL-04-1 Electrical Conductivity Data

Table D.21. Electrical Conductivity Data for Glass LP2-OL-04-1

| Temperature, °C | Conductivity, S/m | 1/T, $K^{-1}$ | ln (ε, S/m) |
|---|---|---|---|
| 950 | 19.23 | 0.000818 | 2.956 |
| 950 | 19.40 | 0.000818 | 2.965 |
| 1250 | 54.31 | 0.000657 | 3.995 |
| 1150 | 42.44 | 0.000703 | 3.748 |
| 1150 | 42.53 | 0.000703 | 3.750 |
| 1050 | 30.20 | 0.000756 | 3.408 |
| 1050 | 30.34 | 0.000756 | 3.413 |

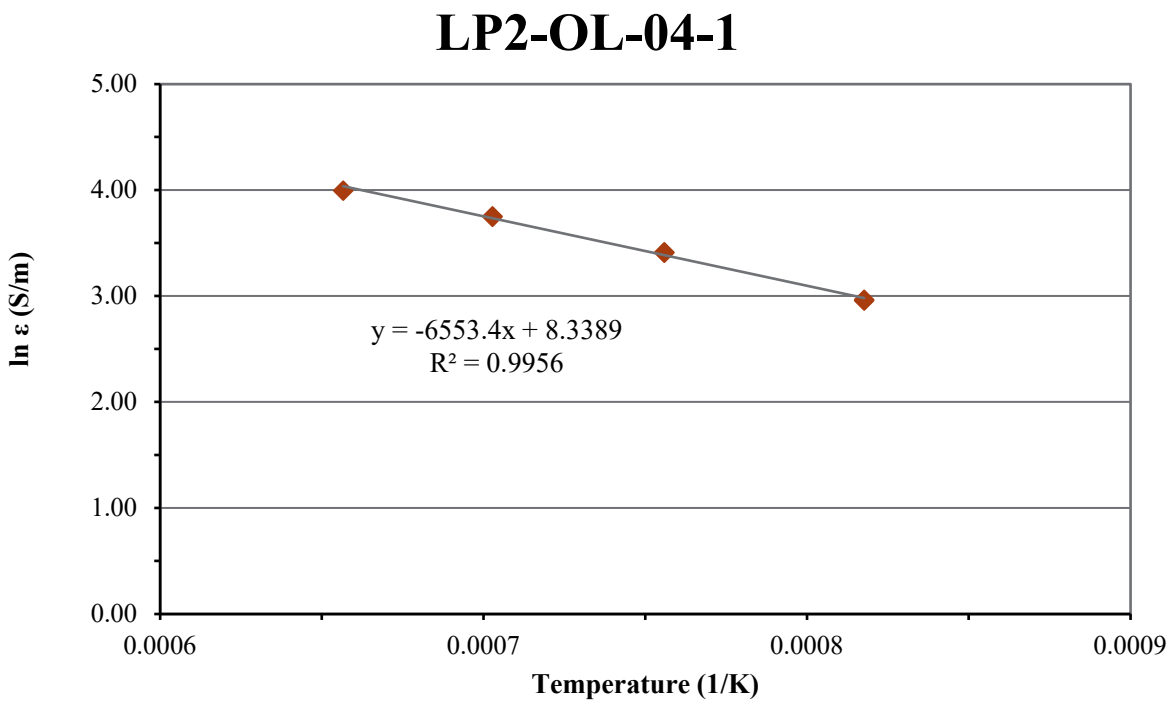


Figure D.21. Electrical Conductivity-Temperature Data and Arrhenius Equation Fit for Glass LP2-OL-04-1

## D.22 Glass LP2-OL-05 Electrical Conductivity Data

Table D.22. Electrical Conductivity Data for Glass LP2-OL-05

| Temperature, °C | Conductivity, S/m | 1/T, $K^{-1}$ | ln (ε, S/m) |
|---|---|---|---|
| 950 | 16.27 | 0.000818 | 2.789 |
| 950 | 16.40 | 0.000818 | 2.797 |
| 1250 | 46.29 | 0.000657 | 3.835 |
| 1250 | 46.13 | 0.000657 | 3.832 |
| 1150 | 35.81 | 0.000703 | 3.578 |
| 1150 | 35.90 | 0.000703 | 3.581 |
| 1050 | 25.42 | 0.000756 | 3.236 |
| 1050 | 25.55 | 0.000756 | 3.241 |

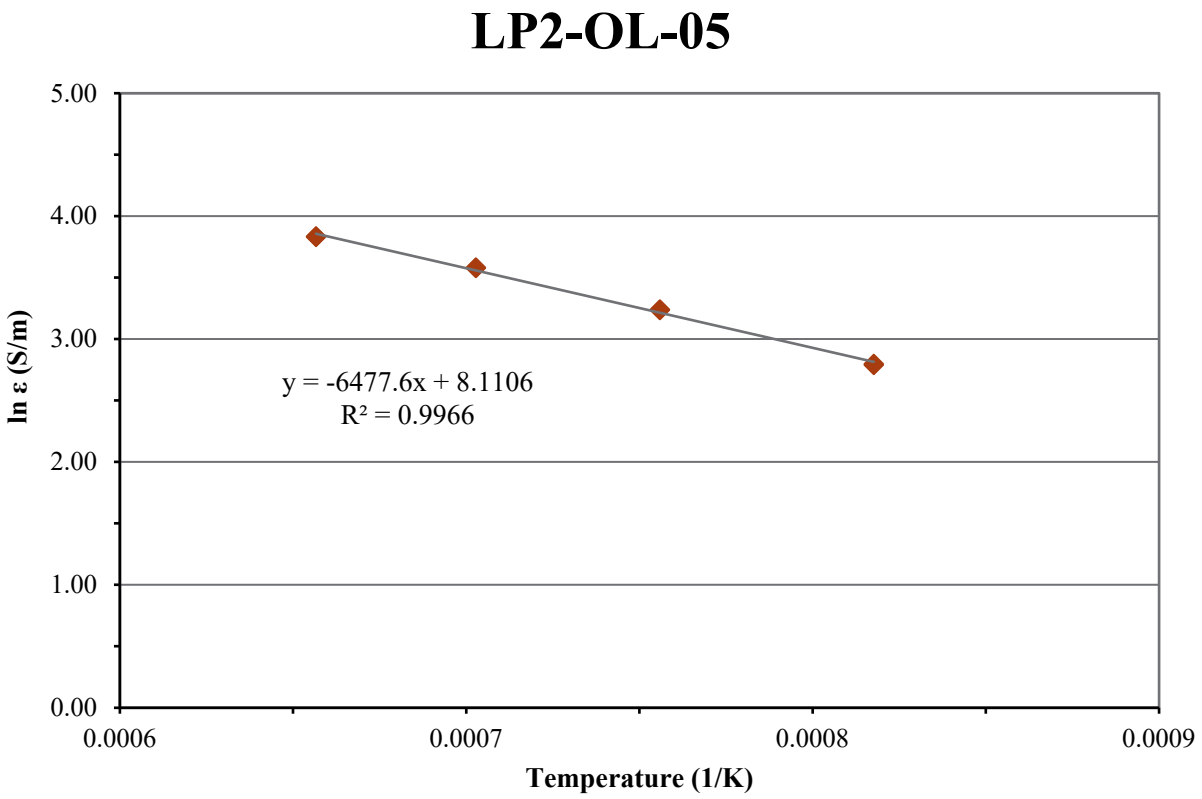


Figure D.22. Electrical Conductivity-Temperature Data and Arrhenius Equation Fit for Glass LP2-OL-05

## D.23 Glass LP2-OL-07-1 Electrical Conductivity Data

Table D.23. Electrical Conductivity Data for Glass LP2-OL-07-1

| Temperature, °C | Conductivity, S/m | 1/T, $K^{-1}$ | ln (ε, S/m) |
|---|---|---|---|
| 950 | 17.50 | 0.000818 | 2.862 |
| 950 | 17.64 | 0.000818 | 2.870 |
| 1250 | 48.69 | 0.000657 | 3.885 |
| 1150 | 37.82 | 0.000703 | 3.633 |
| 1150 | 37.84 | 0.000703 | 3.633 |
| 1050 | 27.05 | 0.000756 | 3.298 |
| 1050 | 27.17 | 0.000756 | 3.302 |

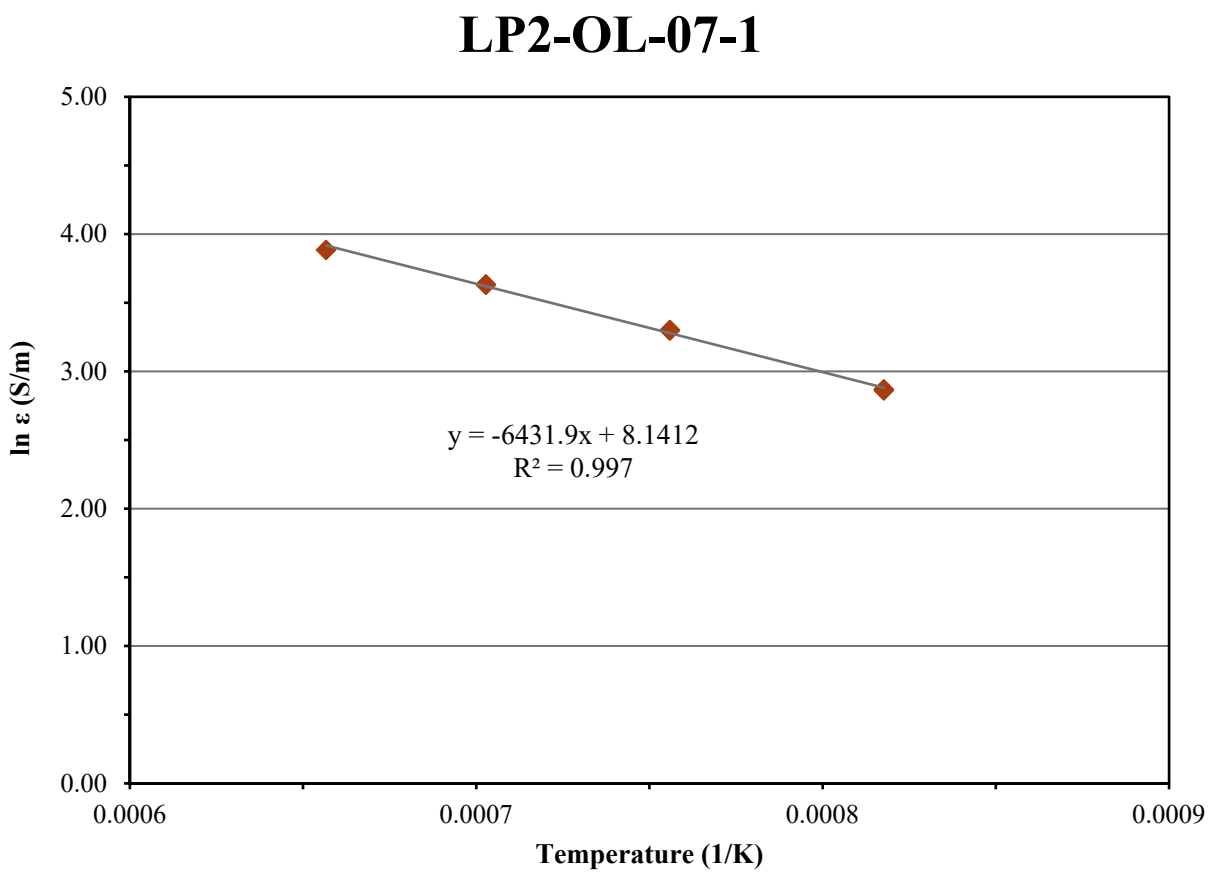


Figure D.23. Electrical Conductivity-Temperature Data and Arrhenius Equation Fit for Glass LP2-OL-07-1

## D.24 Glass LP2-OL-08 MOD Electrical Conductivity Data

Table D.24. Electrical Conductivity Data for Glass LP2-OL-08 MOD

| Temperature, °C | Conductivity, S/m | 1/T, $K^{-1}$ | ln (ε, S/m) |
|---|---|---|---|
| 950 | 36.85 | 0.000818 | 3.607 |
| 950 | 37.08 | 0.000818 | 3.613 |
| 1250 | 80.67 | 0.000657 | 4.390 |
| 1150 | 65.99 | 0.000703 | 4.189 |
| 1150 | 66.09 | 0.000703 | 4.191 |
| 1050 | 51.18 | 0.000756 | 3.935 |
| 1050 | 51.28 | 0.000756 | 3.937 |

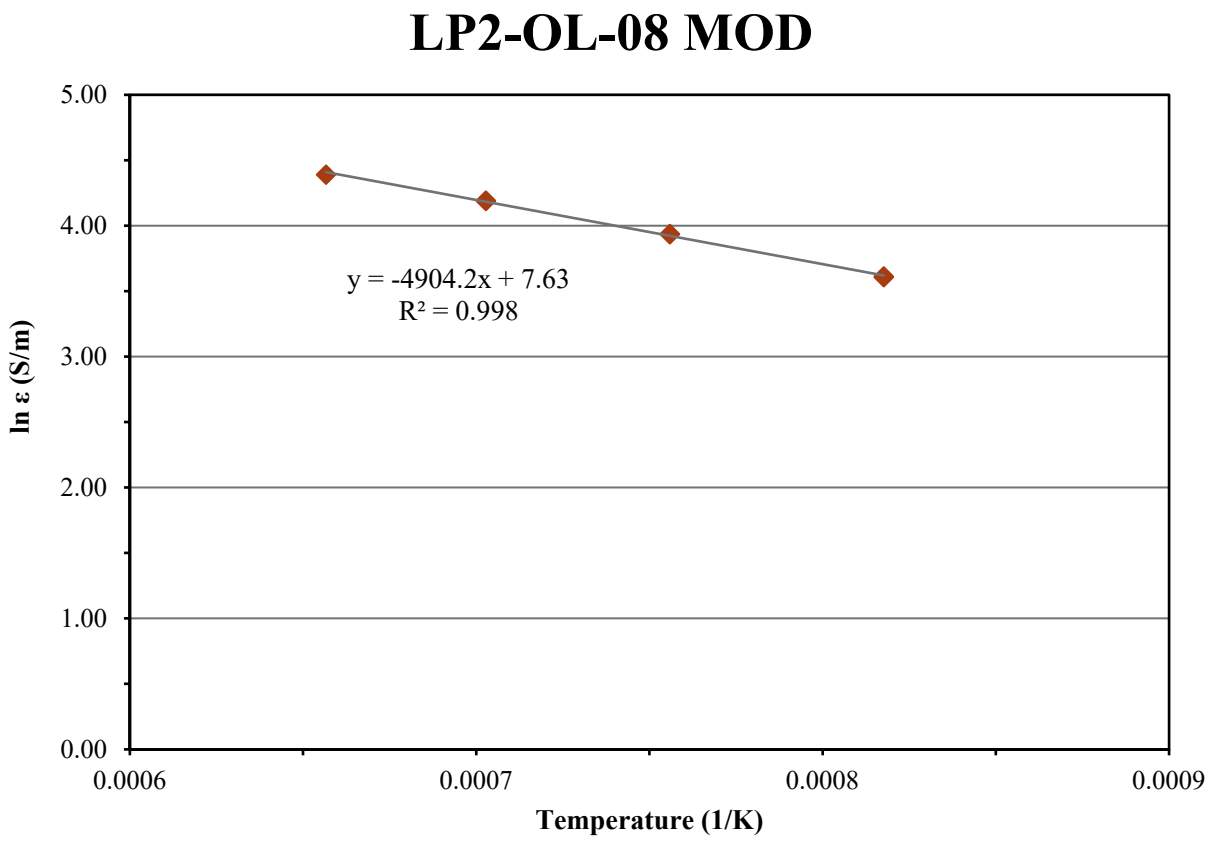


Figure D.24. Electrical Conductivity-Temperature Data and Arrhenius Equation Fit for Glass LP2-OL-08 MOD

## D.25 Glass LP2-OL-09-1 Electrical Conductivity Data

Table D.25. Electrical Conductivity Data for Glass LP2-OL-09-1

| Temperature, °C | Conductivity, S/m | 1/T, $K^{-1}$ | ln (ε, S/m) |
|---|---|---|---|
| 950 | 19.36 | 0.000818 | 2.963 |
| 950 | 19.49 | 0.000818 | 2.970 |
| 1250 | 49.63 | 0.000657 | 3.905 |
| 1250 | 49.52 | 0.000657 | 3.902 |
| 1150 | 39.48 | 0.000703 | 3.676 |
| 1150 | 39.56 | 0.000703 | 3.678 |
| 1050 | 28.89 | 0.000756 | 3.364 |
| 1050 | 29.01 | 0.000756 | 3.368 |

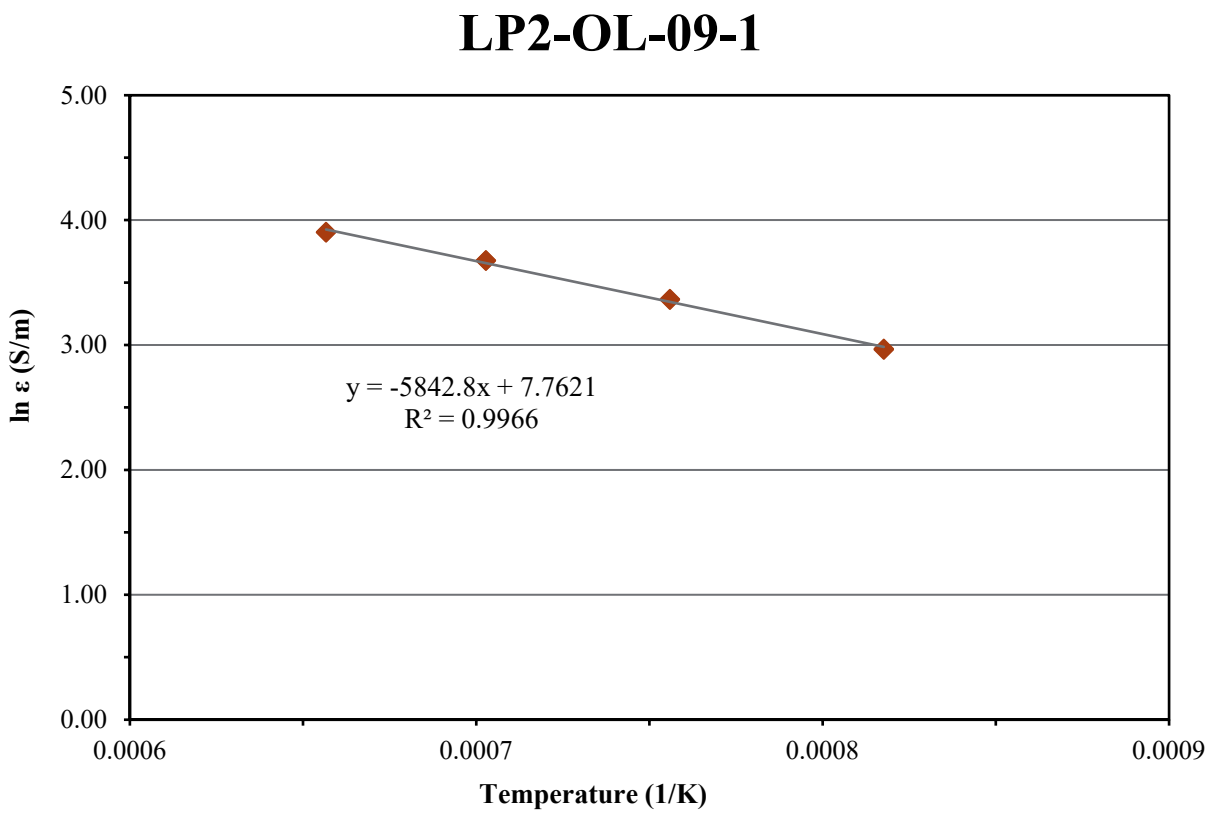


Figure D.25. Electrical Conductivity-Temperature Data and Arrhenius Equation Fit for Glass LP2-OL-09-1

## D.26 Glass LP2-OL-10 MOD Electrical Conductivity Data

Table D.26. Electrical Conductivity Data for Glass LP2-OL-10 MOD

| Temperature, °C | Conductivity, S/m | 1/T, $K^{-1}$ | ln (ε, S/m) |
|---|---|---|---|
| 950 | 17.28 | 0.000818 | 2.850 |
| 950 | 17.43 | 0.000818 | 2.858 |
| 1250 | 47.47 | 0.000657 | 3.860 |
| 1150 | 36.95 | 0.000703 | 3.610 |
| 1150 | 37.05 | 0.000703 | 3.612 |
| 1050 | 26.60 | 0.000756 | 3.281 |
| 1050 | 26.72 | 0.000756 | 3.285 |

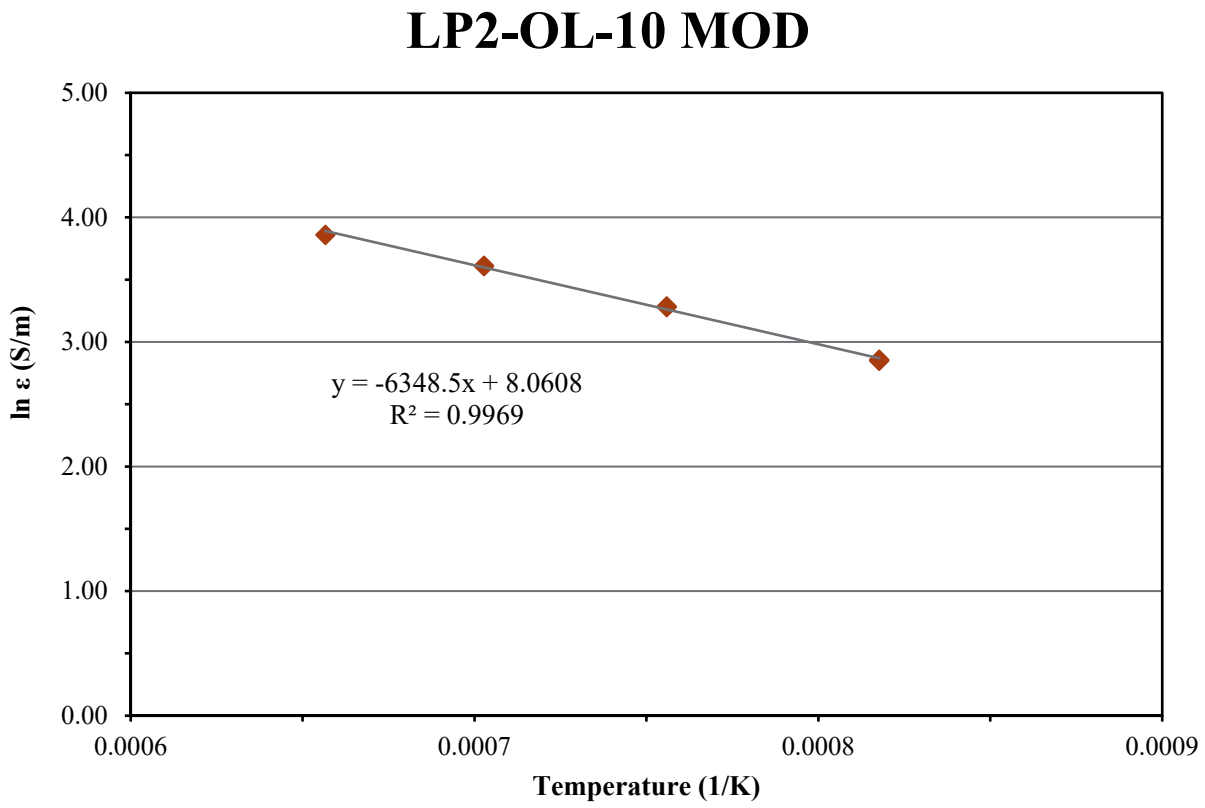


Figure D.26. Electrical Conductivity-Temperature Data and Arrhenius Equation Fit for Glass LP2-OL-10 MOD

## D.27 Glass LP2-OL-11 Electrical Conductivity Data

Table D.27. Electrical Conductivity Data for Glass LP2-OL-11

| Temperature, °C | Conductivity, S/m | 1/T, $K^{-1}$ | ln (ε, S/m) |
|---|---|---|---|
| 950 | 23.42 | 0.000818 | 3.154 |
| 950 | 23.58 | 0.000818 | 3.161 |
| 1250 | 61.58 | 0.000657 | 4.120 |
| 1150 | 48.62 | 0.000703 | 3.884 |
| 1150 | 48.77 | 0.000703 | 3.887 |
| 1050 | 35.57 | 0.000756 | 3.571 |
| 1050 | 35.70 | 0.000756 | 3.575 |

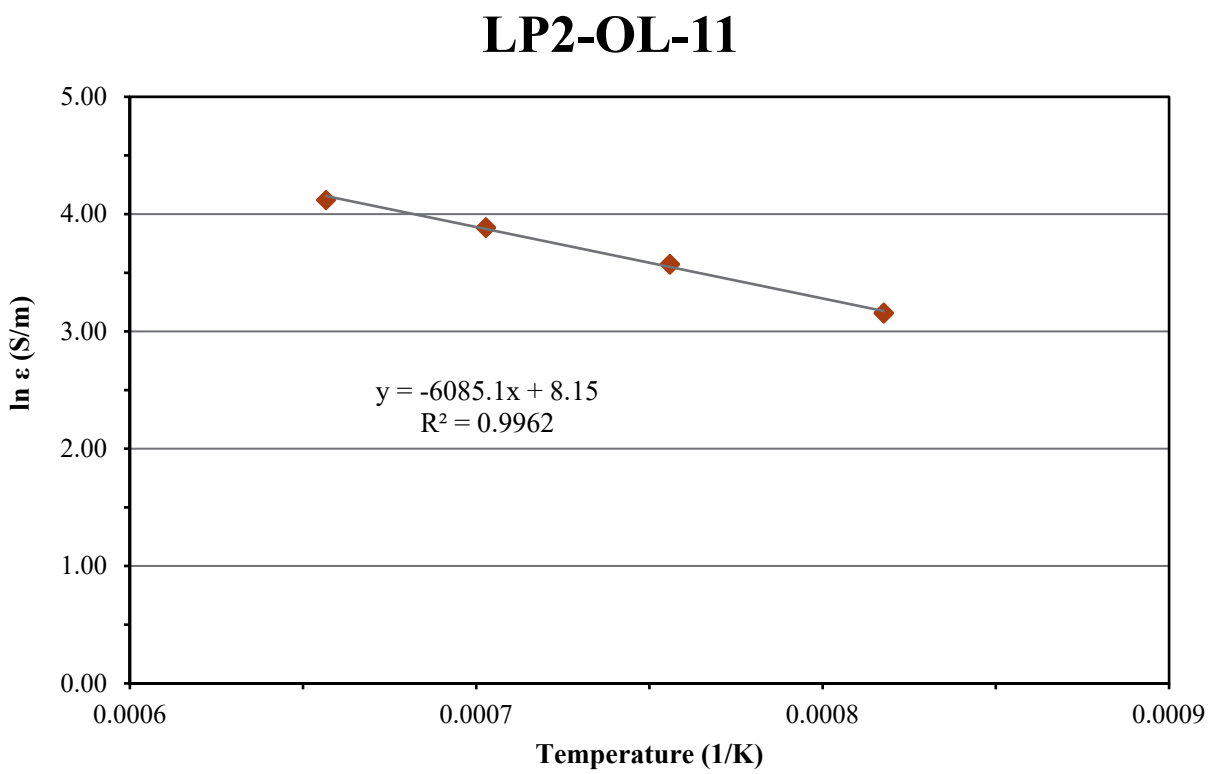


Figure D.27. Electrical Conductivity-Temperature Data and Arrhenius Equation Fit for Glass LP2-OL-11

## D.28 Glass LP2-OL-12 Electrical Conductivity Data

Table D.28. Electrical Conductivity Data for Glass LP2-OL-12

| Temperature, °C | Conductivity, S/m | 1/T, $K^{-1}$ | ln (ε, S/m) |
|---|---|---|---|
| 950 | 32.16 | 0.000818 | 3.471 |
| 950 | 32.33 | 0.000818 | 3.476 |
| 1250 | 74.87 | 0.000657 | 4.316 |
| 1150 | 60.44 | 0.000703 | 4.102 |
| 1150 | 60.68 | 0.000703 | 4.106 |
| 1050 | 45.87 | 0.000756 | 3.826 |
| 1050 | 46.09 | 0.000756 | 3.831 |

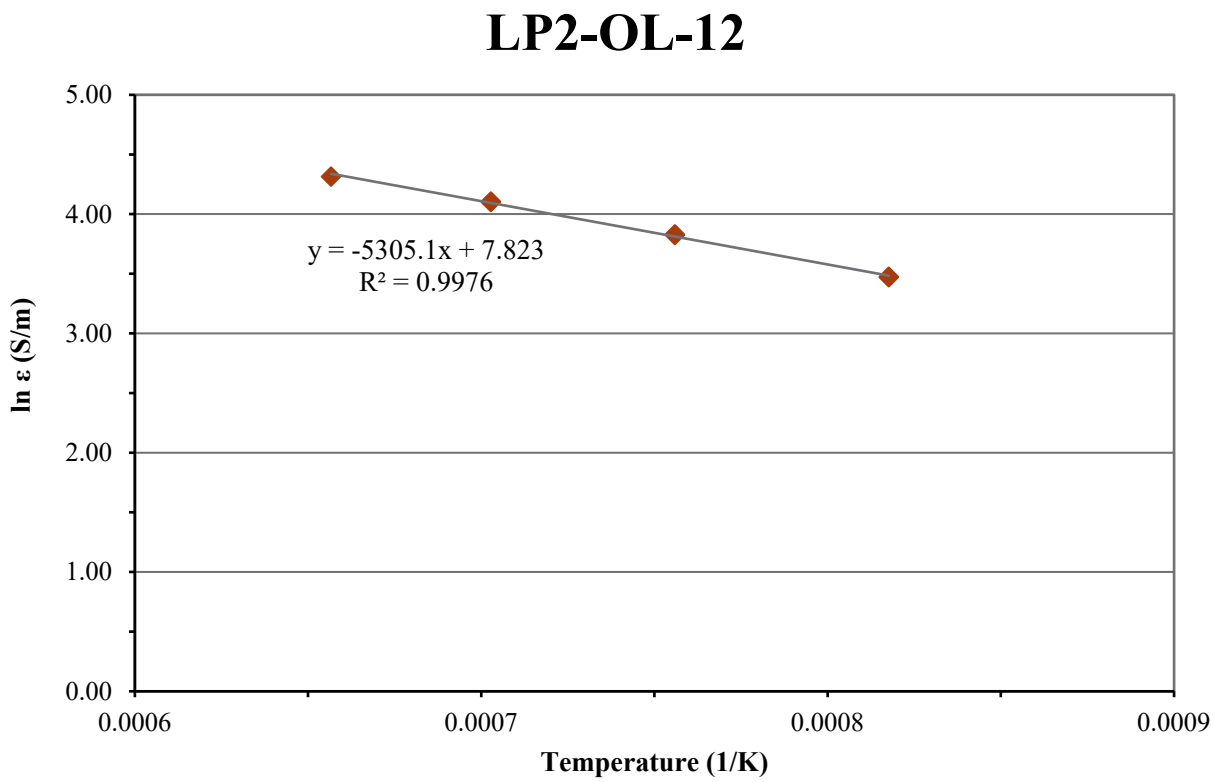


Figure D.28. Electrical Conductivity-Temperature Data and Arrhenius Equation Fit for Glass LP2-OL-12

## D.29 Glass LP2-OL-13 Electrical Conductivity Data

Table D.29. Electrical Conductivity Data for Glass LP2-OL-13

| Temperature, °C | Conductivity, S/m | 1/T, $K^{-1}$ | ln (ε, S/m) |
|---|---|---|---|
| 950 | 29.13 | 0.000818 | 3.372 |
| 950 | 29.43 | 0.000818 | 3.382 |
| 1250 | 69.77 | 0.000657 | 4.245 |
| 1250 | 69.52 | 0.000657 | 4.242 |
| 1150 | 56.89 | 0.000703 | 4.041 |
| 1150 | 57.02 | 0.000703 | 4.043 |
| 1050 | 42.86 | 0.000756 | 3.758 |
| 1050 | 43.01 | 0.000756 | 3.762 |

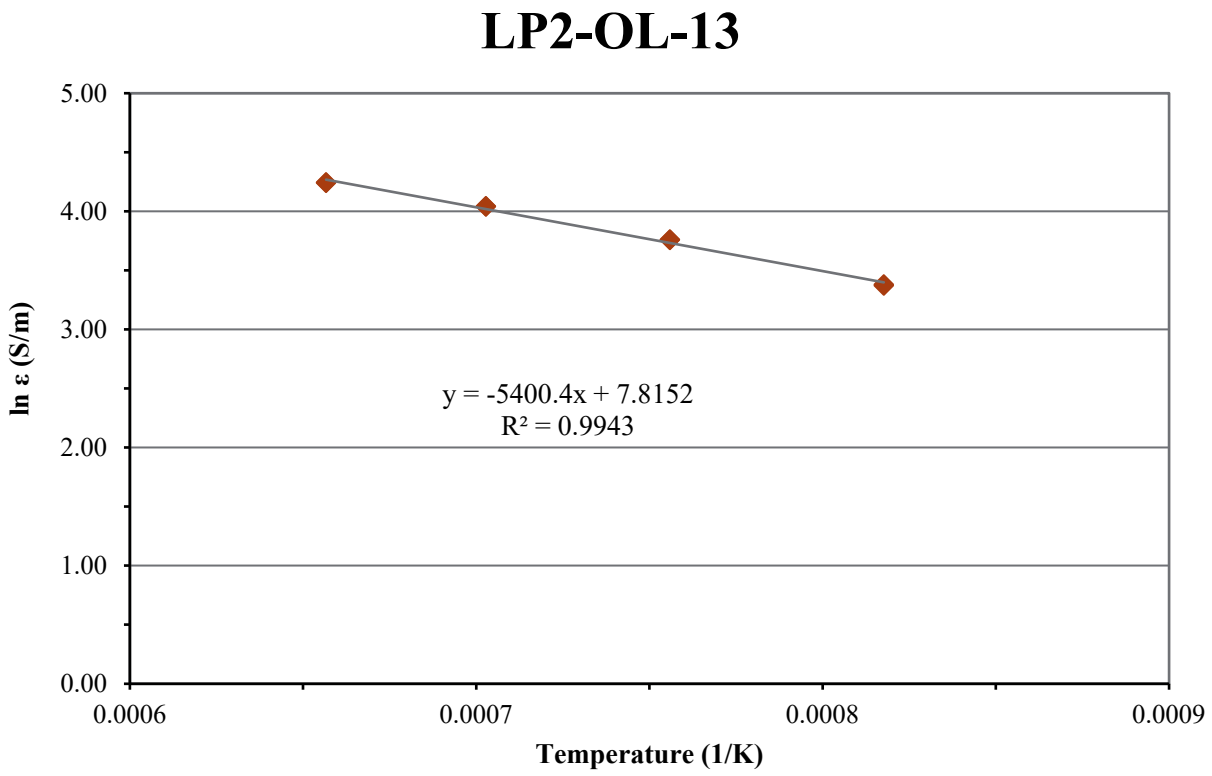


Figure D.29. Electrical Conductivity-Temperature Data and Arrhenius Equation Fit for Glass LP2-OL-13

## D.30 Glass LP2-OL-14 Electrical Conductivity Data

Table D.30. Electrical Conductivity Data for Glass LP2-OL-14

| Temperature, °C | Conductivity, S/m | 1/T, $K^{-1}$ | ln (ε, S/m) |
|---|---|---|---|
| 950 | 25.46 | 0.000818 | 3.237 |
| 950 | 25.64 | 0.000818 | 3.244 |
| 1250 | 64.31 | 0.000657 | 4.164 |
| 1250 | 64.06 | 0.000657 | 4.160 |
| 1150 | 51.32 | 0.000703 | 3.938 |
| 1050 | 37.98 | 0.000756 | 3.637 |
| 1050 | 38.18 | 0.000756 | 3.642 |

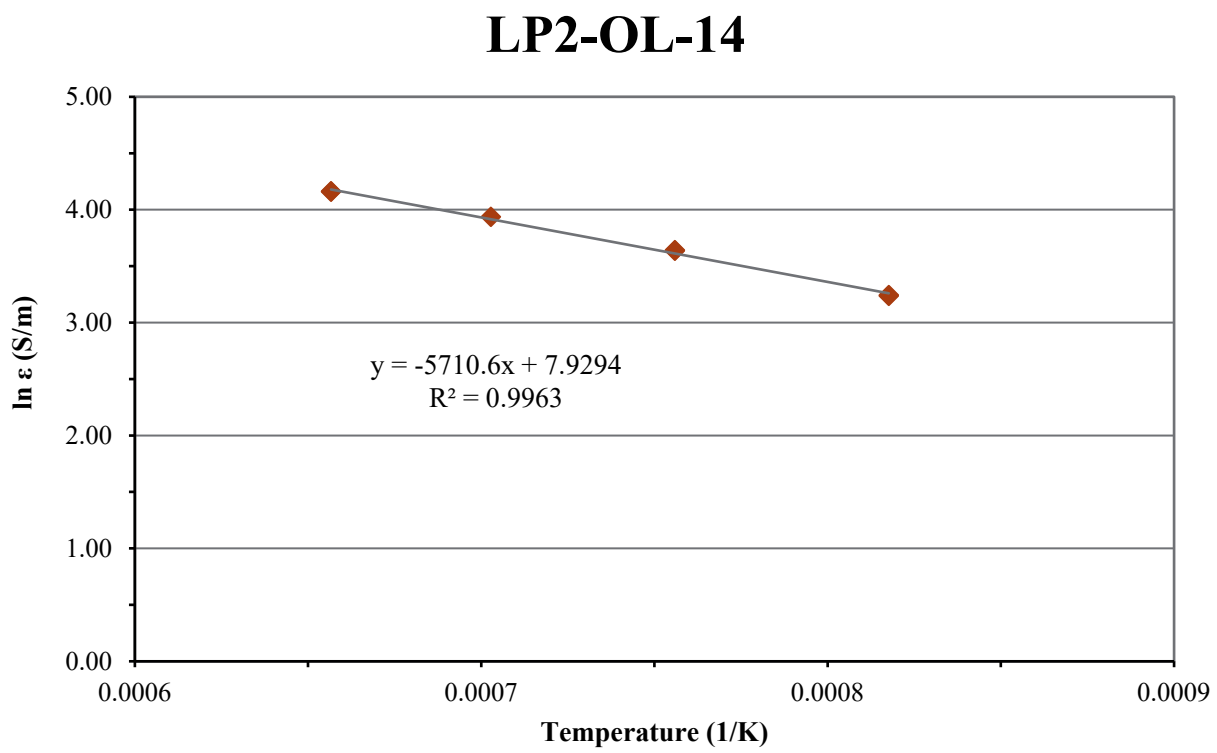


Figure D.30. Electrical Conductivity-Temperature Data and Arrhenius Equation Fit for Glass LP2-OL-14

## D.31 Glass LP2-OL-15 Electrical Conductivity Data

Table D.31. Electrical Conductivity Data for Glass LP2-OL-15

| Temperature, °C | Conductivity, S/m | 1/T, $K^{-1}$ | ln (ε, S/m) |
|---|---|---|---|
| 950 | 16.36 | 0.000818 | 2.795 |
| 950 | 16.52 | 0.000818 | 2.804 |
| 1250 | 53.12 | 0.000657 | 3.973 |
| 1250 | 52.90 | 0.000657 | 3.968 |
| 1150 | 39.76 | 0.000703 | 3.683 |
| 1150 | 39.88 | 0.000703 | 3.686 |
| 1050 | 27.04 | 0.000756 | 3.297 |
| 1050 | 27.20 | 0.000756 | 3.303 |

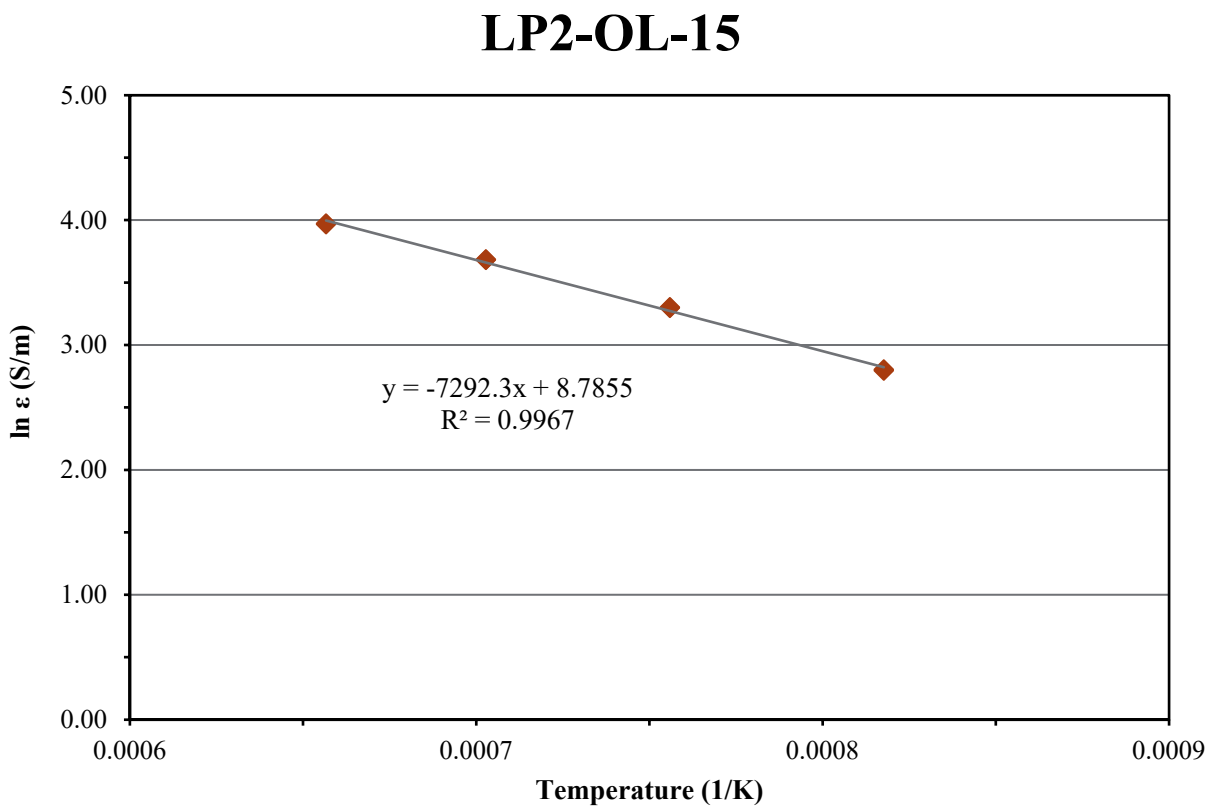


Figure D.31. Electrical Conductivity-Temperature Data and Arrhenius Equation Fit for Glass LP2-OL-15

## D.32 Glass LP2-OL-16 MOD Electrical Conductivity Data

Table D.32. Electrical Conductivity Data for Glass LP2-OL-16 MOD

| Temperature, °C | Conductivity, S/m | 1/T, $K^{-1}$ | ln (ε, S/m) |
|---|---|---|---|
| 950 | 21.94 | 0.000818 | 3.088 |
| 950 | 22.10 | 0.000818 | 3.096 |
| 1250 | 52.45 | 0.000657 | 3.960 |
| 1150 | 42.11 | 0.000703 | 3.740 |
| 1150 | 42.05 | 0.000703 | 3.739 |
| 1050 | 31.69 | 0.000756 | 3.456 |
| 1050 | 31.84 | 0.000756 | 3.461 |

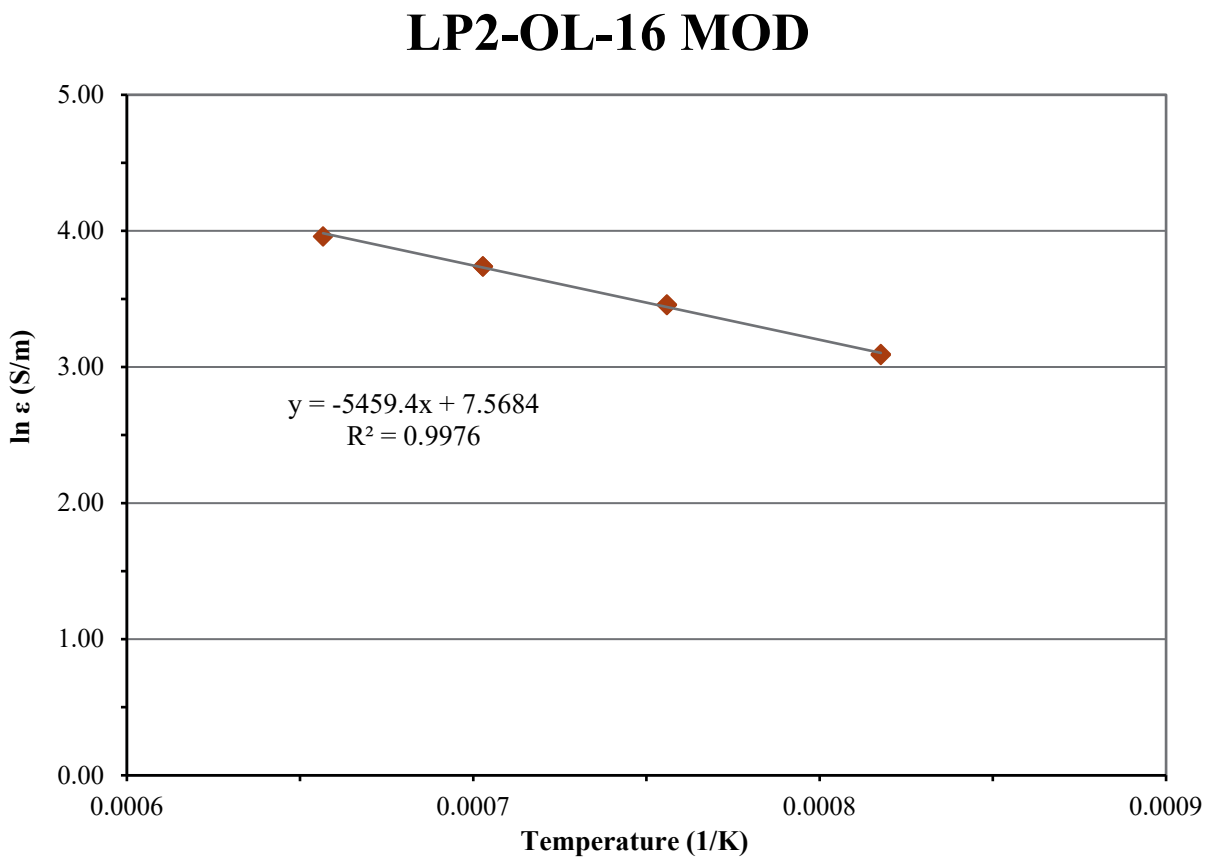


Figure D.32. Electrical Conductivity-Temperature Data and Arrhenius Equation Fit for Glass LP2-OL-16 MOD

## D.33 Glass LP2-OL-17 Electrical Conductivity Data

Table D.33. Electrical Conductivity Data for Glass LP2-OL-17

| Temperature, °C | Conductivity, S/m | 1/T, $K^{-1}$ | ln (ε, S/m) |
|---|---|---|---|
| 950 | 29.46 | 0.000818 | 3.383 |
| 950 | 29.65 | 0.000818 | 3.389 |
| 1250 | 70.24 | 0.000657 | 4.252 |
| 1150 | 56.52 | 0.000703 | 4.035 |
| 1050 | 42.63 | 0.000756 | 3.752 |
| 1050 | 42.74 | 0.000756 | 3.755 |

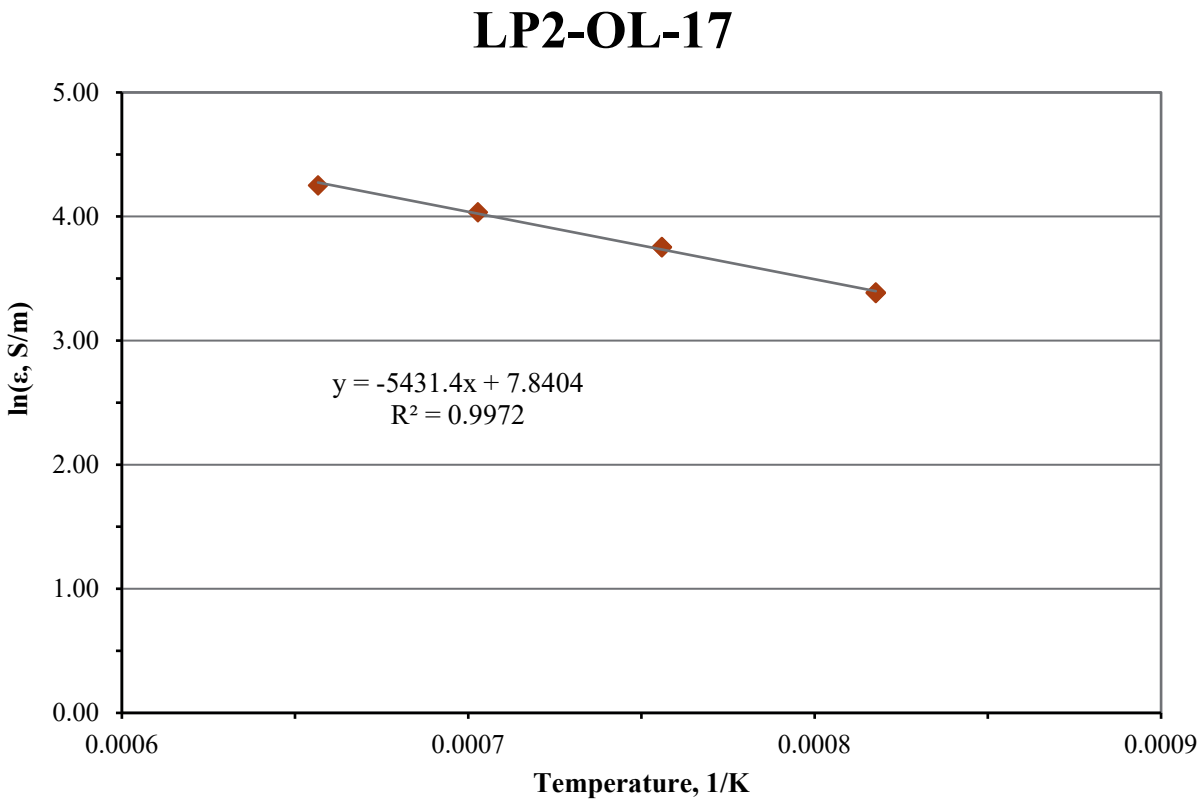


Figure D.33. Electrical Conductivity-Temperature Data and Arrhenius Equation Fit for Glass LP2-OL-17

## D.34 Glass LP2-OL-18 Electrical Conductivity Data

Table D.34. Electrical Conductivity Data for Glass LP2-OL-18

| Temperature, °C | Conductivity, S/m | 1/T, $K^{-1}$ | ln (ε, S/m) |
|---|---|---|---|
| 950 | 19.86 | 0.000818 | 2.989 |
| 950 | 19.99 | 0.000818 | 2.995 |
| 1250 | 56.39 | 0.000657 | 4.032 |
| 1150 | 43.40 | 0.000703 | 3.770 |
| 1150 | 43.60 | 0.000703 | 3.775 |
| 1050 | 30.72 | 0.000756 | 3.425 |
| 1050 | 30.84 | 0.000756 | 3.429 |

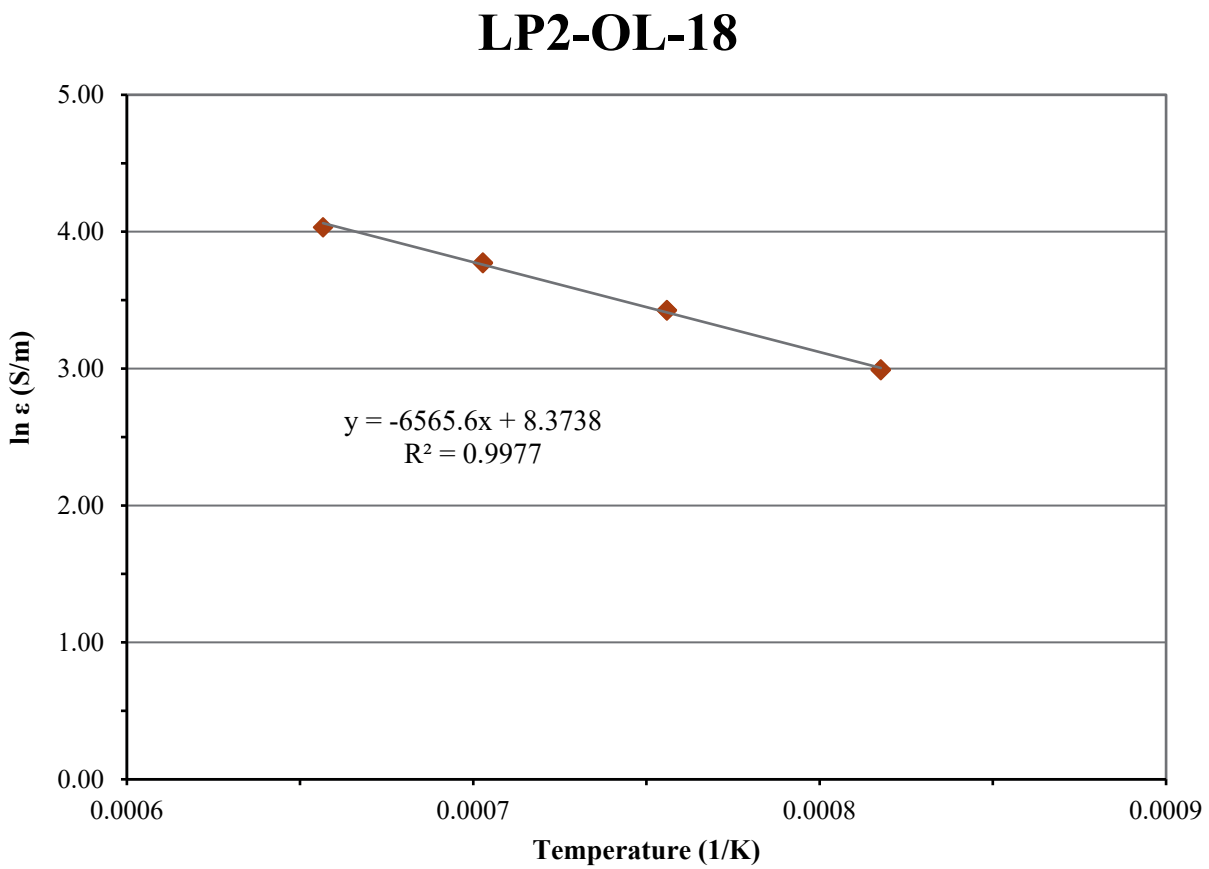


Figure D.34. Electrical Conductivity-Temperature Data and Arrhenius Equation Fit for Glass LP2-OL-18

## D.35 Glass LP2-OL-19 Electrical Conductivity Data

Table D.35. Electrical Conductivity Data for Glass LP2-OL-19

| Temperature, °C | Conductivity, S/m | 1/T, $K^{-1}$ | ln (ε, S/m) |
|---|---|---|---|
| 950 | 21.75 | 0.000818 | 3.080 |
| 950 | 21.89 | 0.000818 | 3.086 |
| 1250 | 57.18 | 0.000657 | 4.046 |
| 1250 | 57.16 | 0.000657 | 4.046 |
| 1150 | 45.11 | 0.000703 | 3.809 |
| 1150 | 45.25 | 0.000703 | 3.812 |
| 1050 | 32.79 | 0.000756 | 3.490 |
| 1050 | 32.91 | 0.000756 | 3.494 |

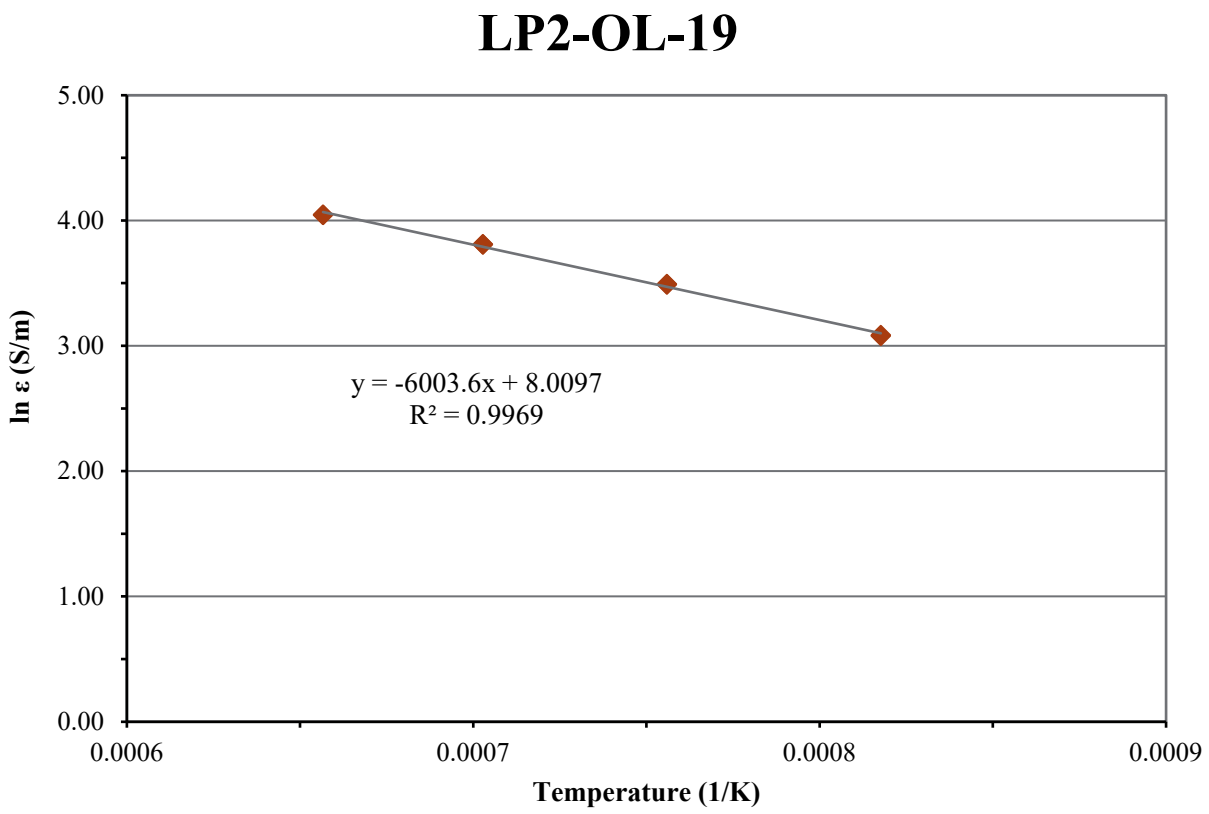


Figure D.35. Electrical Conductivity-Temperature Data and Arrhenius Equation Fit for Glass LP2-OL-19

## D.36 Glass LP2-OL-20 Electrical Conductivity Data

Table D.36. Electrical Conductivity Data for Glass LP2-OL-20

| Temperature, °C | Conductivity, S/m | 1/T, $K^{-1}$ | ln (ε, S/m) |
|---|---|---|---|
| 950 | 29.06 | 0.000818 | 3.369 |
| 950 | 29.23 | 0.000818 | 3.375 |
| 1250 | 66.15 | 0.000657 | 4.192 |
| 1250 | 65.95 | 0.000657 | 4.189 |
| 1150 | 54.17 | 0.000703 | 3.992 |
| 1150 | 54.30 | 0.000703 | 3.994 |
| 1050 | 41.49 | 0.000756 | 3.725 |
| 1050 | 41.61 | 0.000756 | 3.728 |

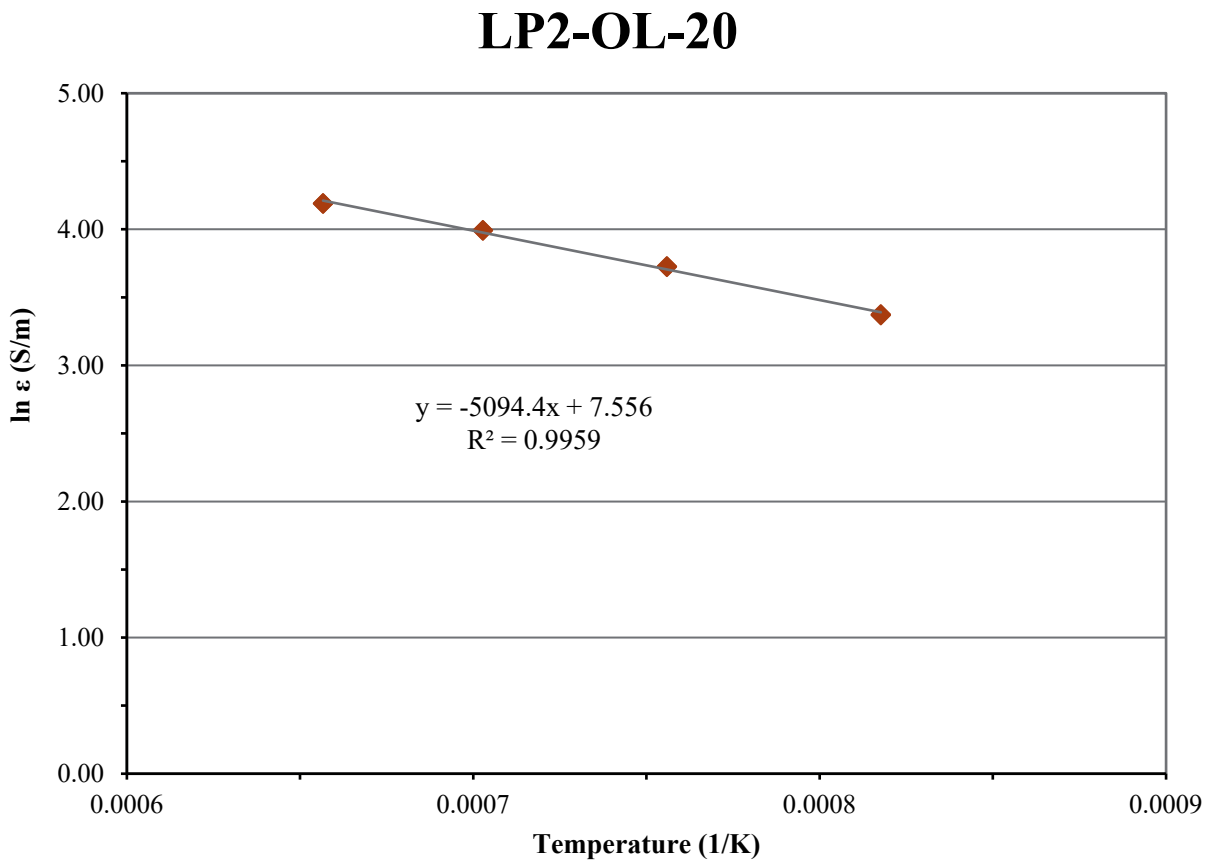


Figure D.36. Electrical Conductivity-Temperature Data and Arrhenius Equation Fit for Glass LP2-OL-20

## D.37 Glass LP2-OL-21 Electrical Conductivity Data

Table D.37. Electrical Conductivity Data for Glass LP2-OL-21

| Temperature, °C | Conductivity, S/m | 1/T, $K^{-1}$ | ln (ε, S/m) |
|---|---|---|---|
| 950 | 25.05 | 0.000818 | 3.221 |
| 950 | 25.22 | 0.000818 | 3.228 |
| 1250 | 62.49 | 0.000657 | 4.135 |
| 1150 | 49.87 | 0.000703 | 3.909 |
| 1150 | 50.00 | 0.000703 | 3.912 |
| 1050 | 37.03 | 0.000756 | 3.612 |
| 1050 | 37.18 | 0.000756 | 3.616 |

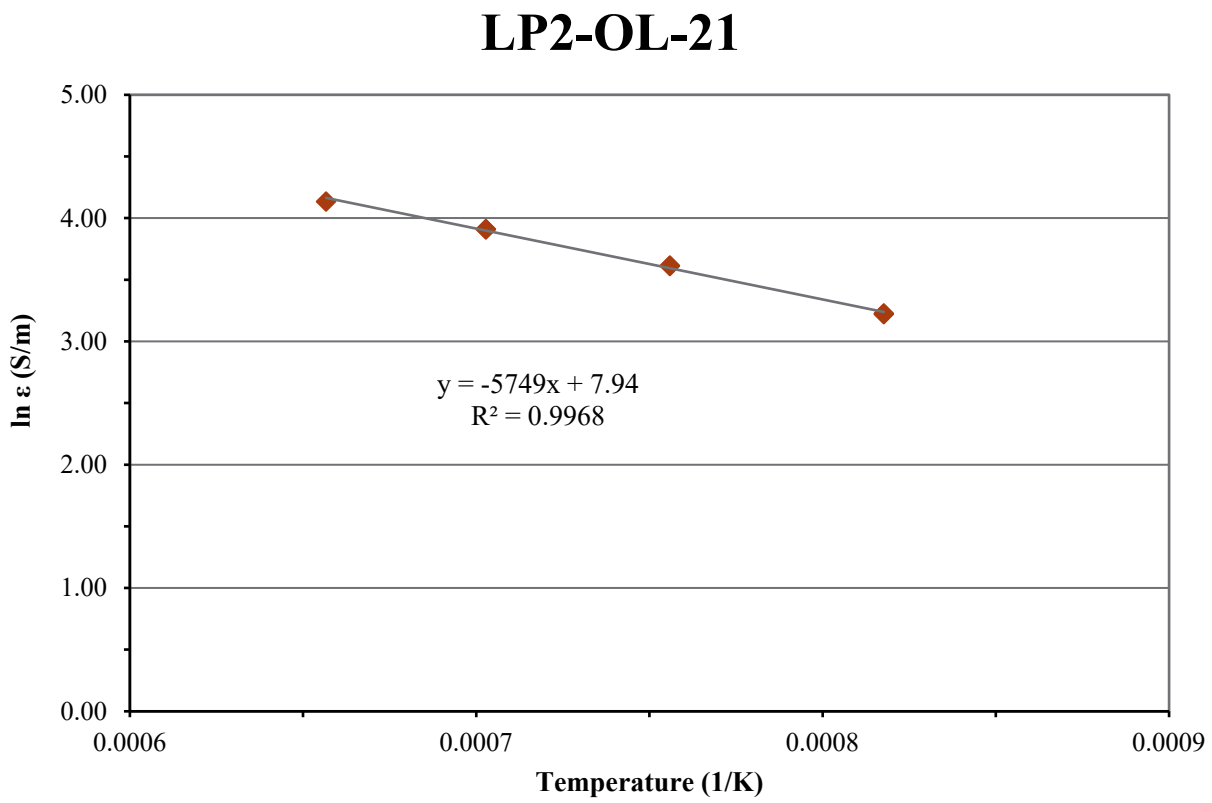


Figure D.37. Electrical Conductivity-Temperature Data and Arrhenius Equation Fit for Glass LP2-OL-21

## D.38 Glass LP2-OL-22 Electrical Conductivity Data

Table D.38. Electrical Conductivity Data for Glass LP2-OL-22

| Temperature, °C | Conductivity, S/m | 1/T, $K^{-1}$ | ln (ε, S/m) |
|---|---|---|---|
| 950 | 17.60 | 0.000818 | 2.868 |
| 950 | 17.74 | 0.000818 | 2.876 |
| 1250 | 53.76 | 0.000657 | 3.985 |
| 1150 | 40.65 | 0.000703 | 3.705 |
| 1150 | 40.75 | 0.000703 | 3.707 |
| 1050 | 28.18 | 0.000756 | 3.338 |
| 1050 | 28.33 | 0.000756 | 3.344 |

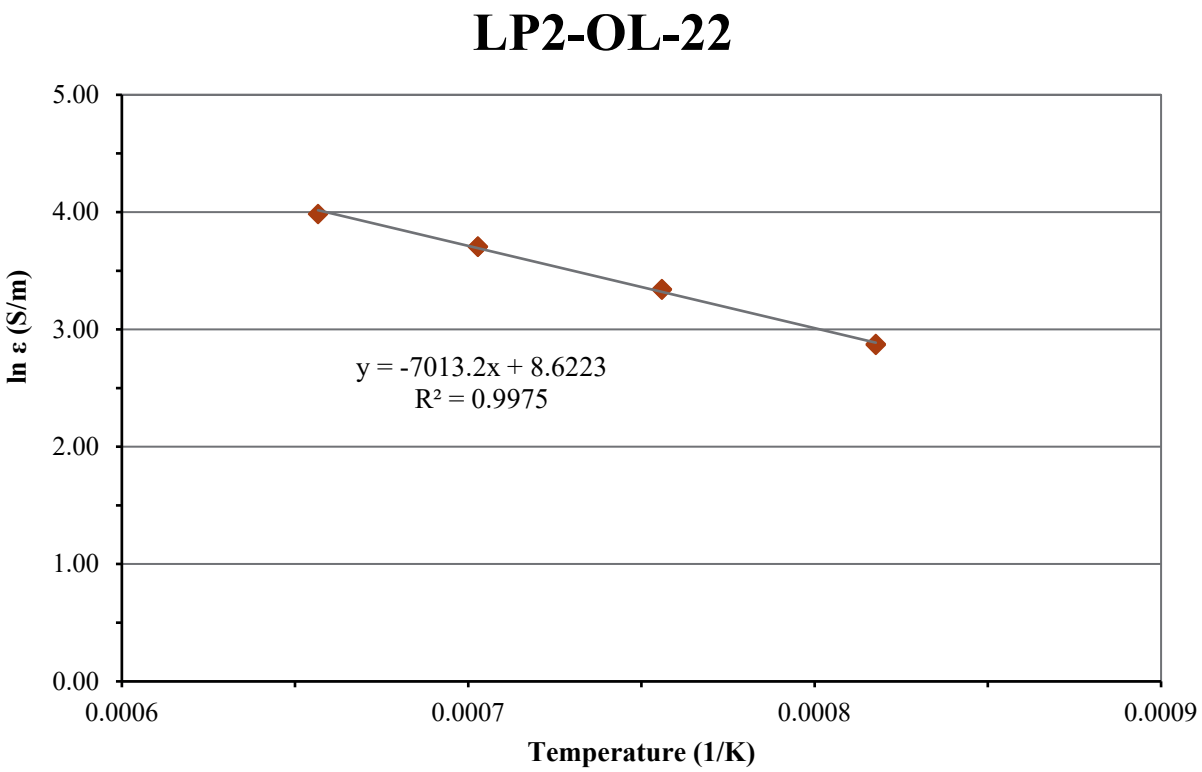


Figure D.38. Electrical Conductivity-Temperature Data and Arrhenius Equation Fit for Glass LP2-OL-22

## D.39 Glass LP2-OL-23 Electrical Conductivity Data

Table D.39. Electrical Conductivity Data for Glass LP2-OL-23

| Temperature, °C | Conductivity, S/m | 1/T, $K^{-1}$ | ln (ε, S/m) |
|---|---|---|---|
| 950 | 18.38 | 0.000818 | 2.911 |
| 950 | 18.52 | 0.000818 | 2.919 |
| 1250 | 55.99 | 0.000657 | 4.025 |
| 1250 | 55.78 | 0.000657 | 4.022 |
| 1150 | 42.51 | 0.000703 | 3.750 |
| 1150 | 42.64 | 0.000703 | 3.753 |
| 1050 | 29.49 | 0.000756 | 3.384 |
| 1050 | 29.63 | 0.000756 | 3.389 |

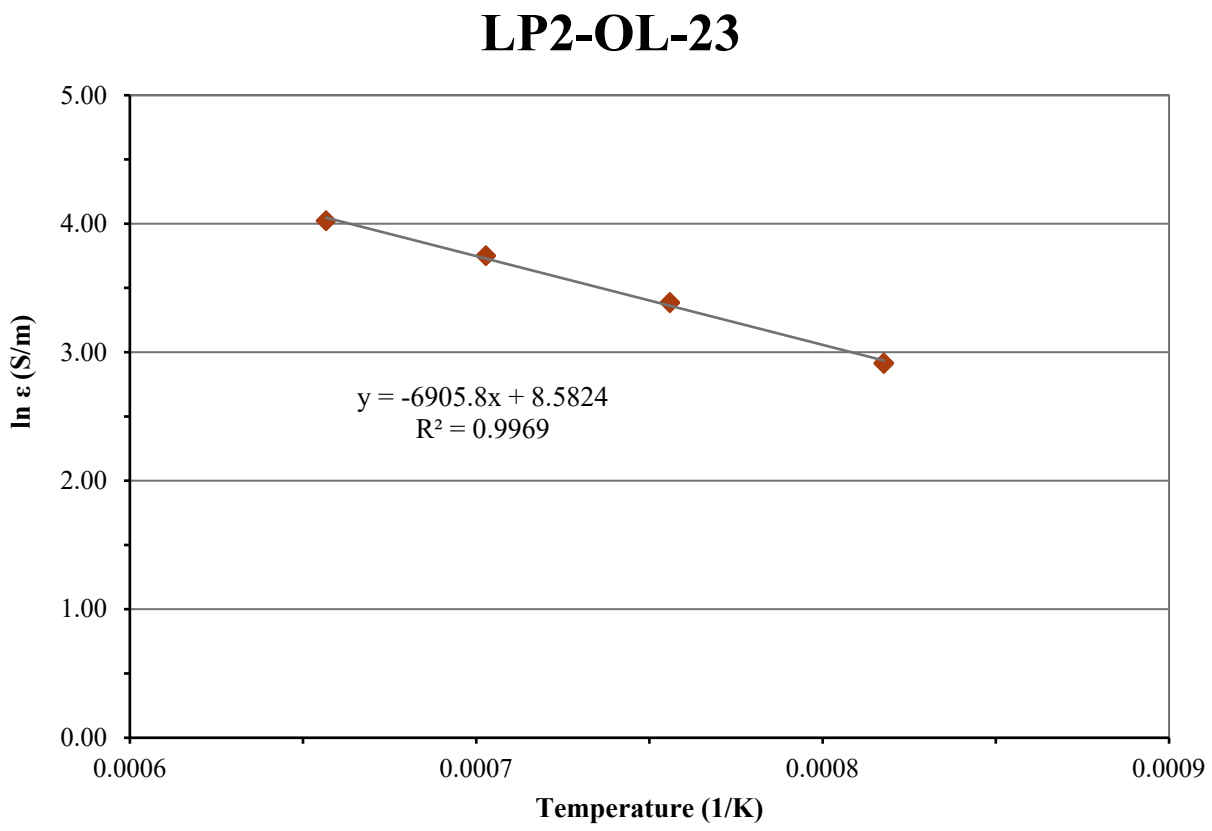


Figure D.39. Electrical Conductivity-Temperature Data and Arrhenius Equation Fit for Glass LP2-OL-23

## D.40 Glass LP2-OL-24 Electrical Conductivity Data

Table D.40. Electrical Conductivity Data for Glass LP2-OL-24

| Temperature, °C | Conductivity, S/m | 1/T, $K^{-1}$ | ln (ε, S/m) |
|---|---|---|---|
| 950 | 27.96 | 0.000818 | 3.331 |
| 950 | 28.13 | 0.000818 | 3.337 |
| 1250 | 64.54 | 0.000657 | 4.167 |
| 1250 | 64.38 | 0.000657 | 4.165 |
| 1150 | 52.60 | 0.000703 | 3.963 |
| 1150 | 52.73 | 0.000703 | 3.965 |
| 1050 | 40.06 | 0.000756 | 3.690 |
| 1050 | 40.24 | 0.000756 | 3.695 |

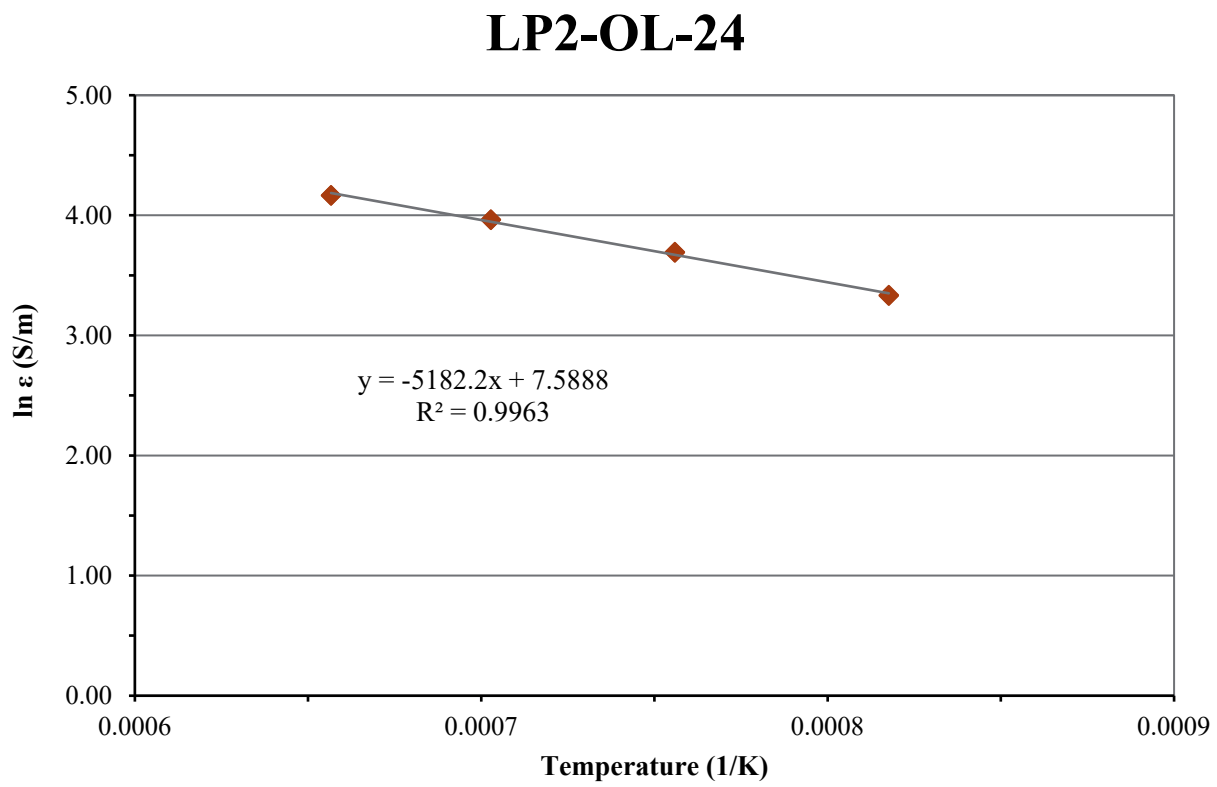


Figure D.40. Electrical Conductivity-Temperature Data and Arrhenius Equation Fit for Glass LP2-OL-24

## D.41 Glass LP2-OL-25 Electrical Conductivity Data

Table D.41. Electrical Conductivity Data for Glass LP2-OL-25

| Temperature, °C | Conductivity, S/m | 1/T, $K^{-1}$ | ln (ε, S/m) |
|---|---|---|---|
| 950 | 29.42 | 0.000818 | 3.382 |
| 950 | 29.61 | 0.000818 | 3.388 |
| 1250 | 68.78 | 0.000657 | 4.231 |
| 1250 | 68.64 | 0.000657 | 4.229 |
| 1150 | 55.78 | 0.000703 | 4.021 |
| 1150 | 55.88 | 0.000703 | 4.023 |
| 1050 | 42.20 | 0.000756 | 3.742 |
| 1050 | 42.30 | 0.000756 | 3.745 |

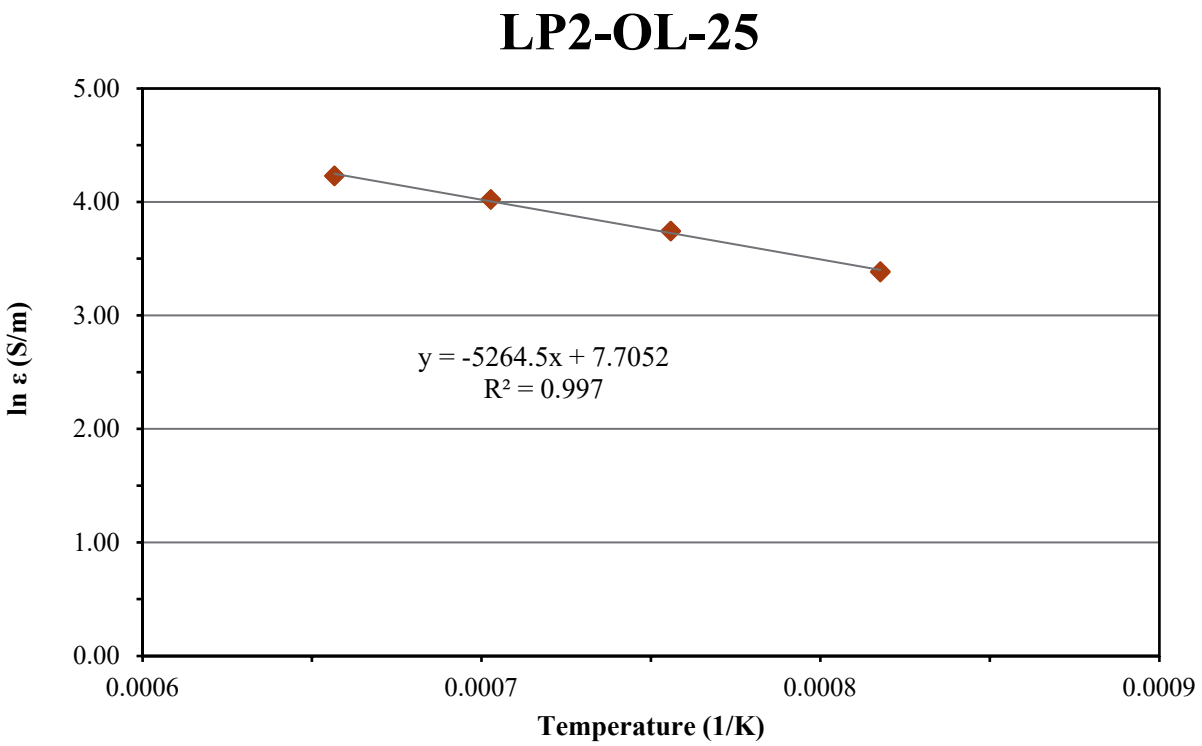


Figure D.41. Electrical Conductivity-Temperature Data and Arrhenius Equation Fit for Glass LP2-OL-25

# Appendix E – Crystal Fraction (CF) of Heat-Treated Glasses Photographs

This appendix contains photos of Phase 2 enhanced LAW glasses after they were heat-treated at 950 °C for 24 hours (CF Heat-Treatment). Each showed different responses to the heat-treatment as indicated by these photos. No photo was taken of glass LP2-IL-01.

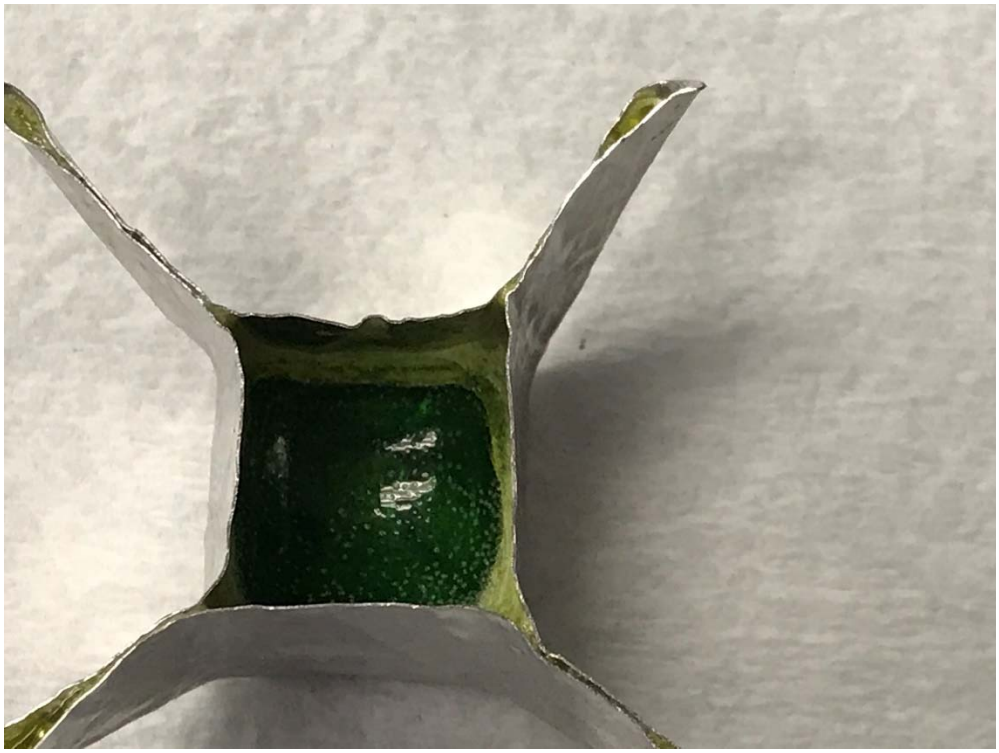

Figure E.1. Glass LP2-IL-02 after CF Heat Treatment at 950 °C for 24 h

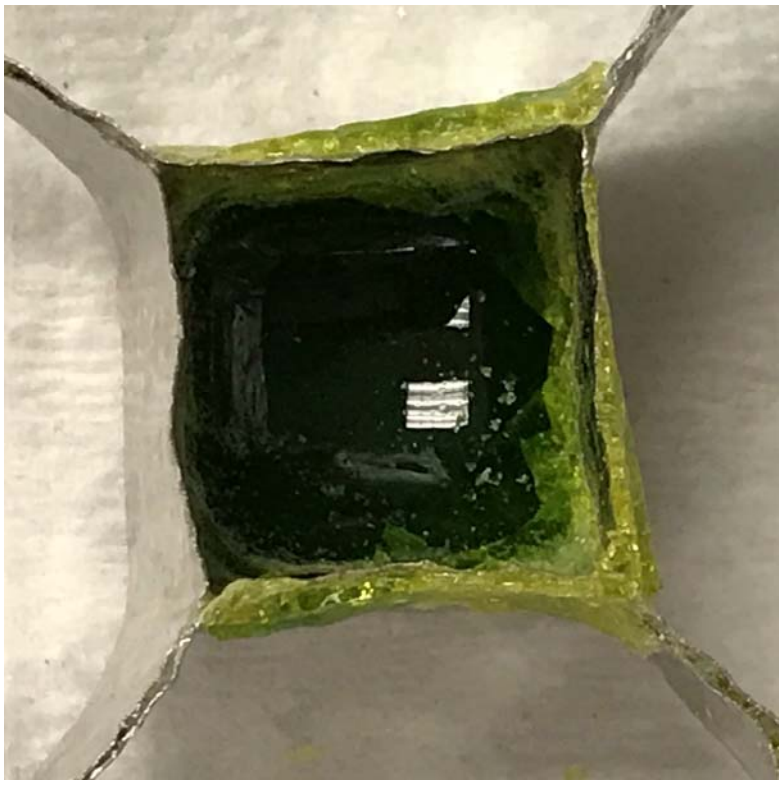

Figure E.2. Glass LP2-IL-03 after CF Heat Treatment at 950 °C for 24 h

Figure E.3. Glass LP2-IL-04 after CF Heat Treatment at 950 °C for 24 h

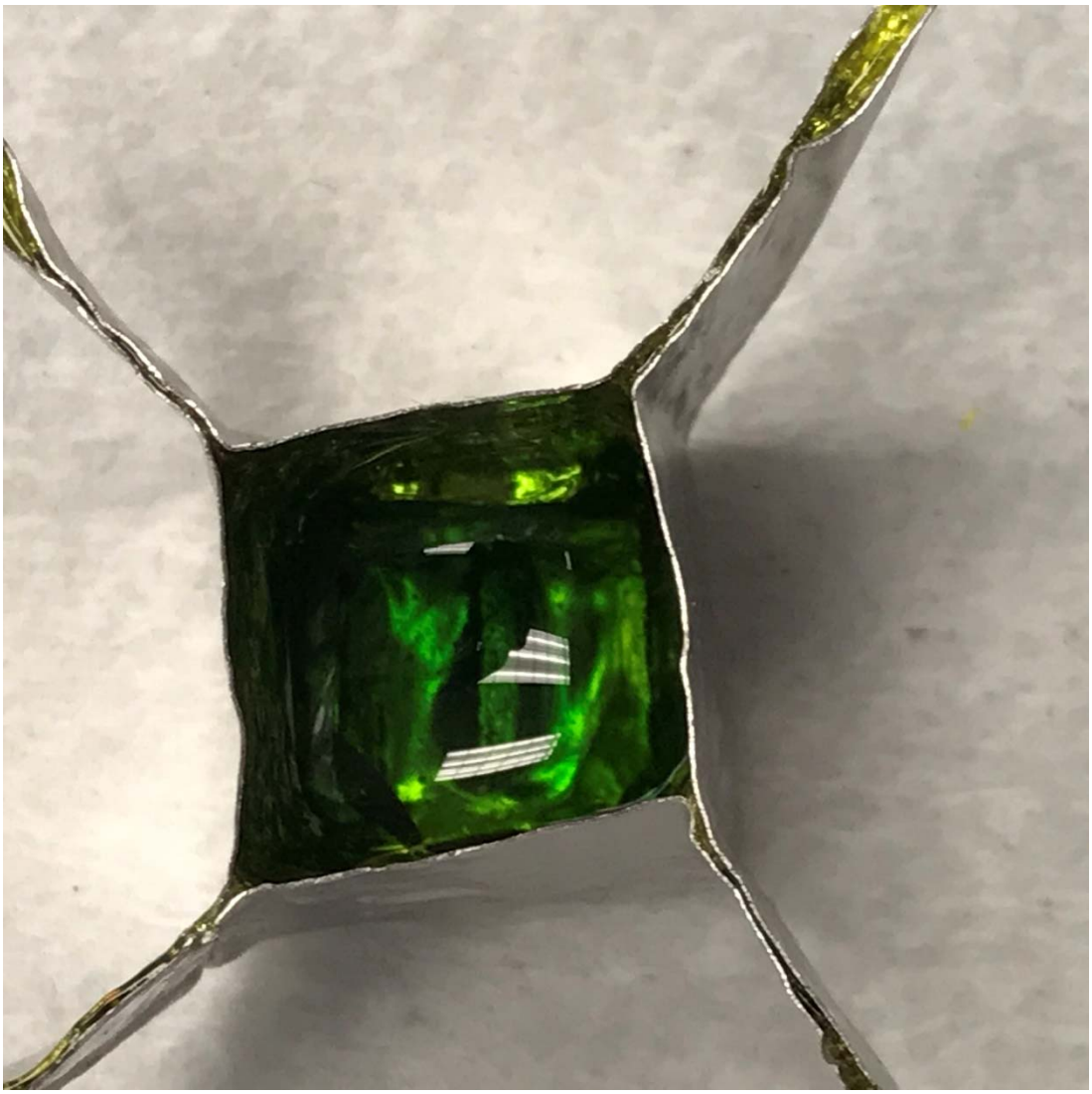

Figure E.4. Glass LP2-IL-05 after CF Heat Treatment at 950 °C for 24 h

Figure E.5. Glass LP2-IL-06 after CF Heat Treatment at 950 °C for 24 h both in Crucible (left) and Magnified 100X (right)

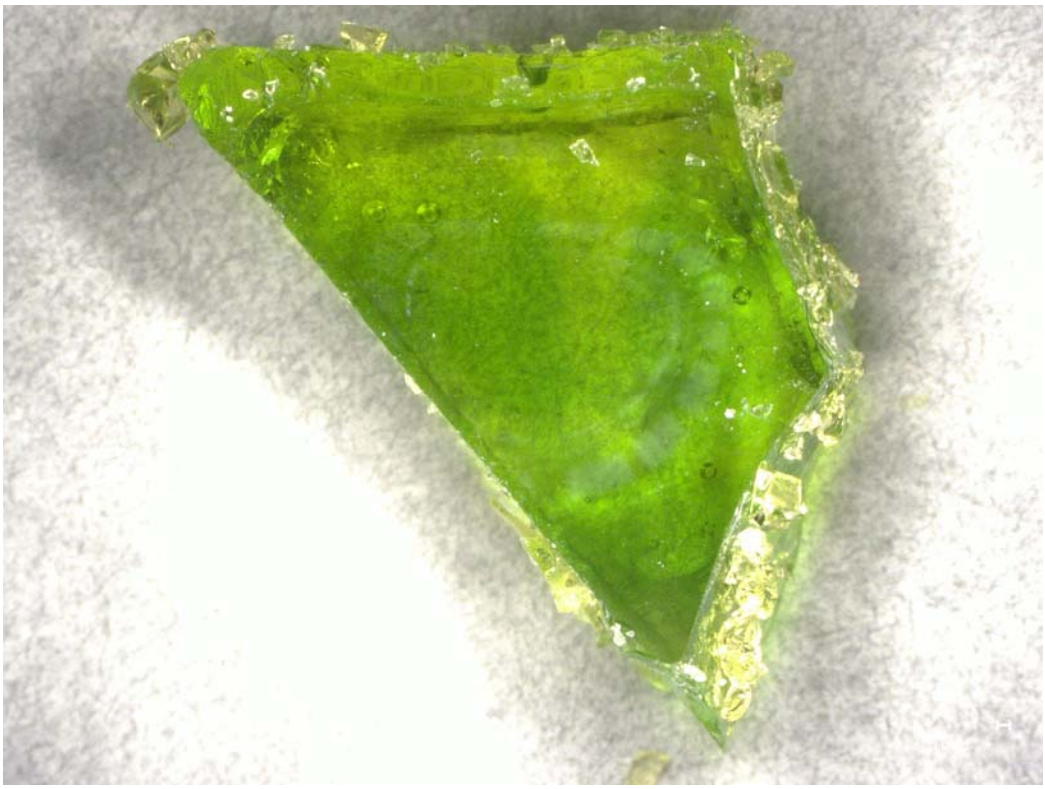

Figure E.6. Glass LP2-IL-07 after CF Heat Treatment at 950 °C for 24 h Magnified 20X


Figure E.7. Glass LP2-IL-08 after CF Heat Treatment at 950 °C for 24 h both in Crucible (top) and Magnified 150X (bottom)

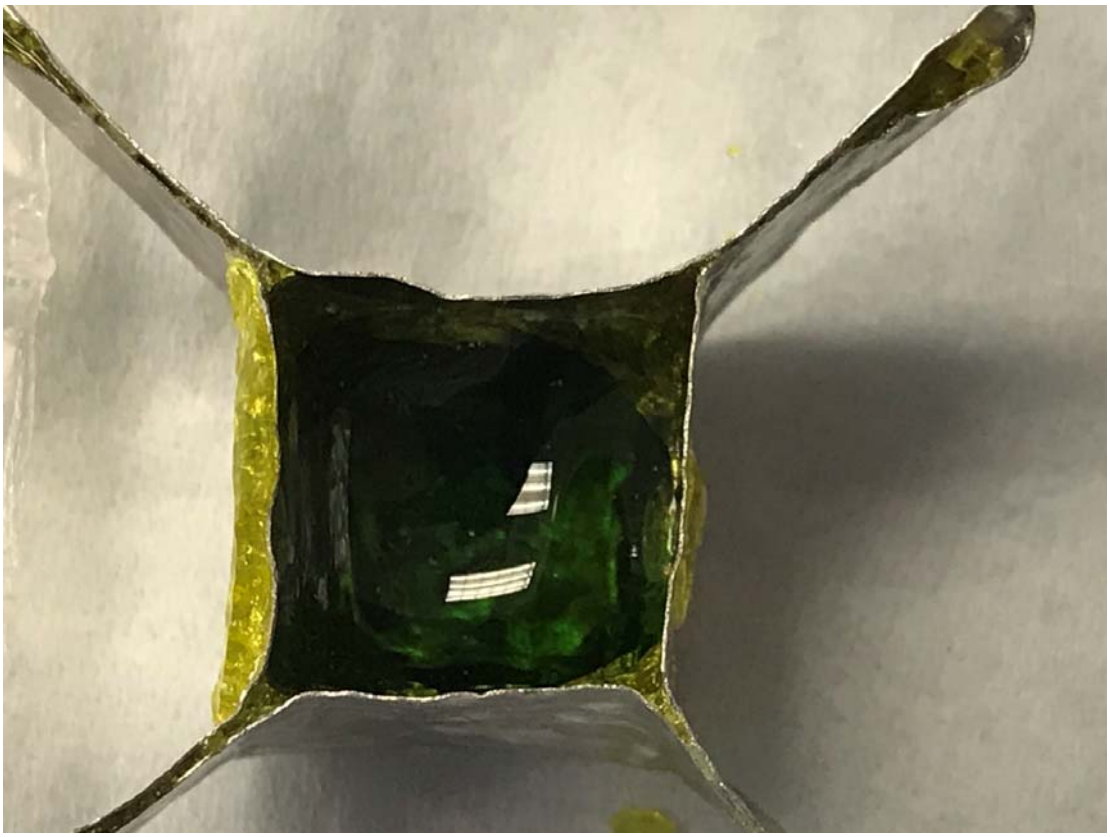

Figure E.8. Glass LP2-IL-09 after CF Heat Treatment at 950 °C for 24 h

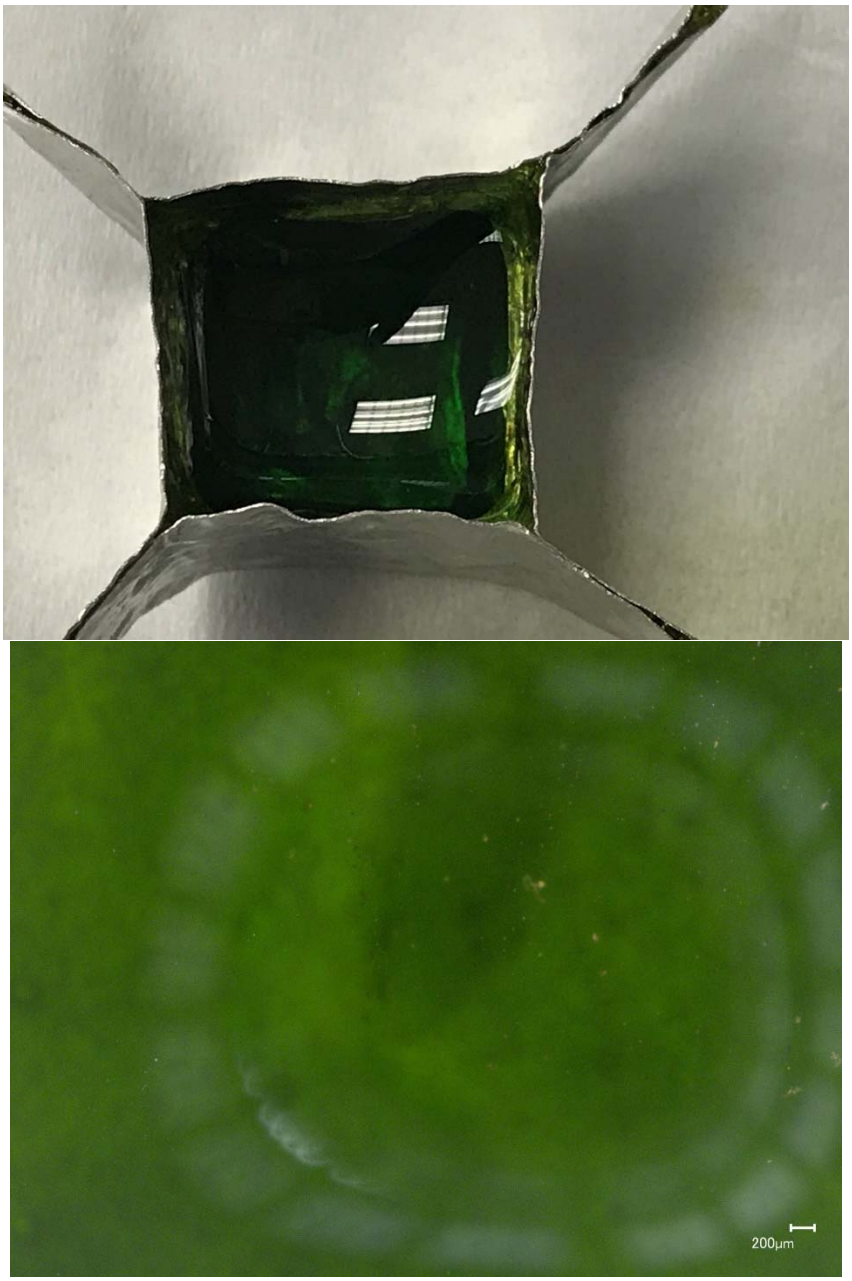


Figure E.9. Glass LP2-IL-10 after CF Heat Treatment at 950 °C for 24 h both in Crucible (top) and Magnified 50X (bottom)


Figure E.10. Glass LP2-IL-11 after CF Heat Treatment at 950 °C for 24 h both in Crucible (top) and Magnified 200X (bottom)

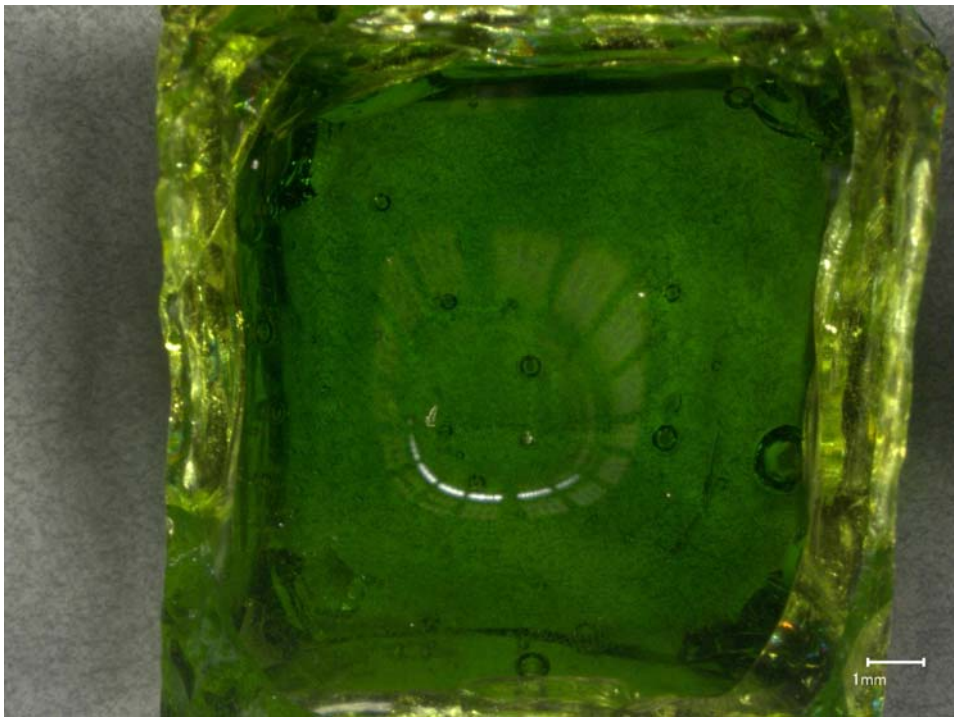


Figure E.11. Glass LP2-IL-12 after CF Heat Treatment at 950 °C for 24 h Magnified 20X

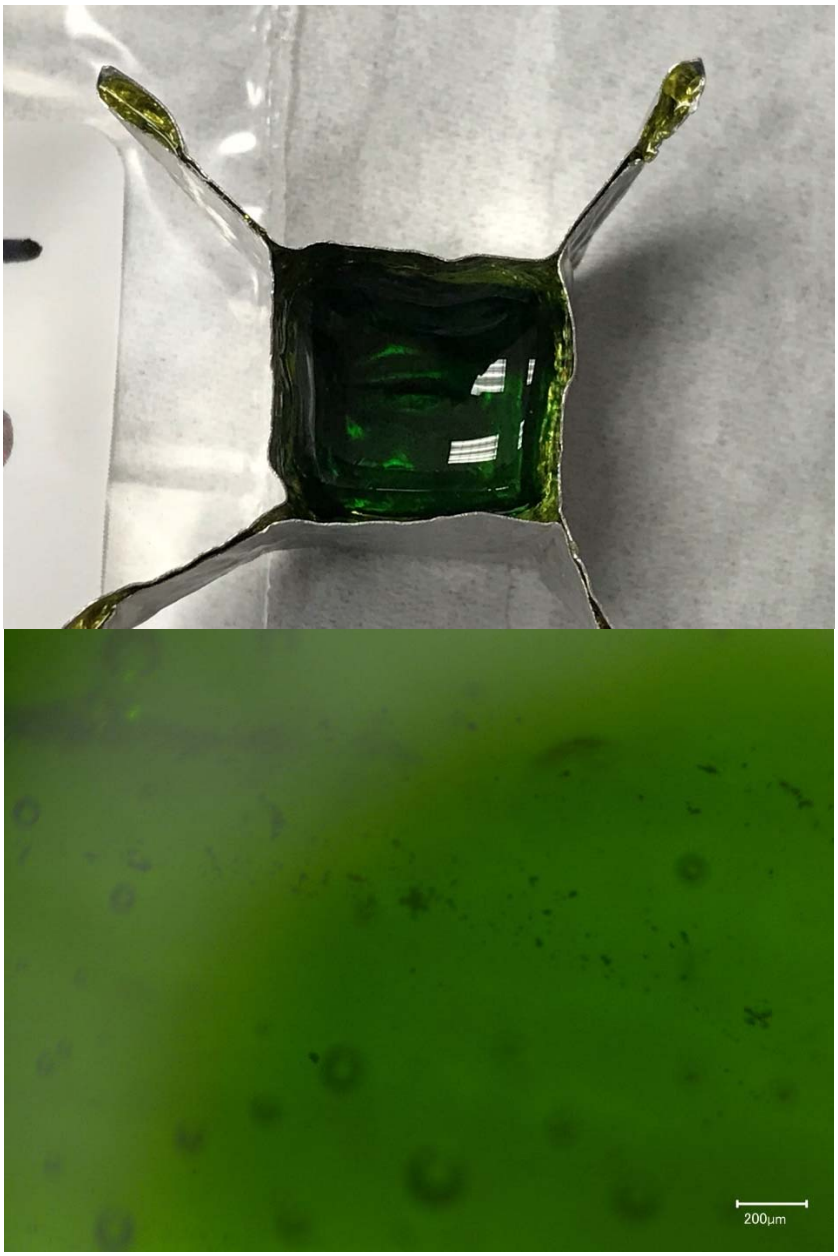


Figure E.12. Glass LP2-IL-13 after CF Heat Treatment at 950 °C for 24 h both in Crucible (top) and Magnified 150X (bottom)

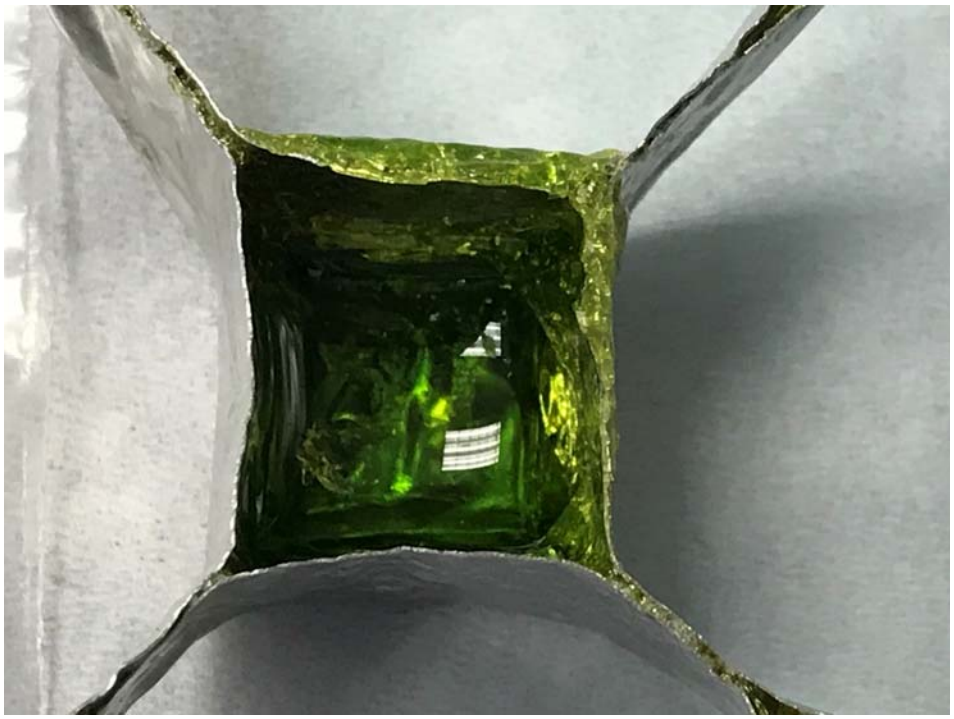

Figure E.13. Glass LP2-IL-14 after CF Heat Treatment at 950 °C for 24 h

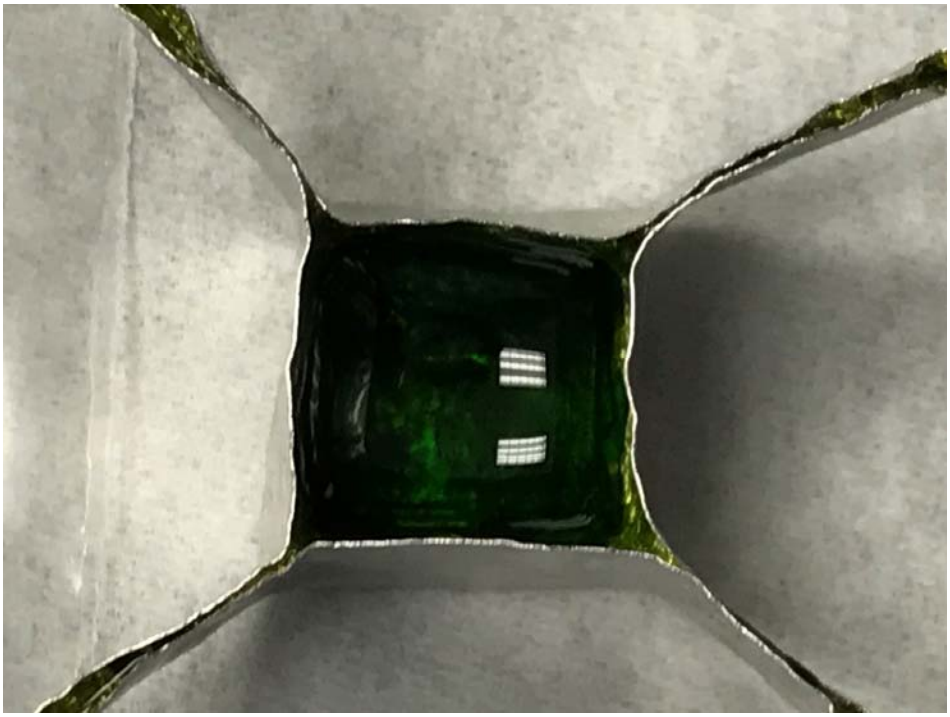

Figure E.14. Glass LP2-IL-15 after CF Heat Treatment at 950 °C for 24 h

Figure E.15. Glass LP2-IL-16 after CF Heat Treatment at 950 °C for 24 h

Figure E.16. Glass LP2-IL-17 after CF Heat Treatment at 950 °C for 24 h

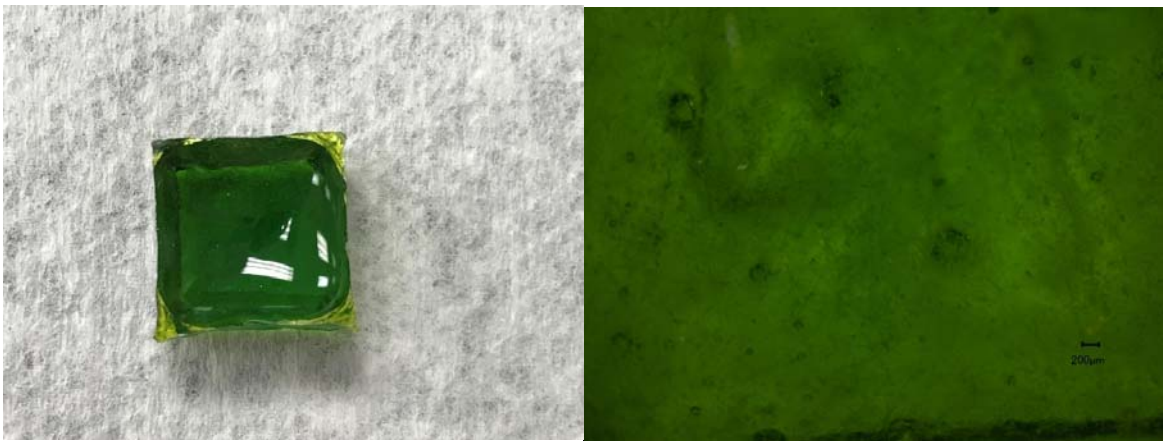

Figure E.17. Glass LP2-OL-01-3 after CF Heat Treatment at 950 °C for 24 h both Glass (left) and Magnified 50X (right)

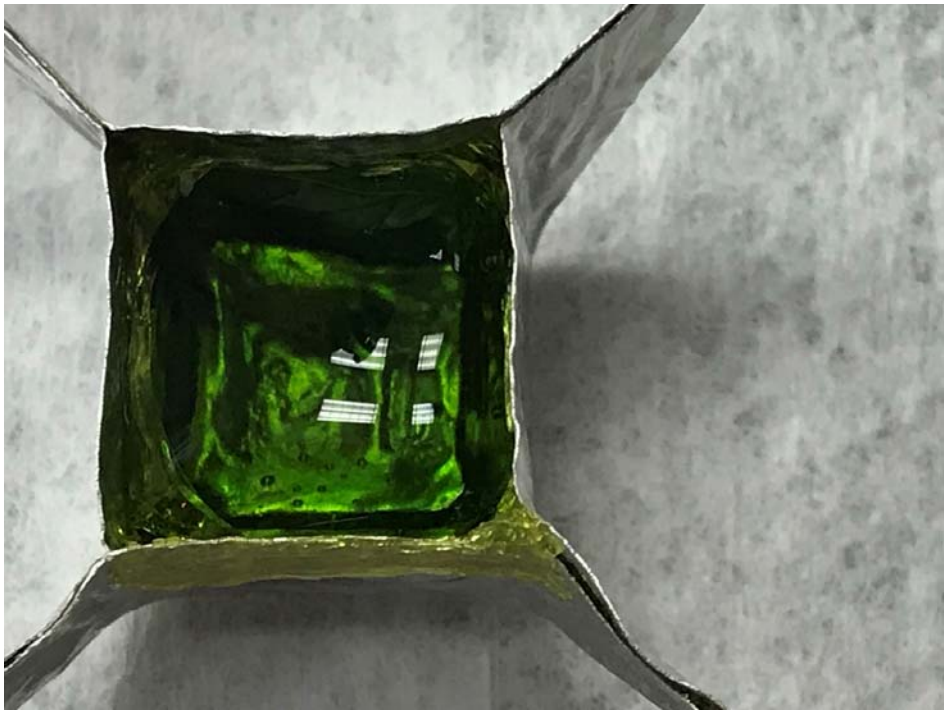

Figure E.18. Glass LP2-OL-02-1 after CF Heat Treatment at 950 °C for 24 h

Figure E.19. Glass LP2-OL-03 MOD2 after CF Heat Treatment at 950 °C for 24 h


Figure E.20. Glass LP2-OL-04-1 after CF Heat Treatment at 950 °C for 24 h both in Crucible (top) and Magnified 30X (bottom)


Figure E.21. Glass LP2-OL-05 after CF Heat Treatment at 950 °C for 24 h both in crucible (top) and magnified 20X (bottom)

Figure E.22. Glass LP2-OL-07-1 after CF Heat Treatment at 950 °C for 24 h

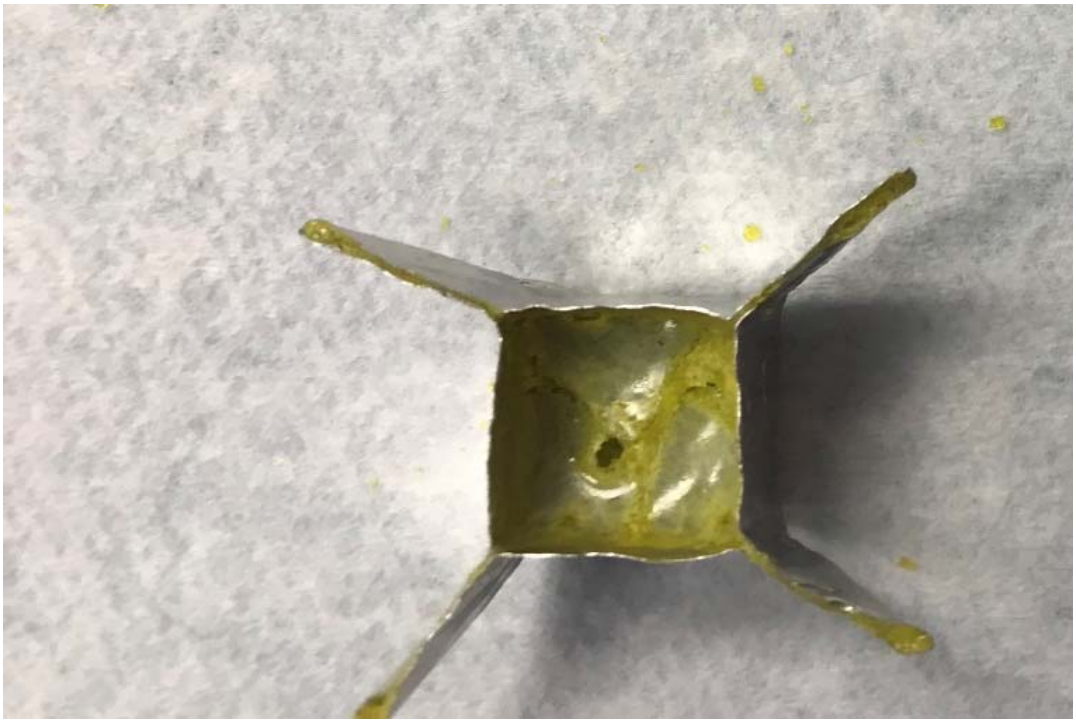

Figure E.23. Glass LP2-OL-08 MOD after CF Heat Treatment at 950 °C for 24 h

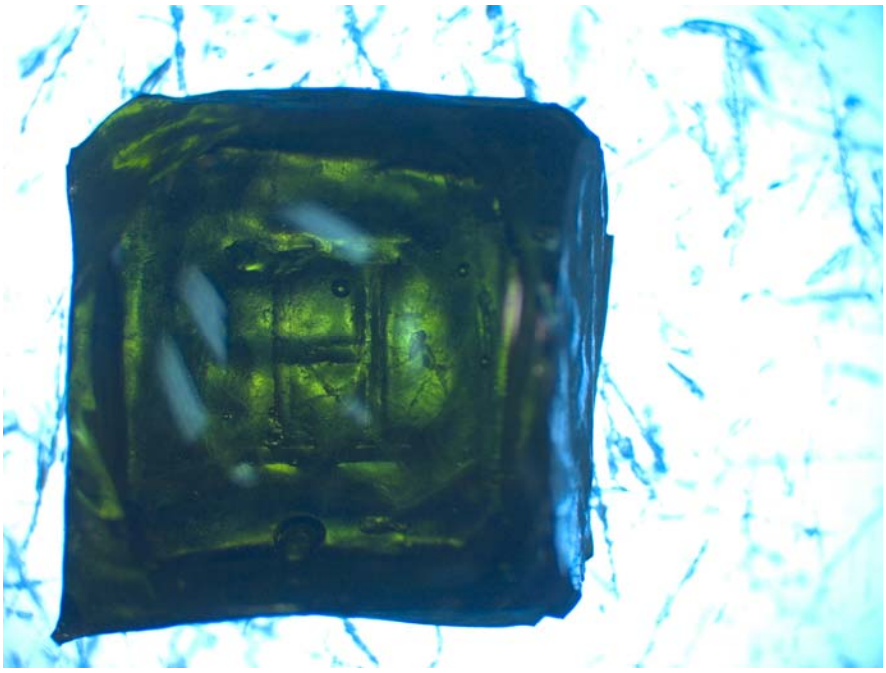

Figure E.24. Glass LP2-OL-09-1 after CF Heat Treatment at 950 °C for 24 h

Figure E.25. Glass LP2-OL-10 MOD after CF Heat Treatment at 950 °C for 24 h

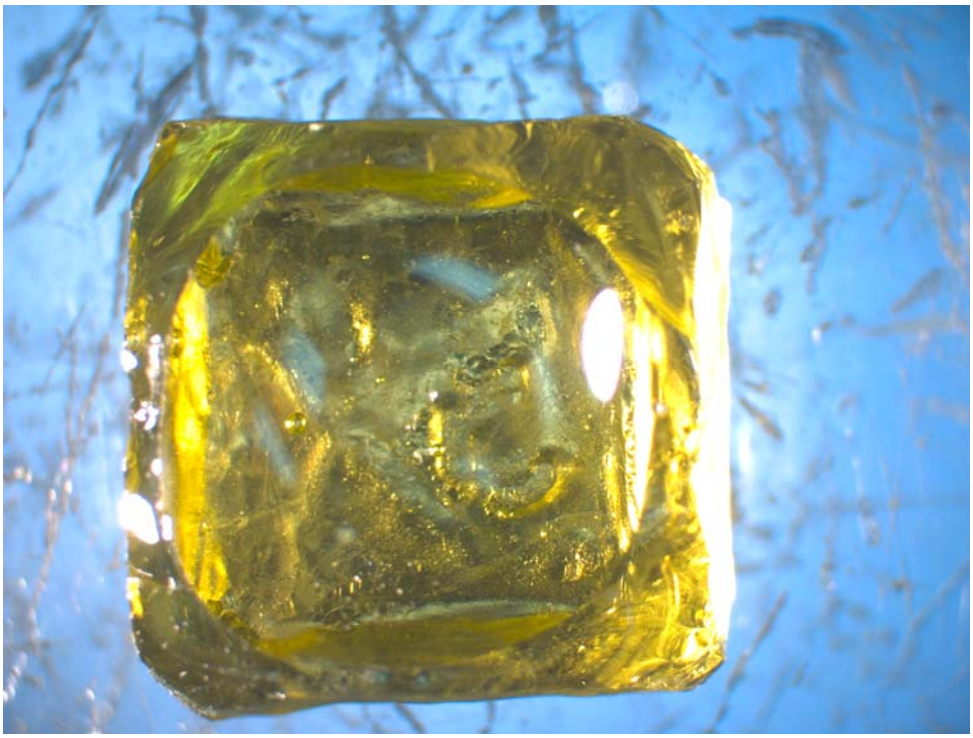

Figure E.26. Glass LP2-OL-11 after CF Heat Treatment at 950 °C for 24 h

Figure E.27. Glass LP2-OL-12 after CF Heat Treatment at 950 °C for 24 h

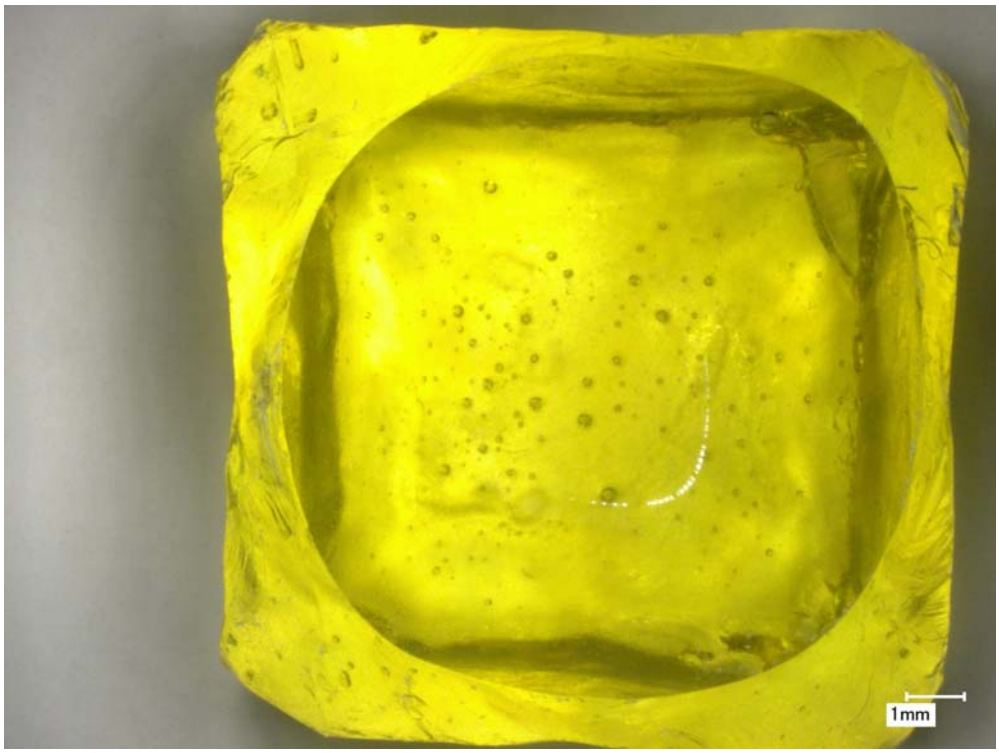


Figure E.28. Glass LP2-OL-13 after CF Heat Treatment at 950 °C for 24 h Magnified 20X

Figure E.29. Glass LP2-OL-14 after CF Heat Treatment at 950 °C for 24 h

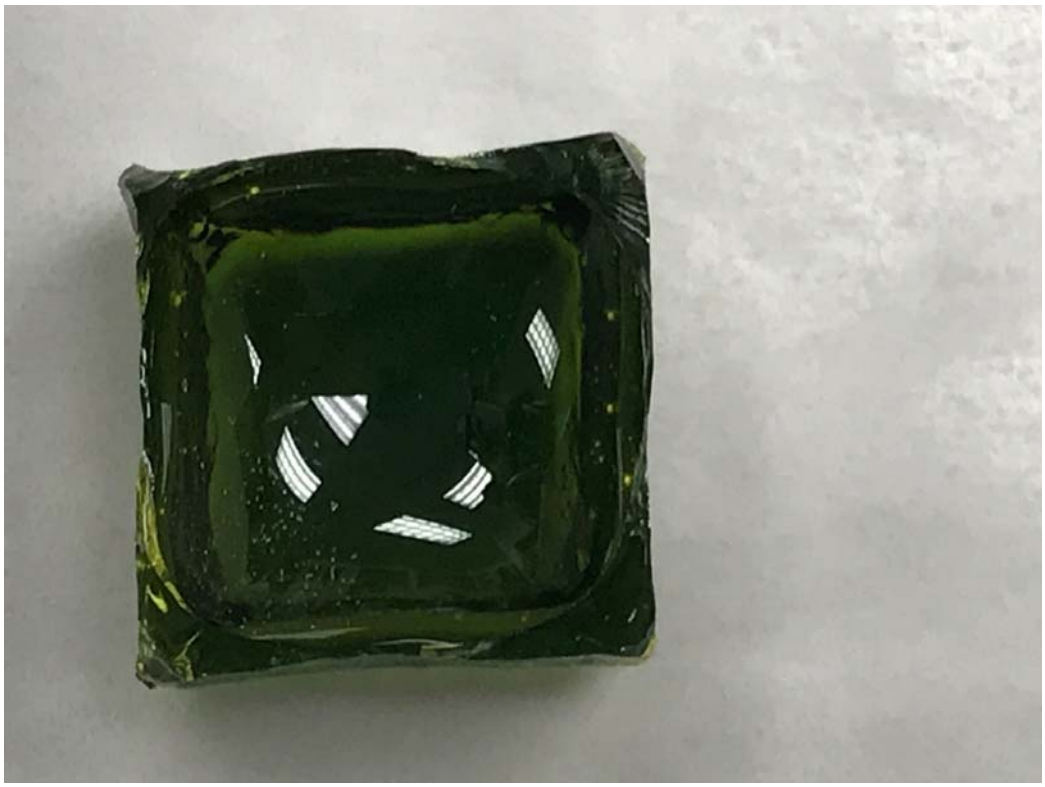

Figure E.30. Glass LP2-OL-15 after CF Heat Treatment at 950 °C for 24 h

Figure E.31. Glass LP2-OL-16 MOD after CF Heat Treatment at 950 °C for 24 h

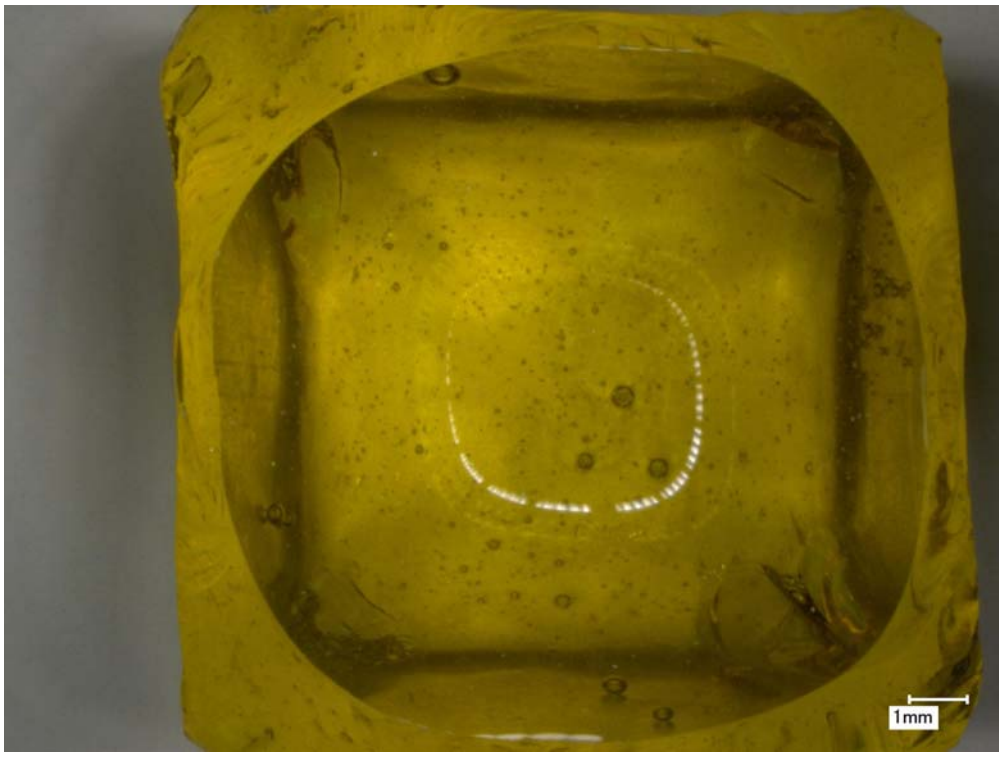


Figure E.32. Glass LP2-OL-17 after CF Heat Treatment at 950 °C for 24 h Magnified 20X

Figure E.33. Glass LP2-OL-18 after CF Heat Treatment at 950 °C for 24 h

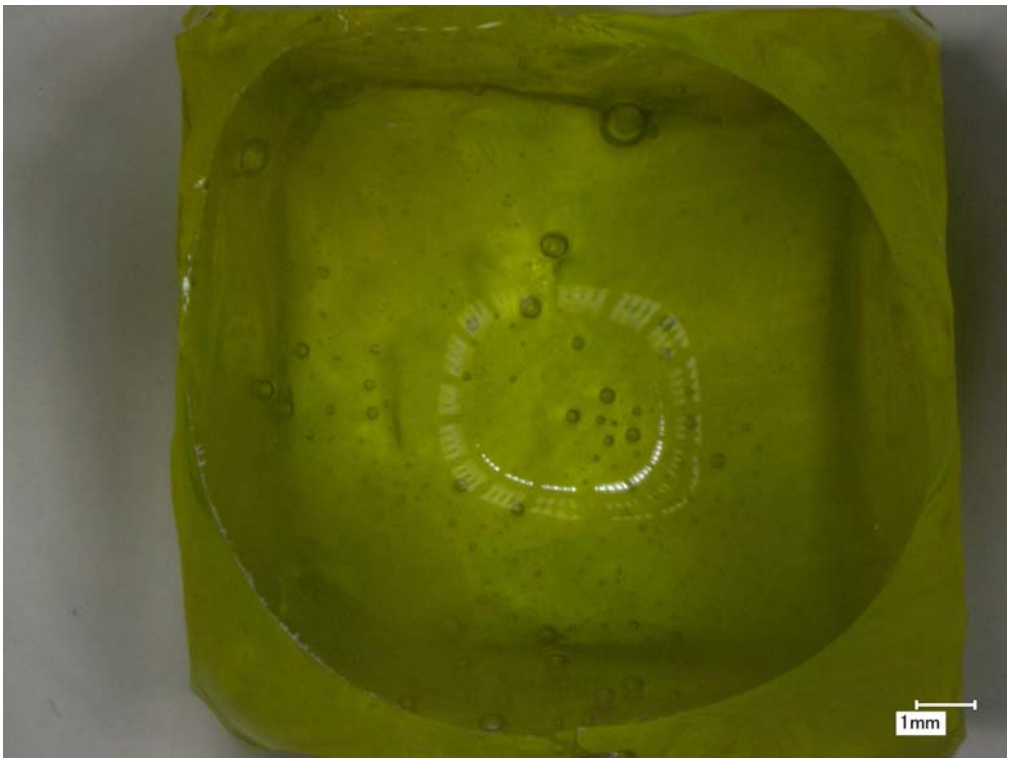


Figure E.34. Glass LP2-OL-19 after CF Heat Treatment at 950 °C for 24 h Magnified 20X

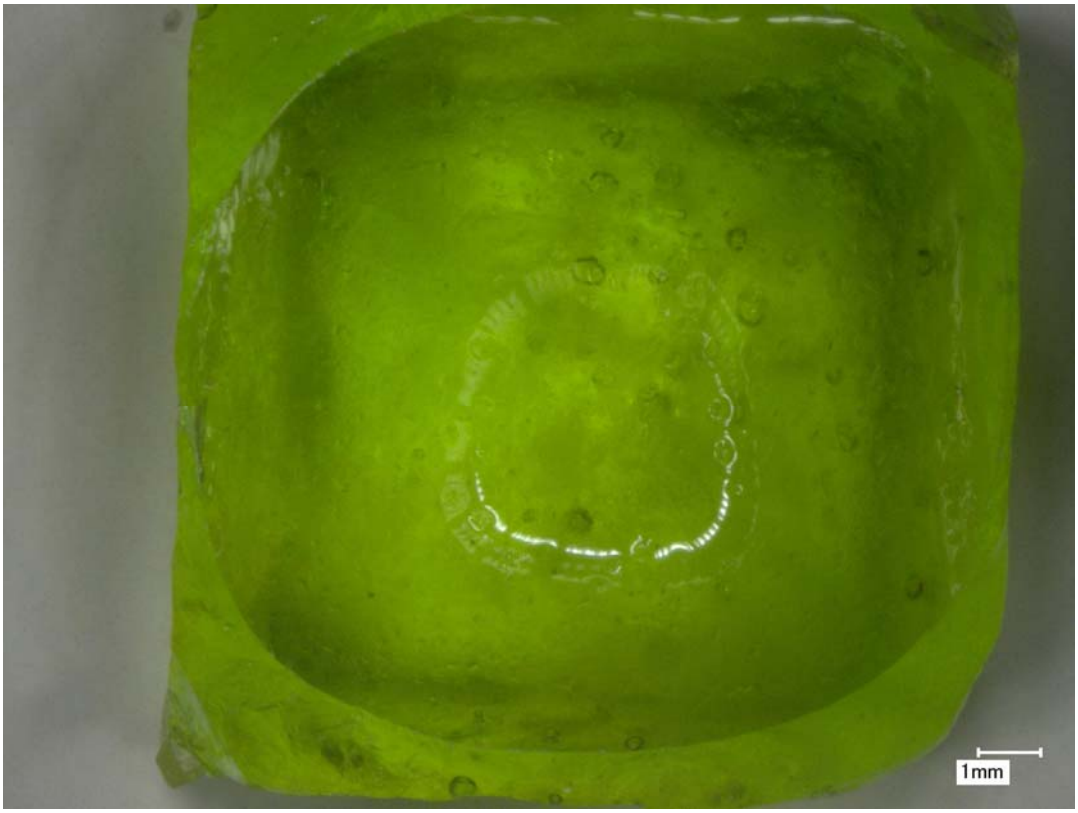


Figure E.35. Glass LP2-OL-20 after CF Heat Treatment at 950 °C for 24 h Magnified 20X

Figure E.36. Glass LP2-OL-21 after CF Heat Treatment at 950 °C for 24 h

Figure E.37. Glass LP2-OL-22 after CF Heat Treatment at 950 °C for 24 h

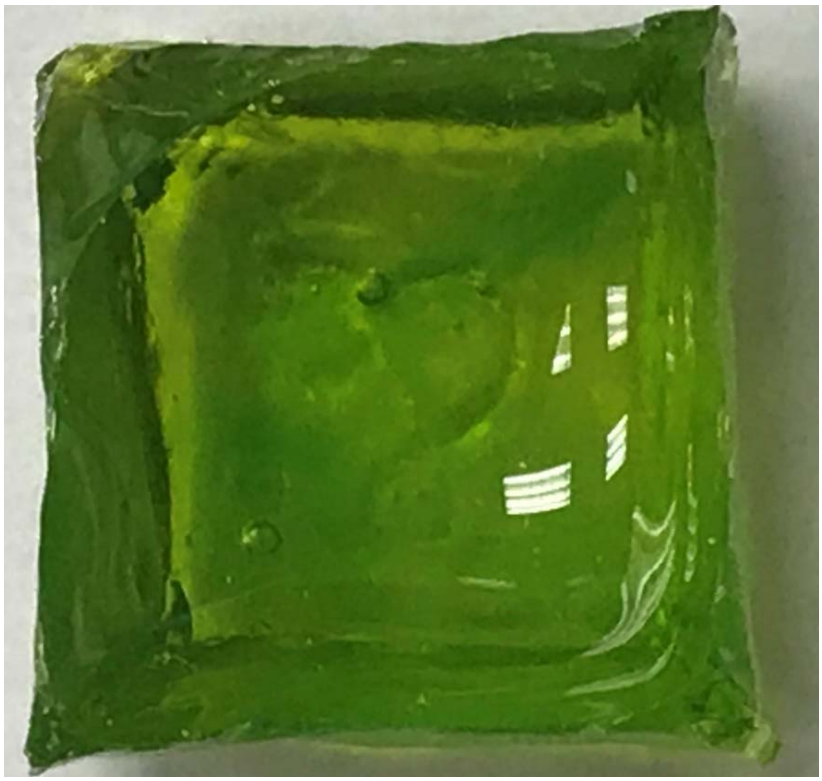

Figure E.38. Glass LP2-OL-23 after CF Heat Treatment at 950° C for 24 h

Figure E.39. Glass LP2-OL-24 after CF Heat Treatment at 950 °C for 24 h

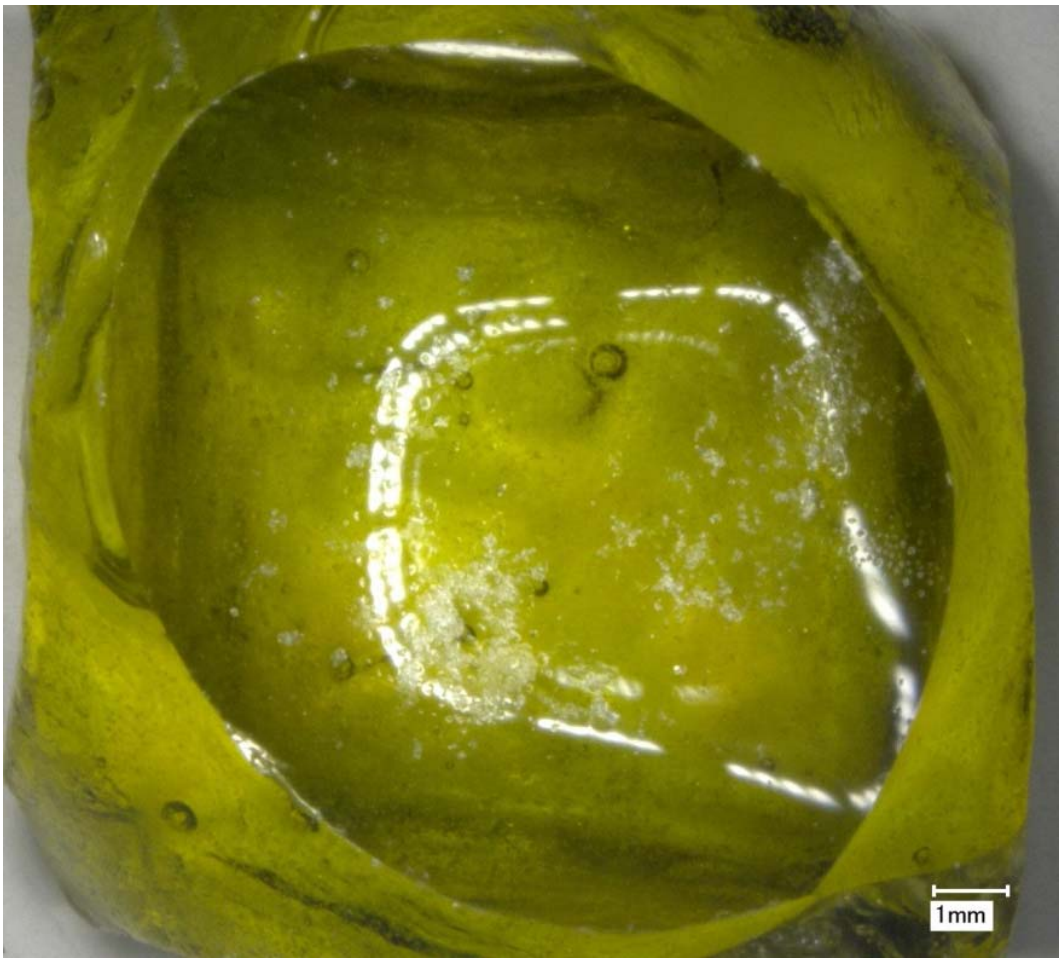


Figure E.40. Glass LP2-OL-25 after CF Heat Treatment at 950 °C for 24 h

# Appendix F – XRD of Heat-Treated Glasses to Determine Crystal Fraction (CF)

This appendix shows the XRD plots of several Phase 2 enhanced LAW glasses after heat-treating (24 hours at 950 °C). These glasses all responded very differently to the heat-treatment from remaining amorphous to developing quite a few crystals of various kinds as shown by the following plots. Some glasses did not contain enough crystals to perform XRD and therefore aren't included here. They were LP2-IL-07, LP2-IL-09, LP2-IL-12, LP2-IL-13, LP2-IL-14, LP2-IL-15, LP2-IL-16, LP2-IL-17, LP2-OL-02-1, LP2-OL-09-1, LP2-OL-11, LP2-OL-12, LP2-OL-14, LP2-OL-15, LP2-OL-21, and LP2-OL-23.

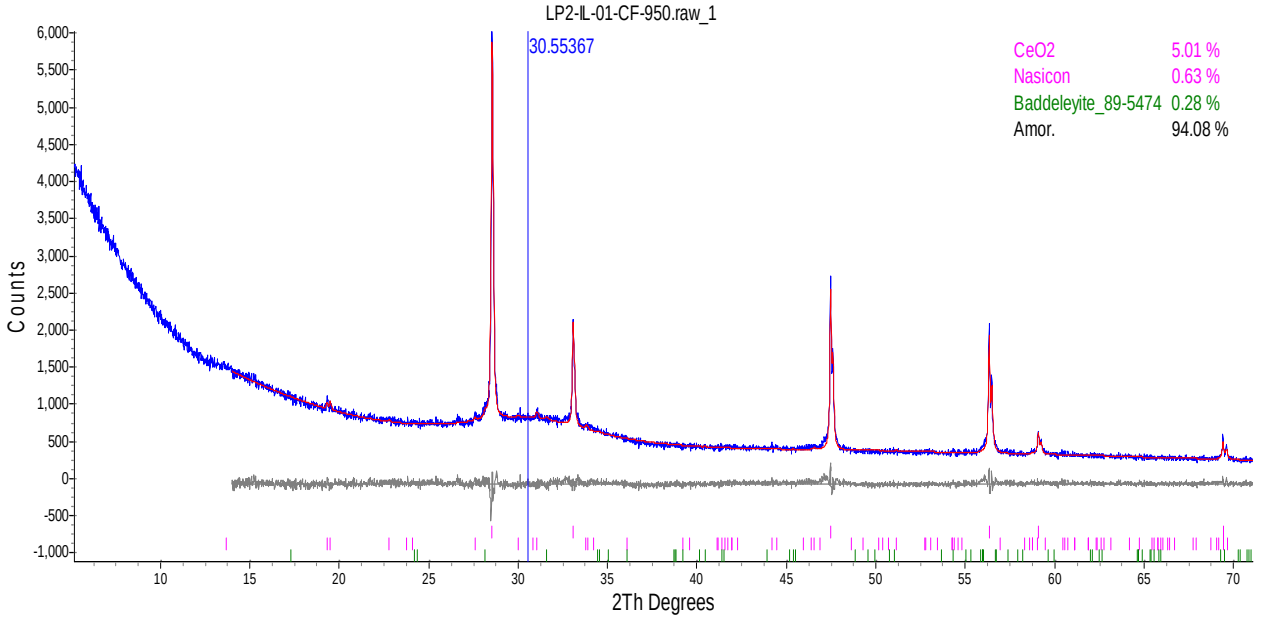


| Phase Name | Wt% of Spiked | Wt% in Spiked Sample | Wt% in Original Sample |
|---|---|---|---|
| $CeO_2$ | 5.007 | 5.007 | 0 |
| Nasicon | 0 | 0.632 | 0.665 |
| Baddeleyite | 0 | 0.279 | 0.294 |

Figure F.1. XRD Spectrum of Heat-Treated Glass LP2-IL-01

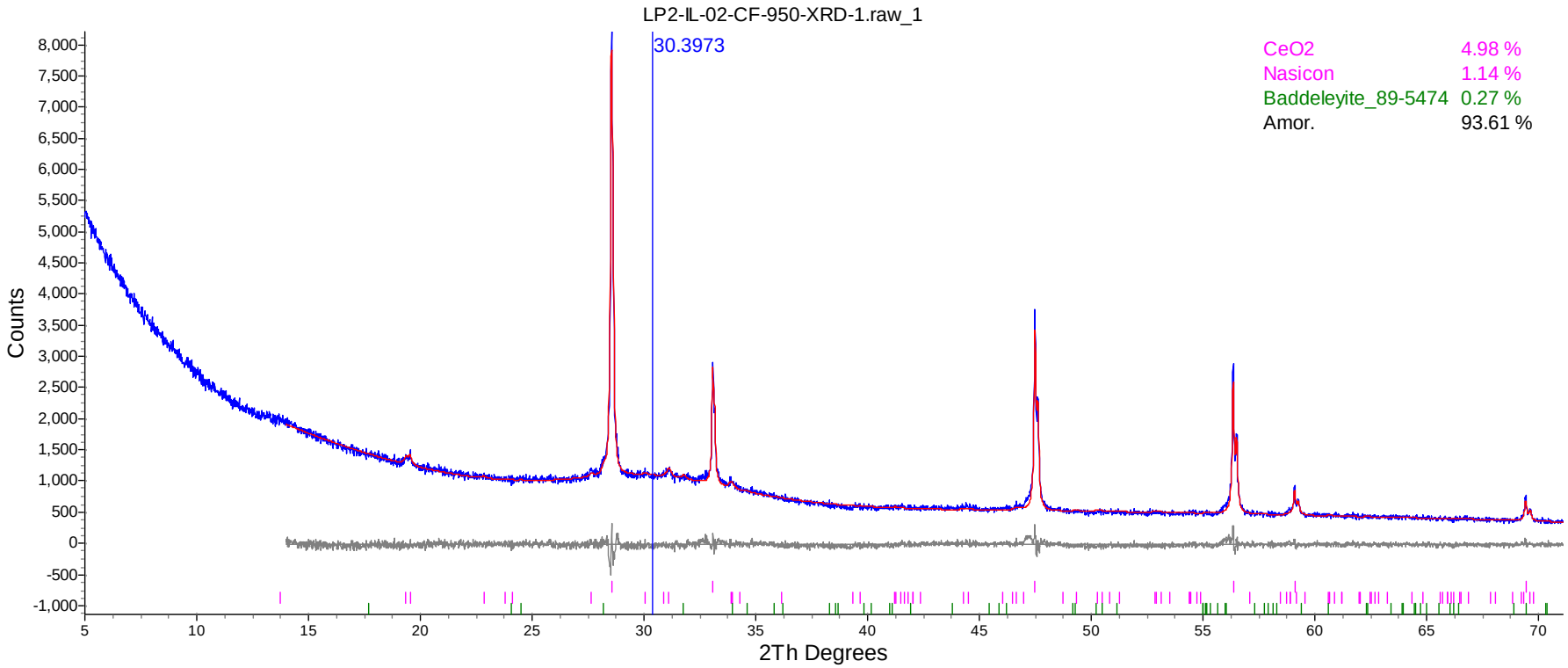


| Phase Name | Wt% of Spiked | Wt% in Spiked Sample | Wt% in Original Sample |
|---|---|---|---|
| $CeO_2$ | 4.976 | 4.976 | 0 |
| Nasicon | 0 | 1.14 | 1.199 |
| Baddeleyite | 0 | 0.272 | 0.286 |

Figure F.2. XRD Spectrum of Heat-Treated Glass LP2-IL-02

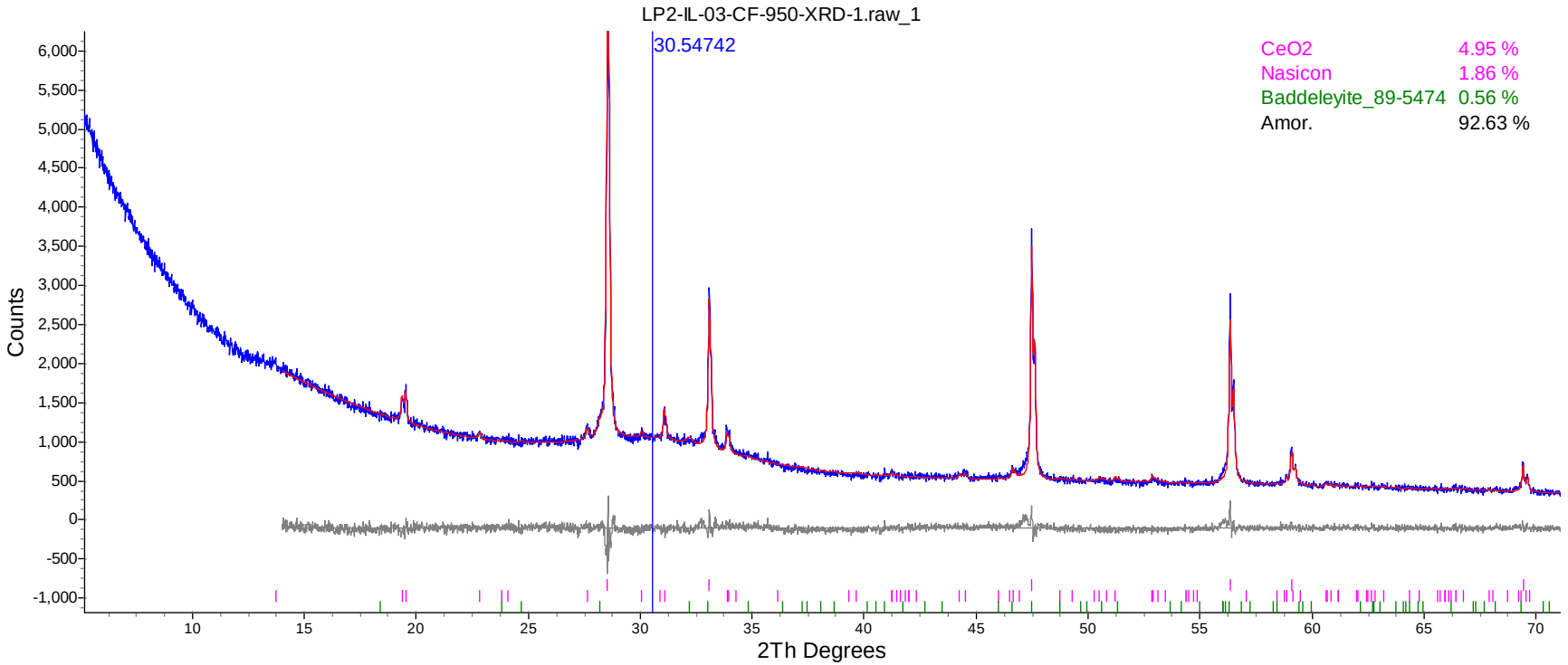


| Phase Name | Wt% of Spiked | Wt% in Spiked Sample | Wt% in Original Sample |
|---|---|---|---|
| $CeO_2$ | 4.98 | 4.98 | 0 |
| Nasicon | 0 | 1.859 | 1.956 |
| Baddeleyite | 0 | 0.557 | 0.586 |

Figure F.3. XRD Spectrum of Heat-Treated Glass LP2-IL-03

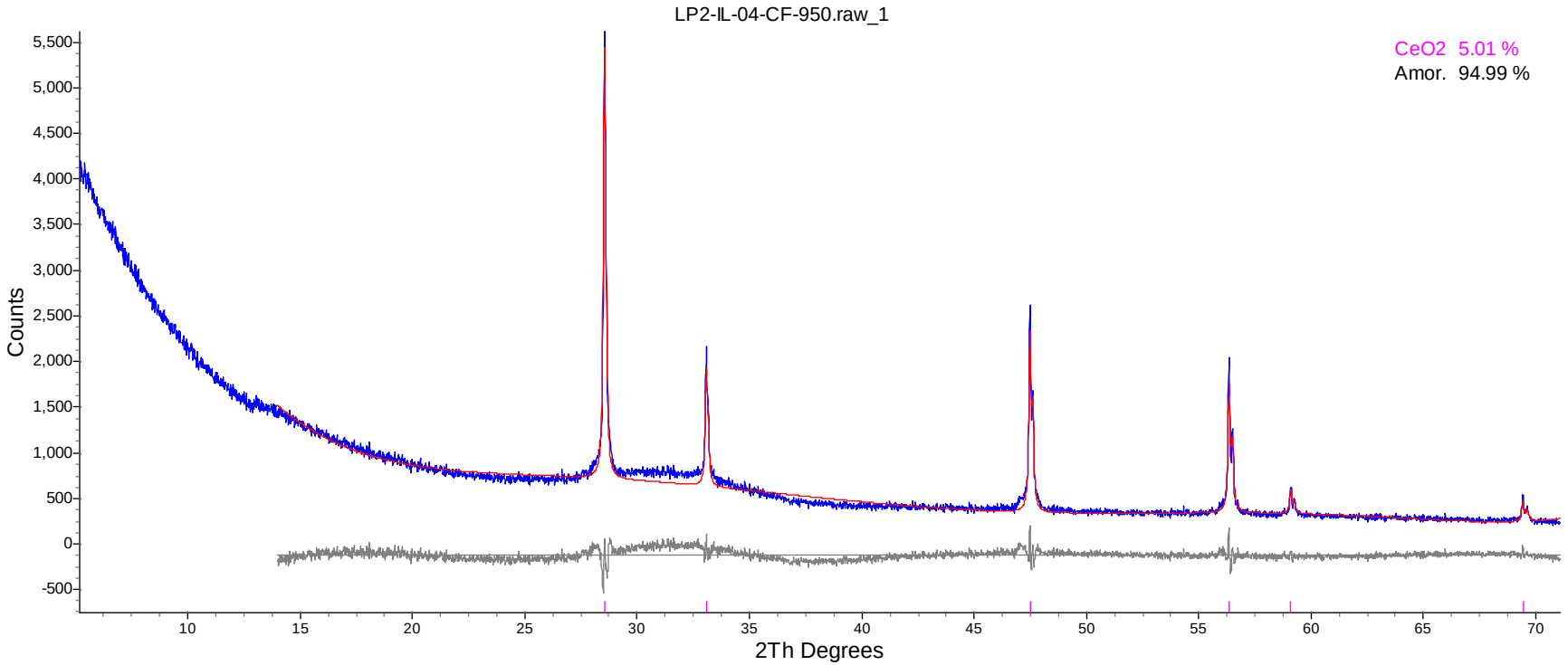


Figure F.4. XRD Spectrum of Heat-Treated Glass LP2-IL-04

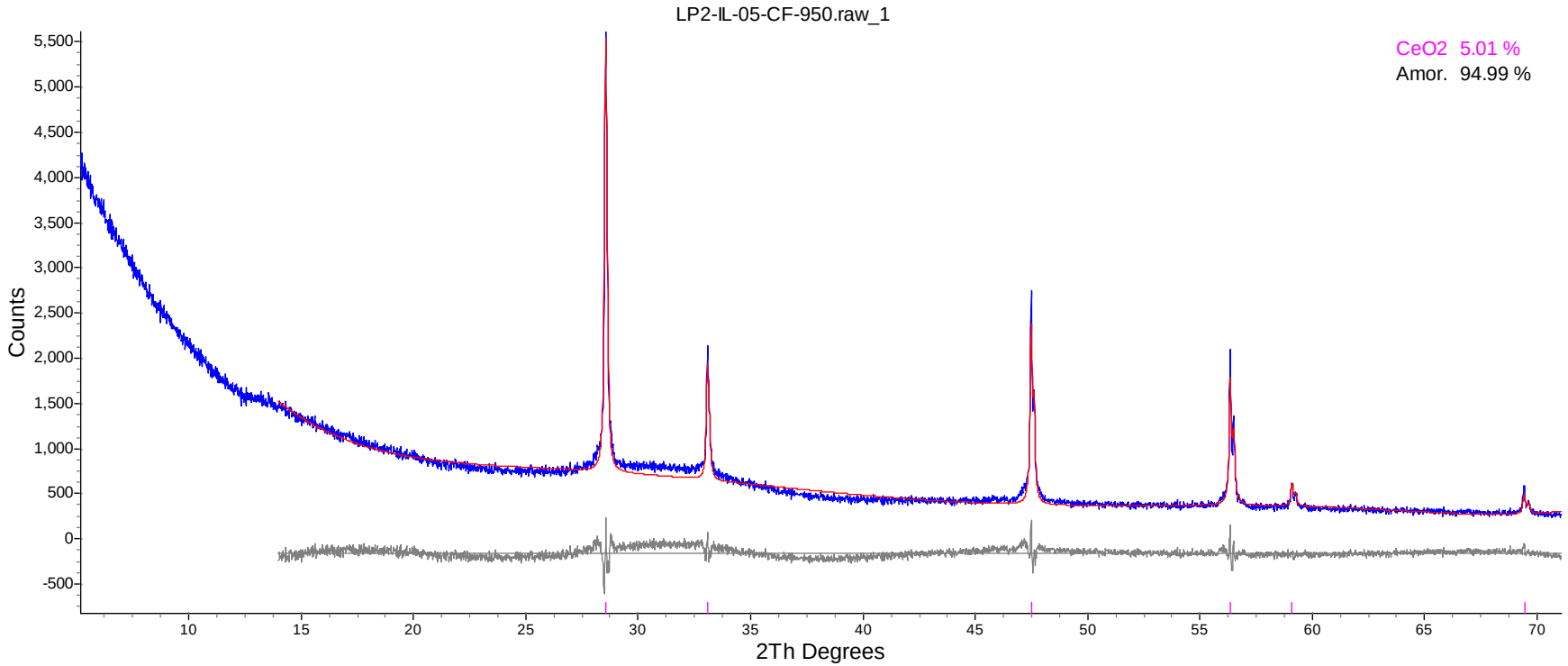


Figure F.5. XRD Spectrum of Heat-Treated Glass LP2-IL-05

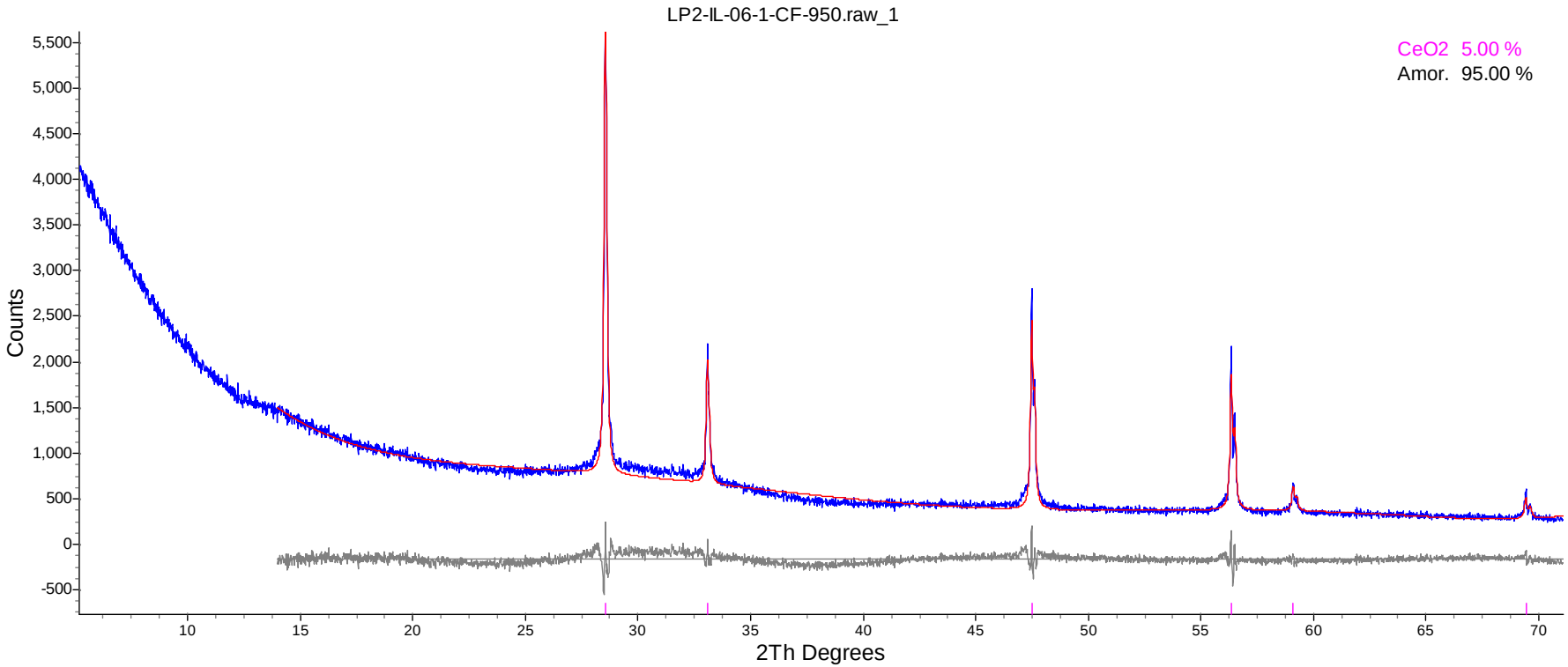


Figure F.6. XRD Spectrum of Heat-Treated Glass LP2-IL-06

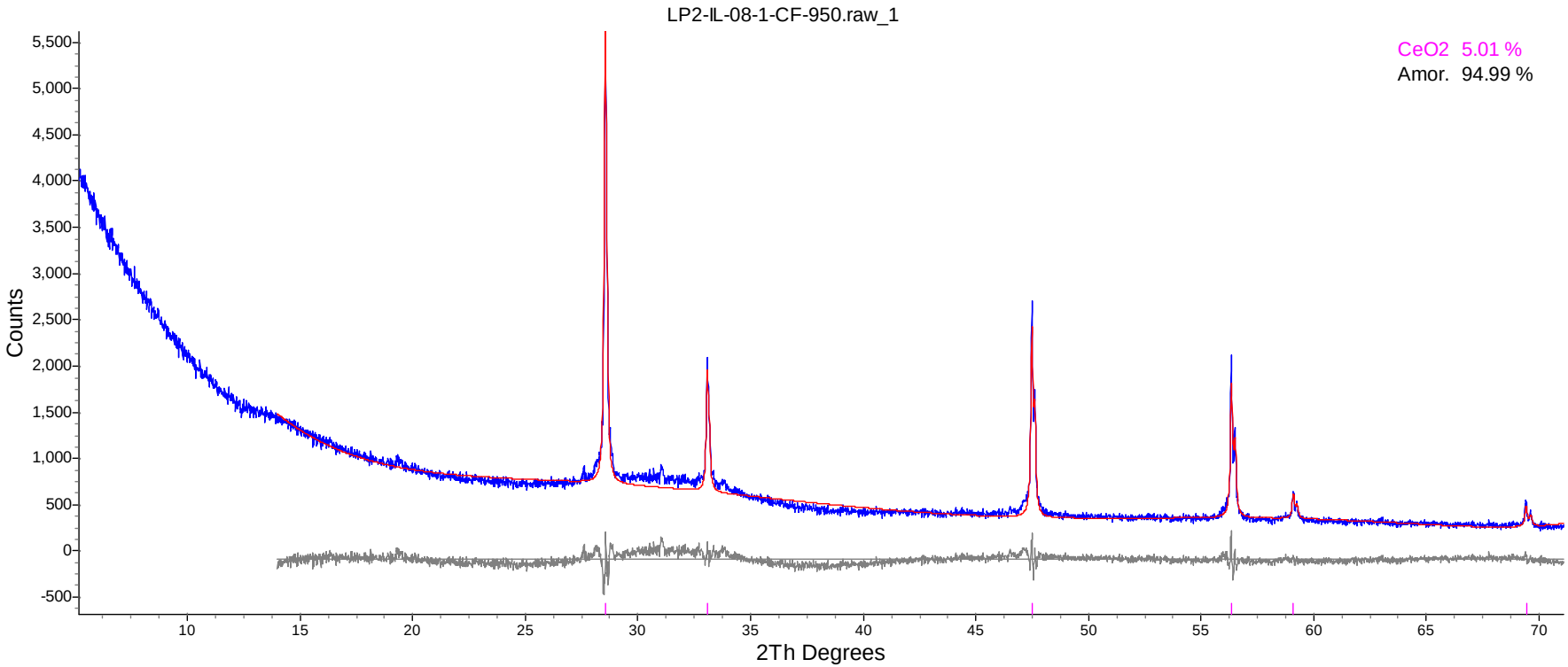


Figure F.7. XRD Spectrum of Heat-Treated Glass LP2-IL-08

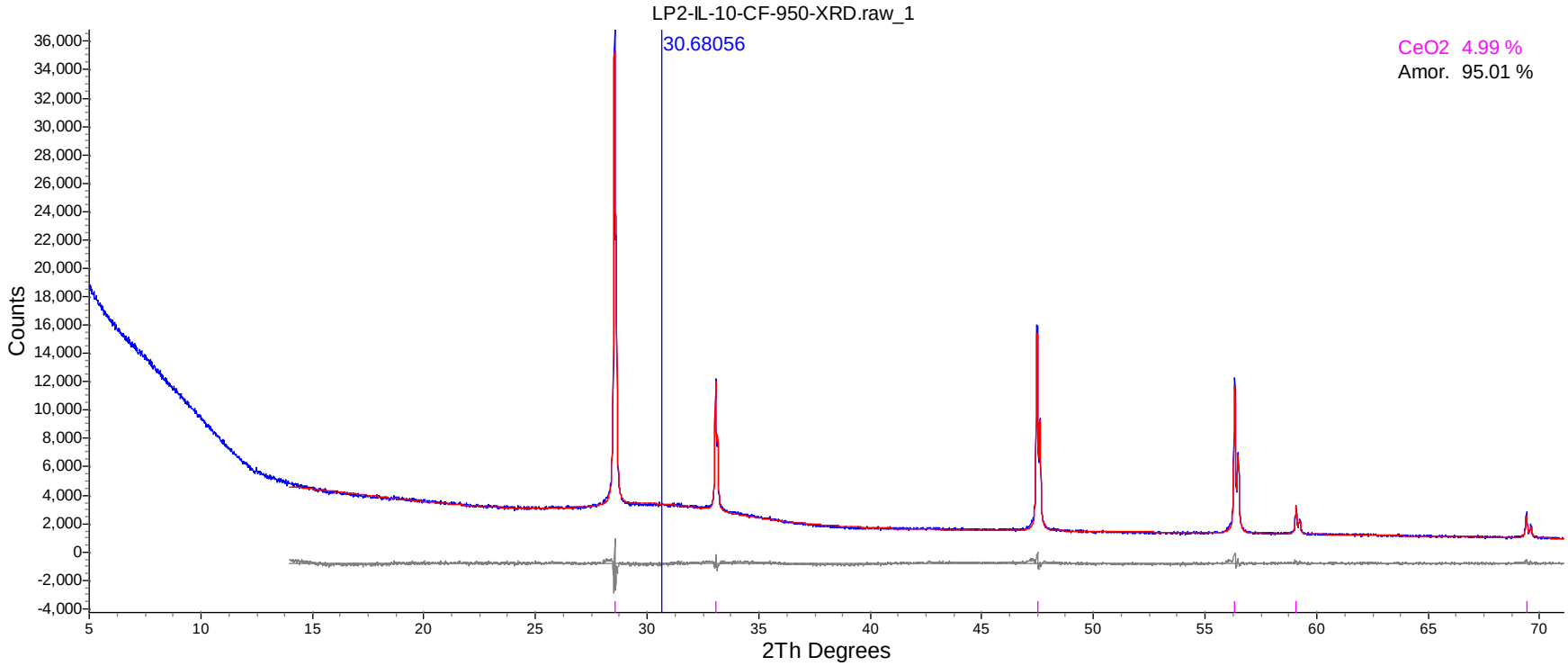


Figure F.8. XRD Spectrum of Heat-Treated Glass LP2-IL-10

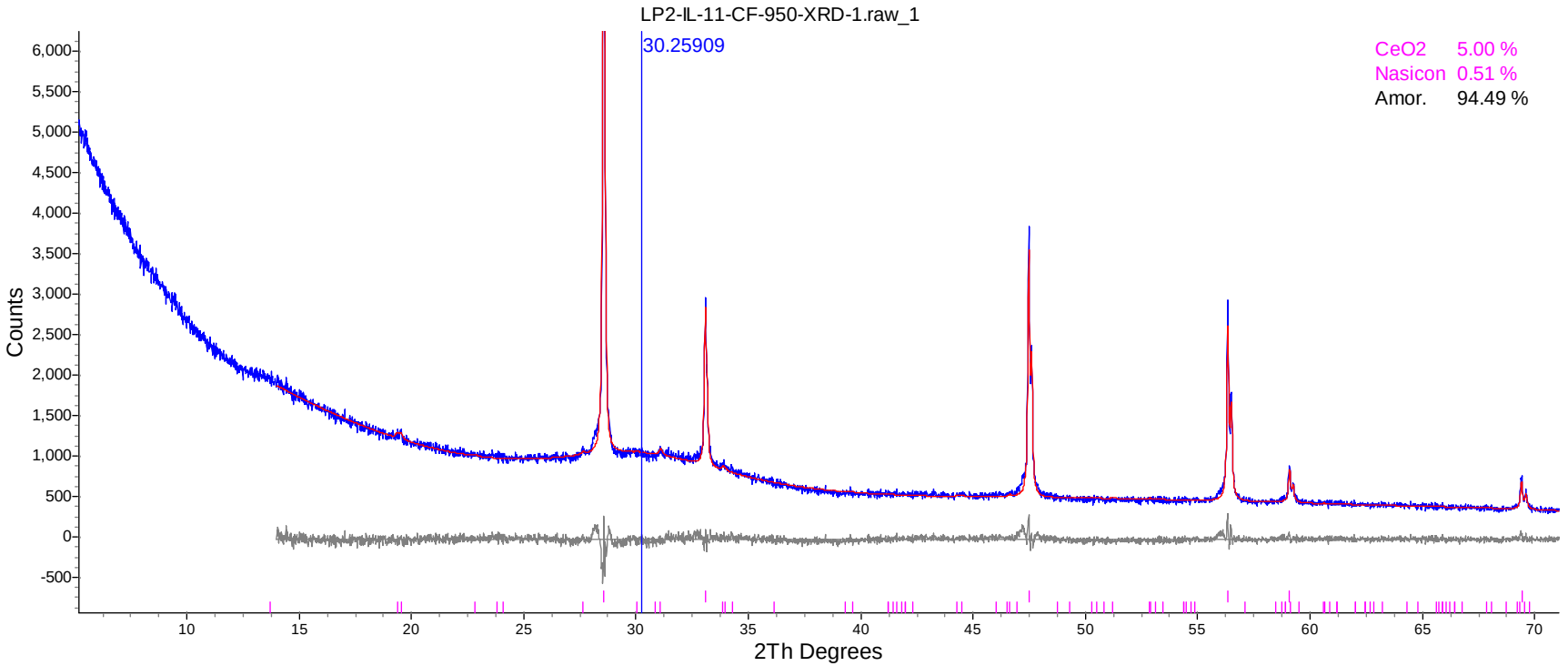


| Phase Name | Wt% of Spiked | Wt% in Spiked Sample | Wt% in Original Sample |
|---|---|---|---|
| $CeO_2$ | 4.999 | 4.999 | 0 |
| Nasicon | 0 | 0.512 | 0.539 |

Figure F.9. XRD Spectrum of Heat-Treated Glass LP2-IL-11

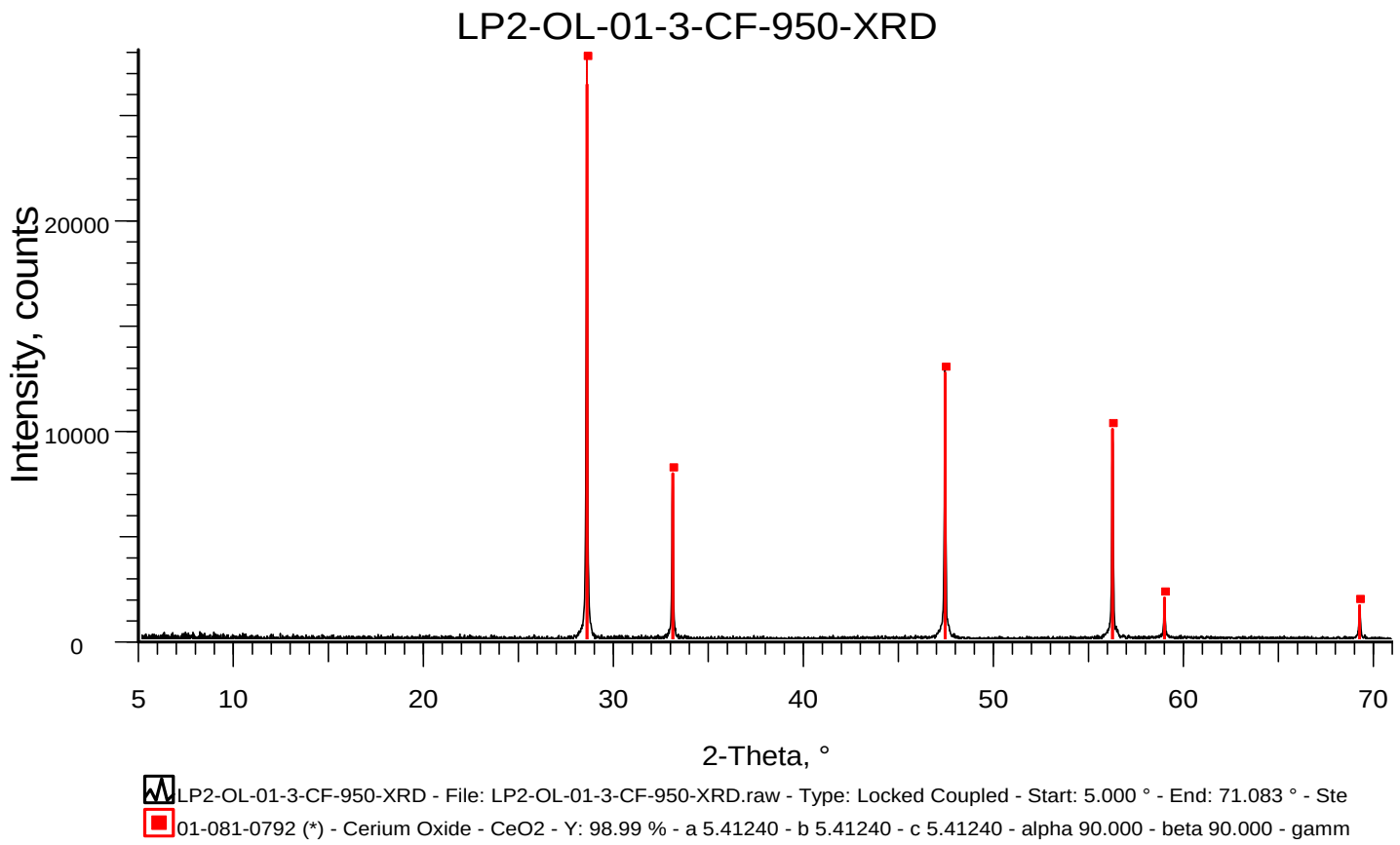


Figure F.10. XRD Spectrum of Heat-Treated Glass LP2-OL-01-3

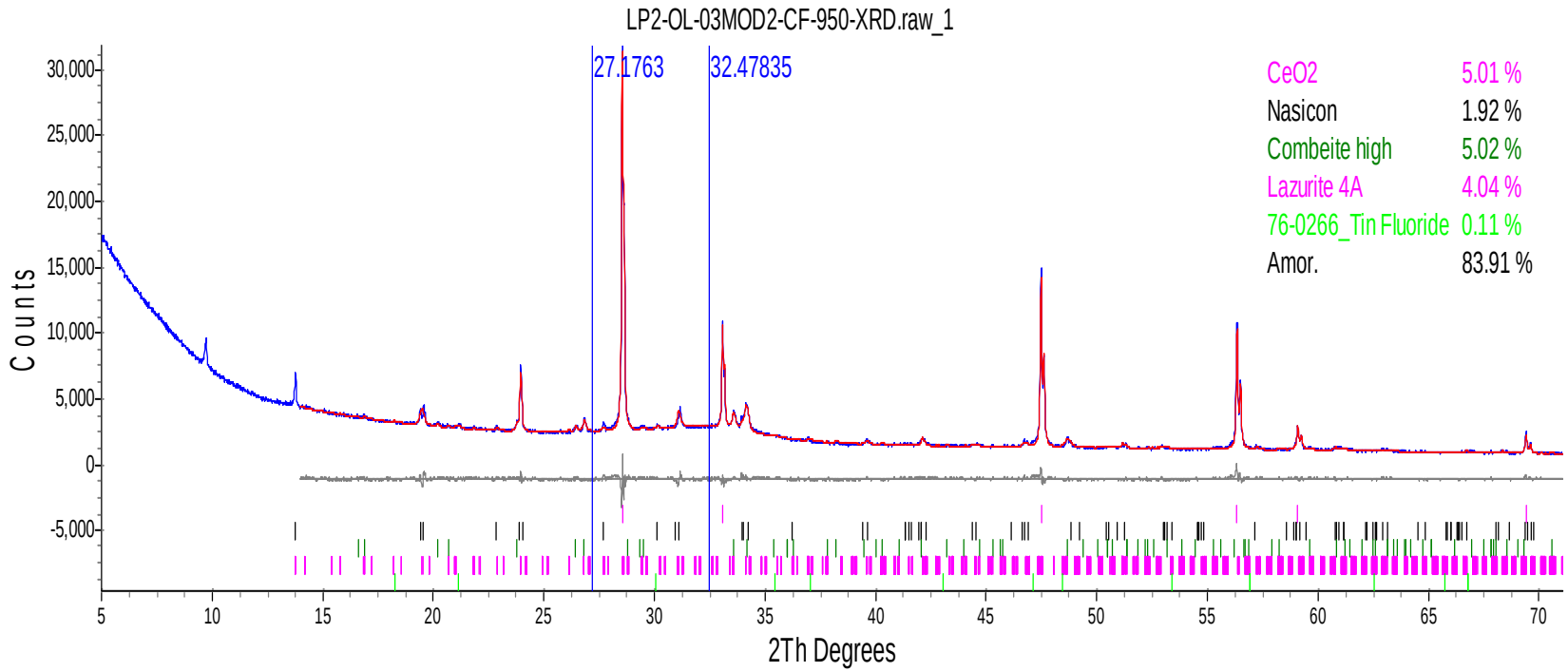


| Phase Name | Wt% of Spiked | Wt% in Spiked Sample | Wt% in Original Sample |
|---|---|---|---|
| $CeO_2$ | 5.011 | 5.011 | 0 |
| Nasicon | 0 | 1.916 | 2.017 |
| Combeite high | 0 | 5.023 | 5.288 |
| Lazurite 4A | 0 | 4.036 | 4.248 |
| Tin Fluoride | 0 | 0.109 | 0.114 |

Figure F.11. XRD Spectrum of Heat-Treated Glass LP2-OL-03-MOD2

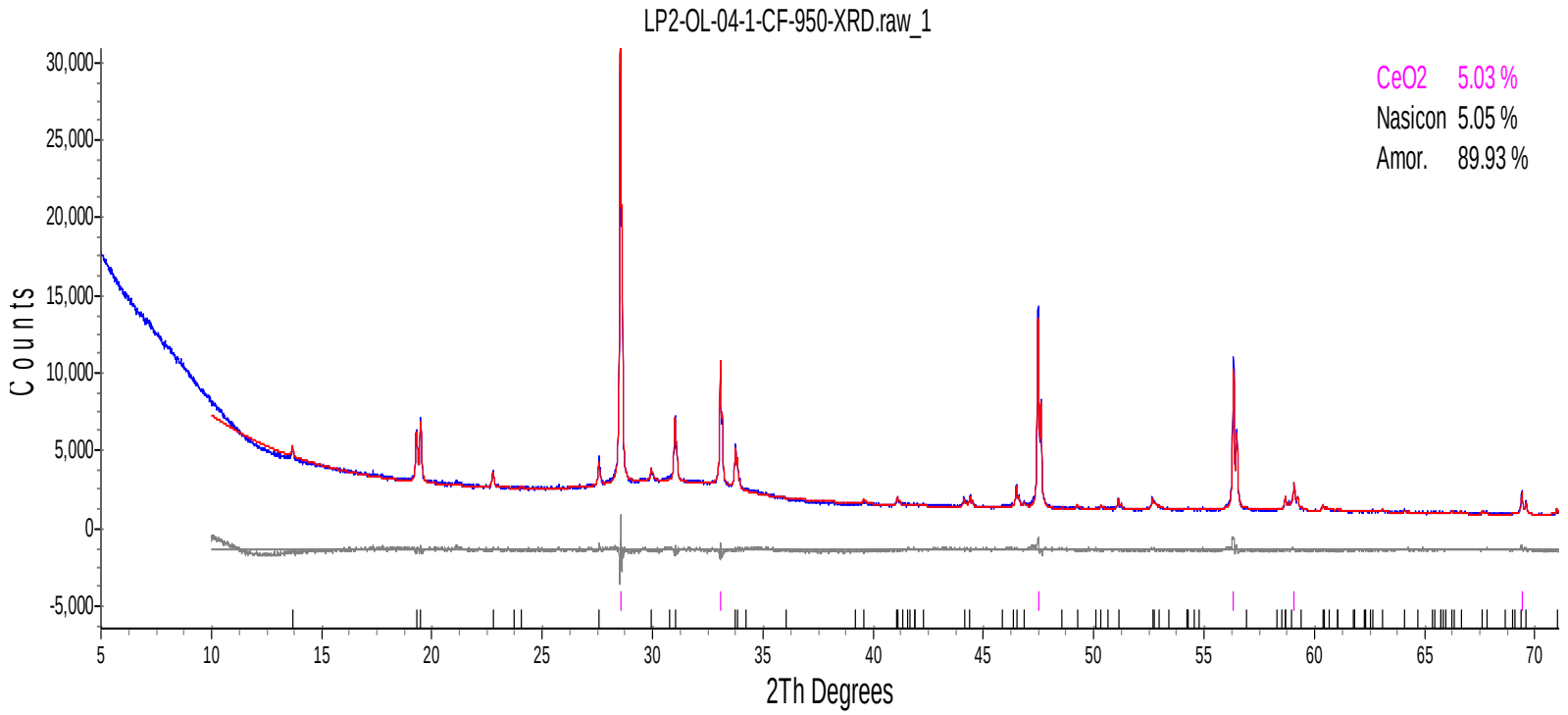


| Phase Name | Wt% of Spiked | Wt% in Spiked Sample | Wt% in Original Sample |
|---|---|---|---|
| $CeO_2$ | 5.025 | 5.025 | 0 |
| Nasicon | 0 | 5.047 | 5.314 |

Figure F.12. XRD Spectrum of Heat-Treated Glass LP2-OL-04-1

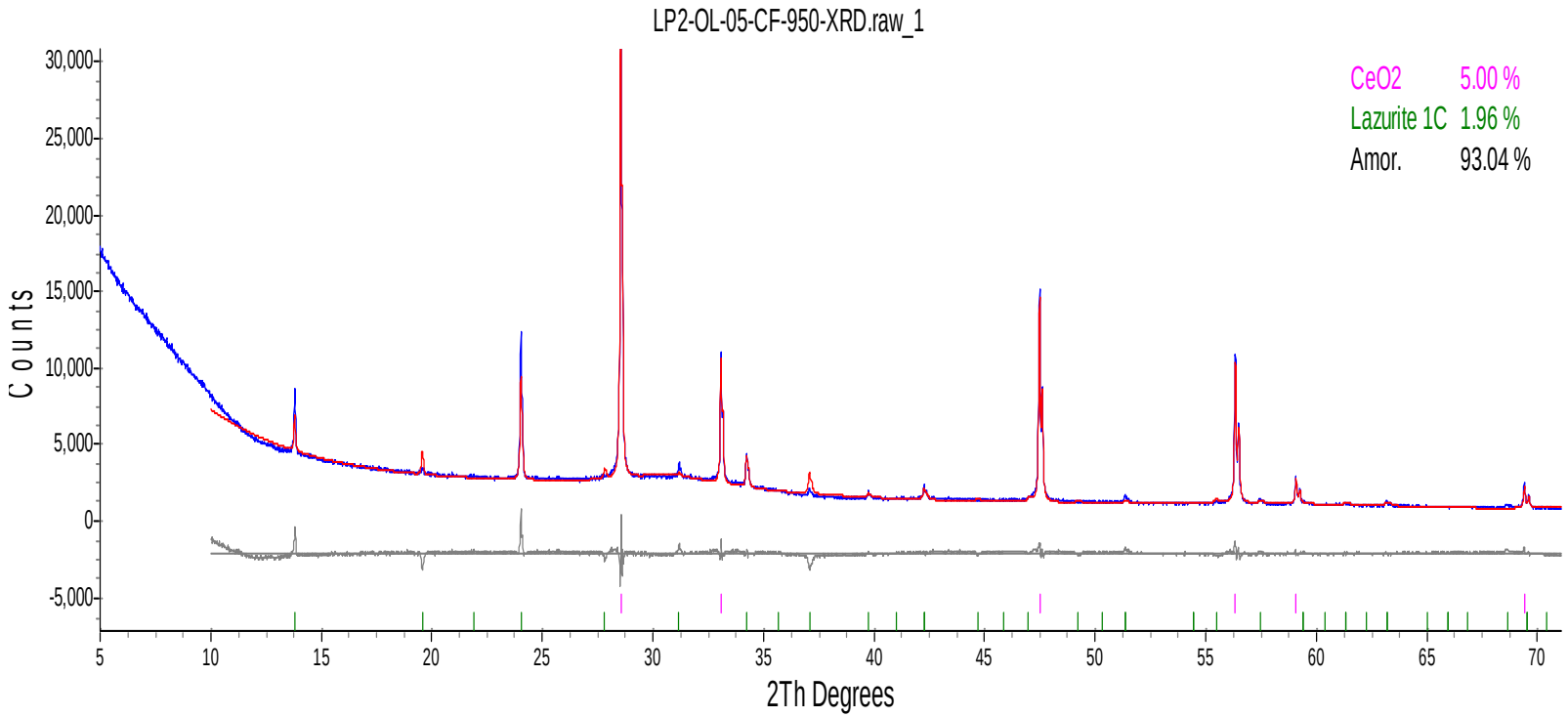


| Phase Name | Wt% of Spiked | Wt% in Spiked Sample | Wt% in Original Sample |
|---|---|---|---|
| $CeO_2$ | 5.001 | 5.001 | 0 |
| Lazurite 1C | 0 | 1.961 | 2.065 |

Figure F.13. XRD Spectrum of Heat-Treated Glass LP2-OL-05

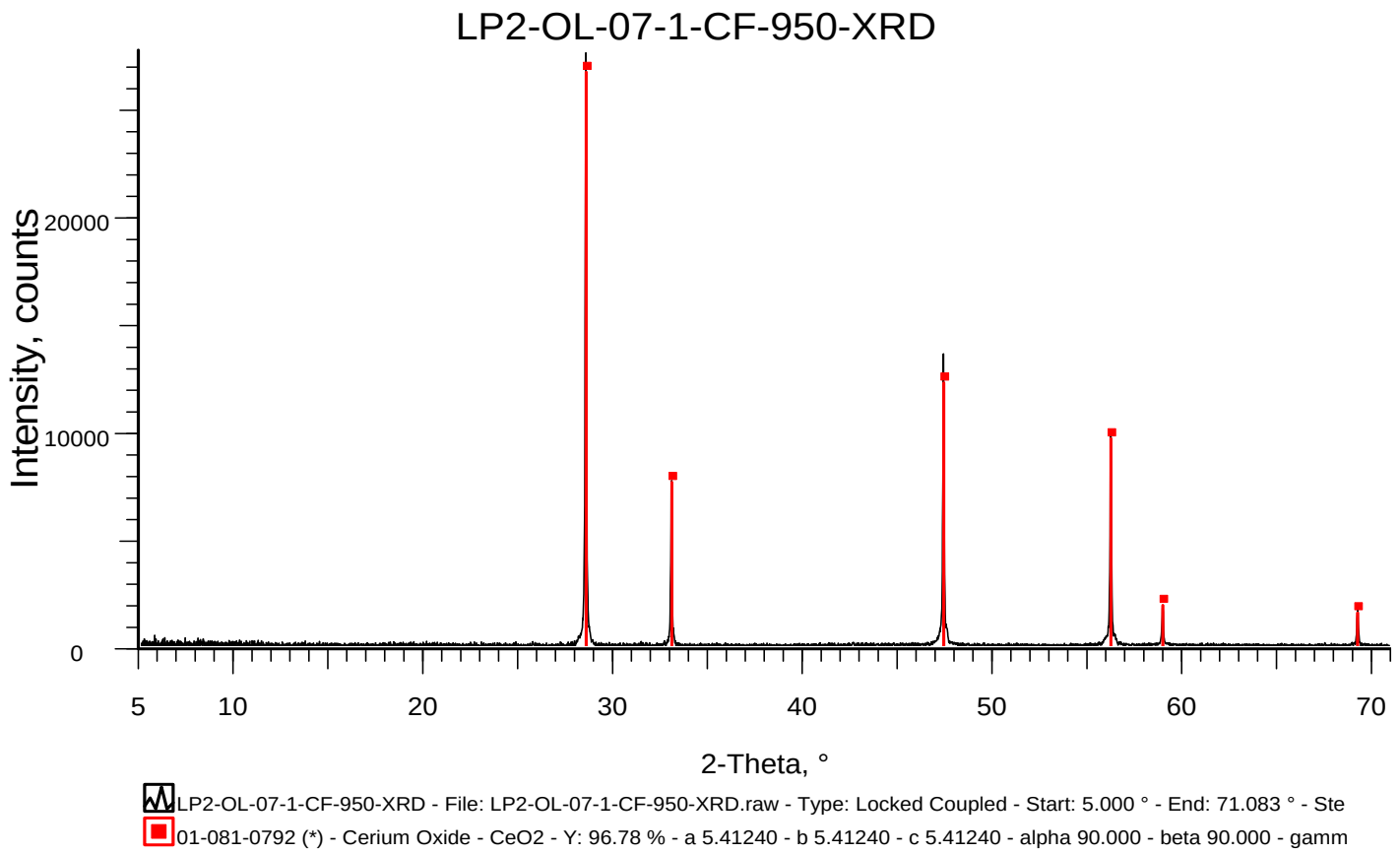


Figure F.14. XRD Spectrum of Heat-Treated Glass LP2-OL-07-1

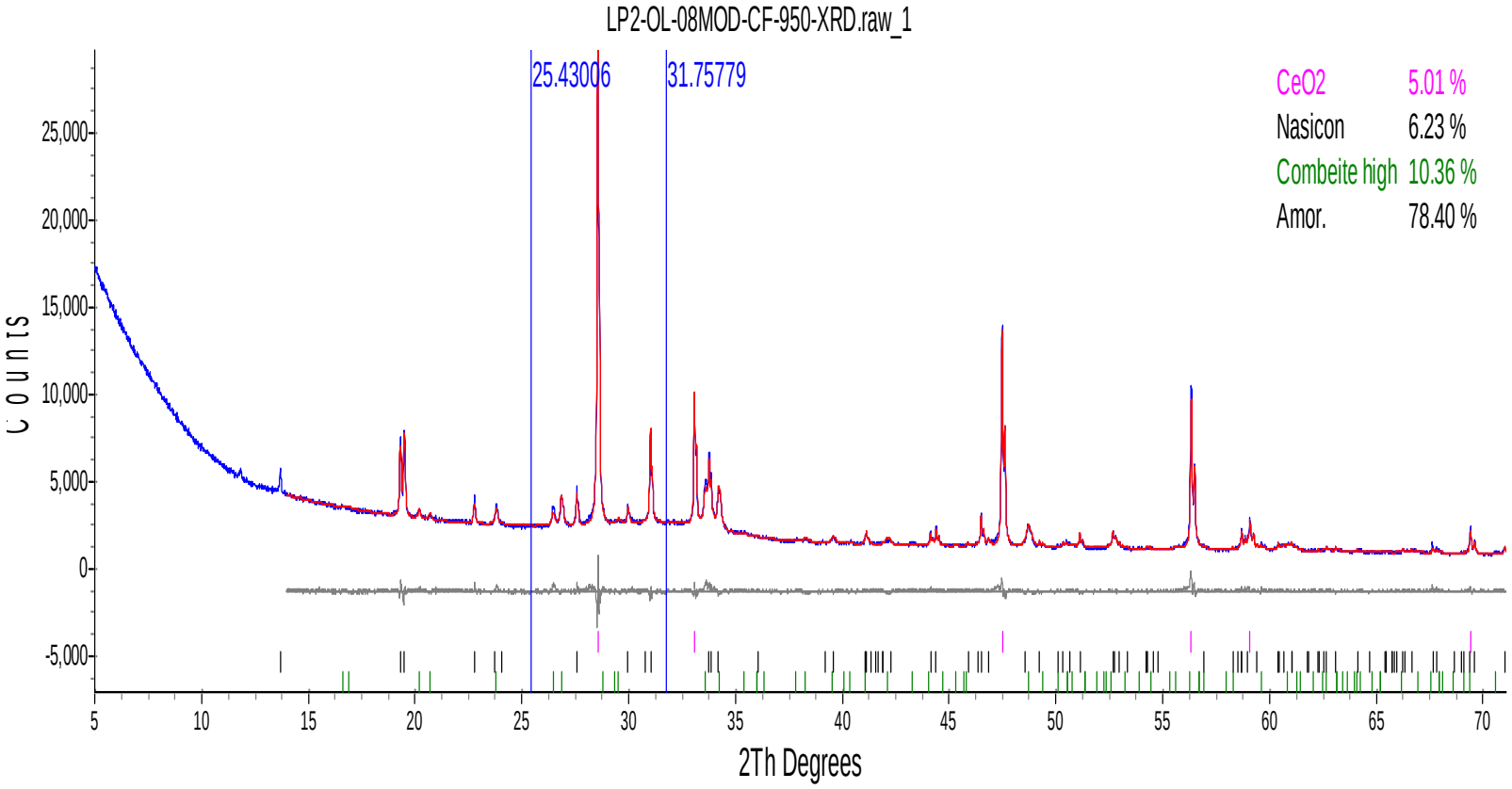


| Phase Name | Wt% of Spiked | Wt% in Spiked Sample | Wt% in Original Sample |
|---|---|---|---|
| $CeO_2$ | 5.011 | 5.011 | 0 |
| Nasicon | 0 | 6.231 | 6.560 |
| Combeite high | 0 | 10.357 | 10.903 |

Figure F.15. XRD Spectrum of Heat-Treated Glass LP2-OL-08 MOD

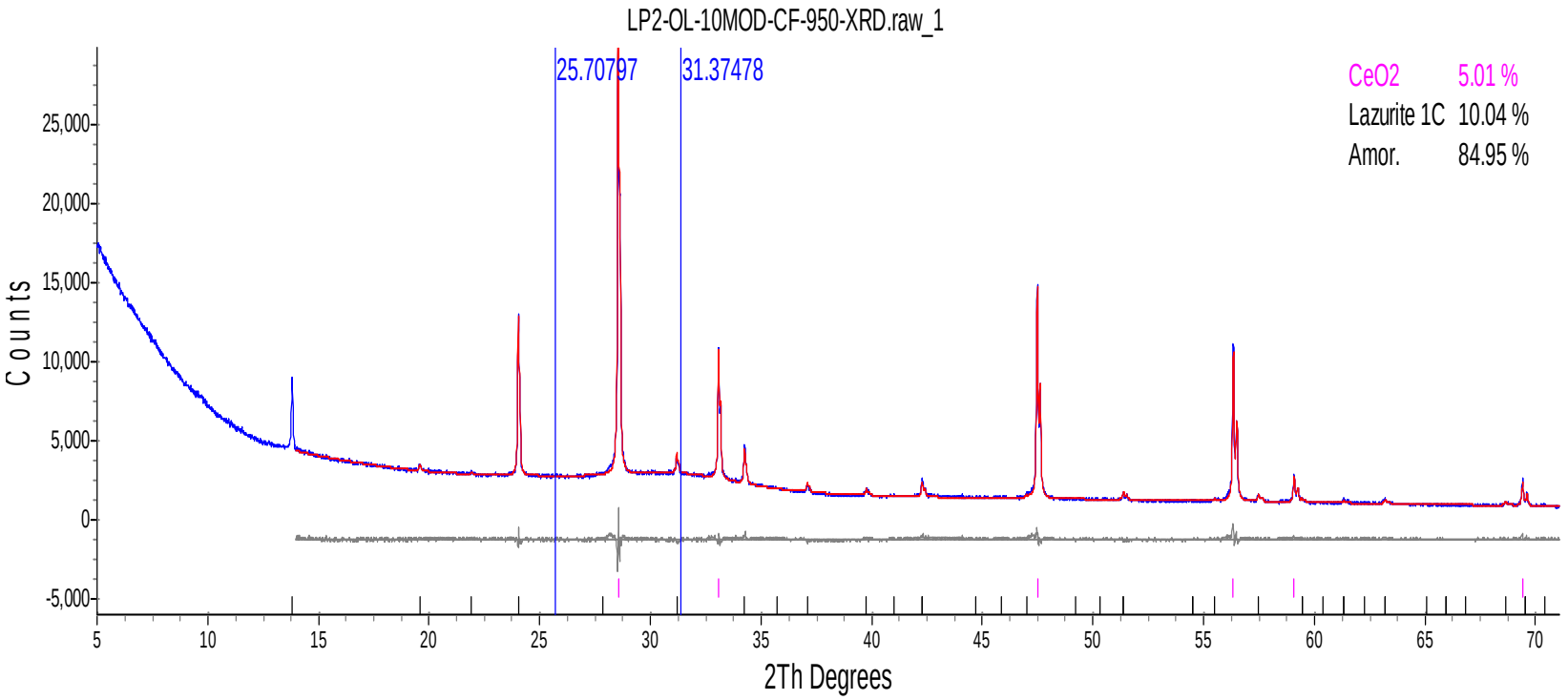


| Phase Name | Wt% of Spiked | Wt% in Spiked Sample | Wt% in Original Sample |
|---|---|---|---|
| $CeO_2$ | 5.006 | 5.006 | 0 |
| Lazurite 1C | 0 | 10.040 | 10.569 |

Figure F.16. XRD Spectrum of Heat-Treated Glass LP2-OL-10 MOD

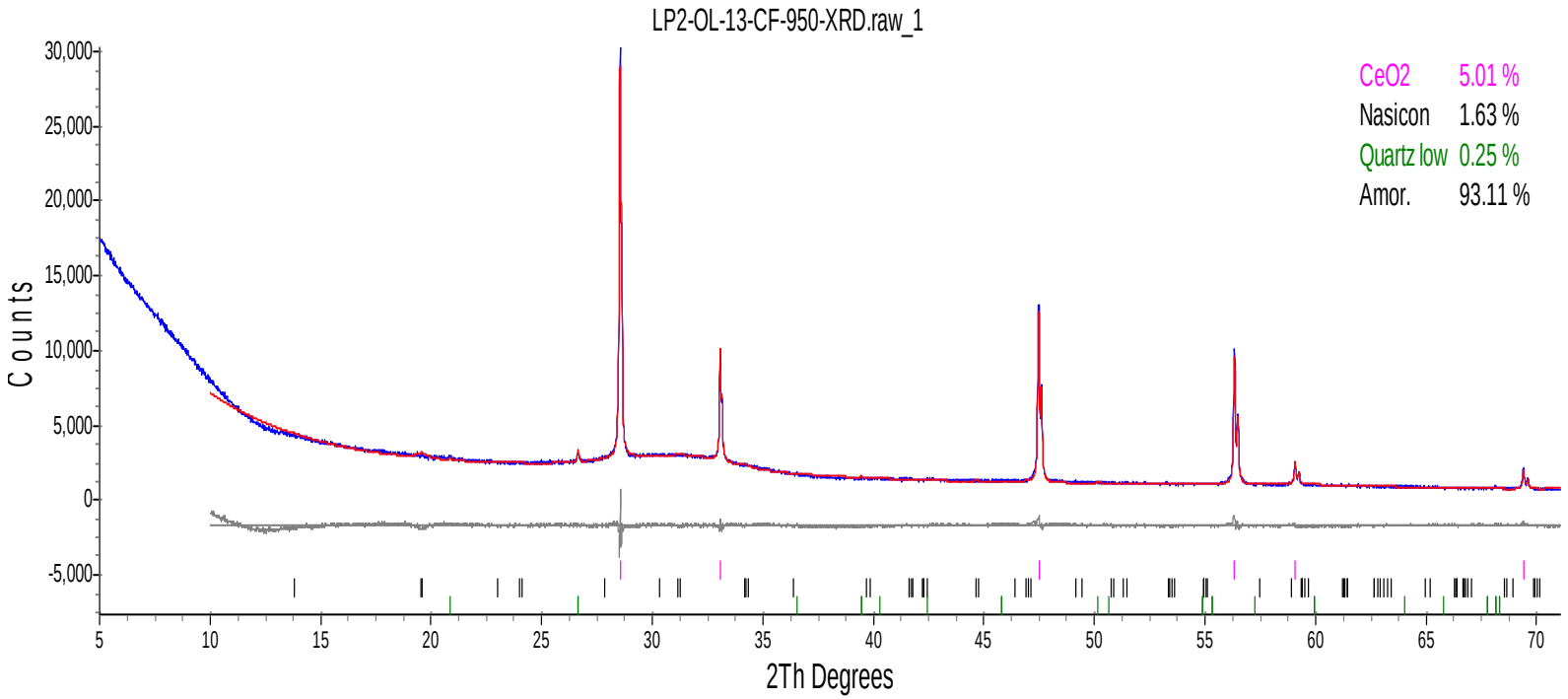


| Phase Name | Wt% of Spiked | Wt% in Spiked Sample | Wt% in Original Sample |
|---|---|---|---|
| $CeO_2$ | 5.008 | 5.008 | 0 |
| Nasicon | 0 | 1.634 | 1.720 |
| Quartz low | 0 | 0.248 | 0.261 |

Figure F.17. XRD Spectrum of Heat-Treated Glass LP2-OL-13

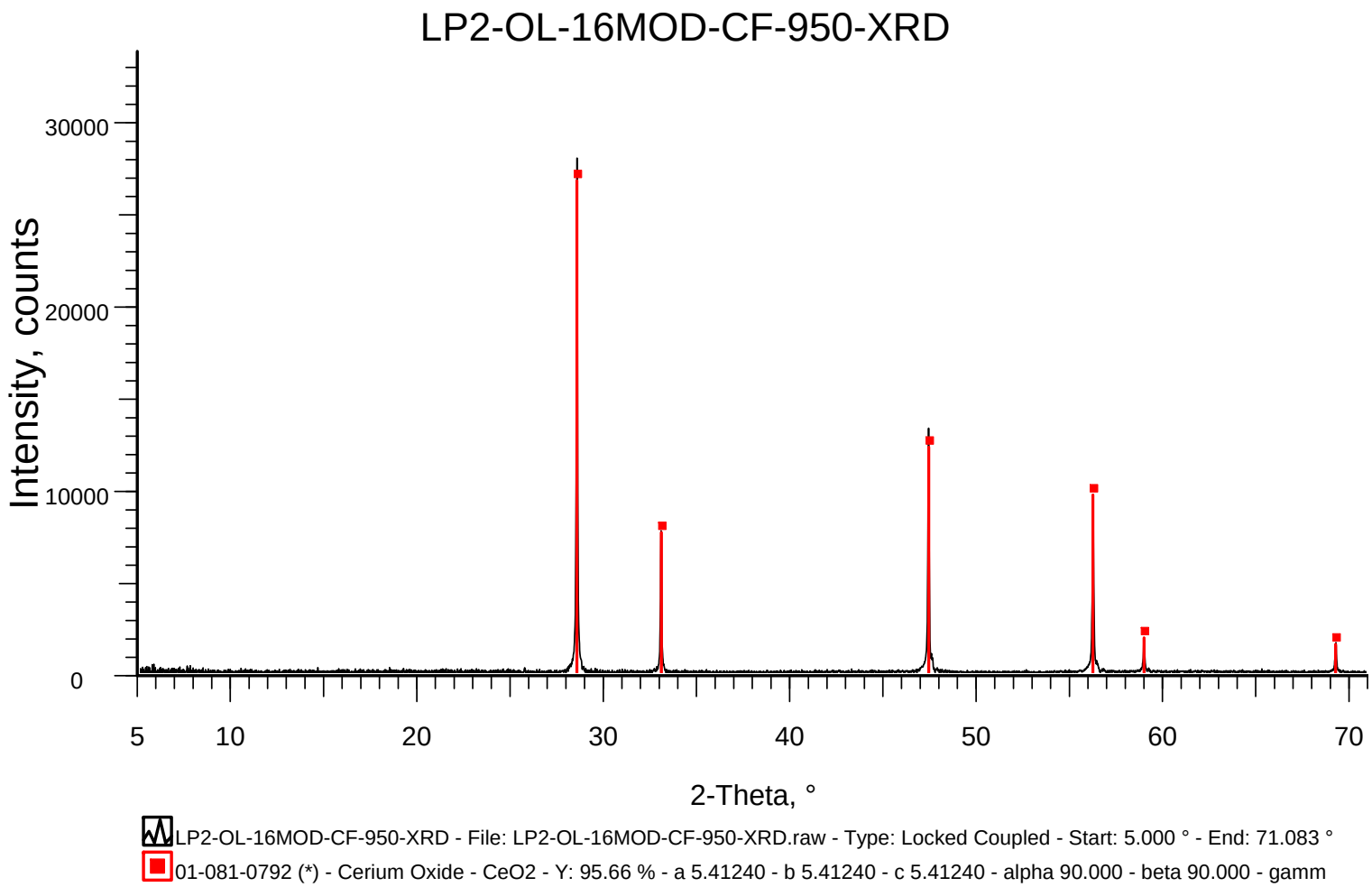


Figure F.18. XRD Spectrum of Heat-Treated Glass LP2-OL-16 MOD

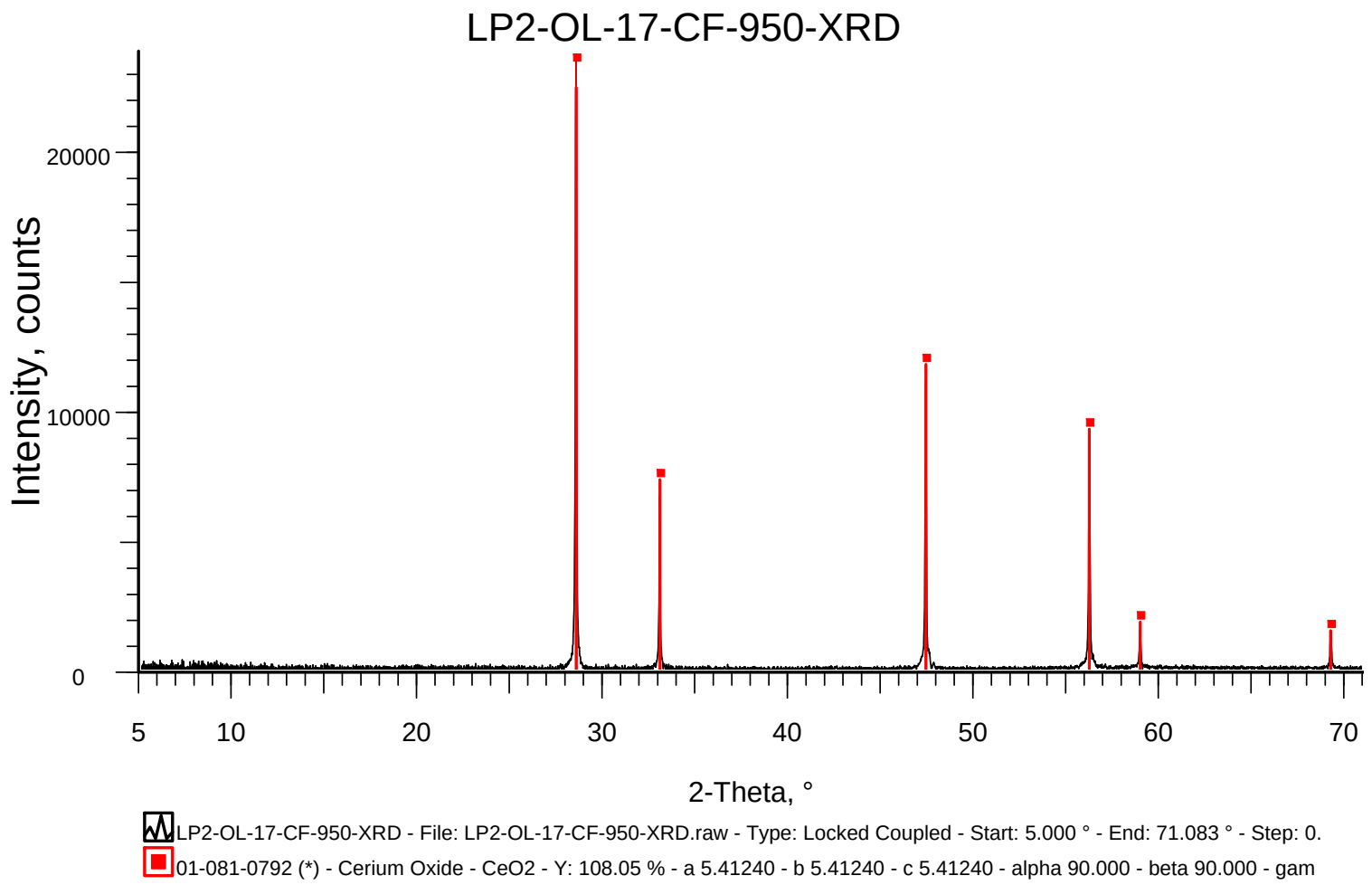


Figure F.19. XRD Spectrum of Heat-Treated Glass LP2-OL-17

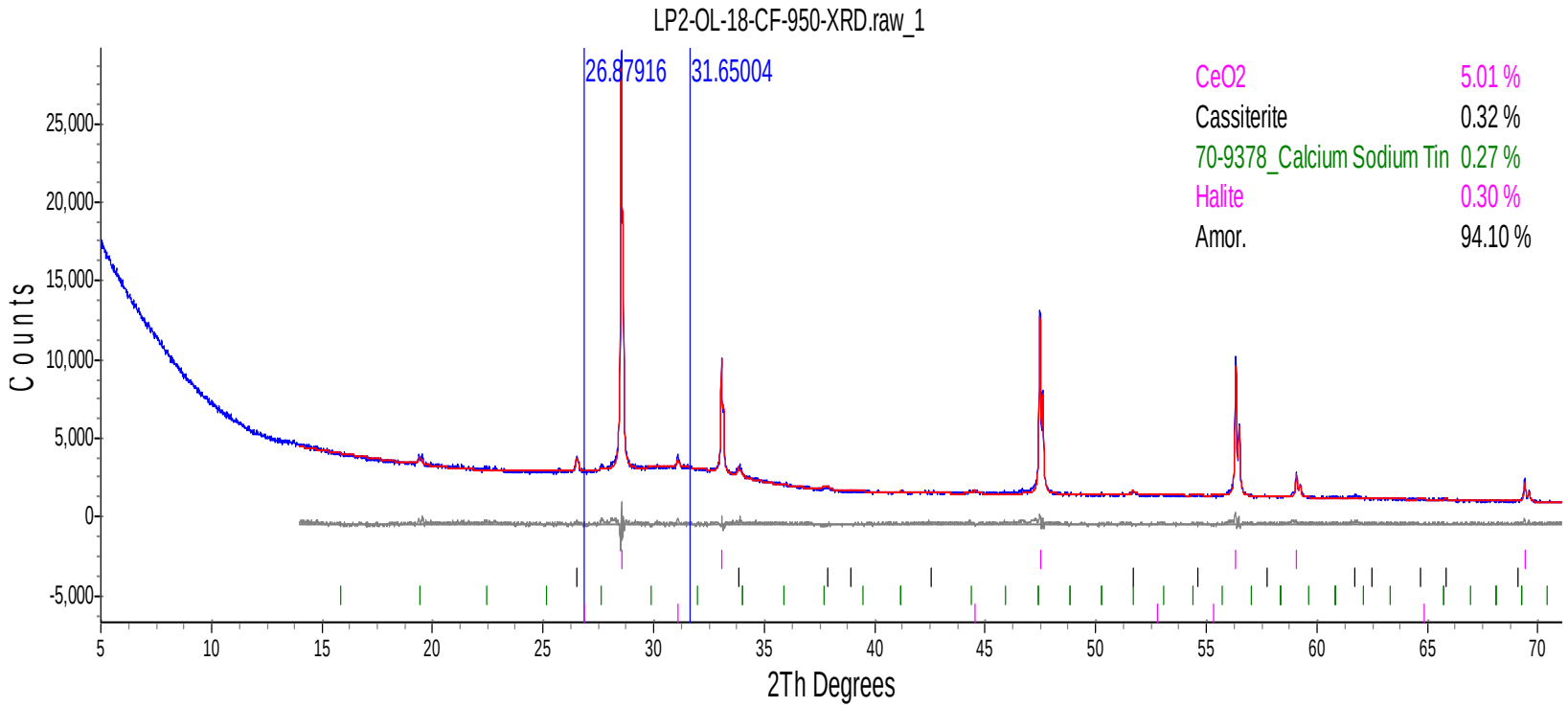


| Phase Name | Wt% of Spiked | Wt% in Spiked Sample | Wt% in Original Sample |
|---|---|---|---|
| $CeO_2$ | 5.010 | 5.010 | 0 |
| Cassiterite | 0 | 0.319 | 0.336 |
| Calcium Sodium Tin | 0 | 0.272 | 0.287 |
| Halite | 0 | 0.297 | 0.313 |

Figure F.20. XRD Spectrum of Heat-Treated Glass LP2-OL-18

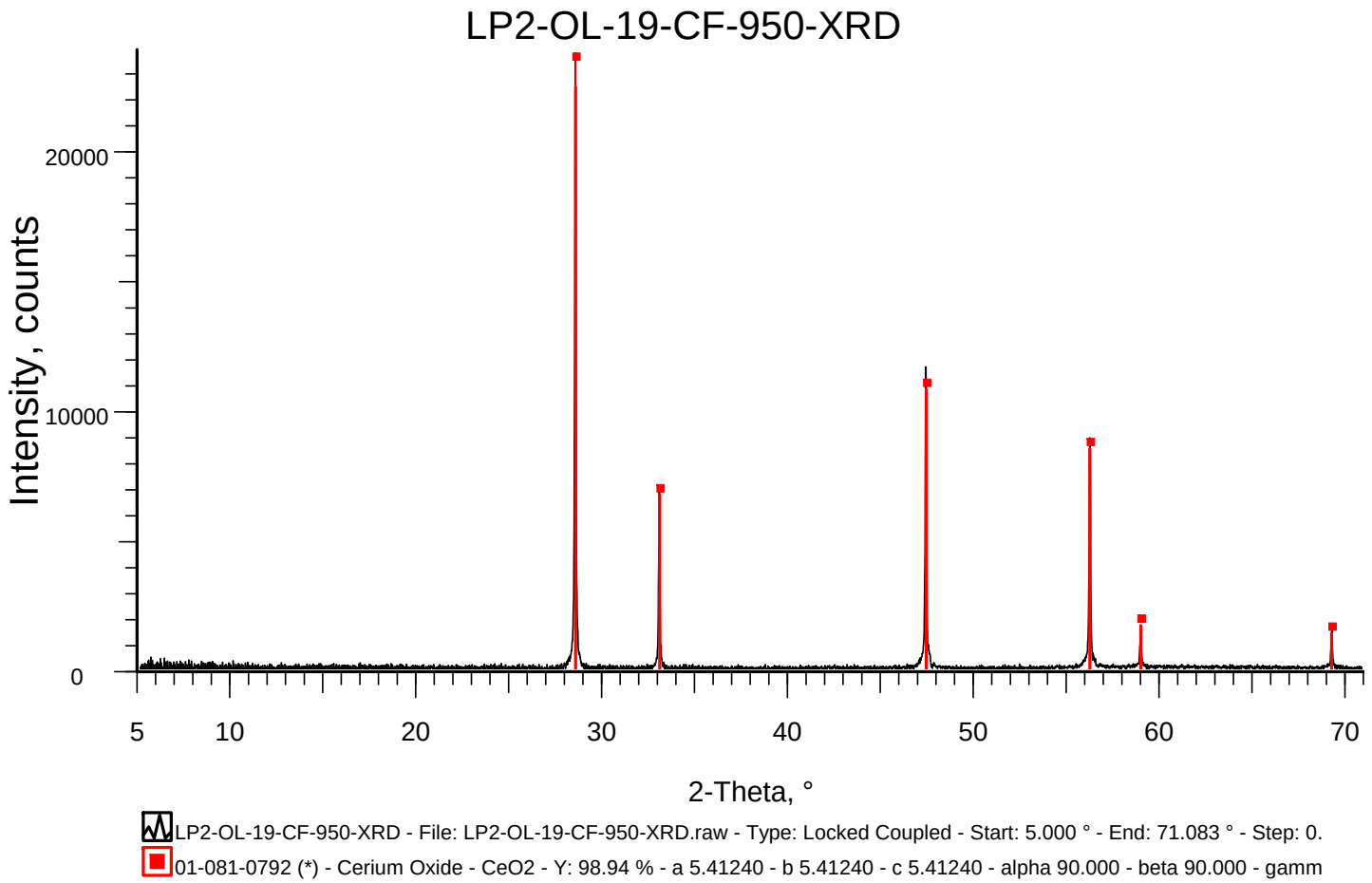


Figure F.21. XRD Spectrum of Heat-Treated Glass LP2-OL-19

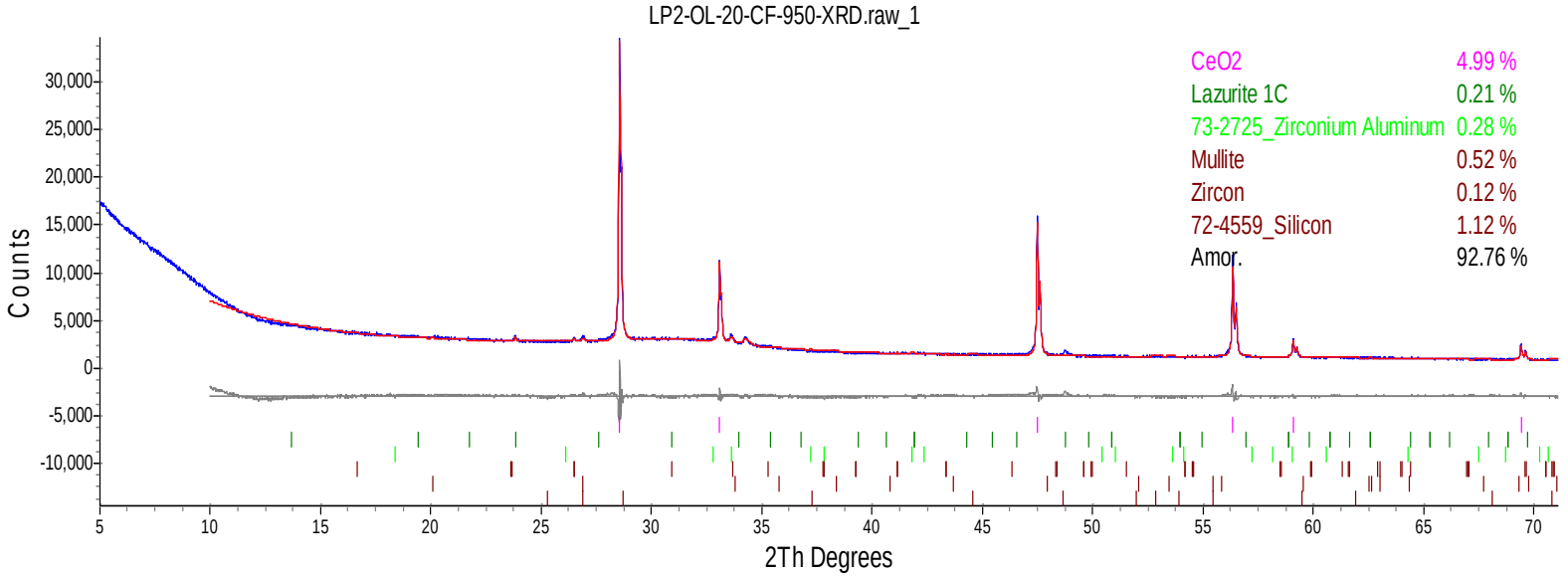


| Phase Name | Wt% of Spiked | Wt% in Spiked Sample | Wt% in Original Sample |
|---|---|---|---|
| $CeO_2$ | 4.985 | 4.985 | 0 |
| Lazurite 1C | 0 | 0.213 | 0.224 |
| Zirconium Aluminum | 0 | 0.277 | 0.292 |
| Mullite | 0 | 0.517 | 0.544 |
| Zircon | 0 | 0.125 | 0.131 |
| Silicon | 0 | 1.121 | 1.180 |

Figure F.22. XRD Spectrum of Heat-Treated Glass LP2-OL-20

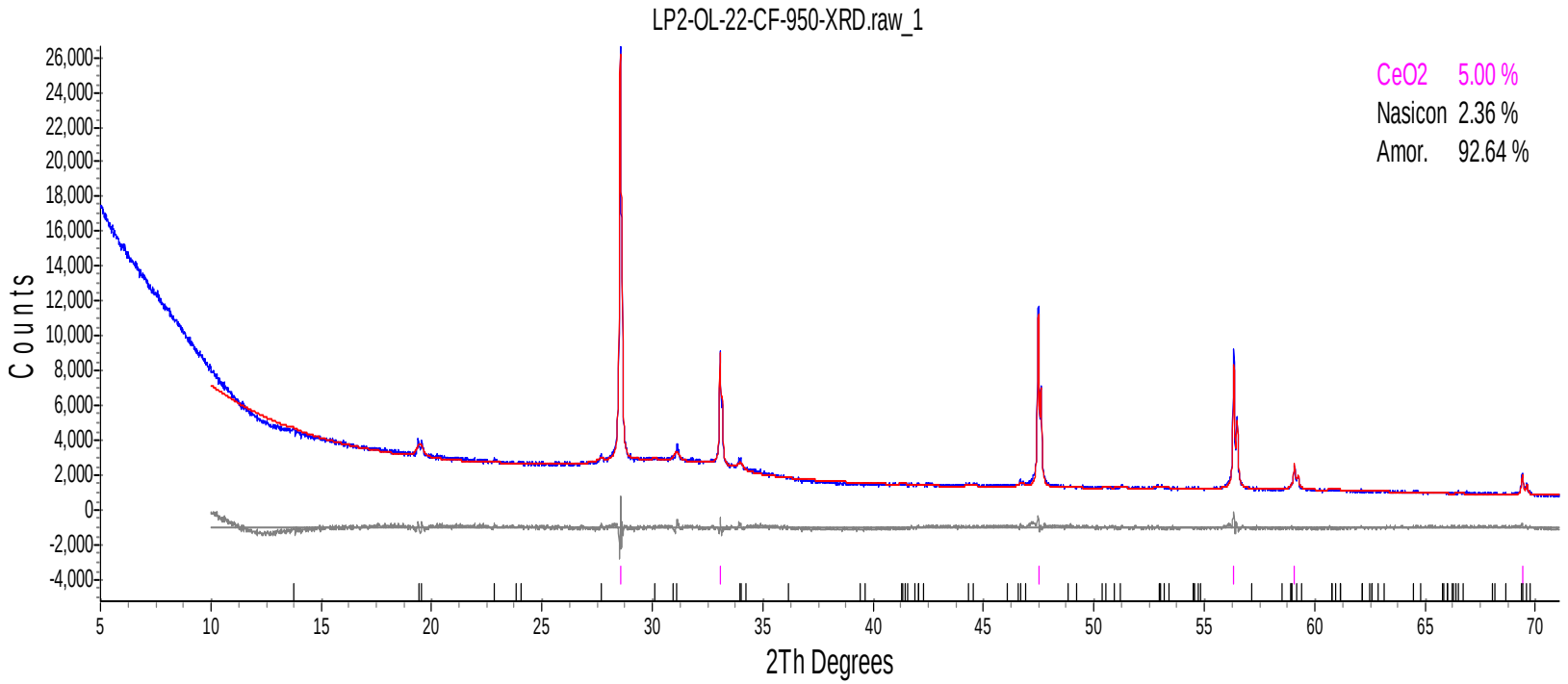


| Phase Name | Wt% of Spiked | Wt% in Spiked Sample | Wt% in Original Sample |
|---|---|---|---|
| $CeO_2$ | 5.004 | 5.004 | 0 |
| Nasicon | 0 | 2.358 | 2.483 |

Figure F.23. XRD Spectrum of Heat-Treated Glass LP2-OL-22

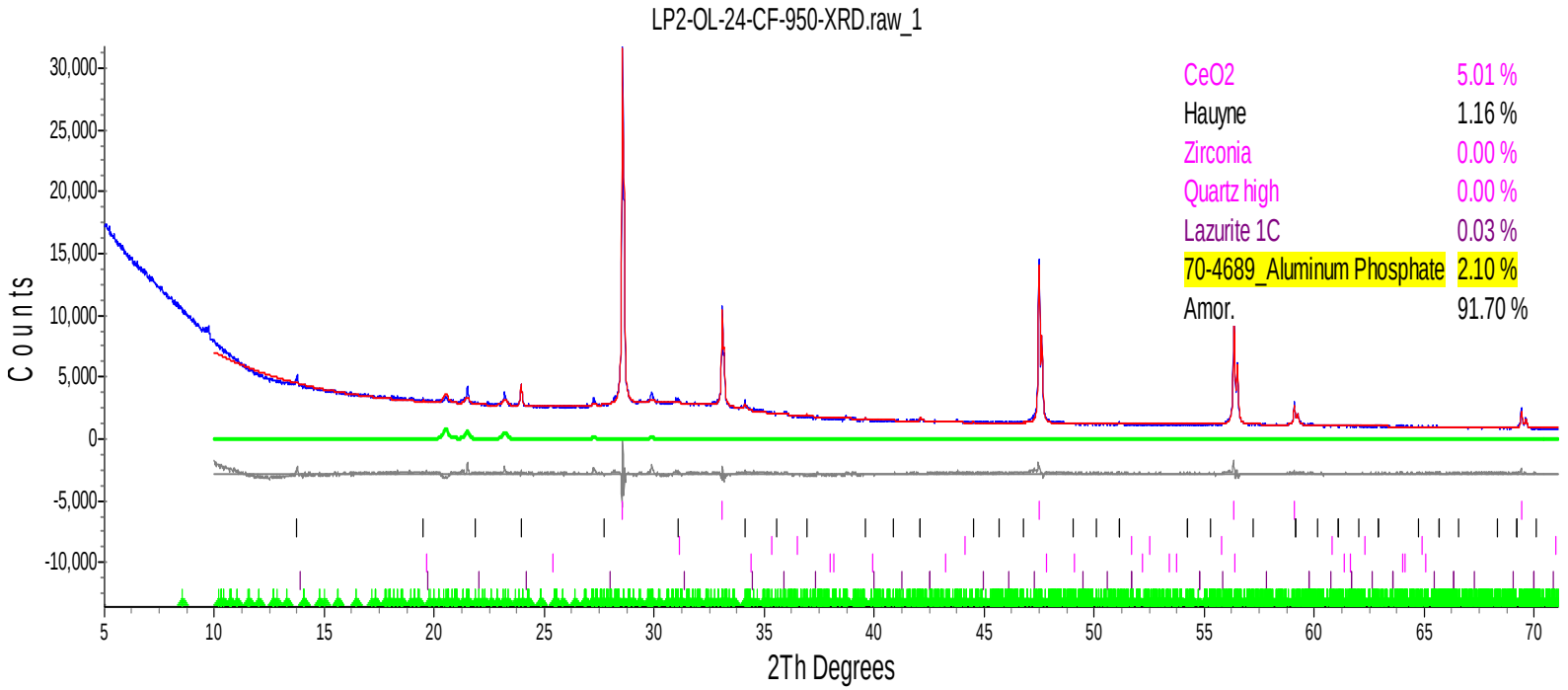


| Phase Name | Wt% of Spiked | Wt% in Spiked Sample | Wt% in Original Sample |
|---|---|---|---|
| $CeO_2$ | 5.007 | 5.007 | 0 |
| Hauyne | 0 | 1.157 | 1.218 |
| Lazurite 1C | 0 | 0.031 | 0.033 |
| Aluminum Phosphate | 0 | 2.105 | 2.216 |

Figure F.24. XRD Spectrum of Heat-Treated Glass LP2-OL-24

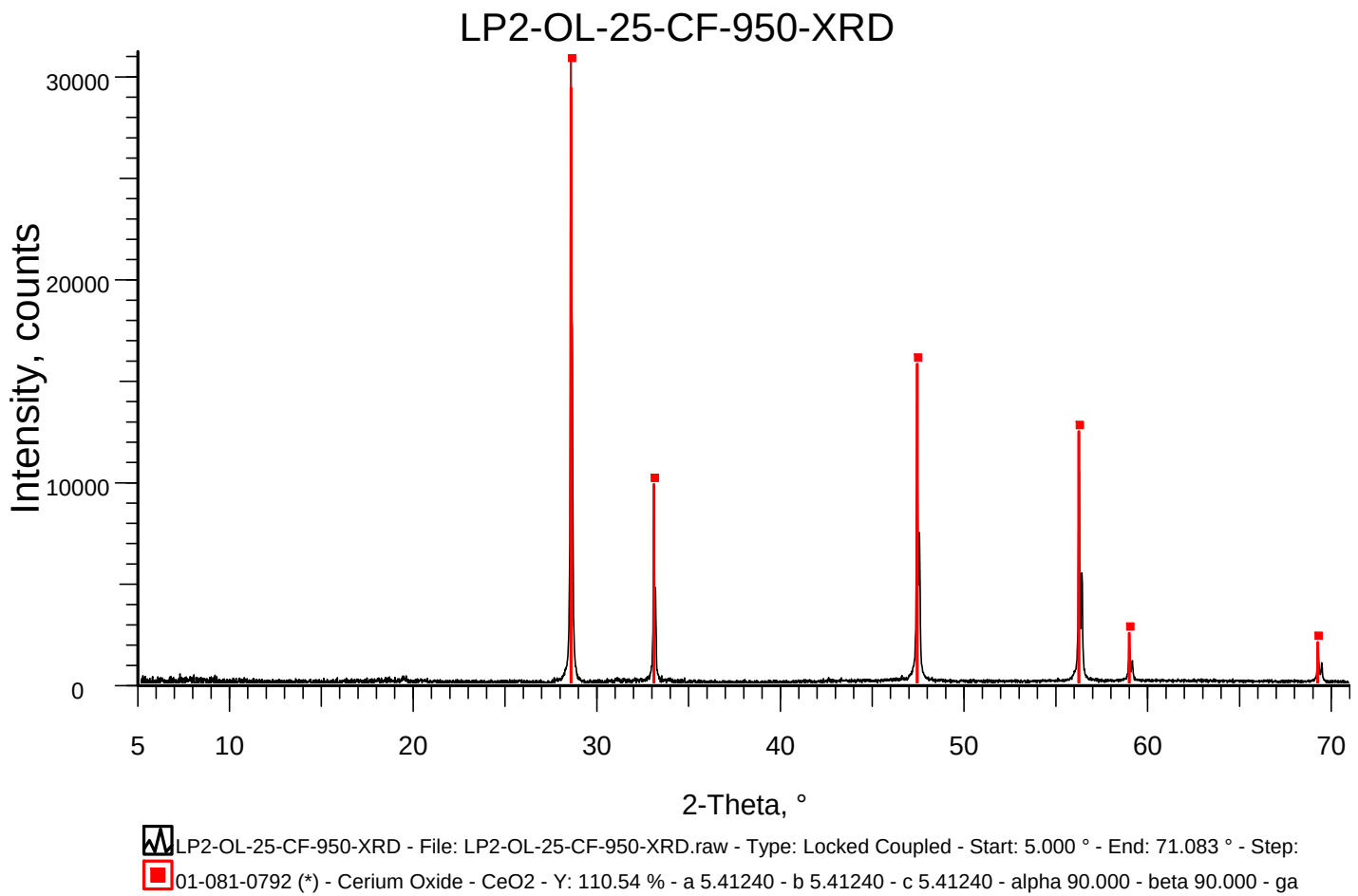


Figure F.25. XRD Spectrum of Heat-Treated Glass LP2-OL-25

# Appendix G – Canister Centerline Cooling (CCC) Glass Photographs

This appendix contains photos of Phase 2 enhanced LAW glasses after they were CCC heat-treated beginning at the glass melting temperature, which is indicated in the picture title. Each showed different responses to the CCC heat-treatment as indicated by these photos.


Figure G.1. Glass LP2-IL-01 after CCC Beginning at 1150 °C both Glass (top) and Magnified 50X (bottom)

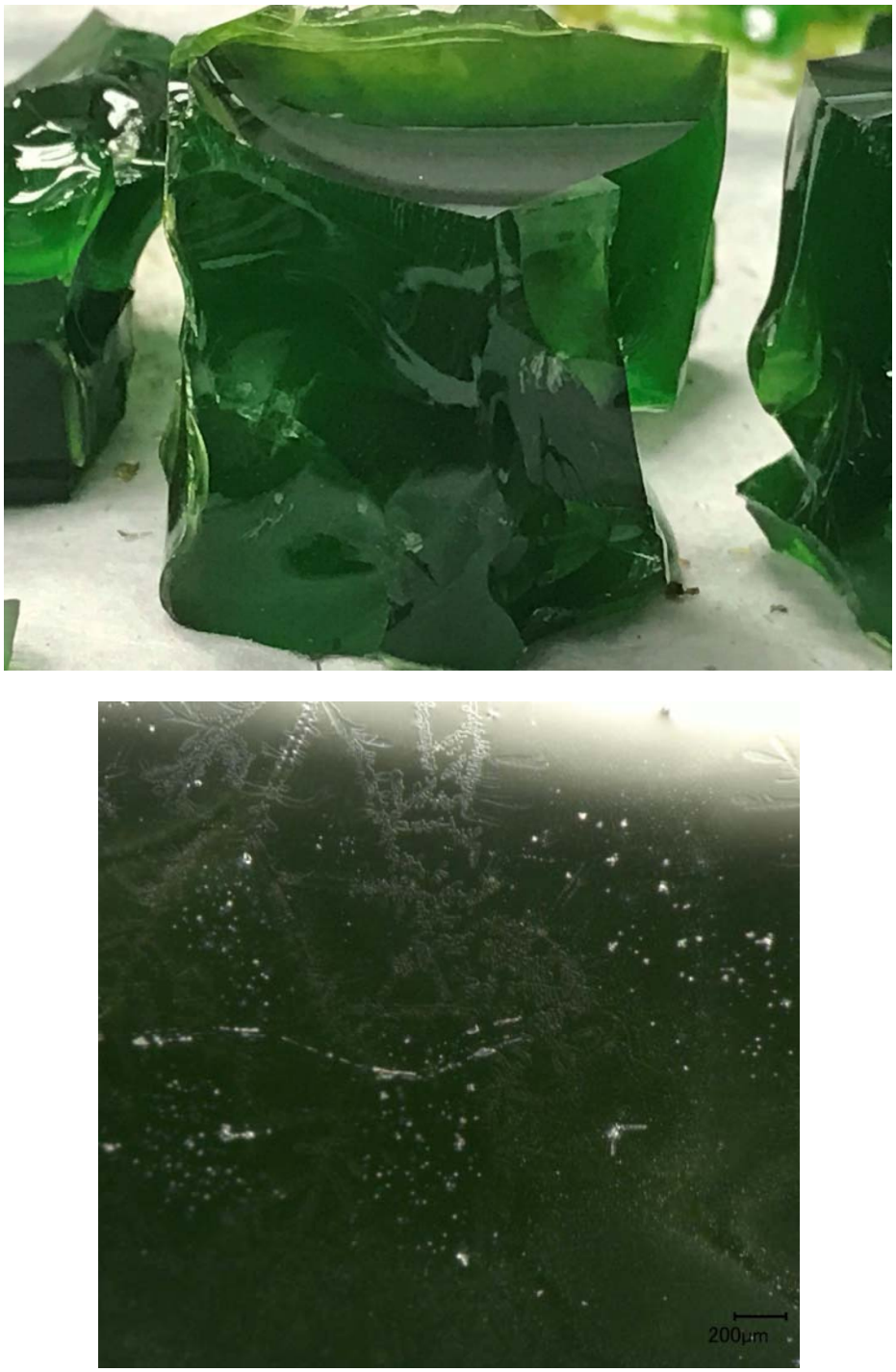


Figure G.2. Glass LP2-IL-02 after CCC Beginning at 1150 °C both Glass (top) and Magnified 100X (bottom)

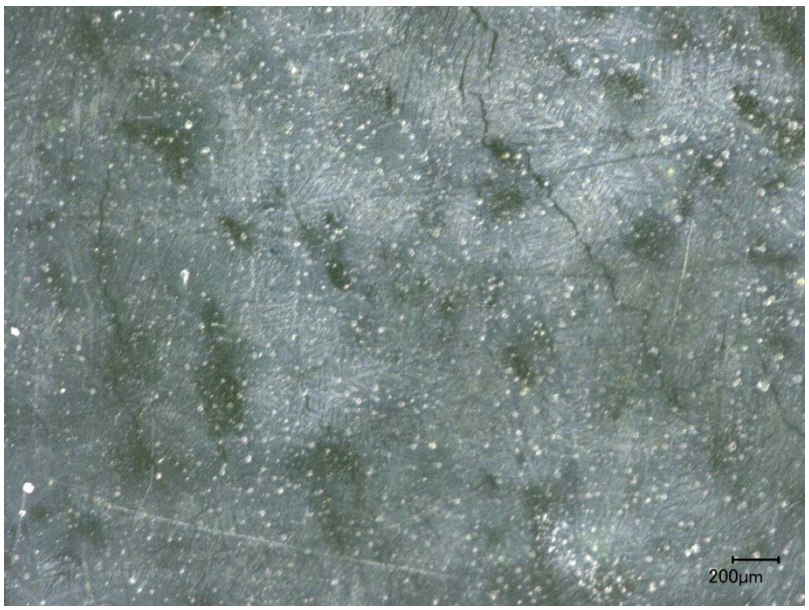


Figure G.3. Glass LP2-IL-03 after CCC Beginning at 1150 °C both Glass (top) and Magnified 100X (bottom)


Figure G.4. Glass LP2-IL-04 after CCC Beginning at 1150 °C both Glass (top) and Magnified 100X (bottom)

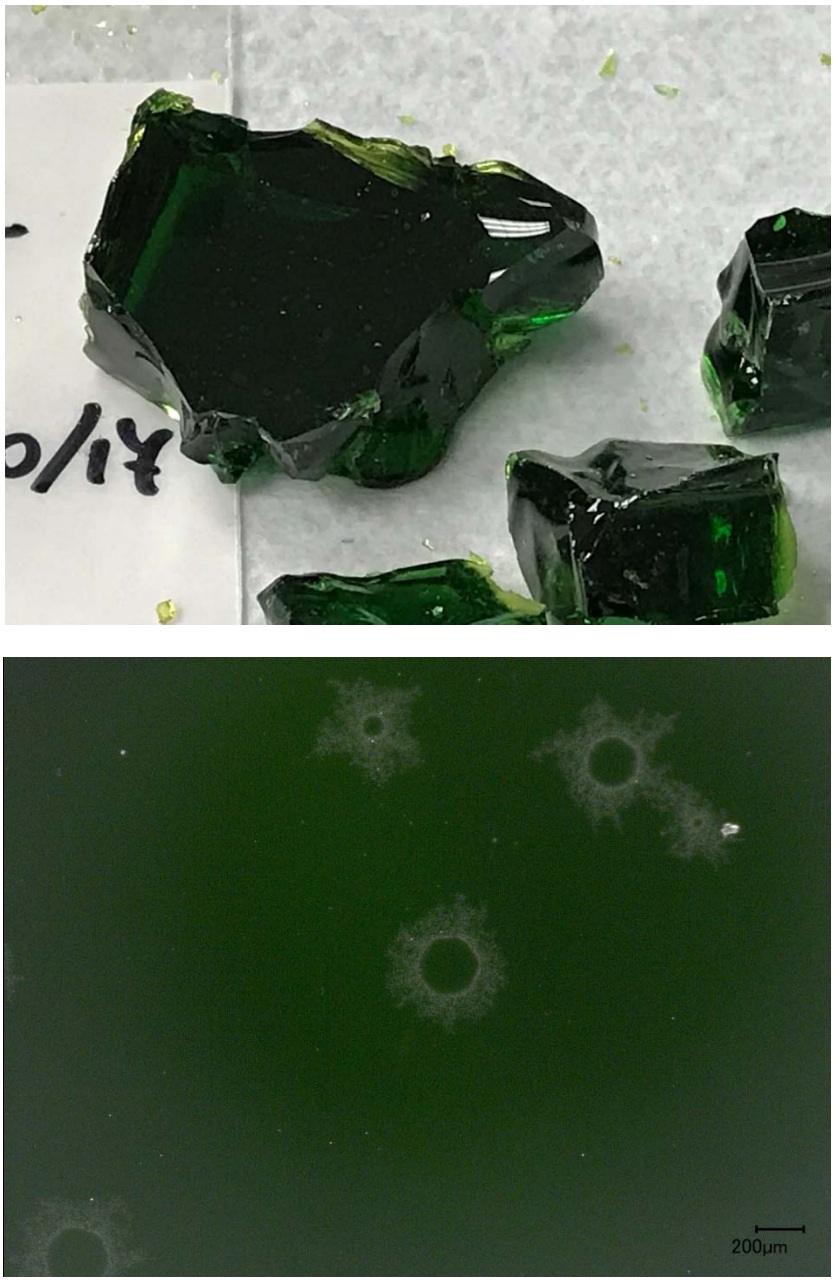


Figure G.5. Glass LP2-IL-05 CCC Beginning at 1150 °C both Glass (top) and Magnified 100X (bottom)


Figure G.6. Glass LP2-IL-06 after CCC Beginning at 1150 °C both Glass (top) and Magnified 100X (bottom)

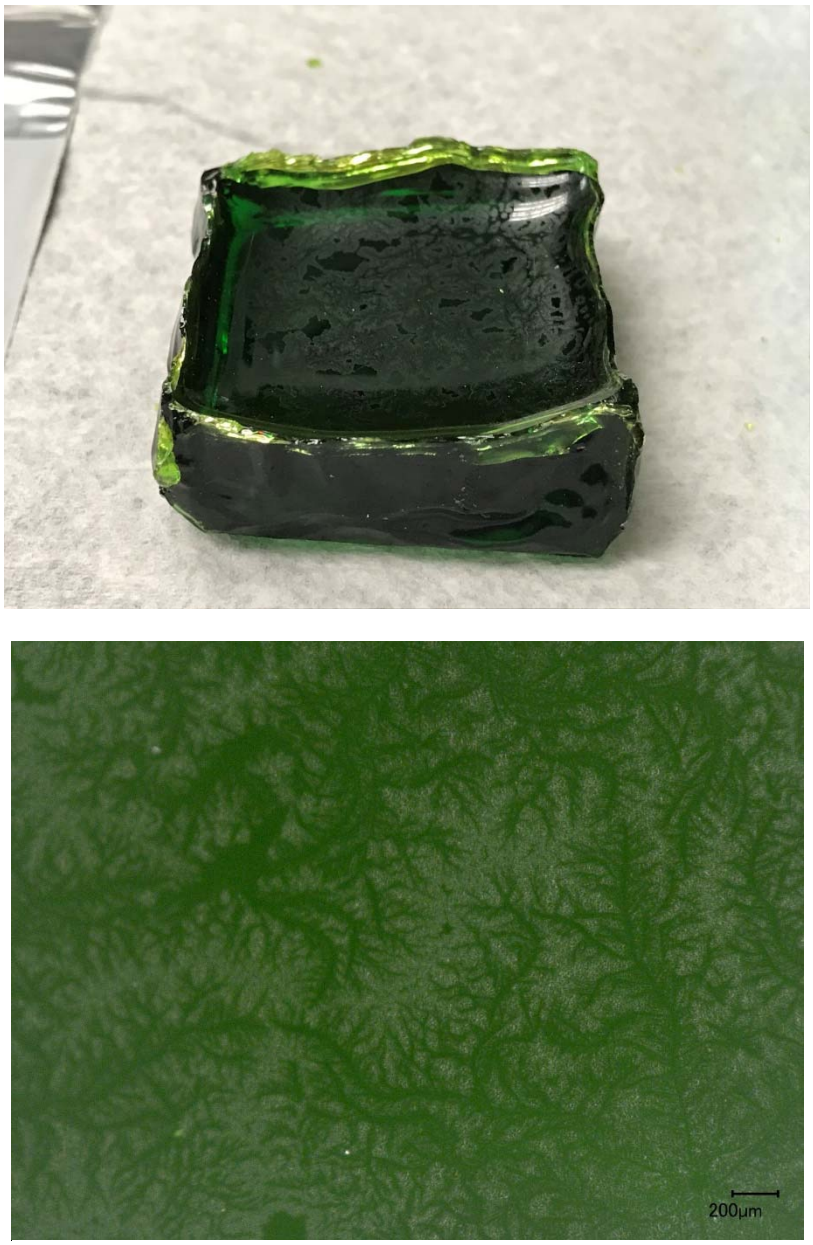


Figure G.7. Glass LP2-IL-07 after CCC Beginning at 1150 °C both Glass (top) and Magnified 100X (bottom)

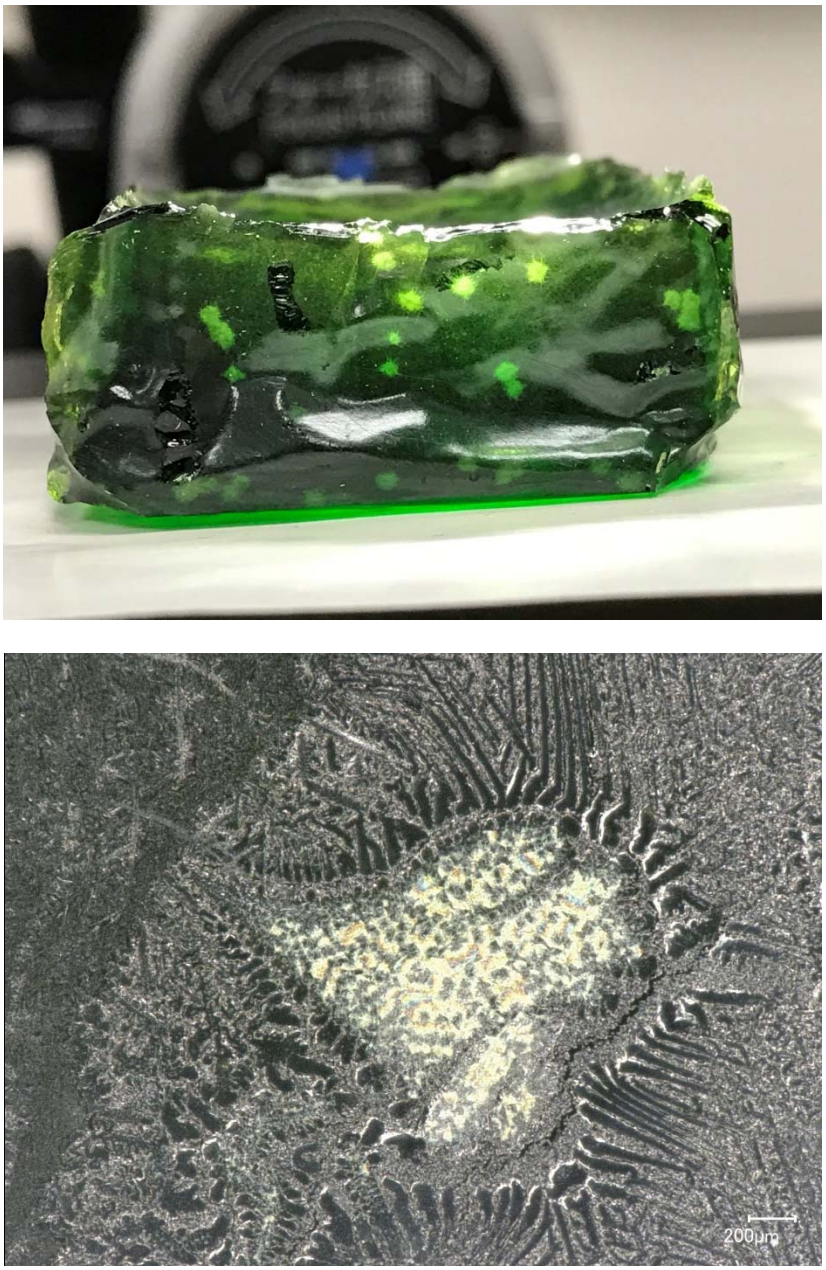


Figure G.8. Glass LP2-IL-08 after CCC Beginning at 1150 °C both Glass (top) and Magnified 100X (bottom)

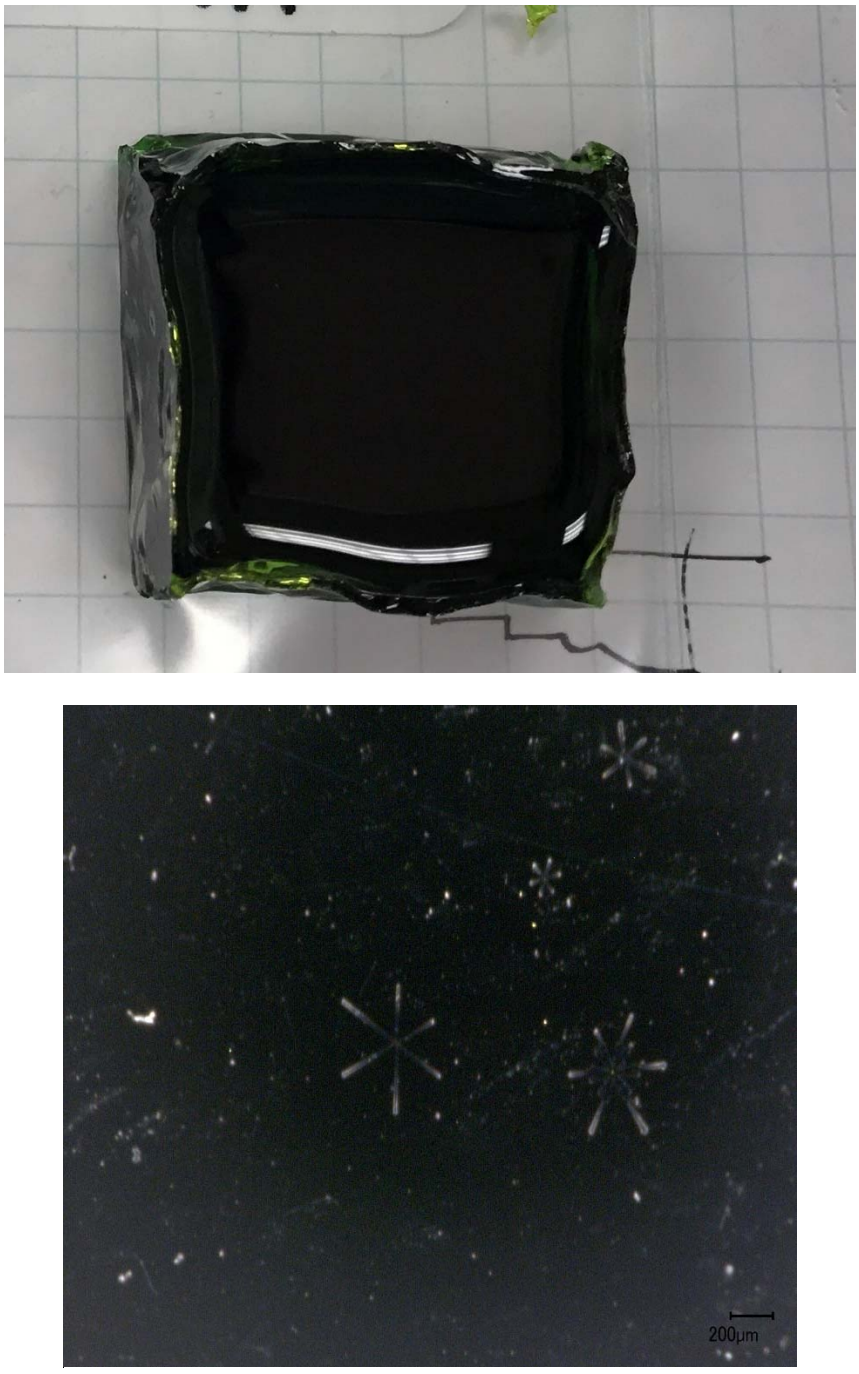


Figure G.9. Glass LP2-IL-09 after CCC Beginning at 1150 °C both Glass (top) and Magnified 100X (bottom)


Figure G.10. Glass LP2-IL-10 CCC Beginning at 1150° C both Glass (top) and Magnified 30X (bottom)

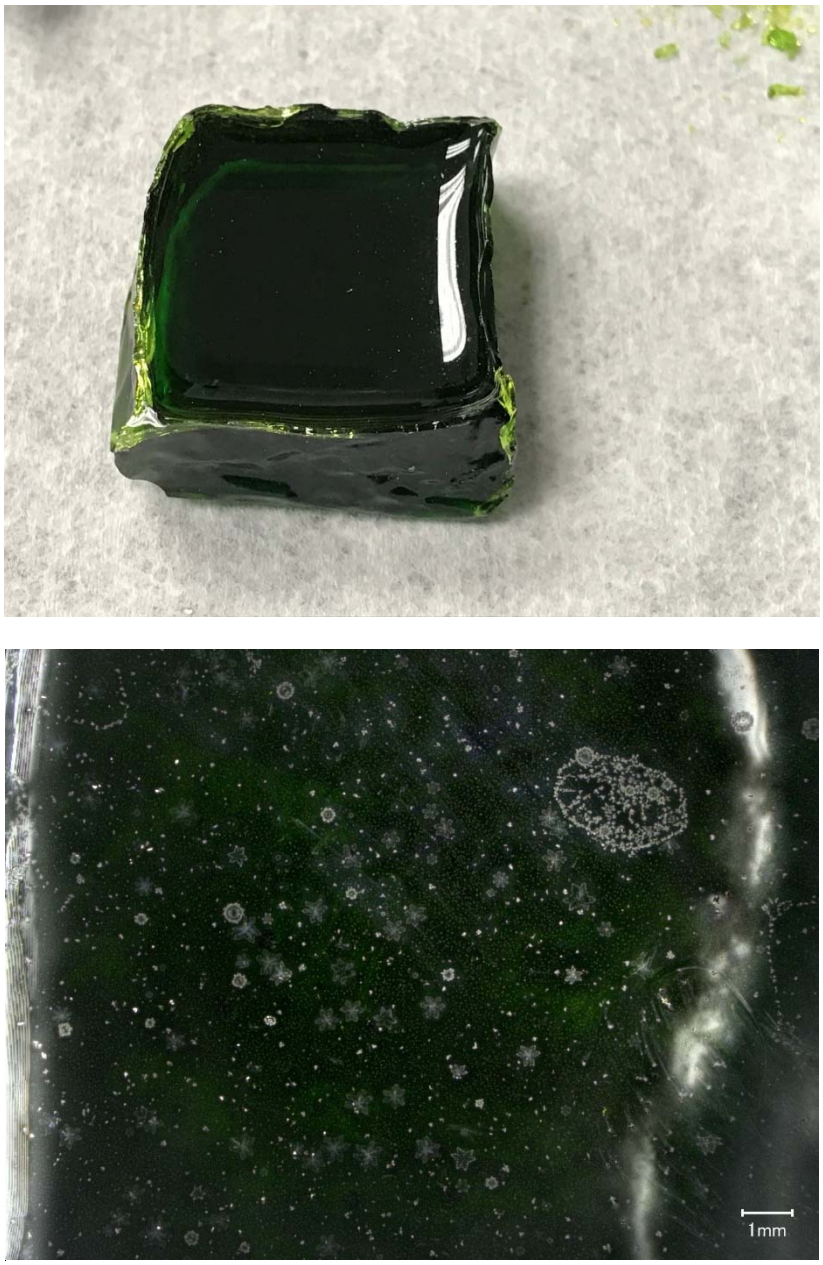


Figure G.11. Glass LP2-IL-11 CCC Beginning at 1150 °C both Glass (top) and Magnified 20X (bottom)


Figure G.12. Glass LP2-IL-12 after CCC Beginning at 1150 °C both Glass (top) and Magnified 50X (bottom)

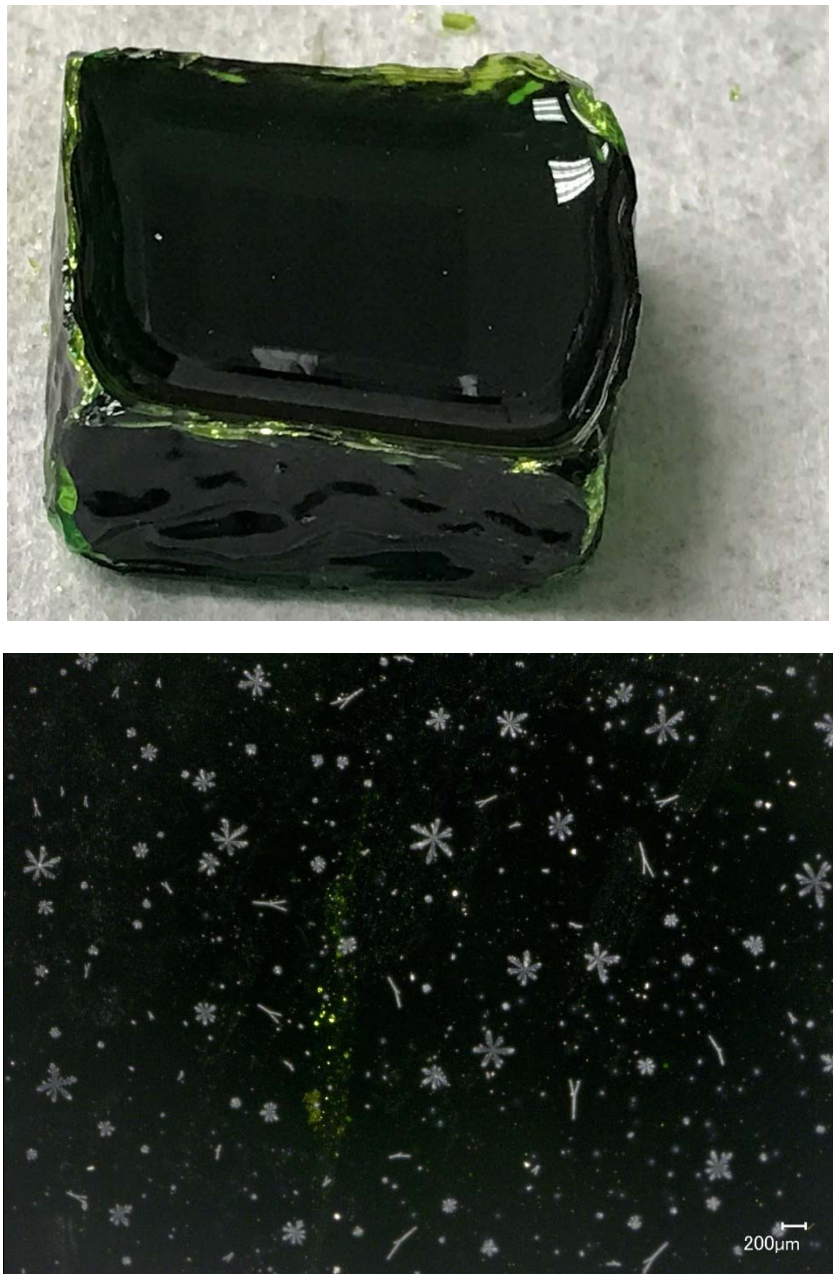


Figure G.13. Glass LP2-IL-13 after CCC Beginning at 1150 °C both Glass (top) and Magnified 50X (bottom)

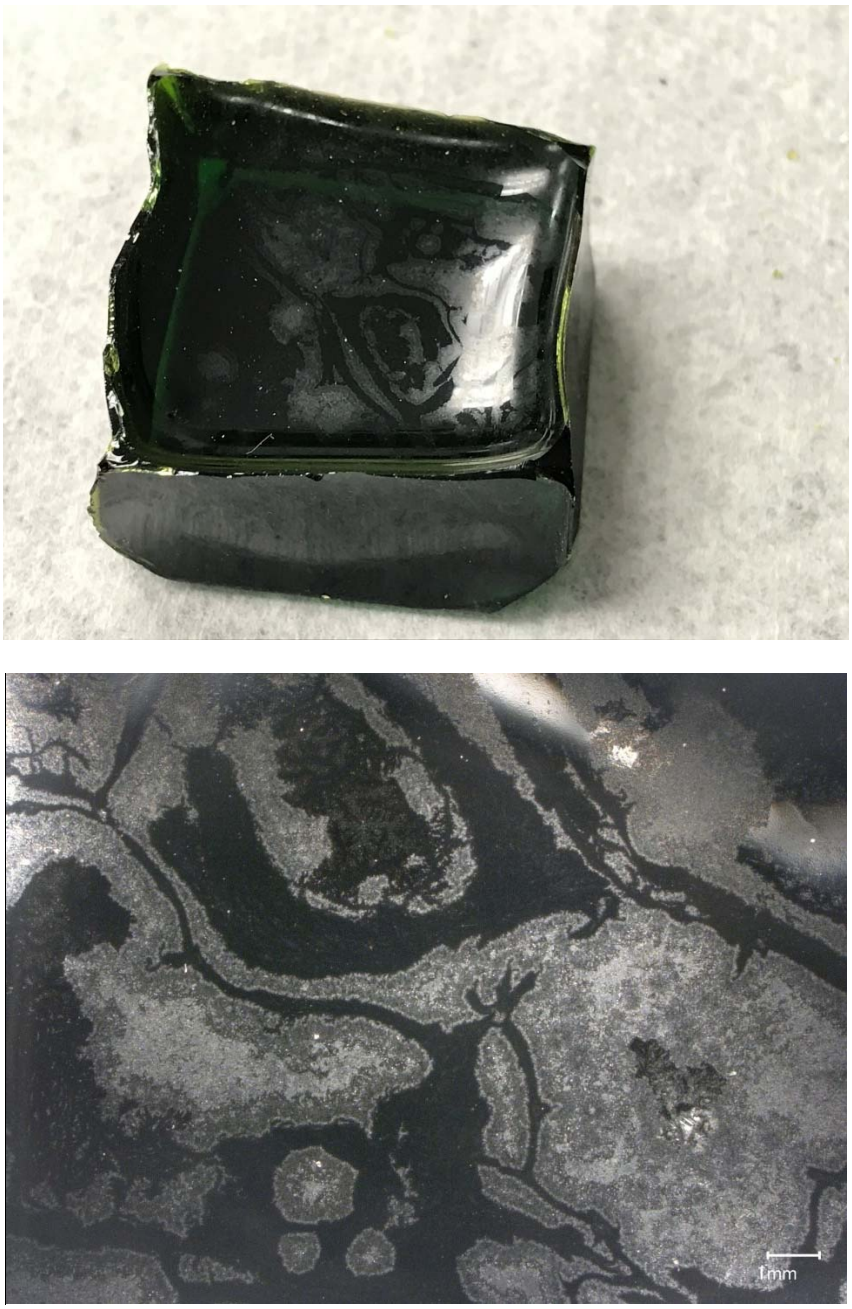


Figure G.14. Glass LP2-IL-14 after CCC Beginning at 1150 °C both Glass (top) and Magnified 20X (bottom)

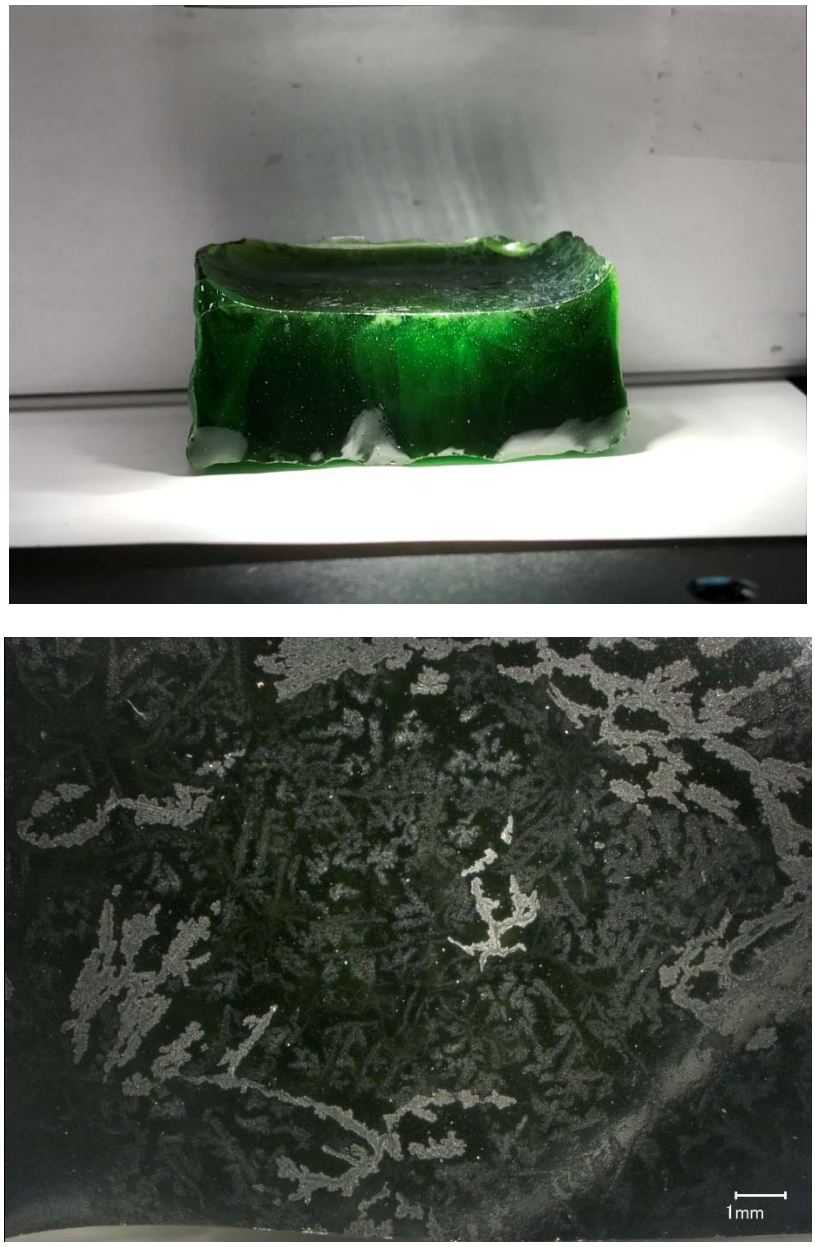


Figure G.15. Glass LP2-IL-15 after CCC Beginning at 1150 °C both Glass (top) and Magnified 20X (bottom)

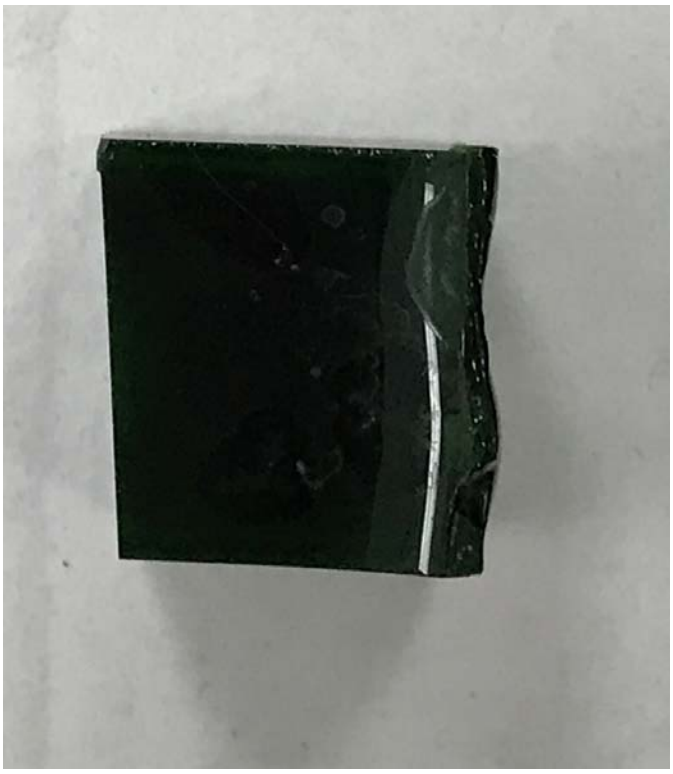

Figure G.16. Glass LP2-IL-16 after CCC Beginning at 1150 °C

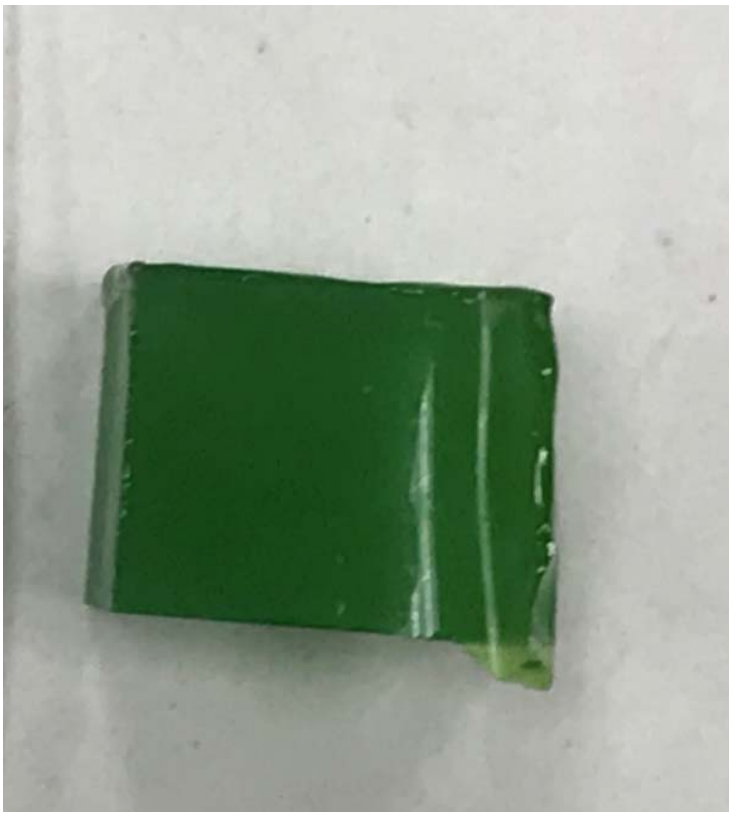

Figure G.17. Glass LP2-IL-17 after CCC Beginning at 1150 °C

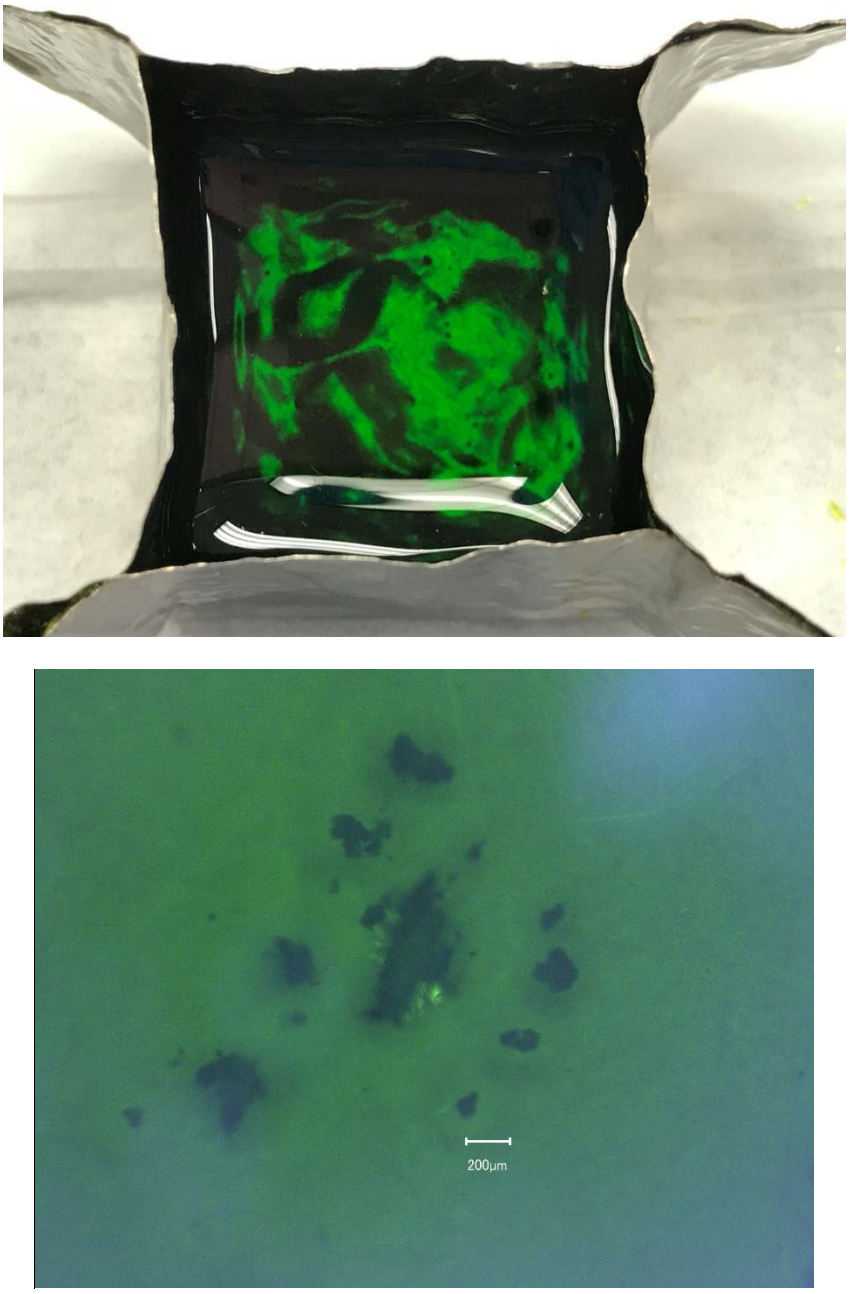


Figure G.18. Glass LP2-OL-01-3 after CCC Beginning at 1150 °C both in Crucible (top) and Magnified 100X (bottom)

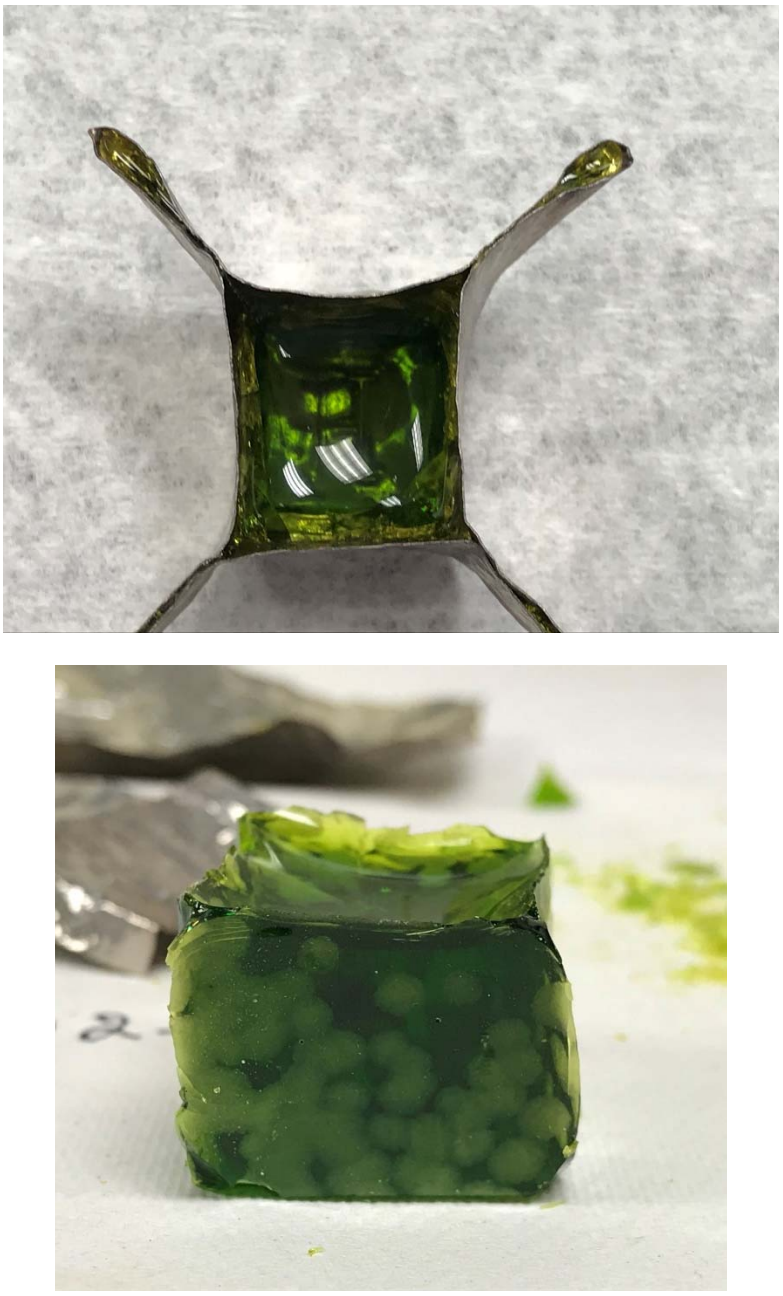

Figure G.19. Glass LP2-OL-02-1 after CCC Beginning at 1150 °C both in Crucible (top) and Glass (bottom)

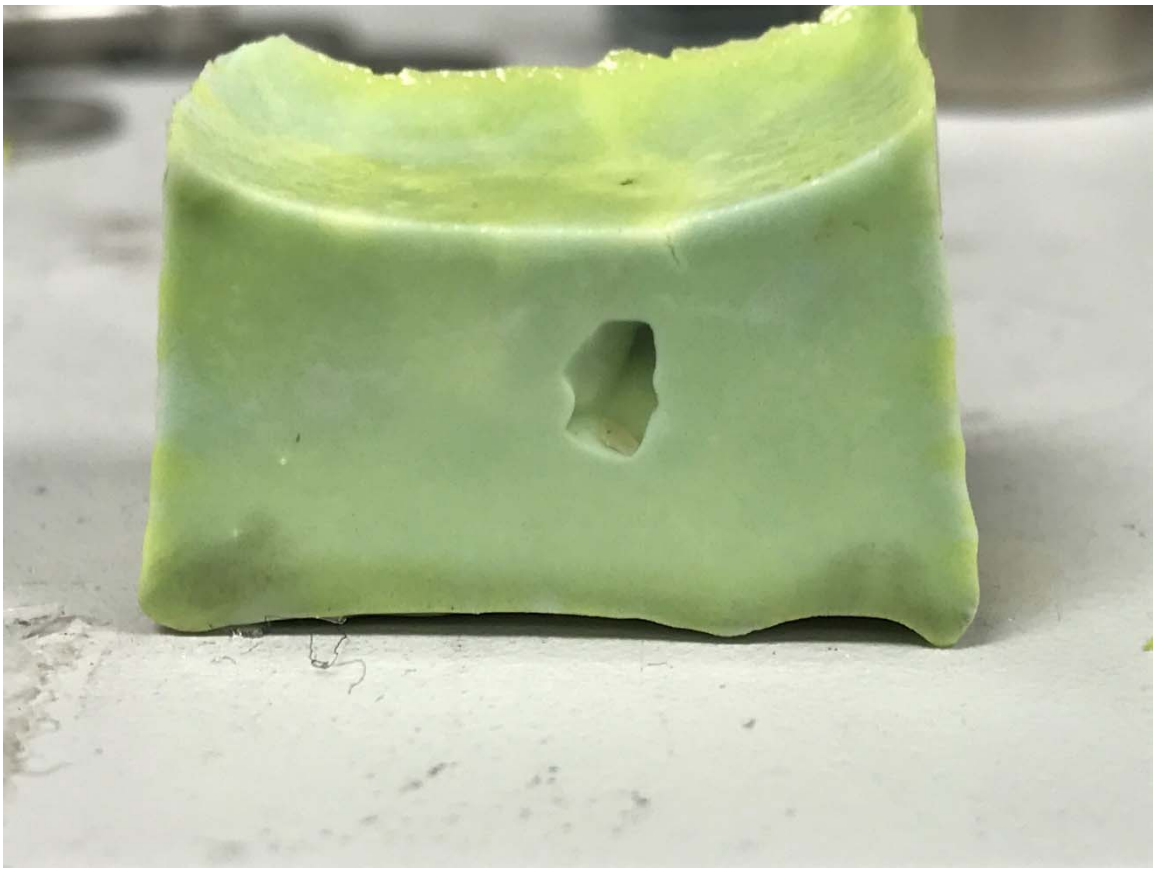

Figure G.20. Glass LP2-OL-03MOD2 after CCC Beginning at 1150 °C

Figure G.21. Glass LP2-OL-04-1 after CCC Beginning at 1150 °C

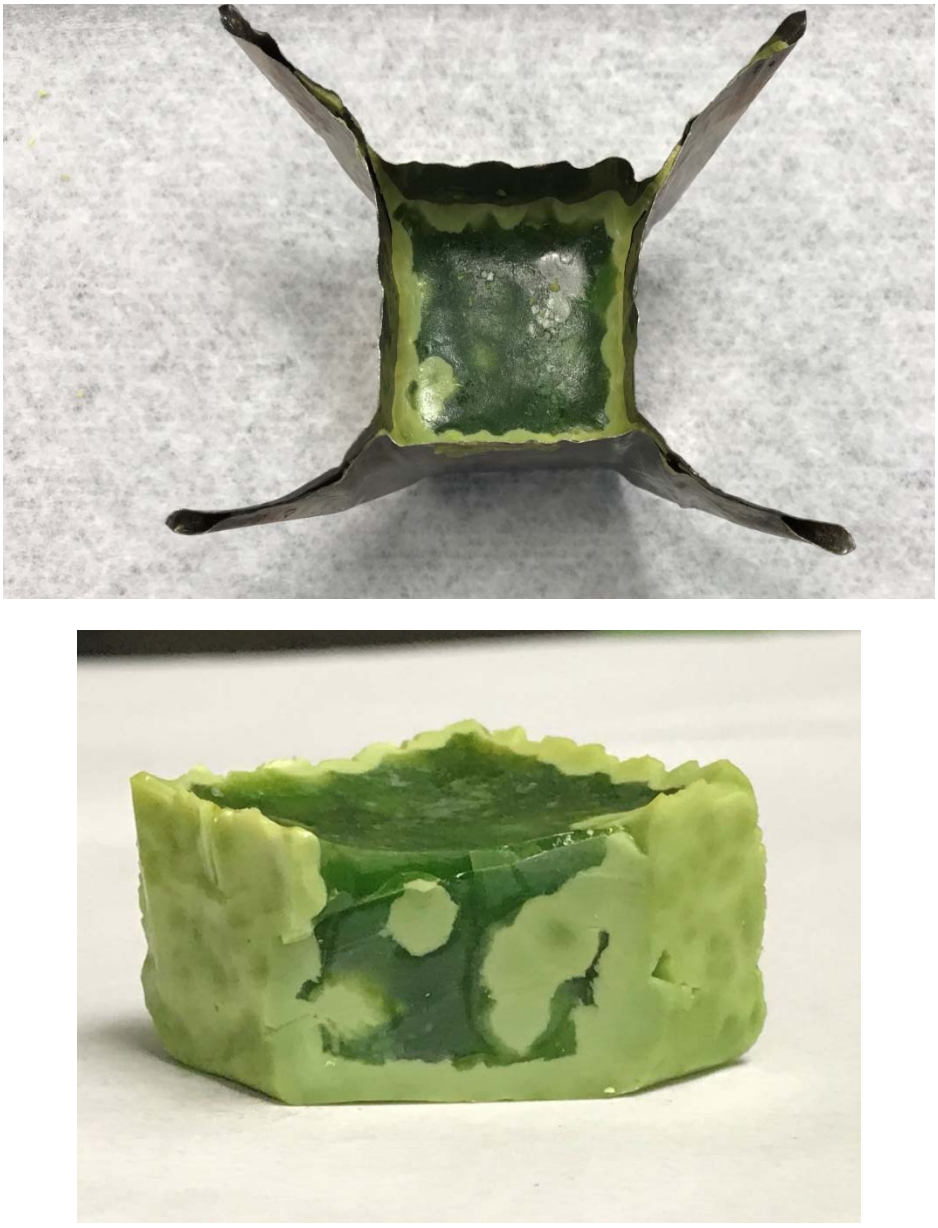

Figure G.22. Glass LP2-OL-05 after CCC Beginning at 1150 °C both in Crucible (top) and Glass (bottom)

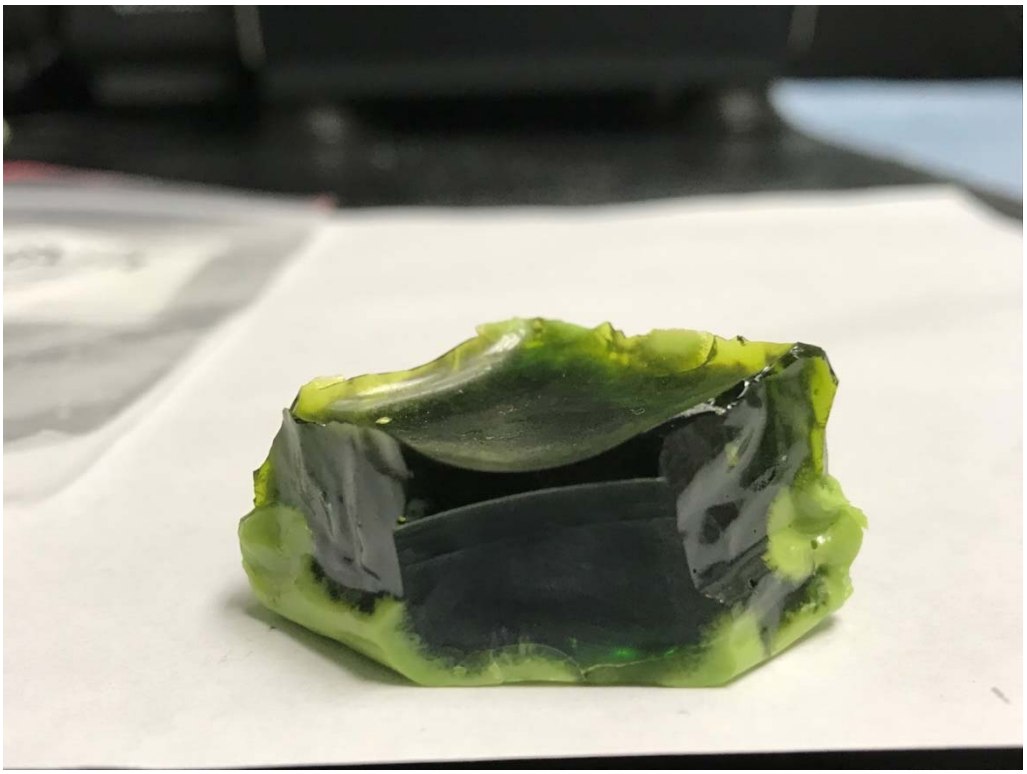

Figure G.23. Glass LP2-OL-07-1 after CCC Beginning at 1150 °C

Figure G.24. Glass LP2-OL-08MOD after CCC Beginning at 1150 °C

Figure G.25. Glass LP2-OL-09-1 after CCC Beginning at 1150 °C

Figure G.26. Glass LP2-OL-10MOD after CCC Beginning at 1150 °C

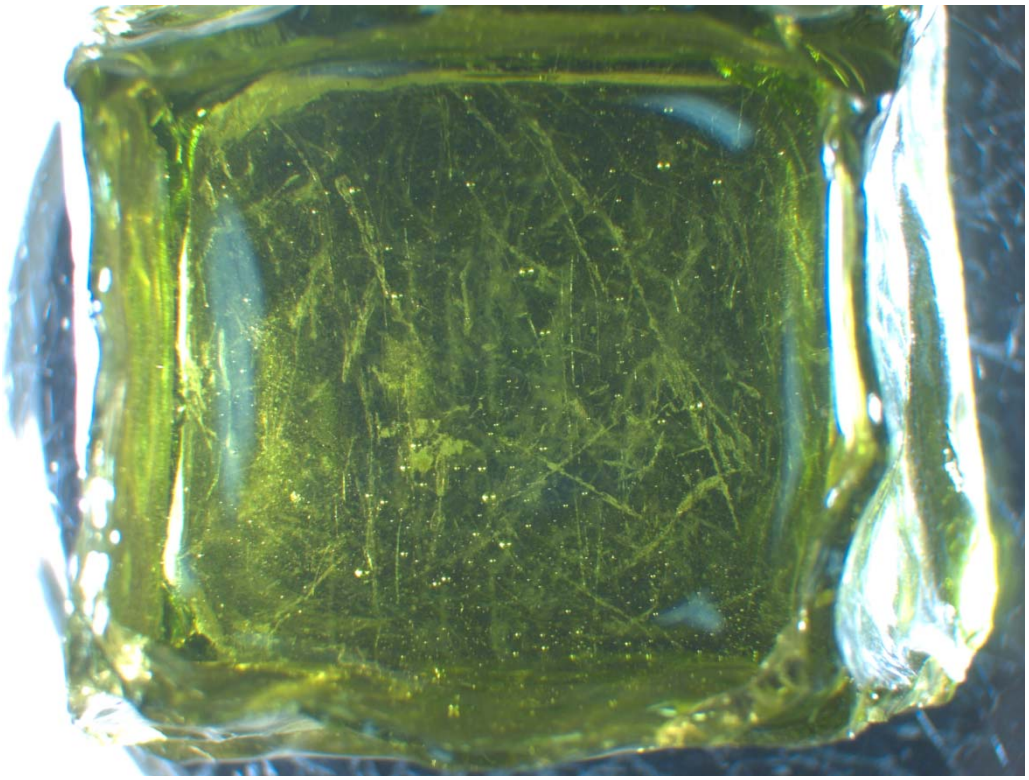

Figure G.27. Glass LP2-OL-11 after CCC Beginning at 1150 °C

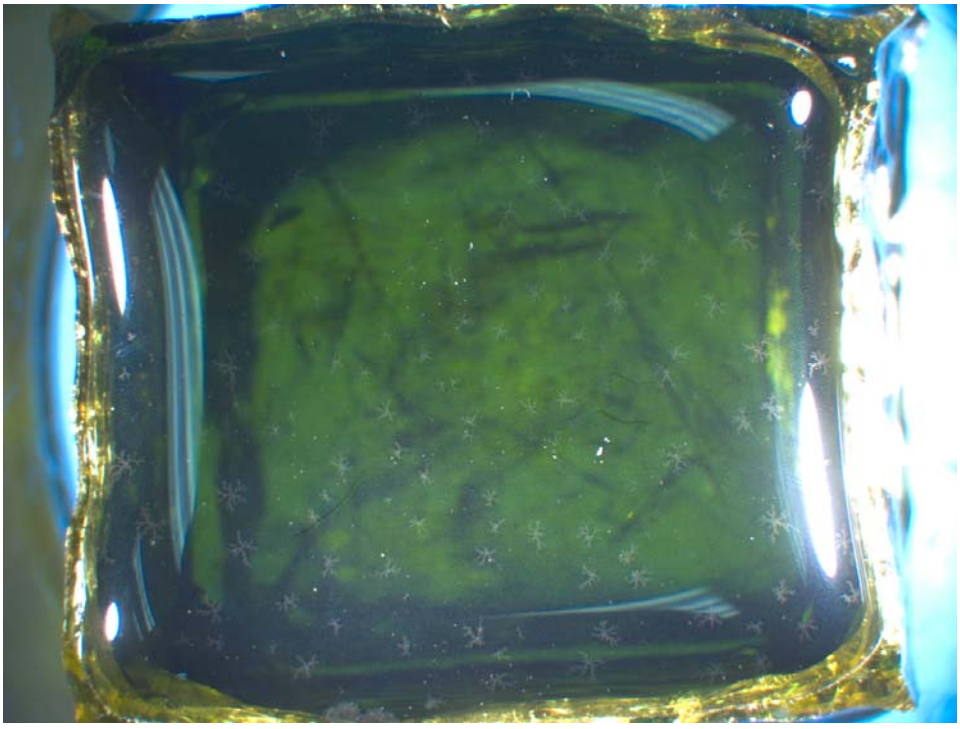

Figure G.28. Glass LP2-OL-12 after CCC Beginning at 1150 °C

Figure G.29. Glass LP2-OL-13 after CCC Beginning at 1150 °C both in Crucible (top) and Glass (bottom)

Figure G.30. Glass LP2-OL-14 after CCC Beginning at 1150 °C

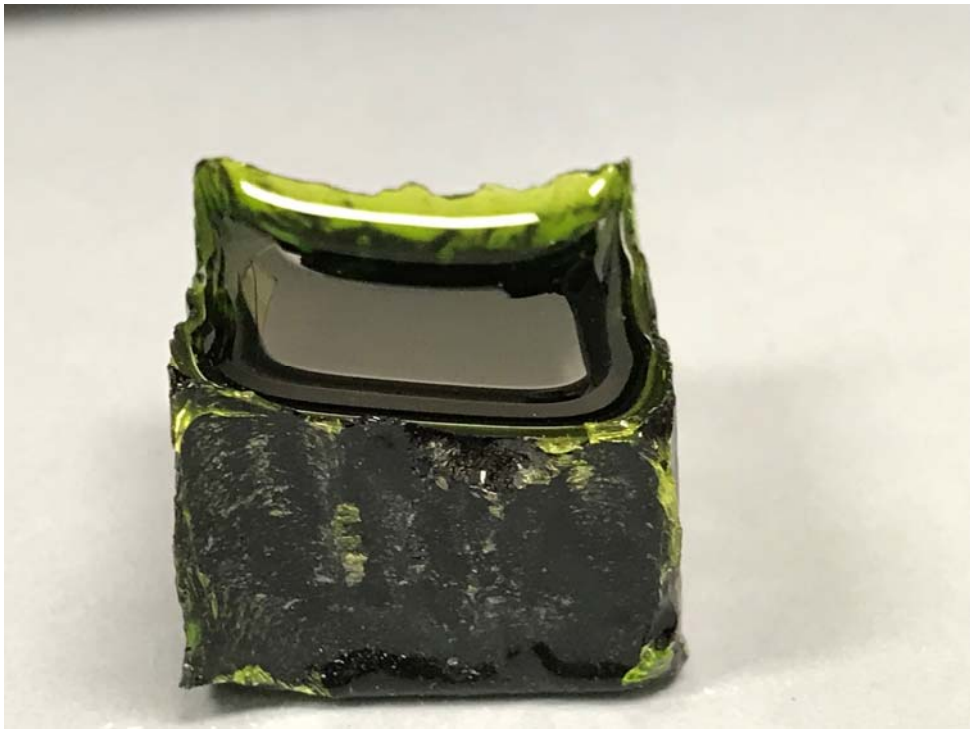

Figure G.31. Glass LP2-OL-15 after CCC Beginning at 1150 °C

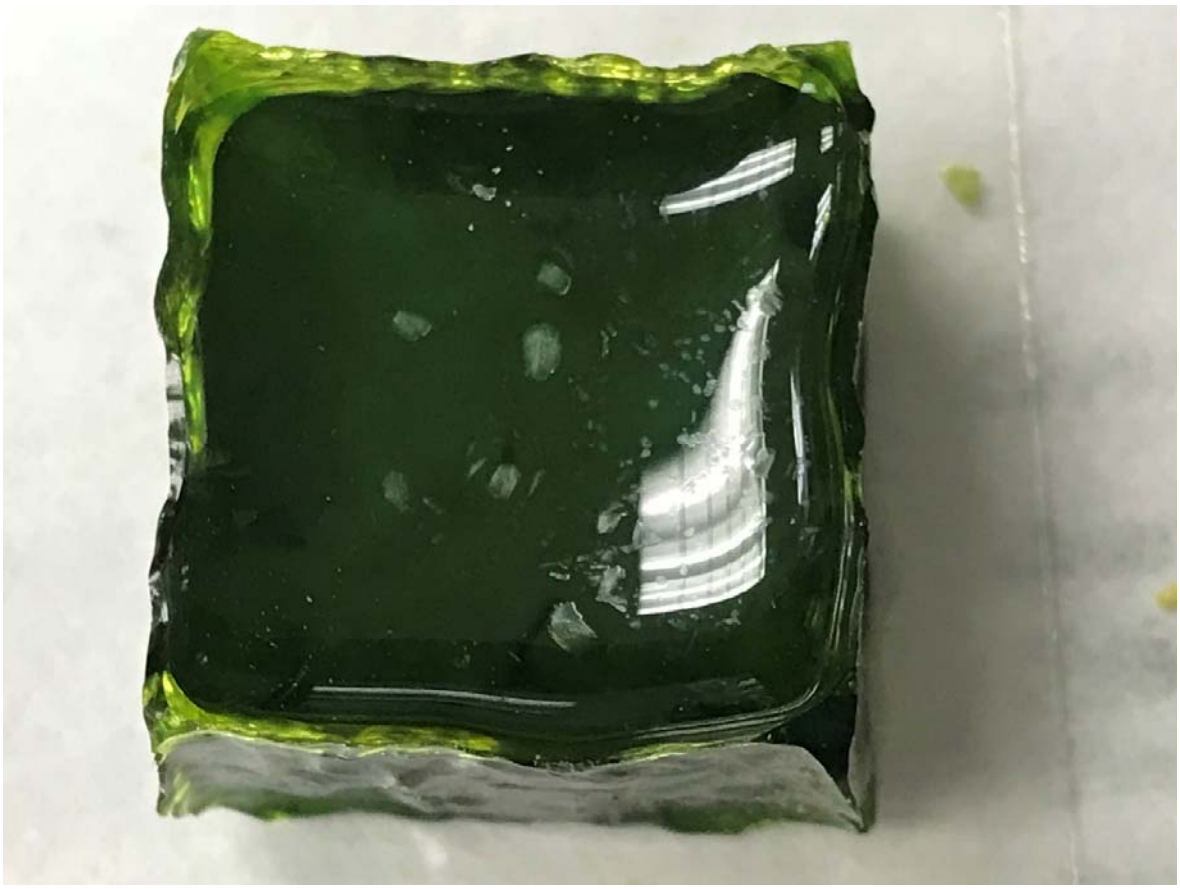

Figure G.32. Glass LP2-OL-16MOD after CCC Beginning at 1150 °C

Figure G.33. Glass LP2-OL-17 after CCC Beginning at 1150 °C

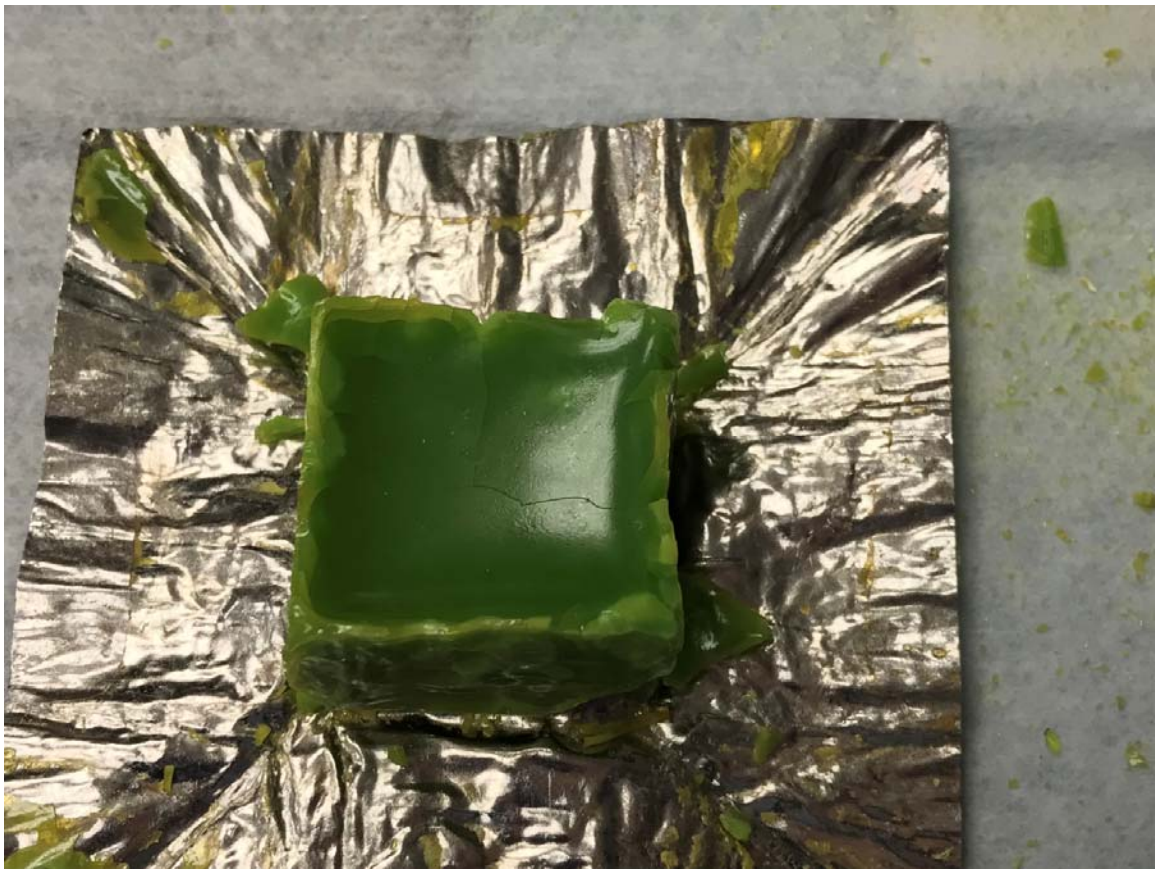

Figure G.34. Glass LP2-OL-18 after CCC Beginning at 1150 °C

Figure G.35. Glass LP2-OL-19 after CCC Beginning at 1150 °C

Figure G.36. Glass LP2-OL-20 after CCC Beginning at 1150 °C

Figure G.37. Glass LP2-OL-21 after CCC Beginning at 1150 °C

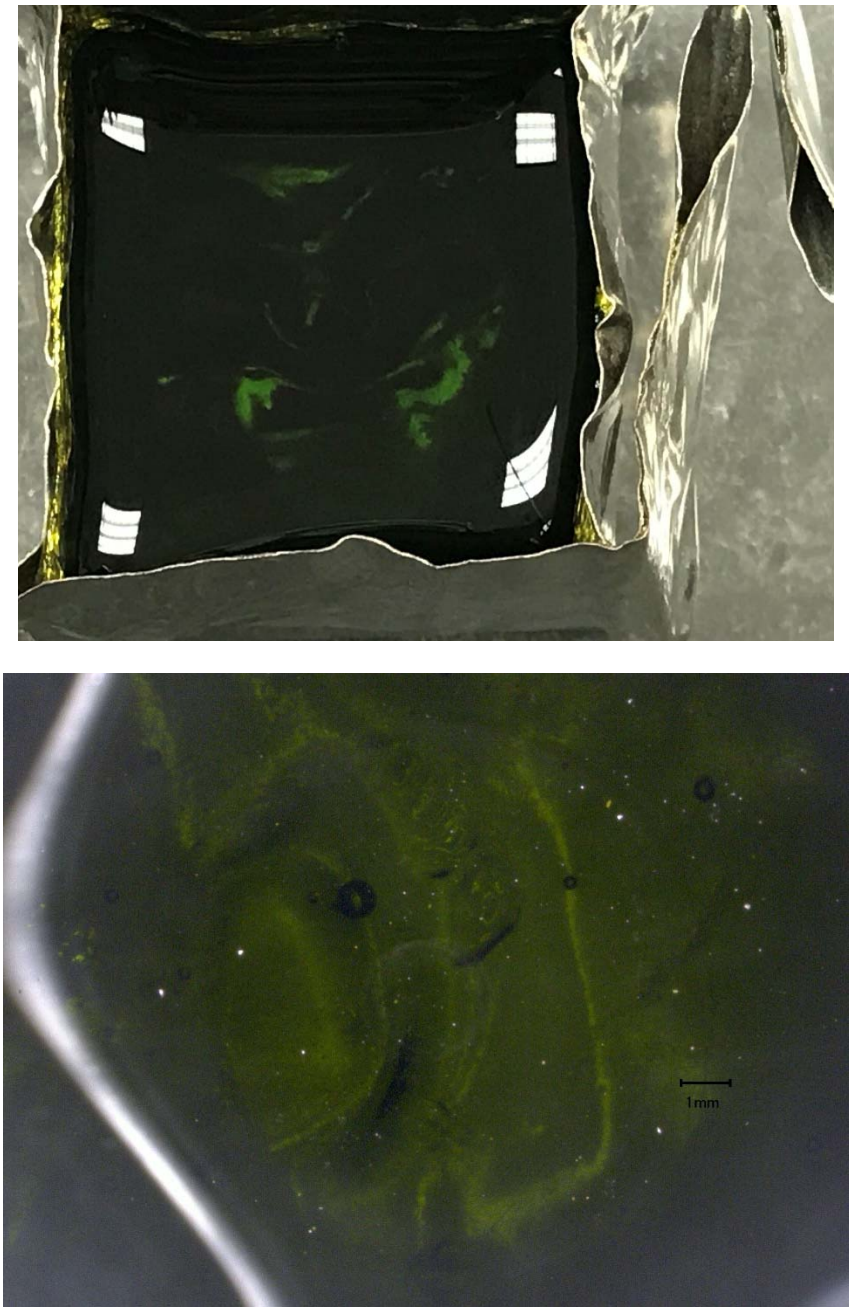


Figure G.38. Glass LP2-OL-22 after CCC Beginning at 1150 °C both in Crucible (top) and Magnified 20X (bottom)

Figure G.39. Glass LP2-OL-23 after CCC Beginning at 1150 °C

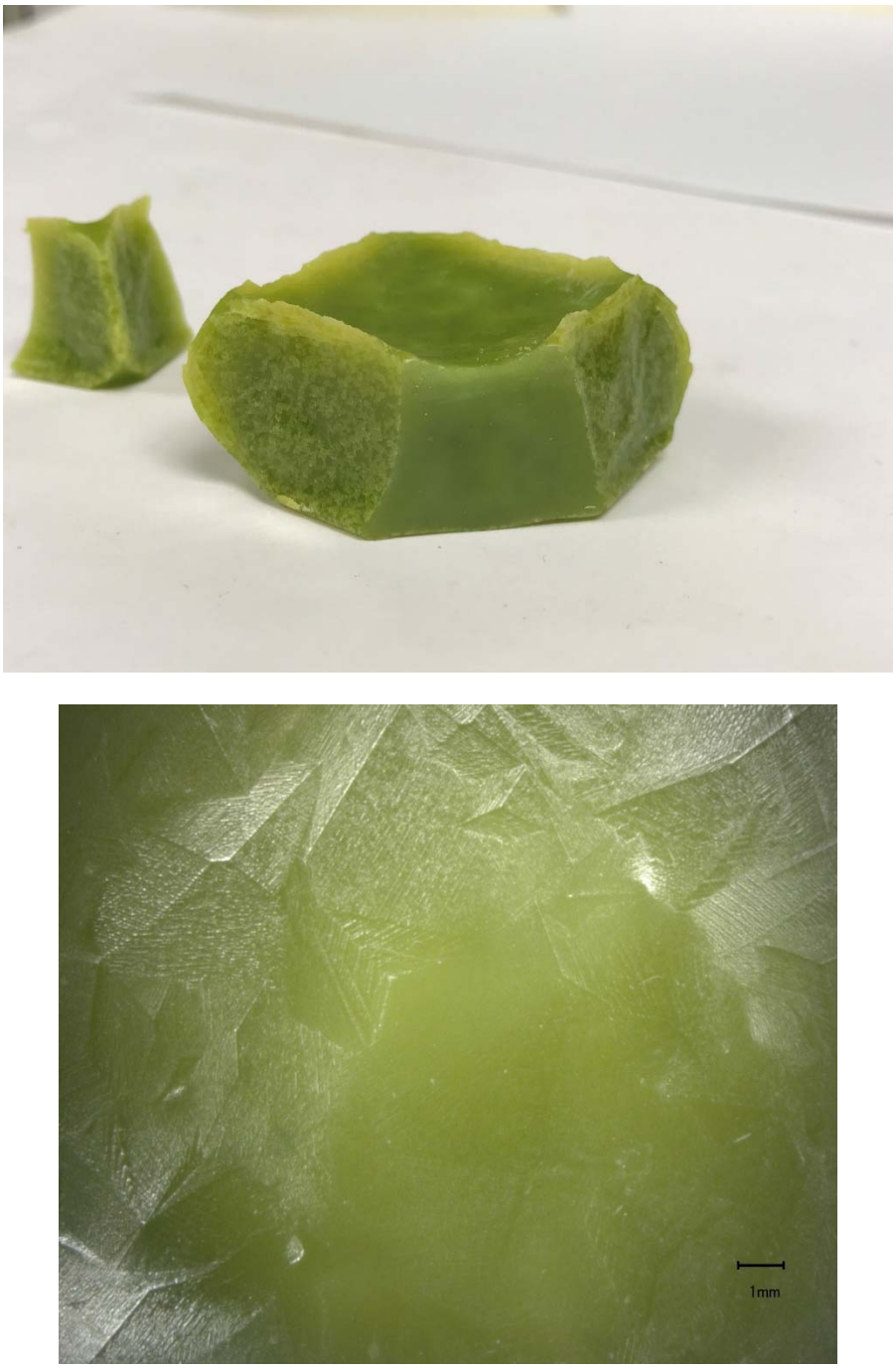


Figure G.40. Glass LP2-OL-24 after CCC Beginning at 1150 °C both Glass (top) and Magnified 20X (bottom)

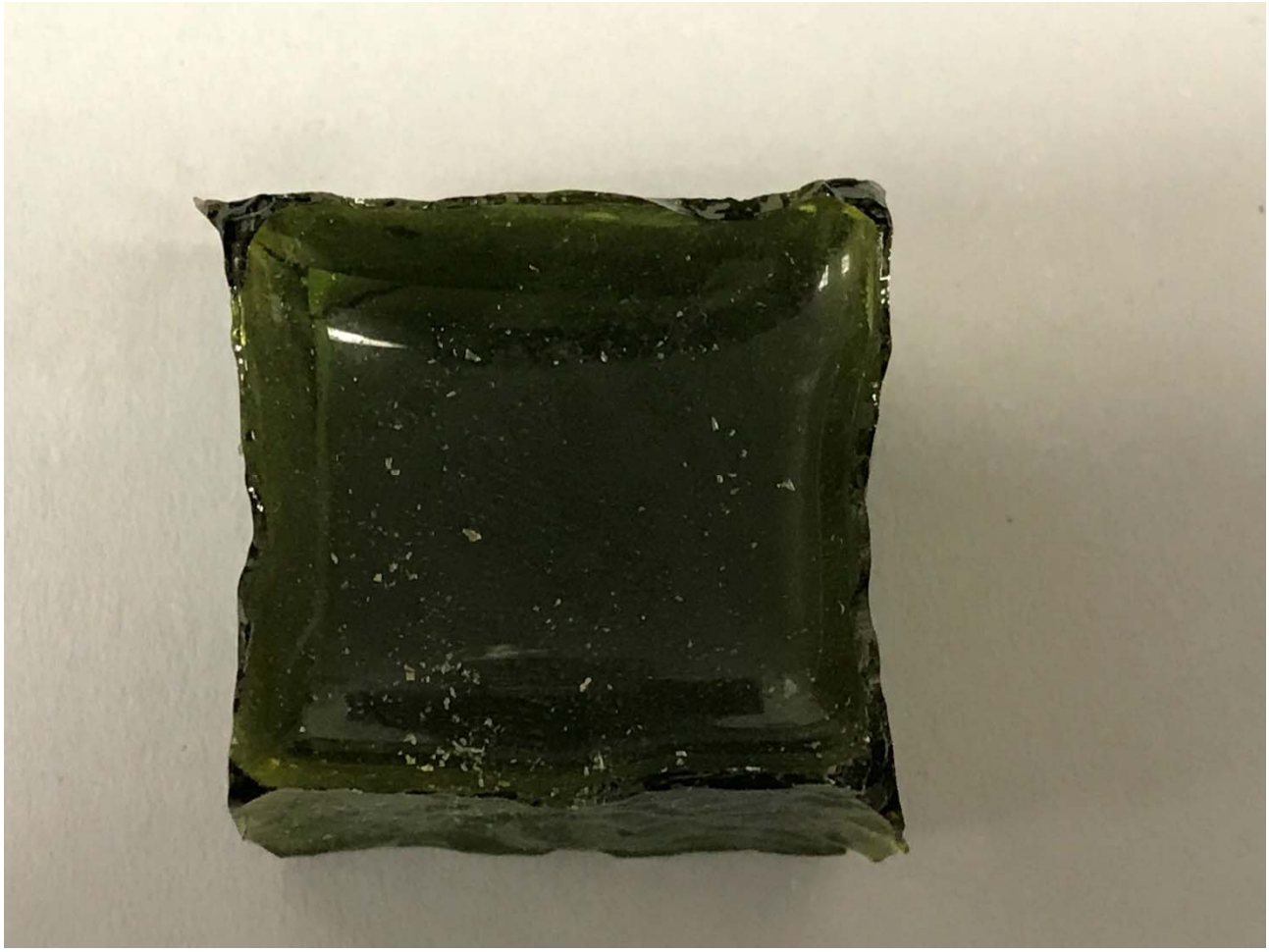

Figure G.41. Glass LP2-OL-25 after CCC Beginning at 1150 °C

# Appendix H – XRD of Canister Centerline Cooling (CCC) Treated Glasses

This appendix shows the XRD plots of several Phase 2 enhanced LAW glasses after CCC heat-treatment. These glasses all responded very differently to the CCC heat-treatment from remaining amorphous to developing quite a few crystals of various kinds as shown by the following plots. Some glasses did not contain enough crystals to perform XRD and therefore are not included here. They were LP2-IL-02, LP2-IL-03, LP2-IL-04, LP2-IL-05, LP2-IL-07, LP2-IL-09, LP2-IL-11, LP2-IL-12, LP2-IL-13, LP2-IL-14, LP2-IL-16, LP2-OL-01-3, LP2-OL-09-1, LP2-OL-11, LP2-OL-12, LP2-OL-15, LP2-OL-21, LP2-OL-22, LP2-OL-23, and LP2-OL-25.

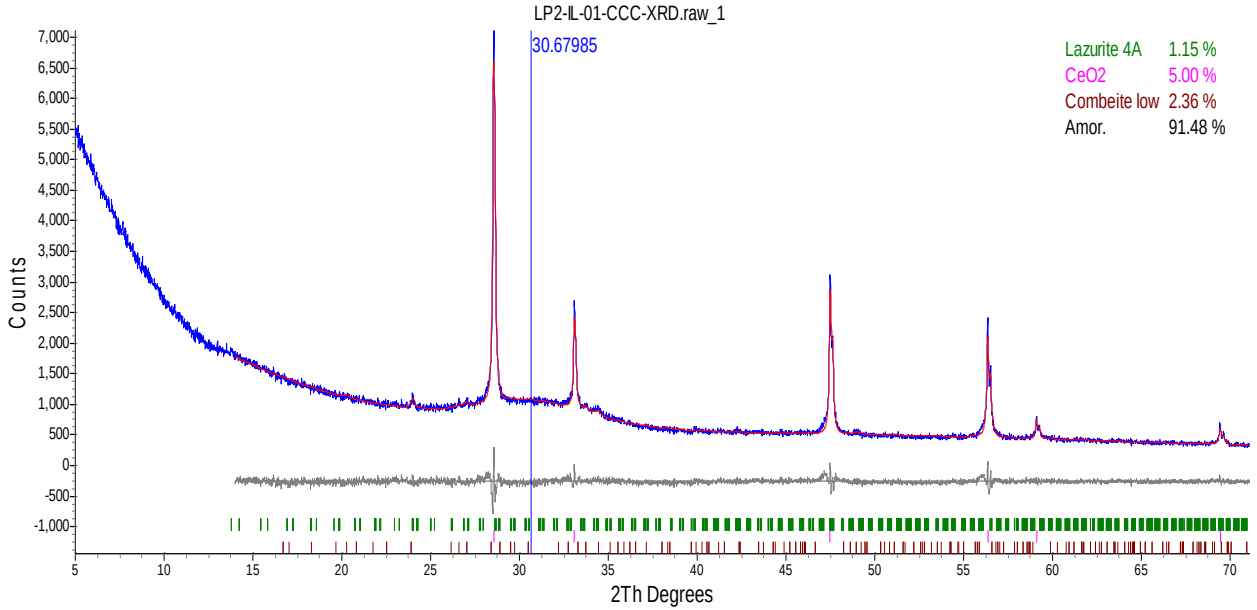


| Phase Name | Wt% of Spiked | Wt% in Spiked Sample | Wt% in Original Sample |
|---|---|---|---|
| $CeO_2$ | 5.004 | 5.004 | 0 |
| Lazurite 4A | 0 | 1.155 | 1.215 |
| Combeite low | 0 | 2.36 | 2.484 |

Figure H.1. XRD Spectrum of CCC-Treated Glass LP2-IL-01

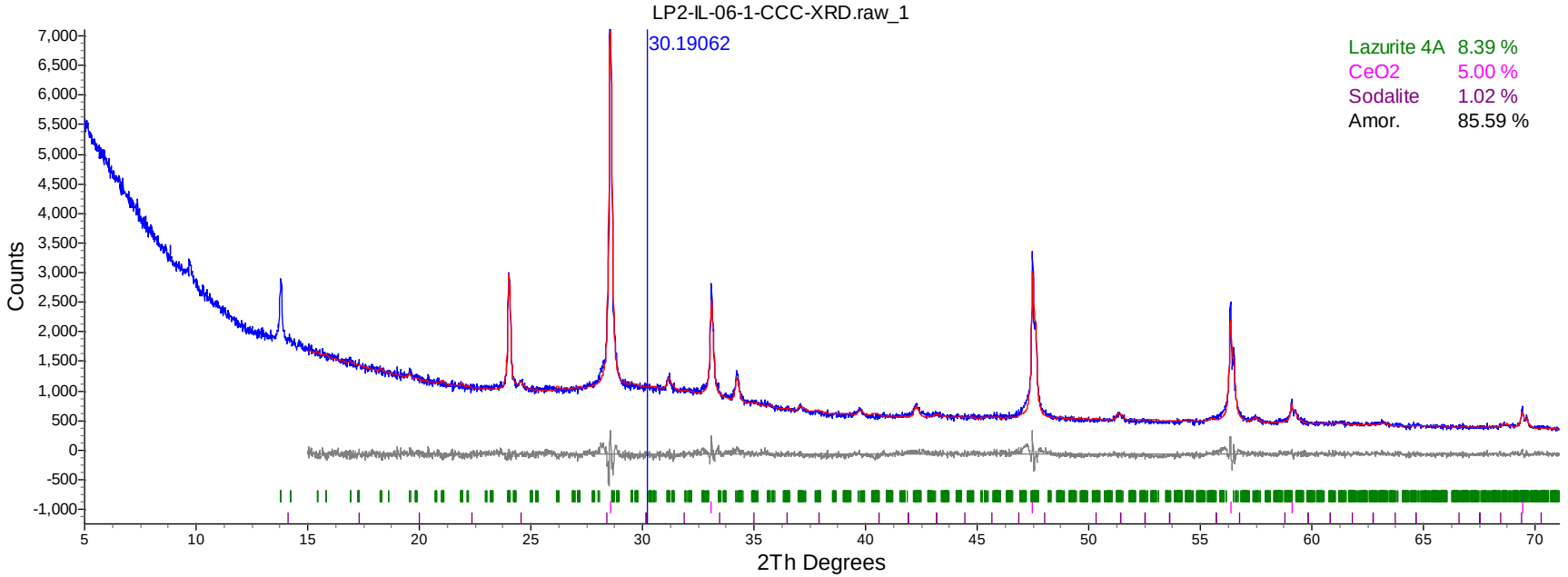


| Phase Name | Wt% of Spiked | Wt% in Spiked Sample | Wt% in Original Sample |
|---|---|---|---|
| $CeO_2$ | 5.001 | 5.001 | 0 |
| Lazurite 4A | 0 | 8.388 | 8.83 |
| Sodalite | 0 | 1.019 | 1.07 |

Figure H.2. XRD Spectrum of CCC-Treated Glass LP2-IL-06

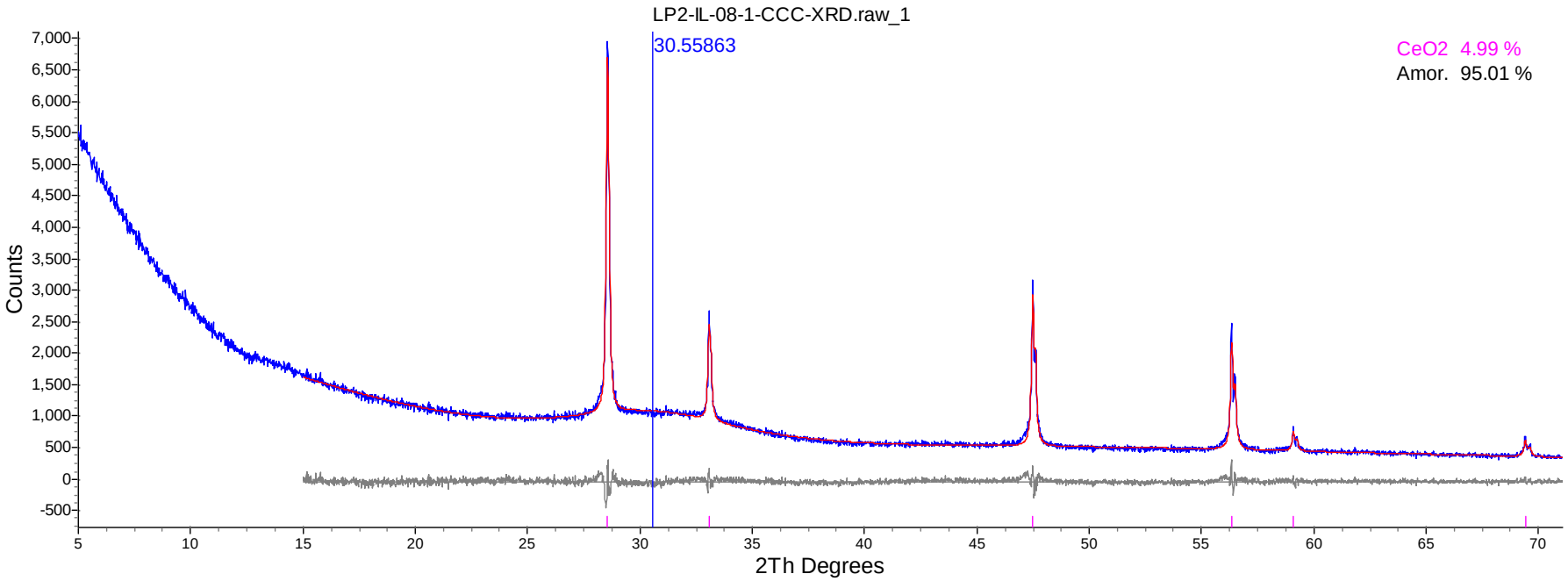


Figure H.3. XRD Spectrum of CCC-Treated Glass LP2-IL-08

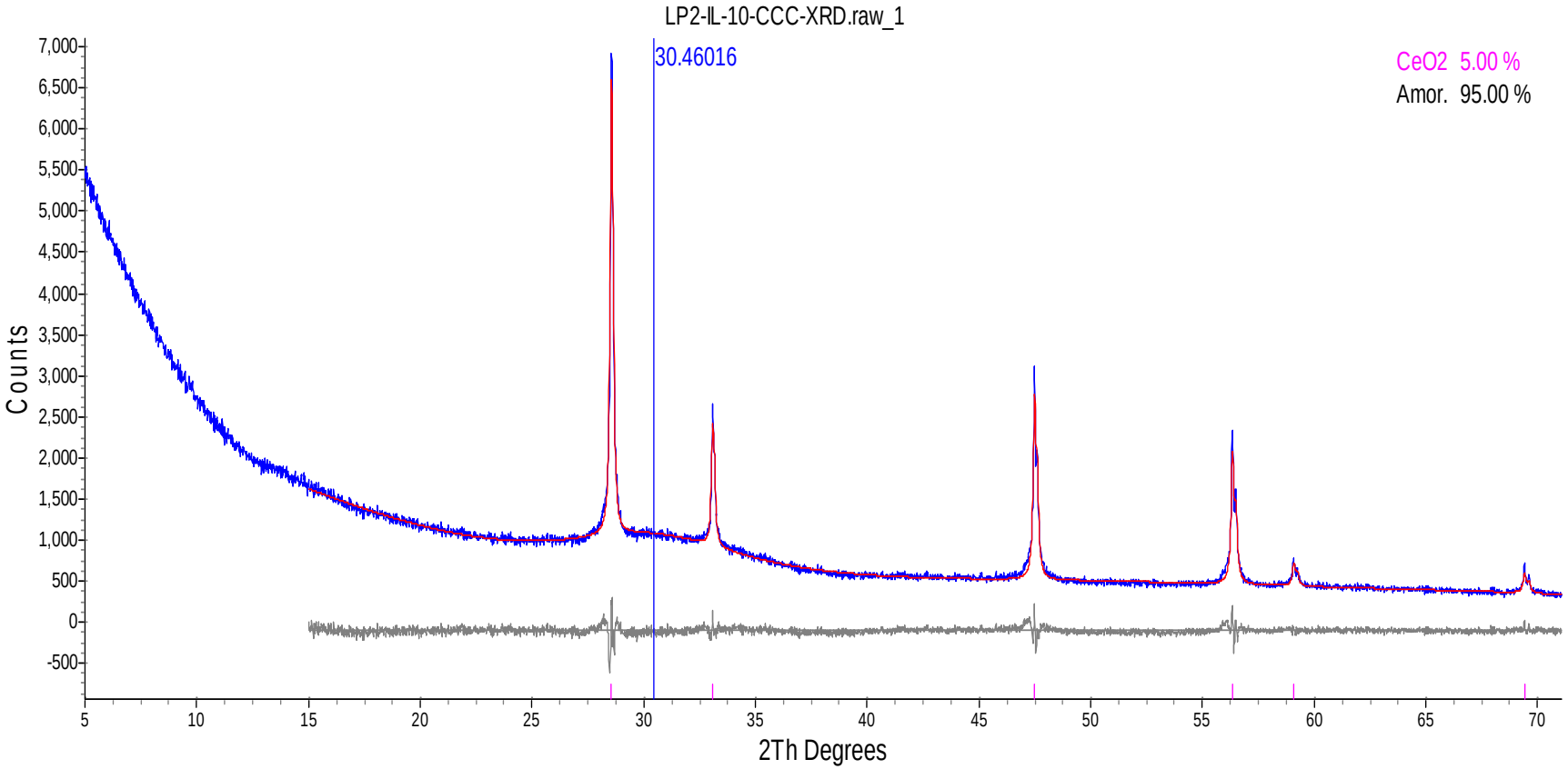


Figure H.4. XRD Spectrum of CCC-Treated Glass LP2-IL-10

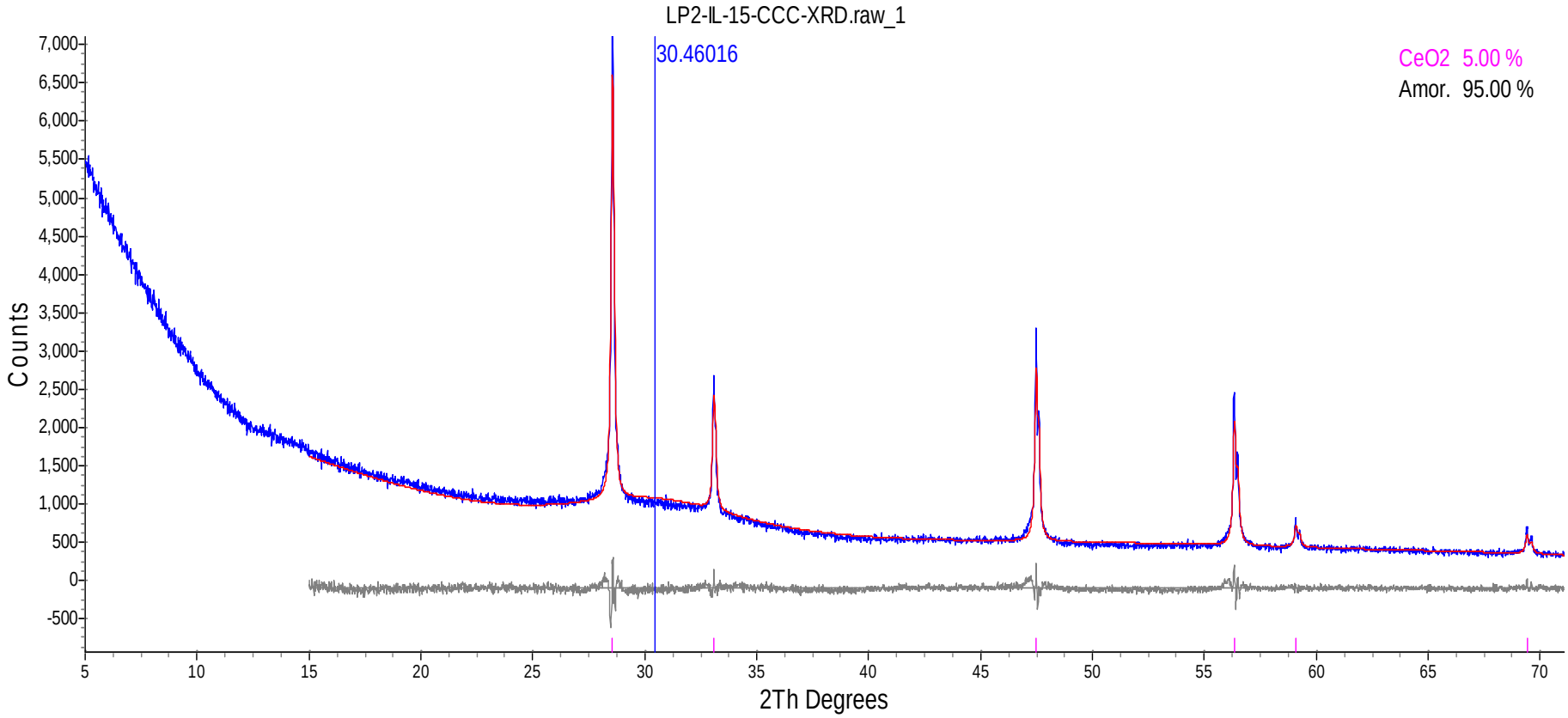


Figure H.5. XRD Spectrum of CCC-Treated Glass LP2-IL-15

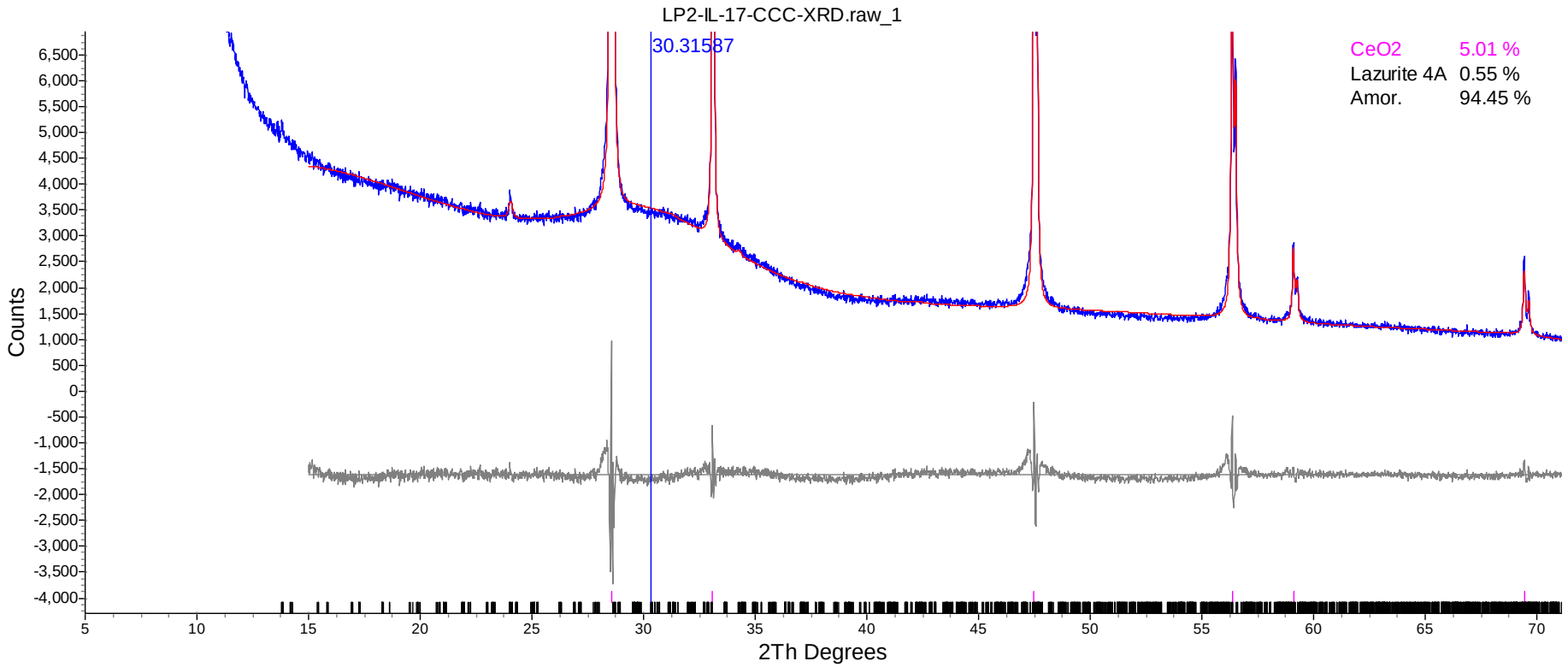


| Phase Name | Wt% of Spiked | Wt% in Spiked Sample | Wt% in Original Sample |
|---|---|---|---|
| $CeO_2$ | 5.007 | 5.007 | 0 |
| Lazurite 4A | 0 | 0.547 | 0.576 |

Figure H.6. XRD Spectrum of CCC-Treated Glass LP2-IL-17

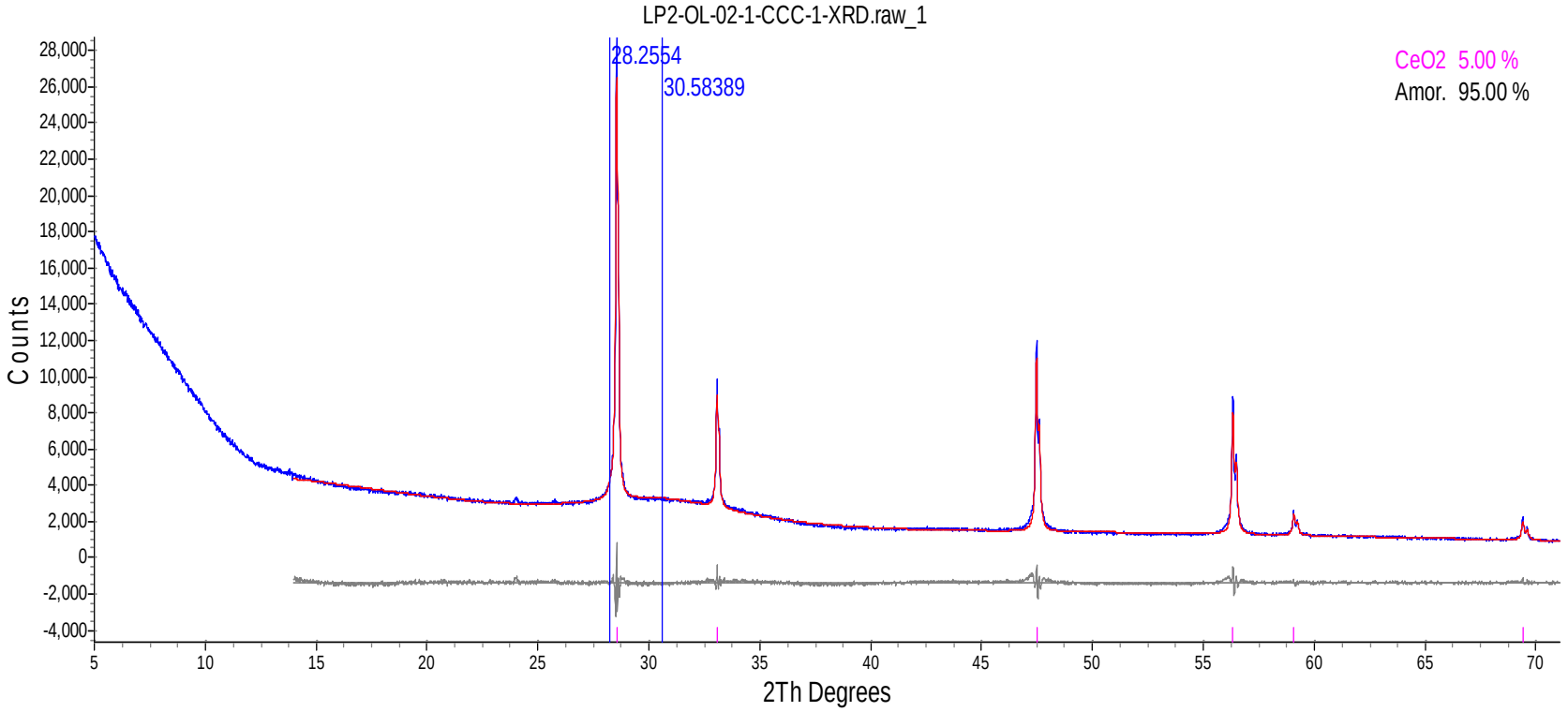


Figure H.7. XRD Spectrum of CCC-Treated Glass LP2-OL-02-1

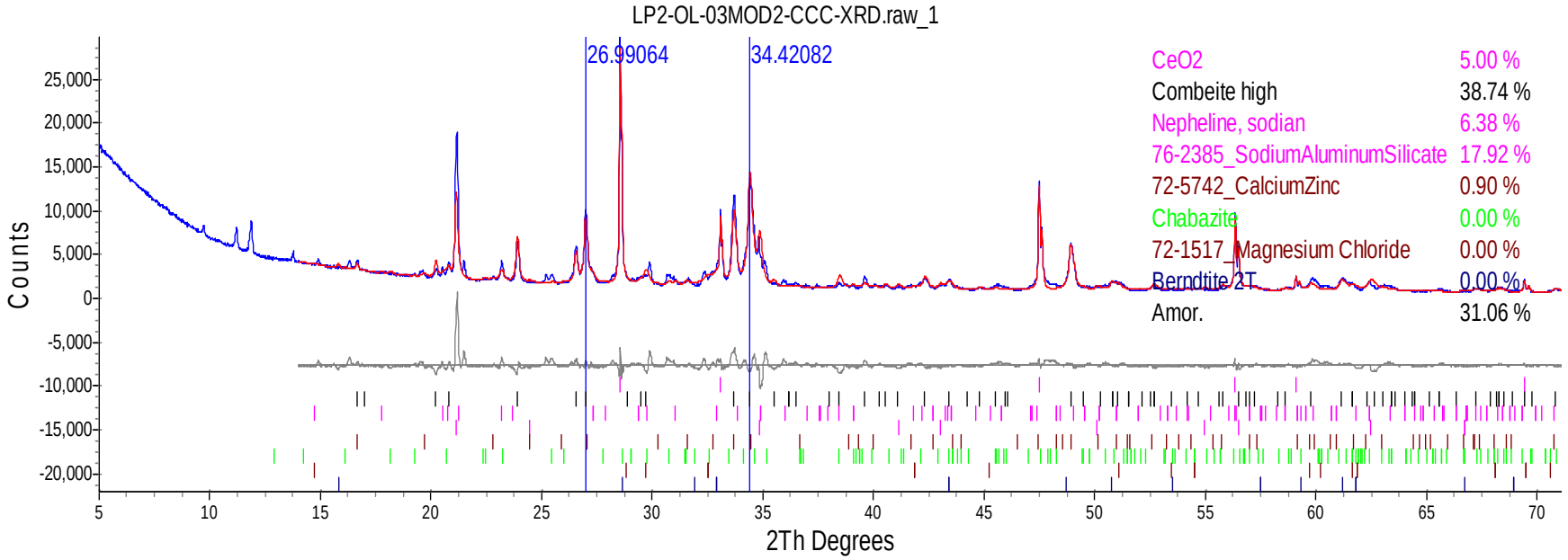


| Phase Name | Wt% of Spiked | Wt% in Spiked Sample | Wt% in Original Sample |
|---|---|---|---|
| $CeO_2$ | 5.003 | 5.003 | 0 |
| Combeite high | 0 | 38.739 | 40.779 |
| Nepheline, sodian | 0 | 6.379 | 6.715 |
| Sodium Aluminum Silicate | 0 | 17.923 | 18.866 |
| Calcium Zinc | 0 | 0.896 | 0.943 |

Figure H.8. XRD Spectrum of CCC-Treated Glass LP2-OL-03 MOD2

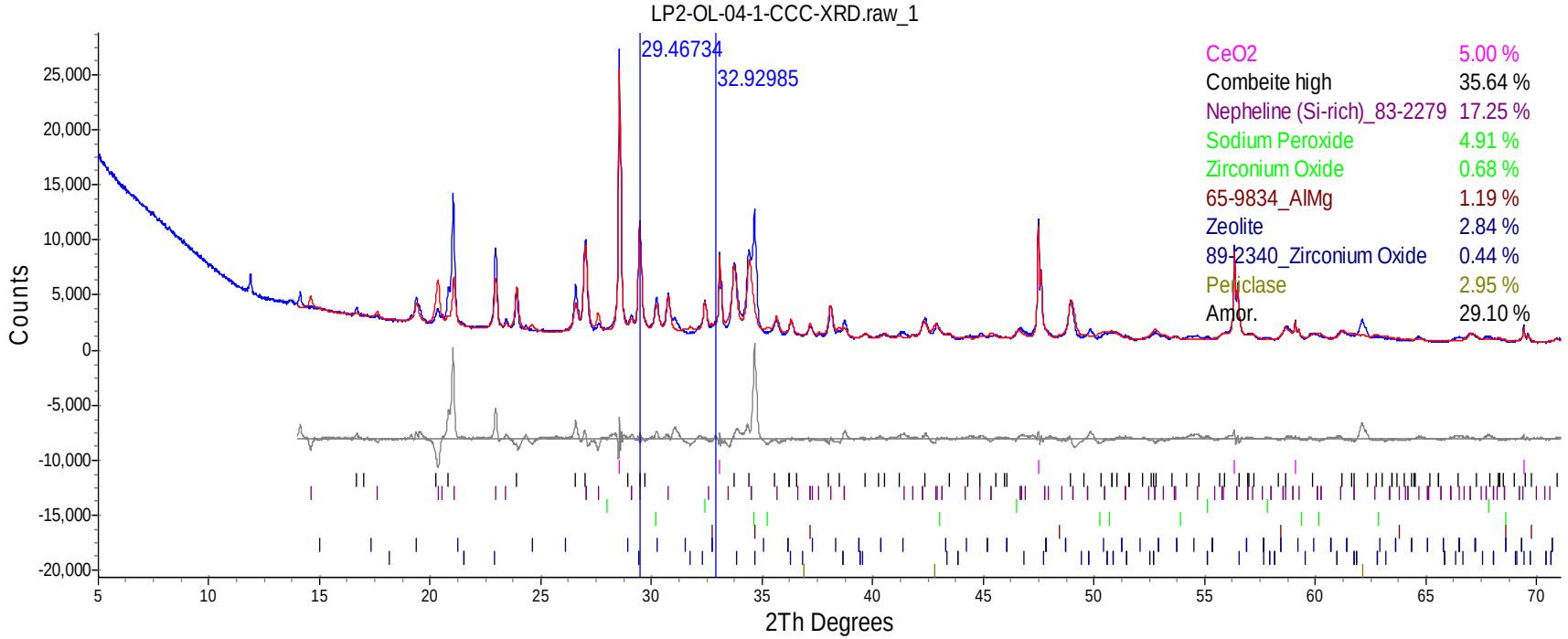


| Phase Name | Wt% of Spiked | Wt% in Spiked Sample | Wt% in Original Sample |
|---|---|---|---|
| $CeO_2$ | 4.998 | 4.998 | 0 |
| Combeite high | 0 | 35.645 | 37.520 |
| Nepheline (Si-rich) | 0 | 17.253 | 18.161 |
| Sodium Peroxide | 0 | 4.914 | 5.173 |
| Zirconium Oxide | 0 | 0.680 | 0.716 |
| 65-9834_AlMg | 0 | 1.186 | 1.248 |
| Zeolite | 0 | 2.835 | 2.984 |
| 89-2340_Zirconium Oxide | 0 | 0.438 | 0.461 |
| Periclase | 0 | 2.955 | 3.110 |

Figure H.9. XRD Spectrum of CCC-Treated Glass LP2-OL-04-1

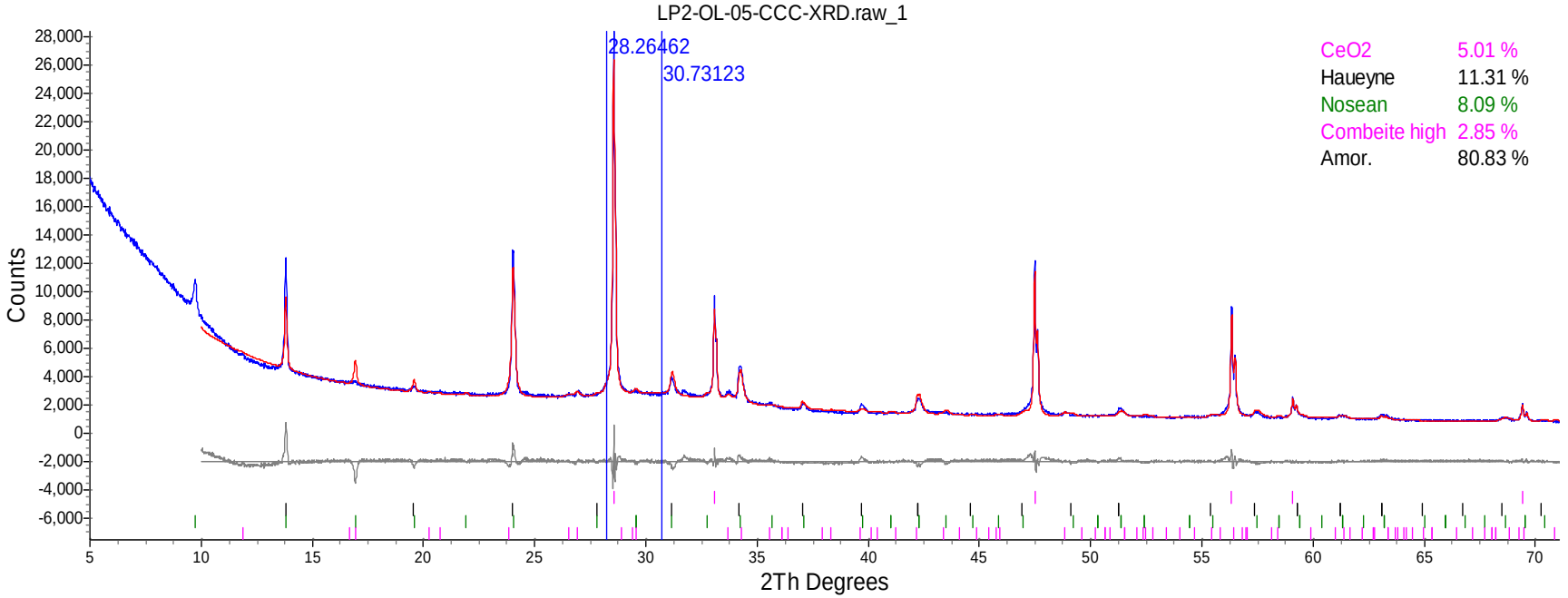


| Phase Name | Wt% of Spiked | Wt% in Spiked Sample | Wt% in Original Sample |
|---|---|---|---|
| $CeO_2$ | 5.008 | 5.008 | 0 |
| Haueyne | 0 | 11.311 | 11.907 |
| Nosean | 0 | 8.088 | 8.514 |
| Combeite high | 0 | 2.849 | 2.999 |

Figure H.10. XRD Spectrum of CCC-Treated Glass LP2-OL-05

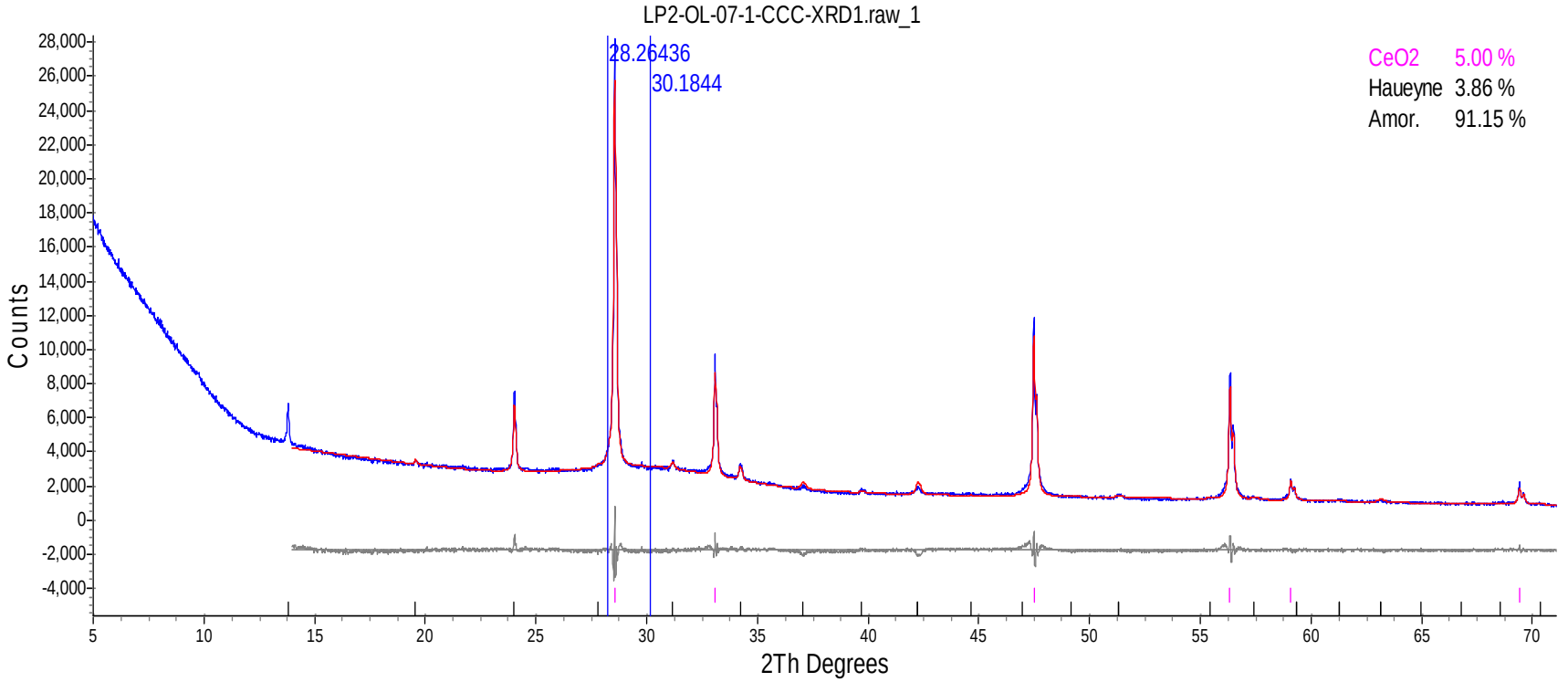


| Phase Name | Wt% of Spiked | Wt% in Spiked Sample | Wt% in Original Sample |
|---|---|---|---|
| $CeO_2$ | 4.995 | 4.995 | 0 |
| Haueyne | 0 | 3.855 | 4.058 |

Figure H.11. XRD Spectrum of CCC-Treated Glass LP2-OL-07-1

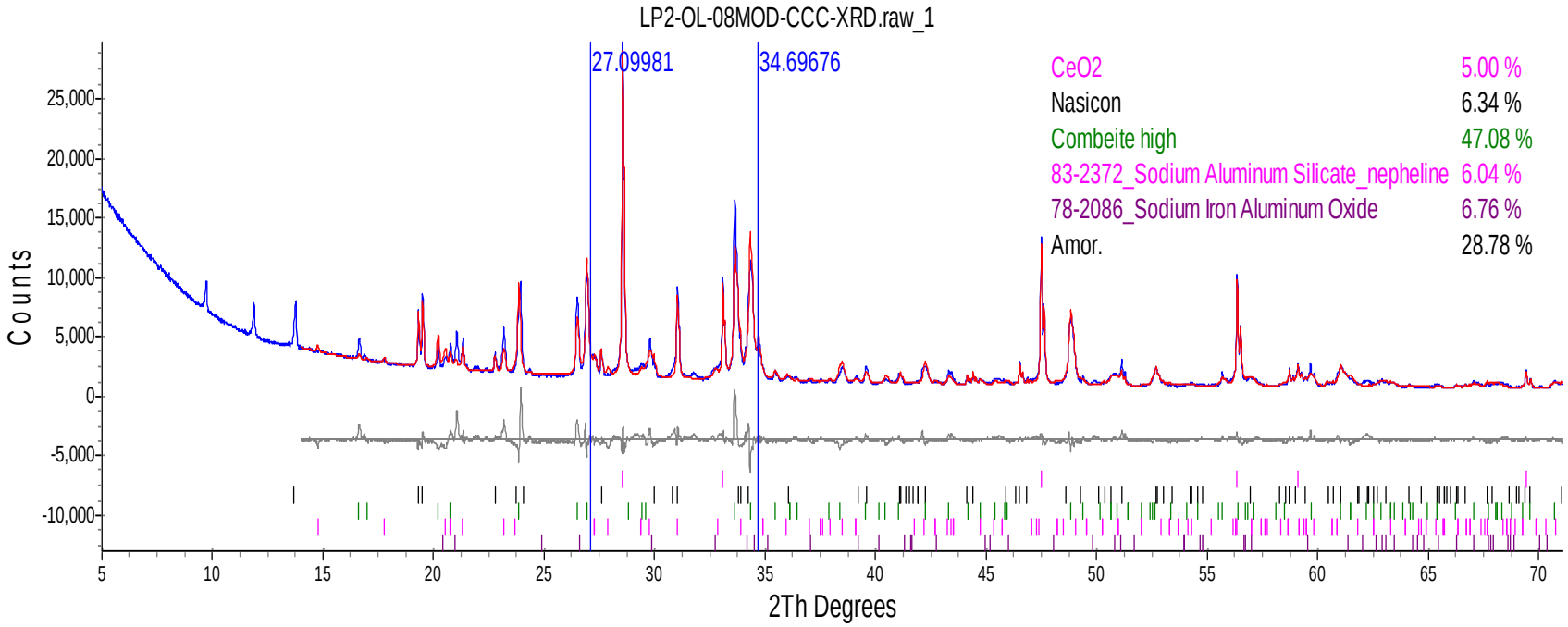


| Phase Name | Wt% of Spiked | Wt% in Spiked Sample | Wt% in Original Sample |
|---|---|---|---|
| $CeO_2$ | 5.001 | 5.001 | 0 |
| Nasicon | 0 | 6.343 | 6.677 |
| Combeite, high | 0 | 47.076 | 49.555 |
| Sodium Aluminum Silicate-Nepheline | 0 | 6.037 | 6.355 |
| Sodium Iron Aluminum Oxide | 0 | 6.763 | 7.119 |

Figure H.12. XRD Spectrum of CCC-Treated Glass LP2-OL-08 MOD

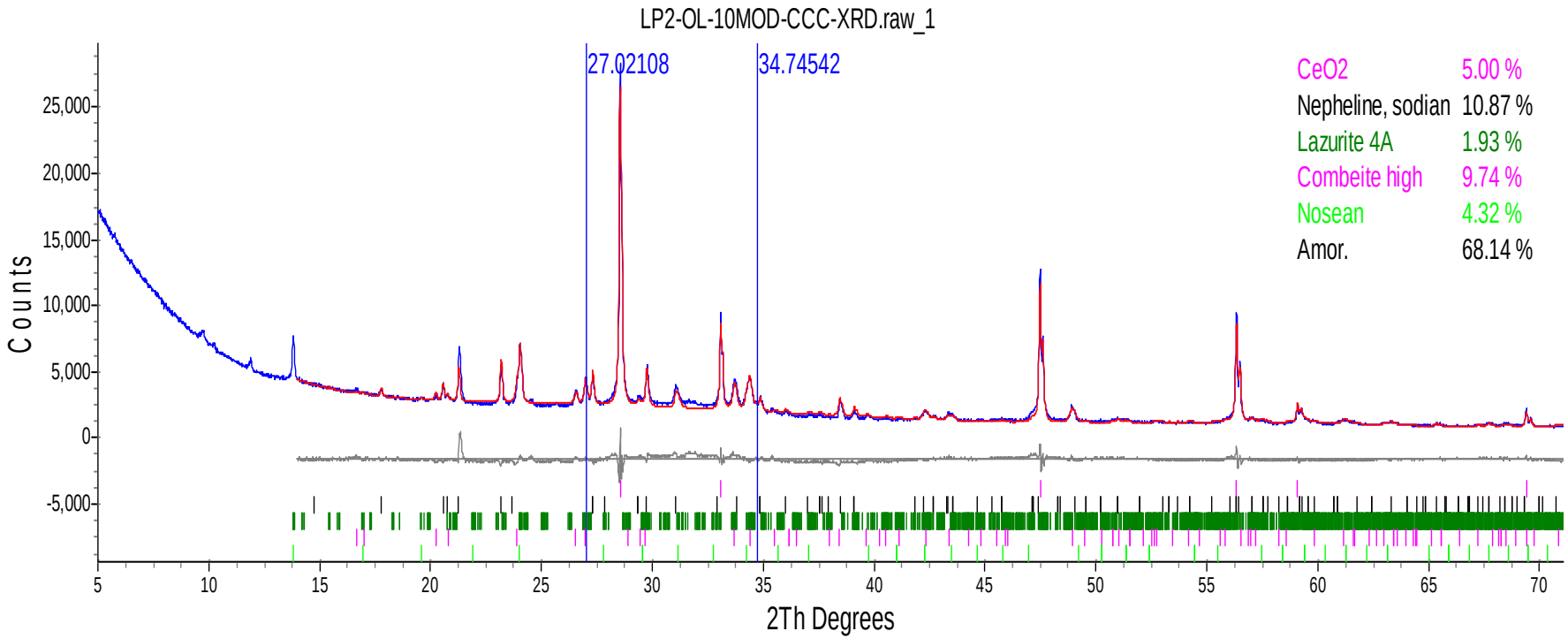


| Phase Name | Wt% of Spiked | Wt% in Spiked Sample | Wt% in Original Sample |
|---|---|---|---|
| $CeO_2$ | 4.995 | 4.995 | 0 |
| Nepheline, sodian | 0 | 10.873 | 11.445 |
| Combeite, high | 0 | 9.739 | 10.251 |
| Lazurite 4A | 0 | 1.934 | 2.035 |
| Nosean | 0 | 4.320 | 4.547 |

Figure H.13. XRD Spectrum of CCC-Treated Glass LP2-OL-10 MOD

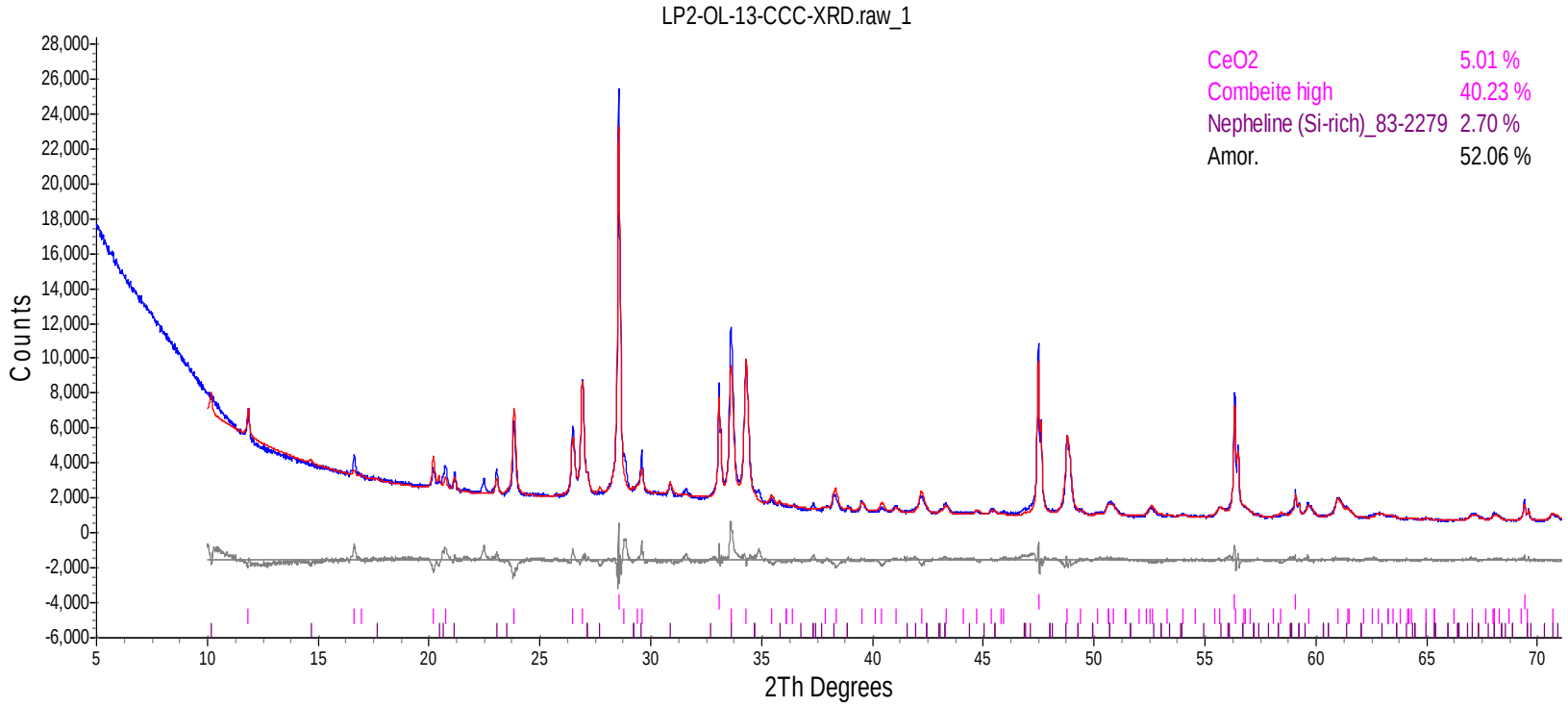


| Phase Name | Wt% of Spiked | Wt% in Spiked Sample | Wt% in Original Sample |
|---|---|---|---|
| $CeO_2$ | 5.007 | 5.007 | 0 |
| Combeite high | 0 | 40.235 | 42.356 |
| Nepheline (Si-rich) | 0 | 2.696 | 2.838 |

Figure H.14. XRD Spectrum of CCC-Treated Glass LP2-OL-13

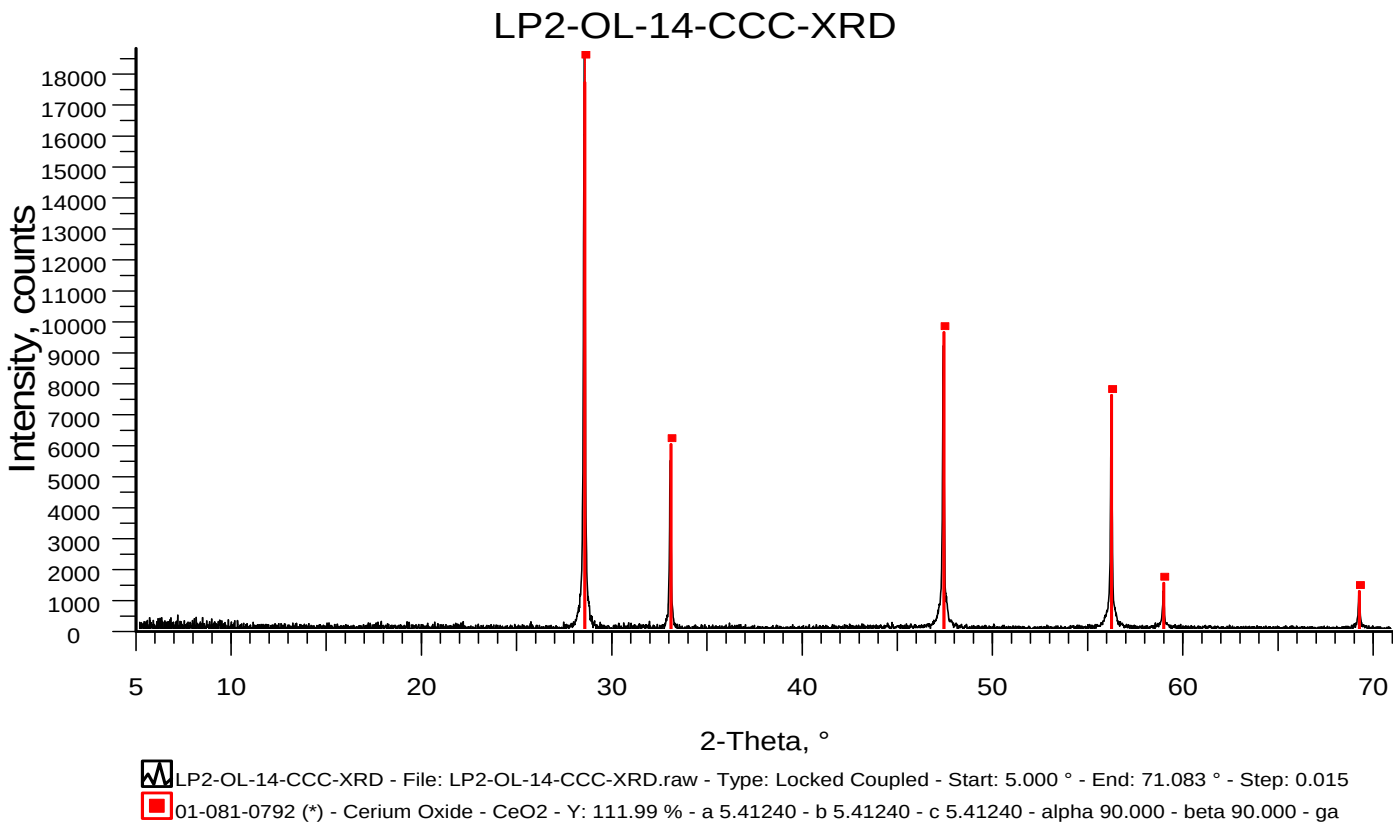


Figure H.15. XRD Spectrum of CCC-Treated Glass LP2-OL-14

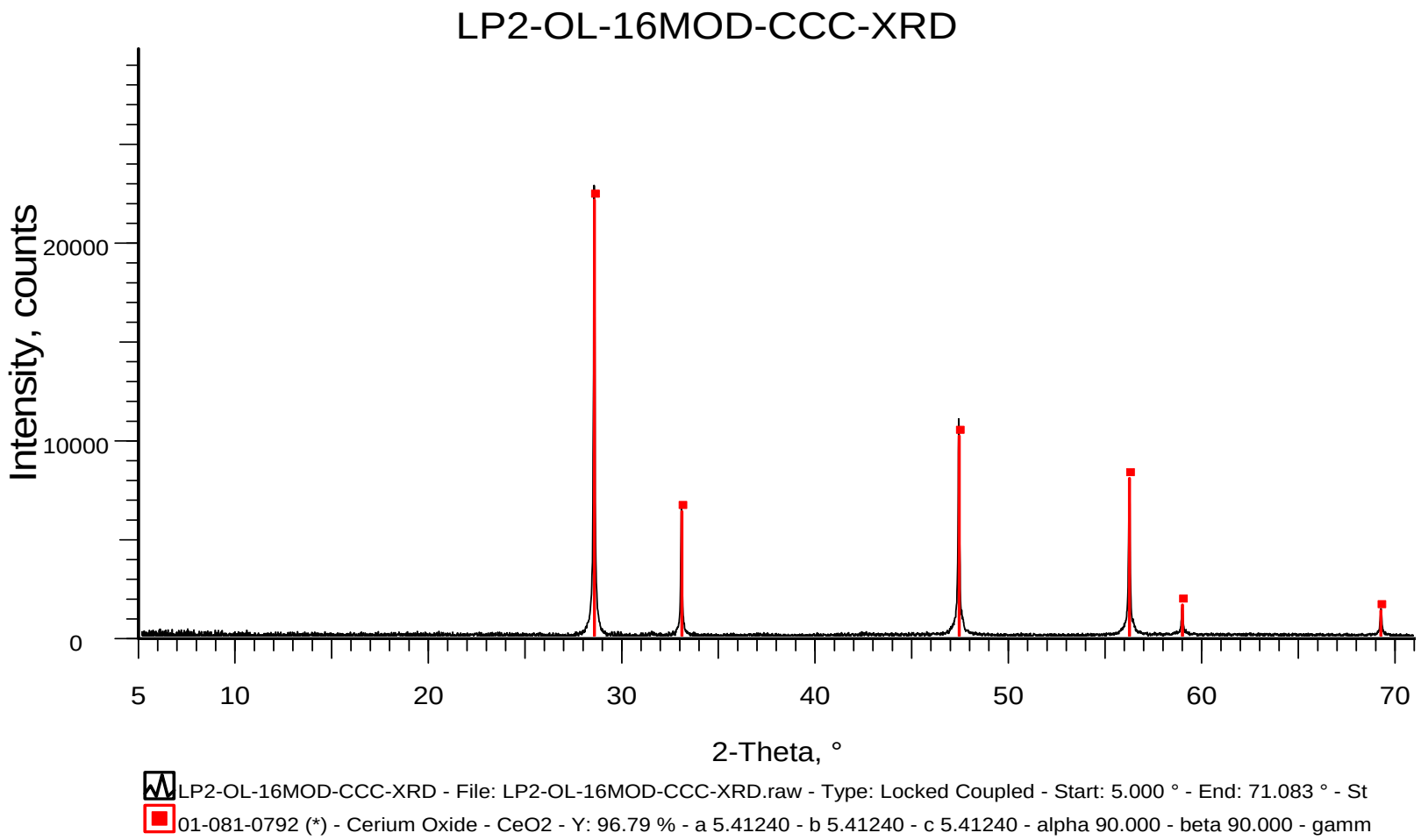


Figure H.16. XRD Spectrum of CCC-Treated Glass LP2-OL-16 MOD

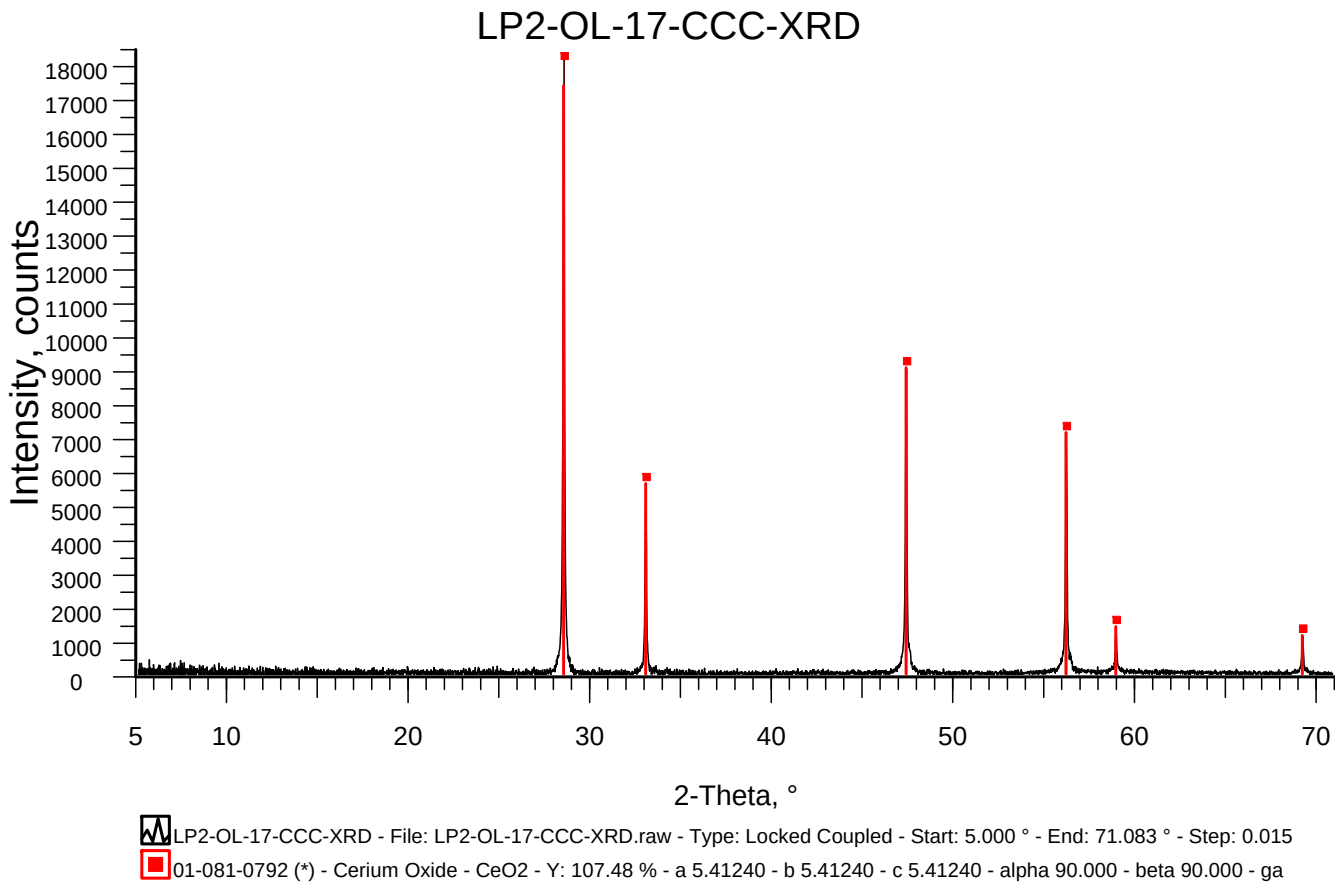


Figure H.17. XRD Spectrum of CCC-Treated Glass LP2-OL-17

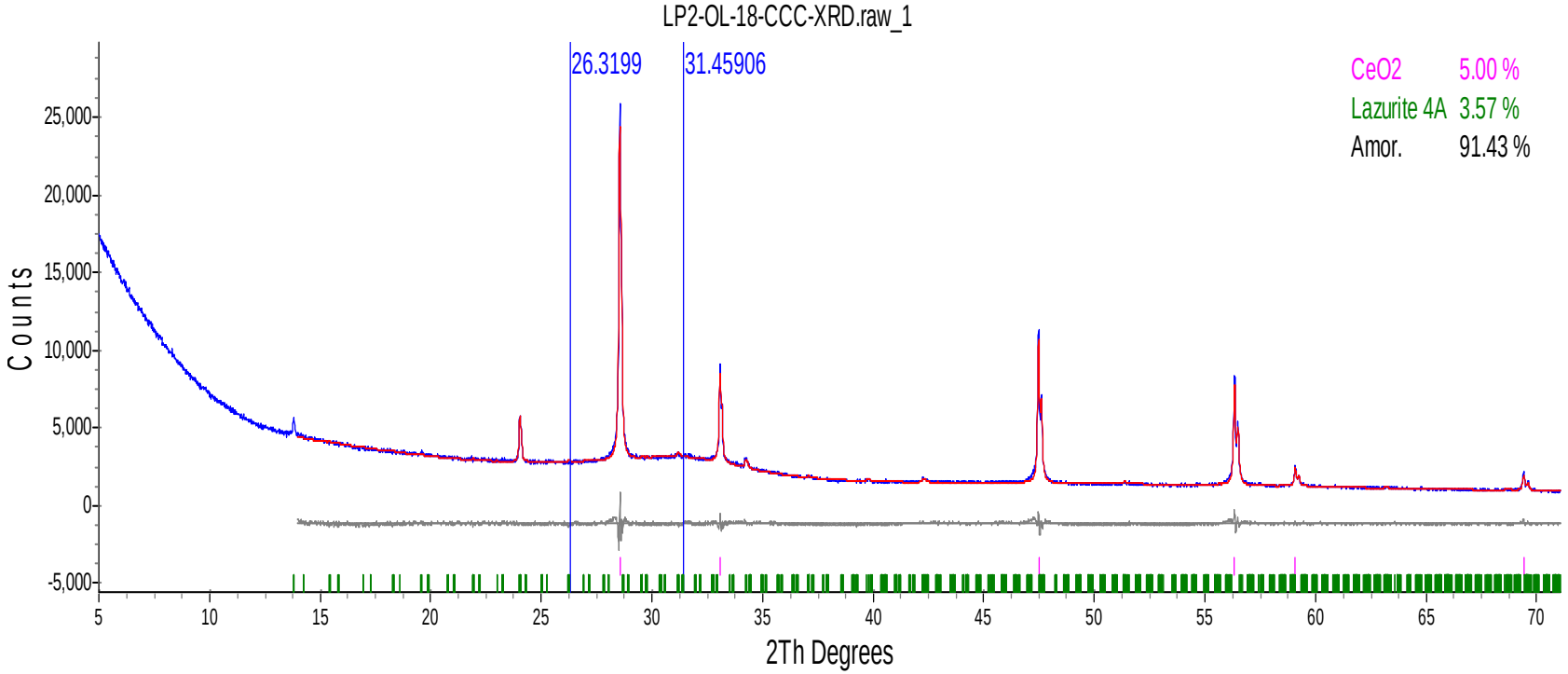


| Phase Name | Wt% of Spiked | Wt% in Spiked Sample | Wt% in Original Sample |
|---|---|---|---|
| $CeO_2$ | 4.997 | 4.997 | 0 |
| Lazurite 4A | 0 | 3.572 | 3.760 |

Figure H.18. XRD Spectrum of CCC-Treated Glass LP2-OL-18

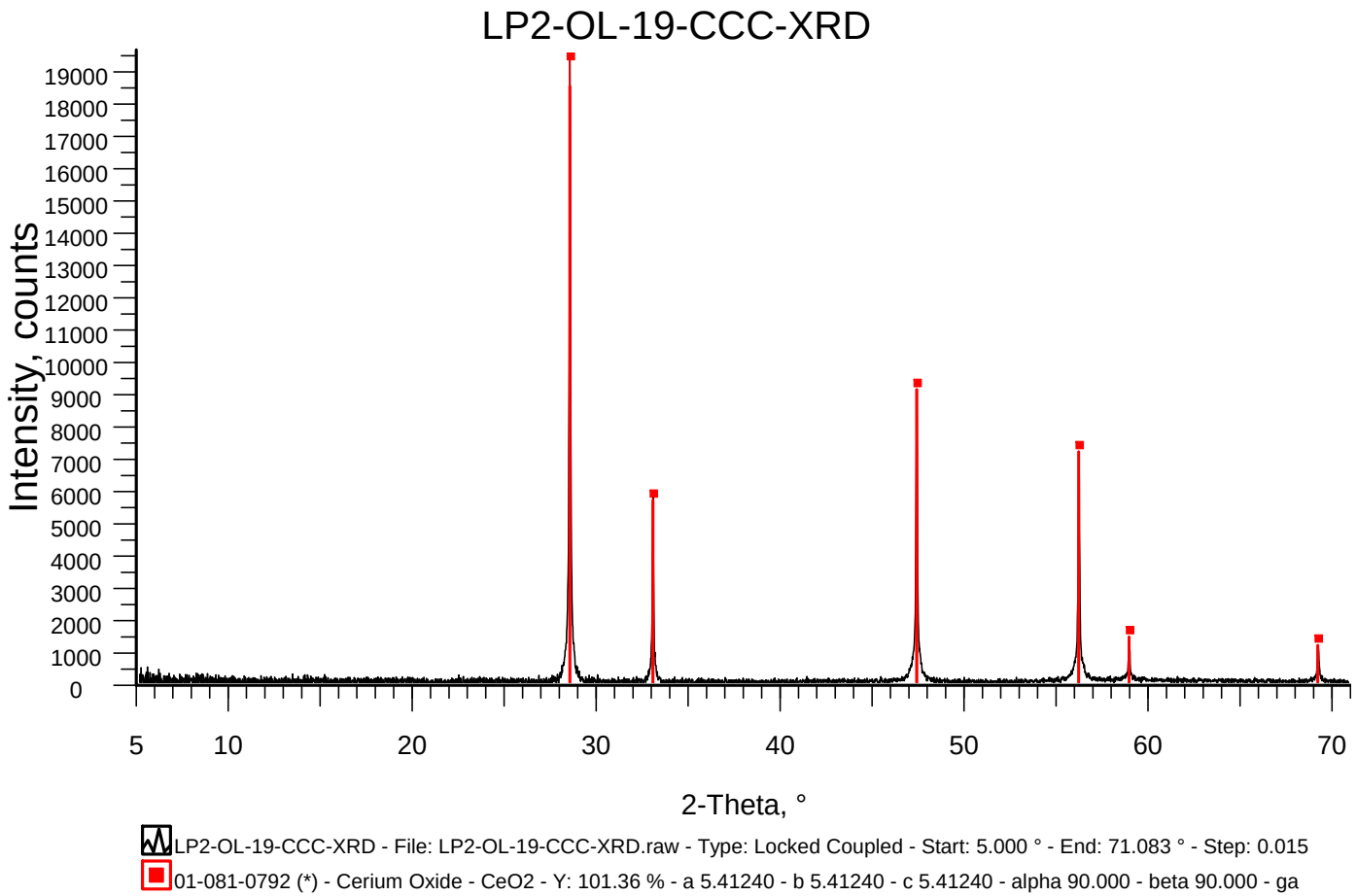


Figure H.19. XRD Spectrum of CCC-Treated Glass LP2-OL-19

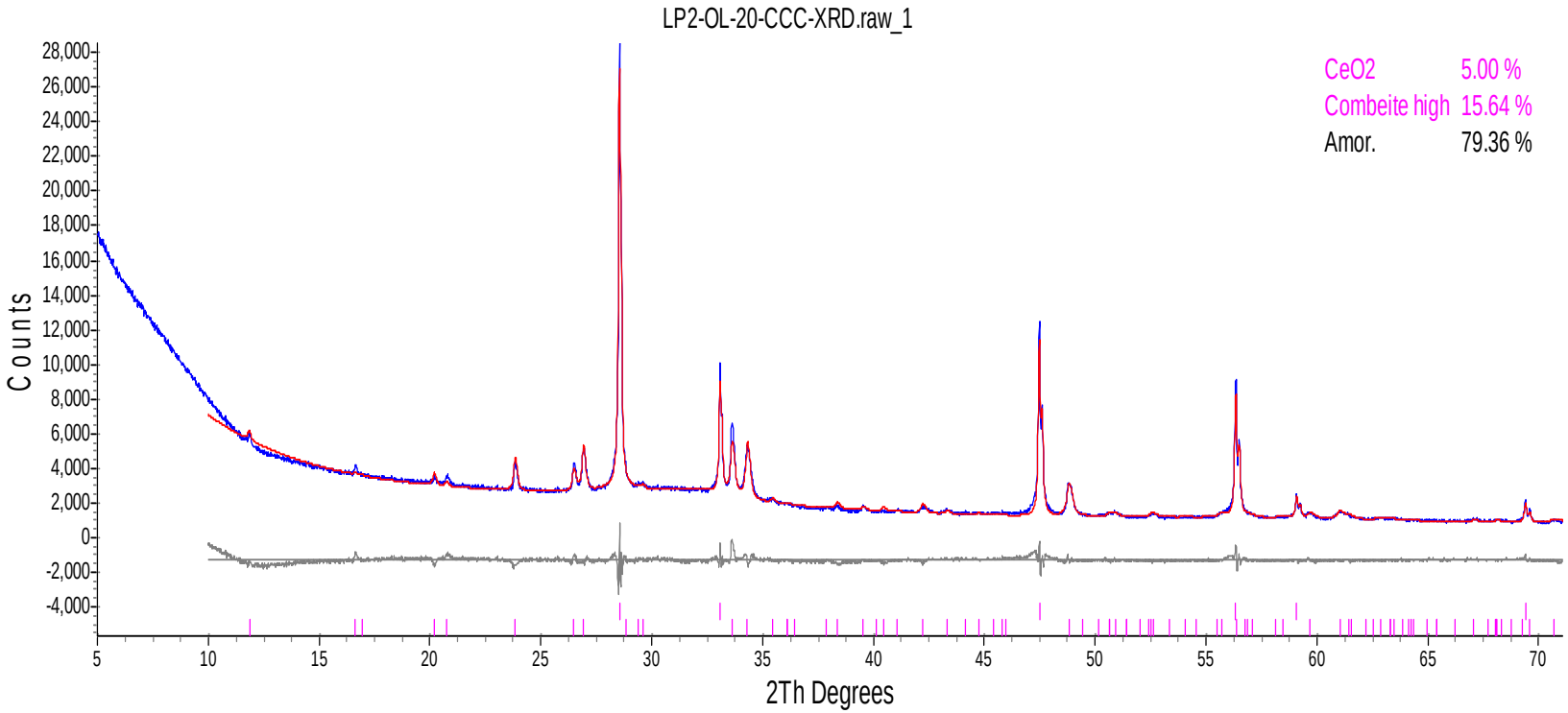


| Phase Name | Wt% of Spiked | Wt% in Spiked Sample | Wt% in Original Sample |
|---|---|---|---|
| $CeO_2$ | 5.001 | 5.001 | 0 |
| Combeite high | 0 | 15.641 | 16.464 |

Figure H.20. XRD Spectrum of CCC-Treated Glass LP2-OL-20

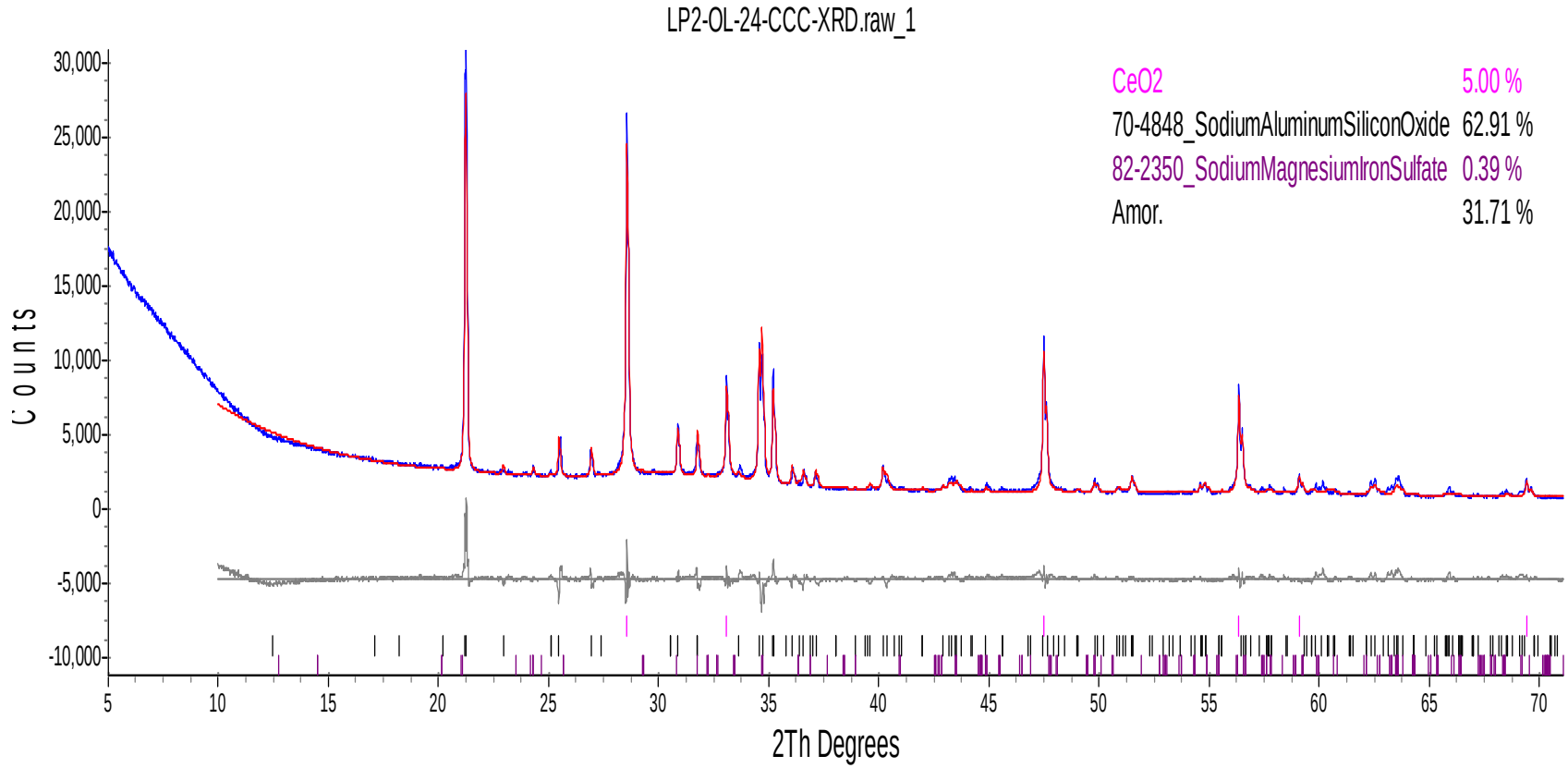


| Phase Name | Wt% of Spiked | Wt% in Spiked Sample | Wt% in Original Sample |
|---|---|---|---|
| $CeO_2$ | 4.997 | 4.997 | 0 |
| SodiumAluminumSiliconOxide | 0 | 62.908 | 62.908 |
| SodiumMagnesiumIronSulfate | 0 | 0.386 | 0.406 |

Figure H.21. XRD Spectrum of CCC-Treated Glass LP2-OL-24

# Appendix I – Vapor Hydration Test (VHT) Results

This appendix shows photos of the VHT samples of Phase 2 enhanced LAW glasses both before and after testing. The glasses tested performed either extremely well or extremely poor, with only four glasses near the corrosion rate limit. These photos show the variation in corrosion with the samples.

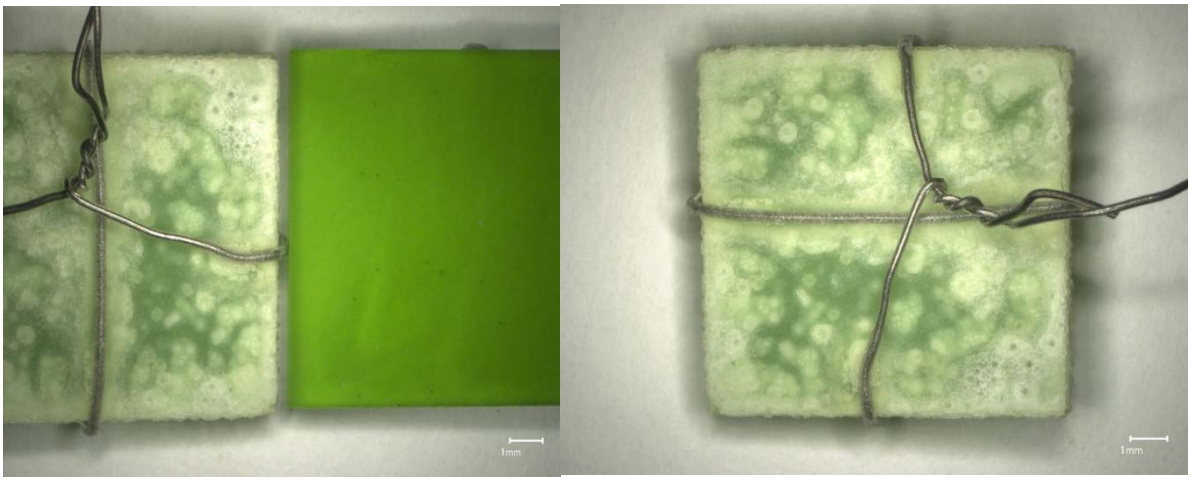

a) Glass square after (left) and before (right) VHT; b) Glass square after VHT

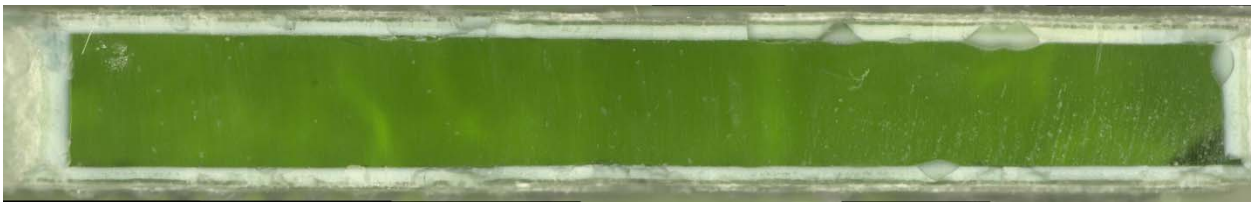

c) Glass cross section magnified after VHT

Figure I.1. Quenched Glass LP2-IL-01 after VHT for 7 Days

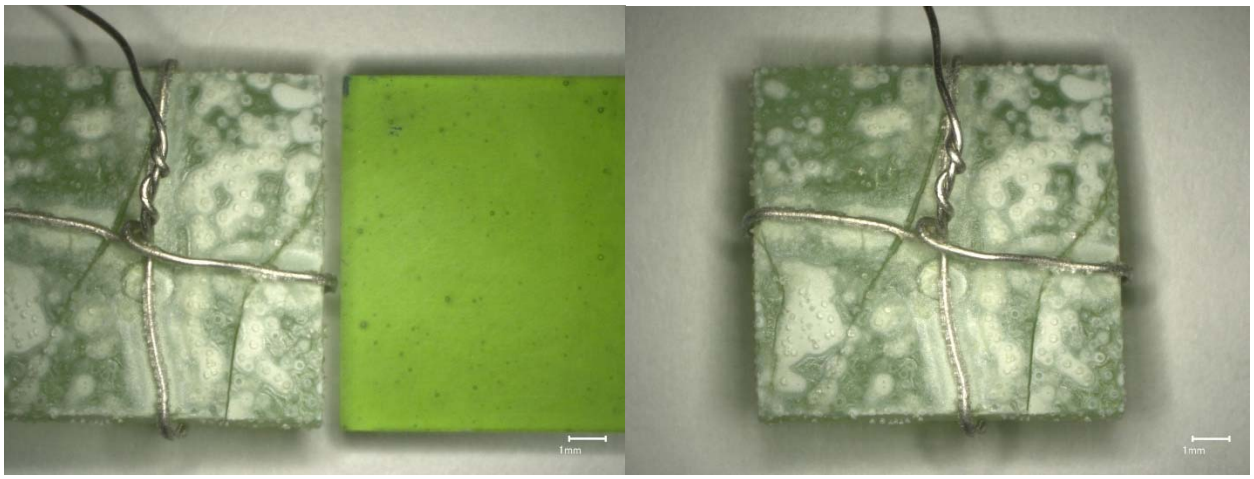

a) Glass square after (left) and before (right) VHT; b) Glass square after VHT

c) Glass cross section magnified after VHT

Figure I.2. Quenched Glass LP2-IL-02 after VHT for 7 Days

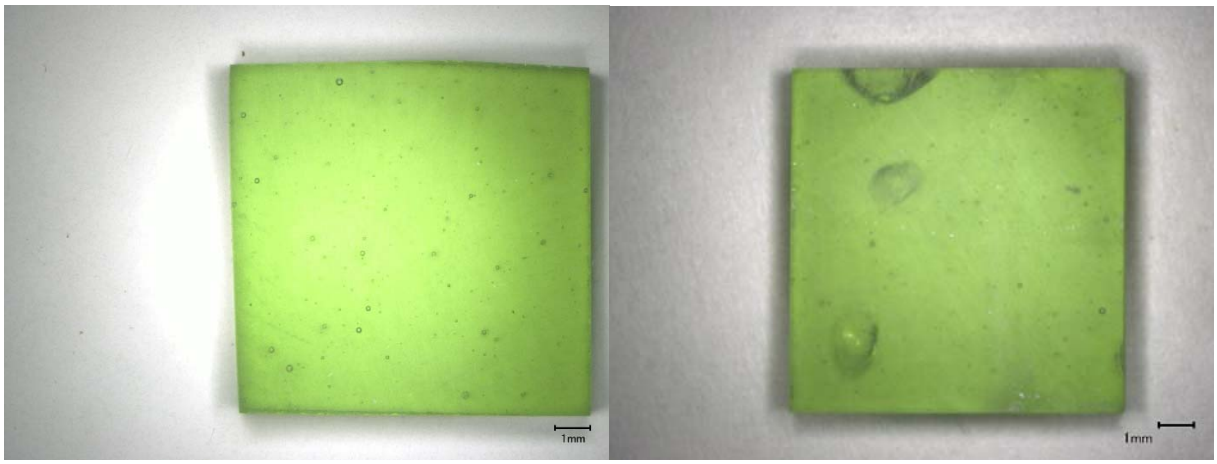

a) Glass square before VHT b) Glass square after VHT

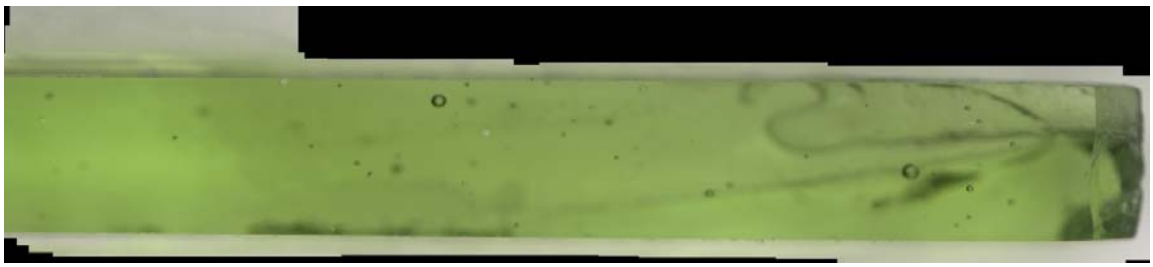

b) Glass cross section magnified after VHT

Figure I.3. Quenched Glass LP2-IL-02 after VHT for 24 Days

a) Glass square after (left) and before (right) VHT; b) Glass square after VHT

c) Glass surface magnified after VHT

Figure I.4. Quenched Glass LP2-IL-03 after VHT for 7 Days

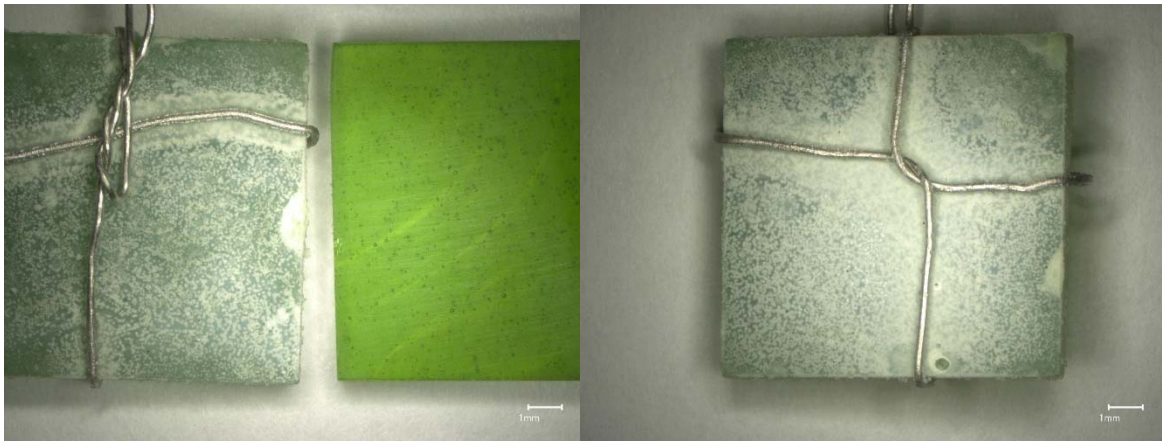

a) Glass square after (left) and before (right) VHT; b) Glass square after VHT

c) Glass cross section magnified after VHT

Figure I.5. Quenched Glass LP2-IL-04 after VHT for 7 Days

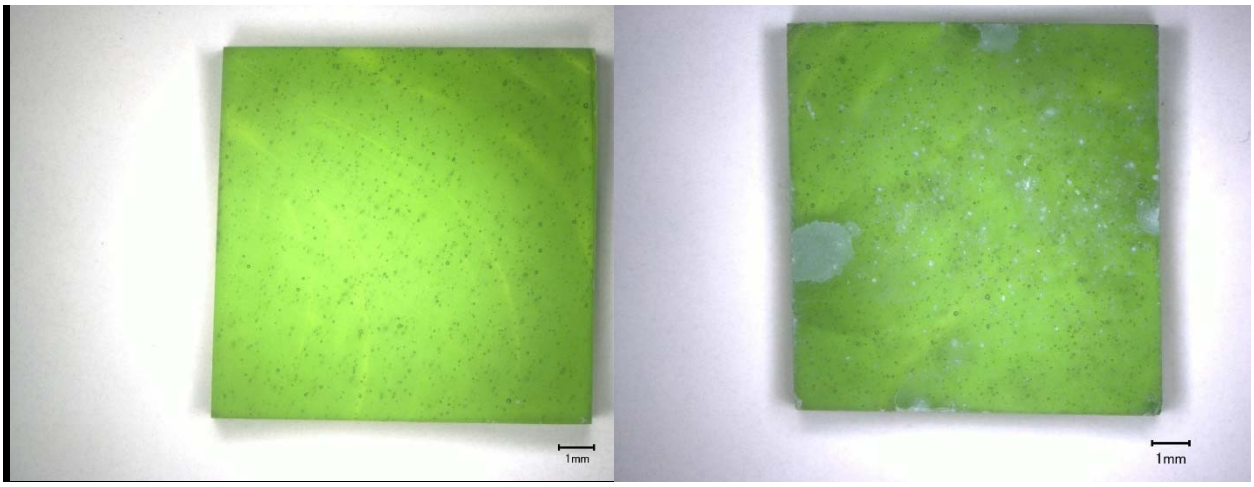


a) Glass square magnified 20X before VHT; b) Glass square magnified 20X after VHT

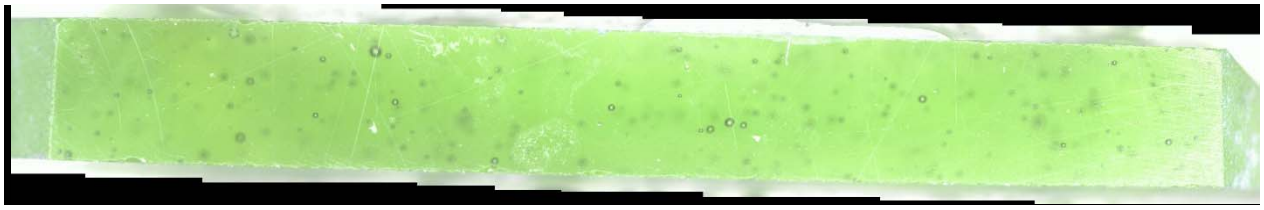

c) Glass cross section magnified after VHT

Figure I.6. Quenched Glass LP2-IL-04 after VHT for 24 Days

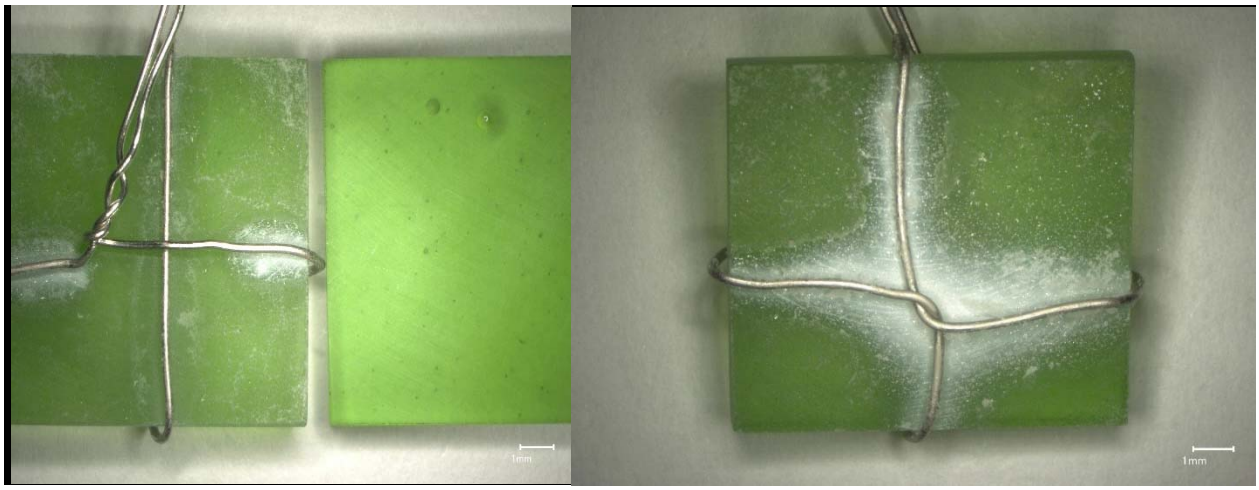


a) Glass square after (left) and before (right) VHT; b) Glass square after VHT

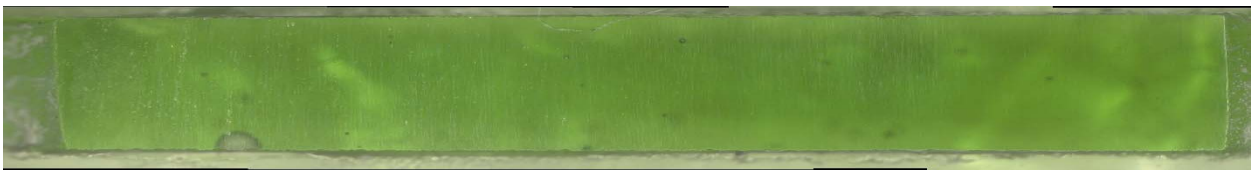

c) Glass cross section magnified after VHT

Figure I.7. Quenched Glass LP2-IL-05 after VHT for 7 Days

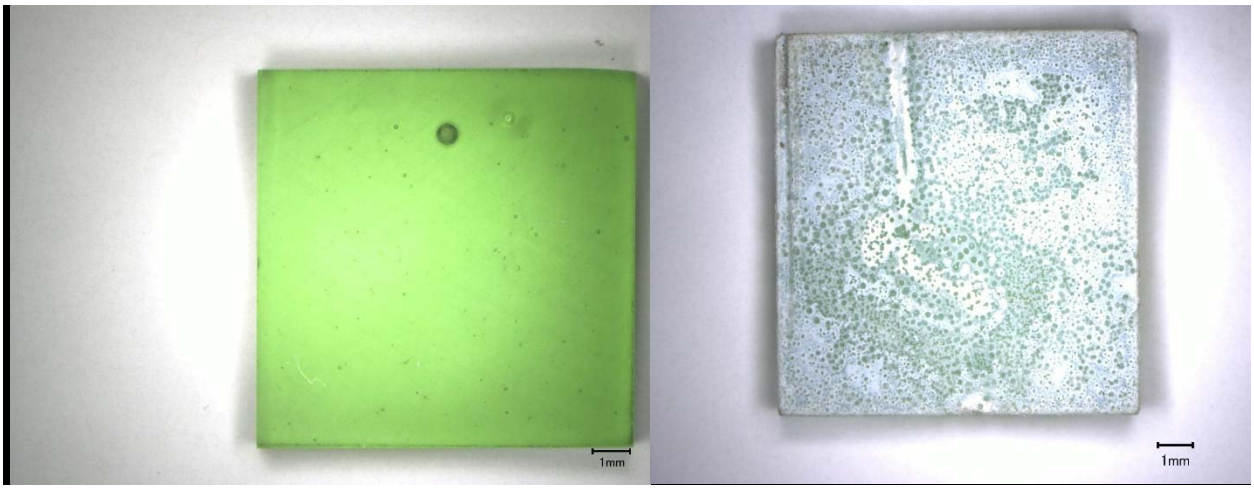


a) Glass square magnified 20X before VHT; b) Glass square magnified 20X after VHT

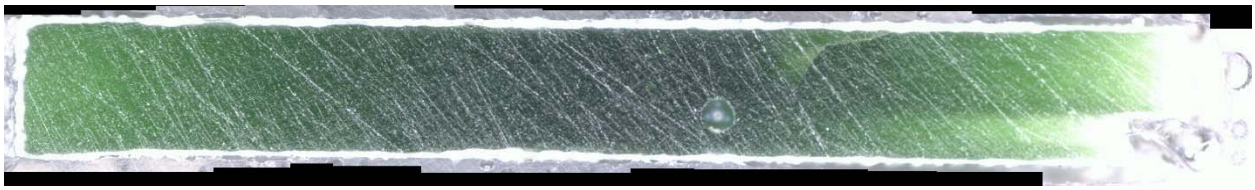

c) Glass cross section magnified after VHT

Figure I.8. Quenched Glass LP2-IL-05 after VHT for 24 Days

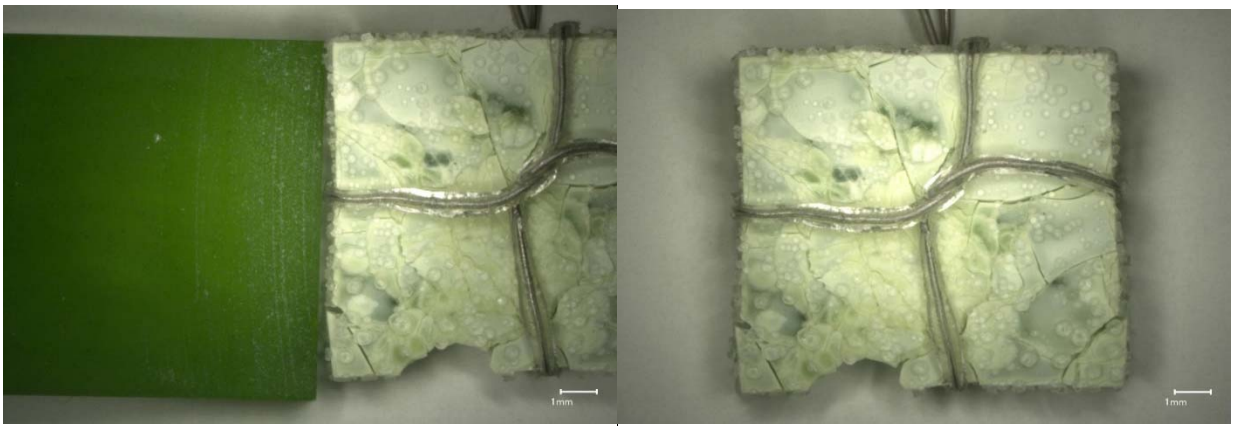


a) Glass square after (right) and before (left) VHT; b) Glass square after VHT

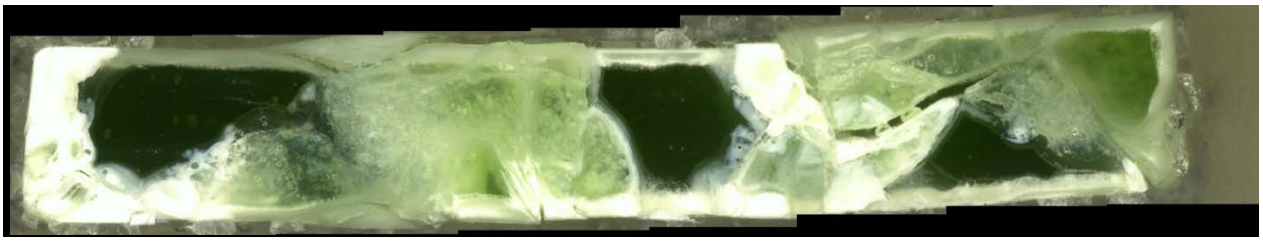

**c**) Glass cross section magnified after VHT

Figure I.9. Quenched Glass LP2-IL-06 after VHT for 7 Days

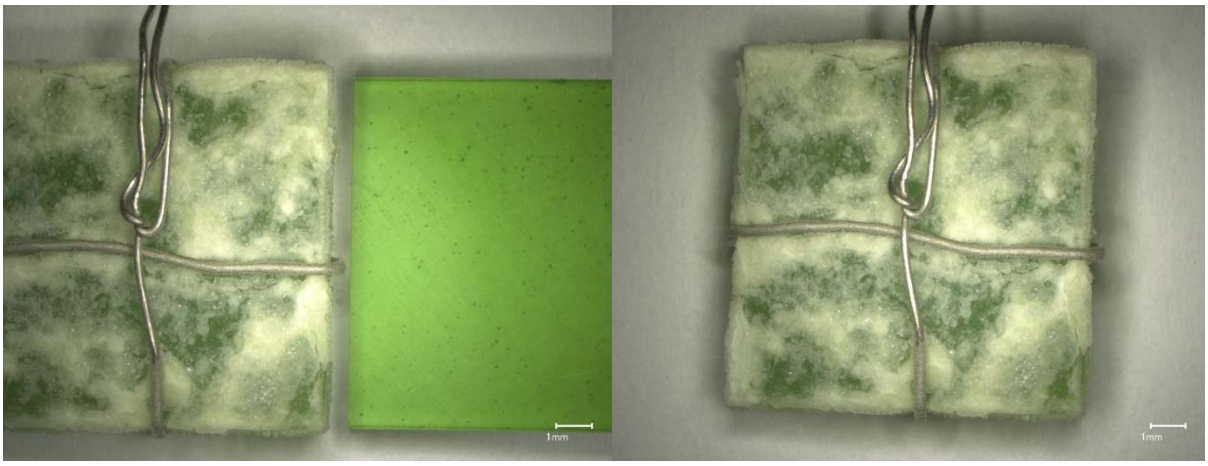

a) Glass square after (left) and before (right) VHT; b) Glass square after VHT

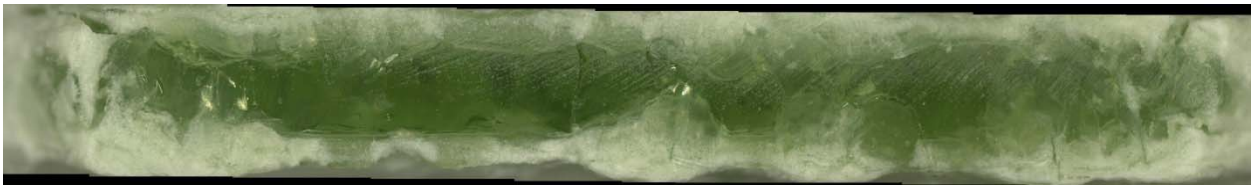

c) Glass cross section magnified after VHT

Figure I.10. Quenched Glass LP2-IL-07 after VHT for 7 Days

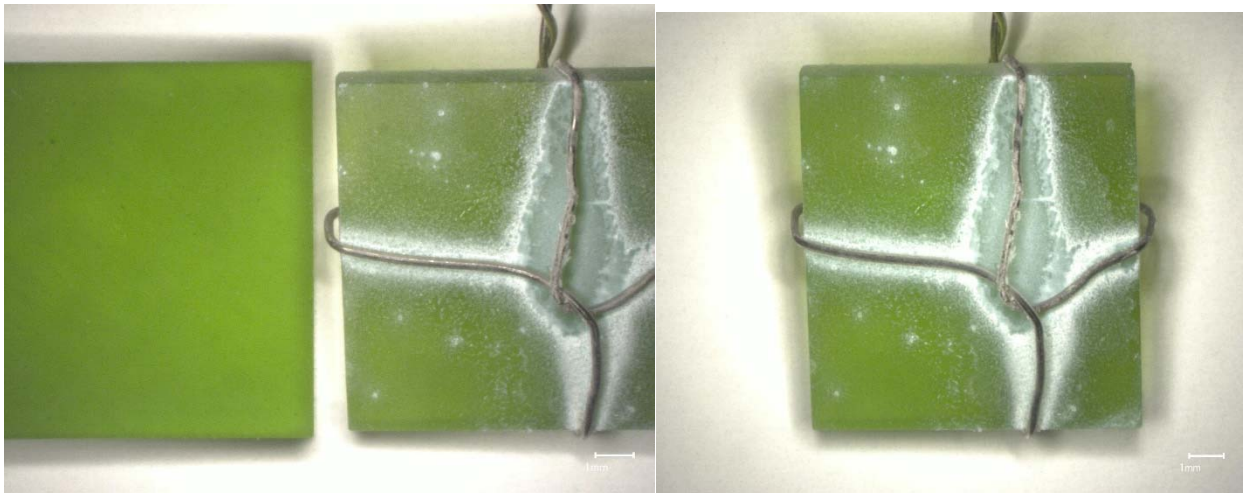

a) Glass square after (right) and before (left) VHT; b) Glass square after VHT

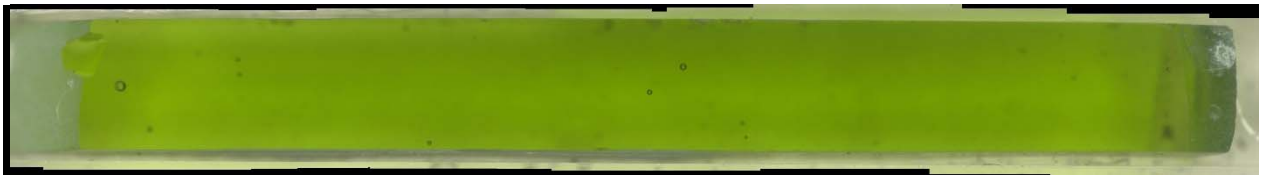

c) Glass cross section magnified after VHT

Figure I.11. Quenched Glass LP2-IL-08 after VHT after 7 Days

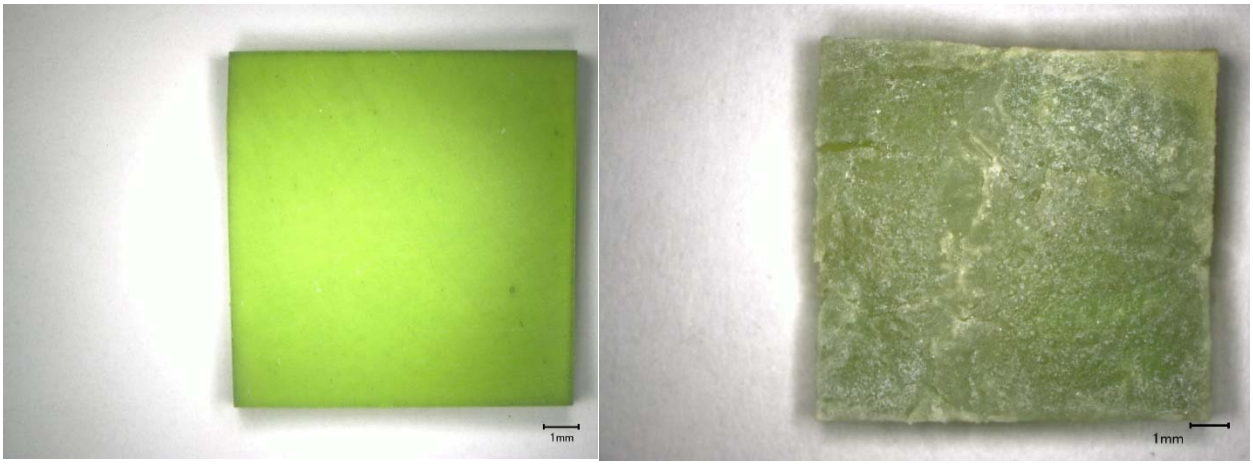


a) Glass square after (right) and before (left) VHT; b) Glass square after VHT

c) Glass cross section magnified after VHT

Figure I.12. Quenched Glass LP2-IL-08 after VHT after 24 Days

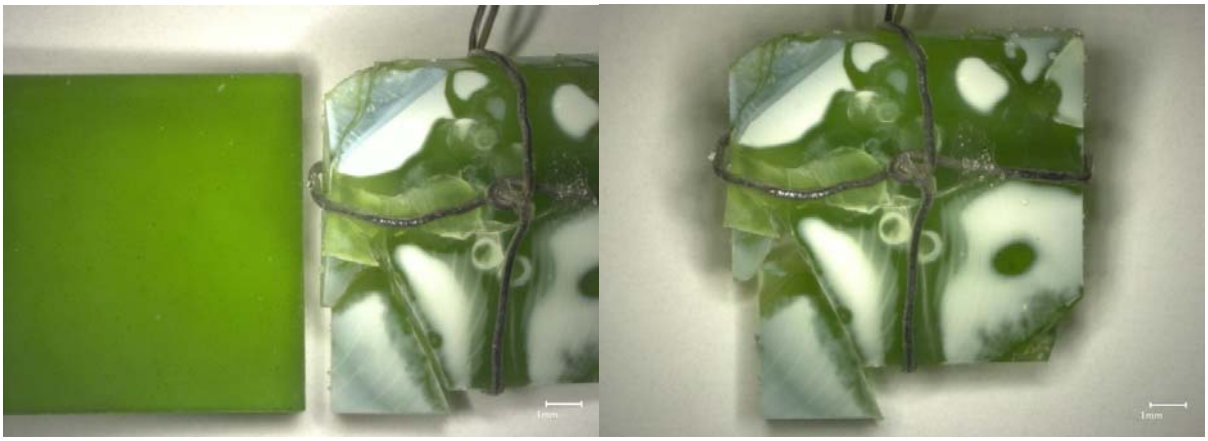

a) Glass square after (right) and before (left) VHT; b) Glass square after VHT

c) Glass cross section magnified after VHT

Figure I.13. Quenched Glass LP2-IL-09 after VHT after 7 Days

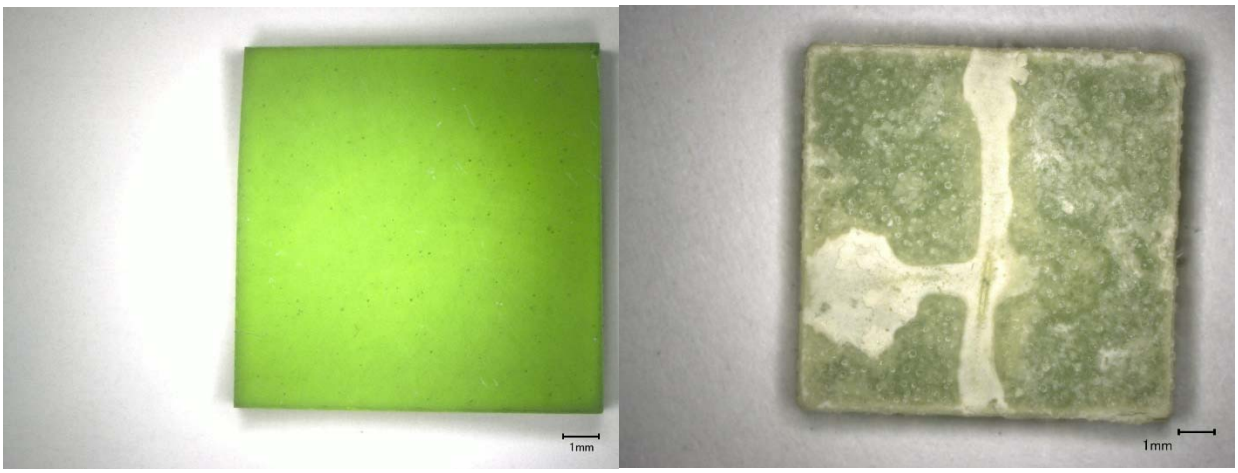


a) Glass square magnified 20X before VHT; b) Glass square magnified 20X after VHT

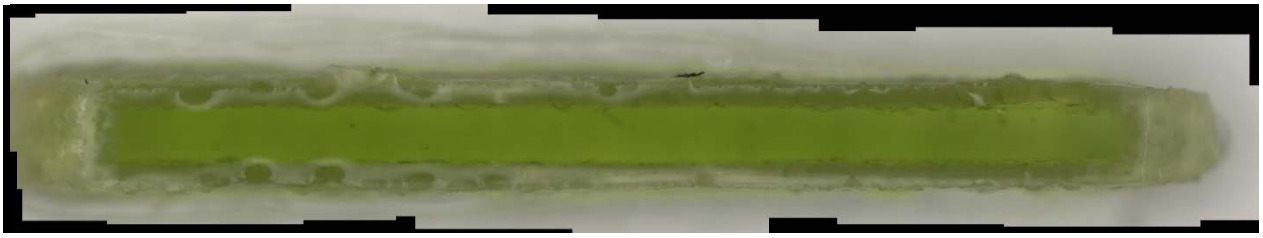

c) Glass cross section magnified after VHT

Figure I.14. Quenched Glass LP2-IL-09 after VHT after 24 Days

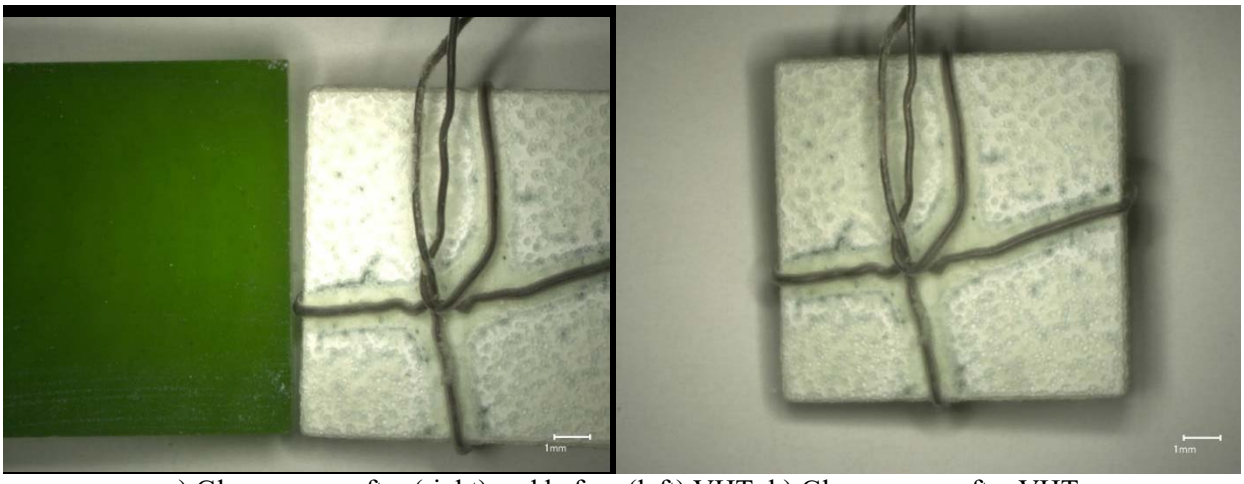


a) Glass square after (right) and before (left) VHT; b) Glass square after VHT

c) Glass cross section magnified after VHT

Figure I.15. Quenched Glass LP2-IL-10 after VHT for 7 Days

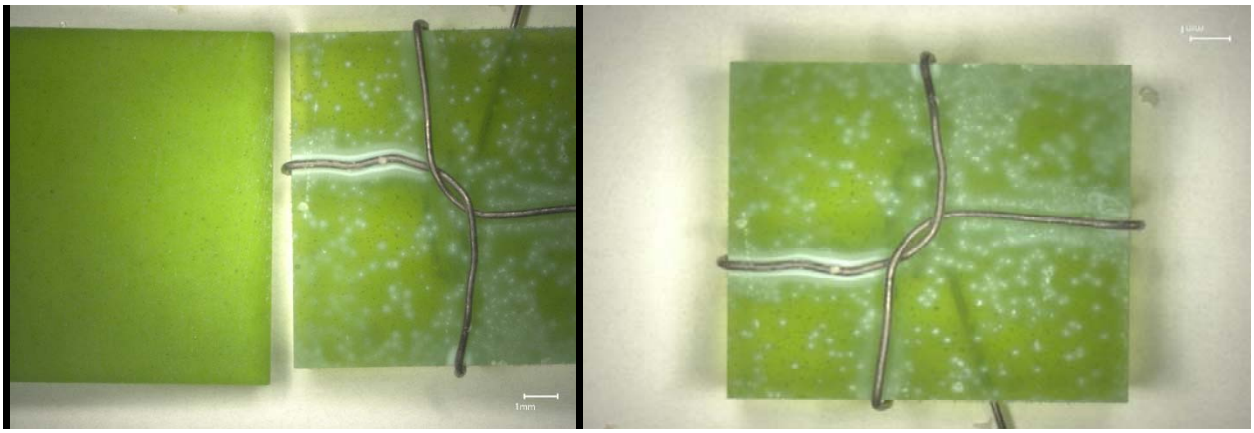

a) Glass square after (right) and before (left) VHT; b) Glass square after VHT

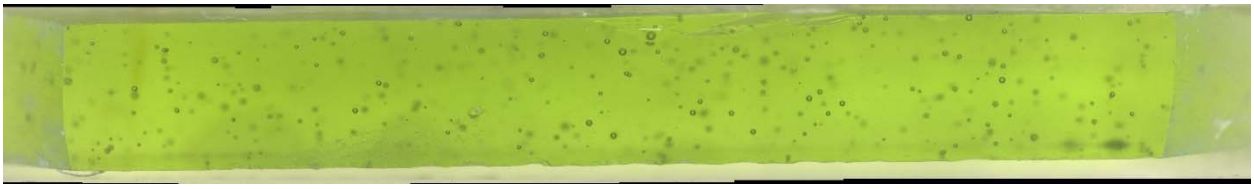

c) Glass cross section magnified after VHT

Figure I.16. Quenched Glass LP2-IL-11 after VHT for 7 Days

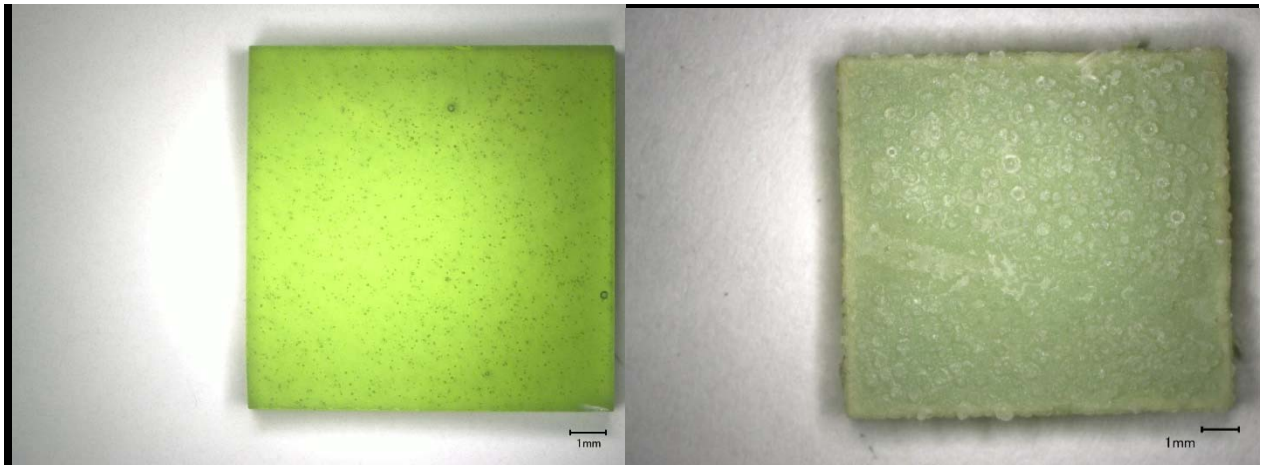

a) Glass square after (right) and before (left) VHT; b) Glass square after VHT

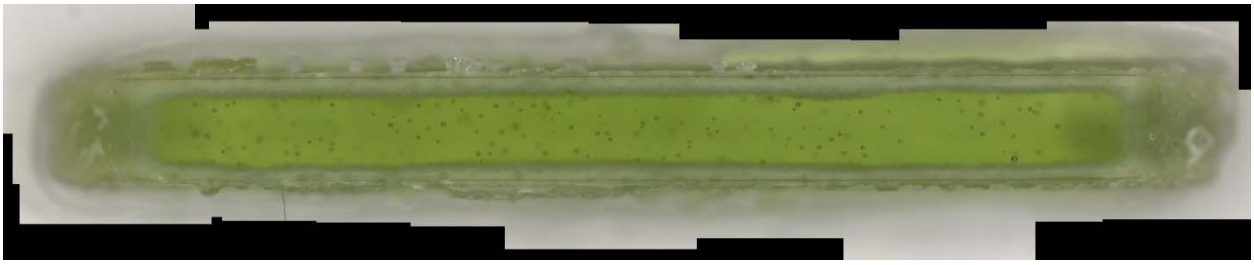

c) Glass cross section magnified after VHT

Figure I.17. Quenched Glass LP2-IL-11 after VHT for 24 Days

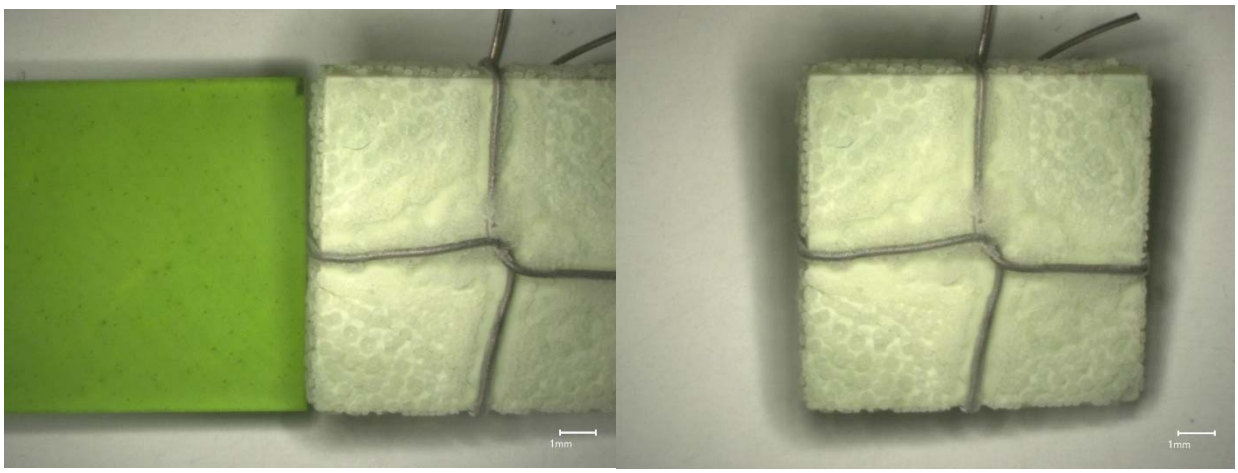

a) Glass square after (right) and before (left) VHT; b) Glass square after VHT

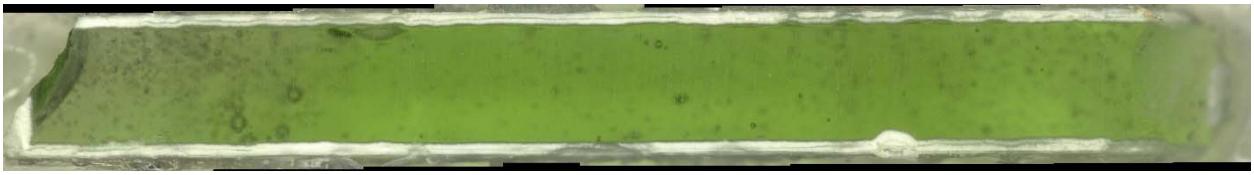

c) Glass cross section magnified after VHT

Figure I.18. Quenched Glass LP2-IL-12 after VHT for 7 Days

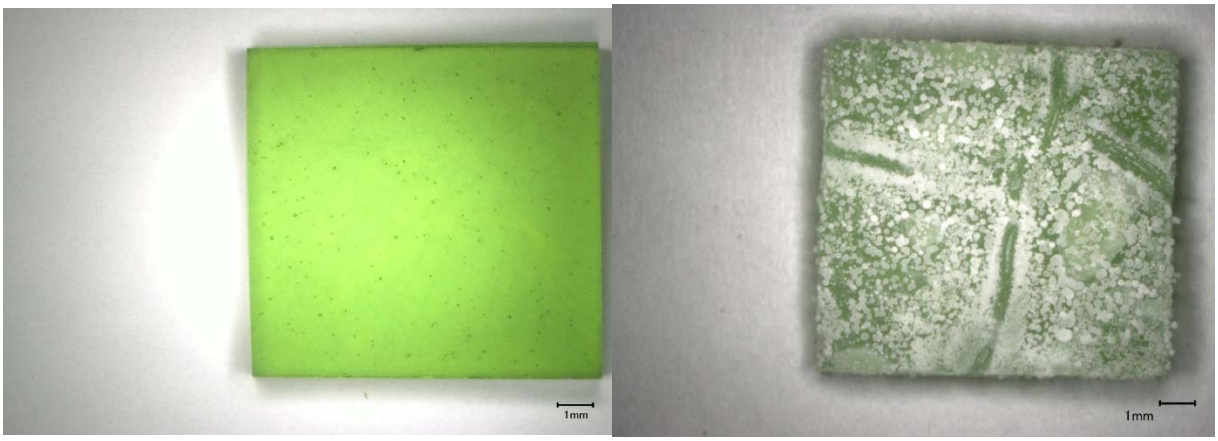

a) Glass square magnified 20X before VHT; b) Glass square magnified 20X after VHT

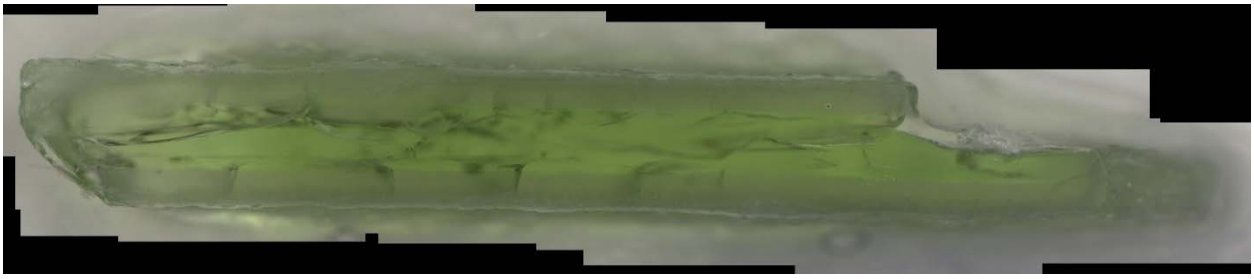

c) Glass surface magnified after VHT

Figure I.19. Quenched Glass LP2-IL-12 after VHT for 24 Days

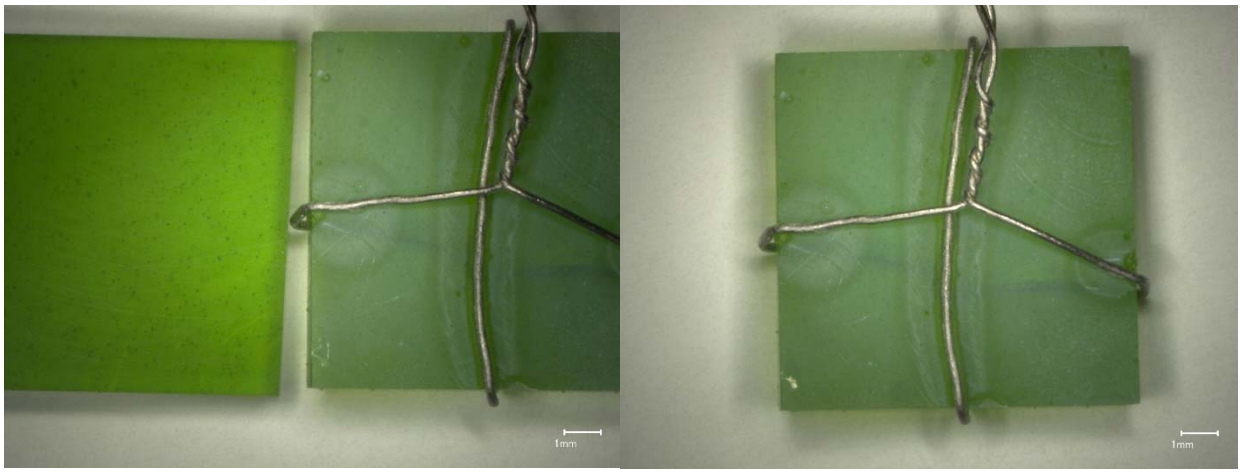

a) Glass square after (right) and before (left) VHT; b) Glass square after VHT

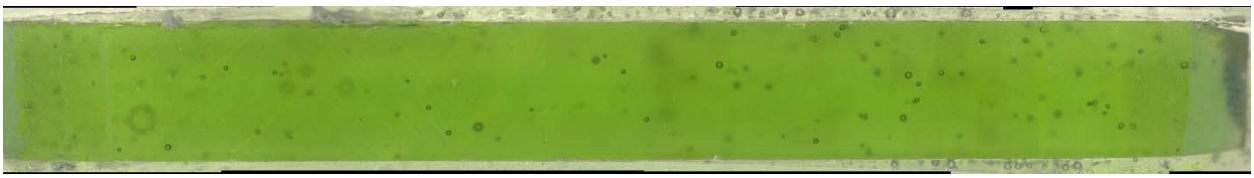

c) Glass cross section magnified after VHT

Figure I.20. Quenched Glass LP2-IL-13 after VHT for 7 Days

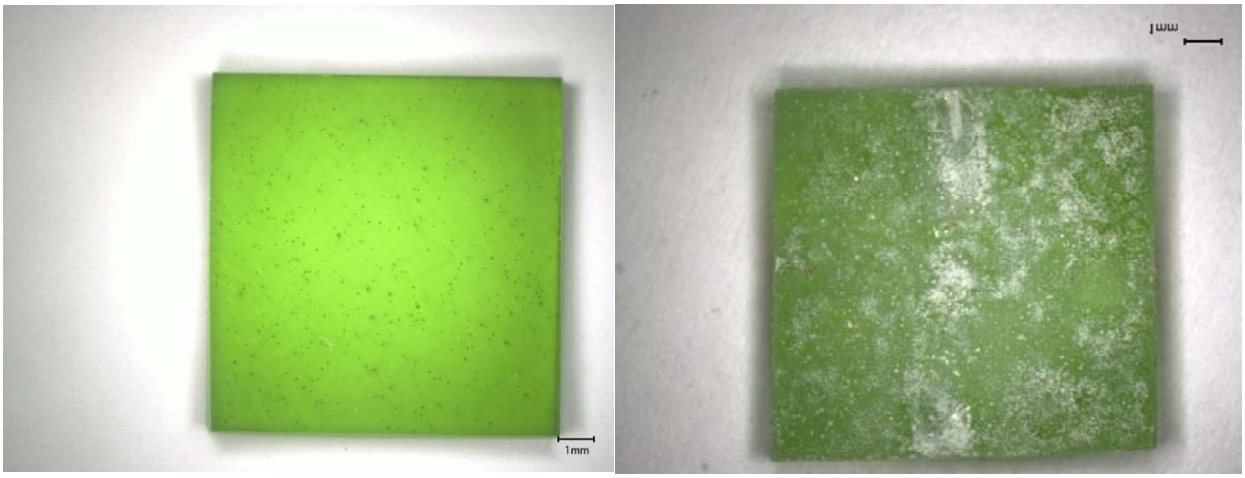

a) Glass square magnified 20X before VHT; b) Glass square magnified 20X after VHT

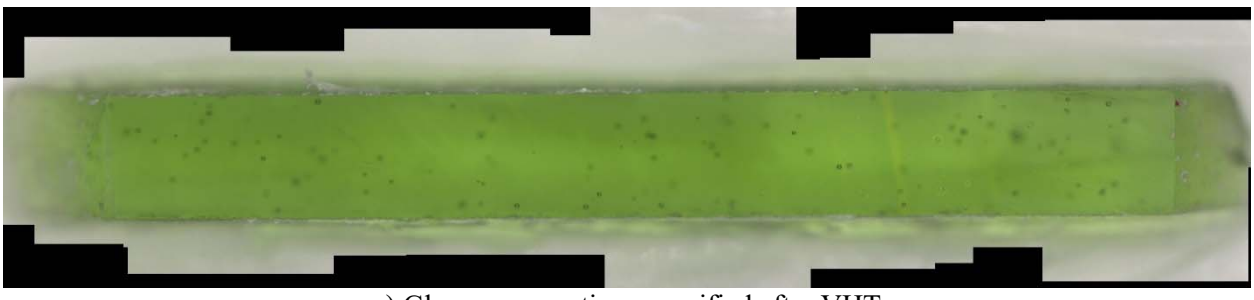

c) Glass cross section magnified after VHT

Figure I.21. Quenched Glass LP2-IL-13 after VHT for 24 Days

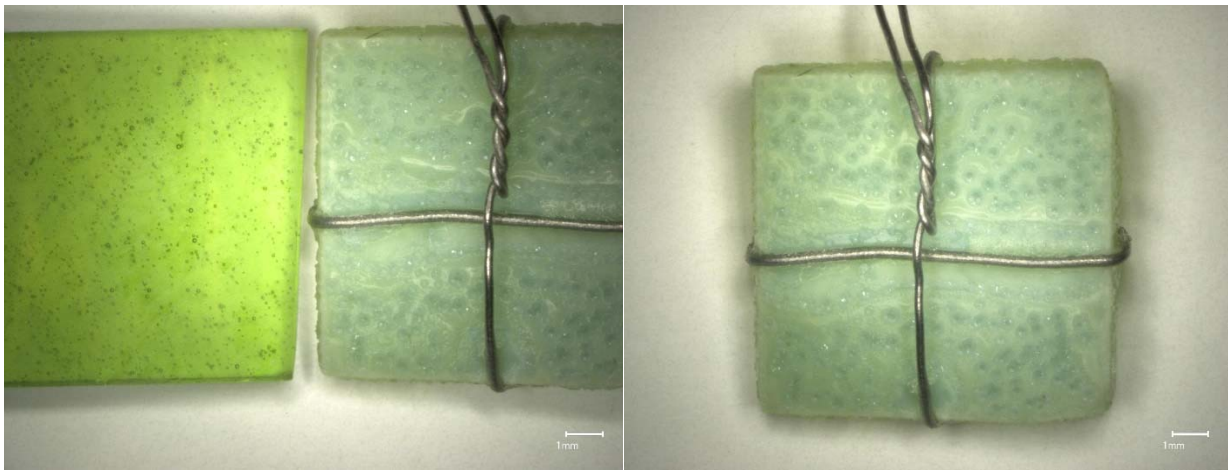

a) Glass square after (right) and before (left) VHT; b) Glass square after VHT

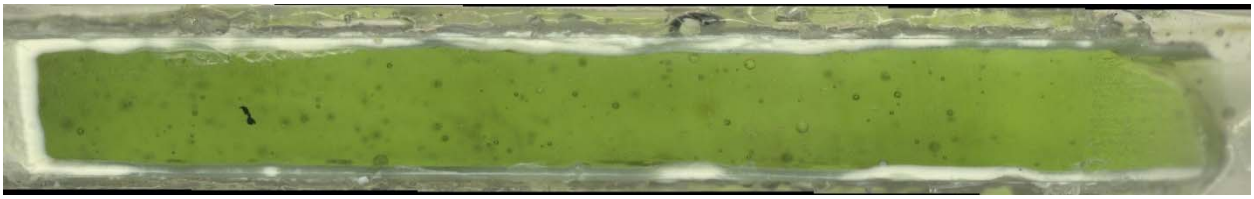

c) Glass cross section magnified after VHT

Figure I.22. Quenched Glass LP2-IL-14 after VHT for 7 Days

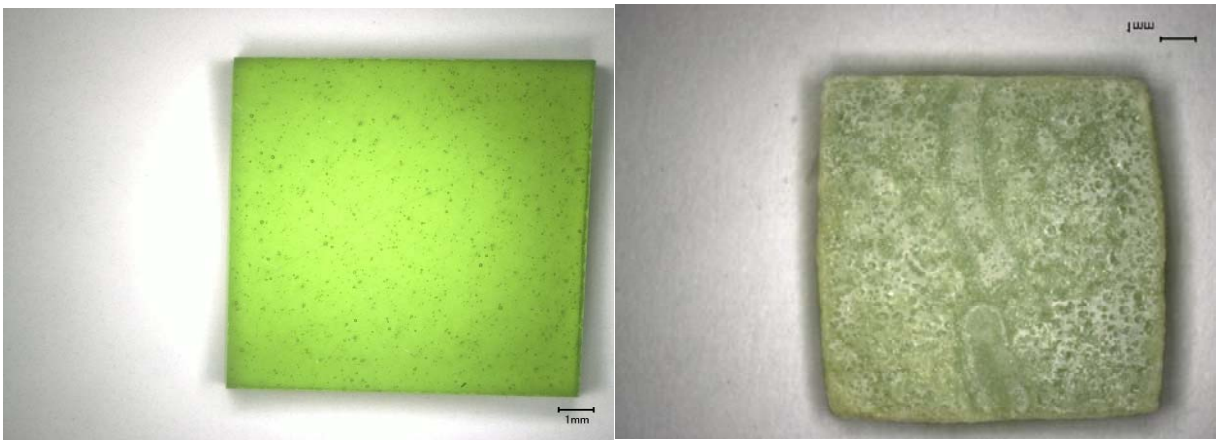

a) Glass square magnified 20X before VHT; b) Glass square magnified 20X after VHT

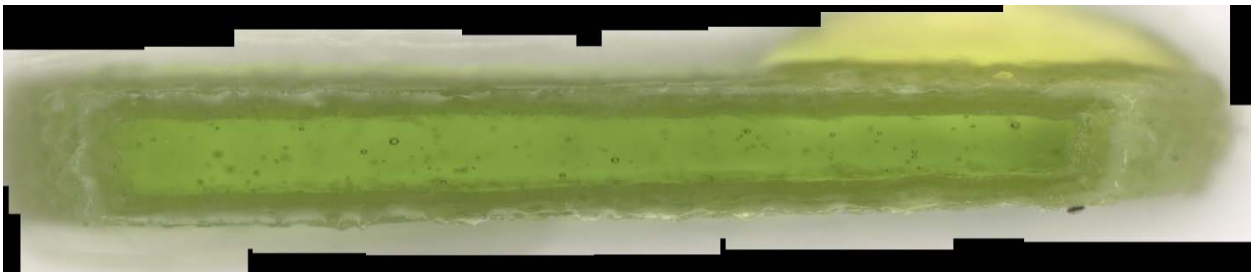

c) Glass cross section magnified after VHT

Figure I.23. Quenched Glass LP2-IL-14 after VHT for 24 Days

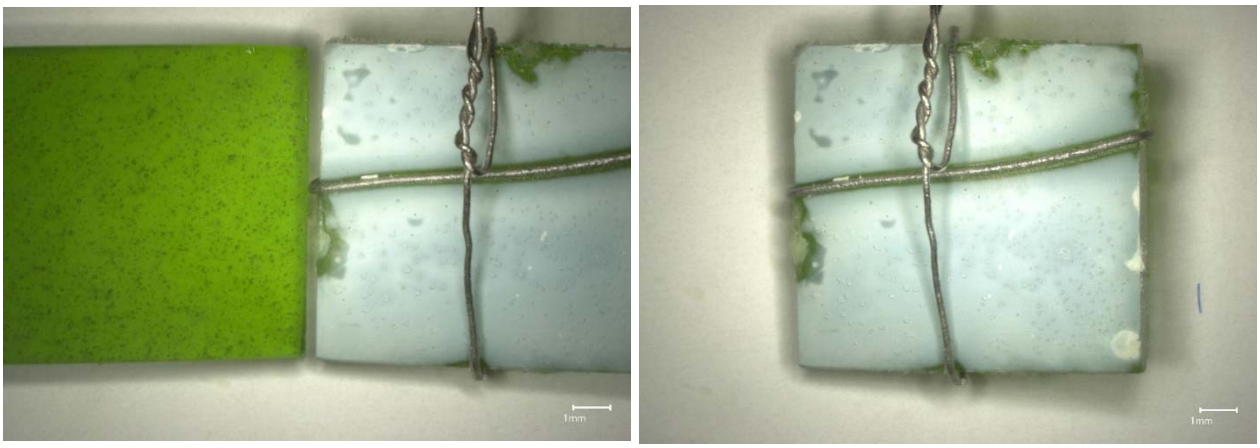

a) Glass square after (right) and before (left) VHT; b) Glass square after VHT

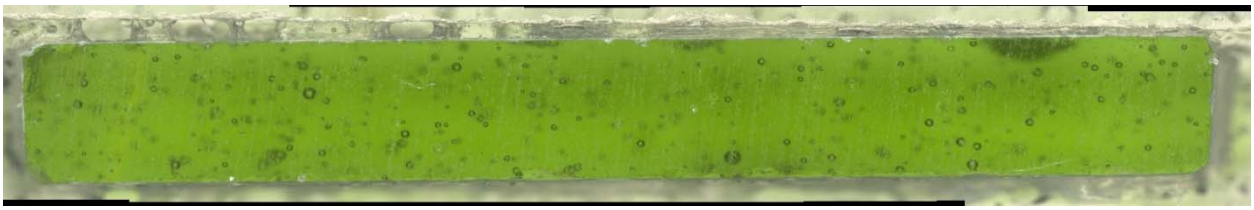

c) Glass cross section magnified after VHT

Figure I.24. Quenched Glass LP2-IL-15 after VHT for 7 Days

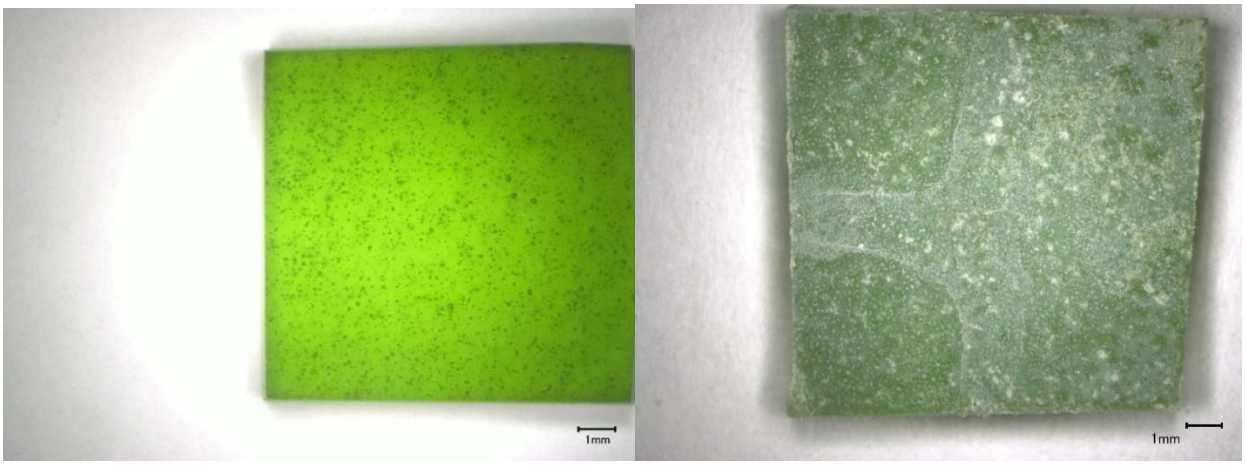

a) Glass square magnified 20X before VHT; b) Glass square magnified 20X after VHT

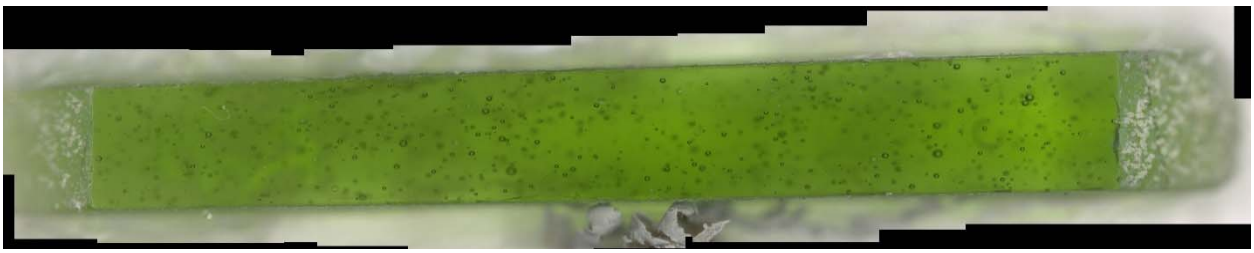

c) Glass cross section magnified after VHT

Figure I.25. Quenched Glass LP2-IL-15 after VHT for 24 Days

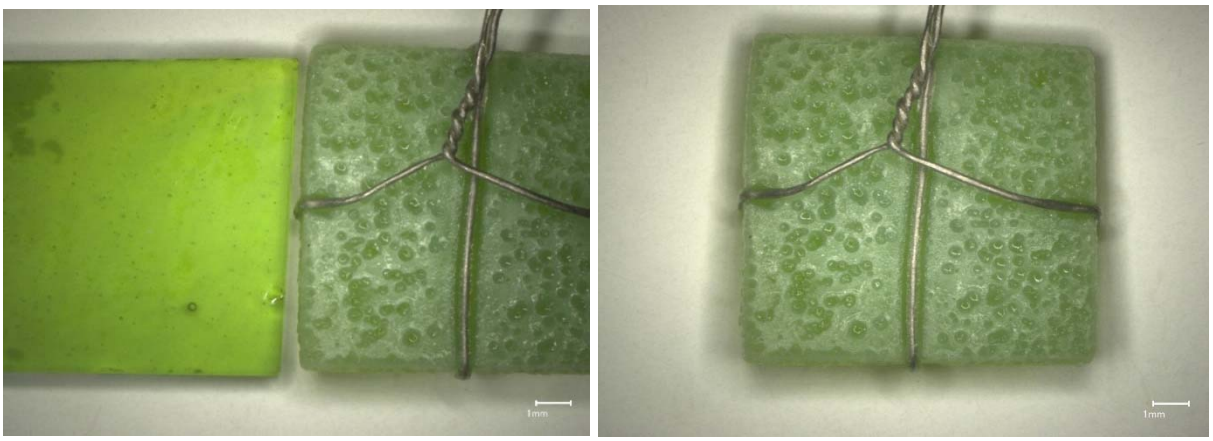

a) Glass square magnified 20X before VHT; b) Glass square magnified 20X after VHT

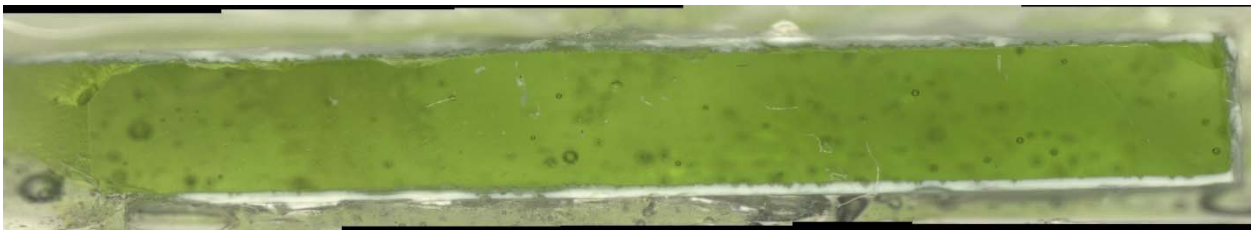

c) Glass cross section magnified after VHT

Figure I.26. Quenched Glass LP2-IL-16 after VHT for 7 Days

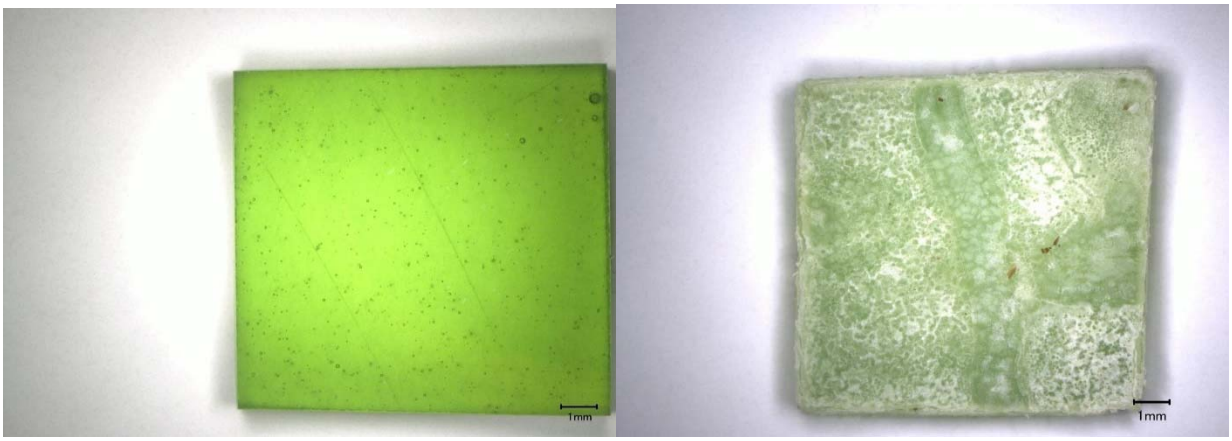

a) Glass square magnified 20X before VHT; b) Glass square magnified 20X after VHT

c) Glass cross section magnified after VHT

Figure I.27. Quenched Glass LP2-IL-16 after VHT for 24 Days

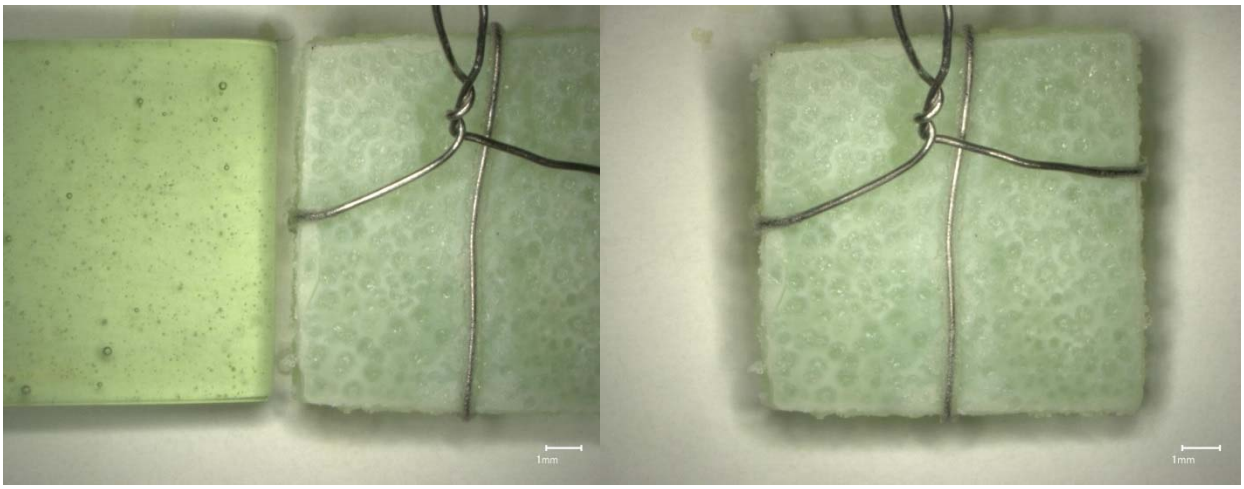

a) Glass square after (right) and before (left) VHT; b) Glass square after VHT

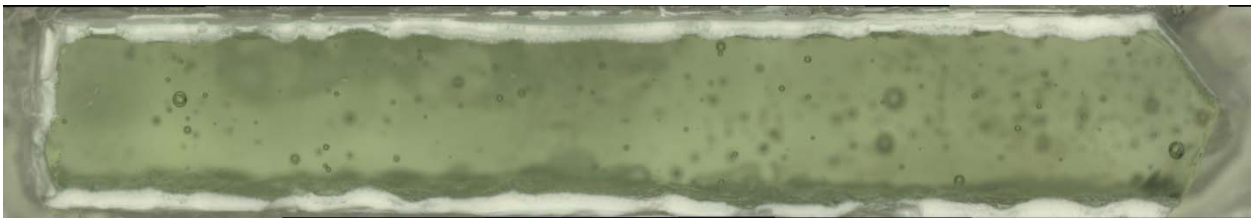

c) Glass cross section magnified after VHT

Figure I.28. Quenched Glass LP2-IL-17 after VHT for 7 Days

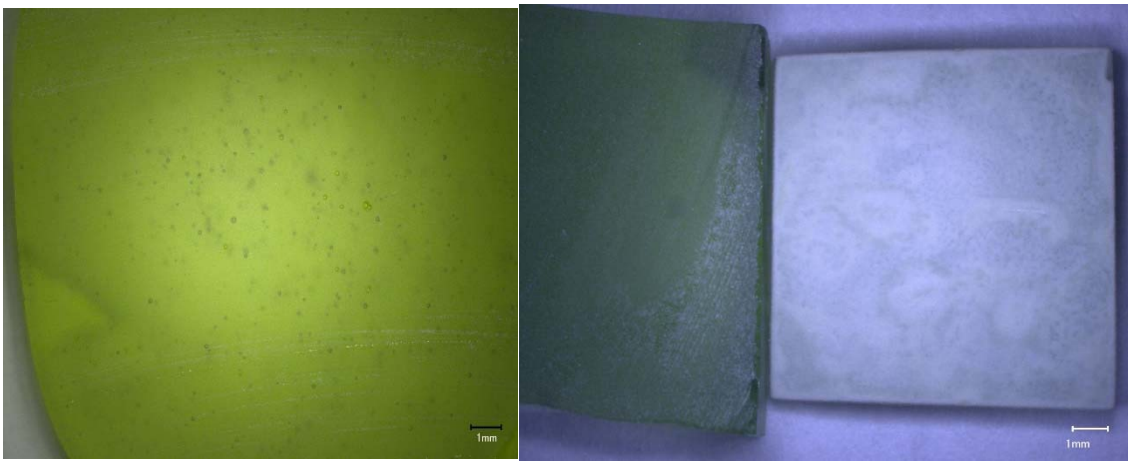

a) Glass square magnified 20X before VHT; b) Glass square after (right) and before (left) VHT

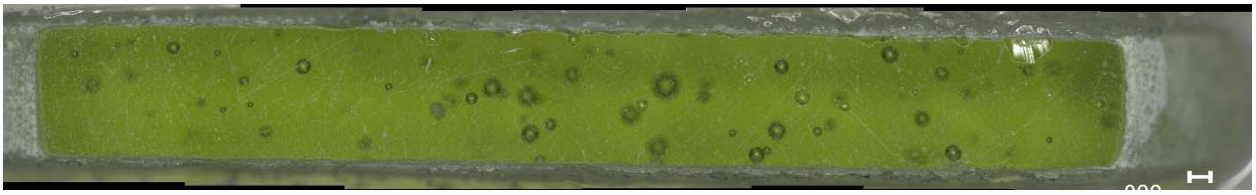

c) Glass cross section magnified after VHT

Figure I.29. Quenched Glass LP2-OL-01-3 after VHT for 11 Days

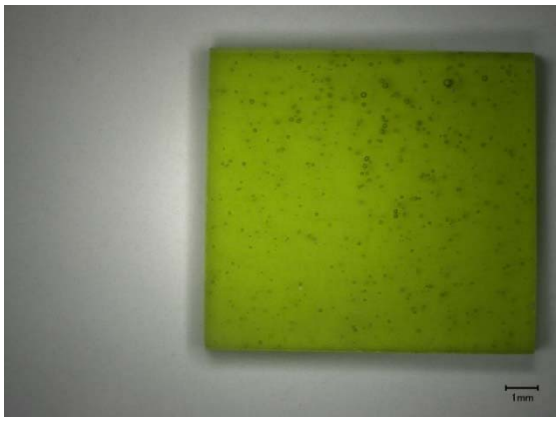

a) Glass square magnified 20X before VHT

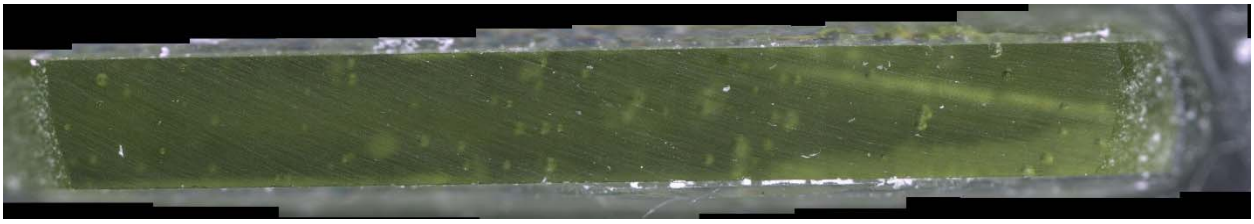

b) Glass cross section magnified after VHT

Figure I.30. Quenched Glass LP2-OL-01-3 after VHT for 24 Days

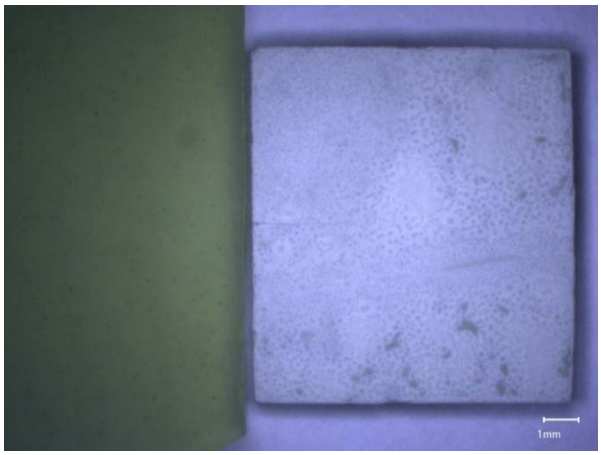

a) Glass square after (right) and before (left) VHT

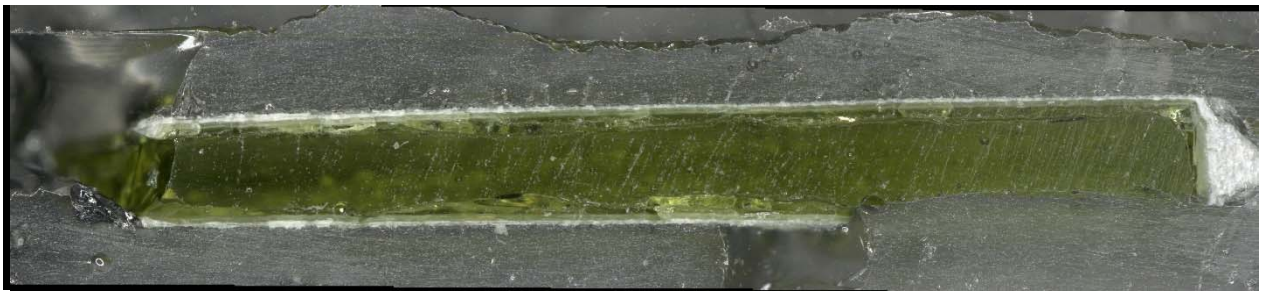

b) Glass cross section magnified after VHT

Figure I.31. Quenched Glass LP2-OL-02-1 after VHT for 11 Days

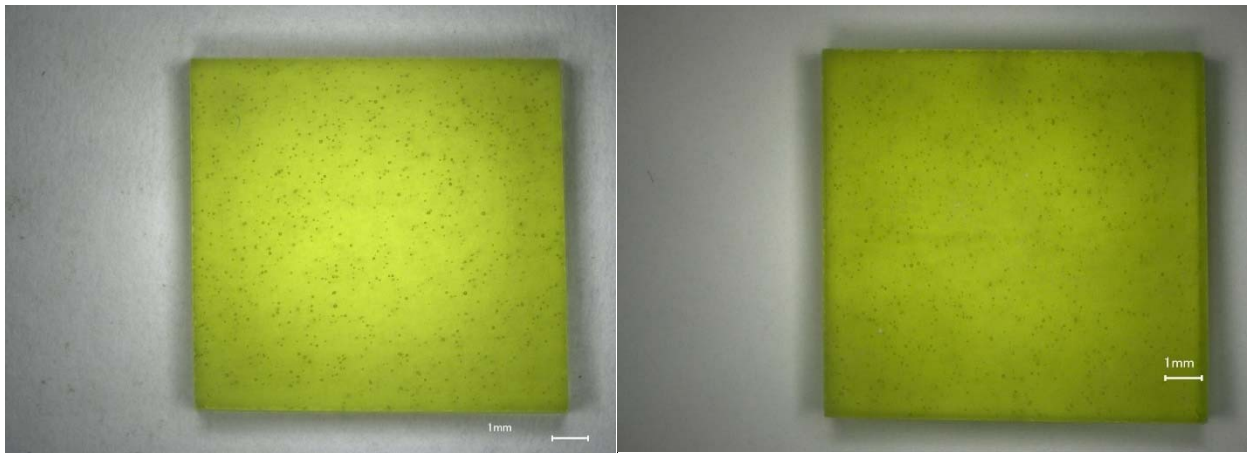


a) Glass square magnified 20X before VHT; b) Glass square magnified 20X after VHT

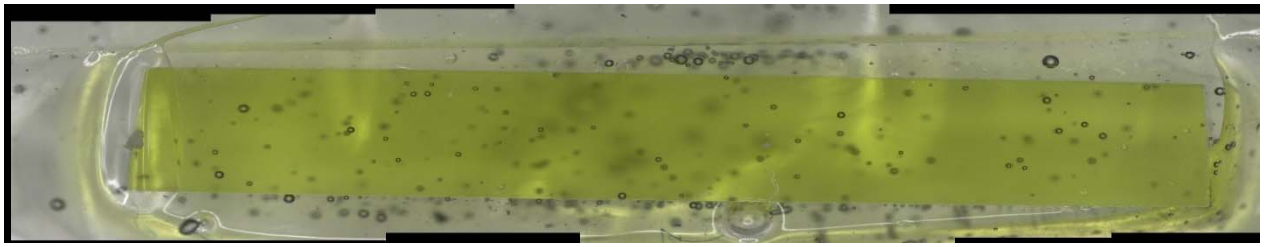

c) Glass cross section magnified after VHT

Figure I.32. Quenched Glass LP2-OL-02-1 after VHT for 24 Days

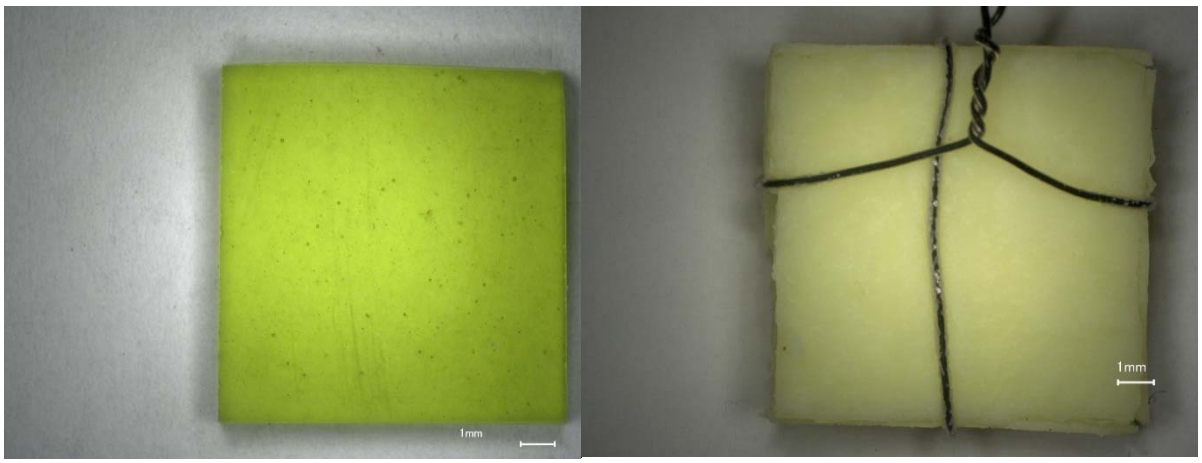


a) Glass square magnified 20X before VHT; b) Glass square magnified 20X after VHT

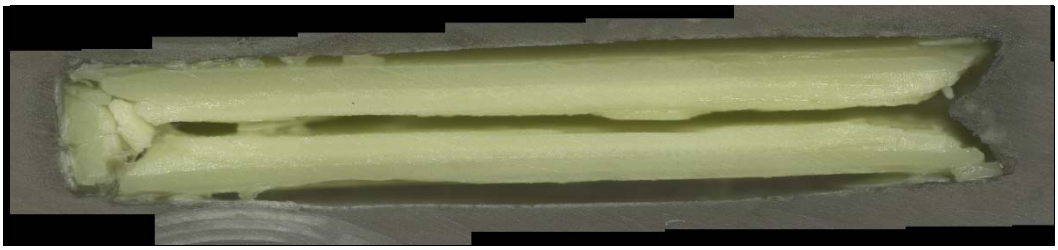

c) Glass cross section magnified after VHT

Figure I.33. Quenched Glass LP2-OL-03 MOD2 after VHT for 24 Days

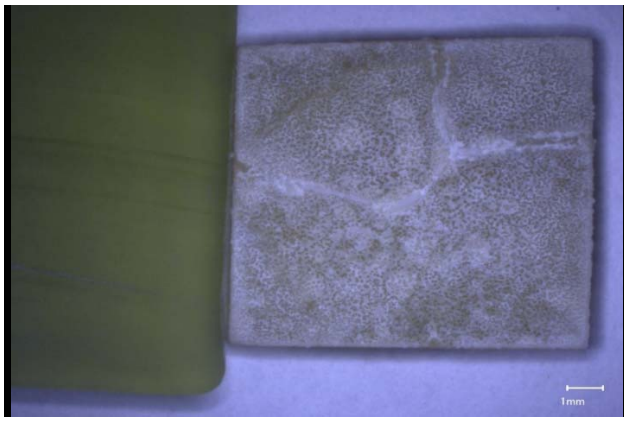


a) Glass square after (right) and before (left) VHT

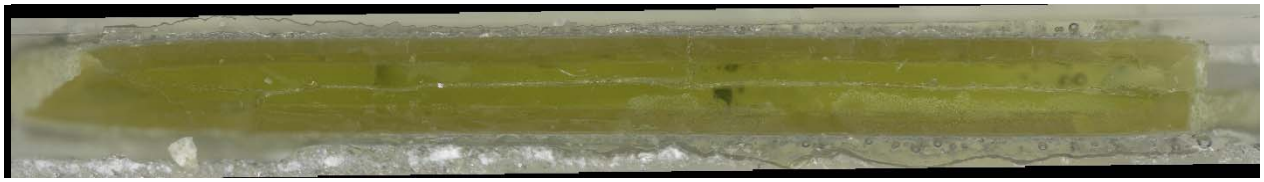

b) Glass cross section magnified after VHT

Figure I.34. Quenched Glass LP2-OL-04-1 after VHT for 11 Days

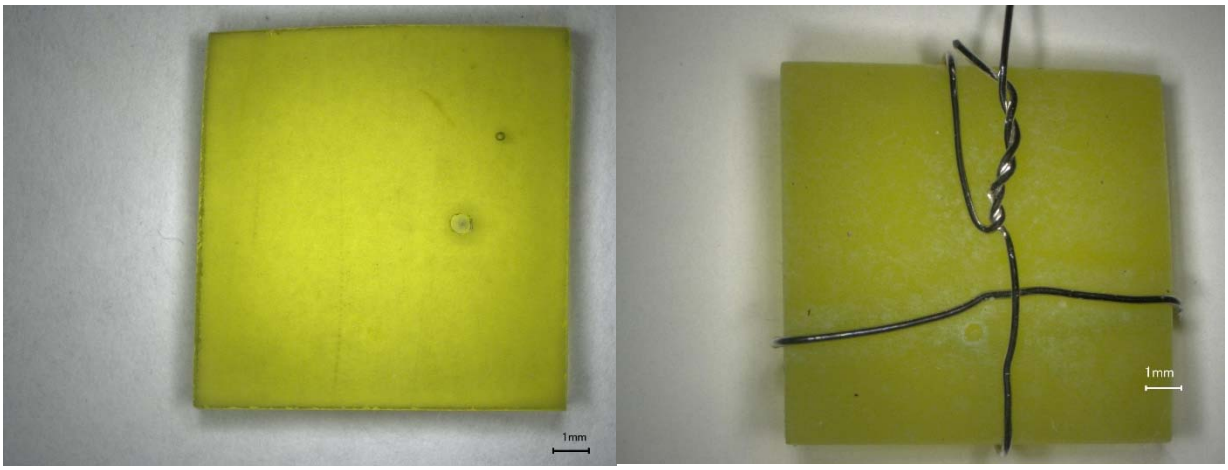


a) Glass square magnified 20X before VHT; b) Glass square magnified 20X after VHT

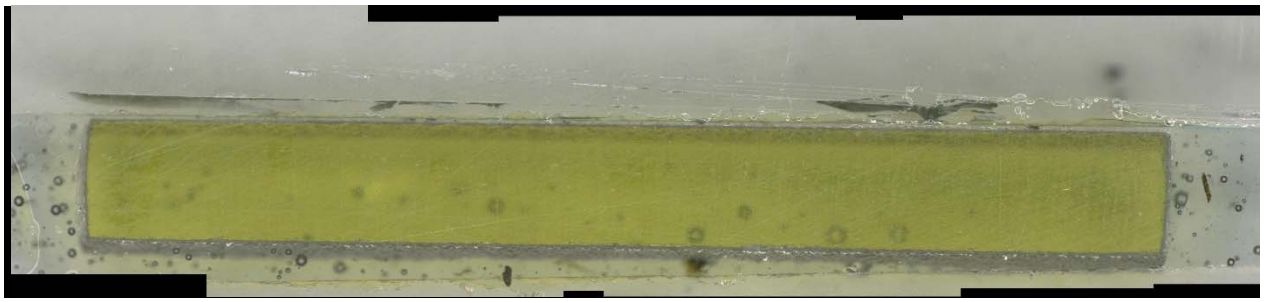

c) Glass cross section magnified after VHT

Figure I.35. Quenched Glass LP2-OL-04-1 after VHT for 24 Days

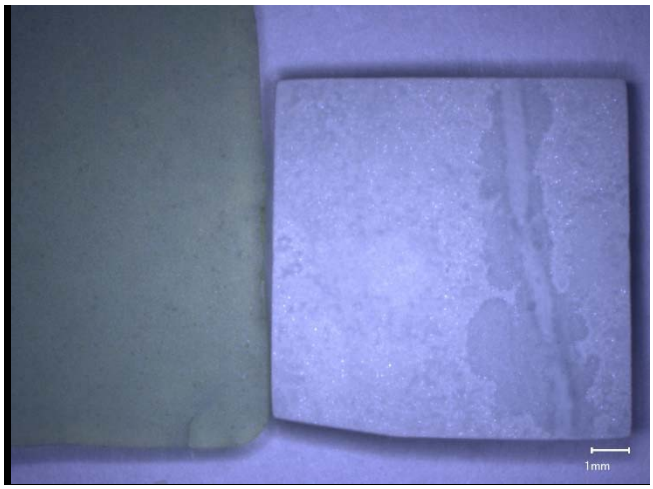


a) Glass square after (right) and before (left) VHT

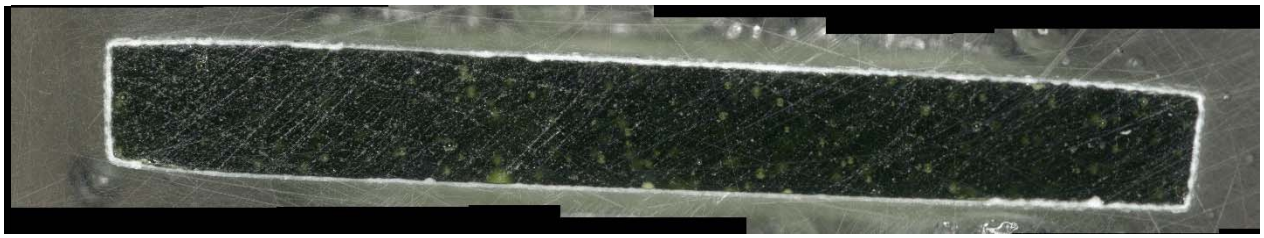

b) Glass cross section magnified after VHT

Figure I.36. Quenched Glass LP2-OL-05 after VHT for 11 Days


a) Glass square magnified 20X before VHT; b) Glass square magnified 20X after VHT

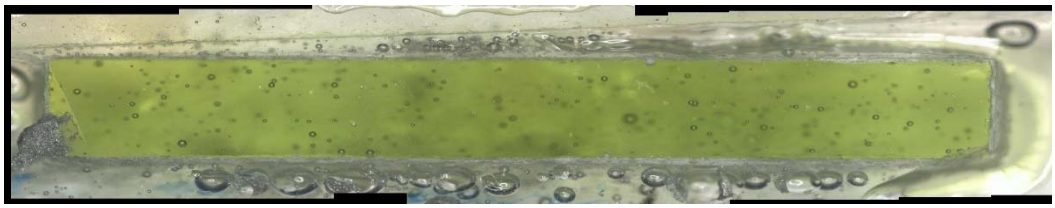

c) Glass cross section magnified after VHT

Figure I.37. Quenched Glass LP2-OL-05 after VHT for 24 Days

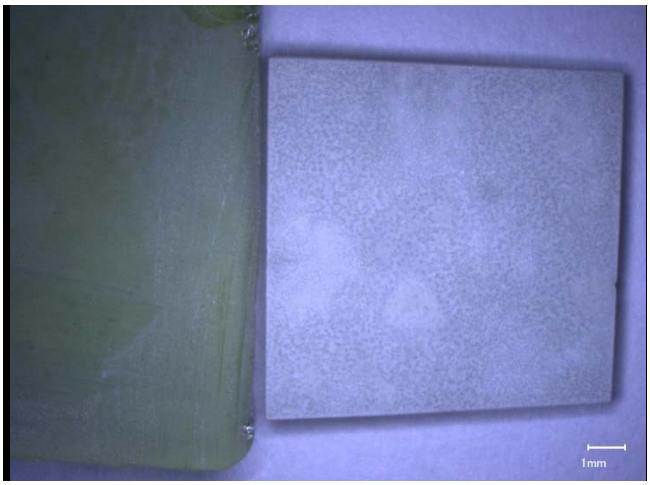


a) Glass square after (right) and before (left) VHT

b) Glass cross section magnified after VHT

Figure I.38. Quenched Glass LP2-OL-07-1 after VHT for 11 Days

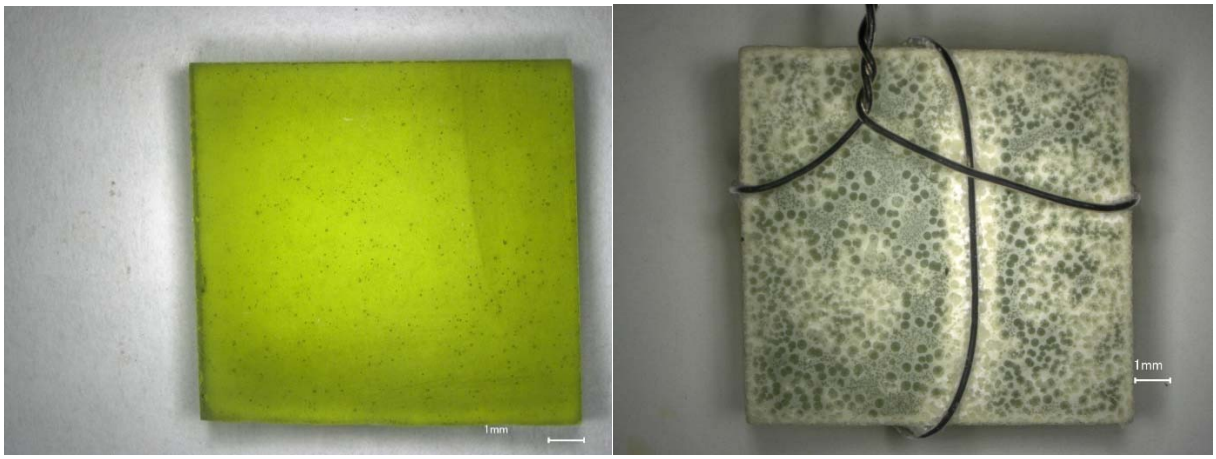


a) Glass square magnified 20X before VHT; b) Glass square magnified 20X after VHT

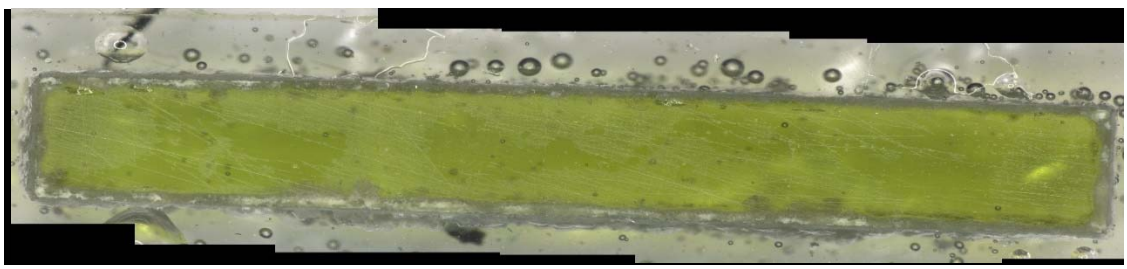

c) Glass cross section magnified after VHT

Figure I.39. Quenched Glass LP2-OL-07-1 after VHT for 24 Days

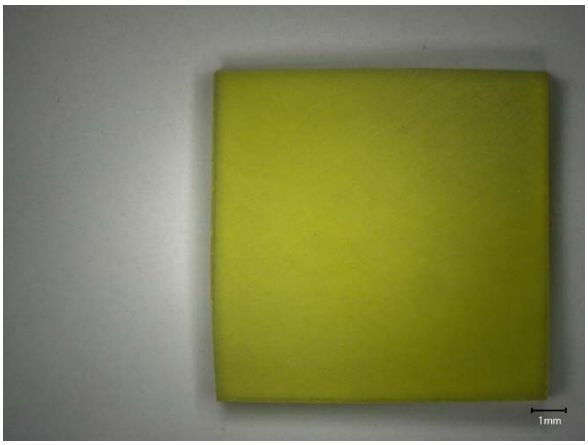

a) Glass square magnified 20X before VHT

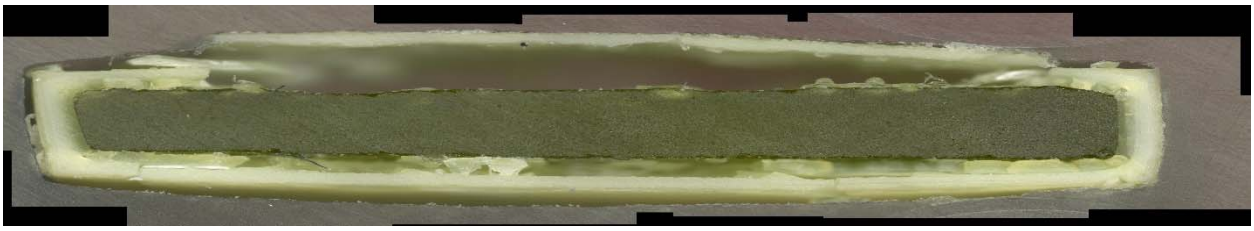

b) Glass cross section magnified after VHT

Figure I.40. Quenched Glass LP2-OL-08MOD after VHT for 7 Days

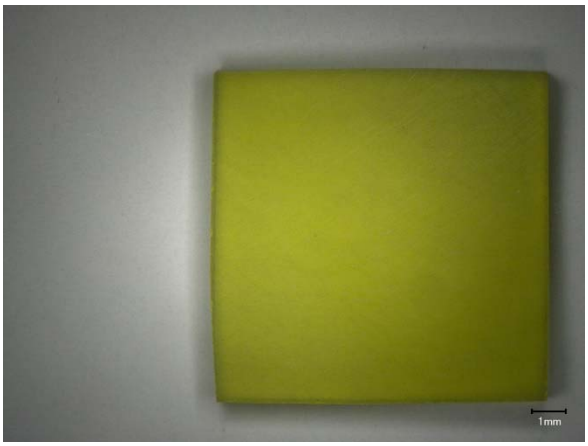

a) Glass square magnified 20X before VHT

b) Glass cross section magnified after VHT

Figure I.41. Quenched Glass LP2-OL-08MOD after VHT for 24 Days

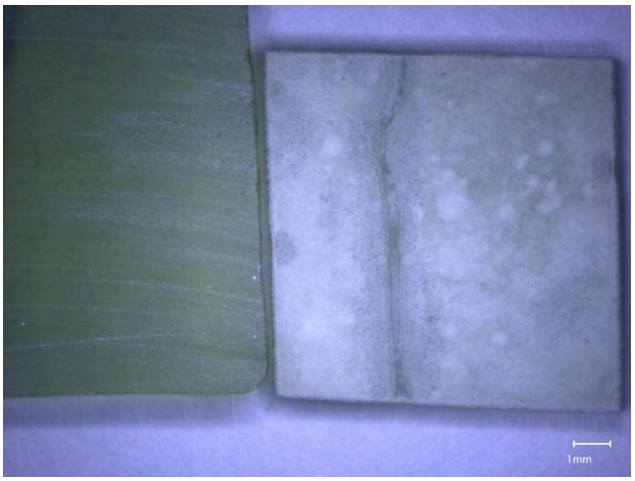


a) Glass square after (right) and before (left) VHT

b) Glass cross section magnified after VHT

Figure I.42. Quenched Glass LP2-OL-09-1 after VHT for 11 Days

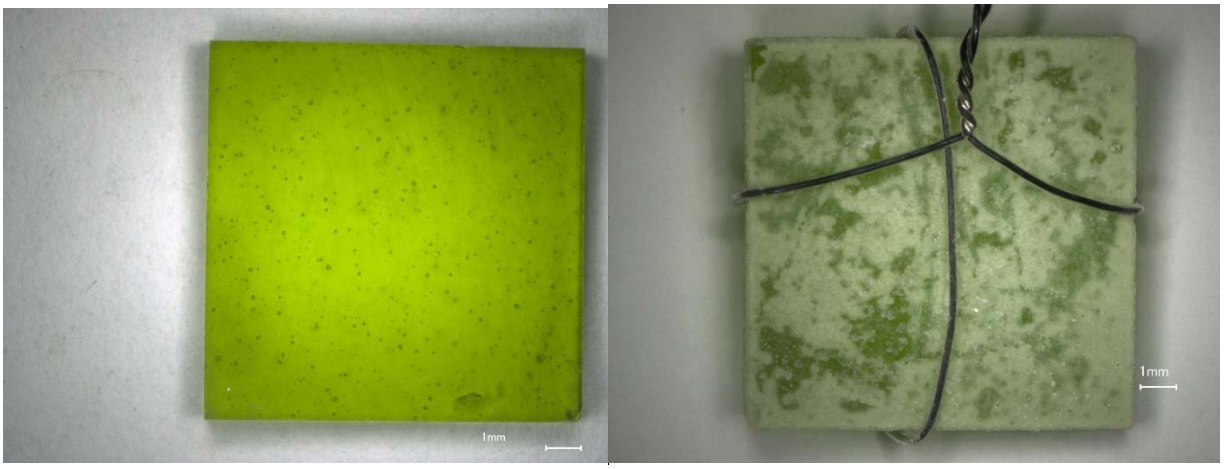


a) Glass square magnified 20X before VHT; b) Glass square magnified 20X after VHT

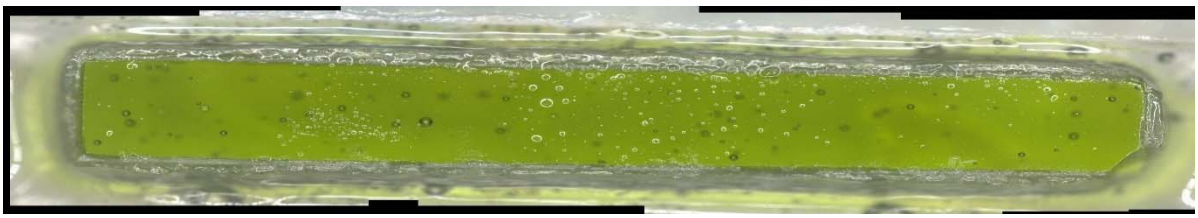

c) Glass cross section magnified after VHT

Figure I.43. Quenched Glass LP2-OL-09-1 after VHT for 24 Days

a) Glass square magnified 20X before VHT

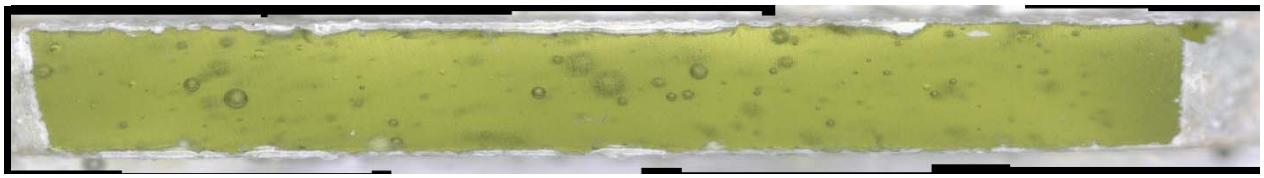

b) Glass cross section magnified after VHT

Figure I.44. Quenched Glass LP2-OL-10MOD after VHT for 24 Days

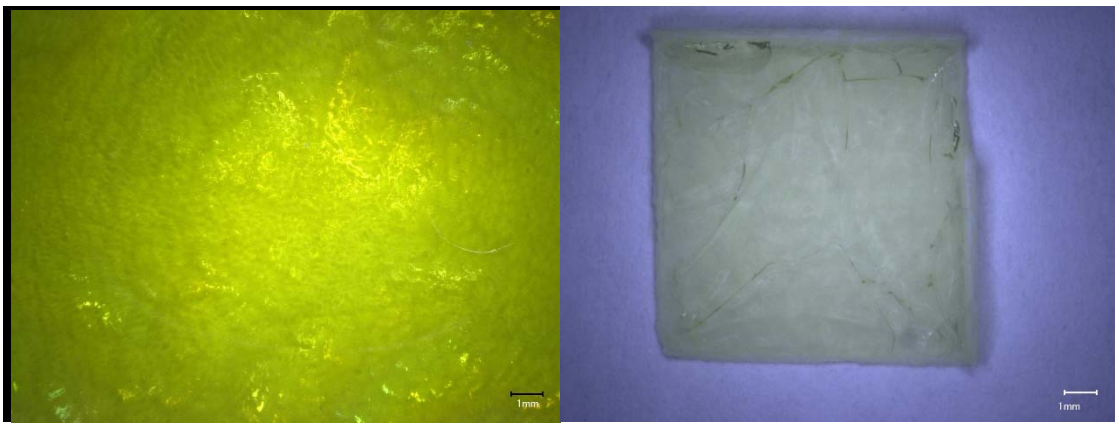

a) Glass square magnified 20X before VHT; b) Glass surface magnified after VHT

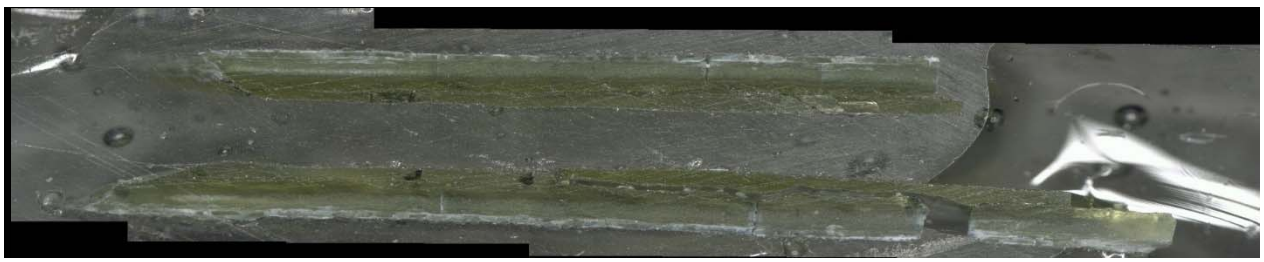

c) Glass cross section magnified after VHT

Figure I.45. Quenched Glass LP2-OL-11 after VHT for 11 Days

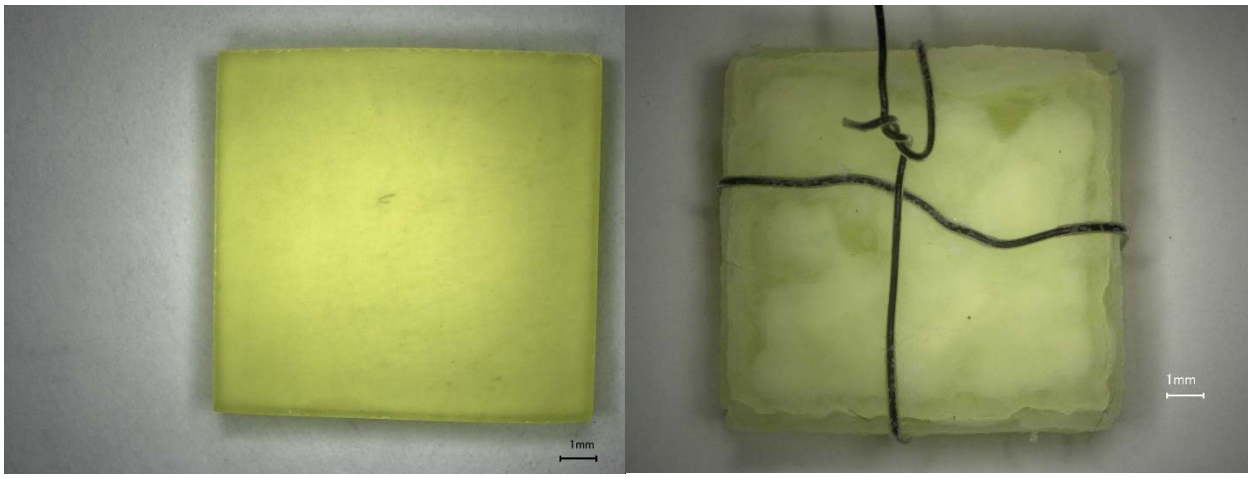


a) Glass square magnified 20X before VHT; b) Glass surface magnified after VHT

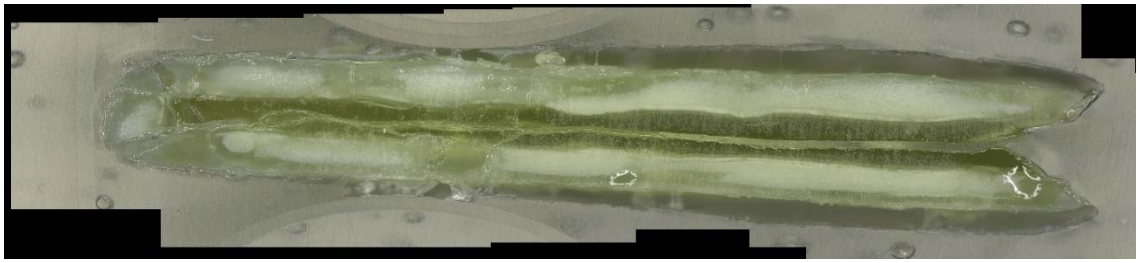

c) Glass cross section magnified after VHT

Figure I.46. Quenched Glass LP2-OL-11 after VHT for 24 Days

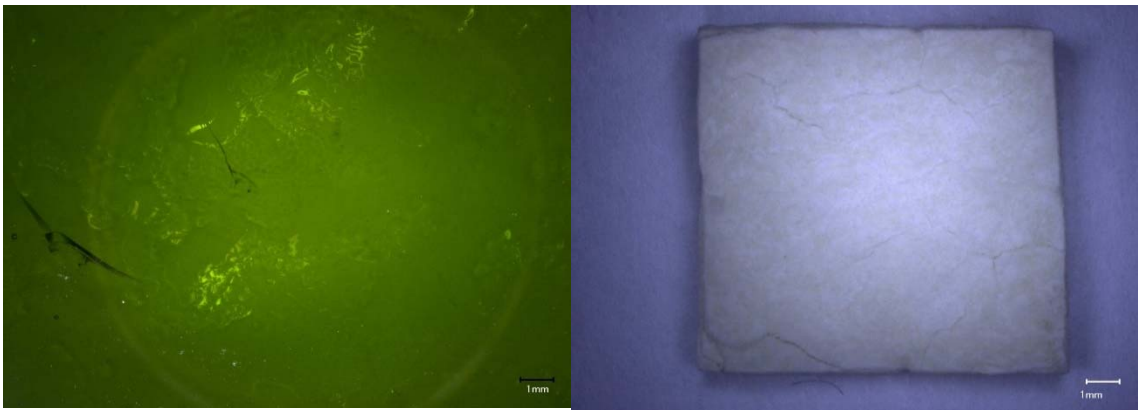


a) Glass square magnified 20X before VHT; b) Glass surface magnified after VHT

c) Glass cross section magnified after VHT

Figure I.47. Quenched Glass LP2-OL-12 after VHT for 11 Days

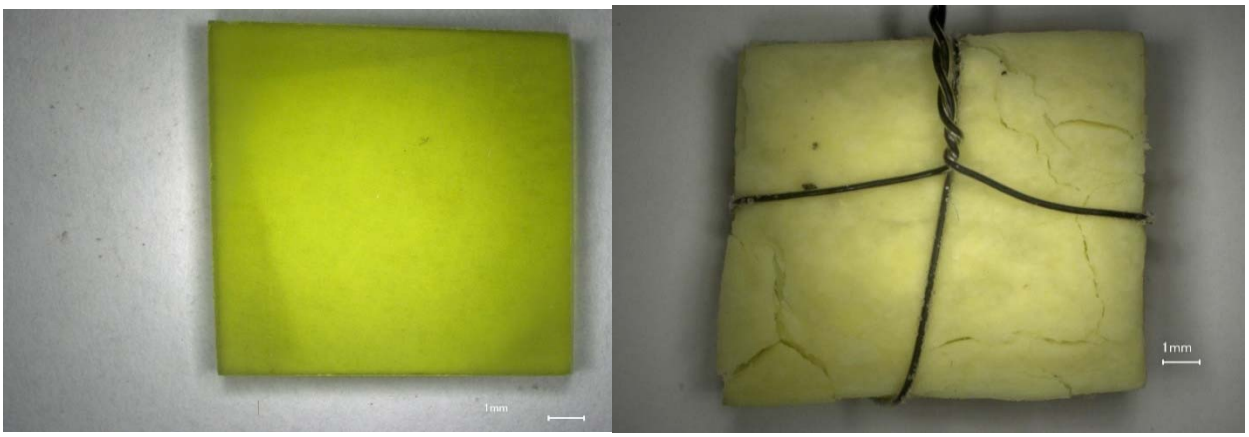

a) Glass square magnified 20X before VHT; b) Glass surface magnified after VHT

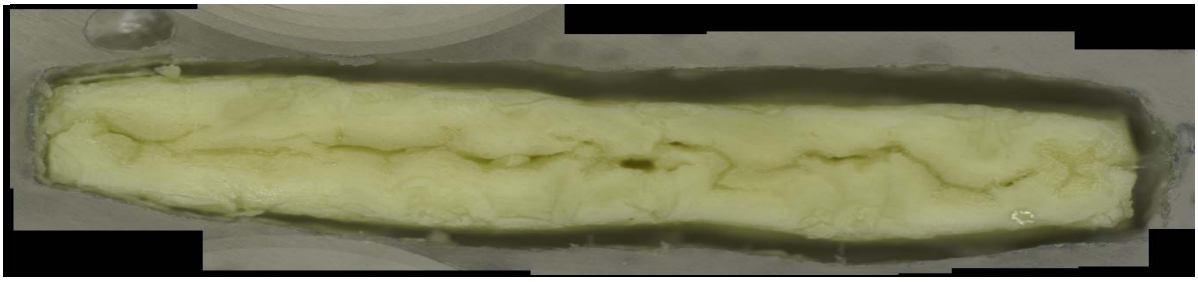

c) Glass cross section magnified after VHT

Figure I.48. Quenched Glass LP2-OL-12 after VHT after 24 Days

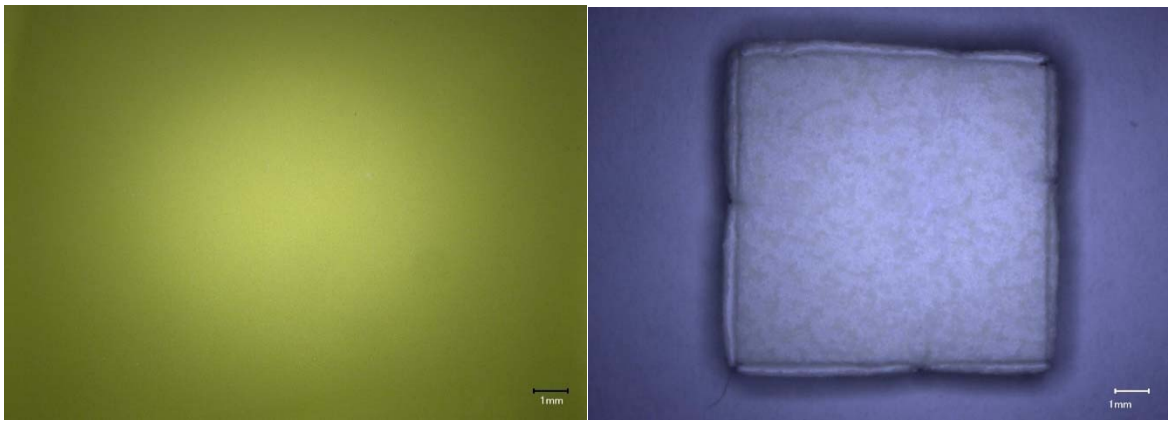

a) Glass square magnified 20X before VHT; b) Glass square magnified 20X after VHT

c) Glass cross section magnified after VHT

Figure I.49. Quenched Glass LP2-OL-13 after VHT after 11 Days

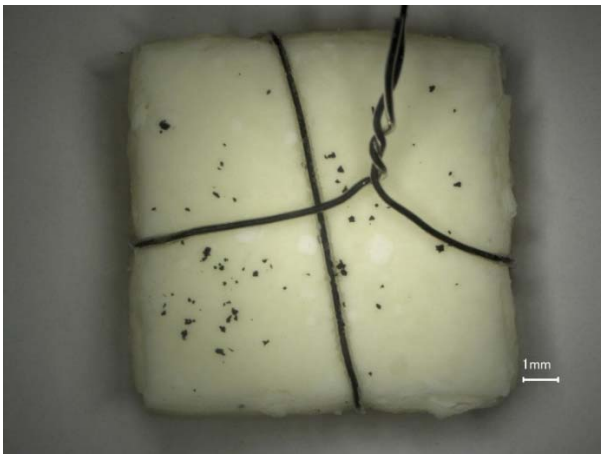


a) Glass square magnified 20X after VHT

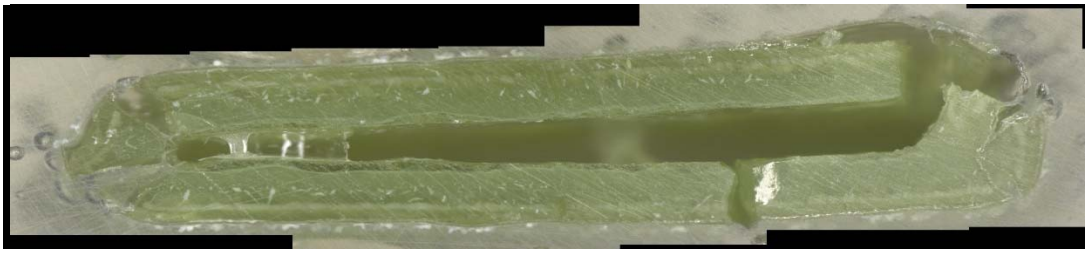

b) Glass cross section magnified after VHT

Figure I.50. Quenched Glass LP2-OL-13 after VHT after 24 Days

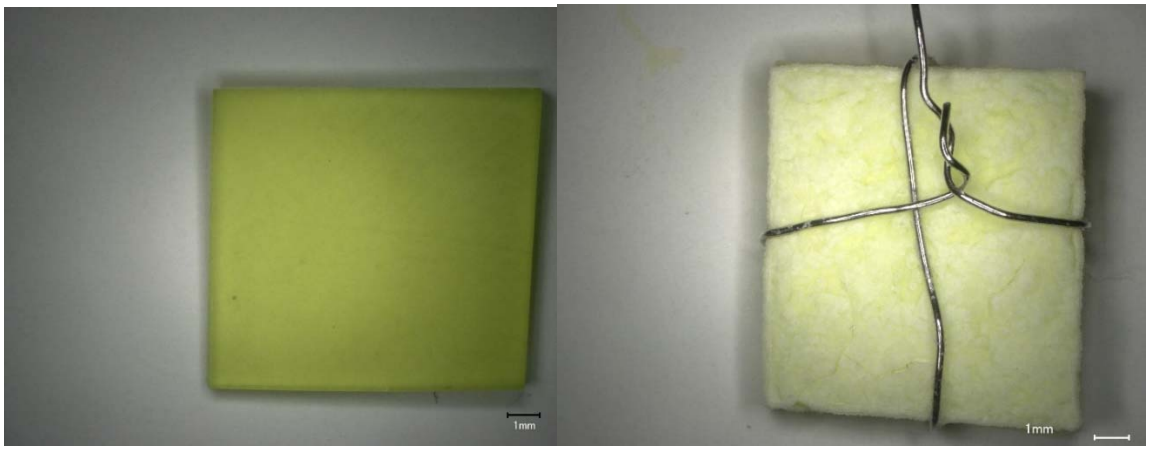


a) Glass square magnified 20X after VHT; b) Glass surface magnified after VHT

c) Glass cross section magnified after VHT

Figure I.51. Quenched Glass LP2-OL-14 after VHT after 7 Days

a) Glass square magnified 20X after VHT; b) Glass surface magnified 30X after VHT

c) Glass cross section magnified after VHT

Figure I.52. Quenched Glass LP2-OL-14 after VHT after 24 Days

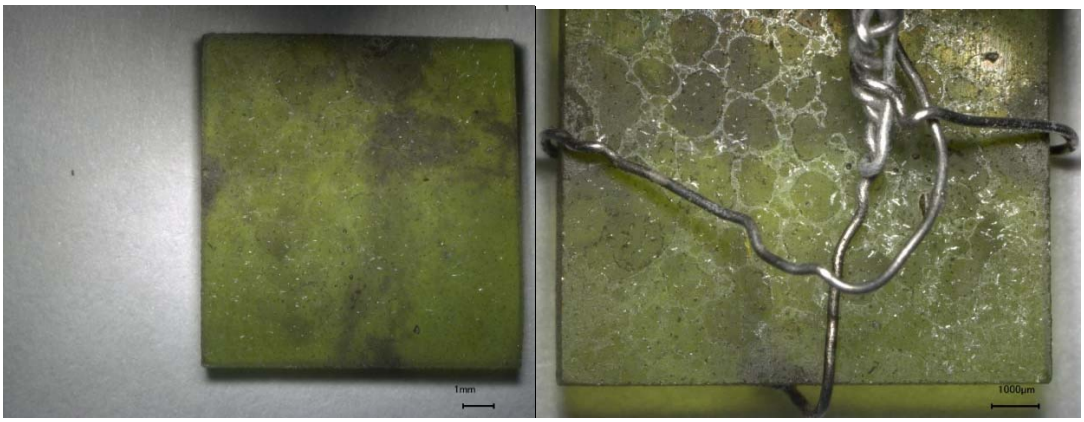

a) Glass square magnified 20X after VHT; b) Glass surface magnified 30X after VHT

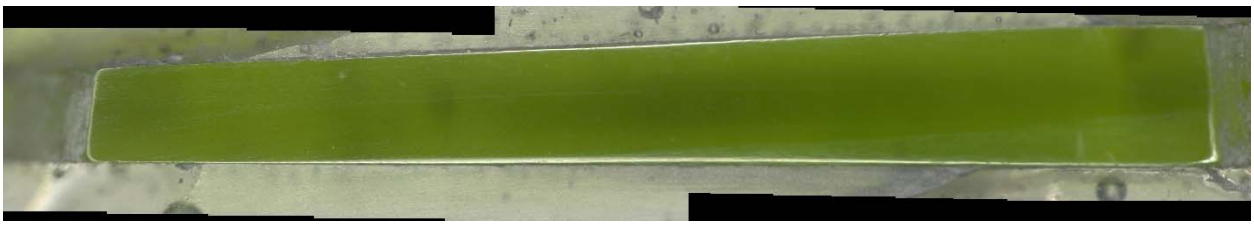

c) Glass cross section magnified after VHT

Figure I.53. Quenched Glass LP2-OL-15 after VHT for 24 Days

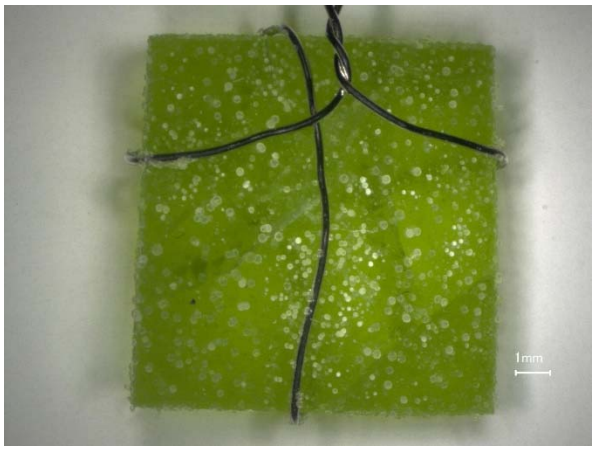


a) Glass surface magnified 20X after VHT

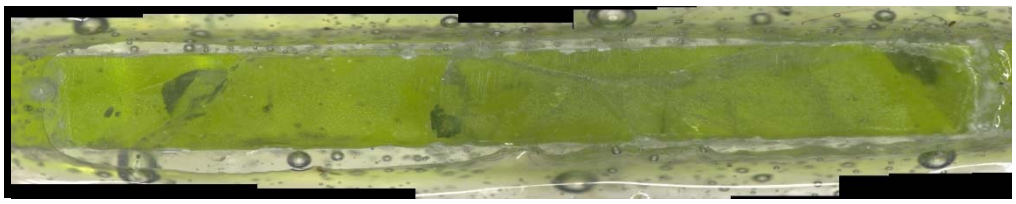

b) Glass cross section magnified after VHT

Figure I.54. Quenched Glass LP2-OL-16MOD after VHT for 24 Days

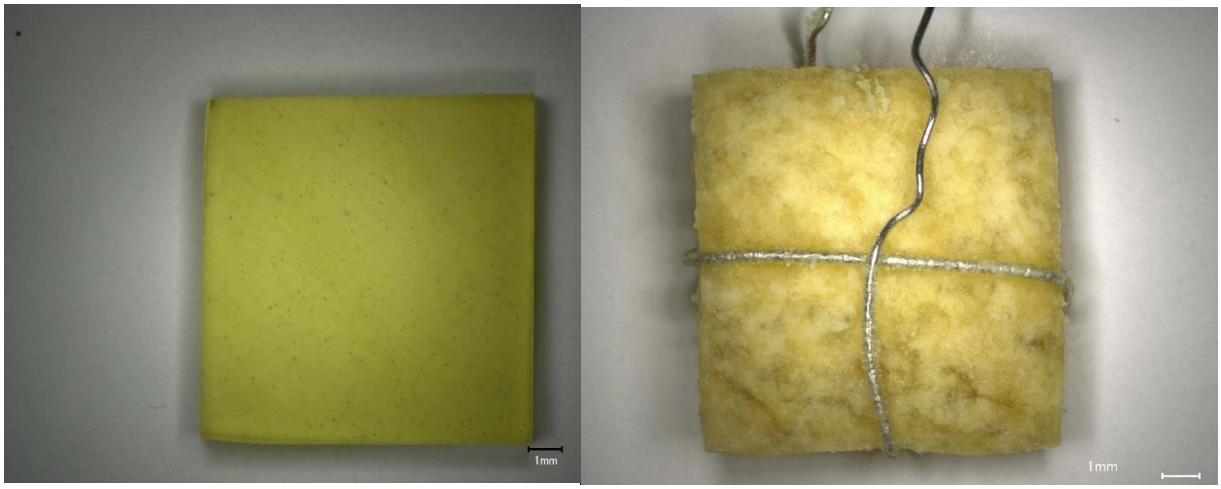


a) Glass square magnified 20X before VHT; b) Glass surface magnified after VHT

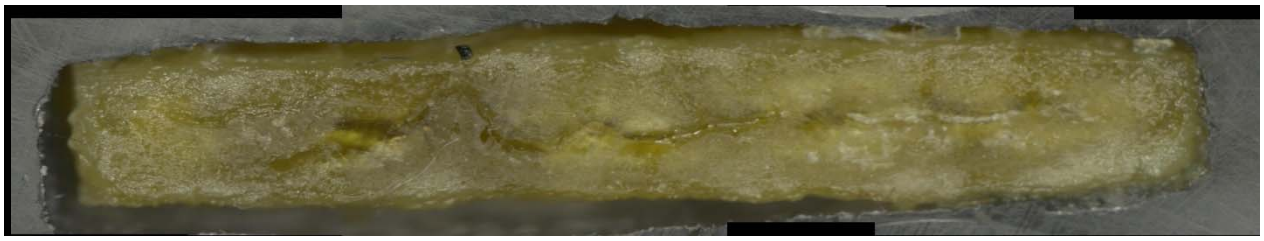

c) Glass cross section magnified after VHT

Figure I.55. Quenched Glass LP2-OL-17 after VHT for 7 Days

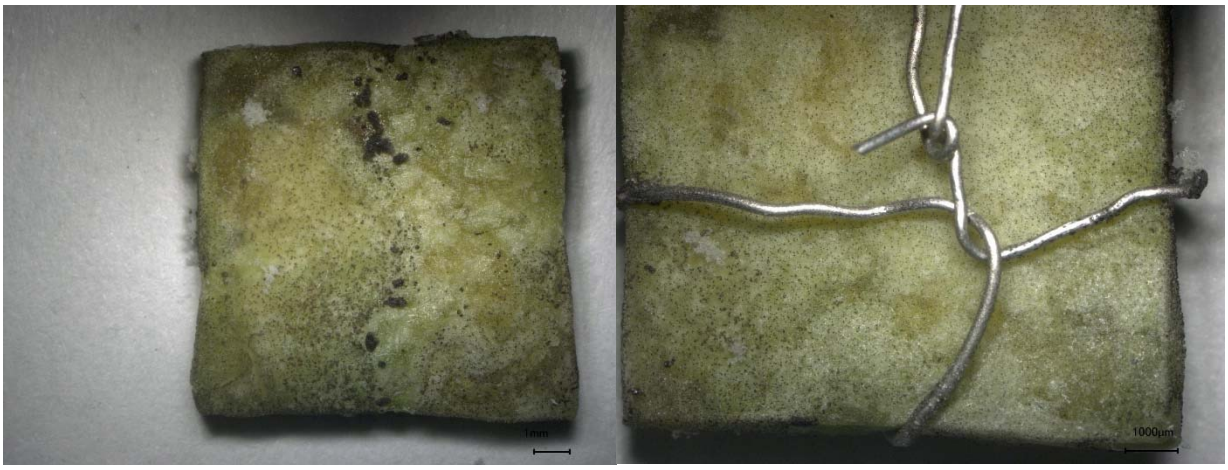

a) Glass square magnified 20X after VHT; b) Glass surface magnified 30X after VHT

c) Glass cross section magnified after VHT

Figure I.56. Quenched Glass LP2-OL-17 after VHT for 24 Days

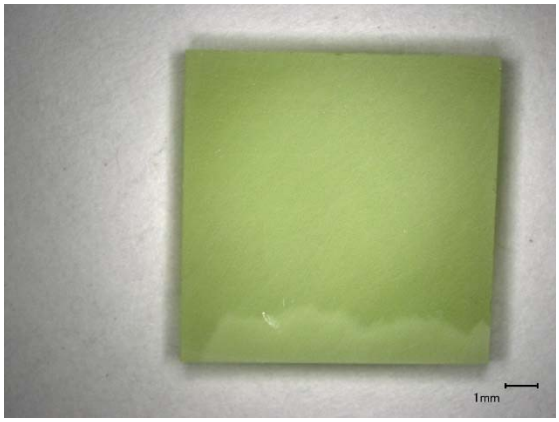

a) Glass square magnified 20X before VHT

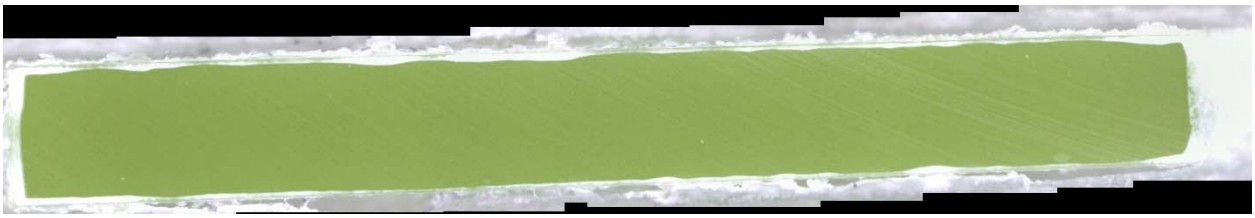

b) Glass cross section magnified after VHT

Figure I.57. Quenched Glass LP2-OL-18 after VHT for 24 Days

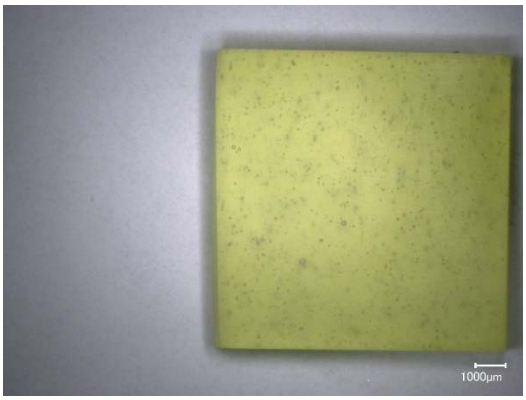


a) Glass square magnified 20X before VHT

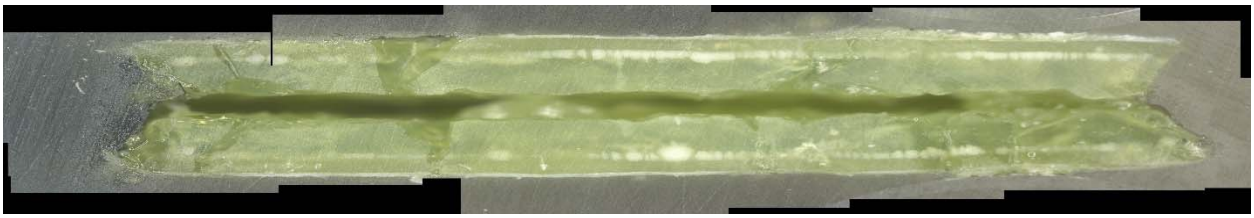

b) Glass cross section magnified after VHT

Figure I.58. Quenched Glass LP2-OL-19 after VHT for 7 Days

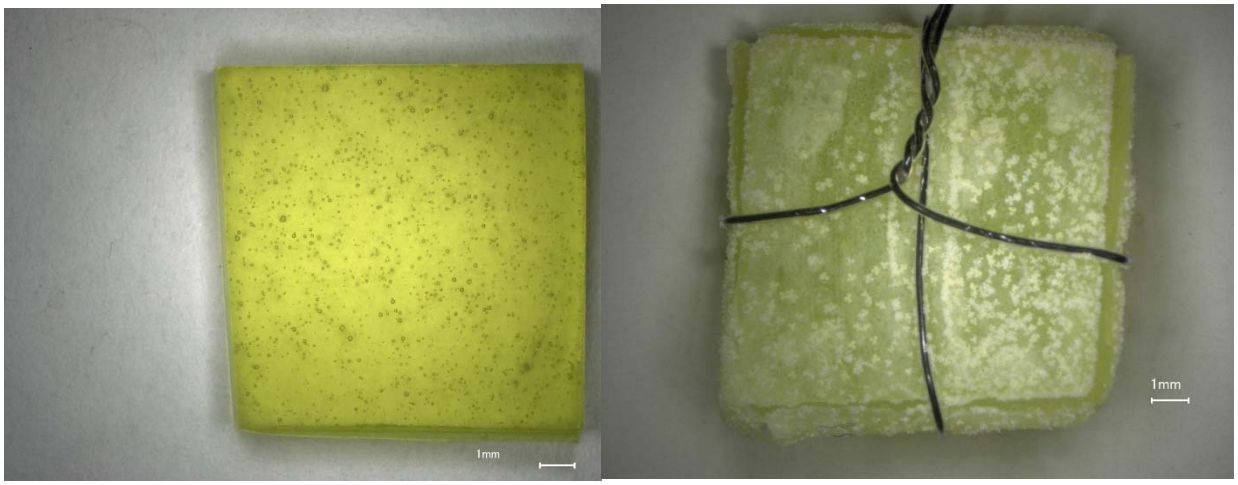


a) Glass square magnified 20X before VHT; b) Glass surface magnified after VHT

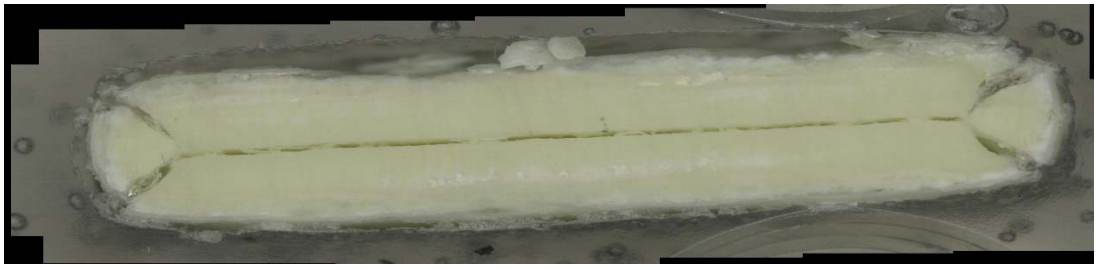

c) Glass cross section magnified after VHT

Figure I.59. Quenched Glass LP2-OL-19 after VHT for 24 Days

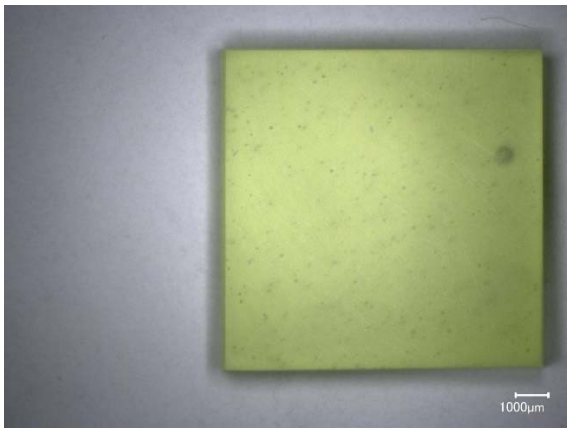


a) Glass square magnified 20X before VHT

b) Glass cross section magnified after VHT

Figure I.60. Quenched Glass LP2-OL-20 after VHT for 7 Days

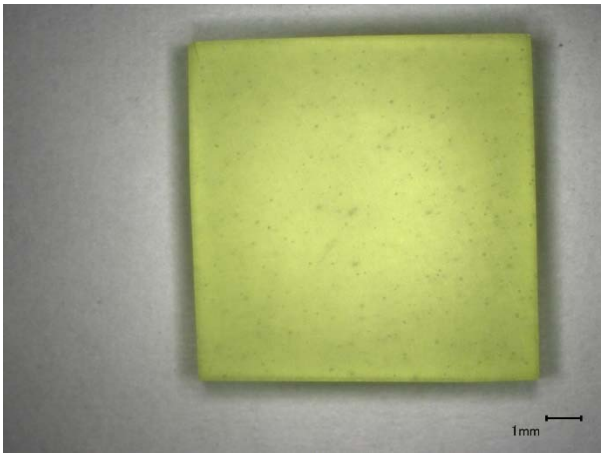


a) Glass square magnified 20X before VHT

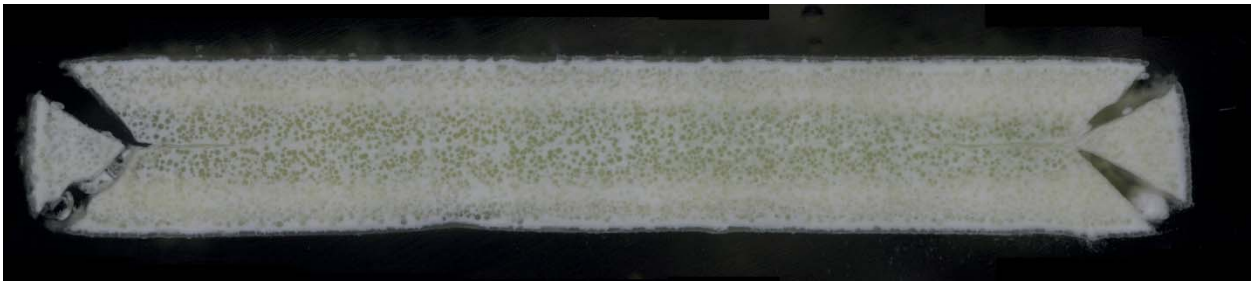

b) Glass cross section magnified after VHT

Figure I.61. Quenched Glass LP2-OL-20 after VHT for 24 Days

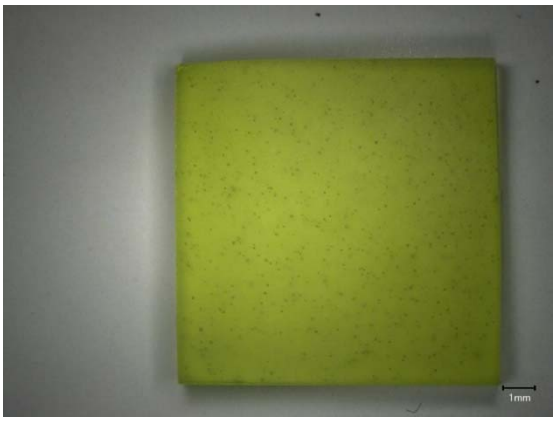

a) Glass square magnified 20X before VHT

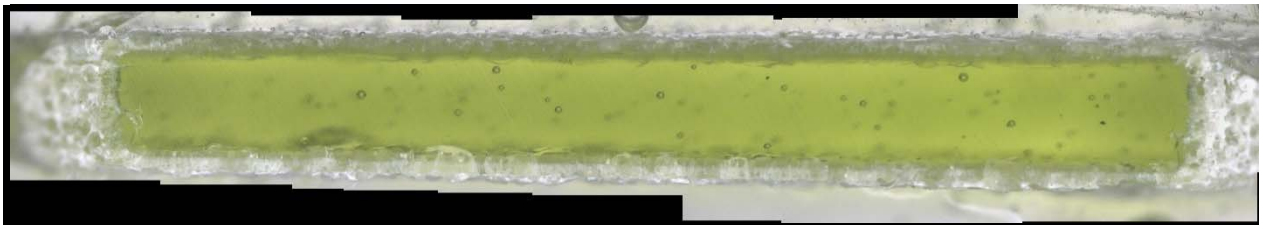

b) Glass cross section magnified after VHT

Figure I.62. Quenched Glass LP2-OL-21 after VHT for 24 Days

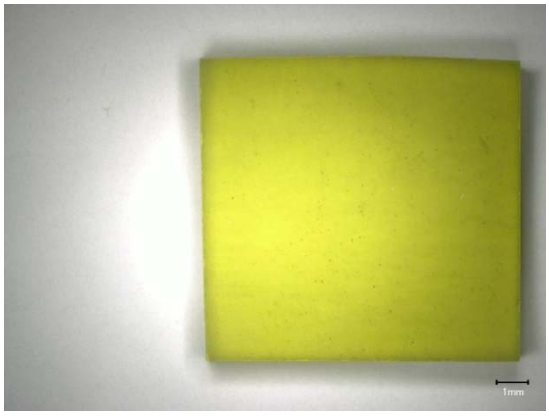

a) Glass square magnified 20X before VHT

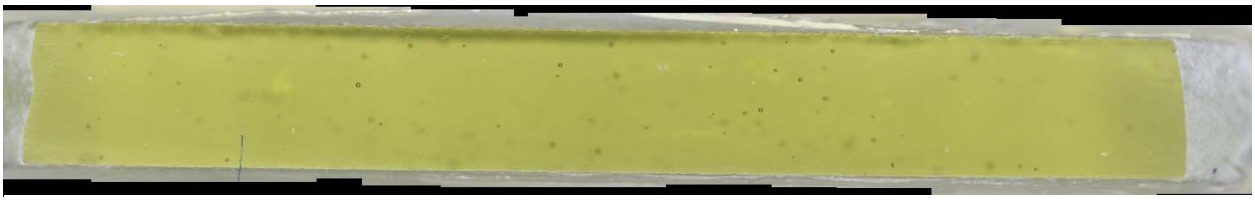

b) Glass cross section magnified after VHT

Figure I.63. Quenched Glass LP2-OL-22 after VHT for 24 Days

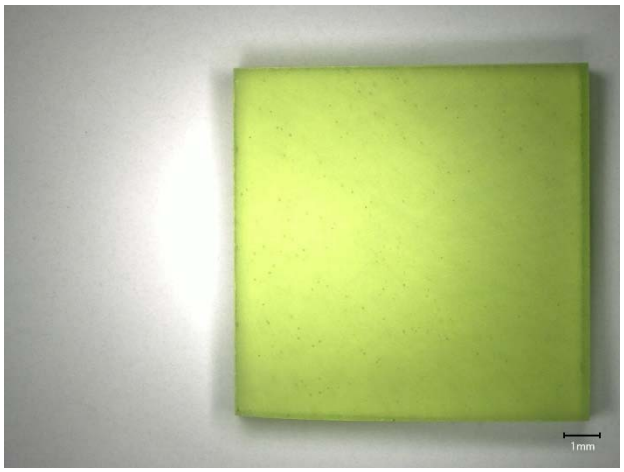

a) Glass square magnified 20X before VHT

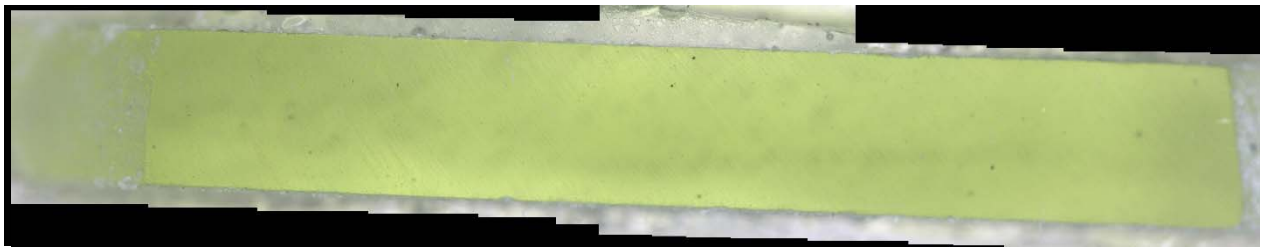

b) Glass cross section magnified after VHT

Figure I.64. Quenched Glass LP2-OL-23 after VHT for 24 Days

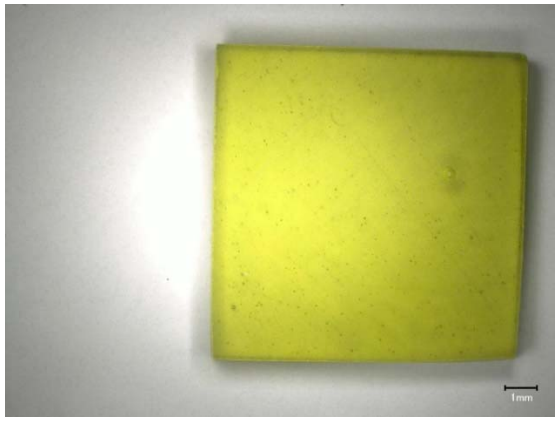

a) Glass square magnified 20X before VHT

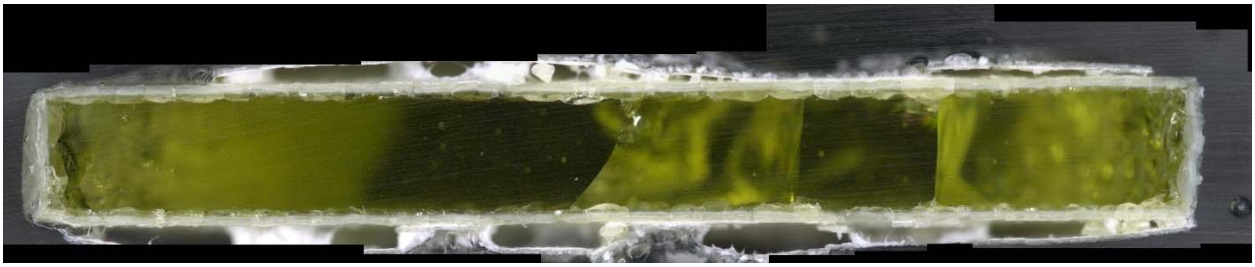

b) Glass cross section magnified after VHT

Figure I.65. Quenched Glass LP2-OL-24 after VHT for 24 Days

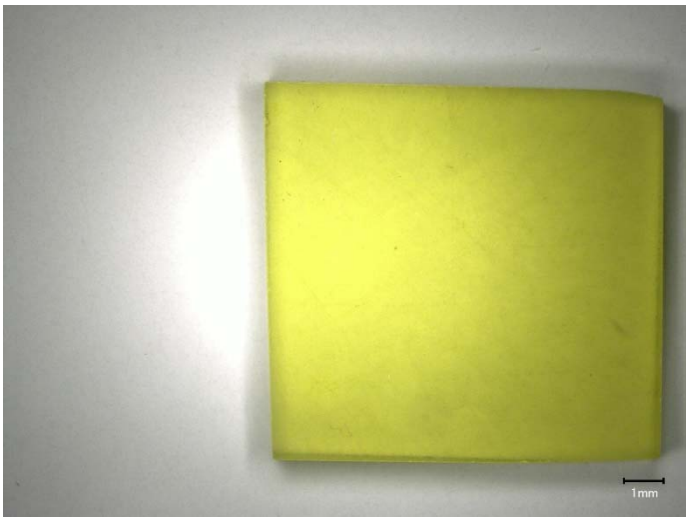


a) Glass square magnified 20X before VHT

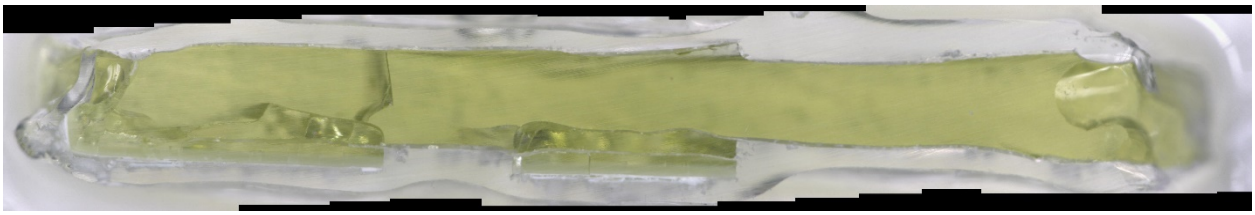

b) Glass cross section magnified after VHT

Figure I.66. Quenched Glass LP2-OL-25 after VHT for 24 Days

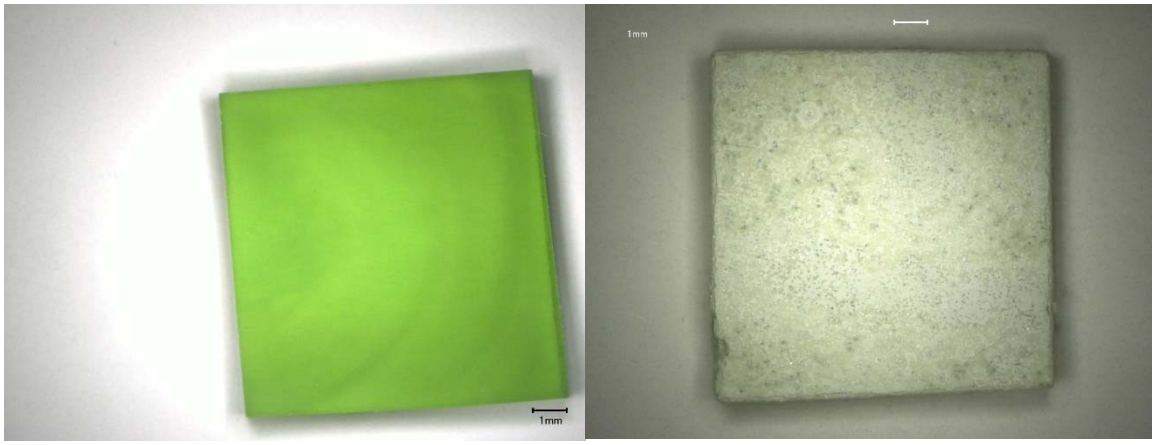


a) Glass square magnified 20X before VHT; b) Glass surface magnified after VHT

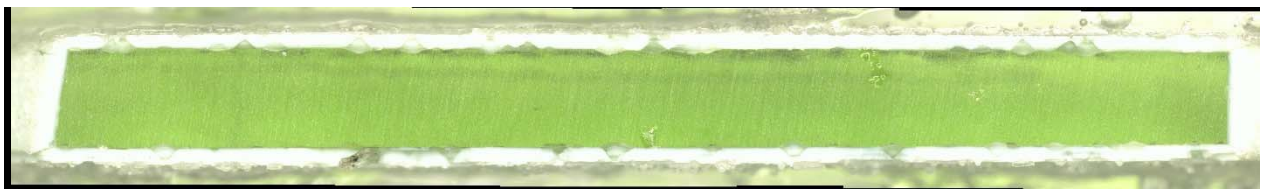

c) Glass cross section magnified after VHT

Figure I.67. CCC-Treated Glass LP2-IL-01 after VHT for 7 Days

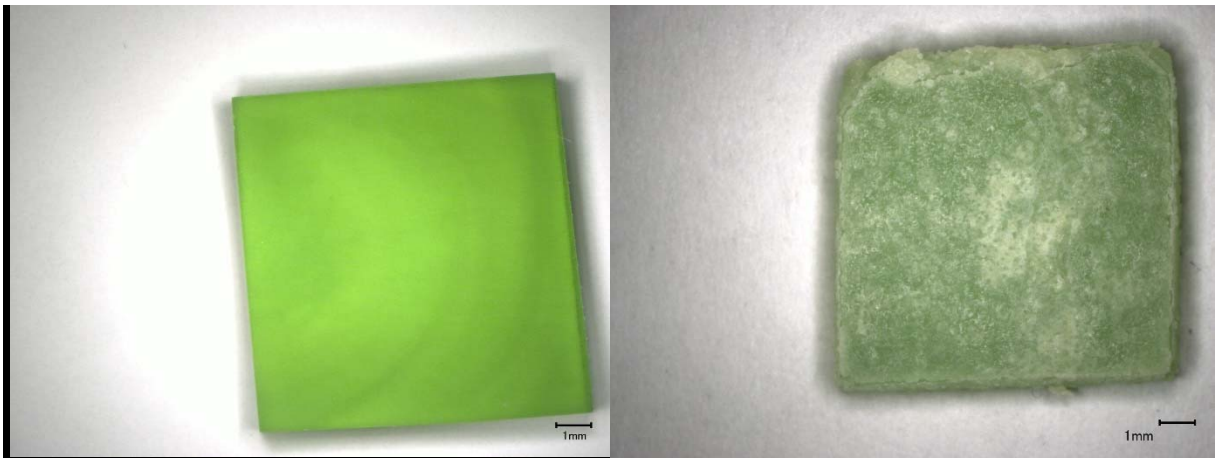


a) Glass square magnified 20X before VHT; b) Glass surface magnified after VHT

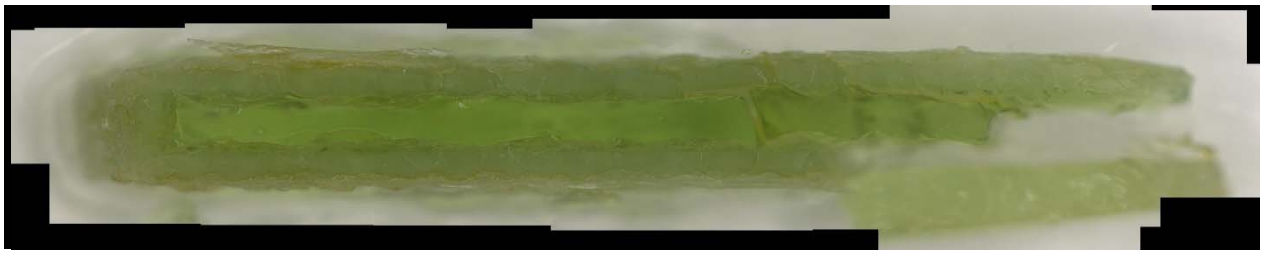

c) Glass cross section magnified after VHT

Figure I.68. CCC-Treated Glass LP2-IL-01 after VHT for 24 Days

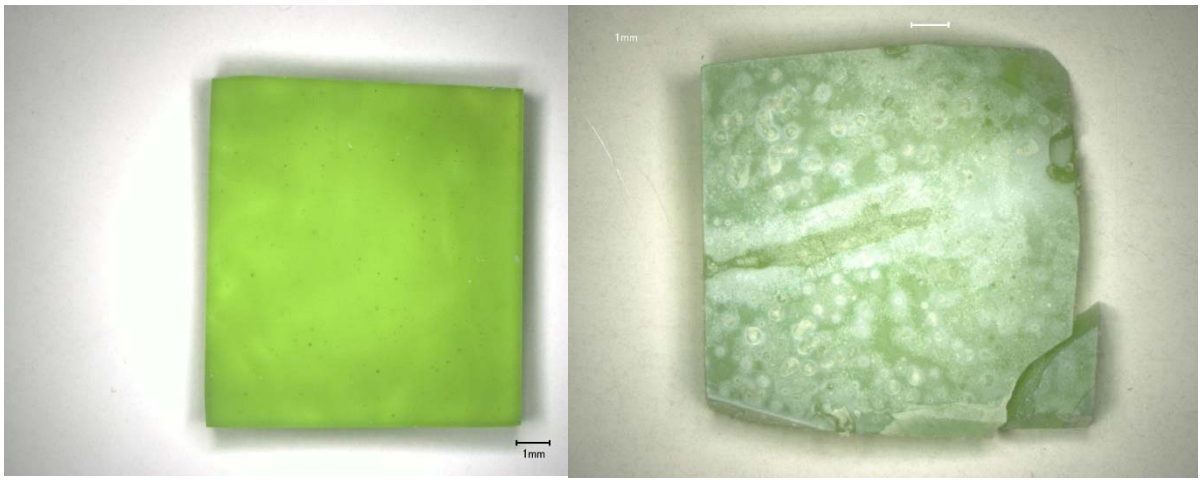


a) Glass square magnified 20X before VHT; b) Glass surface magnified after VHT

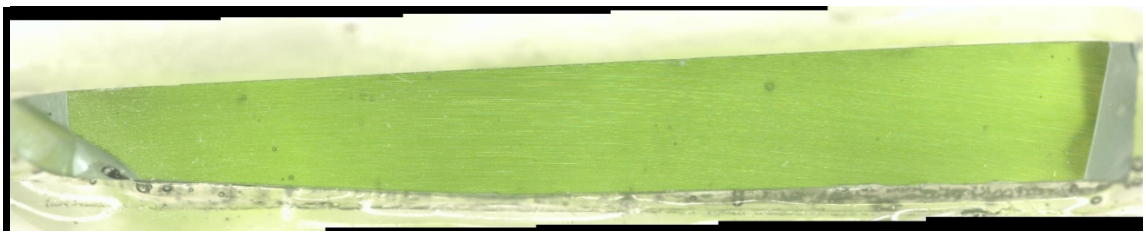

c) Glass cross section magnified after VHT

Figure I.69. CCC-Treated Glass LP2-IL-02 after VHT for 7 Days

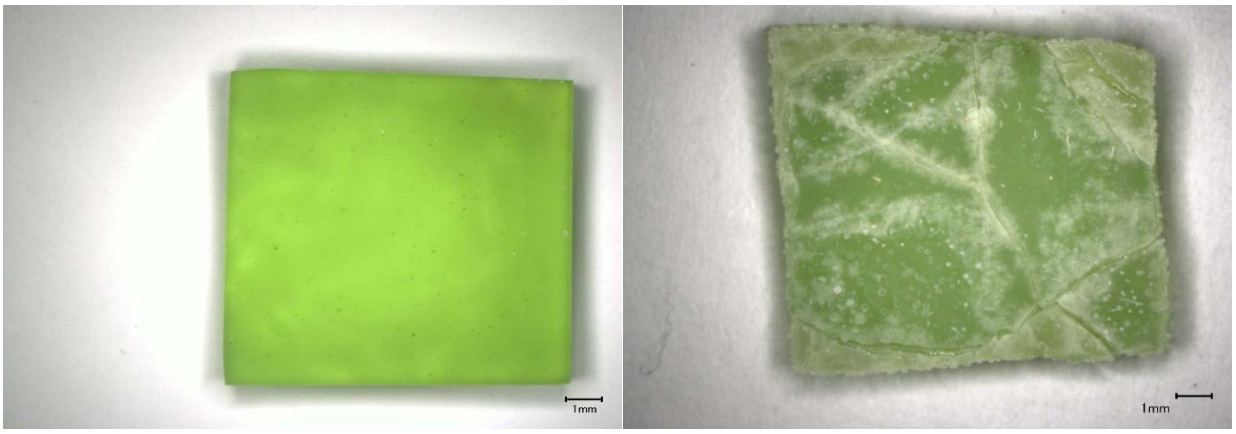


a) Glass square magnified 20X before VHT; b) Glass surface magnified after VHT

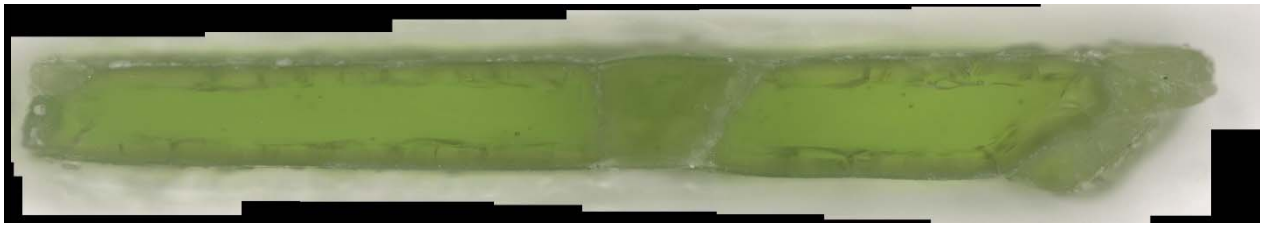

c) Glass cross section magnified after VHT

Figure I.70. CCC-Treated Glass LP2-IL-02 after VHT for 24 Days

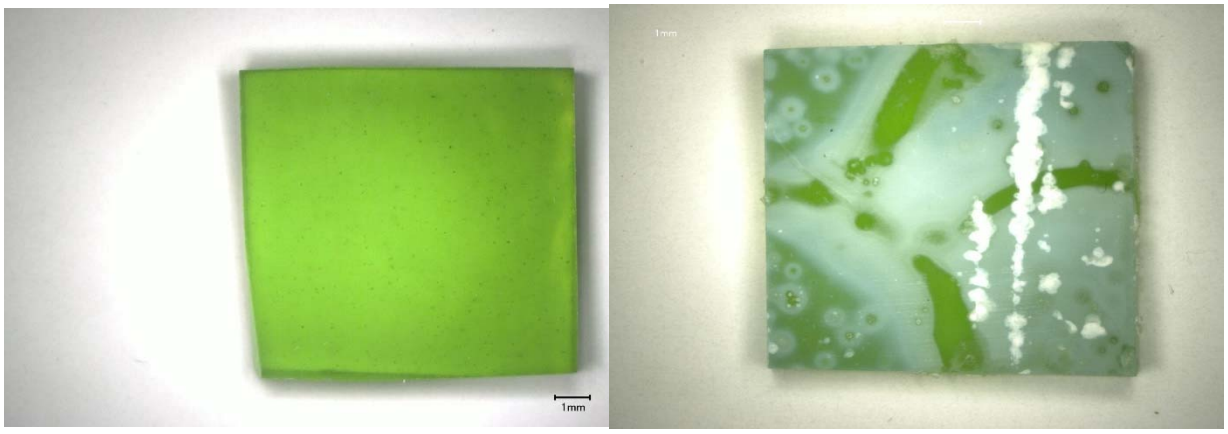


a) Glass square magnified 20X before VHT; b) Glass surface magnified after VHT

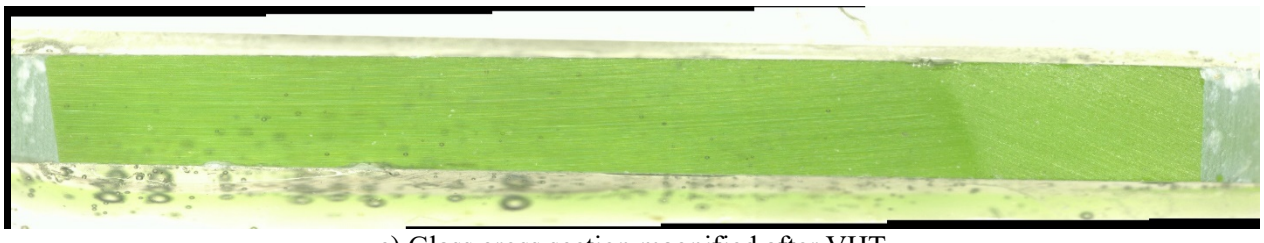

c) Glass cross section magnified after VHT

Figure I.71. CCC-Treated Glass LP2-IL-03 after VHT for 7 Days

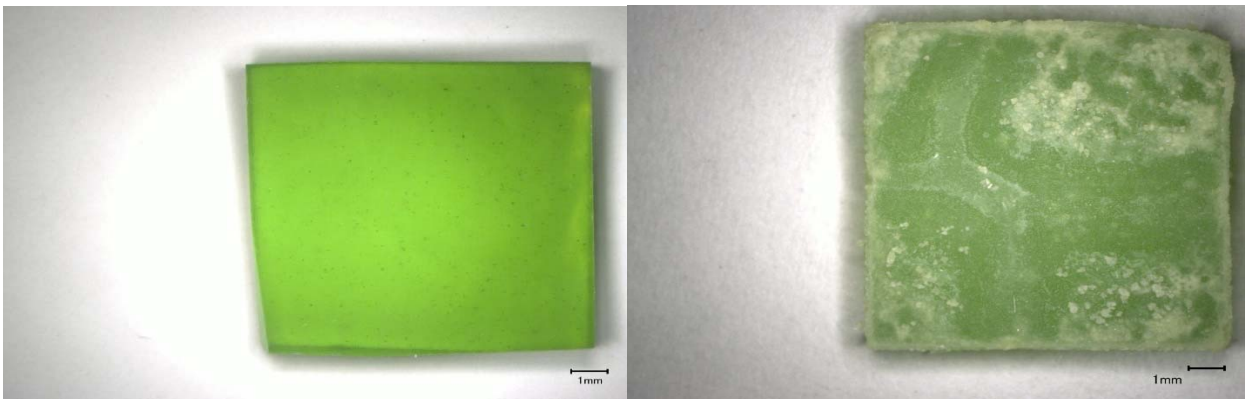


a) Glass square magnified 20X before VHT; b) Glass surface magnified after VHT

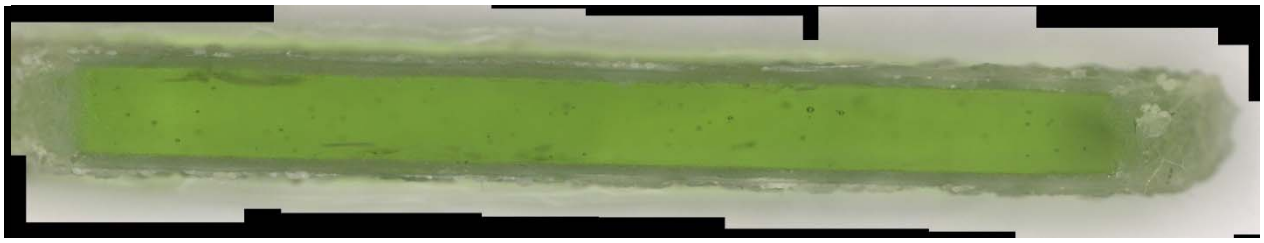

c) Glass cross section magnified after VHT

Figure I.72. CCC-Treated Glass LP2-IL-03 after VHT for 24 Days

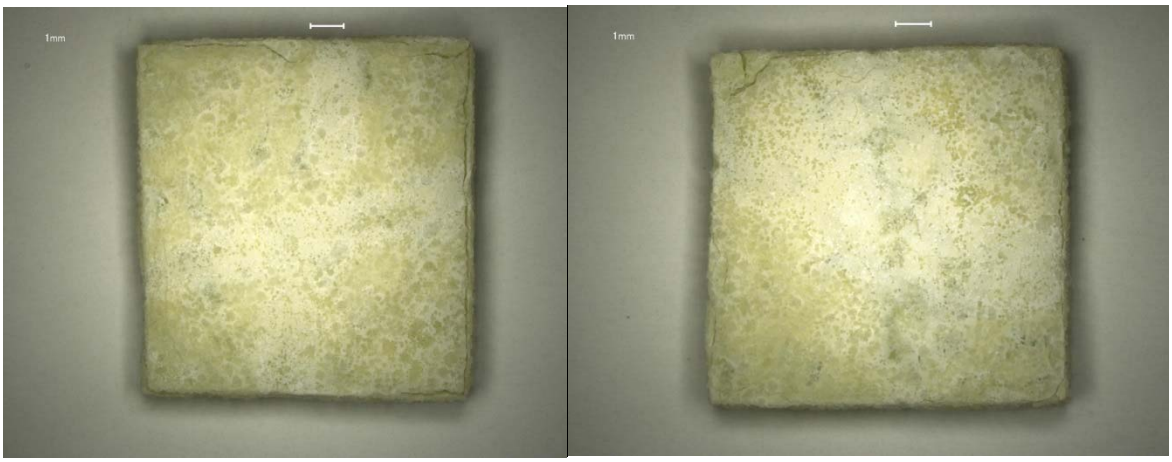


a) Glass square magnified after VHT; b) Glass square magnified after VHT

c) Glass cross section magnified after VHT

Figure I.73. CCC-Treated Glass LP2-IL-04 after VHT for 7 Days

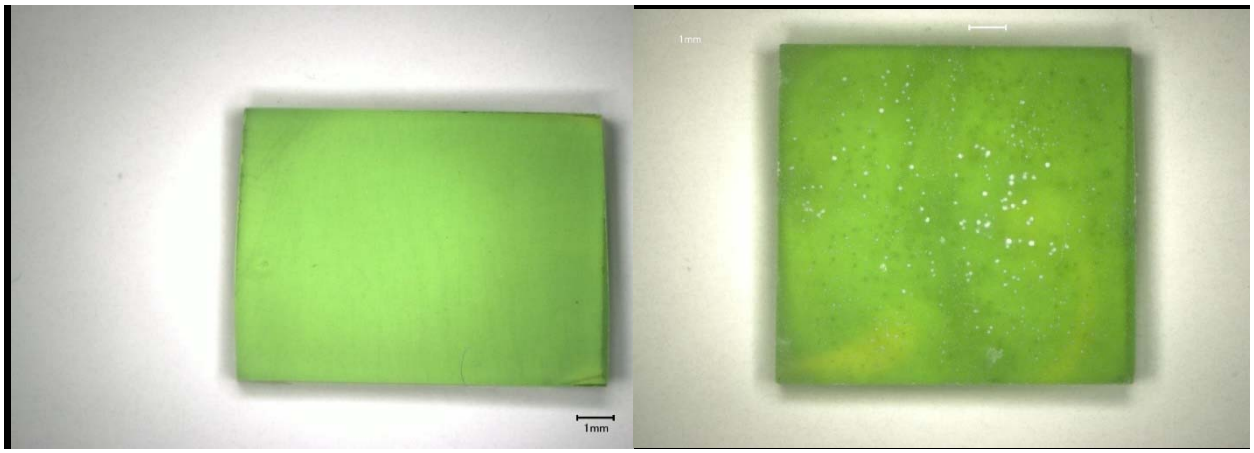

a) Glass square magnified 20X before VHT; b) Glass surface magnified after VHT

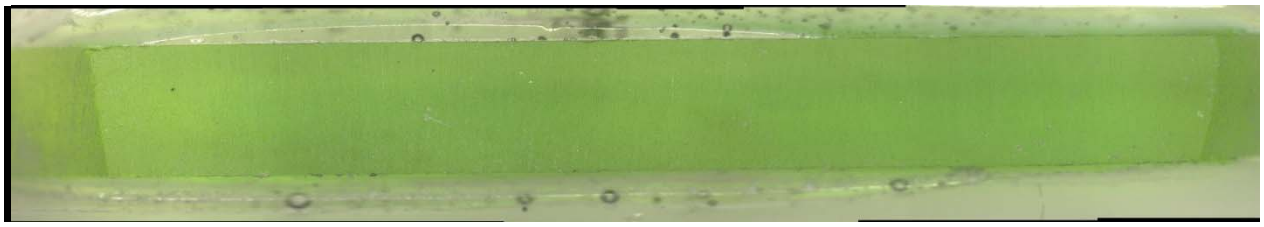

c) Glass cross section magnified after VHT

Figure I.74. CCC-Treated Glass LP2-IL-05 after VHT for 7 Days

a) Glass square magnified 20X before VHT; b) Glass surface magnified after VHT

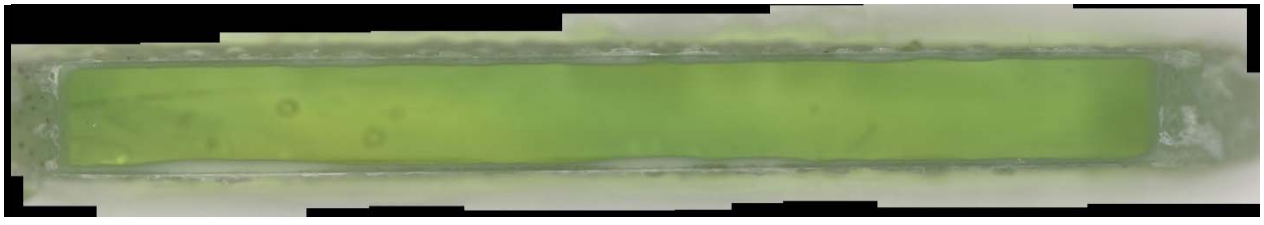

c) Glass cross section magnified after VHT

Figure I.75. CCC-Treated Glass LP2-IL-05 after VHT for 24 Days

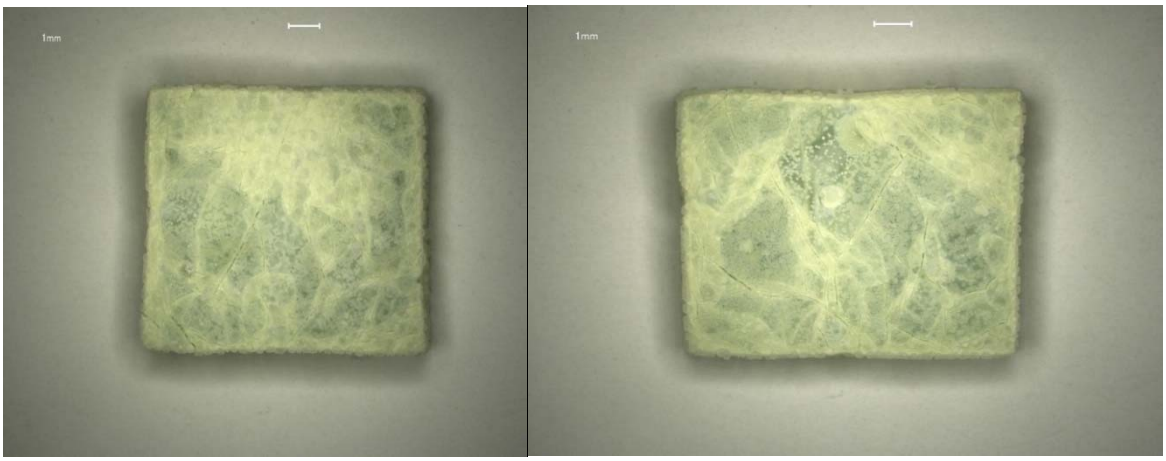

a) Glass square magnified after VHT; b) Glass square magnified after VHT

c) Glass cross section magnified after VHT

Figure I.76. CCC-Treated Glass LP2-IL-06 after VHT for 7 Days

a) Glass square magnified after VHT; b) Glass square magnified after VHT

c) Glass cross section magnified after VHT

Figure I.77. CCC-Treated Glass LP2-IL-07 after VHT for 7 Days

a) Glass square magnified 20X before VHT; b) Glass surface magnified after VHT

c) Glass cross section magnified after VHT

Figure I.78. CCC-Treated Glass LP2-IL-08 after VHT for 7 Days

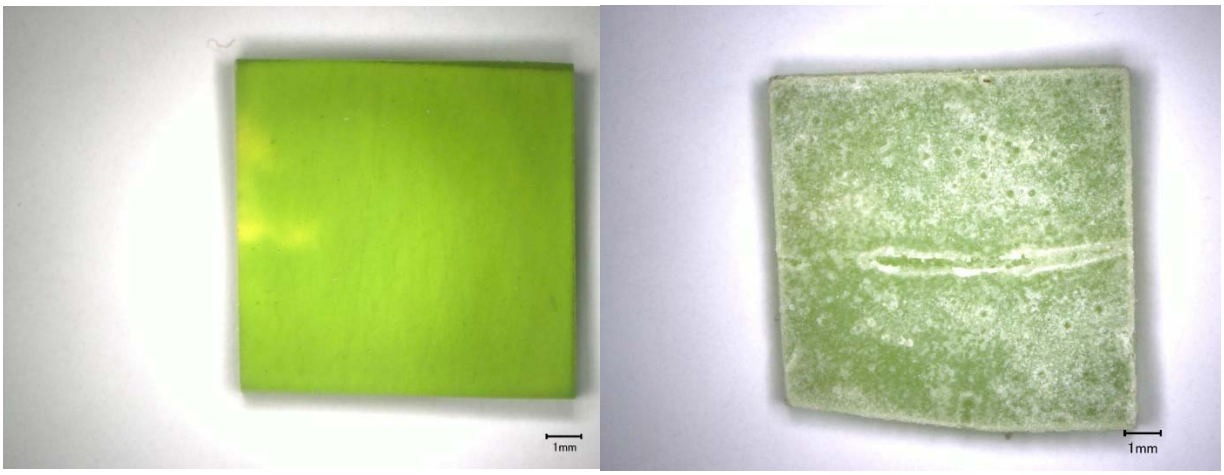

a) Glass square magnified 20X before VHT; b) Glass surface magnified after VHT

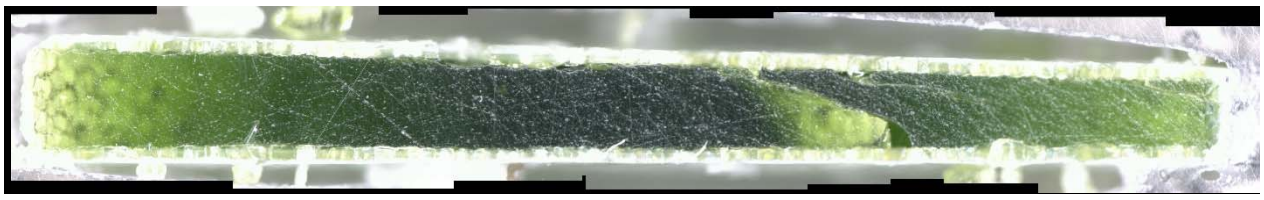

c) Glass cross section magnified after VHT

Figure I.79. CCC-Treated Glass LP2-IL-08 after VHT for 24 Days

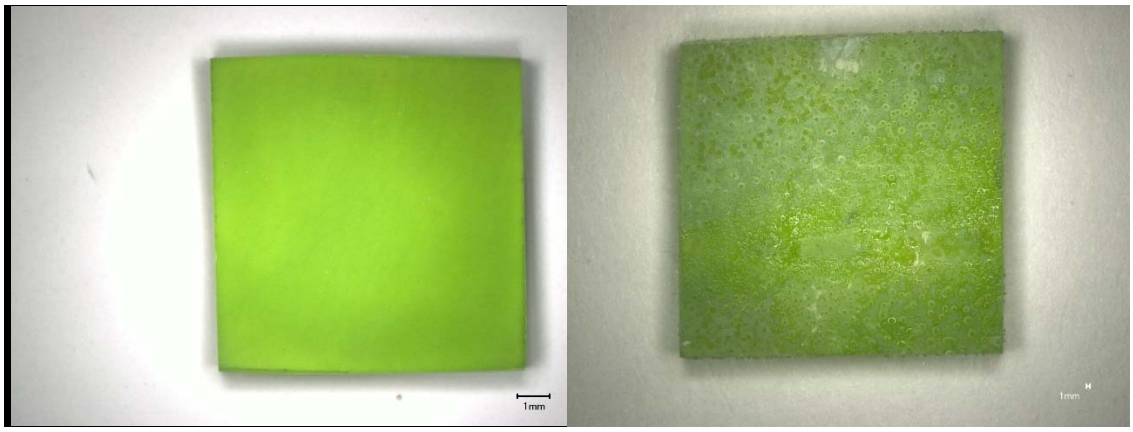

a) Glass square magnified 20X before VHT; b) Glass surface magnified after VHT

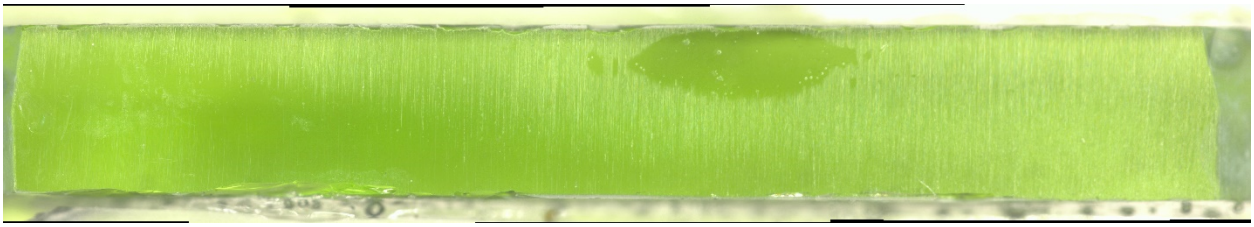

c) Glass cross section magnified after VHT

Figure I.80. CCC-Treated Glass LP2-IL-09 after VHT for 7 Days

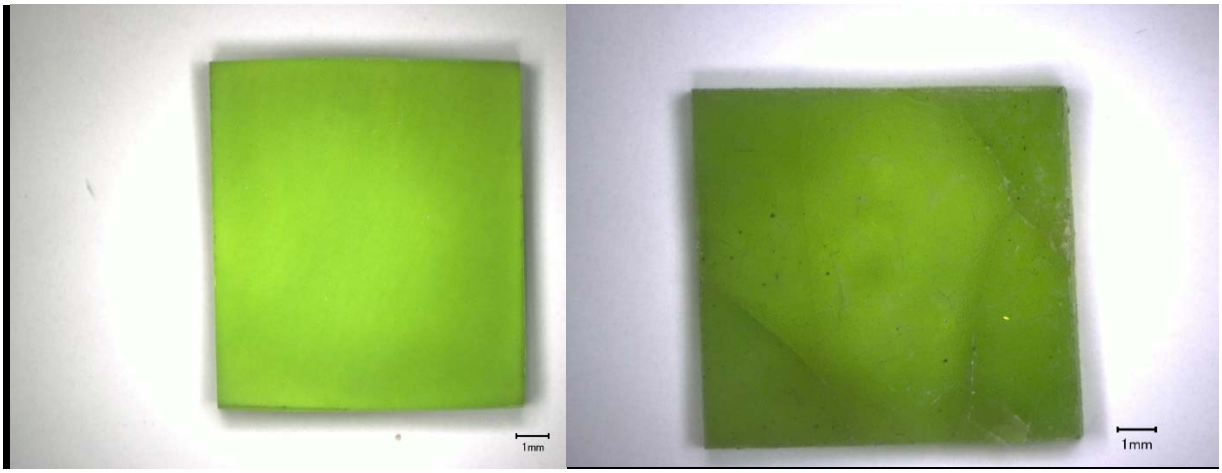

a) Glass square magnified 20X before VHT; b) Glass surface magnified after VHT

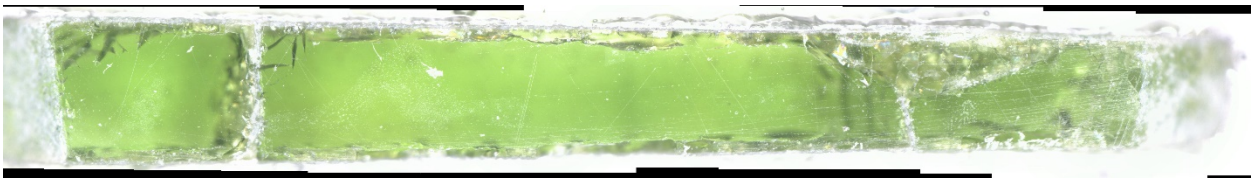

c) Glass cross section magnified after VHT

Figure I.81. CCC-Treated Glass LP2-IL-09 after VHT for 24 Days

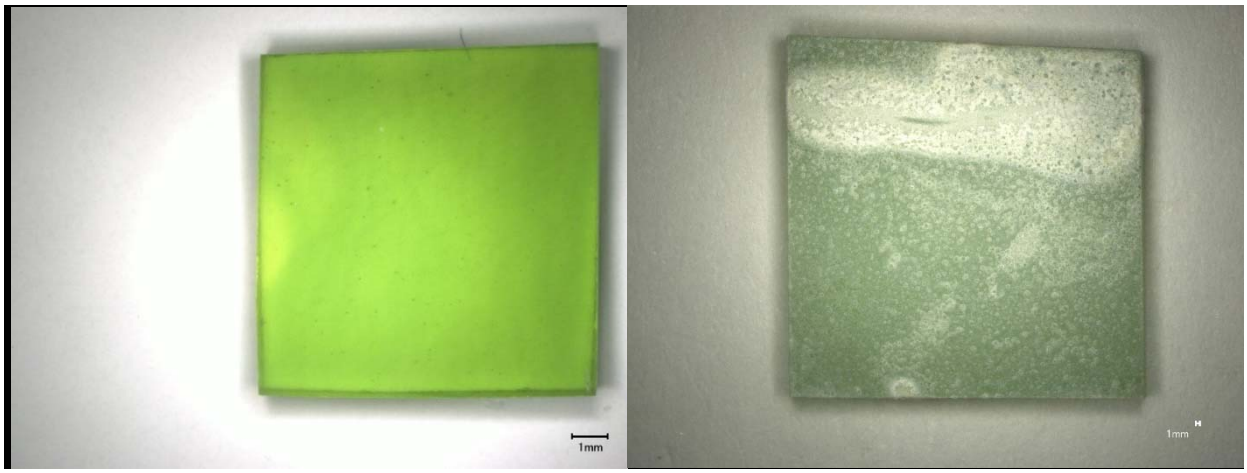


a) Glass square magnified 20X before VHT; b) Glass surface magnified after VHT

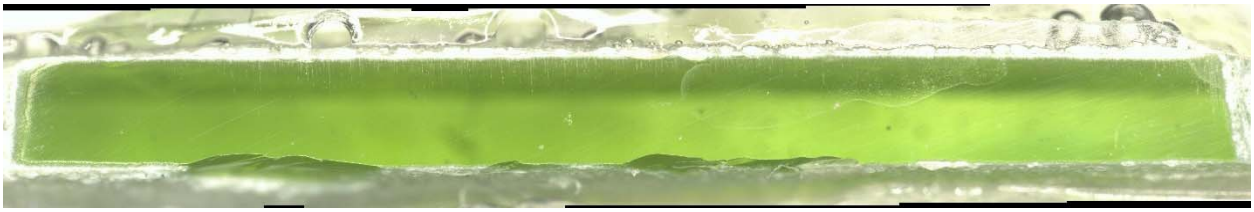

c) Glass cross section magnified after VHT

Figure I.82. CCC-Treated Glass LP2-IL-10 after VHT for 7 Days

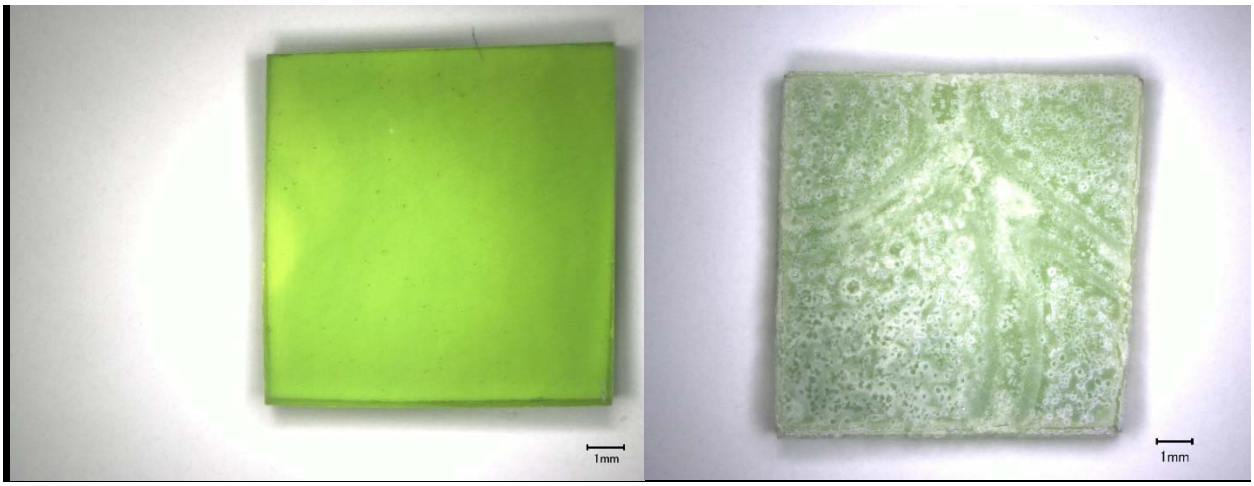


a) Glass square magnified 20X before VHT; b) Glass surface magnified after VHT

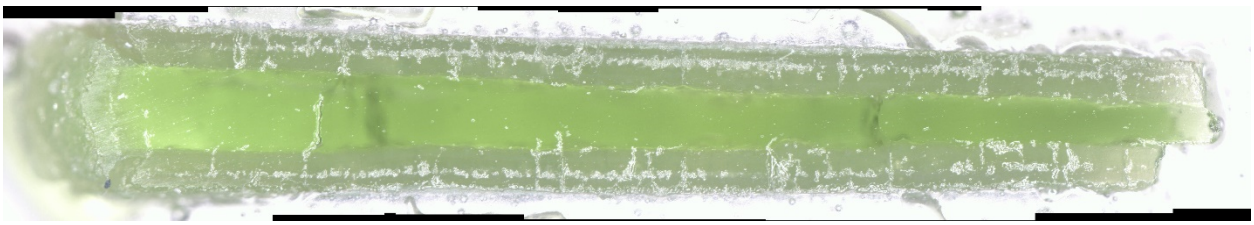

c) Glass cross section magnified after VHT

Figure I.83. CCC-Treated Glass LP2-IL-10 after VHT for 24 Days

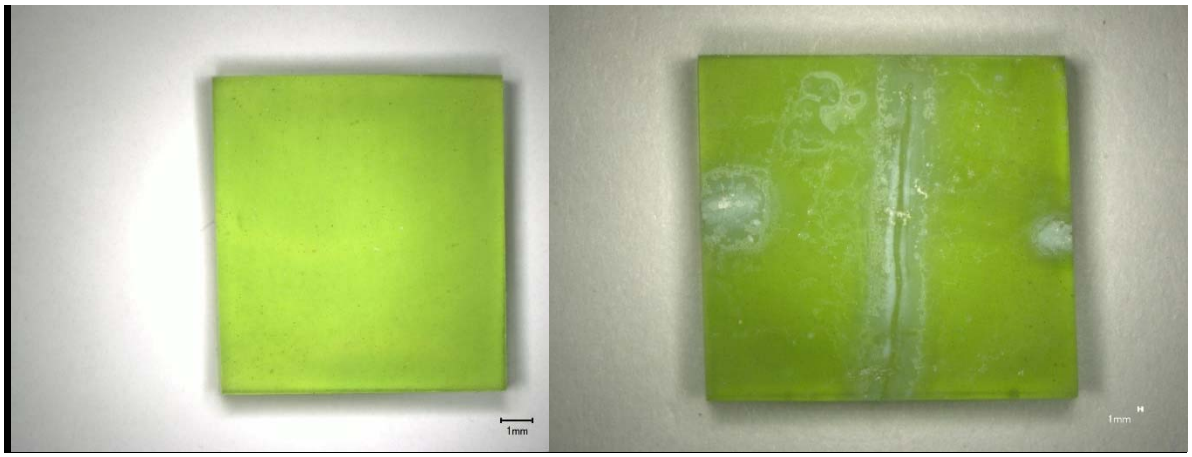

a) Glass square magnified 20X before VHT; b) Glass surface magnified after VHT

c) Glass cross section magnified after VHT

Figure I.84. CCC-Treated Glass LP2-IL-11 after VHT for 7 Days

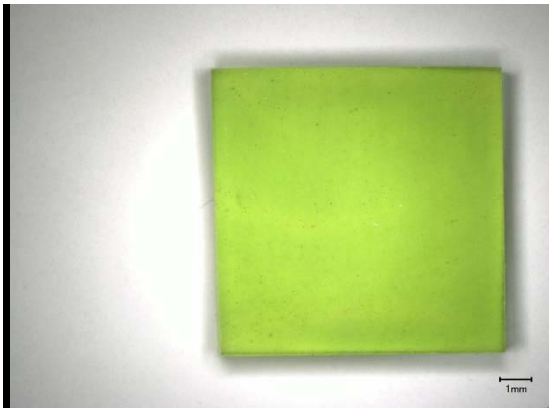

a) Glass square magnified 20X before VHT

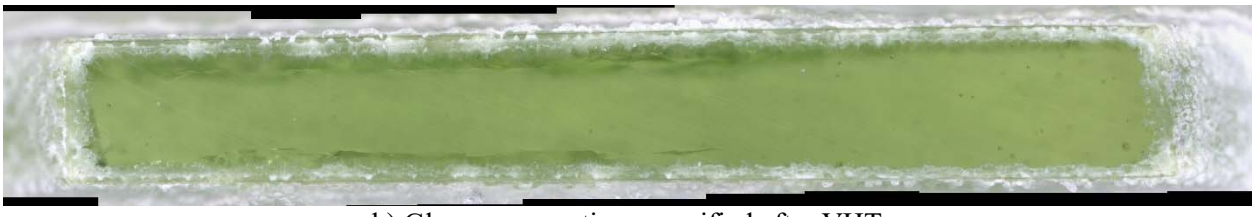

b) Glass cross section magnified after VHT

Figure I.85. CCC-Treated Glass LP2-IL-11 after VHT for 24 Days

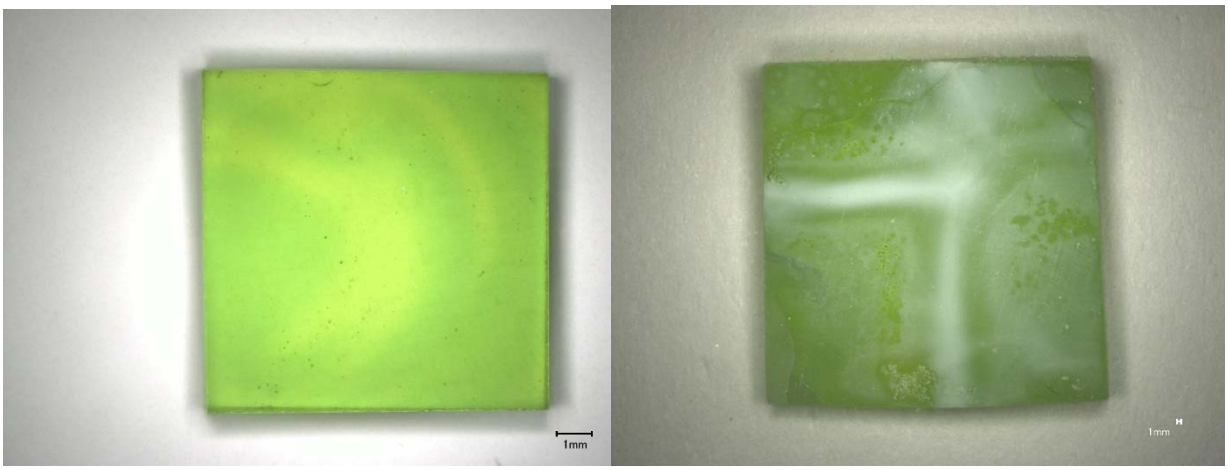

a) Glass square magnified 20X before VHT; b) Glass surface magnified after VHT

c) Glass cross section magnified after VHT

Figure I.86. CCC-Treated Glass LP2-IL-12 after VHT for 7 Days

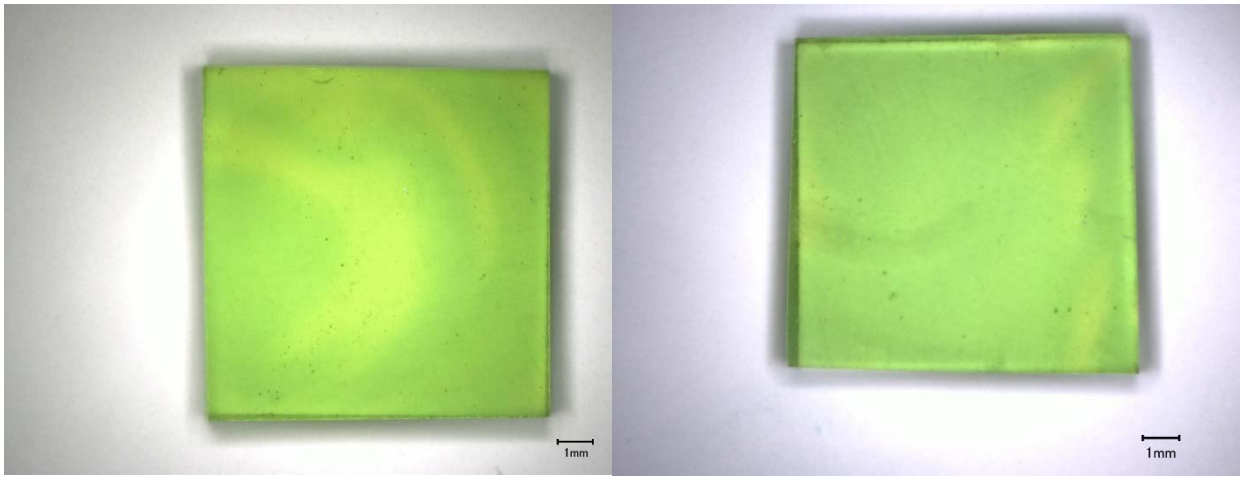

a) Glass square magnified 20X before VHT; b) Glass surface magnified after VHT

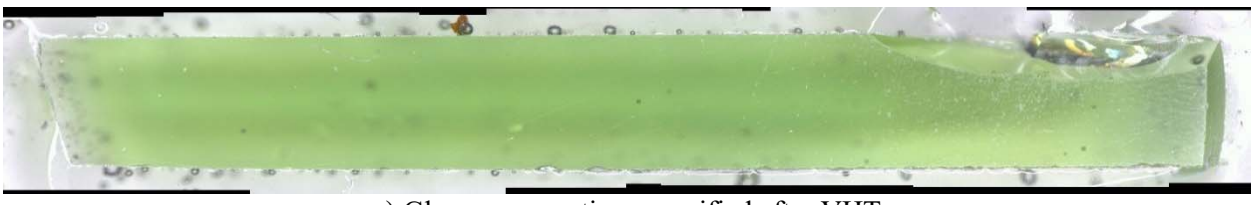

c) Glass cross section magnified after VHT

Figure I.87. CCC-Treated Glass LP2-IL-12 after VHT for 24 Days

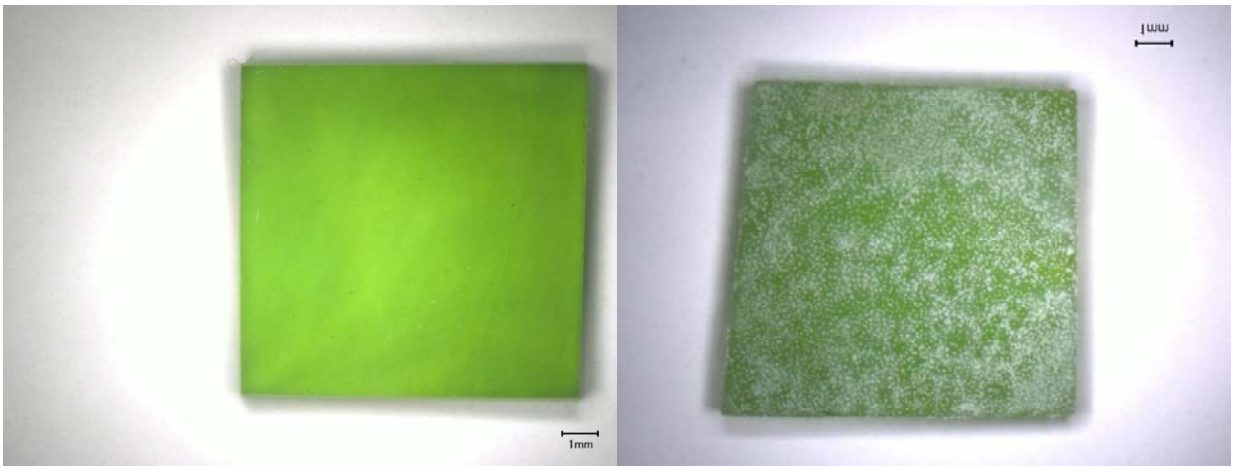

a) Glass square magnified 20X before VHT; b) Glass surface magnified after VHT

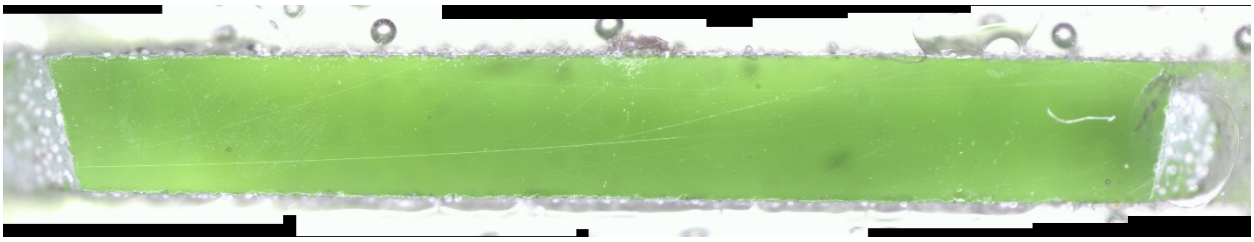

c) Glass cross section magnified after VHT

Figure I.88. CCC-Treated Glass LP2-IL-13 after VHT for 24 Days

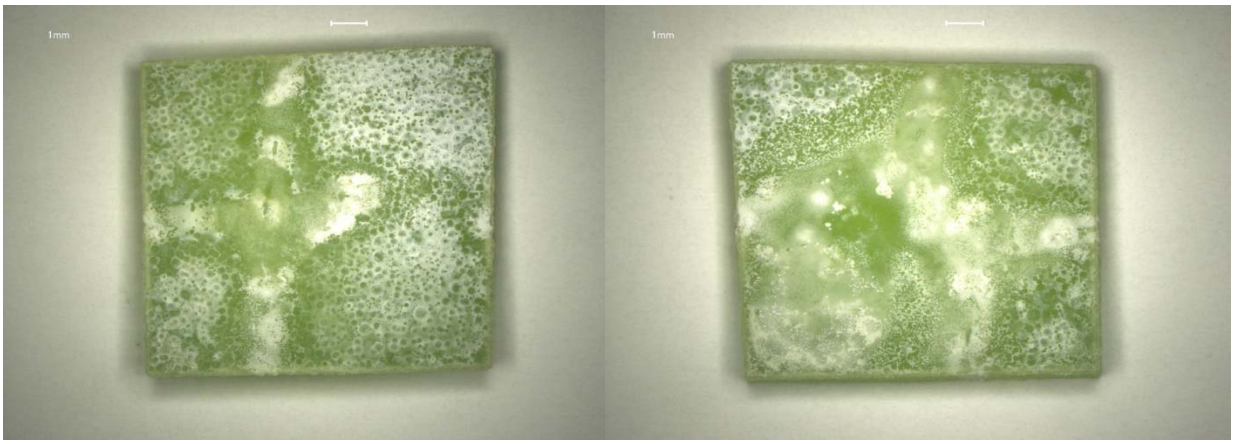

a) Glass square magnified after VHT; b) Glass square magnified after VHT

c) Glass cross section magnified after VHT

Figure I.89. CCC-Treated Glass LP2-IL-14 after VHT for 7 Days

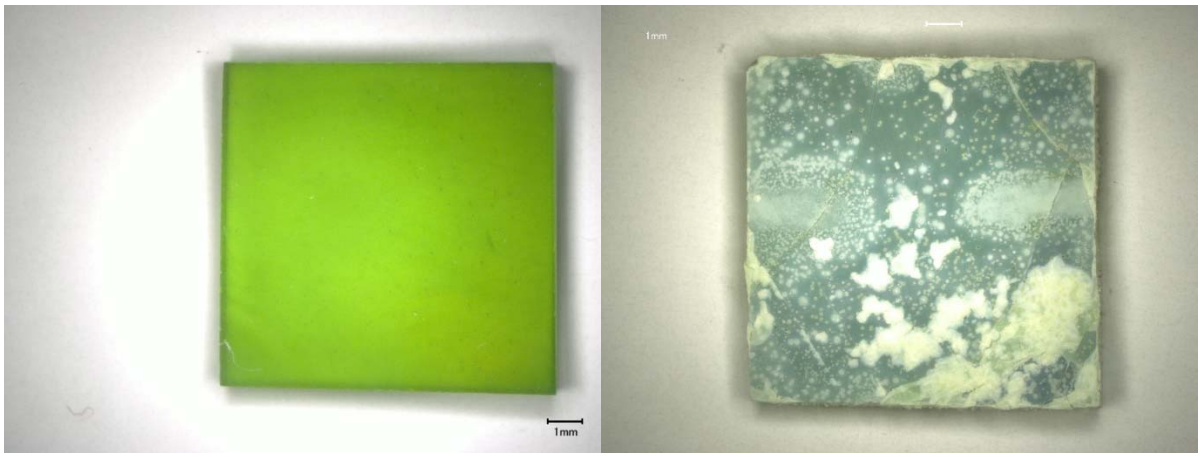


a) Glass square magnified 20X before VHT; b) Glass surface magnified after VHT

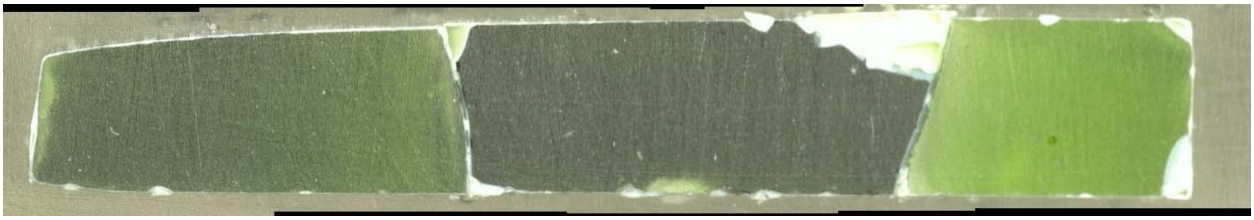

c) Glass cross section magnified after VHT

Figure I.90. CCC-Treated Glass LP2-IL-15 after VHT for 7 Days

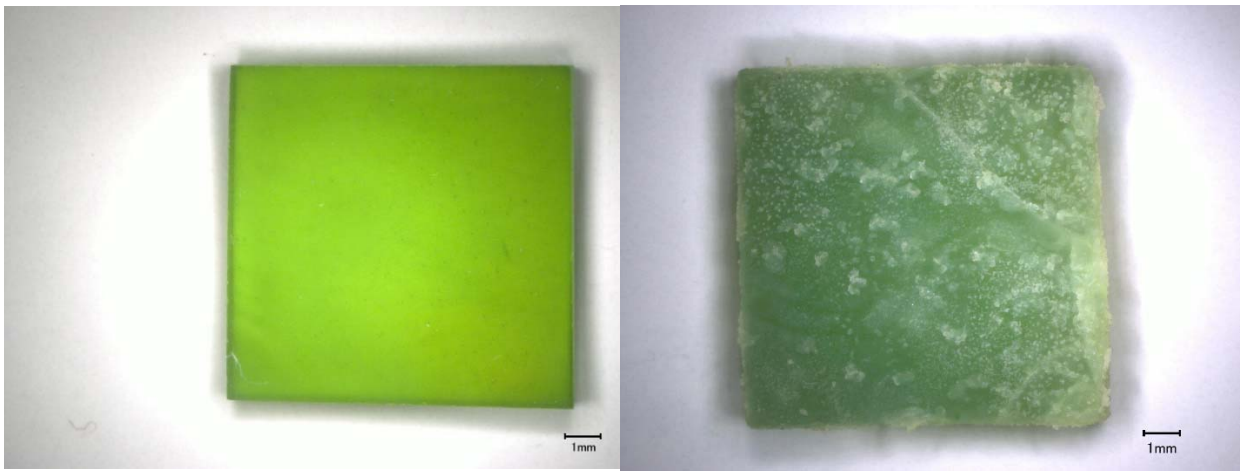


a) Glass square magnified 20X before VHT; b) Glass surface magnified after VHT

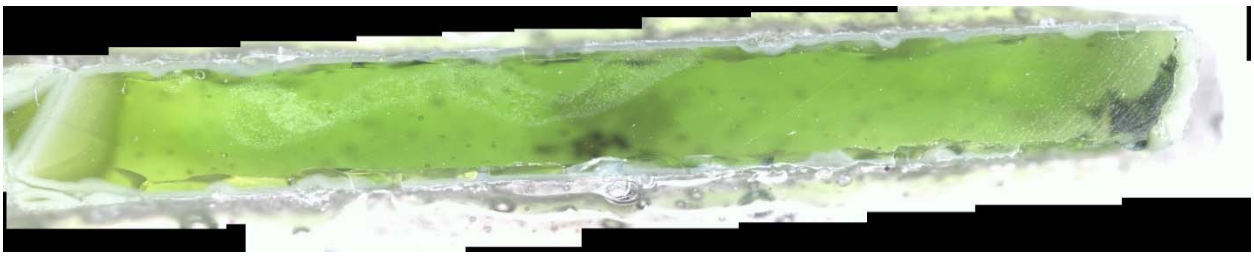

c) Glass cross section magnified after VHT

Figure I.91. CCC-Treated Glass LP2-IL-15 after VHT for 24 Days

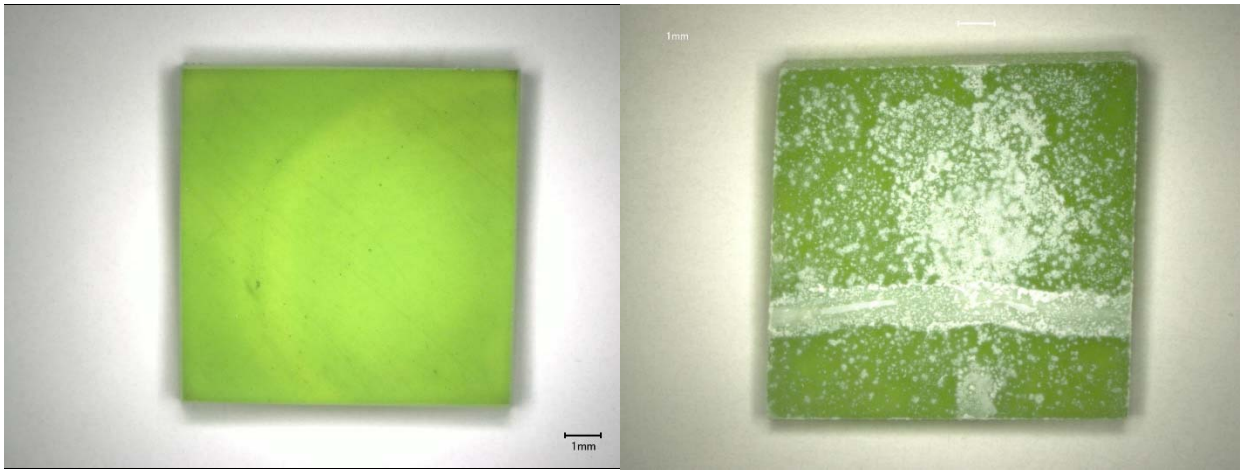


a) Glass square magnified 20X before VHT; b) Glass surface magnified after VHT

c) Glass cross section magnified after VHT

Figure I.92. CCC-Treated Glass LP2-IL-16 after VHT for 24 Days

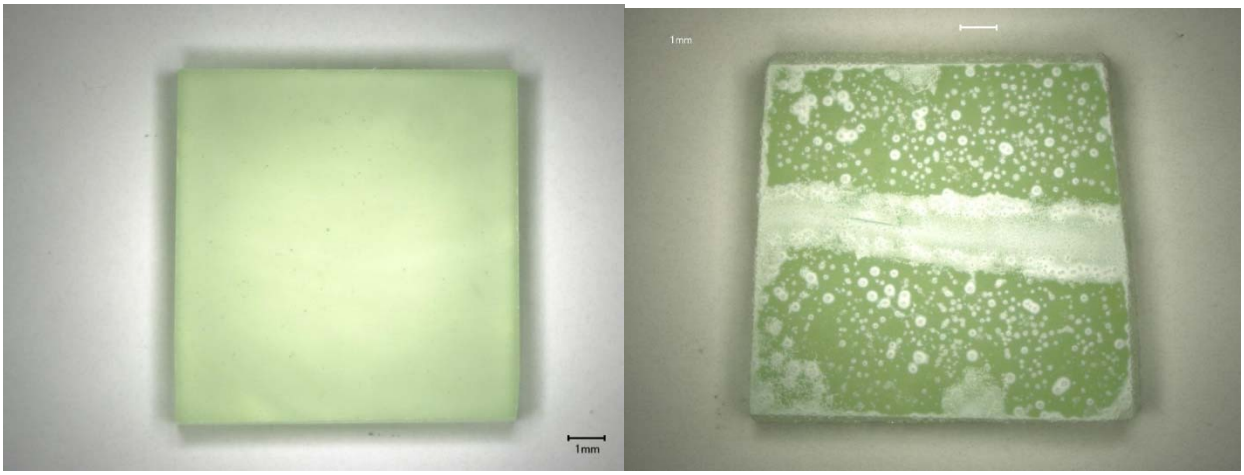


a) Glass square magnified 20X before VHT; b) Glass surface magnified after VHT

c) Glass cross section magnified after VHT

Figure I.93. CCC-Treated Glass LP2-IL-17 after VHT for 7 Days

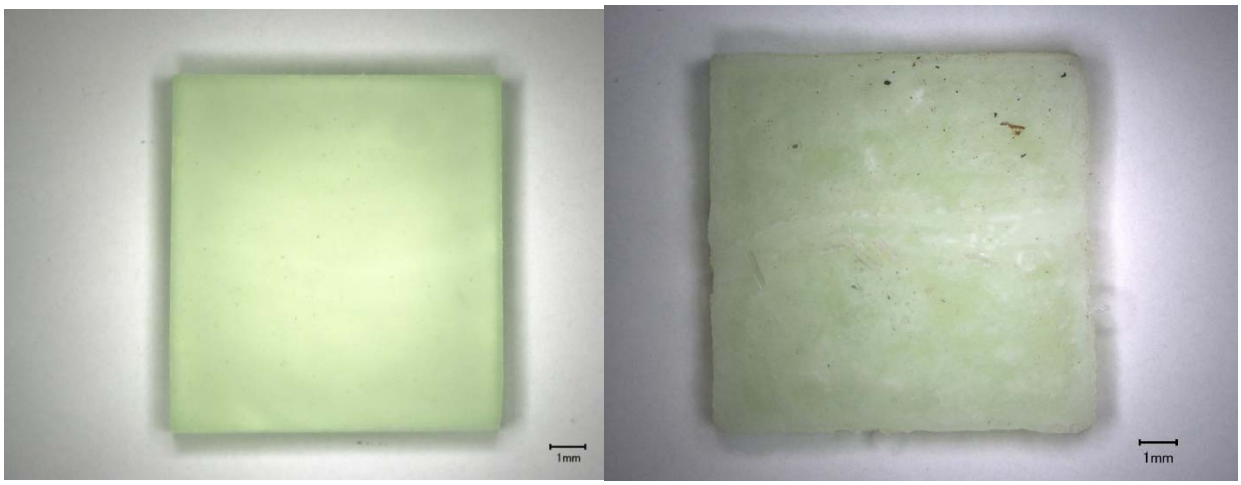


a) Glass square magnified 20X before VHT; b) Glass surface magnified after VHT

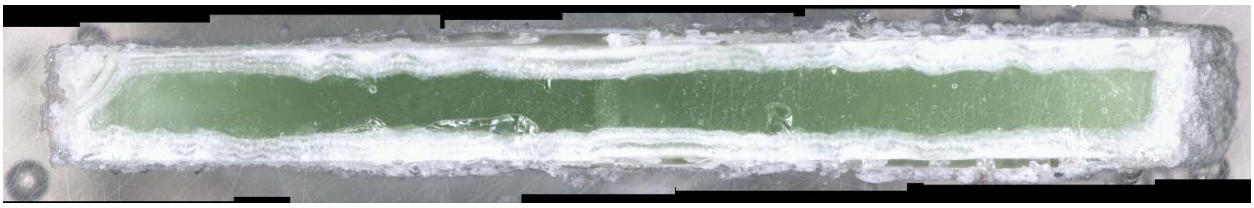

c) Glass cross section magnified after VHT

Figure I.94. CCC-Treated Glass LP2-IL-17 after VHT for 24 Days

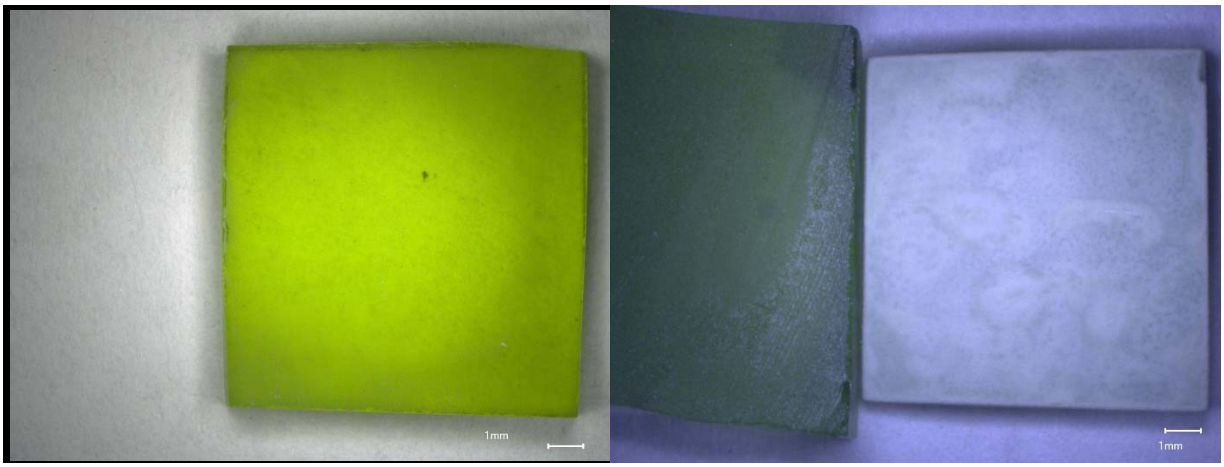


a) Glass square magnified 20X before VHT; b) Glass square after (right) and before (left) VHT

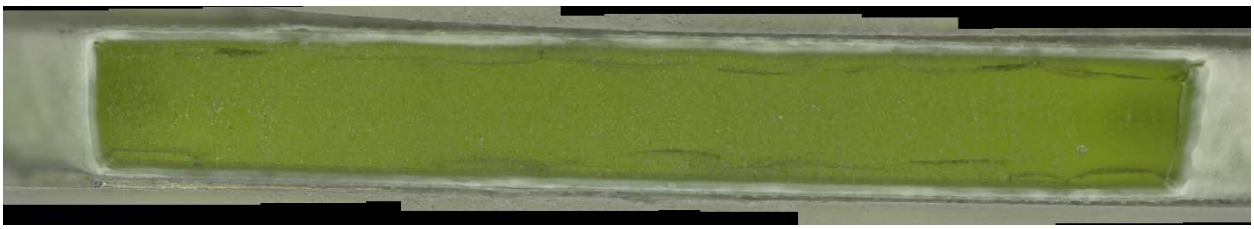

c) Glass cross section magnified after VHT

Figure I.95. CCC-Treated Glass LP2-OL-01-3 after VHT for 11 Days

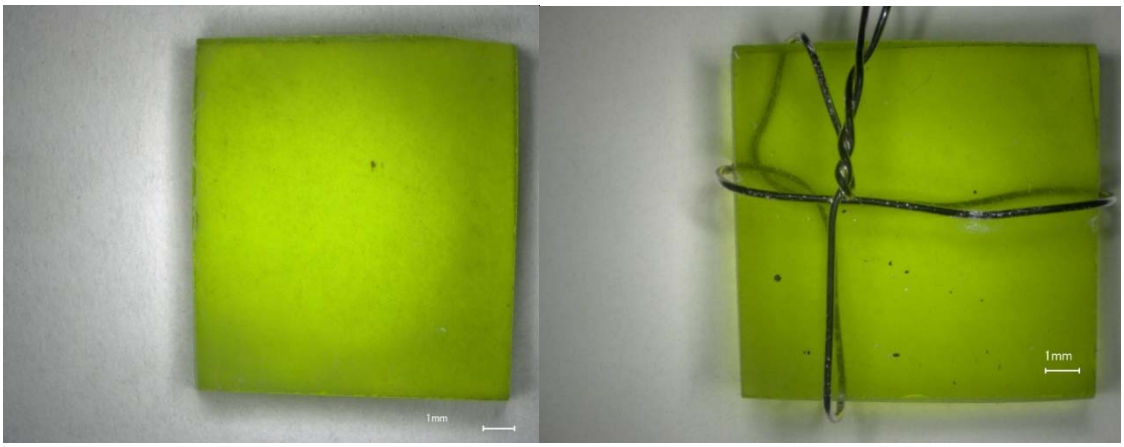


a) Glass square magnified 20X before VHT; b) Glass square magnified 20X after VHT

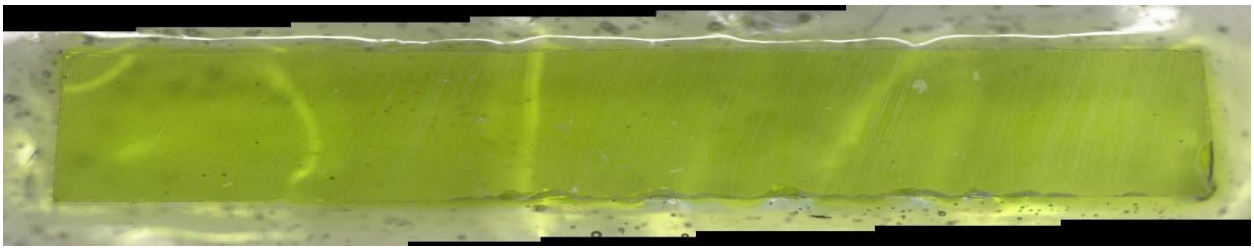

c) Glass cross section magnified after VHT

Figure I.96. CCC-Treated Glass LP2-OL-01-3 after VHT for 24 Days

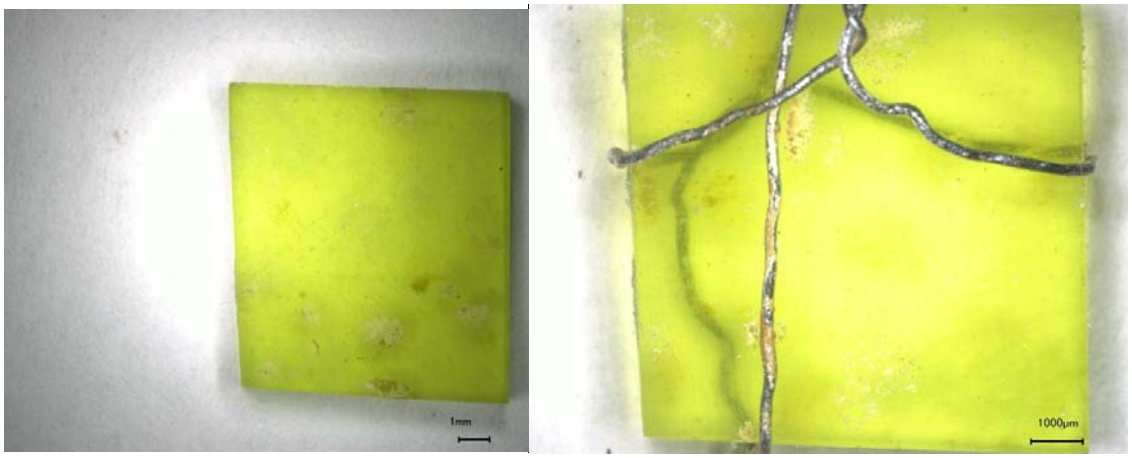


a) Glass square magnified 20X after VHT; b) Glass square magnified 30X after VHT

c) Glass cross section magnified after VHT

Figure I.97. CCC-Treated Glass LP2-OL-02-1 after VHT for 24 Days

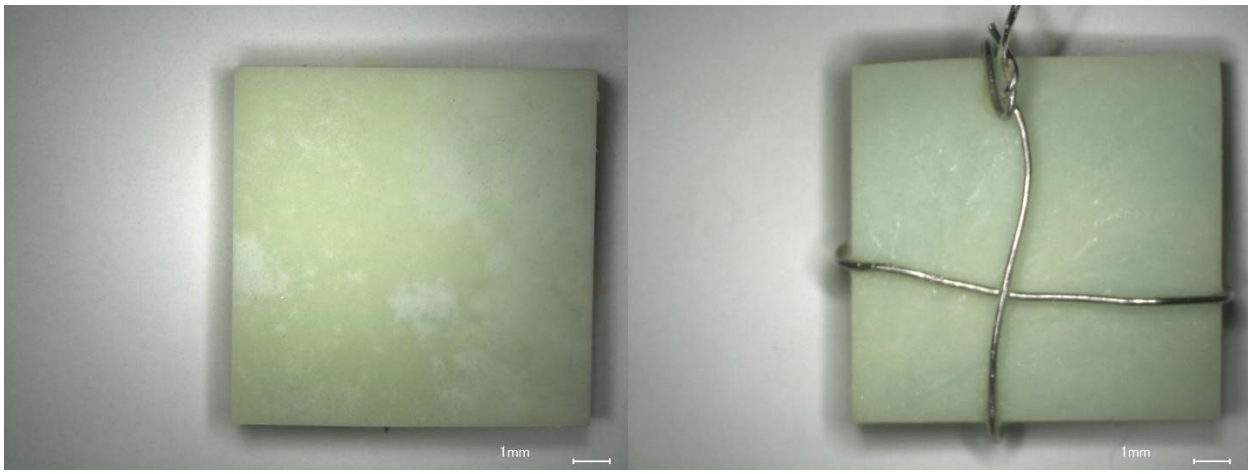


a) Glass square magnified 20X before VHT; b) Glass square magnified after VHT

c) Glass cross section magnified after VHT

Figure I.98. CCC-Treated Glass LP2-OL-03 MOD2 after VHT for 7 Days

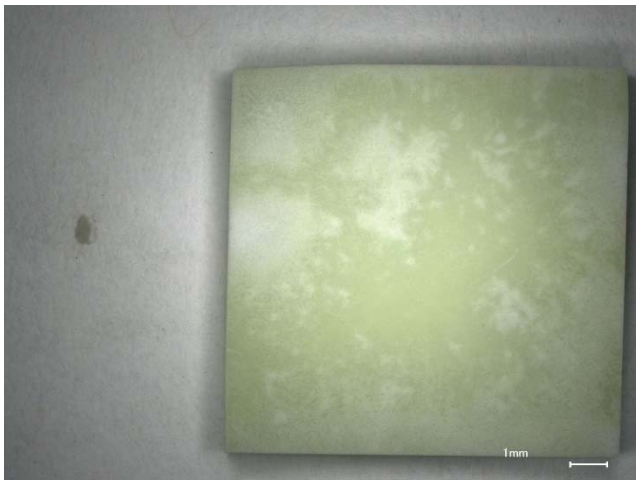


a) Glass square magnified 20X before VHT

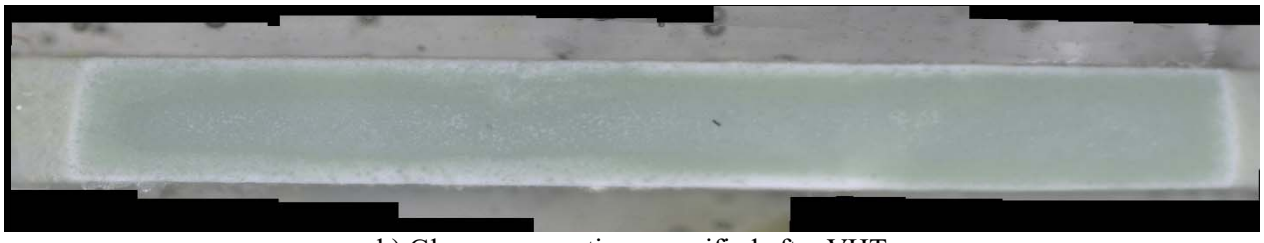

b) Glass cross section magnified after VHT

Figure I.99. CCC-Treated Glass LP2-OL-03 MOD2 after VHT for 24 Days

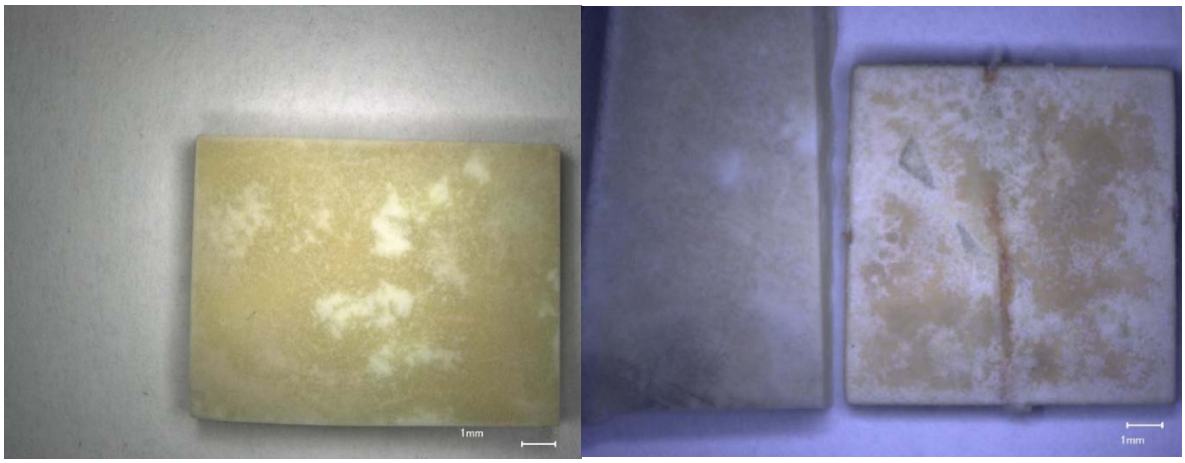

a) Glass square magnified 20X before VHT b) Glass square before (on left) and after (on right) VHT

c) Glass cross section magnified after VHT

Figure I.100. CCC-Treated Glass LP2-OL-04-1 after VHT for 11 Days

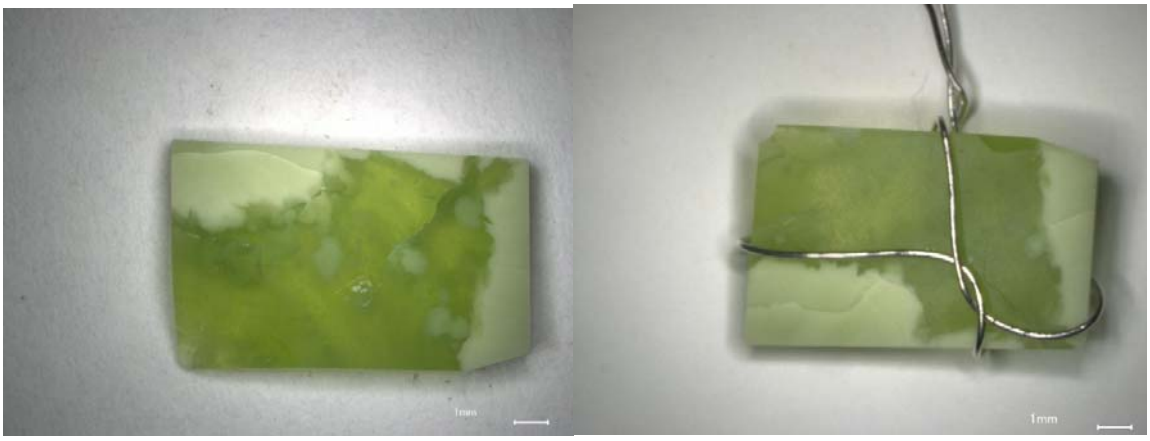

a) Glass square magnified 20X before VHT; b) Glass square magnified after VHT

c) Glass cross section magnified after VHT

Figure I.101. CCC-Treated Glass LP2-OL-05 after VHT for 7 Days

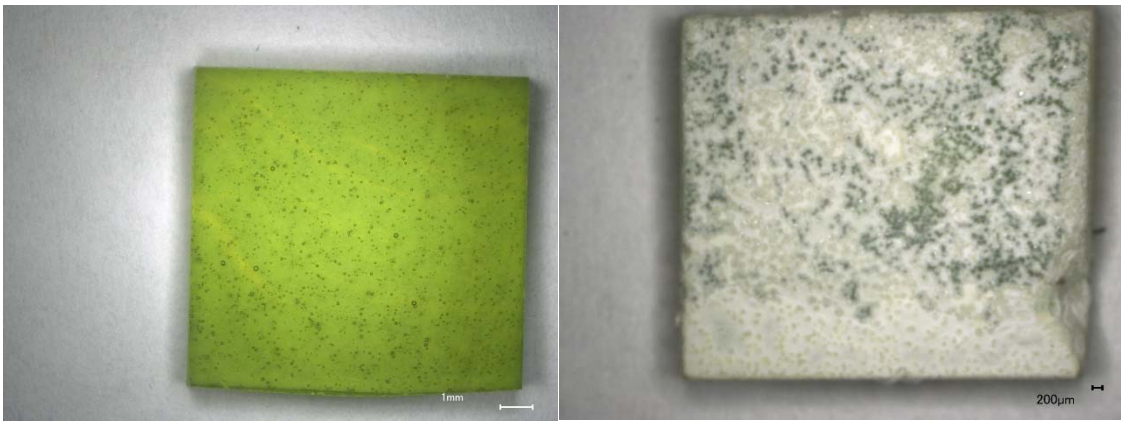


a) Glass square magnified 20X before VHT; b) Glass square magnified after VHT

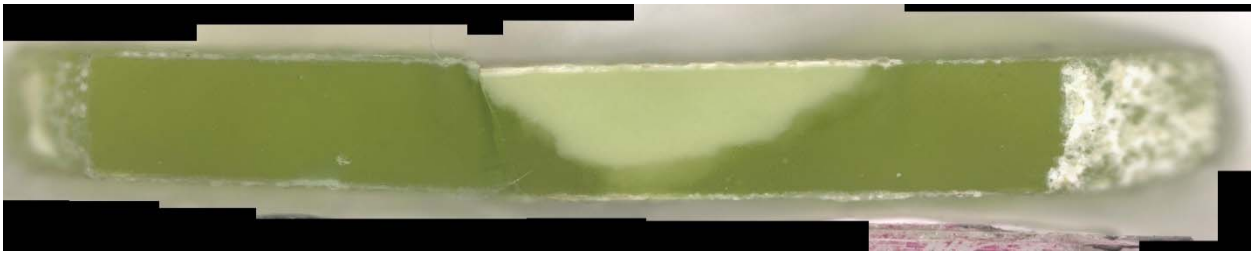

c) Glass cross section magnified after VHT

Figure I.102. CCC-Treated Glass LP2-OL-05 after VHT for 24 Days

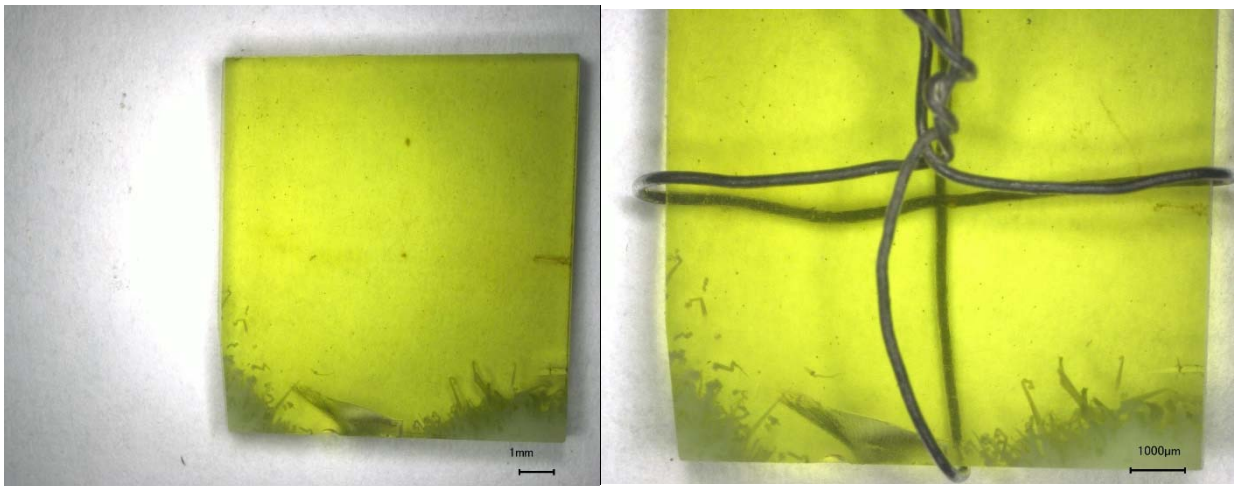


a) Glass square magnified 20X after VHT; b) Glass square magnified 30X after VHT

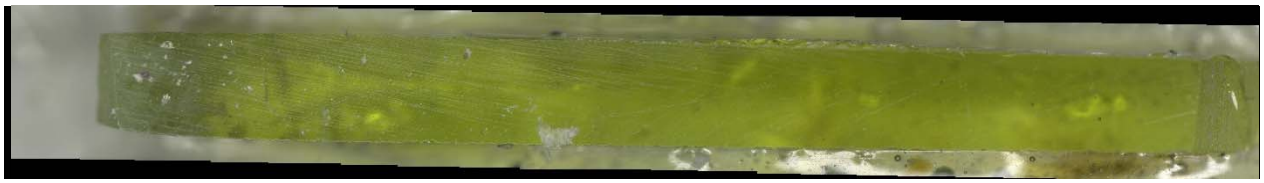

c) Glass cross section magnified after VHT

Figure I.103. CCC-Treated Glass LP2-OL-07-1 after VHT for 24 Days

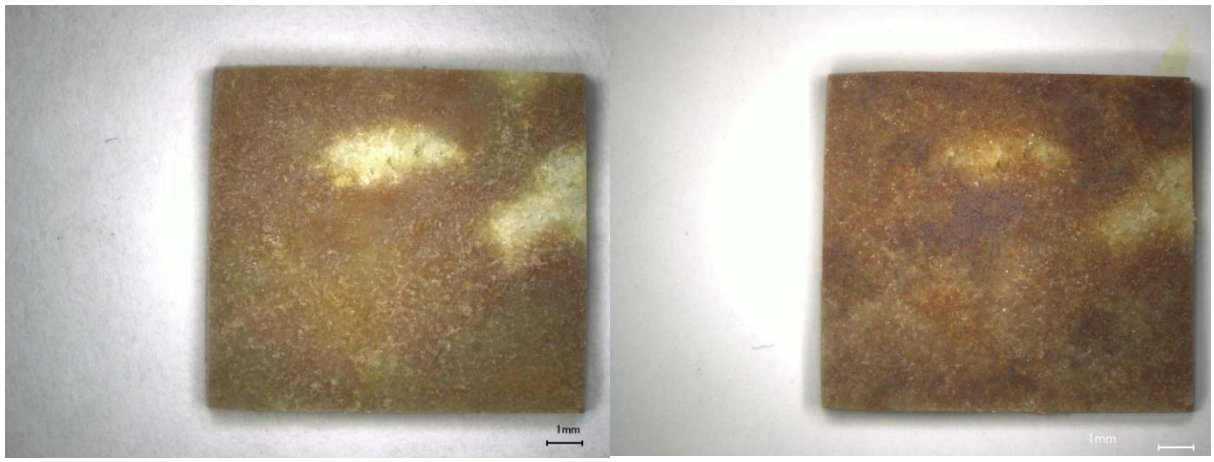


a) Glass square magnified 20X before VHT; b) Glass square magnified after VHT

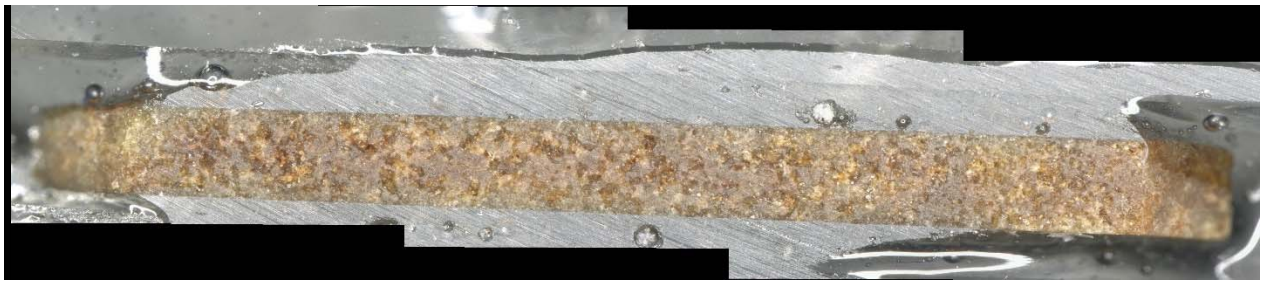

c) Glass cross section magnified after VHT

Figure I.104. CCC-Treated Glass LP2-OL-08MOD after VHT for 7 Days

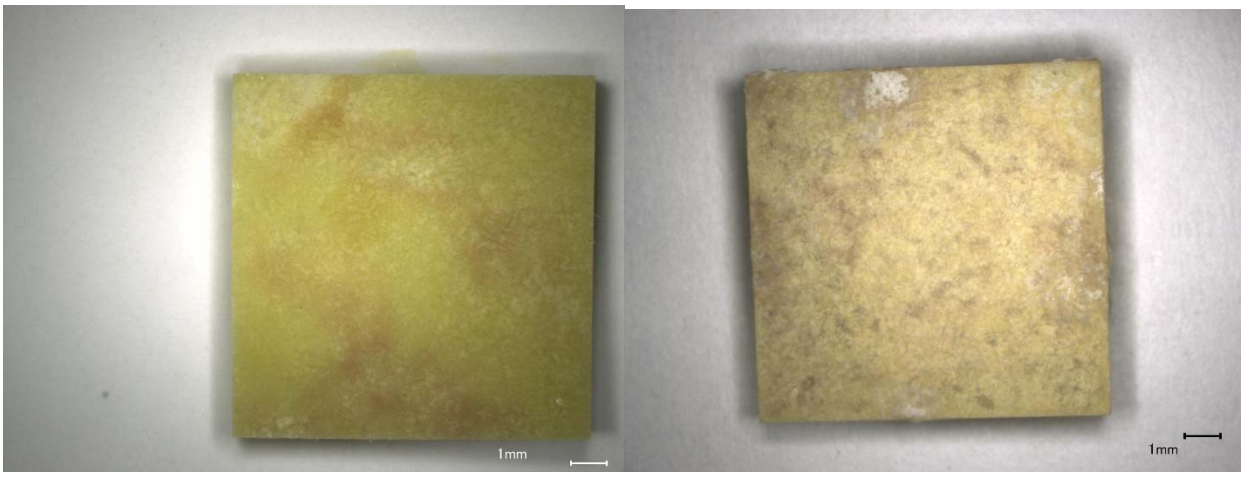


a) Glass square magnified 20X before VHT; b) Glass square magnified after VHT

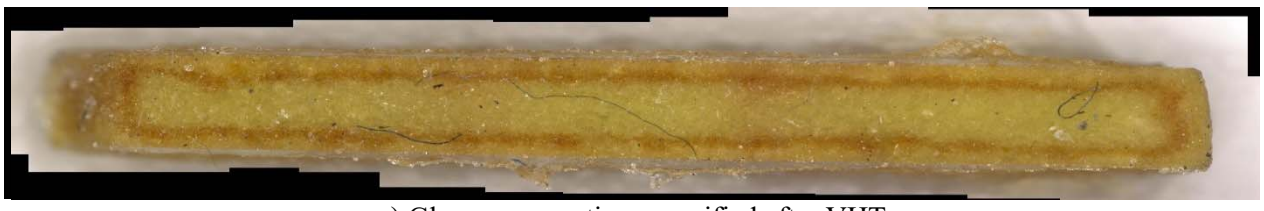

c) Glass cross section magnified after VHT

Figure I.105. CCC-Treated Glass LP2-OL-08MOD after VHT for 24 Days

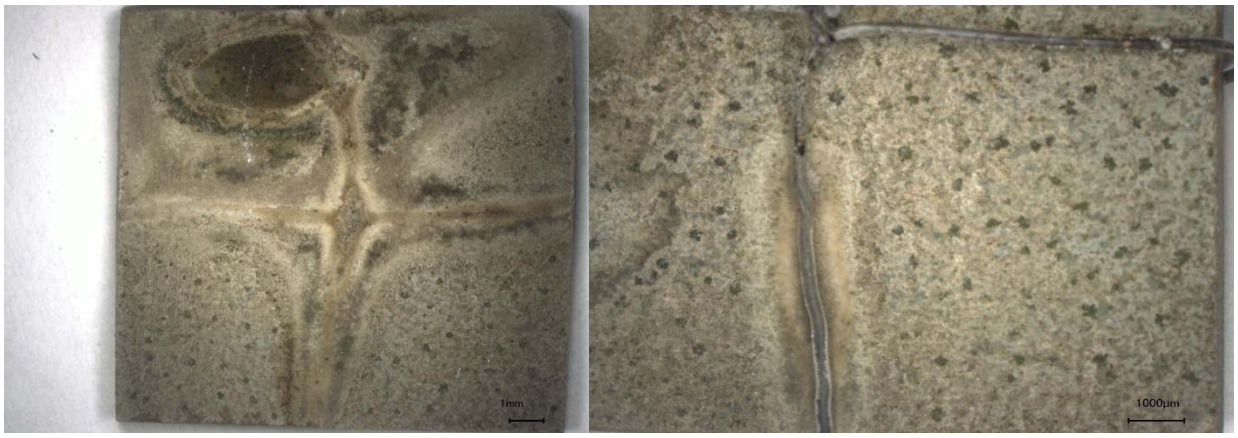


a) Glass square magnified 20X after VHT; b) Glass square magnified 30X after VHT

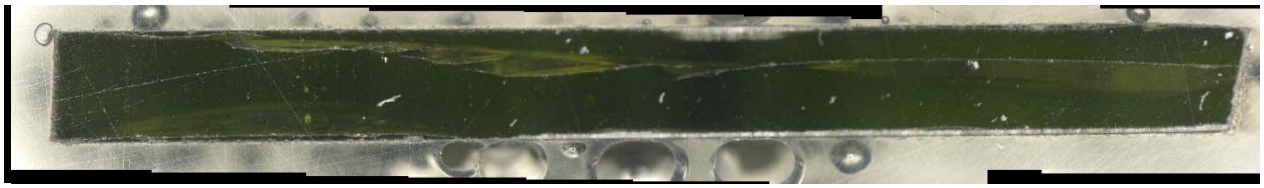

c) Glass cross section magnified after VHT

Figure I.106. CCC-Treated Glass LP2-OL-09-1 after VHT for 24 Days

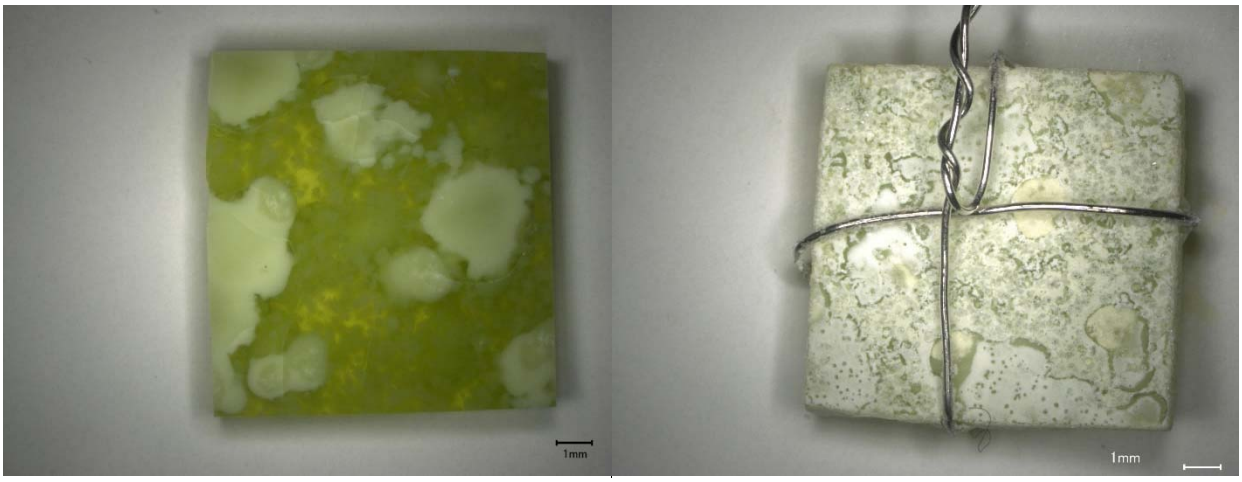


a) Glass square magnified 20X before VHT; b) Glass square magnified after VHT

c) Glass cross section magnified after VHT

Figure I.107. CCC-Treated Glass LP2-OL-10MOD after VHT for 7 Days


a) Glass square magnified 20X before VHT; b) Glass square magnified after VHT

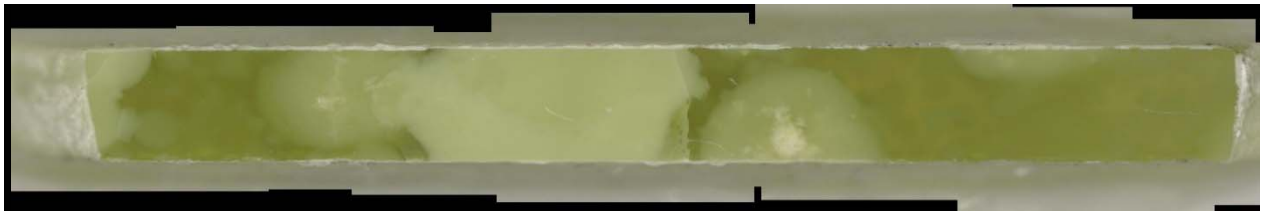

c) Glass cross section magnified after VHT

Figure I.108. CCC-Treated Glass LP2-OL-10MOD after VHT for 24 Days

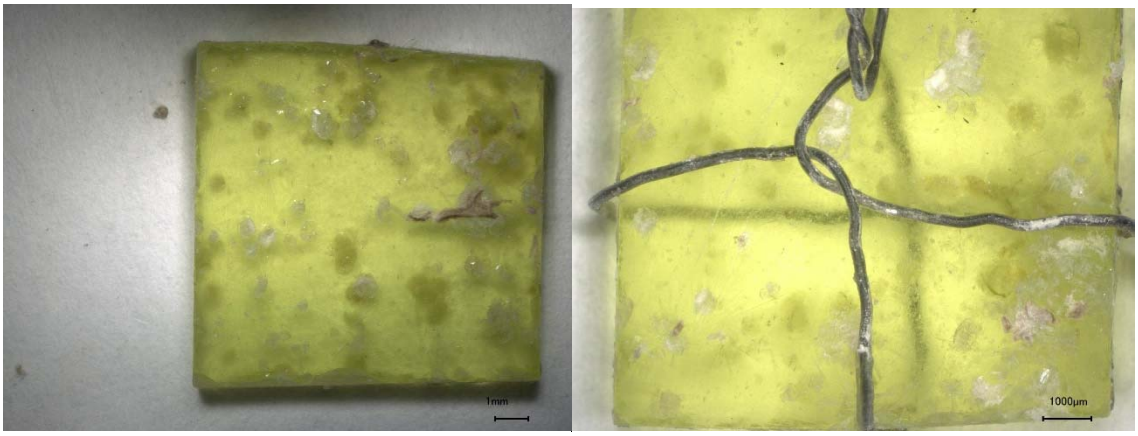


a) Glass square magnified 20X after VHT; b) Glass square magnified 30X after VHT

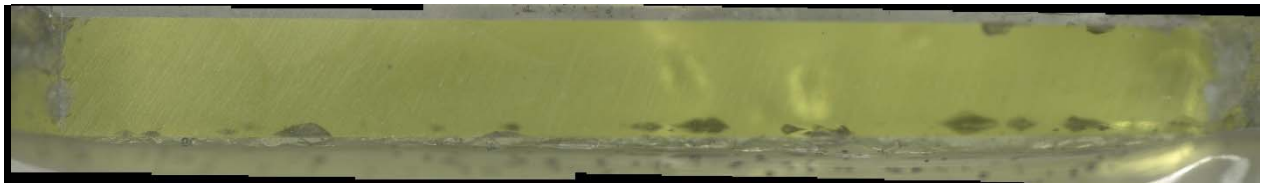

c) Glass cross section magnified after VHT

Figure I.109. CCC-Treated Glass LP2-OL-11 after VHT for 24 Days

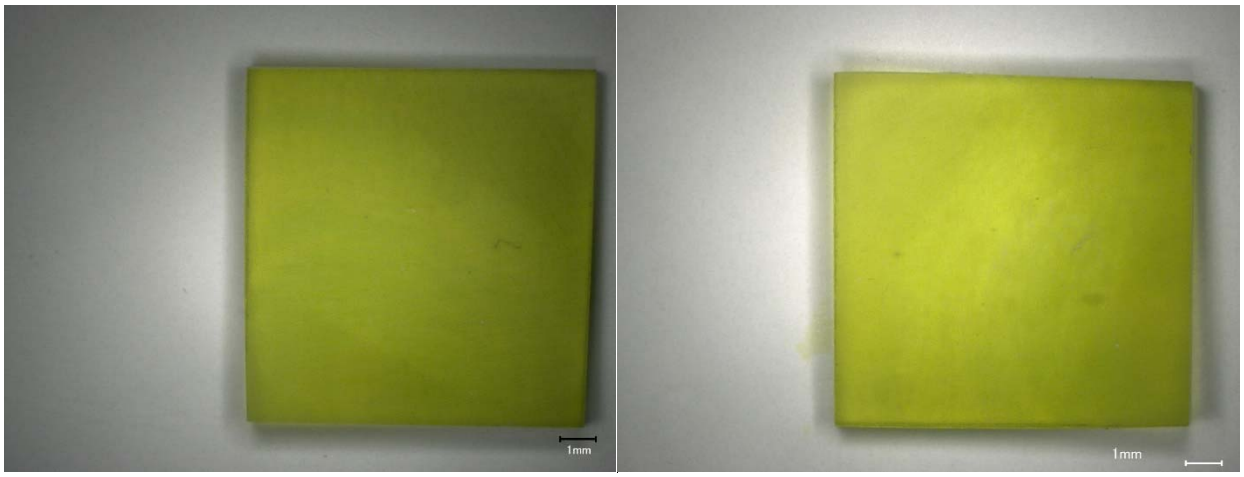


a) Glass square magnified after VHT; b) Glass square magnified after VHT

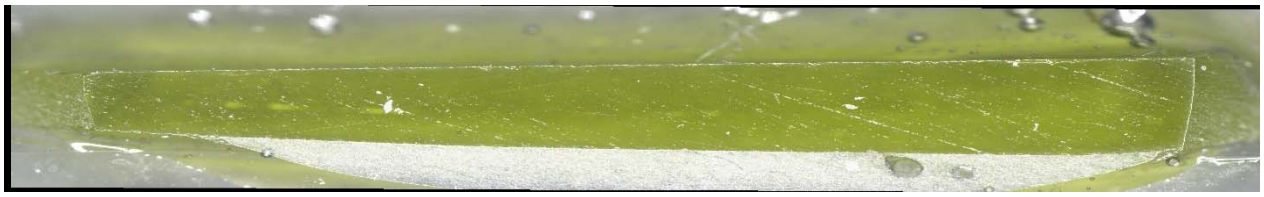

c) Glass cross section magnified after VHT

Figure I.110. CCC-Treated Glass LP2-OL-12 after VHT for 7 Days

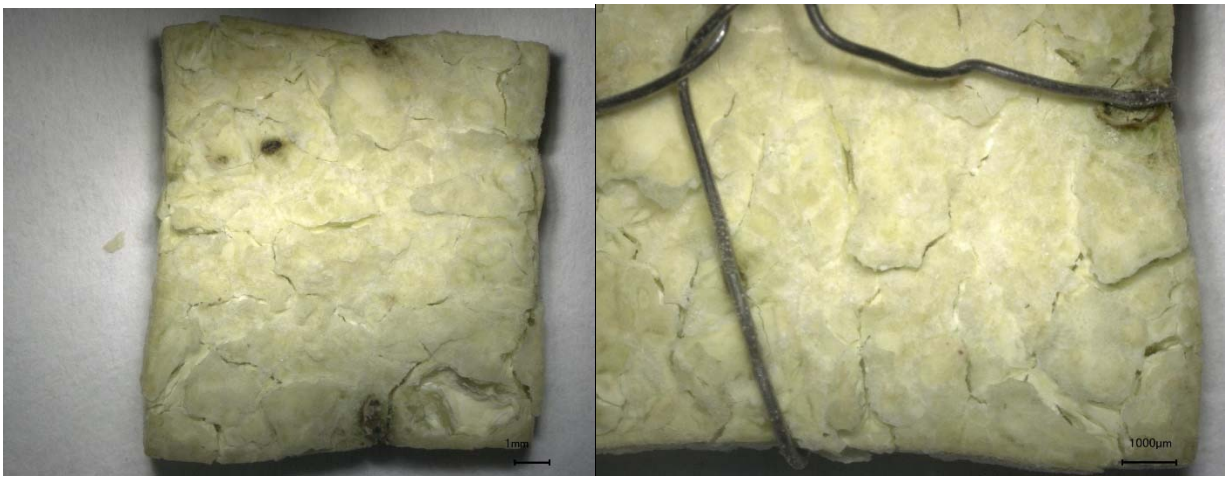


a) Glass square magnified 20X after VHT; b) Glass square magnified 30X after VHT

c) Glass cross section magnified after VHT

Figure I.111. CCC-Treated Glass LP2-OL-12 after VHT for 24 Days

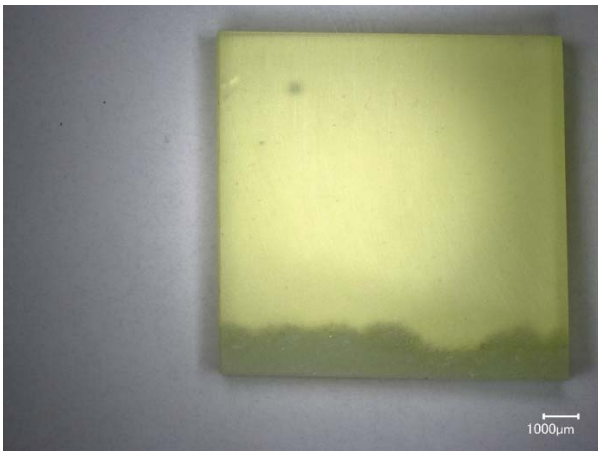


a) Glass square magnified after VHT

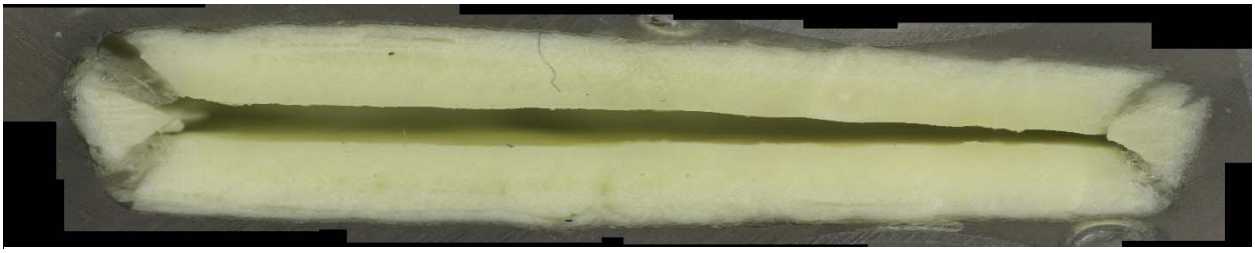

b) Glass cross section magnified after VHT

Figure I.112. CCC-Treated Glass LP2-OL-13 after VHT for 7 Days


a) Glass square magnified 20X after VHT; b) Glass square magnified 30X after VHT

c) Glass cross section magnified after VHT

Figure I.113. CCC-Treated Glass LP2-OL-13 after VHT for 24 Days

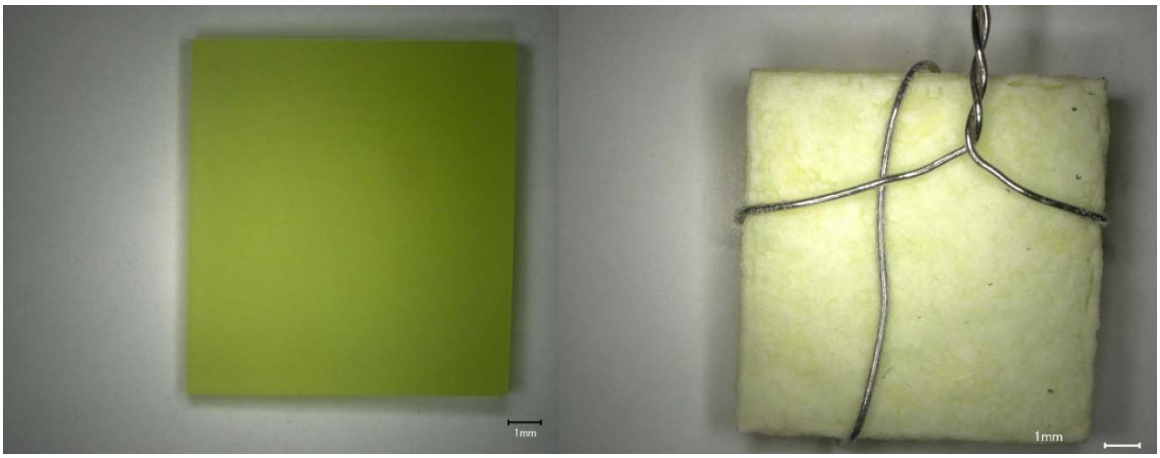


a) Glass square magnified after VHT; b) Glass square magnified after VHT

c) Glass cross section magnified after VHT

Figure I.114. CCC-Treated Glass LP2-OL-14 after VHT for 7 Days

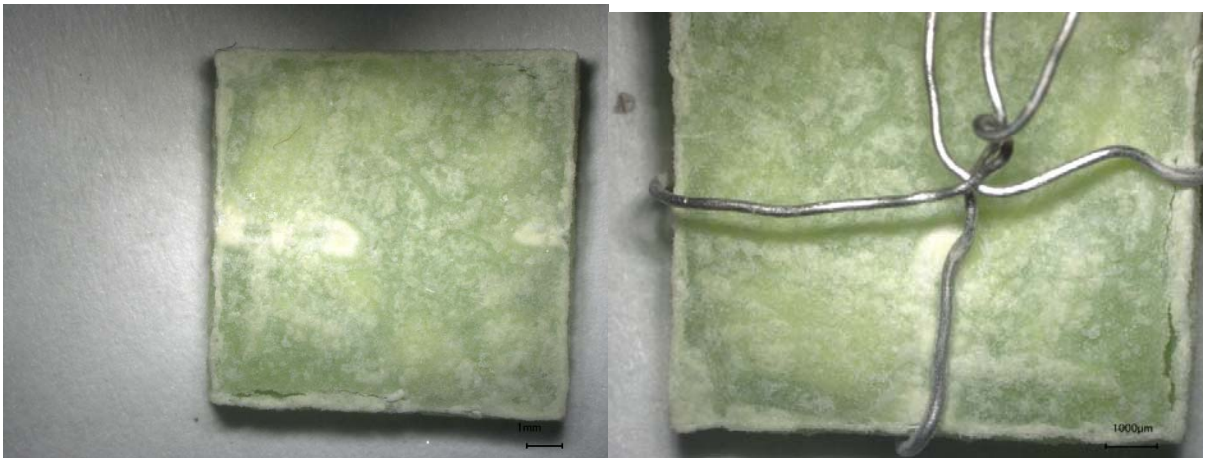


a) Glass square magnified 20X after VHT; b) Glass square magnified 30X after VHT

c) Glass cross section magnified after VHT

Figure I.115. CCC-Treated Glass LP2-OL-14 after VHT for 24 Days

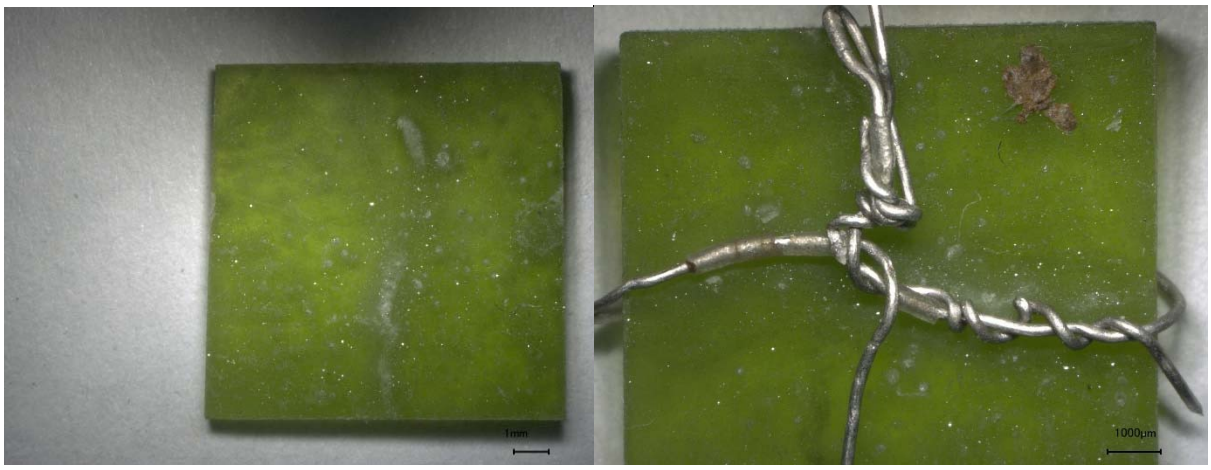


a) Glass square magnified 20X after VHT; b) Glass square magnified 30X after VHT

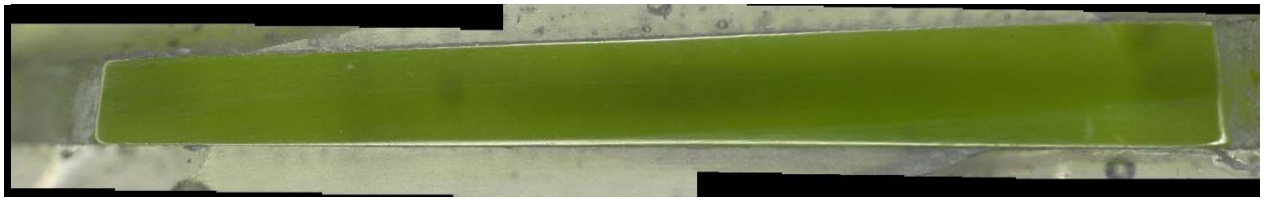

c) Glass cross section magnified after VHT

Figure I.116. CCC-Treated Glass LP2-OL-15 after VHT for 24 Days

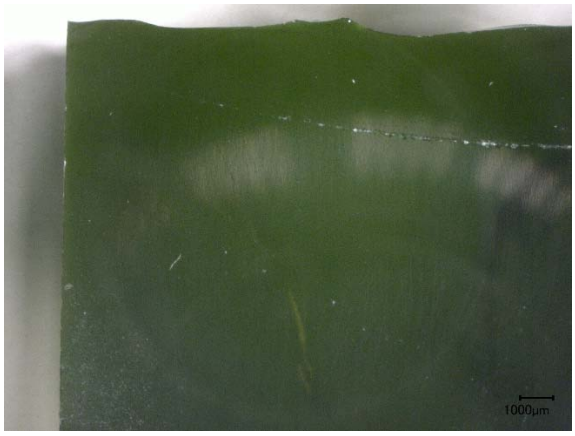


a) Glass square magnified before VHT

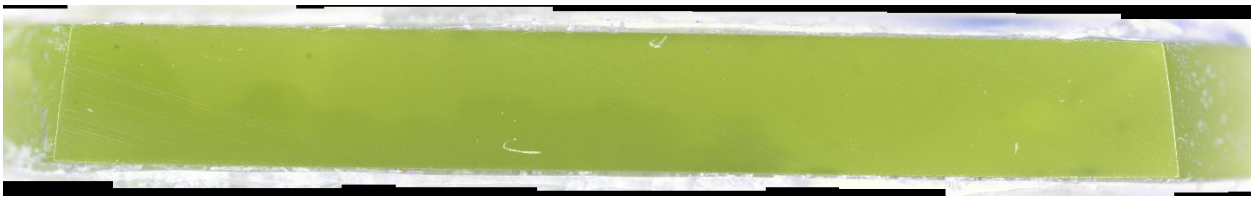

b) Glass cross section magnified after VHT

Figure I.117. CCC-Treated Glass LP2-OL-16MOD after VHT for 24 Days

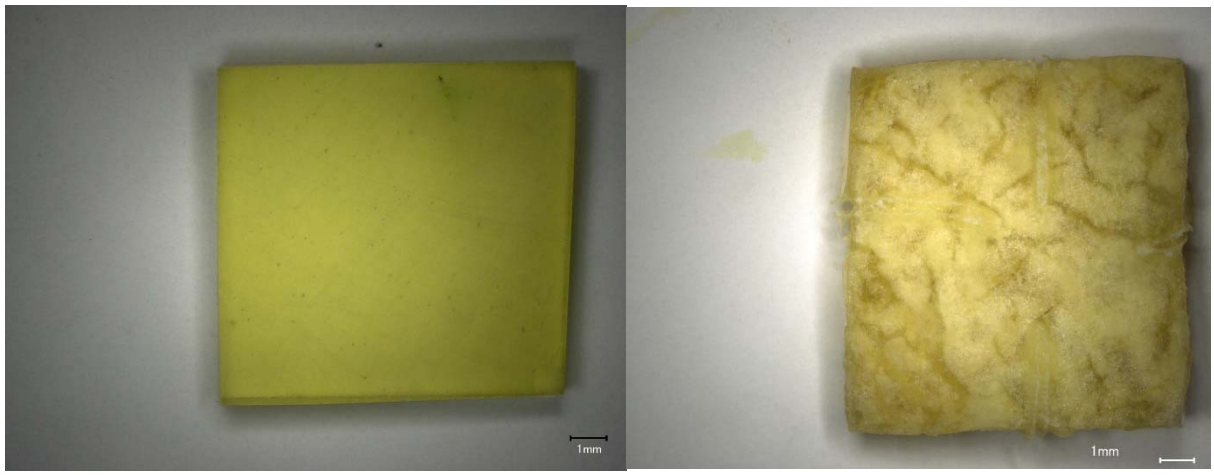

a) Glass square magnified after VHT; b) Glass square magnified after VHT

c) Glass cross section magnified after VHT

Figure I.118. CCC-Treated Glass LP2-OL-17 after VHT for 7 Days

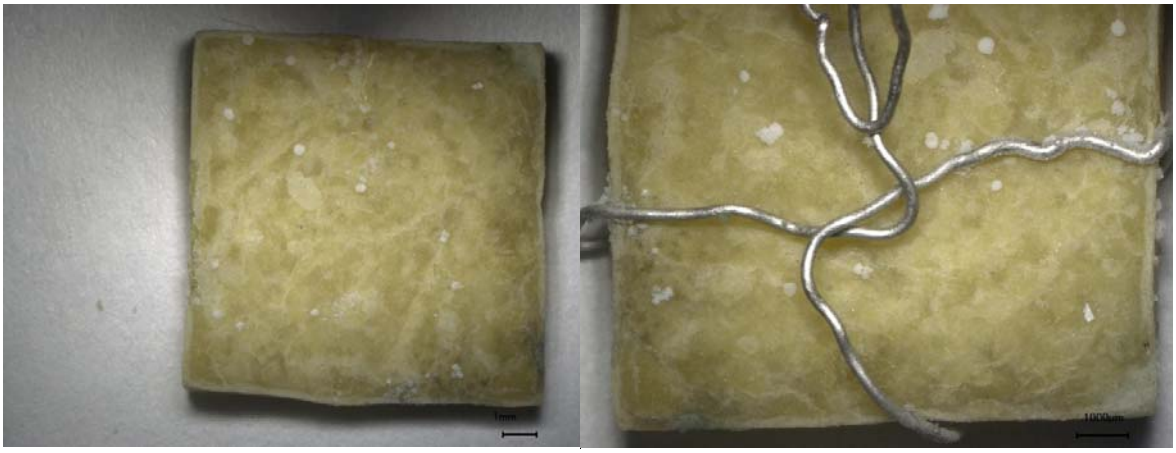

a) Glass square magnified 20X after VHT; b) Glass square magnified 30X after VHT

c) Glass cross section magnified after VHT

Figure I.119. CCC-Treated Glass LP2-OL-17 after VHT for 24 Days

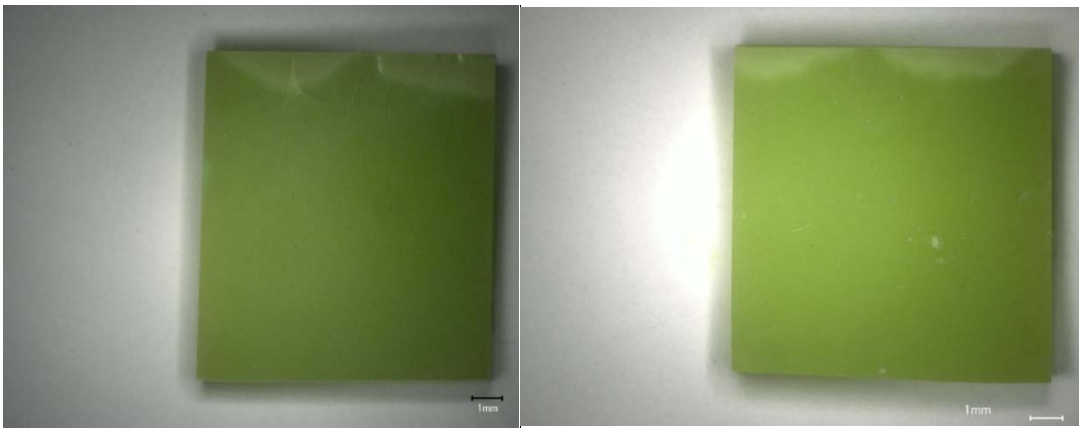

a) Glass square magnified after VHT; b) Glass square magnified after VHT

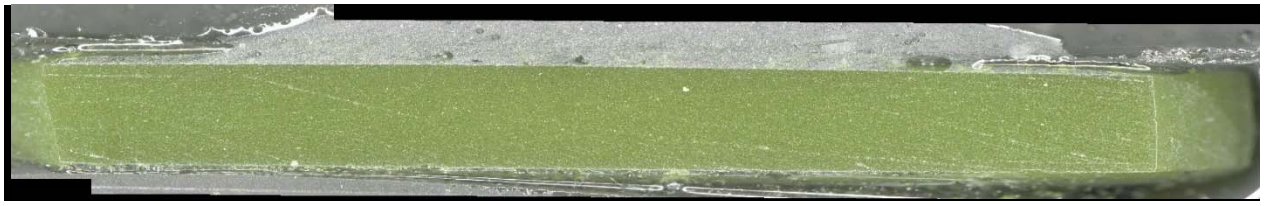

c) Glass cross section magnified after VHT

Figure I.120. CCC-Treated Glass LP2-OL-18 after VHT for 7 Days

a) Glass square magnified after VHT

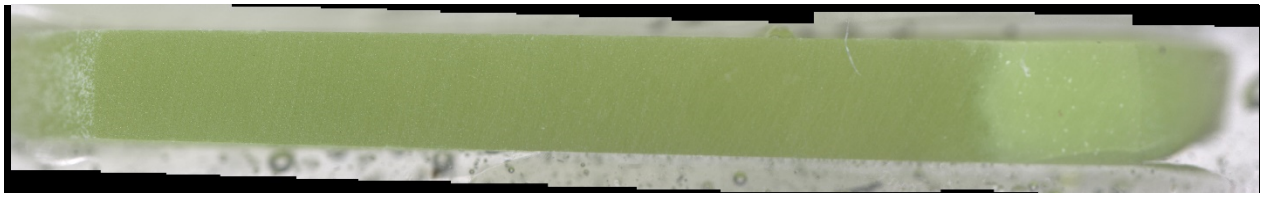

b) Glass cross section magnified after VHT

Figure I.121. CCC-Treated Glass LP2-OL-18 after VHT for 24 Days

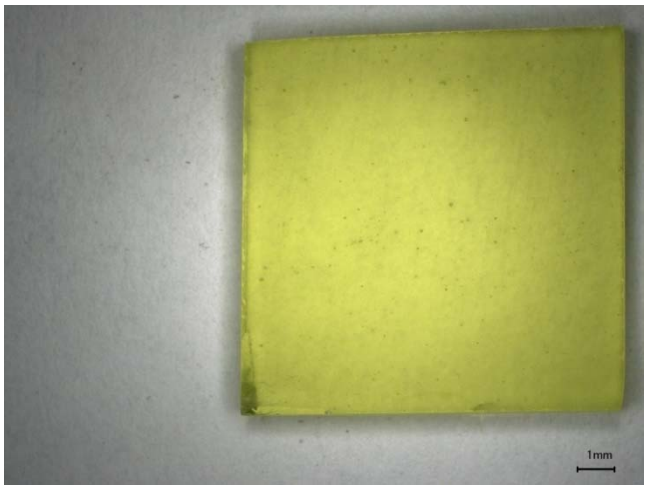


a) Glass square magnified 20X before VHT

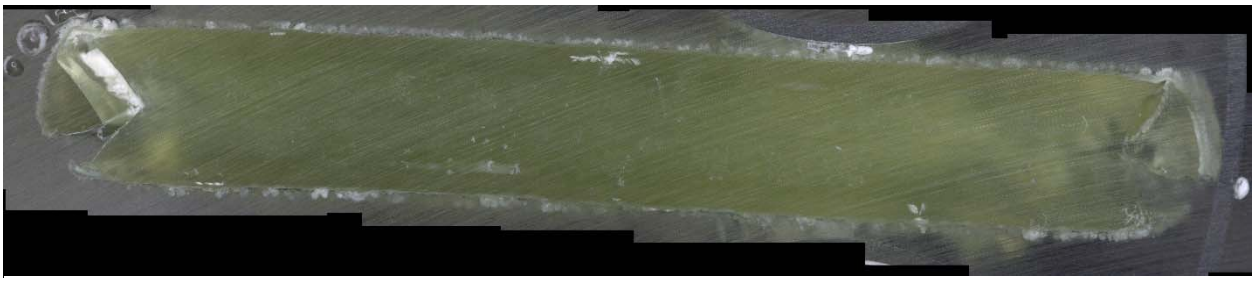

b) Glass cross section magnified after VHT

Figure I.122. CCC-Treated Glass LP2-OL-19 after VHT for 24 Days

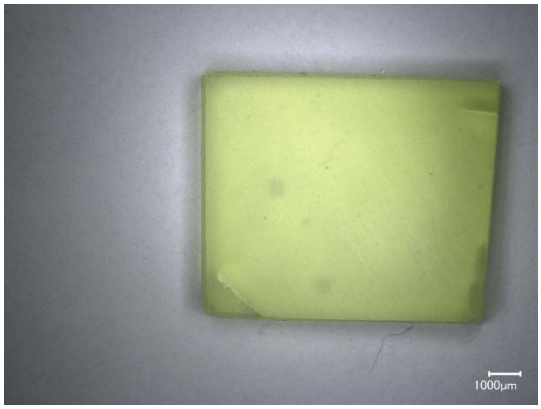


a) Glass square magnified before VHT

b) Glass cross section magnified after VHT

Figure I.123. CCC-Treated Glass LP2-OL-20 after VHT for 7 Days

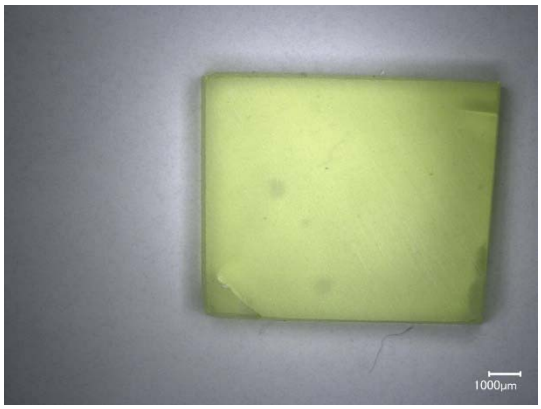


a) Glass square magnified before VHT

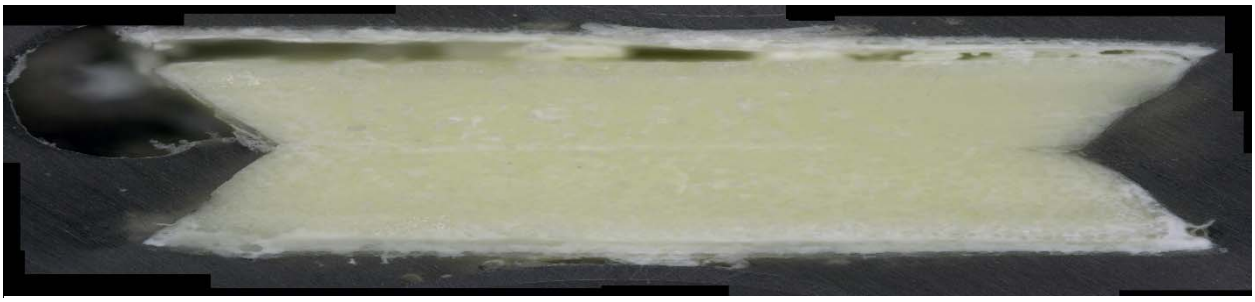

b) Glass cross section magnified after VHT

Figure I.124. CCC-Treated Glass LP2-OL-20 after VHT for 24 Days

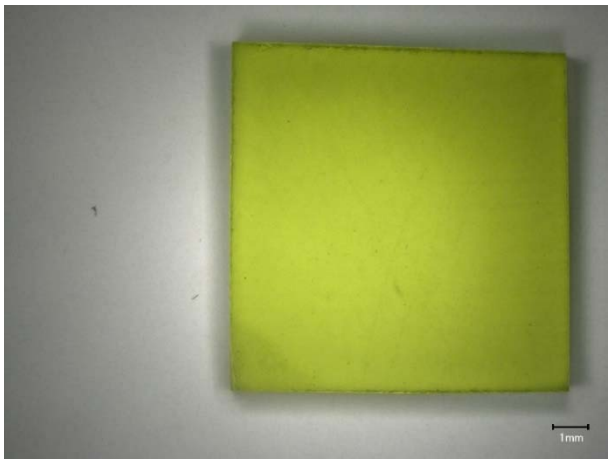


a) Glass square magnified 20X before VHT

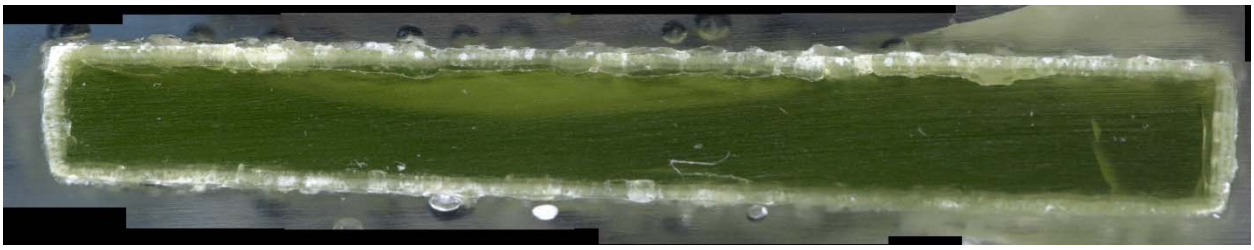

b) Glass cross section magnified after VHT

Figure I.125. CCC-Treated Glass LP2-OL-21 after VHT for 24 Days

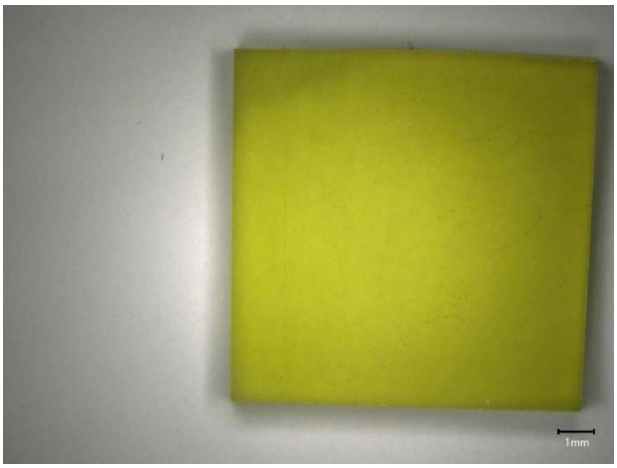


a) Glass square magnified 20X before VHT

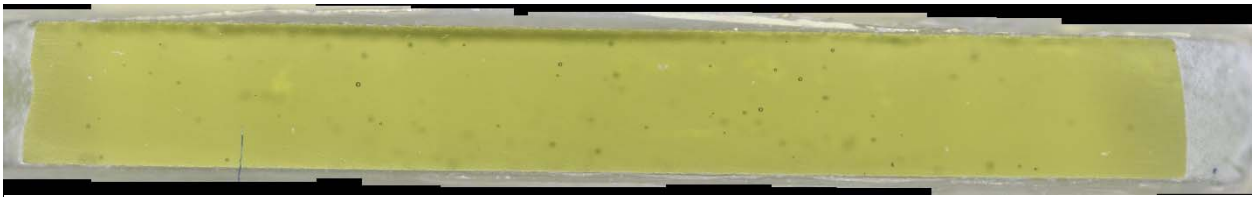

b) Glass cross section magnified after VHT

Figure I.126. CCC-Treated Glass LP2-OL-22 after VHT for 24 Days

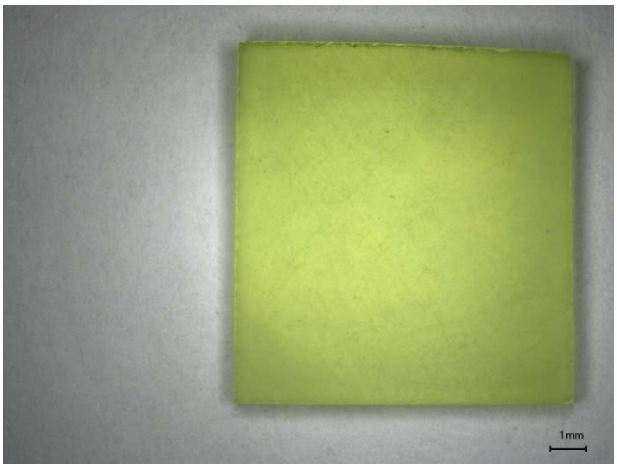


a) Glass square magnified 20X before VHT

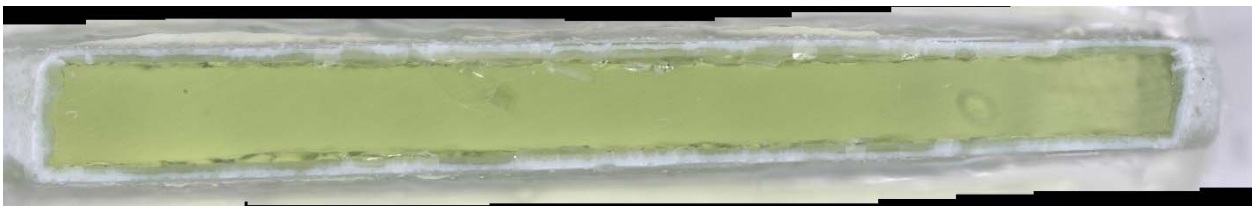

b) Glass cross section magnified after VHT

Figure I.127. CCC-Treated Glass LP2-OL-23 after VHT for 24 Days

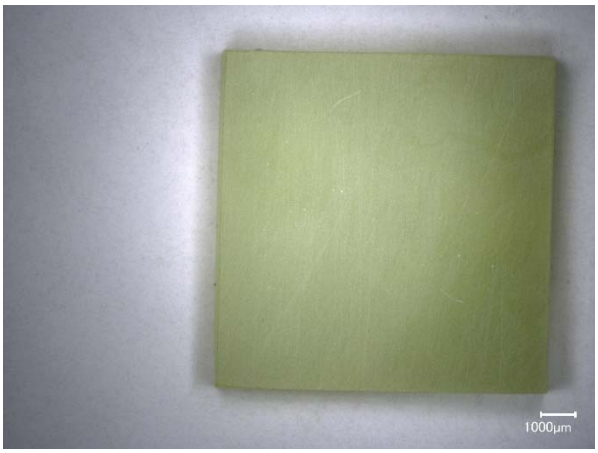


a) Glass square magnified 20X before VHT

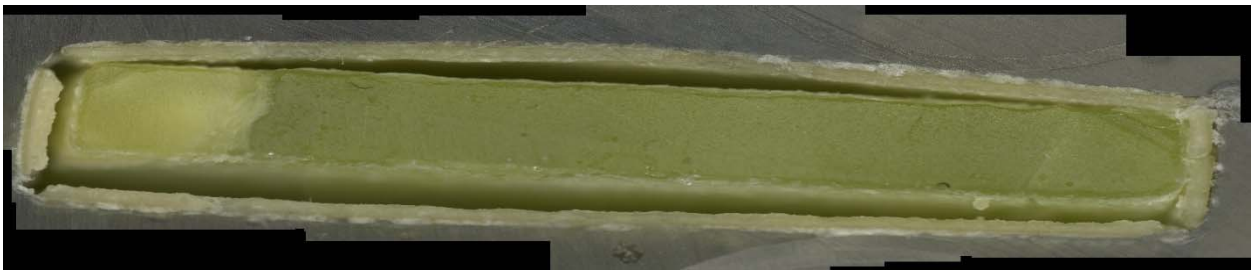

b) Glass cross section magnified after VHT

Figure I.128. CCC-Treated Glass LP2-OL-24 after VHT for 7 Days

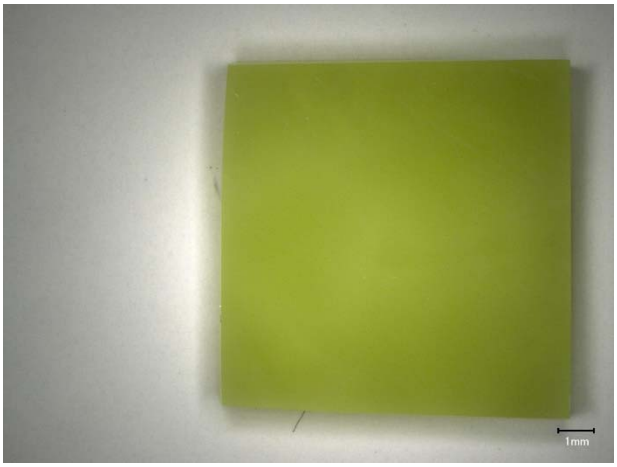


a) Glass square magnified 20X before VHT

b) Glass cross section magnified after VHT

Figure I.129. CCC-Treated Glass LP2-OL-24 after VHT for 24 Days

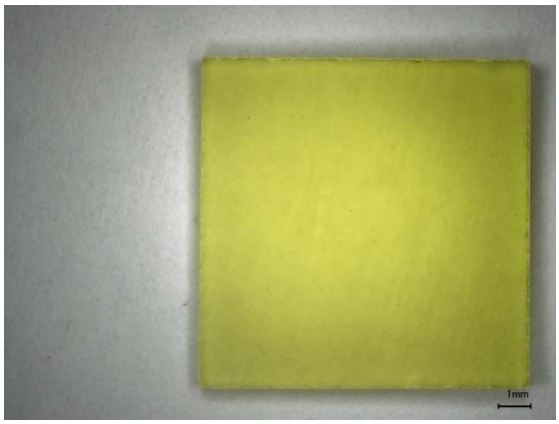


a) Glass square magnified 20X before VHT

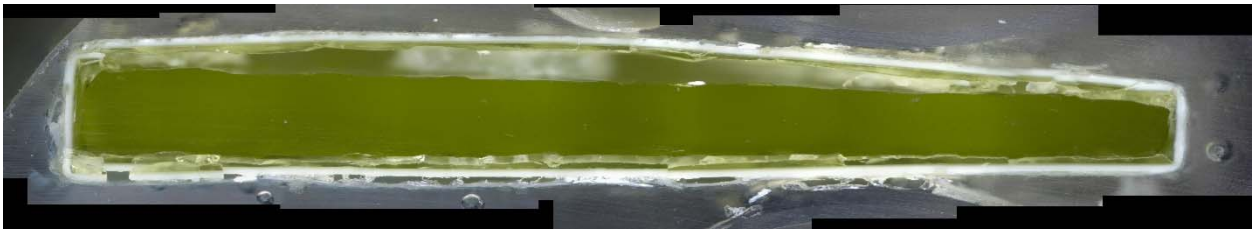

b) Glass cross section magnified after VHT

Figure I.130. CCC-Heat-Treated Glass LP2-OL-25 after VHT for 24 Days

# Appendix J – Composition Analyses for Baseline and Sulfur-Saturated Glasses and Sulfur-Wash Solutions

This appendix presents and compares the normalized compositional analyses of the baseline and sulfur-saturated Phase 2 enhanced LAW glasses and sulfur-wash solutions using ICP-AES and IC. The comparisons in the tables are shown as percentage differences (%Diff). The %Diff results show how much $SO_3$ was retained in the glass. Statistical methods to assess statistically significant differences could have been performed but were beyond the scope of this report (which focuses on data summaries, not data analyses).

Table J.1. Normalized Measured Compositions (mass fractions) for Baseline and Sulfur-Saturated Versions of the LAW Phase 2 Glasses

| | Glass ID | | | | | | | | | | | |
|---|---|---|---|---|---|---|---|---|---|---|---|---|
| | LP2-IL-01 | | | LP2-IL-02 | | | LP2-IL-03 | | | LP2-IL-04 | | |
| Components | Measured Baseline | Sulfur-saturated | % Diff | Measured Baseline | Sulfur-saturated | % Diff | Measured Baseline | Sulfur-saturated | % Diff | Measured Baseline | Sulfur-saturated | % Diff |
| $Al_2O_3$ | 0.07001 | 0.07404 | 5.75 | 0.07342 | 0.07801 | 6.26 | 0.08262 | 0.08096 | -2.00 | 0.07263 | 0.07345 | 1.13 |
| $B_2O_3$ | 0.07736 | 0.07793 | 0.74 | 0.08213 | 0.08147 | -0.79 | 0.08749 | 0.08428 | -3.66 | 0.08283 | 0.07990 | -3.54 |
| CaO | 0.07986 | 0.07412 | -7.18 | 0.02326 | 0.02101 | -9.67 | 0.02392 | 0.02172 | -9.17 | 0.07667 | 0.07125 | -7.07 |
| Cl | 0.00126 | 0.00054 | -57.12 | 0.00116 | 0.00059 | -49.37 | 0.00268 | 0.00124 | -53.67 | 0.00228 | 0.00090 | -60.27 |
| $Cr_2O_3$ | 0.00527 | 0.00311 | -41.01 | 0.00375 | 0.00293 | -22.01 | 0.00532 | 0.00396 | -25.65 | 0.00524 | 0.00291 | -44.42 |
| F | 0.00228 | 0.00196 | -14.11 | 0.00221 | 0.00186 | -15.65 | 0.00473 | 0.00395 | -16.54 | 0.00465 | 0.00396 | -14.88 |
| $Fe_2O_3$ | 0.00220 | 0.01289 | 486 | 0.00609 | 0.00489 | -19.59 | 0.00226 | 0.00494 | 118 | 0.01076 | 0.01029 | -4.41 |
| $K_2O$ | 0.02012 | 0.01492 | -25.87 | 0.02003 | 0.01492 | -25.50 | 0.00832 | 0.00668 | -19.70 | 0.01958 | 0.01496 | -23.63 |
| MgO | 0.00319 | 0.00285 | -10.73 | 0.00988 | 0.00935 | -5.35 | 0.00320 | 0.00296 | -7.45 | 0.00992 | 0.00927 | -6.53 |
| $Na_2O$ | 0.22549 | 0.22672 | 0.55 | 0.22616 | 0.23456 | 3.71 | 0.22624 | 0.23429 | 3.56 | 0.22565 | 0.23256 | 3.06 |
| $P_2O_5$ | 0.00670 | 0.00458 | -31.62 | 0.00522 | 0.00440 | -15.73 | 0.00847 | 0.00881 | 3.98 | 0.00841 | 0.00947 | 12.61 |
| $SiO_2$ | 0.39635 | 0.39641 | 0.01 | 0.42962 | 0.43239 | 0.64 | 0.43294 | 0.42542 | -1.74 | 0.40010 | 0.39631 | -0.95 |
| $SO_3$ | 0.00817 | 0.01558 | 90.68 | 0.00799 | 0.01195 | 49.57 | 0.00216 | 0.01232 | 470 | 0.00231 | 0.01542 | 569 |
| $SnO_2$ | 0.00511 | 0.00549 | 7.53 | 0.02540 | 0.02460 | -3.16 | 0.02631 | 0.02495 | -5.18 | 0.02652 | 0.02478 | -6.58 |
| $V_2O_5$ | 0.02036 | 0.01739 | -14.55 | 0.00495 | 0.00446 | -10.04 | 0.00492 | 0.00452 | -8.17 | 0.00491 | 0.00450 | -8.41 |
| ZnO | 0.02460 | 0.02329 | -5.33 | 0.02651 | 0.02478 | -6.53 | 0.03239 | 0.03115 | -3.83 | 0.02426 | 0.02348 | -3.21 |
| $ZrO_2$ | 0.05166 | 0.04817 | -6.76 | 0.05221 | 0.04783 | -8.40 | 0.04603 | 0.04784 | 3.93 | 0.02329 | 0.02661 | 14.24 |

(a) Measured concentrations below detection limits were treated as 0.

Table J.1. Normalized Measured Compositions (mass fractions) for Baseline and Sulfur-Saturated Versions of the LAW Phase 2 Glasses (cont.)

| | Glass ID | | | | | | | | | | | |
|---|---|---|---|---|---|---|---|---|---|---|---|---|
| | LP2-IL-05 | | | LP2-IL-06 | | | LP2-IL-07 | | | LP2-IL-08 | | |
| Components | Measured Baseline | Sulfur-saturated | % Diff | Measured Baseline | Sulfur-saturated | % Diff | Measured Baseline | Sulfur-saturated | % Diff | Measured Baseline | Sulfur-saturated | % Diff |
| $Al_2O_3$ | 0.07135 | 0.07312 | 2.48 | 0.10244 | 0.10824 | 5.66 | 0.07047 | 0.07224 | 2.51 | 0.07303 | 0.07256 | -0.65 |
| $B_2O_3$ | 0.11564 | 0.11672 | 0.93 | 0.11929 | 0.12035 | 0.89 | 0.12042 | 0.11834 | -1.73 | 0.08590 | 0.07933 | -7.66 |
| CaO | 0.07316 | 0.06700 | -8.42 | 0.02261 | 0.02241 | -0.92 | 0.05416 | 0.05179 | -4.38 | 0.08193 | 0.08139 | -0.66 |
| Cl | 0.00247 | 0.00119 | -51.64 | 0.00215 | 0.00095 | -55.95 | 0.00272 | 0.00131 | -51.97 | 0.00208 | 0.00093 | -55.49 |
| $Cr_2O_3$ | 0.00374 | 0.00313 | -16.08 | 0.00516 | 0.00375 | -27.30 | 0.00371 | 0.00324 | -12.74 | 0.00513 | 0.00367 | -28.43 |
| F | 0.00446 | 0.00361 | -19.04 | 0.00418 | 0.00359 | -14.14 | 0.00470 | 0.00383 | -18.50 | 0.00448 | 0.00395 | -11.81 |
| $Fe_2O_3$ | 0.00228 | 0.00299 | 31.35 | 0.00215 | 0.00319 | 48.60 | 0.00124 | 0.00217 | 74.89 | 0.00998 | 0.01022 | 2.39 |
| $K_2O$ | 0.00534 | 0.00461 | -13.68 | 0.01974 | 0.01597 | -19.08 | 0.02002 | 0.01641 | -18.02 | 0.00543 | 0.00445 | -17.93 |
| MgO | 0.00309 | 0.00311 | 0.86 | 0.00973 | 0.00975 | 0.18 | 0.00971 | 0.00981 | 0.97 | 0.00983 | 0.01020 | 3.75 |
| $Na_2O$ | 0.20913 | 0.21747 | 3.99 | 0.21949 | 0.20777 | -5.34 | 0.22232 | 0.22183 | -0.22 | 0.21148 | 0.21074 | -0.35 |
| $P_2O_5$ | 0.00758 | 0.00987 | 30.22 | 0.00859 | 0.00941 | 9.51 | 0.00752 | 0.00994 | 32.21 | 0.00875 | 0.01079 | 23.31 |
| $SiO_2$ | 0.39199 | 0.38281 | -2.34 | 0.38627 | 0.39313 | 1.78 | 0.40786 | 0.40423 | -0.89 | 0.40317 | 0.40539 | 0.55 |
| $SO_3$ | 0.00215 | 0.01520 | 608 | 0.00771 | 0.01076 | 39.66 | 0.00789 | 0.01694 | 115 | 0.00771 | 0.01445 | 87.47 |
| $SnO_2$ | 0.02638 | 0.02437 | -7.61 | 0.00819 | 0.00849 | 3.74 | 0.00382 | 0.00447 | 17.05 | 0.00405 | 0.00464 | 14.57 |
| $V_2O_5$ | 0.00490 | 0.00449 | -8.31 | 0.01008 | 0.00946 | -6.14 | 0.00490 | 0.00478 | -2.58 | 0.00488 | 0.00490 | 0.30 |
| ZnO | 0.02432 | 0.02297 | -5.52 | 0.02318 | 0.02359 | 1.75 | 0.03151 | 0.03193 | 1.31 | 0.03142 | 0.03191 | 1.57 |
| $ZrO_2$ | 0.05203 | 0.04731 | -9.09 | 0.04905 | 0.04919 | 0.28 | 0.02701 | 0.02675 | -0.96 | 0.05075 | 0.05048 | -0.53 |

(a) Measured concentrations below detection limits were treated as 0.

Table J.1. Normalized Measured Compositions (mass fractions) for Baseline and Sulfur-Saturated Versions of the LAW Phase 2 Glasses (cont.)

| | Glass ID | | | | | | | | | | | |
|---|---|---|---|---|---|---|---|---|---|---|---|---|
| | LP2-IL-09 | | | LP2-IL-10 | | | LP2-IL-11 | | | LP2-IL-12 | | |
| Components | Baseline | Sulfur-saturated | % Diff | Baseline | Sulfur-saturated | % Diff | Baseline | Sulfur-saturated | % Diff | Baseline | Sulfur-saturated | % Diff |
| $Al_2O_3$ | 0.07171 | 0.07125 | -0.64 | 0.09284 | 0.09480 | 2.12 | 0.08736 | 0.08614 | -1.40 | 0.07026 | 0.07232 | 2.93 |
| $B_2O_3$ | 0.12318 | 0.11481 | -6.80 | 0.10302 | 0.09238 | -10.33 | 0.08531 | 0.07834 | -8.17 | 0.08091 | 0.07834 | -3.19 |
| CaO | 0.02312 | 0.02272 | -1.70 | 0.05345 | 0.05139 | -3.84 | 0.03365 | 0.03317 | -1.44 | 0.03473 | 0.03331 | -4.10 |
| Cl | 0.00122 | 0.00057 | -52.99 | 0.00140 | 0.00060 | -57.60 | 0.00208 | 0.00103 | -50.45 | 0.00262 | 0.00116 | -55.58 |
| $Cr_2O_3$ | 0.00518 | 0.00319 | -38.37 | 0.00445 | 0.00275 | -38.25 | 0.00370 | 0.00266 | -28.08 | 0.00374 | 0.00325 | -12.95 |
| F | 0.00226 | 0.00183 | -19.04 | 0.00276 | 0.00227 | -17.80 | 0.00442 | 0.00375 | -15.02 | 0.00464 | 0.00371 | -19.90 |
| $Fe_2O_3$ | 0.00951 | 0.00951 | 0.06 | 0.00566 | 0.00571 | 0.98 | 0.00978 | 0.00981 | 0.34 | 0.00122 | 0.00217 | 78.19 |
| $K_2O$ | 0.00552 | 0.00472 | -14.55 | 0.01107 | 0.00872 | -21.22 | 0.01946 | 0.01644 | -15.54 | 0.00539 | 0.00486 | -9.98 |
| MgO | 0.00988 | 0.00992 | 0.37 | 0.00642 | 0.00665 | 3.53 | 0.00296 | 0.00311 | 4.85 | 0.00987 | 0.01004 | 1.70 |
| $Na_2O$ | 0.23805 | 0.23367 | -1.84 | 0.22411 | 0.22978 | 2.53 | 0.21512 | 0.21933 | 1.96 | 0.23030 | 0.23416 | 1.68 |
| $P_2O_5$ | 0.00633 | 0.00440 | -30.58 | 0.00618 | 0.00614 | -0.63 | 0.00776 | 0.00994 | 28.01 | 0.00770 | 0.01001 | 30.02 |
| $SiO_2$ | 0.37725 | 0.39030 | 3.46 | 0.39623 | 0.39539 | -0.21 | 0.39371 | 0.39869 | 1.27 | 0.44635 | 0.43373 | -2.83 |
| $SO_3$ | 0.00215 | 0.01501 | 599 | 0.00481 | 0.01396 | 190 | 0.00201 | 0.01236 | 516 | 0.00210 | 0.01536 | 630 |
| $SnO_2$ | 0.02152 | 0.02075 | -3.56 | 0.01532 | 0.01418 | -7.44 | 0.02570 | 0.02386 | -7.17 | 0.00417 | 0.00476 | 14.24 |
| $V_2O_5$ | 0.02026 | 0.01854 | -8.51 | 0.00962 | 0.00958 | -0.49 | 0.02003 | 0.01850 | -7.65 | 0.02042 | 0.01900 | -6.94 |
| ZnO | 0.03170 | 0.03229 | 1.85 | 0.02807 | 0.02827 | 0.71 | 0.03116 | 0.03203 | 2.80 | 0.02416 | 0.02377 | -1.59 |
| $ZrO_2$ | 0.05117 | 0.04652 | -9.09 | 0.03460 | 0.03744 | 8.21 | 0.05579 | 0.05084 | -8.86 | 0.05143 | 0.05004 | -2.71 |

(a) Measured concentrations below detection limits were treated as 0.

Table J.1. Normalized Measured Compositions (mass fractions) for Baseline and Sulfur-Saturated Versions of the LAW Phase 2 Glasses (cont.)

| | Glass ID | | | | | | | | | | | |
|---|---|---|---|---|---|---|---|---|---|---|---|---|
| | LP2-IL-13 | | | LP2-IL-14 | | | LP2-IL-15 | | | LP2-IL-16 | | |
| Components | Baseline | Sulfur-saturated | % Diff | Baseline | Sulfur-saturated | % Diff | Baseline | Sulfur-saturated | % Diff | Baseline | Sulfur-saturated | % Diff |
| $Al_2O_3$ | 0.07355 | 0.07262 | -1.26 | 0.08276 | 0.08510 | 2.83 | 0.07174 | 0.07204 | 0.42 | 0.09590 | 0.09580 | -0.11 |
| $B_2O_3$ | 0.11142 | 0.10652 | -4.39 | 0.11539 | 0.11371 | -1.45 | 0.10492 | 0.10096 | -3.78 | 0.09270 | 0.08939 | -3.57 |
| CaO | 0.02617 | 0.02564 | -2.03 | 0.04203 | 0.04136 | -1.60 | 0.02211 | 0.02117 | -4.23 | 0.05348 | 0.05259 | -1.66 |
| Cl | 0.00129 | 0.00062 | -51.63 | 0.00248 | 0.00096 | -61.41 | 0.00258 | 0.00112 | -56.57 | 0.00141 | 0.00066 | -52.96 |
| $Cr_2O_3$ | 0.00517 | 0.00443 | -14.33 | 0.00373 | 0.00218 | -41.51 | 0.00527 | 0.00437 | -17.10 | 0.00445 | 0.00314 | -29.43 |
| F | 0.00205 | 0.00176 | -14.24 | 0.00431 | 0.00347 | -19.39 | 0.00423 | 0.00339 | -19.72 | 0.00267 | 0.00231 | -13.56 |
| $Fe_2O_3$ | 0.00969 | 0.01072 | 10.53 | 0.00933 | 0.01027 | 10.02 | 0.00956 | 0.01070 | 11.91 | 0.00566 | 0.00670 | 18.26 |
| $K_2O$ | 0.01958 | 0.01698 | -13.29 | 0.00552 | 0.00450 | -18.50 | 0.00551 | 0.00461 | -16.36 | 0.01103 | 0.00855 | -22.45 |
| MgO | 0.00296 | 0.00288 | -2.75 | 0.00303 | 0.00293 | -3.27 | 0.00304 | 0.00298 | -2.06 | 0.00650 | 0.00637 | -2.08 |
| $Na_2O$ | 0.21781 | 0.22109 | 1.51 | 0.23981 | 0.23442 | -2.25 | 0.21466 | 0.21425 | -0.19 | 0.22807 | 0.21737 | -4.69 |
| $P_2O_5$ | 0.00610 | 0.00478 | -21.61 | 0.00793 | 0.00862 | 8.62 | 0.00938 | 0.00923 | -1.56 | 0.00626 | 0.00597 | -4.63 |
| $SiO_2$ | 0.44078 | 0.43353 | -1.65 | 0.39041 | 0.39545 | 1.29 | 0.44227 | 0.44901 | 1.52 | 0.39722 | 0.40721 | 2.51 |
| $SO_3$ | 0.00202 | 0.01265 | 526 | 0.00783 | 0.01524 | 94.57 | 0.00753 | 0.01276 | 69.45 | 0.00493 | 0.01366 | 177 |
| $SnO_2$ | 0.00437 | 0.00554 | 26.71 | 0.00481 | 0.00505 | 5.05 | 0.02447 | 0.02448 | 0.04 | 0.01462 | 0.01513 | 3.45 |
| $V_2O_5$ | 0.00488 | 0.00467 | -4.32 | 0.00497 | 0.00453 | -8.85 | 0.02054 | 0.01841 | -10.37 | 0.00973 | 0.00926 | -4.86 |
| ZnO | 0.02403 | 0.02408 | 0.20 | 0.02415 | 0.02453 | 1.61 | 0.02428 | 0.02366 | -2.56 | 0.02800 | 0.02833 | 1.17 |
| $ZrO_2$ | 0.04812 | 0.05150 | 7.03 | 0.05151 | 0.04767 | -7.44 | 0.02793 | 0.02687 | -3.79 | 0.03735 | 0.03757 | 0.59 |

(a) Measured concentrations below detection limits were treated as 0.

Table J.1. Normalized Measured Compositions (mass fractions) for Baseline and Sulfur-Saturated Versions of the LAW Phase 2 Glasses (cont.)

| | Glass ID | | | | | | | | | | | |
|---|---|---|---|---|---|---|---|---|---|---|---|---|
| | LP2-IL-17 | | | LP2-OL-01-3 | | | LP2-OL-02-1 | | | LP2-OL-03 MOD2 | | |
| Components | Baseline | Sulfur-saturated | % Diff | Baseline | Sulfur-saturated | % Diff | Baseline | Sulfur-saturated | % Diff | Baseline | Sulfur-saturated | % Diff |
| $Al_2O_3$ | 0.08765 | 0.08998 | 2.66 | 0.05842 | 0.05588 | -4.35 | 0.09054 | 0.09253 | 2.20 | 0.10010 | 0.09978 | -0.32 |
| $B_2O_3$ | 0.10513 | 0.10534 | 0.21 | 0.06190 | 0.05609 | -9.40 | 0.09156 | 0.09020 | -1.49 | 0.05829 | 0.05673 | -2.68 |
| CaO | 0.02781 | 0.02749 | -1.13 | 0.08716 | 0.08425 | -3.34 | 0.05031 | 0.05158 | 2.52 | 0.11064 | 0.10937 | -1.15 |
| Cl | 0.00063 | 0.0000[a] | -- | 0.0000[a] | 0.0000[a] | -- | 0.00145 | 0.0000[a] | -- | 0.00069 | 0.0000[a] | -- |
| $Cr_2O_3$ | 0.00088 | 0.0000[a] | -- | 0.00735 | 0.00310 | -57.79 | 0.00555 | 0.00240 | -56.80 | 0.00702 | 0.00227 | -67.64 |
| F | 0.00088 | 0.00078 | -11.37 | 0.00074 | 0.00060 | -18.34 | 0.00258 | 0.00189 | -26.72 | 0.00104 | 0.0000[a] | -- |
| $Fe_2O_3$ | 0.00167 | 0.00301 | 80.77 | 0.00429 | 0.0000[a] | -- | 0.01003 | 0.00627 | -37.51 | 0.00482 | 0.0000[a] | -- |
| $K_2O$ | 0.00564 | 0.00458 | -18.73 | 0.0000[a] | 0.0000[a] | -- | 0.00970 | 0.00690 | -28.87 | 0.0000[a] | 0.0000[a] | -- |
| MgO | 0.00980 | 0.00975 | -0.53 | 0.01315 | 0.01303 | -0.91 | 0.00649 | 0.00640 | -1.38 | 0.01380 | 0.01428 | 3.49 |
| $Na_2O$ | 0.22943 | 0.22585 | -1.56 | 0.20078 | 0.20383 | 1.52 | 0.22577 | 0.22629 | 0.23 | 0.26820 | 0.27679 | 3.20 |
| $P_2O_5$ | 0.00178 | 0.0000[a] | -- | 0.0000[a] | 0.0000[a] | -- | 0.00573 | 0.00521 | -9.06 | 0.00184 | 0.00167 | -9.57 |
| $SiO_2$ | 0.42028 | 0.42201 | 0.41 | 0.49166 | 0.49686 | 1.06 | 0.40808 | 0.41159 | 0.86 | 0.34949 | 0.35015 | 0.19 |
| $SO_3$ | 0.00964 | 0.01354 | 40.48 | 0.00158 | 0.01472 | 832 | 0.00475 | 0.01110 | 134 | 0.00743 | 0.01478 | 99.04 |
| $SnO_2$ | 0.00128 | 0.0000[a] | -- | 0.0000[a] | 0.0000[a] | -- | 0.01704 | 0.01669 | -2.08 | 0.03037 | 0.02756 | -9.23 |
| $V_2O_5$ | 0.02110 | 0.01972 | -6.56 | 0.0000[a] | 0.0000[a] | -- | 0.00945 | 0.00896 | -5.17 | 0.0000[a] | 0.0000[a] | -- |
| ZnO | 0.02977 | 0.03058 | 2.73 | 0.01972 | 0.01975 | 0.14 | 0.02672 | 0.02748 | 2.84 | 0.02139 | 0.02107 | -1.48 |
| $ZrO_2$ | 0.04666 | 0.04737 | 1.52 | 0.05326 | 0.05190 | -2.56 | 0.03425 | 0.03452 | 0.80 | 0.02490 | 0.02556 | 2.66 |

(a) Measured concentrations below detection limits were treated as 0.

Table J.1. Normalized Measured Compositions (mass fractions) for Baseline and Sulfur-Saturated Versions of the LAW Phase 2 Glasses (cont.)

| | Glass ID | | | | | | | | | | | |
|---|---|---|---|---|---|---|---|---|---|---|---|---|
| | LP2-OL-04-1 | | | LP2-OL-05 | | | LP2-OL-07-1 | | | LP2-OL-08 MOD | | |
| Components | Baseline | Sulfur-saturated | % Diff | Baseline | Sulfur-saturated | % Diff | Baseline | Sulfur-saturated | % Diff | Baseline | Sulfur-saturated | % Diff |
| $Al_2O_3$ | 0.10384 | 0.10117 | -2.58 | 0.12057 | 0.12202 | 1.20 | 0.09726 | 0.09594 | -1.36 | 0.05880 | 0.05839 | -0.69 |
| $B_2O_3$ | 0.06410 | 0.05760 | -10.13 | 0.06112 | 0.06087 | -0.41 | 0.12595 | 0.11522 | -8.52 | 0.06160 | 0.05874 | -4.65 |
| CaO | 0.07453 | 0.07589 | 1.82 | 0.11020 | 0.10712 | -2.79 | 0.08235 | 0.07517 | -8.71 | 0.10746 | 0.10819 | 0.68 |
| Cl | 0.0000[a] | 0.0000[a] | -- | 0.00298 | 0.00192 | -35.73 | 0.00208 | 0.00133 | -36.25 | 0.00061 | 0.0000[a] | -- |
| $Cr_2O_3$ | 0.00643 | 0.0000[a] | -- | 0.00393 | 0.00162 | -58.83 | 0.00596 | 0.00273 | -54.30 | 0.00708 | 0.00358 | -49.43 |
| F | 0.00081 | 0.00071 | -12.23 | 0.00607 | 0.00496 | -18.29 | 0.00125 | 0.00108 | -13.29 | 0.00079 | 0.00067 | -14.13 |
| $Fe_2O_3$ | 0.01898 | 0.01486 | -21.72 | 0.01955 | 0.01503 | -23.12 | 0.01368 | 0.00980 | -28.32 | 0.01929 | 0.01581 | -18.07 |
| $K_2O$ | 0.05390 | 0.04039 | -25.08 | 0.0000[a] | 0.0000[a] | -- | 0.00215 | 0.00139 | -35.60 | 0.0000[a] | 0.0000[a] | -- |
| MgO | 0.01280 | 0.01328 | 3.74 | 0.0000[a] | 0.0000[a] | -- | 0.01004 | 0.01030 | 2.58 | 0.0000[a] | 0.0000[a] | -- |
| $Na_2O$ | 0.20210 | 0.21319 | 5.49 | 0.19398 | 0.19564 | 0.86 | 0.19756 | 0.19775 | 0.09 | 0.25410 | 0.25814 | 1.59 |
| $P_2O_5$ | 0.0000[a] | 0.0000[a] | -- | 0.01491 | 0.00828 | -44.50 | 0.00267 | 0.0000[a] | -- | 0.00232 | 0.00212 | -8.58 |
| $SiO_2$ | 0.36880 | 0.38057 | 3.19 | 0.41476 | 0.42776 | 3.13 | 0.38301 | 0.40925 | 6.85 | 0.36207 | 0.36070 | -0.38 |
| $SO_3$ | 0.00158 | 0.01091 | 592 | 0.00948 | 0.01416 | 49.36 | 0.01033 | 0.01620 | 56.86 | 0.00646 | 0.01885 | 192 |
| $SnO_2$ | 0.0000[a] | 0.0000[a] | -- | 0.0000[a] | 0.0000[a] | -- | 0.0000[a] | 0.0000[a] | -- | 0.00482 | 0.00283 | -41.16 |
| $V_2O_5$ | 0.0000[a] | 0.0000[a] | -- | 0.0000[a] | 0.0000[a] | -- | 0.00949 | 0.00961 | 1.34 | 0.04025 | 0.03784 | -5.99 |
| ZnO | 0.03538 | 0.03692 | 4.35 | 0.02039 | 0.02016 | -1.11 | 0.03118 | 0.03013 | -3.36 | 0.02061 | 0.02086 | 1.22 |
| $ZrO_2$ | 0.05675 | 0.05451 | -3.95 | 0.02205 | 0.02047 | -7.18 | 0.02504 | 0.02410 | -3.78 | 0.05375 | 0.05328 | -0.88 |

(a) Measured concentrations below detection limits were treated as 0.

Table J.1. Normalized Measured Compositions (mass fractions) for Baseline and Sulfur-Saturated Versions of the LAW Phase 2 Glasses (cont.)

| | Glass ID | | | | | | | | | | | |
|---|---|---|---|---|---|---|---|---|---|---|---|---|
| | LP2-OL-09-1 | | | LP2-OL-10 MOD | | | LP2-OL-11 | | | LP2-OL-12 | | |
| Components | Baseline | Sulfur-saturated | % Diff | Baseline | Sulfur-saturated | % Diff | Baseline | Sulfur-saturated | % Diff | Baseline | Sulfur-saturated | % Diff |
| $Al_2O_3$ | 0.12079 | 0.11592 | -4.03 | 0.11691 | 0.11888 | 1.69 | 0.05581 | 0.05658 | 1.39 | 0.05847 | 0.05673 | -2.99 |
| $B_2O_3$ | 0.14041 | 0.13041 | -7.13 | 0.05750 | 0.05903 | 2.66 | 0.13417 | 0.13139 | -2.07 | 0.13930 | 0.13156 | -5.55 |
| CaO | 0.01981 | 0.01921 | -3.06 | 0.10955 | 0.11469 | 4.69 | 0.07935 | 0.07791 | -1.82 | 0.08039 | 0.07617 | -5.25 |
| Cl | 0.0000[a] | 0.0000[a] | -- | 0.00386 | 0.00114 | -70.36 | 0.00052 | 0.0000[a] | -- | 0.00353 | 0.00230 | -34.68 |
| $Cr_2O_3$ | 0.00703 | 0.00380 | -45.99 | 0.00413 | 0.00123 | -70.27 | 0.00407 | 0.00141 | -65.28 | 0.00697 | 0.00382 | -45.27 |
| F | 0.00068 | 0.0000[a] | -- | 0.00662 | 0.00512 | -22.74 | 0.00078 | 0.00071 | -9.37 | 0.00594 | 0.00515 | -13.36 |
| $Fe_2O_3$ | 0.00580 | 0.0000[a] | -- | 0.01961 | 0.01508 | -23.10 | 0.00334 | 0.0000[a] | -- | 0.01888 | 0.01462 | -22.56 |
| $K_2O$ | 0.0000[a] | 0.0000[a] | -- | 0.0000[a] | 0.0000[a] | -- | 0.05406 | 0.04438 | -17.91 | 0.0000[a] | 0.0000[a] | -- |
| MgO | 0.0000[a] | 0.0000[a] | -- | 0.0000[a] | 0.0000[a] | -- | 0.01350 | 0.01309 | -3.00 | 0.01342 | 0.01318 | -1.83 |
| $Na_2O$ | 0.194503 | 0.20269 | 3.92 | 0.20971 | 0.20855 | -0.55 | 0.20419 | 0.21275 | 4.19 | 0.24666 | 0.24494 | -0.69 |
| $P_2O_5$ | 0.00245 | 0.0000[a] | -- | 0.01761 | 0.01326 | -24.66 | 0.00237 | 0.00209 | -11.81 | 0.01451 | 0.01221 | -15.82 |
| $SiO_2$ | 0.40663 | 0.42397 | 4.27 | 0.39293 | 0.40356 | 2.70 | 0.37129 | 0.37122 | -0.02 | 0.36839 | 0.37624 | 2.14 |
| $SO_3$ | 0.00110 | 0.01081 | 884 | 0.00734 | 0.01116 | 52.11 | 0.00149 | 0.01485 | 897 | 0.00139 | 0.02354 | 1595 |
| $SnO_2$ | 0.01562 | 0.01386 | -11.27 | 0.00268 | 0.0000[a] | -- | 0.00268 | 0.0000[a] | -- | 0.0000[a] | 0.0000[a] | -- |
| $V_2O_5$ | 0.03841 | 0.03657 | -4.78 | 0.0000[a] | 0.0000[a] | -- | 0.0000[a] | 0.0000[a] | -- | 0.0000[a] | 0.0000[a] | -- |
| ZnO | 0.01978 | 0.01976 | -0.12 | 0.02057 | 0.02160 | 5.00 | 0.01983 | 0.01939 | -2.19 | 0.02041 | 0.02037 | -0.16 |
| $ZrO_2$ | 0.02645 | 0.02301 | -12.98 | 0.03099 | 0.02671 | -13.81 | 0.05255 | 0.05423 | 3.19 | 0.02178 | 0.01917 | -11.98 |

(a) Measured concentrations below detection limits were treated as 0.

Table J.1. Normalized Measured Compositions (mass fractions) for Baseline and Sulfur-Saturated Versions of the LAW Phase 2 Glasses (cont.)

| | Glass ID | | | | | | | | | | | |
|---|---|---|---|---|---|---|---|---|---|---|---|---|
| | LP2-OL-13 | | | LP2-OL-14 | | | LP2-OL-15 | | | LP2-OL-16 MOD | | |
| Components | Baseline | Sulfur-saturated | % Diff | Baseline | Sulfur-saturated | % Diff | Baseline | Sulfur-saturated | % Diff | Baseline | Sulfur-saturated | % Diff |
| $Al_2O_3$ | 0.05757 | 0.05750 | -0.12 | 0.05829 | 0.05714 | -1.98 | 0.05918 | 0.05586 | -5.62 | 0.05396 | 0.05536 | 2.59 |
| $B_2O_3$ | 0.06076 | 0.05884 | -3.17 | 0.14430 | 0.12904 | -10.58 | 0.14187 | 0.13080 | -7.80 | 0.07203 | 0.07225 | 0.30 |
| CaO | 0.11149 | 0.11173 | 0.22 | 0.07495 | 0.06913 | -7.77 | 0.10887 | 0.09947 | -8.63 | 0.03020 | 0.03130 | 3.64 |
| Cl | 0.00306 | 0.00141 | -53.95 | 0.0000[a] | 0.0000[a] | -- | 0.0000[a] | 0.0000[a] | -- | 0.00051 | 0.0000[a] | -- |
| $Cr_2O_3$ | 0.00383 | 0.00150 | -60.75 | 0.00706 | 0.00329 | -53.38 | 0.00707 | 0.00355 | -49.69 | 0.00700 | 0.00335 | -52.07 |
| F | 0.00609 | 0.00508 | -16.63 | 0.00074 | 0.00056 | -23.47 | 0.00071 | 0.00061 | -15.29 | 0.00074 | 0.00055 | -25.29 |
| $Fe_2O_3$ | 0.00374 | 0.0000[a] | -- | 0.00301 | 0.0000[a] | -- | 0.02051 | 0.01445 | -29.55 | 0.01853 | 0.01457 | -2137 |
| $K_2O$ | 0.05696 | 0.04621 | -18.88 | 0.05870 | 0.04594 | -21.74 | 0.0000[a] | 0.0000[a] | -- | 0.0000[a] | 0.0000[a] | -- |
| MgO | 0.0000[a] | 0.0000[a] | -- | 0.0000[a] | 0.0000[a] | -- | 0.0000[a] | 0.0000[a] | -- | 0.01282 | 0.01278 | -0.31 |
| $Na_2O$ | 0.21019 | 0.22292 | 6.06 | 0.19924 | 0.20788 | 4.34 | 0.1545 | 0.20206 | 3.38 | 0.20194 | 0.19897 | -1.47 |
| $P_2O_5$ | 0.01803 | 0.01754 | -2.68 | 0.0000[a] | 0.0000[a] | -- | 0.0000[a] | 0.0000[a] | -- | 0.00201 | 0.00174 | -13.60 |
| $SiO_2$ | 0.36058 | 0.35975 | -0.23 | 0.35491 | 0..38266 | 7.82 | 0.37227 | 0.38387 | 3.12 | 0.49174 | 0.49760 | 1.19 |
| $SO_3$ | 0.00104 | 0.01555 | 1389 | 0.01581 | 0.02619 | 65.67 | 0.00122 | 0.01975 | 1525 | 0.00883 | 0.01195 | 35.31 |
| $SnO_2$ | 0.00284 | 0.0000[a] | -- | 0.0000[a] | 0.0000[a] | -- | 0.03536 | 0.03202 | -9.44 | 0.00434 | 0.00271 | -37.48 |
| $V_2O_5$ | 0.04059 | 0.03757 | -7.43 | 0.04181 | 0.03768 | -9.88 | 0.0000[a] | 0.0000[a] | -- | 0.03717 | 0.03634 | -2.23 |
| ZnO | 0.03764 | 0.03784 | 0.55 | 0.02122 | 0.02023 | -4.67 | 0.03626 | 0.03452 | -4.79 | 0.03389 | 0.03503 | 3.36 |
| $ZrO_2$ | 0.02559 | 0.02654 | 3.70 | 0.01997 | 0.02026 | 1.45 | 0.02124 | 0.02305 | 8.51 | 0.02429 | 0.02550 | 4.98 |

(a) Measured concentrations below detection limits were treated as 0.

Table J.1. Normalized Measured Compositions (mass fractions) for Baseline and Sulfur-Saturated Versions of the LAW Phase 2 Glasses (cont.)

| | Glass ID | | | | | | | | | | | |
|---|---|---|---|---|---|---|---|---|---|---|---|---|
| | LP2-OL-17 | | | LP2-OL-18 | | | LP2-OL-19 | | | LP2-OL-20 | | |
| Components | Baseline | Sulfur-saturated | % Diff | Baseline | Sulfur-saturated | % Diff | Baseline | Sulfur-saturated | % Diff | Baseline | Sulfur-saturated | % Diff |
| $Al_2O_3$ | 0.05860 | 0.05800 | -1.04 | 0.05964 | 0.06124 | 2.68 | 0.05998 | 0.06054 | 0.94 | 0.05705 | 0.05664 | -0.72 |
| $B_2O_3$ | 0.06334 | 0.05781 | -8.73 | 0.06122 | 0.06237 | 1.87 | 0.06362 | 0.06162 | -3.14 | 0.05947 | 0.05695 | -4.25 |
| CaO | 0.04452 | 0.04505 | 1.19 | 0.08913 | 0.09224 | 3.48 | 0.03694 | 0.03724 | 0.82 | 0.08273 | 0.08171 | -1.23 |
| Cl | 0.00337 | 0.00190 | -43.55 | 0.00329 | 0.00100 | -69.45 | 0.00058 | 0.0000[a] | -- | 0.00066 | 0.0000[a] | -- |
| $Cr_2O_3$ | 0.00387 | 0.0000[a] | -- | 0.00679 | 0.00259 | -61.81 | 0.00447 | 0.00129 | -71.17 | 0.00444 | 0.00190 | -57.14 |
| F | 0.00618 | 0.00516 | -16.52 | 0.00651 | 0.00543 | -16.64 | 0.00085 | 0.00072 | -15.19 | 0.00083 | 0.00080 | -3.91 |
| $Fe_2O_3$ | 0.01812 | 0.01475 | -18.61 | 0.00477 | 0.0000[a] | -- | 0.02075 | 0.01610 | -22.42 | 0.00549 | 0.0000[a] | -- |
| $K_2O$ | 0.05520 | 0.04621 | -16.29 | 0.0000[a] | 0.0000[a] | -- | 0.05945 | 0.04915 | -17.31 | 0.0000[a] | 0.0000[a] | -- |
| MgO | 0.01320 | 0.01315 | -0.35 | 0.01324 | 0.01339 | 1.19 | 0.0000[a] | 0.0000[a] | -- | 0.0000[a] | 0.0000[a] | -- |
| $Na_2O$ | 0.21027 | 0.22342 | 6.26 | 0.20963 | 0.20648 | -1.50 | 0.20207 | 0.21311 | 5.47 | 0.26211 | 0.27016 | 3.07 |
| $P_2O_5$ | 0.01499 | 0.01196 | -20.22 | 0.01320 | 0.01033 | -21.71 | 0.00255 | 0.00212 | -16.93 | 0.00220 | 0.00181 | -17.47 |
| $SiO_2$ | 0.38970 | 0.39368 | 1.02 | 0.35247 | 0.36750 | 4.26 | 0.45472 | 0.46307 | 1.84 | 0.45702 | 0.44846 | -1.87 |
| $SO_3$ | 0.00141 | 0.01789 | 1165 | 0.01036 | 0.01249 | 20.56 | 0.00653 | 0.01018 | 55.77 | 0.00123 | 0.01915 | 1455 |
| $SnO_2$ | 0.03482 | 0.03300 | -5.24 | 0.03975 | 0.03796 | -4.50 | 0.03820 | 0.03679 | -3.68 | 0.00265 | 0.0000[a] | -- |
| $V_2O_5$ | 0.03928 | 0.03669 | -6.58 | 0.04104 | 0.03862 | -5.90 | 0.0000[a] | 0.0000[a] | -- | 0.0000[a] | 0.0000[a] | -- |
| ZnO | 0.02015 | 0.02054 | 1.92 | 0.03829 | 0.03976 | 3.83 | 0.02118 | 0.02160 | 1.98 | 0.03813 | 0.03731 | -215 |
| $ZrO_2$ | 0.02297 | 0.02080 | -9.44 | 0.05066 | 0.04859 | -4.10 | 0.02812 | 0.02646 | -5.90 | 0.02599 | 0.02510 | -3.41 |

(a) Measured concentrations below detection limits were treated as 0.

Table J.1. Normalized Measured Compositions (mass fractions) for Baseline and Sulfur-Saturated Versions of the LAW Phase 2 Glasses (cont.)

| | Glass ID | | | | | | | | | | | |
|---|---|---|---|---|---|---|---|---|---|---|---|---|
| | LP2-OL-21 | | | LP2-OL-22 | | | LP2-OL-23 | | | LP2-OL-24 | | |
| Components | Baseline | Sulfur-saturated | % Diff | Baseline | Sulfur-saturated | % Diff | Baseline | Sulfur-saturated | % Diff | Baseline | Sulfur-saturated | % Diff |
| $Al_2O_3$ | 0.09221 | 0.09287 | 0.71 | 0.06779 | 0.06749 | -0.44 | 0.05545 | 0.05433 | -2.01 | 0.11546 | 0.11707 | 1.40 |
| $B_2O_3$ | 0.09296 | 0.09166 | -1.40 | 0.06123 | 0.05988 | -2.21 | 0.13342 | 0.12699 | -4.82 | 0.05877 | 0.05568 | -5.25 |
| CaO | 0.05053 | 0.05065 | 0.23 | 0.11149 | 0.10966 | -1.64 | 0.10498 | 0.10592 | 0.90 | 0.07516 | 0.07456 | -0.80 |
| Cl | 0.00160 | 0.00072 | -54.87 | 0.0000[a] | 0.0000[a] | -- | 0.00056 | 0.0000[a] | -- | 0.00062 | 0.0000[a] | -- |
| $Cr_2O_3$ | 0.00545 | 0.00213 | -60.89 | 0.00391 | 0.00147 | -62.40 | 0.00425 | 0.00220 | -48.32 | 0.00426 | 0.00146 | -65.81 |
| F | 0.00274 | 0.00232 | -15.26 | 0.00078 | 0.00067 | -13.72 | 0.00072 | 0.00055 | -24.10 | 0.00096 | 0.00072 | -25.32 |
| $Fe_2O_3$ | 0.00939 | 0.00603 | -35.75 | 0.01975 | 0.01552 | -21.43 | 0.00602 | 0.0000[a] | -- | 0.01940 | 0.01478 | -23.83 |
| $K_2O$ | 0.01041 | 0.00810 | -22.12 | 0.0000[a] | 0.0000[a] | -- | 0.0000[a] | 0.0000[a] | -- | 0.0000[a] | 0.0000[a] | -- |
| MgO | 0.00634 | 0.00661 | 4.38 | 0.0000[a] | 0.0000[a] | -- | 0.01313 | 0.01363 | 3.75 | 0.01368 | 0.01377 | 0.68 |
| $Na_2O$ | 0.21651 | 0.22456 | 3.72 | 0.20025 | 0.20704 | 3.39 | 0.20573 | 0.20888 | 1.53 | 0.25558 | 0.25489 | -0.27 |
| $P_2O_5$ | 0.00623 | 0.00549 | -11.80 | 0.00286 | 0.00252 | -12.03 | 0.00196 | 0.00195 | -0.36 | 0.00194 | 0.00195 | 030 |
| $SiO_2$ | 0.41480 | 0.41268 | -0.51 | 0.37796 | 0.37600 | -0.52 | 0.36620 | 0.37287 | 1.82 | 0.34382 | 0.34754 | 1.08 |
| $SO_3$ | 0.00495 | 0.01128 | 128 | 0.00108 | 0.01180 | 990 | 0.01167 | 0.01737 | 48.92 | 0.00130 | 0.01421 | 997 |
| $SnO_2$ | 0.01770 | 0.01607 | -9.20 | 0.03716 | 0.03551 | -4.43 | 0.03565 | 0.03392 | -4.85 | 0.00253 | 0.0000[a] | -- |
| $V_2O_5$ | 0.00937 | 0.00895 | -4.44 | 0.04064 | 0.03749 | -7.74 | 0.0000[a] | 0.0000[a] | -- | 0.04135 | 0.03775 | -8.72 |
| ZnO | 0.02702 | 0.02730 | 1.06 | 0.02082 | 0.02044 | -1.84 | 0.03437 | 0.03512 | 2.20 | 0.03857 | 0.03839 | -0.46 |
| $ZrO_2$ | 0.03181 | 0.03257 | 2.39 | 0.05426 | 0.05450 | 0.45 | 0.02588 | 0.02626 | 1.47 | 0.02660 | 0.02724 | 2.39 |

(a) Measured concentrations below detection limits were treated as 0.

Table J.1. Normalized Measured Compositions (mass fractions) for Baseline and Sulfur-Saturated Versions of the LAW Phase 2 Glasses (cont.)

| | Glass ID | | |
|---|---|---|---|
| | LP2-OL-25 | | |
| Components | Baseline | Sulfur-saturated | % Diff |
| $Al_2O_3$ | 0.05918 | 0.05884 | -0.58 |
| $B_2O_3$ | 0.13734 | 0.13380 | -2.58 |
| CaO | 0.02686 | 0.02783 | 3.64 |
| Cl | 0.00059 | 0.0000[a] | -- |
| $Cr_2O_3$ | 0.00411 | 0.00150 | -63.5 |
| F | 0.00078 | 0.00073 | -6.75 |
| $Fe_2O_3$ | 0.02038 | 0.01574 | -22.76 |
| $K_2O$ | 0.0000[a] | 0.0000[a] | -- |
| MgO | 0.0000[a] | 0.0000[a] | -- |
| $Na_2O$ | 0.24420 | 0.24933 | 2.10 |
| $P_2O_5$ | 0.00286 | 0.00261 | -8.55 |
| $SiO_2$ | 0.36664 | 0.36533 | -0.36 |
| $SO_3$ | 0.00809 | 0.01293 | 59.94 |
| $SnO_2$ | 0.03797 | 0.03622 | -4.62 |
| $V_2O_5$ | 0.0000[a] | 0.0000[a] | -- |
| ZnO | 0.03618 | 0.03776 | 4.37 |
| $ZrO_2$ | 0.05482 | 0.05739 | 4.68 |

(a) Measured concentrations below detection limits were treated as 0.

Table J.2. Measured Concentrations for the Sulfur-Wash Solutions from Phase 2 Enhanced LAW Glasses (mg/L)

| Component | LP2-IL-01 | LP2-IL-02 | LP2-IL-03 | LP2-IL-04 | LP2-IL-05 | LP2-IL-06 | LP2-IL-07 | LP2-IL-08 | LP2-IL-09 | LP2-IL-10 |
|---|---|---|---|---|---|---|---|---|---|---|
| Al | <1.00 | <1.00 | 1.29 | <1.00 | <1.00 | <1.00 | <1.00 | <1.00 | <1.00 | <1.00 |
| B | 21.1 | 26.4 | 27.3 | 19.0 | 24.4 | 32.6 | 27.2 | 16.8 | 27.6 | 20.1 |
| Ca | 2.30 | 1.41 | <1.00 | 1.96 | <1.00 | 2.30 | 2.99 | 1.61 | 1.31 | 3.53 |
| Cr | 34.5 | 21.9 | 36.0 | 617 | 12.9 | 37.7 | 14.3 | 43.6 | 39.5 | 44.7 |
| Fe | <1.00 | <1.00 | <1.00 | <1.00 | <1.00 | <1.00 | <1.00 | <1.00 | <1.00 | <1.00 |
| K | 82.5 | 106 | 40.6 | 110 | 23.5 | 103 | 90.5 | 32.1 | 15.0 | 53.1 |
| Li | <1.00 | <1.00 | <1.00 | <1.00 | <1.00 | <1.00 | <1.00 | <1.00 | <1.00 | <1.00 |
| Mg | <1.00 | <1.00 | <1.00 | <1.00 | <1.00 | <1.00 | <1.00 | <1.00 | <1.00 | <1.00 |
| Na | 653 | 957 | 1030 | 793 | 698 | 996 | 775 | 885 | 602 | 819 |
| P | 5.95 | 15.0 | 32.0 | 16.1 | 7.10 | 21.1 | 10.2 | 7.73 | 8.48 | 9.88 |
| S | 373 | 606 | 561 | 487 | 414 | 604 | 495 | 544 | 332 | 508 |
| Si | 19.7 | 13.0 | 15.8 | 8.38 | 9.56 | 6.17 | 8.67 | 6.70 | 17.8 | 8.06 |
| Sn | <1.00 | <1.00 | 1.28 | <1.00 | <1.00 | <1.00 | <1.00 | <1.00 | <1.00 | <1.00 |
| V | 22.7 | 6.06 | 7.83 | 5.69 | 3.73 | 16.1 | 4.30 | 4.80 | 19.2 | 10.7 |
| Zn | <1.00 | <1.00 | <1.00 | <1.00 | <1.00 | <1.00 | <1.00 | <1.00 | <1.00 | <1.00 |
| Zr | <1.00 | <1.00 | <1.00 | <1.00 | <1.00 | <1.00 | <1.00 | <1.00 | <1.00 | <1.00 |
| Cl | <10.0 | 12.0 | 30.3 | 16.7 | 20.4 | 27.4 | 24.3 | 19.7 | <10.0 | 10.9 |
| F | <10.0 | <10.0 | 13.7 | <10.1 | <10.0 | <10.0 | <10.0 | <10.0 | <10.0 | <10.0 |
| $PO_4$ | <100 | <100 | <100 | <100 | <100 | <100 | <100 | <100 | <100 | <100 |
| $SO_4$ | 1130 | 1780 | 1680 | 1450 | 1240 | 1780 | 1450 | 1600 | 996 | 1503.33 |

Table J.2. Measured Concentrations for the Sulfur-Wash Solutions from LAW Phase 2 Glasses (mg/L) (cont)

| Component | LP2-IL-11 | LP2-IL-12 | LP2-IL-13 | LP2-IL-14 | LP2-IL-15 | LP2-IL-16 | LP2-IL-17 | LP2-OL-01-3 | LP2-OL-02-1 | LP2-OL-03MOD2 |
|---|---|---|---|---|---|---|---|---|---|---|
| Al | <1.00 | <1.00 | <1.00 | <1.00 | <1.00 | <1.00 | <1.00 | <1.00 | 9.47 | 1.42 |
| B | 17.3 | 19.5 | 25.3 | 24.7 | 23.0 | 23.0 | 26.8 | 10.3 | 23.4 | 13.4 |
| Ca | 1.36 | 1.58 | 2.60 | 2.66 | <1.00 | 1.63 | 5.16 | 7.42 | 5.73 | 4.33 |
| Cr | 28.2 | 17.1 | 18.9 | 31.3 | 21.5 | 35.5 | 1.79 | 63.6 | 50.4 | 88.0 |
| Fe | <1.00 | <1.00 | <1.00 | <1.00 | <1.00 | <1.00 | <1.00 | <1.00 | <1.00 | <1.00 |
| K | 79.3 | 18.7 | 88.3 | 20.1 | 22.2 | 56.9 | 25.2 | <1.00 | 46.7 | <1.00 |
| Li | <1.00 | <1.00 | <1.00 | <1.00 | <1.00 | <1.00 | <1.00 | <1.00 | <1.00 | <1.00 |
| Mg | <1.00 | <1.00 | <1.00 | <1.00 | <1.00 | <1.00 | <1.00 | <1.00 | <1.00 | <1.00 |
| Na | 774 | 814 | 770 | 779 | 939 | 853 | 883 | 767 | 774 | 852 |
| P | 20.9 | 20.5 | 10.2 | 16.0 | 21.7 | 9.45 | 5.06 | <1.00 | 8.21 | 3.69 |
| S | 546 | 464 | 503 | 410 | 542 | 521 | 587 | 457 | 422 | 418 |
| Si | 7.61 | 16.9 | 9.67 | 7.92 | 9.81 | 7.61 | 10.1 | 5.50 | 36.3 | 6.09 |
| Sn | <1.00 | <1.00 | <1.00 | <1.00 | <1.00 | <1.00 | <1.00 | <1.00 | <1.00 | <1.00 |
| V | 31.7 | 28.4 | 4.22 | 4.90 | 27.1 | 11.0 | 21.7 | <1.00 | 10.0 | <1.00 |
| Zn | <1.00 | <1.00 | <1.00 | <1.00 | <1.00 | <1.00 | <1.00 | <1.00 | <1.00 | <1.00 |
| Zr | <1.00 | <1.00 | <1.00 | <1.00 | <1.00 | <1.00 | <1.00 | <1.00 | <1.00 | <1.00 |
| Cl | 23.0 | 21.5 | 11.5 | 15.9 | 28.7 | 12.8 | <10.0 | <10.0 | <10.0 | <10.0 |
| F | <1.00 | <10.0 | <10.0 | <10.0 | <1.00 | <10.0 | <10.0 | <10.0 | <10.0 | <10.0 |
| $PO_4$ | <100 | <100 | <100 | <100 | <100 | <100 | <100 | <10.0 | 17.1 | <10.0 |
| $SO_4$ | 1360 | 1360 | 1490 | 1360 | 1620 | 1540 | 1730 | 1450 | 1360 | 1430 |

Table J.2. Measured Concentrations for the Sulfur-Wash Solutions from LAW Phase 2 Glasses (mg/L) (cont)

| Component | LP2-OL-04-1 | LP2-OL-05 | LP2-OL-07-1 | LP2-OL-08MOD | LP2-OL-09-1 | LP2-OL-10MOD | LP2-OL-11 | LP2-OL-12 | LP2-OL-13 | LP2-OL-14 |
|---|---|---|---|---|---|---|---|---|---|---|
| Al | 1.79 | 1.31 | 1.01 | <1.00 | <1.00 | <1.00 | <1.00 | <1.00 | <1.00 | <1.00 |
| B | 15.1 | 14.1 | 24.5 | 17.0 | 33.1 | 9.91 | 75.3 | 40.2 | 103 | 44.7 |
| Ca | <1.00 | <1.00 | 19.5 | 11.9 | 10.2 | 4.78 | 10.6 | <1.00 | <1.00 | 9.13 |
| Cr | 108 | 32.0 | 61.1 | 68.7 | 56.0 | 42.1 | 73.5 | 57.0 | 204 | 57.3 |
| Fe | <1.00 | <1 | <1.00 | <1.00 | <1.00 | <1.00 | <1.00 | <1.00 | <1.00 | <1.00 |
| K | 397 | <1.00 | 10.8 | <1.00 | <1.00 | <1.00 | 523 | <1.00 | 1430 | 243 |
| Li | <1.00 | <1.00 | <1.00 | <1.00 | <1.00 | <1.00 | <1.00 | <1.00 | <1.00 | <1.00 |
| Mg | <1.00 | <1.00 | <1.00 | <1.00 | <1.00 | <1.00 | <1.00 | <1.00 | <1.00 | <1.00 |
| Na | 642 | 1090 | 1030 | 830 | 913 | 910 | 1060 | 744 | 3240 | 669 |
| P | 2.60 | 3.03 | <1.00 | 2.27 | 5.33 | 9.24 | 2.05 | 8.93 | 25.3 | <1.00 |
| S | 470 | 656 | 609 | 382 | 497 | 513 | 699 | 324 | 1770 | 387 |
| Si | 6.01 | 6.46 | 6.72 | 19.0 | 7.13 | 2.74 | 27.2 | 29.1 | 154 | 26.9 |
| Sn | <1.00 | <1.00 | <1.00 | <1.00 | <1.00 | <1.00 | <1.00 | <1.00 | <1.00 | <1.00 |
| V | <1.00 | <1.00 | 8.46 | 63.5 | 56.4 | <1.00 | <1.00 | <1.00 | 387 | 49.9 |
| Zn | <1.00 | <1.00 | <1.00 | <1.00 | <1.00 | <1.00 | <1.00 | <1.00 | <1.00 | <1.00 |
| Zr | <1.00 | <1.00 | <1.00 | <1.00 | <1.00 | <1.00 | <1.00 | <1.00 | <1.00 | <1.00 |
| Cl | <10.0 | 46.8 | 21.8 | <10.0 | <10.0 | 21.8 | <10.0 | 23.9 | 117 | <10.0 |
| F | <10.0 | 26.4 | <10.0 | <10.0 | <10.0 | 20.6 | <10.0 | 17.8 | 107 | <10.0 |
| $PO_4$ | <10.0 | <10.0 | <10.0 | <10.0 | <10.0 | 18.4 | <10.0 | 18.1 | 56.6 | <10.0 |
| $SO_4$ | 1440 | 2090 | 1830 | 1210 | 1600 | 1620 | 2160 | 1040 | 5480 | 1230 |

Table J.2. Measured Concentrations for the Sulfur-Wash Solutions from LAW Phase 2 Glasses (mg/L) (cont)

| Component | LP2-OL-15 | LP2-OL-16MOD | LP2-OL-17 | LP2-OL-18 | LP2-OL-19 | LP2-OL-20 | LP2-OL-21 | LP2-OL-22 | LP2-OL-23 | LP2-OL-24 | LP2-OL-25 |
|---|---|---|---|---|---|---|---|---|---|---|---|
| Al | <1.00 | <1.00 | <1.00 | <1.00 | <1.00 | <1.00 | <1.00 | <1.00 | <1.00 | 1.51 | <1.00 |
| B | 23.3 | 11.0 | 19.0 | 13.0 | 20.0 | 10.8 | 21.9 | 18.2 | 28.6 | 12.4 | 69.2 |
| Ca | 13.0 | 10.3 | <1.00 | 8.05 | 2.26 | <1.00 | <1.00 | 23.7 | 20.6 | 8.19 | 1.82 |
| Cr | 46.2 | 59.2 | 39.2 | 82.4 | 52.5 | 27.9 | 53.0 | 51.6 | 27.3 | 36.3 | 54.3 |
| Fe | <1.00 | <1.00 | <1.00 | <1.00 | <1.00 | <1.00 | <1.00 | <1.00 | <1.00 | <1.00 | <1.00 |
| K | <1.00 | <1.00 | 256 | <1.00 | 358 | <1.00 | 46.0 | 2.21 | <1.00 | <1.00 | <1.00 |
| Li | <1.00 | <1.00 | <1.00 | <1.00 | <1.00 | <1.00 | <1.00 | <1.00 | <1.00 | <1.00 | <1.00 |
| Mg | <1.00 | <1.00 | <1.00 | <1.00 | <1.00 | <1.00 | <1.00 | <1.00 | <1.00 | <1.00 | <1.00 |
| Na | 673 | 935 | 726 | 1020 | 880 | 623 | 807 | 1157 | 777 | 718 | 1330 |
| P | <1.00 | 4.65 | 28.0 | 9.12 | 6.24 | 1.99 | 8.26 | 1.44 | 2.10 | 3.05 | 8.12 |
| S | 369 | 514 | 377 | 510 | 627 | 349 | 449 | 646 | 447 | 372 | 737 |
| Si | 11.4 | 5.84 | 25.2 | 8.11 | 12.0 | 16.3 | 10.2 | 17.3 | 12.7 | 8.85 | 16.1 |
| Sn | <1.00 | <1.00 | <1.00 | <1.00 | <1.00 | <1.00 | <1.00 | <1.00 | <1.00 | <1.00 | <1.00 |
| V | <1.00 | 42.4 | 90.1 | 79.6 | <1.00 | <1.00 | 11.0 | 78.6 | <1.00 | 67.5 | <1.00 |
| Zn | <1.00 | <1.00 | <1.00 | <1.00 | <1.00 | <1.00 | <1.00 | <1.00 | <1.00 | <1.00 | <1.00 |
| Zr | <1.00 | <1.00 | <1.00 | <1.00 | <1.00 | <1.00 | <1.00 | <1.00 | <1.00 | <1.00 | <1.00 |
| Cl | <10.0 | <10.0 | 27.6 | 23.1 | <10.0 | <10.0 | 13.8 | <10.0 | <10.0 | <10.0 | <10.0 |
| F | <10.0 | <10.0 | 24.9 | 19.2 | <10.0 | <10.0 | <10.0 | <10.0 | <10.0 | <10.0 | <10.0 |
| $PO_4$ | <10.0 | <10.0 | 64.2 | 20.2 | 13.6 | <10.0 | 15.7 | <10.0 | <10.0 | <10.0 | 17.9 |
| $SO_4$ | 1200 | 1620 | 1160 | 1690 | 1930 | 1130 | 1360 | 2020 | 1380 | 1160 | 2270 |

PNNL-28838 Rev 2
EWG-RPT-021 Rev. 2

# Pacific Northwest National Laboratory

902 Battelle Boulevard
P.O. Box 999
Richland, WA 99354
1-888-375-PNNL (7665)

***www.pnnl.gov***